

AD-A276 485



**THREE-DIMENSIONAL VELOCITY MEASUREMENTS
ON A 6:1 PROLATE SPHEROID
AT 10° ANGLE OF ATTACK**

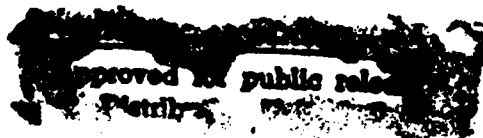
VPI-AOE-202

Christopher J. Chesnakas, Roger L. Simpson and Michael M. Madden
Department of Aerospace and Ocean Engineering
Virginia Polytechnic Institute and State University
Blacksburg, Virginia 24061

January 18, 1994
(revised)

DTIC
S ELECTE D
MAR 03 1994
E

94-07076



94 3 03 021

REPORT DOCUMENTATION PAGE

Form Approved
OMB No. 0704-0188

Public reporting burden for this collection of information is estimated to average 1 hour per response, including the time for reviewing instructions, searching existing data sources, gathering and maintaining the data needed, and completing and reviewing the collection of information. Send comments regarding this burden estimate or any other aspect of this collection of information, including suggestions for reducing this burden, to Washington Headquarters Services, Directorate for Information Operations and Reports, 1215 Jefferson Davis Highway, Suite 1204, Arlington, VA 22202-4302, and to the Office of Management and Budget, Paperwork Reduction Project (0704-0188), Washington, DC 20503.

1. AGENCY USE ONLY (Leave blank)		2. REPORT DATE Jan. 18, 1994	3. REPORT TYPE AND DATES COVERED Technical 5/16/91 - 3/15/93
4. TITLE AND SUBTITLE Three-Dimensional Velocity Measurements on a 6:1 Prolate Spheroid at 10° Angle of Attack			5. FUNDING NUMBERS N00014-91-J-1 732
6. AUTHOR(S) Christopher J. Chesnakas, Roger L. Simpson and Michael M. Madden			
7. PERFORMING ORGANIZATION NAME(S) AND ADDRESS(ES) Aerospace and Ocean Engineering Department Virginia Polytechnic Institute and State University Blacksburg, VA 24061-0203			8. PERFORMING ORGANIZATION REPORT NUMBER VPI-AOE-202
9. SPONSORING/MONITORING AGENCY NAME(S) AND ADDRESS(ES) Advanced Research Projects Agency 370 Fairfax Drive, Suite 100, Arlington, VA 22203-1714 through Office of Naval Research, Applied Hydrodynamics 800 N. Quincy St., Arlington, VA 22217			10. SPONSORING/MONITORING AGENCY REPORT NUMBER
11. SUPPLEMENTARY NOTES			
12a. DISTRIBUTION/AVAILABILITY STATEMENT Approved for public releases, distribution unlimited			12b. DISTRIBUTION CODE
13. ABSTRACT (Maximum 200 words) The flow in the cross-flow separation region of a 6:1 prolate spheroid at 10° angle of attack, $Re_L = 4.20 \times 10^6$, was investigated using a novel 3-D fiber-optic Laser Doppler Velocimeter (LDV). The probe was used to measure three simultaneous, orthogonal velocity components from within the model. The design and operation of this LDV probe is described and velocity, Reynolds stress, and velocity triple product measurements are presented from the inner boundary layer through the boundary-layer edge.			
14. SUBJECT TERMS Three Dimensional Separation Turbulence Laser-Doppler Velocimetry			15. NUMBER OF PAGES 217
			16. PRICE CODE
17. SECURITY CLASSIFICATION OF REPORT Unclassified	18. SECURITY CLASSIFICATION OF THIS PAGE Unclassified	19. SECURITY CLASSIFICATION OF ABSTRACT Unclassified	20. LIMITATION OF ABSTRACT None

THREE-DIMENSIONAL VELOCITY MEASUREMENTS ON A 6:1 PROLATE SPHEROID AT 10° ANGLE OF ATTACK

VPI-AOE-202

Christopher J. Chesnakas, Roger L. Simpson and Michael M. Madden
Department of Aerospace and Ocean Engineering
Virginia Polytechnic Institute and State University
Blacksburg, Virginia 24061

January 18, 1994
(revised)

Accession For	
NTIS	<input checked="" type="checkbox"/>
CRA&I	<input checked="" type="checkbox"/>
DTIC	<input type="checkbox"/>
TAB	<input type="checkbox"/>
Unannounced	<input type="checkbox"/>
Justification	
By	
Distribution /	
Availability Codes	
Dist	Avail and/or Special
A-1	

ABSTRACT

The flow in the cross-flow separation region of a 6:1 prolate spheroid at 10° angle of attack, $Re_L = 4.20 \times 10^6$, was investigated using a novel 3-D fiber-optic Laser Doppler Velocimeter (LDV). The probe was used to measure three simultaneous, orthogonal velocity components from within the model. The design and operation of this LDV probe is described and velocity, Reynolds stress, and velocity triple product measurements are presented from the inner boundary layer through the boundary-layer edge.

TABLE OF CONTENTS

LIST OF TABLES	ii
LIST OF FIGURES	iv
NOMENCLATURE	x
1.0 INTRODUCTION	1
2.0 EXPERIMENTAL FACILITY	2
2.1 Wind Tunnel	2
2.2 Model	2
2.3 Fiber-Optic Probe	2
2.4 Seeding System	4
2.5 Test Conditions	4
2.6 Measurement Uncertainty	5
3.0 RESULTS	5
4.0 DISCUSSION	8
5.0 CONCLUSIONS	8
APPENDIX A: OIL FLOW AND SURFACE PRESSURE MEASUREMENTS	202
A.1 Surface Oil Flow Visualization	202
A.2 Surface Pressure Measurements	202
ACKNOWLEDGEMENTS	215
REFERENCES	216

LIST OF TABLES

Table 1.	Boundary-layer profile summary.	10
Table 2.	Boundary-layer profile at $x/L = 0.400$, $\phi = 90^\circ$	11
Table 3.	Boundary-layer profile at $x/L = 0.400$, $\phi = 100^\circ$	12
Table 4.	Boundary-layer profile at $x/L = 0.400$, $\phi = 110^\circ$	13
Table 5.	Boundary-layer profile at $x/L = 0.400$, $\phi = 120^\circ$	14
Table 6.	Boundary-layer profile at $x/L = 0.400$, $\phi = 130^\circ$	15
Table 7.	Boundary-layer profile at $x/L = 0.400$, $\phi = 140^\circ$	16
Table 8.	Boundary-layer profile at $x/L = 0.400$, $\phi = 150^\circ$	17
Table 9.	Boundary-layer profile at $x/L = 0.400$, $\phi = 160^\circ$	18
Table 10.	Boundary-layer profile at $x/L = 0.400$, $\phi = 170^\circ$	19
Table 11.	Boundary-layer profile at $x/L = 0.400$, $\phi = 180^\circ$	20
Table 12.	Boundary-layer profile at $x/L = 0.600$, $\phi = 90^\circ$	21
Table 13.	Boundary-layer profile at $x/L = 0.600$, $\phi = 100^\circ$	22
Table 14.	Boundary-layer profile at $x/L = 0.600$, $\phi = 110^\circ$	23
Table 15.	Boundary-layer profile at $x/L = 0.600$, $\phi = 120^\circ$	24
Table 16.	Boundary-layer profile at $x/L = 0.600$, $\phi = 130^\circ$	25
Table 17.	Boundary-layer profile at $x/L = 0.600$, $\phi = 140^\circ$	26
Table 18.	Boundary-layer profile at $x/L = 0.600$, $\phi = 150^\circ$	27
Table 19.	Boundary-layer profile at $x/L = 0.600$, $\phi = 160^\circ$	28
Table 20.	Boundary-layer profile at $x/L = 0.600$, $\phi = 170^\circ$	29
Table 21.	Boundary-layer profile at $x/L = 0.600$, $\phi = 180^\circ$	30
Table 22.	Boundary-layer profile at $x/L = 0.752$, $\phi = 120^\circ$	31
Table 23.	Boundary-layer profile at $x/L = 0.752$, $\phi = 123^\circ$	32
Table 24.	Boundary-layer profile at $x/L = 0.752$, $\phi = 125^\circ$	33
Table 25.	Boundary-layer profile at $x/L = 0.762$, $\phi = 120^\circ$	34
Table 26.	Boundary-layer profile at $x/L = 0.762$, $\phi = 123^\circ$	35
Table 27.	Boundary-layer profile at $x/L = 0.762$, $\phi = 125^\circ$	36
Table 28.	Boundary-layer profile at $x/L = 0.772$, $\phi = 105^\circ$	37
Table 29.	Boundary-layer profile at $x/L = 0.772$, $\phi = 110^\circ$	38
Table 30.	Boundary-layer profile at $x/L = 0.772$, $\phi = 115^\circ$	39
Table 31.	Boundary-layer profile at $x/L = 0.772$, $\phi = 120^\circ$	40
Table 32.	Boundary-layer profile at $x/L = 0.772$, $\phi = 123^\circ$	41
Table 33.	Boundary-layer profile at $x/L = 0.772$, $\phi = 125^\circ$	42
Table 34.	Boundary-layer profile at $x/L = 0.772$, $\phi = 130^\circ$	43
Table 35.	Boundary-layer y-derivatives at $x/L = 0.400$, $\phi = 90^\circ$	44
Table 36.	Boundary-layer y-derivatives at $x/L = 0.400$, $\phi = 100^\circ$	45
Table 37.	Boundary-layer y-derivatives at $x/L = 0.400$, $\phi = 110^\circ$	46
Table 38.	Boundary-layer y-derivatives at $x/L = 0.400$, $\phi = 120^\circ$	47
Table 39.	Boundary-layer y-derivatives at $x/L = 0.400$, $\phi = 130^\circ$	48
Table 40.	Boundary-layer y-derivatives at $x/L = 0.400$, $\phi = 140^\circ$	49
Table 41.	Boundary-layer y-derivatives at $x/L = 0.400$, $\phi = 150^\circ$	50
Table 42.	Boundary-layer y-derivatives at $x/L = 0.400$, $\phi = 160^\circ$	51
Table 43.	Boundary-layer y-derivatives at $x/L = 0.400$, $\phi = 170^\circ$	52
Table 44.	Boundary-layer y-derivatives at $x/L = 0.400$, $\phi = 180^\circ$	53
Table 45.	Boundary-layer y-derivatives at $x/L = 0.600$, $\phi = 90^\circ$	54
Table 46.	Boundary-layer y-derivatives at $x/L = 0.600$, $\phi = 100^\circ$	55

Table 47.	Boundary-layer y-derivatives at $x/L = 0.600$, $\phi = 110^\circ$.	56
Table 48.	Boundary-layer y-derivatives at $x/L = 0.600$, $\phi = 120^\circ$.	57
Table 49.	Boundary-layer y-derivatives at $x/L = 0.600$, $\phi = 130^\circ$.	58
Table 50.	Boundary-layer y-derivatives at $x/L = 0.600$, $\phi = 140^\circ$.	59
Table 51.	Boundary-layer y-derivatives at $x/L = 0.600$, $\phi = 150^\circ$.	60
Table 52.	Boundary-layer y-derivatives at $x/L = 0.600$, $\phi = 160^\circ$.	61
Table 53.	Boundary-layer y-derivatives at $x/L = 0.600$, $\phi = 170^\circ$.	62
Table 54.	Boundary-layer y-derivatives at $x/L = 0.600$, $\phi = 180^\circ$.	63
Table 55.	Boundary-layer y-derivatives at $x/L = 0.752$, $\phi = 120^\circ$.	64
Table 56.	Boundary-layer y-derivatives at $x/L = 0.752$, $\phi = 123^\circ$.	65
Table 57.	Boundary-layer y-derivatives at $x/L = 0.752$, $\phi = 125^\circ$.	66
Table 58.	Boundary-layer y-derivatives at $x/L = 0.762$, $\phi = 120^\circ$.	67
Table 59.	Boundary-layer y-derivatives at $x/L = 0.762$, $\phi = 123^\circ$.	68
Table 60.	Boundary-layer y-derivatives at $x/L = 0.762$, $\phi = 125^\circ$.	69
Table 61.	Boundary-layer y-derivatives at $x/L = 0.772$, $\phi = 105^\circ$.	70
Table 62.	Boundary-layer y-derivatives at $x/L = 0.772$, $\phi = 110^\circ$.	71
Table 63.	Boundary-layer y-derivatives at $x/L = 0.772$, $\phi = 115^\circ$.	72
Table 64.	Boundary-layer y-derivatives at $x/L = 0.772$, $\phi = 120^\circ$.	73
Table 65.	Boundary-layer y-derivatives at $x/L = 0.772$, $\phi = 123^\circ$.	74
Table 66.	Boundary-layer y-derivatives at $x/L = 0.772$, $\phi = 125^\circ$.	75
Table 67.	Boundary-layer y-derivatives at $x/L = 0.772$, $\phi = 130^\circ$.	76
Table 68.	Circumferential profile at $x/L = 0.772$, $r = 0.25$ cm, $\phi = 115 - 130^\circ$.	77

LIST OF FIGURES

Figure 1.	Flow lines in the separation region of the prolate spheroid	78
Figure 2.	3-D, fiber-optic, boundary-layer LDV probe	79
Figure 3.	Prolate spheroid streamwise momentum thickness Reynolds number.	80
Figure 4.	Prolate spheroid wall flow angle.	81
Figure 5.	Prolate spheroid skin friction coefficient.	82
Figure 6.	Boundary-layer velocity profiles, $x/L = 0.400$, $\phi = 90^\circ$	83
Figure 7.	Boundary-layer velocity profiles, $x/L = 0.400$, $\phi = 100^\circ$	83
Figure 8.	Boundary-layer velocity profiles, $x/L = 0.400$, $\phi = 110^\circ$	84
Figure 9.	Boundary-layer velocity profiles, $x/L = 0.400$, $\phi = 120^\circ$	84
Figure 10.	Boundary-layer velocity profiles, $x/L = 0.400$, $\phi = 130^\circ$	85
Figure 11.	Boundary-layer velocity profiles, $x/L = 0.400$, $\phi = 140^\circ$	85
Figure 12.	Boundary-layer velocity profiles, $x/L = 0.400$, $\phi = 150^\circ$	86
Figure 13.	Boundary-layer velocity profiles, $x/L = 0.400$, $\phi = 160^\circ$	86
Figure 14.	Boundary-layer velocity profiles, $x/L = 0.400$, $\phi = 170^\circ$	87
Figure 15.	Boundary-layer velocity profiles, $x/L = 0.400$, $\phi = 180^\circ$	87
Figure 16.	Boundary-layer velocity profiles, $x/L = 0.600$, $\phi = 90^\circ$	88
Figure 17.	Boundary-layer velocity profiles, $x/L = 0.600$, $\phi = 100^\circ$	88
Figure 18.	Boundary-layer velocity profiles, $x/L = 0.600$, $\phi = 110^\circ$	89
Figure 19.	Boundary-layer velocity profiles, $x/L = 0.600$, $\phi = 120^\circ$	89
Figure 20.	Boundary-layer velocity profiles, $x/L = 0.600$, $\phi = 130^\circ$	90
Figure 21.	Boundary-layer velocity profiles, $x/L = 0.600$, $\phi = 140^\circ$	90
Figure 22.	Boundary-layer velocity profiles, $x/L = 0.600$, $\phi = 150^\circ$	91
Figure 23.	Boundary-layer velocity profiles, $x/L = 0.600$, $\phi = 160^\circ$	91
Figure 24.	Boundary-layer velocity profiles, $x/L = 0.600$, $\phi = 170^\circ$	92
Figure 25.	Boundary-layer velocity profiles, $x/L = 0.600$, $\phi = 180^\circ$	92
Figure 26.	Boundary-layer velocity profiles, $x/L = 0.752$, $\phi = 120^\circ$	93
Figure 27.	Boundary-layer velocity profiles, $x/L = 0.752$, $\phi = 123^\circ$	93
Figure 28.	Boundary-layer velocity profiles, $x/L = 0.752$, $\phi = 125^\circ$	94
Figure 29.	Boundary-layer velocity profiles, $x/L = 0.762$, $\phi = 120^\circ$	94
Figure 30.	Boundary-layer velocity profiles, $x/L = 0.762$, $\phi = 123^\circ$	95
Figure 31.	Boundary-layer velocity profiles, $x/L = 0.762$, $\phi = 125^\circ$	95
Figure 32.	Boundary-layer velocity profiles, $x/L = 0.772$, $\phi = 105^\circ$	96
Figure 33.	Boundary-layer velocity profiles, $x/L = 0.772$, $\phi = 110^\circ$	96
Figure 34.	Boundary-layer velocity profiles, $x/L = 0.772$, $\phi = 115^\circ$	97
Figure 35.	Boundary-layer velocity profiles, $x/L = 0.772$, $\phi = 120^\circ$	97
Figure 36.	Boundary-layer velocity profiles, $x/L = 0.772$, $\phi = 123^\circ$	98
Figure 37.	Boundary-layer velocity profiles, $x/L = 0.772$, $\phi = 125^\circ$	98
Figure 38.	Boundary-layer velocity profiles, $x/L = 0.772$, $\phi = 130^\circ$	99
Figure 39.	Johnston hodograph, $x/L = 0.400$, $\phi = 90^\circ$	100
Figure 40.	Johnston hodograph, $x/L = 0.400$, $\phi = 100^\circ$	100
Figure 41.	Johnston hodograph, $x/L = 0.400$, $\phi = 110^\circ$	101
Figure 42.	Johnston hodograph, $x/L = 0.400$, $\phi = 120^\circ$	101
Figure 43.	Johnston hodograph, $x/L = 0.400$, $\phi = 130^\circ$	102
Figure 44.	Johnston hodograph, $x/L = 0.400$, $\phi = 140^\circ$	102
Figure 45.	Johnston hodograph, $x/L = 0.400$, $\phi = 150^\circ$	103
Figure 46.	Johnston hodograph, $x/L = 0.400$, $\phi = 160^\circ$	103

Figure 47.	Johnston hodograph, $x/L = 0.400$, $\phi = 170^\circ$.	104
Figure 48.	Johnston hodograph, $x/L = 0.400$, $\phi = 180^\circ$.	104
Figure 49.	Johnston hodograph, $x/L = 0.600$, $\phi = 90^\circ$.	105
Figure 50.	Johnston hodograph, $x/L = 0.600$, $\phi = 100^\circ$.	105
Figure 51.	Johnston hodograph, $x/L = 0.600$, $\phi = 110^\circ$.	106
Figure 52.	Johnston hodograph, $x/L = 0.600$, $\phi = 120^\circ$.	106
Figure 53.	Johnston hodograph, $x/L = 0.600$, $\phi = 130^\circ$.	107
Figure 54.	Johnston hodograph, $x/L = 0.600$, $\phi = 140^\circ$.	107
Figure 55.	Johnston hodograph, $x/L = 0.600$, $\phi = 150^\circ$.	108
Figure 56.	Johnston hodograph, $x/L = 0.600$, $\phi = 160^\circ$.	108
Figure 57.	Johnston hodograph, $x/L = 0.600$, $\phi = 170^\circ$.	109
Figure 58.	Johnston hodograph, $x/L = 0.600$, $\phi = 180^\circ$.	109
Figure 59.	Johnston hodograph, $x/L = 0.752$, $\phi = 120^\circ$.	110
Figure 60.	Johnston hodograph, $x/L = 0.752$, $\phi = 123^\circ$.	110
Figure 61.	Johnston hodograph, $x/L = 0.752$, $\phi = 125^\circ$.	111
Figure 62.	Johnston hodograph, $x/L = 0.762$, $\phi = 120^\circ$.	111
Figure 63.	Johnston hodograph, $x/L = 0.762$, $\phi = 123^\circ$.	112
Figure 64.	Johnston hodograph, $x/L = 0.762$, $\phi = 125^\circ$.	112
Figure 65.	Johnston hodograph, $x/L = 0.772$, $\phi = 105^\circ$.	113
Figure 66.	Johnston hodograph, $x/L = 0.772$, $\phi = 110^\circ$.	113
Figure 67.	Johnston hodograph, $x/L = 0.772$, $\phi = 115^\circ$.	114
Figure 68.	Johnston hodograph, $x/L = 0.772$, $\phi = 120^\circ$.	114
Figure 69.	Johnston hodograph, $x/L = 0.772$, $\phi = 123^\circ$.	115
Figure 70.	Johnston hodograph, $x/L = 0.772$, $\phi = 125^\circ$.	115
Figure 71.	Johnston hodograph, $x/L = 0.772$, $\phi = 130^\circ$.	116
Figure 72.	Boundary-layer normal-stress profiles, $x/L = 0.400$, $\phi = 90^\circ$.	117
Figure 73.	Boundary-layer normal-stress profiles, $x/L = 0.400$, $\phi = 100^\circ$.	117
Figure 74.	Boundary-layer normal-stress profiles, $x/L = 0.400$, $\phi = 110^\circ$.	118
Figure 75.	Boundary-layer normal-stress profiles, $x/L = 0.400$, $\phi = 120^\circ$.	118
Figure 76.	Boundary-layer normal-stress profiles, $x/L = 0.400$, $\phi = 130^\circ$.	119
Figure 77.	Boundary-layer normal-stress profiles, $x/L = 0.400$, $\phi = 140^\circ$.	119
Figure 78.	Boundary-layer normal-stress profiles, $x/L = 0.400$, $\phi = 150^\circ$.	120
Figure 79.	Boundary-layer normal-stress profiles, $x/L = 0.400$, $\phi = 160^\circ$.	120
Figure 80.	Boundary-layer normal-stress profiles, $x/L = 0.400$, $\phi = 170^\circ$.	121
Figure 81.	Boundary-layer normal-stress profiles, $x/L = 0.400$, $\phi = 180^\circ$.	121
Figure 82.	Boundary-layer normal-stress profiles, $x/L = 0.600$, $\phi = 90^\circ$.	122
Figure 83.	Boundary-layer normal-stress profiles, $x/L = 0.600$, $\phi = 100^\circ$.	122
Figure 84.	Boundary-layer normal-stress profiles, $x/L = 0.600$, $\phi = 110^\circ$.	123
Figure 85.	Boundary-layer normal-stress profiles, $x/L = 0.600$, $\phi = 120^\circ$.	123
Figure 86.	Boundary-layer normal-stress profiles, $x/L = 0.600$, $\phi = 130^\circ$.	124
Figure 87.	Boundary-layer normal-stress profiles, $x/L = 0.600$, $\phi = 140^\circ$.	124
Figure 88.	Boundary-layer normal-stress profiles, $x/L = 0.600$, $\phi = 150^\circ$.	125
Figure 89.	Boundary-layer normal-stress profiles, $x/L = 0.600$, $\phi = 160^\circ$.	125
Figure 90.	Boundary-layer normal-stress profiles, $x/L = 0.600$, $\phi = 170^\circ$.	126
Figure 91.	Boundary-layer normal-stress profiles, $x/L = 0.600$, $\phi = 180^\circ$.	126
Figure 92.	Boundary-layer normal-stress profiles, $x/L = 0.752$, $\phi = 120^\circ$.	127
Figure 93.	Boundary-layer normal-stress profiles, $x/L = 0.752$, $\phi = 123^\circ$.	127
Figure 94.	Boundary-layer normal-stress profiles, $x/L = 0.752$, $\phi = 125^\circ$.	128
Figure 95.	Boundary-layer normal-stress profiles, $x/L = 0.762$, $\phi = 120^\circ$.	128
Figure 96.	Boundary-layer normal-stress profiles, $x/L = 0.762$, $\phi = 123^\circ$.	129

Figure 197. Boundary-layer profiles of velocity triple products (1), $x/L = 0.600$, $\phi = 120^\circ$.	181
Figure 198. Boundary-layer profiles of velocity triple products (2), $x/L = 0.600$, $\phi = 120^\circ$.	181
Figure 199. Boundary-layer profiles of velocity triple products (1), $x/L = 0.600$, $\phi = 130^\circ$.	182
Figure 200. Boundary-layer profiles of velocity triple products (2), $x/L = 0.600$, $\phi = 130^\circ$.	182
Figure 201. Boundary-layer profiles of velocity triple products (1), $x/L = 0.600$, $\phi = 140^\circ$.	183
Figure 202. Boundary-layer profiles of velocity triple products (2), $x/L = 0.600$, $\phi = 140^\circ$.	183
Figure 203. Boundary-layer profiles of velocity triple products (1), $x/L = 0.600$, $\phi = 150^\circ$.	184
Figure 204. Boundary-layer profiles of velocity triple products (2), $x/L = 0.600$, $\phi = 150^\circ$.	184
Figure 205. Boundary-layer profiles of velocity triple products (1), $x/L = 0.600$, $\phi = 160^\circ$.	185
Figure 206. Boundary-layer profiles of velocity triple products (2), $x/L = 0.600$, $\phi = 160^\circ$.	185
Figure 207. Boundary-layer profiles of velocity triple products (1), $x/L = 0.600$, $\phi = 170^\circ$.	186
Figure 208. Boundary-layer profiles of velocity triple products (2), $x/L = 0.600$, $\phi = 170^\circ$.	186
Figure 209. Boundary-layer profiles of velocity triple products (1), $x/L = 0.600$, $\phi = 180^\circ$.	187
Figure 210. Boundary-layer profiles of velocity triple products (2), $x/L = 0.600$, $\phi = 180^\circ$.	187
Figure 211. Boundary-layer profiles of velocity triple products (1), $x/L = 0.752$, $\phi = 120^\circ$.	188
Figure 212. Boundary-layer profiles of velocity triple products (2), $x/L = 0.752$, $\phi = 120^\circ$.	188
Figure 213. Boundary-layer profiles of velocity triple products (1), $x/L = 0.752$, $\phi = 123^\circ$.	189
Figure 214. Boundary-layer profiles of velocity triple products (2), $x/L = 0.752$, $\phi = 123^\circ$.	189
Figure 215. Boundary-layer profiles of velocity triple products (1), $x/L = 0.752$, $\phi = 125^\circ$.	190
Figure 216. Boundary-layer profiles of velocity triple products (2), $x/L = 0.752$, $\phi = 125^\circ$.	190
Figure 217. Boundary-layer profiles of velocity triple products (1), $x/L = 0.762$, $\phi = 120^\circ$.	191
Figure 218. Boundary-layer profiles of velocity triple products (2), $x/L = 0.762$, $\phi = 120^\circ$.	191
Figure 219. Boundary-layer profiles of velocity triple products (1), $x/L = 0.762$, $\phi = 123^\circ$.	192
Figure 220. Boundary-layer profiles of velocity triple products (2), $x/L = 0.762$, $\phi = 123^\circ$.	192
Figure 221. Boundary-layer profiles of velocity triple products (1), $x/L = 0.762$, $\phi = 125^\circ$.	193
Figure 222. Boundary-layer profiles of velocity triple products (2), $x/L = 0.762$, $\phi = 125^\circ$.	193
Figure 223. Boundary-layer profiles of velocity triple products (1), $x/L = 0.772$, $\phi = 105^\circ$.	194
Figure 224. Boundary-layer profiles of velocity triple products (2), $x/L = 0.772$, $\phi = 105^\circ$.	194
Figure 225. Boundary-layer profiles of velocity triple products (1), $x/L = 0.772$, $\phi = 110^\circ$.	195
Figure 226. Boundary-layer profiles of velocity triple products (2), $x/L = 0.772$, $\phi = 110^\circ$.	195
Figure 227. Boundary-layer profiles of velocity triple products (1), $x/L = 0.772$, $\phi = 115^\circ$.	196
Figure 228. Boundary-layer profiles of velocity triple products (2), $x/L = 0.772$, $\phi = 115^\circ$.	196
Figure 229. Boundary-layer profiles of velocity triple products (1), $x/L = 0.772$, $\phi = 120^\circ$.	197
Figure 230. Boundary-layer profiles of velocity triple products (2), $x/L = 0.772$, $\phi = 120^\circ$.	197
Figure 231. Boundary-layer profiles of velocity triple products (1), $x/L = 0.772$, $\phi = 123^\circ$.	198
Figure 232. Boundary-layer profiles of velocity triple products (2), $x/L = 0.772$, $\phi = 123^\circ$.	198
Figure 233. Boundary-layer profiles of velocity triple products (1), $x/L = 0.772$, $\phi = 125^\circ$.	199
Figure 234. Boundary-layer profiles of velocity triple products (2), $x/L = 0.772$, $\phi = 125^\circ$.	199
Figure 235. Boundary-layer profiles of velocity triple products (1), $x/L = 0.772$, $\phi = 130^\circ$.	200
Figure 236. Boundary-layer profiles of velocity triple products (2), $x/L = 0.772$, $\phi = 130^\circ$.	200
Figure 237. Circumferential profile of wall-normal velocity, $x/L = 0.772$, $r = 0.25$ cm.	201
Figure 238. Circumferential profile of flow angle, $x/L = 0.772$, $r = 0.25$ cm.	201
Figure A1. Primary separation location comparison, $\alpha = 10^\circ$.	203
Figure A2. Oil flow pattern at $\alpha = 10^\circ$, $Re_L = 4.20 \times 10^6$.	204
Figure A3. Mean and rms pressure distributions at $x/L = 0.0000$.	205
Figure A4. Mean and rms pressure distributions at $x/L = 0.1079$.	206
Figure A5. Mean and rms pressure distributions at $x/L = 0.2315$.	207
Figure A6. Mean and rms pressure distributions at $x/L = 0.3145$.	208
Figure A7. Mean and rms pressure distributions at $x/L = 0.4396$.	209
Figure A8. Mean and rms pressure distributions at $x/L = 0.5646$.	210

Figure A9. Mean and rms pressure distributions at $x/L = 0.6892$	211
Figure A10. Mean and rms pressure distributions at $x/L = 0.7725$	212
Figure A11. Mean and rms pressure distributions at $x/L = 0.8346$	213
Figure A12. Mean and rms pressure distributions at $x/L = 0.8962$	214

NOMENCLATURE

C_f	Coefficient of friction, $2\tau_w / \rho U_e^2$
L	Length of model, 1.37 m
r	Radial coordinate, from model surface
Re	Reynolds number
U	Identical to U_{fs}
U_e	Total velocity at the edge of the boundary layer
U_b	Velocity component in the x - r plane, parallel to the model surface (+ downstream)
U_{fs}	Velocity component in the plane tangent to the model surface, parallel to the edge velocity
U_∞	Wind tunnel approach velocity
V	Identical to V_{fs}
V_b	Velocity component perpendicular to the model surface (+ outward)
V_{fs}	Identical to V_b
W	Identical to W_{fs}
W_s	Circumferential velocity component (+ in windward direction)
W_{fs}	Velocity component in the plane tangent to the model surface, perpendicular to the edge velocity
x	Axial coordinate, from nose of model
β	Flow angle, $\arctan(W_b / U_b)$
δ	Boundary layer thickness
θ	Boundary-layer streamwise momentum thickness
ρ	Density
τ	Shear stress
ϕ	Circumferential coordinate, from windward side

Subscripts

b	In the body-surface coordinate system
e	At the boundary-layer edge
fs	In the local-freestream coordinate system
w	At the wall

1.0 INTRODUCTION

The phenomenon of three-dimensional separation of the flow about a body, though quite common, is both difficult to model and poorly understood. Indeed, since — unlike in two-dimensional flow separation — three-dimensional flow separation is rarely associated with the vanishing of the wall shear stress, it can often be difficult to even identify the presence or precise location of 3-D flow separation.

In order to better understand three-dimensional flow separation, several groups have studied the flow about a 6 to 1 prolate spheroid at angle of attack. This flow is a well-defined, relatively simple 3-D flow which exhibits all the fundamental transition and separation phenomena of three-dimensional flow. The flow about the prolate spheroid is schematically illustrated in Figure 1. The flow separating from the lee-side of the prolate spheroid, at the point marked S_1 , rolls up into a strong vortex on each side of the body. This primary vortex is accompanied by several smaller vortices, which separate from the surface at the points S_2 and S_3 . The flow reattaches at points, R_1 and R_2 . The complex interactions between vortices result in a highly skewed, and thus three-dimensional, boundary layer.

Previous works by Meier et al. (1984 & 1986), Kreplin et al. (1985) and Vollmers et al. (1985) at the DFVLR (now the DLR) and Barveris and Chanetz (1986) and Chanetz and Délery (1988) at ONERA have documented the surface flow, surface pressure, skin friction and mean velocity around the prolate spheroid. Previous work at VPI by Ahn (1992) has documented the Reynolds number and angle of attack effects on the boundary-layer transition and separation phenomena for this flow. Barber and Simpson (1991) thoroughly documented the mean and turbulent velocities in the cross-flow separation region, but due to the limitations of their instrumentation — five-hole pressure probes and crossed hot wires — they obtained no data within the inner boundary layer.

Because of simple geometry and the extent of the experimental data obtained, this flowfield has made an excellent test case for three-dimensional computational models. A recent study by AGARD (1990) used the DFVLR and ONERA data for comparison to three-dimensional computations utilizing integral boundary-layer, algebraic mixing-length, and eddy-viscosity turbulence models. The AGARD study found that all of the computational models experienced difficulties in calculating the flowfield in the cross-flow separation region. Gee et al. (1992) were able to get somewhat better results calculating the flow about the 6:1 prolate spheroid using versions of the Baldwin-Lomax and Johnson-King turbulence models modified for three dimensions, but stated that "more experimental data may be required before a better understanding of the effects of turbulence models on flow parameters can be gained."

The present work extends the knowledge of this 3-D separated flow with measurements of the total velocity vector, as well as the full Reynolds stress tensor and velocity triple products, throughout the boundary layer in the cross-flow separation region. Previous to this work, little data on the Reynolds stress tensor was available, and no data on the velocity triple products existed. In addition, the data which were available did not extend to the sublayer.

The present measurements were accomplished using a miniature, three-dimensional, fiber-optic LDV designed specifically for this application. The probe was placed within the model, and all beams passed through a window molded to the shape of the model so that the flow was virtually undisturbed by the instrumentation. The probe was configured to measure three simultaneous, orthogonal velocity components. In this way, the total velocity vector and Reynolds stress tensor were obtained with maximum accuracy.

2.0 EXPERIMENTAL FACILITY

2.1 Wind Tunnel

The Virginia Polytechnic Institute and State University Stability Wind Tunnel is a continuous, closed test section, single return, subsonic wind tunnel with 7 m long, interchangeable round and square test sections. For these tests a 1.8×1.8 m square test section was used. The tunnel provides a maximum speed of 67 m/s and unit Reynolds number of 4.36×10^6 per meter. The 9:1 contraction ratio and seven anti-turbulence screens provide for very low turbulence levels — on the order of 0.03% or less. Temperature stabilization is provided by the air exchange tower located between the fan and the settling chamber.

2.2 Model

The 6 to 1 prolate spheroid model used in this experiment is 1.37 m (54 in.) in length and 0.229 m (9 in.) in diameter. The model is constructed in three sections, each with a 6.3 mm thick fiberglass skin bonded to an aluminum frame. A circumferential trip, consisting of posts 1.2 mm in diameter, 0.7 mm high spaced 2.5 mm apart, was placed around the nose of the model at $x/L = 0.2$ in order to stabilize the location of the separation. In the rear section of the model is a 30×150 mm, 0.75 mm thick window to allow optical access to the flow in the vicinity of $x/L = 0.75$. The window is molded to the curvature of the model to minimize flow disturbances, and is flush with the model surface within 0.1 mm. Wax is used to smooth any steps which existed between the window and model skin. There is a similar window in the model about $x/L = 0.6$. Because of the symmetry of the model, this same window can be used for measurements near $x/L = 0.4$ with the model turned around. The model is supported in the wind tunnel with a rear-mounted, 0.75 m long sting connected to a vertical post coming through the wind tunnel floor.

2.3 Fiber-Optic Probe

The objective of this research was to measure the complete velocity vector and full Reynolds stress tensor throughout the boundary layer in the cross-flow separation region of the 6:1 prolate spheroid. Measurements as close to the wall as possible were desired. These requirements led to the design of a unique, three-component, fiber-optic LDV probe.

The probe was designed to measure three simultaneous, orthogonal velocity components. In this way, the three correlated velocities can be used to calculate all Reynolds stress terms, and the measurement accuracy of a third component is not compromised by a small coupling angle.

All optics for the probe were placed inside the model, and light was transmitted and received through a thin plastic window molded to the shape of the model. This placement of the probe provides three benefits: (1) the flow remains undisturbed by the presence of the probe, (2) the probe can be mounted directly to the frame of the model so that relative motion between the measurement volume of the probe and the model itself is extremely small, and (3) the probe can be physically close to the measuring volume, so short focal length-transmitting and receiving optics can be used to maximize the signal-to-noise ratio.

As was noted above, molding the window to conform to the shape of the model has the benefit of minimizing the flow disturbances caused by the probe. Unfortunately, curving the window in such a way also causes light passing through it to be distorted, or defocused. There is no way of eliminating this "lensing" effect of a curved window, but by making the window thin, the effect can be minimized. The window in this model was made of the thinnest (0.75 mm), high quality, moldable

optical sheet available, and was found to produce no significant defocusing of the laser beams passing through it.

A drawing of the probe placed inside the model is shown in Figure 2. As can be seen from this drawing, the probe is, by necessity, compact. The complete 3-D fiber-optic probe head weighs less than 1.1 kg and occupies a volume of less than $21 \times 9 \times 4.5$ cm. When the probe is mounted on a two-component traverse, the package is still smaller than $21 \times 11.7 \times 8.25$ cm. This small size allows for the probe to be placed inside the model with sufficient clearance for traversing and the connection of fiber-optic and electrical cables.

The probe consists of three sets of optics — two transmitting and one receiving. The outermost assemblies shown in Figure 2 are the two transmitting optics assemblies. These two assemblies are oriented at 90° to one another. The transmitting optics assembly located toward the center of the model transmits three green beams (514.5 nm) from an etalon-tuned, argon-ion laser — one Bragg shifted at -27 MHz, one shifted at +40 MHz, and one unshifted. The beams are configured to measure two, orthogonal, frequency-separated velocity components — one in the circumferential direction and one at 135° to the model axis in the plane of the lower part of the figure. The blue transmitting optics are shown toward the end of the model in Figure 2, and transmit two blue (488 nm) beams about an axis at 90° to the green beams. One of the blue beams is Bragg shifted by 40 MHz. The beams are transmitted in the plane of the figure, so that they measure a velocity component at 45° to the model axis. The laser light is brought from the laser into the probe through single-mode, polarization-preserving fibers.

The transmitting optics assemblies each have a focal length of 88 mm. This allows measurements to be made up to 40 mm from the probe. Collimated beams of roughly 1.1 mm in diameter are focused by the transmitting lenses to a spot only 55 μ m in diameter. Fringe spacing is approximately 5 μ m. In order to minimize reflections from the window, the transmitting beams are p-polarized with respect to the window. Since the transmitted beams are at roughly 45° to the window, which is not far from the Brewster angle of 56° , 99% of the light is transmitted through the uncoated window.

Scattered light is collected through a 60 mm, f/2.4 receiving optics assembly located in the center of the probe, at 45° to each of the transmitting optics assemblies. In this way, off-axis, back-scatter light collection is employed, the effective probe volume is roughly spherical with a diameter of 55 μ m, and any beam reflections from the window do not reflect into the receiving optics. Collected light is relayed from the probe to two photomultiplier tubes through a 62.5 μ m gradient index fiber. Before the photomultiplier tubes, the light is separated into blue and green components by a dichroic filter.

Signals from the photomultiplier tubes are downmixed and analyzed using three Macrodyne FDP3100 frequency domain signal processors. In these processors, a fast Fourier transform is performed on each incoming Doppler burst to determine the peak frequency of the burst. Under conditions of high noise and low signal strength, these processors are capable of (1) discriminating valid Doppler bursts from random "noise bursts", and (2) accurately finding the peak Doppler frequency in very low signal-to-noise ratio (SNR) bursts. Both of these capabilities are essential for obtaining data in the near-wall region, where flare from the window can be significant. If the processor is not capable of analyzing low SNR bursts, no measurements can be made in this region, and if the processor is not capable of discriminating valid Doppler bursts from bursts of high amplitude noise, the measured velocities will not be representative of the flow. The processors were used in coincidence mode — with a coincidence window of 5 to 8 μ s, depending on the measurement position — to ensure that all three velocity measurements were correlated. This correlation is essential if the Reynolds shear stress terms are to be measured. The coincident data rate varied from approximately 30 /s near the wall to 150 /s at the edge of the boundary layer. This was approximately 60 to 70% of the non-coincident data rate.

The probe was mounted to the frame of the model on a two component traverse. With this traverse, the probe could be remotely positioned ± 2.5 cm in the axial direction by turning a cable connected to the lead screw of a linear stage. The probe could be positioned ± 2.5 cm in the radial direction with a remotely-controlled, motorized stage. The motorized stage was powered by a rotary-encoded servo-motor, which was geared to yield 20,157 encoder counts per centimeter. Positioning of the measurement volume in the circumferential direction was accomplished by rotating the model about its primary axis. The probe sting was indexed so that this rotation could be measured $\pm 0.1^\circ$.

2.4 Seeding System

Polystyrene latex (PSL) spheres $0.7 \mu\text{m}$ in diameter were used to seed the flow about the 6:1 prolate spheroid. The seed was suspended in ethanol and introduced into the flow using two Spraying Systems Incorporated air-atomizing paint spray nozzles placed just downstream of the turbulence reducing screens. These nozzles produced a fine spray of the liquid droplets. The ethanol in these droplets rapidly evaporated leaving individual PSL particles in the flow. The arrangement of the two nozzles produced a localized region of seeded flow extending a minimum of 10 cm on all sides of the model.

2.5 Test Conditions

All tests were performed at a 10° angle of attack with at a Reynolds number based on the model length and free-stream velocity of 4.20×10^6 . Measurements were performed at 5 axial locations — $x/L = 0.400, 0.600, 0.752, 0.762$ and 0.772 . Surface oil flow visualizations by Ahn (1992), reproduced in Appendix A, indicated that the primary separation is not yet developed at $x/L = 0.400$, is incipient at $x/L = 0.600$, and is well developed at $x/L = 0.772$. Measurements were therefore made across the lee-side flowfield at $x/L = 0.400$ and 0.600 in order to define the flow conditions which exist before, and near the start of, separation, and measurements were made about the primary separation line at $x/L = 0.752$ and 0.762 and 0.772 in order to closely examine the conditions which exist at the open, 3-D separation.

At each axial location, several boundary-layer profiles were measured. Each boundary-layer profile consisted of measurements at 13 to 17 points, from approximately 0.01 cm from the model surface out to 2.5 cm from the model surface in the radial direction. At each point, 16,384 coincident, 3-D velocity realizations were acquired.

The boundary-layer profile measurements are presented here in a local-freestream coordinate system, with y_{fs} perpendicular to the model surface, x_{fs} perpendicular to y_{fs} and in the direction of the mean velocity at the edge of the boundary layer, and z_{fs} completing the right-hand rule. (For this measurement set, the windward side of the model is always in the $+z_{fs}$ direction.) U_{fs} , V_{fs} and W_{fs} are the velocity components in the x_{fs} , y_{fs} and z_{fs} directions, respectively. For brevity, the velocity components in the local-freestream coordinates will be referred to here as U , V and W . The measured flow angles at the boundary-layer edge, relative to the axial direction, are listed in Table 1.

At $x/L = 0.772$, a series of velocity measurements were performed at a distance of 0.25 cm from the model surface, in 1° increments from 115° to 130° . This circumferential profile was intended to identify the exact location of the open separation line. The circumferential profile measurements are presented here in a body-surface coordinate system, with y_b perpendicular to the model surface, x_b perpendicular to y_b in the axial-radial plane, and z_b in the circumferential direction. U_b , V_b and W_b are the velocity components in the x_b , y_b and z_b directions, respectively.

The convention is used here of capital letters representing the time averaged velocity quantities, and lowercase letters representing the unsteady quantities.

2.6 Measurement Uncertainty

The probe was calibrated by measuring the frequency of signals generated by light scattered from the edge of a rotating wheel of known diameter and angular velocity. In this way, the fringe spacing, and thus the frequency-to-velocity conversion factor, was calibrated to $\pm 0.5\%$. The directional ambiguity of the measurements is estimated to be less than 0.5° . The accuracy of the Reynolds stress terms is limited primarily by statistical uncertainties — that is the uncertainty of estimating the sample variance or covariance with a finite sample size. The uncertainty in the normal stress terms, u_{ii} , was estimated to be $\pm 2\%$ of u_{ii} and the uncertainty in the shear stress terms, $-u_{ij}$, is estimated to be $\pm 3\%$ of the quantity

$$\sqrt{\overline{u_i u_i} \cdot \overline{u_j u_j} + 2 \cdot \overline{u_i u_j}^2}$$

It should be noted that, due to the measurement of three orthogonal velocity components, the uncertainty is the same independent of direction. This is particularly notable for the quantity $-\overline{vw}$, which in most studies of 3-D turbulent flow is either not measured, or of poor accuracy.

The high resolution of the probe traverse and the direct mounting of the probe to the model frame provides for excellent positioning accuracy — estimated at $\pm 10\mu\text{m}$ — and the small size of the roughly spherical measuring volume (approximately $55\mu\text{m}$ in diameter) provides for excellent spatial resolution. The circumferential location of the measurement, ϕ , was determined using an indexed dial on the probe sting, and was measured to $\pm 0.1^\circ$.

Measurements at locations near the surface of the model exhibited large instantaneous velocity variations — indicating that there could be a velocity bias error in the ensemble-averaged velocity calculations. To correct for this velocity bias, all measurements are averaged using a weighting factor of 1 over the total measured velocity. That is, an inverse-velocity weighting scheme is employed. In addition, very near the surface of the model, the measurement-volume diameter ($55\mu\text{m}$) becomes comparable to the scale of the flow gradients — indicating that the ensemble-averaged velocity calculations could be influenced by the flow gradients. To correct for this gradient broadening, all computed components are corrected by a scheme similar to that of Durst et al. (1992). Since the measurement volume size is relatively small, the corrections for gradient broadening are only significant for the points closest to the wall. At the point closest to the wall, the corrections are still small — generally less than 0.2% for the mean velocities and less than 10% for the Reynolds stress terms.

3.0 RESULTS

The boundary-layer parameters for all the measured boundary-layer profiles are summarized in Table 1. For each measurement location, the flow angle at the boundary-layer edge, β_* , the boundary-layer edge velocity, U_* , the boundary layer thickness, δ , the streamwise momentum thickness, θ , the Reynolds number based on the streamwise momentum thickness, Re_θ , the flow angle at the wall, β_w , and the skin friction coefficient, C_f are listed.

The boundary layer thickness is calculated by finding the point where the velocity magnitude is 99% of the maximum value in the profile. Due to the difficulty of defining a velocity at “infinity” in a three-dimensional, curving flow with some experimental uncertainty in U , δ is accurate to no

better than 10%, and should be used for reference only. The streamwise momentum thickness is calculated from the equation

$$\theta = \int_0^{\delta} \frac{U}{U_e} \left(1 - \frac{U}{U_e} \right) dy$$

and the skin friction is calculated using the Spalding wall law,

$$y^+ = u^+ + \frac{1}{E} \left[e^{ku^+} - 1 - ku^+ - \frac{(ku^+)^2}{2} - \frac{(ku^+)^3}{6} - \frac{(ku^+)^4}{24} \right]$$

with the substitutions

$$u^+ = \frac{U}{U_e} / \sqrt{\frac{C_f}{2}} \quad y^+ = \frac{r + \Delta r}{L} Re_L \frac{U_e}{V_\infty} \sqrt{\frac{C_f}{2}}$$

In this way, the skin friction coefficient (and the term Δr , which is a term correcting for any error in the traverse zero point) can be calculated from a least squares fit of this equation to the measured U/U_e vs. r/L pairs. In order to avoid any three-dimensional effects, only the points measured within the collateral wall region are used for this least squares fit. It should be noted that the skin friction coefficient, C_f , is based on the local boundary layer edge velocity, U_e , and not the wind tunnel velocity.

Data from Table 1 are plotted in Figures 3, 4, and 5. It can be seen in these figures that, as the flow moves downstream, the momentum thickness increases, the wall flow angle becomes more positive, and the skin friction coefficient decreases. Over the range of circumferential angles measured at $x/L = 0.752$ through 0.772 , there is no local minima or maxima in any of these quantities. However, at $x/L = 0.772$ there is a small kink in both the profiles of C_f and β_w at $\phi = 123^\circ$. Since this is approximately the point of the primary separation, it is believed that these kinks are due to the separation. The kinks in these profiles are small, however, and the possibility exists that they are just an artifact of the measurement uncertainty.

At $x/L = 0.600$ there are very clear local extrema in the momentum thickness, wall flow angle, and skin friction plots. These local extrema are not, however, coincident. The maximum wall flow angle lags the minimum skin friction line by approximately 15° . The point of maximum momentum thickness is approximately halfway between the minimum skin friction and the maximum wall flow angle. It should be noted that the location of the minimum skin friction, at approximately $\phi = 145^\circ$, agrees quite well with that found by Kreplin et al. (1985), which is shown in Appendix A.

At $x/L = 0.400$ there are local extrema in momentum thickness and in skin friction, but not in the wall flow angle. The wall flow angle increases continuously from $\phi = 90^\circ$ to 180° . The point of maximum momentum thickness lags the point of minimum skin friction by about 20° . The point of minimum skin friction, at approximately $\phi = 150^\circ$, is slightly displaced from the value of $\phi = 160^\circ$ found by Kreplin et al.

The measured quantities at all points measured in these boundary-layer profiles are listed in Tables 2 through 34 and are plotted in Figures 6 through 236. All data is in a local-freestream coordinate system, as explained in Section 2.5, *Test Conditions*, and all velocities are normalized by the local boundary-layer edge velocity, U_e . Shown in Tables 35 through 67 are the first and second derivatives, with respect to the radial direction, of the mean velocity terms and the Reynolds stress terms. These derivatives were found by applying a parabolic, least-squares fit to five points about

each radial location. At the second point from the wall, a four-point curve fit was used to find the derivatives, and at the point closest to the wall, the derivatives were extrapolated from the derivatives calculated for the second, third and fourth points from the wall.

In order to clearly show the near-wall, mean-flow three dimensionality, U and W have been plotted as hodographs in Figures 29 through 51. The Johnston Hodograph, as explained in Cooke and Hall (1962), is a plot of U vs. W (normalized by U_e) across the boundary layer in the local-freestream coordinate system (U aligned with the flow at the edge of the boundary layer, W tangent to the model surface). In such a plot, W is zero both at the wall, where U is also zero, and at the edge of the boundary layer, where U/U_e is 1 and the flow is aligned with the coordinate system. Johnston hypothesized that in a 3-D boundary layer, such a plot would show two distinct regions of the flow. The outer region of the flow would start on the plot at $U/U_e = 1$, $W/U_e = 0$, and have a negative slope, thus showing more turning of the flow in the outer boundary layer as the wall is approached. The inner region of the flow, roughly corresponding to the viscous sublayer and transition layer, would be collateral, and thus would start on the plot at $U = 0$, $W = 0$ (the wall) and have a constant, positive slope. This is precisely the behavior seen in most of these figures. There are some exceptions to this behavior, however. First, for the two profiles at $\phi = 180^\circ$ ($x/L = 0.400$ and 0.600), the flow is clearly two dimensional. At $x/L = 0.600$, $\phi = 100^\circ$, the wall flow angle, as shown in Figure 4, is near an inflection point, and the boundary-layer three-dimensionality is not adequately described by Johnston's simplified model.

Plots of the Reynolds normal stresses are shown in Figures 72 through 104. From these figures it can be seen that the maximum value of the normal stress occurs quite far down in the boundary layer in these profiles, and always well within the collateral wall region. The normal stress is dominated by \overline{uu} with \overline{vv} , the smallest of the three normal stresses, becoming negligible near the wall, and \overline{ww} always intermediate in magnitude. It should also be noted that for the measurements at $x/L = 0.752$, 0.762 and 0.772 , as the measurements move across the separation line (at approximately $\phi = 123^\circ$), and the boundary layer becomes more three dimensional, the maximum normal stress decreases. Similarly, at $x/L = 0.600$, the profiles near $\phi = 90^\circ$ and 180° — in which the hodographs exhibit the least three-dimensionality — exhibit the greatest maximum shear stress. This same trend has been noted in direct numerical simulations of a simple, 3-D, turbulent boundary layer by Sendstad and Moin (1992).

Plots of the Reynolds shear stresses are shown in Figures 105 through 137. Perhaps the most notable feature in these plots is the large magnitude of $-\overline{uw}$ near the wall in the more highly three-dimensional regions — three or four times the magnitude of $-\overline{uv}$. The terms containing $-\overline{uw}$ are generally neglected in the boundary-layer equations — since they appear only as x -derivatives. Due to the large magnitude of this stress, it seems that the neglect of these terms may not be justified in all cases. More investigation needs to be done on this point. For the downstream locations, the shear stress terms do not go to zero as one would expect at the edge of the boundary-layer. This source of this non-zero shear stress outside the boundary layer appears to be unsteadiness of the cross-flow separation on the prolate spheroid, which has been documented with Particle Displacement Velocimetry studies of the flow about the prolate spheroid by Fu et al. (1992).

Plots of the velocity triple products are shown in Figures 138 through 236. Knowledge of these terms is necessary if higher order turbulence models utilizing equations for the shear stresses are to be evaluated. As can be seen from these plots, $\overline{u^3}$ becomes quite large and positive near the wall, apparently due to the wall's limiting influence on the magnitude of negative u events. For most of these profiles, $\overline{uw^2}$ — which appears in the turbulent transport term of the \overline{uw} equation — is several times larger than $\overline{uv^2}$, which appears in the turbulent transport term of the \overline{uv} equation. This suggests that the turbulent structure is changing rapidly in the third dimension near the separation line.

Measurements were also made at $x/L = 0.772$, at a radius of 0.25 cm, from $\phi = 115^\circ$ to 130° in one-degree increments. This circumferential traverse was intended to precisely identify the location of the primary separation line at $x/L = 0.772$. Ahn (1992) had previously found from surface oil flows

that the primary separation line at these conditions is approximately at 124° . The results of this circumferential traverse are listed in Table 68, and the V and β profiles are plotted in Figures 237 and 238, respectively. From Figure 237 it can be seen that V reaches a maximum at 123° and in Figure 238 it can be seen that there is a slight discontinuity in the plot of β vs. ϕ between 122° and 123° . It appears, then, that the primary separation line at $x/L = 0.772$ lies at $\phi = 123^\circ$.

4.0 DISCUSSION

As was noted in the above section describing the fiber-optic LDV probe, the primary goal of this research was to make total velocity vector and full Reynolds stress tensor measurements as close to the wall of the model as possible with maximum accuracy. In order to achieve these goals, a miniature, 3-D LDV probe of a unique design was developed. In practice, these design goals were met with the following qualifications.

The greatest limitation on positioning accuracy is actually caused not by the probe itself, but by the wind tunnel in which these measurements were made. This wind tunnel does not have the provision of temperature control, so that the temperature in the test section varies with the outside temperature. It was found that through the day, as the tunnel air heats up, the model expands slightly. This slight expansion is not normally a problem, but when attempting to make measurements less than 0.01 cm from the model wall, the small expansion is noticeable. The model expansion changes the zero position of the traverse relative to the model. It was therefore necessary to make measurements close to the wall only after the tunnel had heated up sufficiently, and only immediately after the traverse zero had been set. After all measurements in the profile were complete, the zero was then corrected by fitting the points nearest the wall to the Spalding wall law, as described in Section 3.0, *Results*.

The factor which, in practice, limits how near to the wall measurements can be obtained is the deposition of seed on the window. Due to the geometry of the experimental setup — with both transmitting beams and collected light passing through the window — flare from seed on the windows finds its way into the collection optics and tends to saturate the photomultiplier tubes when the measurement volume is positioned within about two probe diameters of the window. With careful cleaning of the window, the probe can be positioned to within 0.005 cm (approximately 1 probe diameter) of the window without excessive flare. However, the low velocity at this location, in conjunction with the very small probe volume, causes the data rate to be low, and makes it impossible to obtain a sufficiently large data sample before new seed deposition leads, once again, to PM tube saturation. Measurements are therefore limited to no closer than about 0.01 cm from the wall.

5.0 CONCLUSIONS

A novel two-color, three-component LDV probe was developed to measure three simultaneous velocity components in the boundary layer of a 6 to 1 prolate spheroid. This probe was placed inside the model, with all transmitted and reflected light passing through a window molded to the curvature of the model, so that the flow was virtually undisturbed by the presence of the probe. All measurements were made at 10° angle of attack and $Re_L = 4.20 \times 10^6$. Boundary-layer profiles were measured across the lee side of the model at $x/L = 0.400$ and 0.600 , and about the primary separation line at $x/L = 0.752$, 0.762 and 0.772 . Measurements of all mean velocity components, the full Reynolds stress tensor and all velocity triple products were obtained from less than 0.01 cm from the wall out to the edge of the boundary layer. The geometry of the probe was such that all measured terms were of high accuracy, even the normally difficult to obtain $-\overline{vw}$. These measurements show

clearly the increasing three-dimensionality of the boundary layer across the separation line and the changes in turbulence with this increasing three-dimensionality.

$$x/L = 0.400$$

ϕ	Edge Conditions			Momentum Thickness		Wall Conditions	
	(deg.) β	(/Uinf) U	(cm) δ	(cm) θ	Re	(deg.) β	($\times 10^3$) Cl
90	-17.06	1.067	0.388	0.047	1545	-18.07	4.11
100	-16.10	1.064	0.422	0.052	1701	-17.13	3.88
110	-15.50	1.067	0.479	0.061	1982	-15.12	3.63
120	-14.40	1.060	0.527	0.069	2246	-11.95	3.46
130	-12.49	1.054	0.588	0.078	2505	-9.18	3.34
140	-10.33	1.046	0.555	0.087	2787	-6.44	3.27
150	-7.83	1.036	0.711	0.094	2993	-3.86	3.19
160	-5.28	1.041	0.791	0.102	3242	-1.43	3.28
170	-2.29	1.033	0.927	0.104	3304	-0.09	3.54
180	0.87	1.043	0.709	0.090	2887	0.72	3.28

$$x/L = 0.600$$

ϕ	Edge Conditions			Momentum Thickness		Wall Conditions	
	(deg.) β	(/Uinf) U	(cm) δ	(cm) θ	Re	(deg.) β	($\times 10^3$) Cl
90	-17.10	1.090	0.652	0.081	2693	-18.60	3.50
100	-16.50	1.080	0.764	0.096	3169	-19.70	3.12
110	-15.70	1.080	0.865	0.107	3531	-15.00	2.92
120	-14.00	1.080	1.043	0.140	4621	-10.50	2.58
130	-12.70	1.060	1.228	0.178	5776	-5.28	2.33
140	-11.30	1.060	1.486	0.220	7138	-0.98	2.09
150	-9.09	1.050	1.681	0.250	8051	1.93	2.09
160	-6.51	1.050	1.785	0.244	7860	3.01	2.22
170	-3.85	1.040	1.843	0.218	6954	2.06	2.50
180	-0.33	1.040	1.677	0.182	6119	-0.75	2.63

$$x/L = 0.752$$

ϕ	Edge Conditions			Momentum Thickness		Wall Conditions	
	(deg.) β	(/Uinf) U	(cm) δ	(cm) θ	Re	(deg.) β	($\times 10^3$) Cl
120	-13.77	1.026	1.396	0.205	6438	-2.09	2.10
123	-13.82	1.024	1.489	0.226	7088	-0.25	1.96
125	-12.66	1.034	1.595	0.249	7869	0.57	1.84

$$x/L = 0.762$$

ϕ	Edge Conditions			Momentum Thickness		Wall Conditions	
	(deg.) β	(/Uinf) U	(cm) δ	(cm) θ	Re	(deg.) β	($\times 10^3$) Cl
120	-13.43	1.032	1.426	0.215	6783	-0.63	2.05
123	-13.15	1.027	1.589	0.242	7606	0.82	1.91
125	-12.74	1.033	1.644	0.258	8148	2.55	1.84

$$x/L = 0.772$$

ϕ	Edge Conditions			Momentum Thickness		Wall Conditions	
	(deg.) β	(/Uinf) U	(cm) δ	(cm) θ	Re	(deg.) β	($\times 10^3$) Cl
105	-16.67	1.027	0.933	0.125	3930	-11.10	2.86
110	-15.50	1.033	1.093	0.155	4918	-7.57	2.55
115	-14.86	1.027	1.250	0.180	5670	-3.86	2.25
120	-14.55	1.023	1.419	0.212	6646	-0.48	2.07
123	-14.30	1.016	1.538	0.239	7427	1.23	1.83
125	-13.77	1.020	1.640	0.256	8004	3.35	1.71
130	-13.65	1.017	1.873	0.305	9512	5.64	1.56

Table 1. Boundary-layer profile summary.

$x/L = 0.400$ $\alpha = 10 \text{ deg.}$
 $Re = 4.2E+06$ $\phi = 90 \text{ deg.}$

Local-Freestream Coordinates

r		y+	(deg.)	(/ Ue)			(/ Ue ² x1000)					
(cm)	(/ δ)		Beta bs	U	V	W	uu	vv	ww	-uv	-uw	-vw
0.005	0.0139	8	-18.07	0.301	0.001	-0.005	15.950	0.229	1.978	0.894	0.297	0.016
0.009	0.0243	14	-18.23	0.434	0.002	-0.009	17.940	0.557	2.818	1.435	0.587	-0.004
0.013	0.0346	20	-18.46	0.515	0.004	-0.013	15.750	1.000	3.452	1.928	0.461	0.027
0.019	0.0501	29	-18.28	0.586	0.003	-0.012	12.290	1.553	3.886	2.055	0.228	0.034
0.025	0.0656	38	-18.40	0.616	0.004	-0.014	10.610	1.881	4.134	1.999	0.243	-0.009
0.032	0.0836	48	-18.39	0.634	0.003	-0.015	9.736	1.996	4.147	2.003	0.106	0.054
0.042	0.1094	63	-18.72	0.665	0.004	-0.019	7.959	2.266	4.003	1.945	0.048	0.033
0.057	0.1481	85	-18.64	0.704	0.003	-0.019	6.745	2.341	3.846	1.788	-0.042	0.093
0.077	0.1998	115	-18.57	0.734	0.004	-0.019	6.194	2.334	3.595	1.697	-0.022	0.175
0.122	0.3159	182	-18.37	0.789	0.004	-0.018	5.173	2.238	3.243	1.520	-0.066	0.105
0.197	0.5094	293	-18.12	0.862	0.006	-0.016	4.226	1.905	2.636	1.250	-0.099	0.157
0.297	0.7675	441	-17.57	0.940	0.006	-0.008	2.715	1.326	1.692	0.803	-0.158	0.134
0.398	1.0260	589	-17.06	0.994	0.006	0.000	1.047	0.664	0.634	0.249	-0.131	0.037
0.598	1.5420	885	-16.49	1.016	0.004	0.010	0.099	0.098	0.114	-0.022	-0.036	-0.035
0.997	2.5740	1478	-16.11	1.011	-0.001	0.017	0.070	0.086	0.092	-0.031	-0.026	-0.038
1.497	3.8640	2218	-15.69	1.004	-0.002	0.024	0.085	0.084	0.163	-0.036	-0.001	-0.026
1.998	5.1550	2960	-15.51	1.000	-0.006	0.027	0.079	0.089	0.090	-0.030	-0.026	-0.017

r		y+	(/Ue ³ x10 ⁶)								
(cm)	(/δ)		U ³	V ³	W ³	U ² V	U ² W	UV ²	V ² W	UW ²	VW ²
0.005	0.0139	8	1198.00	-22.47	-0.17	-97.24	-14.79	10.50	-2.87	124.60	2.36
0.009	0.0243	14	137.80	-18.16	-16.33	-33.51	-3.23	15.07	-4.74	118.40	6.35
0.013	0.0346	20	-341.50	-16.52	-17.70	57.20	11.01	1.84	-6.12	71.79	6.59
0.019	0.0501	29	-433.30	-6.05	-5.98	118.30	9.59	-21.08	-2.46	32.16	7.27
0.025	0.0656	38	-351.60	3.79	2.89	112.90	20.02	-26.10	1.35	-3.66	17.42
0.032	0.0836	48	-278.20	5.75	-4.45	107.60	12.88	-31.80	-0.16	-4.10	16.51
0.042	0.1094	63	-164.20	15.90	6.97	71.47	8.60	-29.40	-0.03	-17.56	18.74
0.057	0.1481	85	-64.04	24.76	-4.21	43.06	1.65	-25.54	-1.46	-13.19	17.32
0.077	0.1998	115	-66.40	24.44	-6.87	38.81	-0.37	-26.31	-1.06	-9.84	15.41
0.122	0.3159	182	-55.89	28.71	-5.68	33.33	-2.21	-26.94	1.11	-15.36	10.91
0.197	0.5094	293	-86.36	33.56	9.60	37.10	-2.90	-32.02	-0.86	-24.50	12.69
0.297	0.7675	441	-90.49	37.37	-9.08	38.70	-10.69	-36.17	-0.83	-28.57	15.45
0.398	1.0260	589	-38.39	16.19	-7.92	17.17	-9.77	-16.50	4.94	-14.93	7.87
0.598	1.5420	885	6.69	0.44	-1.38	-0.13	-5.88	-2.28	8.21	-4.26	0.73
0.997	2.5740	1478	6.30	0.29	-1.89	-0.31	-5.77	-2.41	7.82	-4.13	0.56
1.497	3.8640	2218	6.25	0.47	-1.20	-0.10	-5.99	-2.18	7.43	-3.40	1.47
1.998	5.1550	2960	6.06	0.85	-2.63	-0.27	-5.33	-2.12	7.33	-3.91	0.44

Table 2. Boundary-layer profile at $x/L = 0.400$, $\phi = 90^\circ$.

$x/L = 0.400$ $\alpha = 10 \text{ deg.}$
 $Re = 4.2E+06$ $\phi = 100 \text{ deg.}$

Local-Freestream Coordinates

r		y+	(deg.)	(/ Ue)			(/ Ue ² x1000)					
(cm)	(/δ)		Beta _{bs}	U	V	W	uu	vv	ww	-uv	-uw	-vw
0.009	0.0216	13	-17.13	0.422	0.002	-0.008	17.800	0.539	2.711	1.297	0.464	0.035
0.013	0.0311	19	-17.22	0.489	0.003	-0.010	15.640	0.841	3.253	1.751	0.650	-0.023
0.017	0.0405	25	-17.59	0.532	-0.000	-0.014	14.110	1.250	3.579	2.002	0.410	0.040
0.023	0.0548	33	-17.43	0.579	0.003	-0.013	11.770	1.581	3.826	1.936	0.298	0.018
0.029	0.0690	42	-17.54	0.607	0.004	-0.015	10.440	1.903	4.049	2.016	0.186	0.051
0.036	0.0856	52	-17.39	0.635	0.001	-0.014	8.766	2.115	4.047	1.968	0.129	0.065
0.046	0.1093	66	-17.68	0.660	0.005	-0.018	7.596	2.326	4.009	1.965	0.132	0.049
0.061	0.1449	88	-17.75	0.689	0.004	-0.020	6.649	2.349	3.761	1.834	0.062	0.063
0.081	0.1923	116	-17.76	0.721	0.004	-0.021	6.043	2.261	3.538	1.606	0.085	0.069
0.126	0.2990	181	-17.79	0.773	0.006	-0.023	5.074	2.190	3.253	1.420	-0.097	0.126
0.201	0.4768	289	-17.63	0.844	0.010	-0.023	4.141	1.947	2.722	1.200	-0.264	0.232
0.301	0.7138	432	-17.50	0.921	0.006	-0.023	2.832	1.356	1.852	0.838	-0.146	0.126
0.401	0.9509	576	-17.04	0.981	0.006	-0.016	1.402	0.738	0.867	0.382	-0.132	0.088
0.601	1.4250	863	-16.10	1.018	0.009	0.000	0.105	0.132	0.107	-0.030	-0.029	-0.045
1.001	2.3730	1437	-15.82	1.013	0.006	0.005	0.080	0.096	0.089	-0.044	-0.039	-0.050
1.501	3.5590	2155	-15.46	1.005	0.005	0.011	0.075	0.067	0.136	-0.029	0.015	-0.006
2.001	4.7440	2872	-15.16	1.000	0.004	0.016	0.061	0.084	0.073	-0.022	-0.017	-0.020

r		y+	(/ Ue ³ x10 ⁶)								
(cm)	(/δ)		u ³	v ³	w ³	u ² v	u ² w	uv ²	v ² w	uw ²	vw ²
0.009	0.0216	13	216.70	-9.85	-14.68	-40.77	6.74	17.52	-3.63	113.10	5.87
0.013	0.0311	19	-217.90	-14.18	-17.37	33.39	18.12	7.42	-3.17	80.88	5.07
0.017	0.0405	25	-367.60	-3.33	-15.49	81.61	16.72	-7.56	-7.16	49.02	9.49
0.023	0.0548	33	-377.50	-8.35	-8.87	95.05	7.08	-10.74	-2.78	18.55	10.64
0.029	0.0690	42	-335.80	13.00	-10.62	105.00	8.93	-28.56	-6.39	6.88	16.20
0.036	0.0856	52	-231.60	12.07	-1.27	84.87	3.60	-26.54	-0.21	-6.31	14.10
0.046	0.1093	66	-125.50	31.36	3.05	72.09	-11.99	-41.26	-2.04	-13.50	18.52
0.061	0.1449	88	-81.01	22.80	0.24	52.76	-0.63	-26.79	-2.99	-5.35	16.18
0.081	0.1923	116	-56.15	23.86	-1.92	39.16	1.76	-22.86	2.64	-7.63	12.68
0.126	0.2990	181	-58.99	29.52	-1.98	38.11	-3.46	-27.83	1.93	-18.72	13.37
0.201	0.4768	289	-63.93	29.89	-7.97	34.11	-1.85	-30.16	0.29	-25.75	17.75
0.301	0.7138	432	-71.97	23.92	-4.75	27.90	-7.63	-26.96	3.22	-26.84	14.25
0.401	0.9509	576	-50.45	15.61	-8.64	20.15	-9.60	-18.93	4.30	-18.98	8.77
0.601	1.4250	863	6.34	0.67	-1.16	-0.17	-6.10	-2.18	8.18	-4.07	0.86
1.001	2.3730	1437	5.97	0.43	-1.60	-0.25	-5.96	-2.10	7.92	-3.90	0.55
1.501	3.5590	2155	5.94	0.23	-2.08	-0.11	-6.11	-2.01	7.28	-3.09	1.32
2.001	4.7440	2872	5.49	0.40	-2.19	-0.34	-5.52	-2.23	7.05	-3.73	0.11

Table 3. Boundary-layer profile at $x/L = 0.400$, $\phi = 100^\circ$.

$$x/L = 0.400 \quad \alpha = 10 \text{ deg.}$$

$$Re = 4.2E+06 \quad \phi = 110 \text{ deg.}$$

Local-Freestream Coordinates

r		y+	(deg.)	(/ Ue)			(/ Ue ² x1000)					
(cm)	(/ δ)		Beta bs	U	V	W	uu	vv	ww	-uv	-uw	-vw
0.008	0.0159	11	-15.12	0.380	0.002	0.002	17.510	0.423	2.378	1.129	0.300	0.055
0.012	0.0242	16	-15.22	0.445	-0.000	0.002	15.870	0.674	2.955	1.583	0.262	0.049
0.016	0.0326	22	-15.33	0.496	0.001	0.002	14.390	0.974	3.307	1.780	0.239	0.011
0.022	0.0451	30	-15.53	0.545	0.001	-0.000	11.980	1.359	3.565	1.902	0.143	0.041
0.028	0.0576	38	-15.44	0.576	0.003	0.001	10.350	1.702	3.775	1.895	0.035	0.025
0.035	0.0723	48	-15.48	0.605	0.000	0.000	8.905	1.967	3.823	1.927	0.148	-0.022
0.045	0.0932	62	-15.63	0.633	0.003	-0.001	7.536	2.136	3.700	1.856	0.013	0.015
0.060	0.1245	83	-15.89	0.661	0.002	-0.004	6.598	2.226	3.742	1.762	0.069	0.021
0.080	0.1662	111	-15.92	0.694	0.002	-0.005	5.881	2.335	3.475	1.677	0.087	0.039
0.125	0.2602	173	-16.26	0.752	0.002	-0.010	5.161	2.210	3.295	1.529	0.063	0.045
0.200	0.4169	278	-16.26	0.819	0.006	-0.011	4.260	1.955	2.902	1.226	0.016	0.060
0.300	0.6257	417	-16.47	0.895	0.004	-0.015	3.212	1.528	2.138	0.939	-0.049	0.103
0.400	0.8346	556	-16.25	0.956	0.009	-0.013	1.962	0.968	1.257	0.542	-0.072	0.074
0.599	1.2520	835	-15.50	1.016	0.013	0.000	0.213	0.229	0.172	-0.037	-0.053	-0.054
1.000	2.0880	1392	-15.24	1.011	0.009	0.005	0.084	0.105	0.106	-0.052	-0.037	-0.046
1.500	3.1320	2087	-14.76	1.004	0.012	0.013	0.083	0.079	0.180	-0.032	0.010	-0.017
1.999	4.1760	2782	-14.59	1.000	0.011	0.016	0.081	0.089	0.131	-0.038	-0.020	-0.014

r		y+	(/ Ue ³ x10 ⁶)								
(cm)	(/ δ)		u ³	v ³	w ³	u ² v	u ² w	uv ²	v ² w	uw ²	vw ²
0.008	0.0159	11	465.30	-10.53	-5.31	-56.69	-15.08	15.43	-4.83	110.70	5.89
0.012	0.0242	16	-87.03	-16.50	-4.48	-1.45	3.43	15.24	-1.61	92.87	6.64
0.016	0.0326	22	-311.90	-11.94	-10.95	59.94	-0.85	2.72	-4.13	69.56	4.59
0.022	0.0451	30	-325.30	-4.97	-9.69	76.48	14.79	-6.20	-3.22	35.41	10.99
0.028	0.0576	38	-299.30	-1.14	-8.13	105.00	0.31	-20.79	0.68	21.01	12.19
0.035	0.0723	48	-206.50	6.72	-2.78	85.86	7.15	-23.58	1.78	-2.05	13.96
0.045	0.0932	62	-144.00	20.97	-4.31	75.25	-2.30	-32.47	-2.81	1.40	12.57
0.060	0.1245	83	-59.88	24.22	0.17	47.75	-2.34	-24.54	-2.14	-12.99	17.93
0.080	0.1662	111	-47.42	28.04	1.10	41.31	-5.76	-26.66	-0.58	-2.98	12.18
0.125	0.2602	173	-24.14	18.67	0.94	19.60	-5.20	-16.36	1.50	-9.19	9.93
0.200	0.4169	278	-51.41	16.93	-1.26	21.29	-0.26	-16.17	4.39	-12.24	6.64
0.300	0.6257	417	-68.28	23.66	-6.70	29.02	-2.12	-24.89	4.13	-25.54	13.10
0.400	0.8346	556	-63.39	18.37	-4.87	23.19	-6.56	-22.32	3.87	-23.31	10.86
0.599	1.2520	835	3.53	3.16	-1.32	1.62	-6.16	-3.28	7.89	-4.10	1.45
1.000	2.0880	1392	5.66	0.71	-1.72	-0.15	-5.92	-1.81	7.62	-3.60	0.59
1.500	3.1320	2087	5.53	0.55	-3.85	-0.10	-6.23	-1.87	6.93	-2.19	1.47
1.999	4.1760	2782	5.41	0.61	-5.71	-0.14	-5.72	-1.79	6.74	-3.10	0.59

Table 4. Boundary-layer profile at $x/L = 0.400$, $\phi = 110^\circ$.

$x/L = 0.400$ $\alpha = 10 \text{ deg.}$
 $Re = 4.2E+06$ $\phi = 120 \text{ deg.}$

Local-Freestream Coordinates

r		y+	(deg.)	(/ Ue)			(/ Ue ² x1000)					
(cm)	(/δ)		Beta_bs	U	V	W	uu	vv	ww	-uv	-uw	-vw
0.006	0.0123	9	-11.95	0.317	0.000	0.014	15.570	0.267	2.160	0.950	-0.496	0.074
0.010	0.0199	14	-12.50	0.403	-0.000	0.013	15.740	0.524	2.560	1.400	-0.112	0.062
0.014	0.0275	20	-12.72	0.467	0.000	0.014	14.540	0.828	3.013	1.678	-0.062	0.064
0.021	0.0389	28	-12.87	0.522	0.001	0.014	12.310	1.327	3.513	1.860	-0.035	0.097
0.026	0.0503	36	-13.03	0.558	0.002	0.013	10.370	1.570	3.666	1.840	0.105	0.050
0.034	0.0636	45	-13.11	0.583	0.001	0.013	8.846	1.790	3.730	1.828	0.071	0.037
0.043	0.0825	59	-13.16	0.615	0.002	0.013	7.600	2.055	3.730	1.750	0.026	0.061
0.058	0.1110	79	-13.48	0.643	0.001	0.010	6.404	2.148	3.664	1.604	0.087	0.057
0.079	0.1490	106	-13.66	0.675	0.002	0.009	5.907	2.263	3.441	1.656	0.053	0.050
0.123	0.2343	167	-13.99	0.726	0.004	0.005	5.192	2.227	3.349	1.536	0.018	0.052
0.198	0.3766	268	-14.51	0.793	0.007	-0.002	4.386	1.993	2.953	1.247	0.119	0.011
0.298	0.5664	403	-14.85	0.865	0.005	-0.007	3.524	1.631	2.385	0.995	0.034	0.052
0.398	0.7561	538	-14.80	0.931	0.007	-0.007	2.424	1.116	1.530	0.697	-0.016	0.050
0.599	1.1360	808	-14.40	1.011	0.014	0.000	0.341	0.293	0.253	0.013	-0.052	-0.017
0.999	1.8950	1348	-13.99	1.013	0.013	0.007	0.067	0.101	0.070	-0.036	-0.022	-0.030
1.498	2.8430	2023	-13.56	1.004	0.016	0.015	0.060	0.060	0.120	-0.023	0.002	-0.014
1.998	3.7920	2698	-13.39	1.000	0.018	0.017	0.059	0.069	0.084	-0.026	-0.018	-0.017

r		y+	(Ue ³ x10 ⁶)								
(cm)	(/δ)		U ³	V ³	W ³	U ² V	U ² W	UV ²	V ² W	UW ²	VW ²
0.006	0.0123	9	868.00	-19.47	13.26	-80.19	30.64	13.92	0.44	126.20	0.16
0.010	0.0199	14	173.00	-14.31	9.58	-29.71	-4.71	14.38	-1.95	93.22	3.32
0.014	0.0275	20	-192.30	-15.19	6.68	40.60	-18.01	2.72	0.38	71.70	8.37
0.021	0.0389	28	-304.90	2.15	1.93	77.07	-4.77	-10.38	-7.31	44.71	10.00
0.026	0.0503	36	-296.70	3.72	-8.61	84.18	8.31	-18.66	-3.82	18.35	10.23
0.034	0.0636	45	-220.80	3.91	-1.01	80.05	-10.63	-20.51	-0.20	8.86	8.15
0.043	0.0825	59	-135.80	13.76	-13.19	67.38	-3.96	-25.87	-4.77	-0.16	14.05
0.058	0.1110	79	-51.66	19.62	-8.01	36.18	-0.81	-18.60	-4.43	-4.11	12.94
0.079	0.1490	106	-46.36	27.60	-6.60	37.62	-3.76	-27.69	-2.80	-8.44	12.46
0.123	0.2343	167	-23.93	19.57	1.65	23.98	-0.90	-16.69	-2.40	-11.35	9.29
0.198	0.3766	268	-33.51	16.34	0.56	15.92	-2.23	-13.99	4.56	-11.85	10.33
0.298	0.5664	403	-62.93	25.61	4.58	26.98	-3.64	-27.15	3.23	-23.56	11.65
0.398	0.7561	538	-69.56	21.52	-1.45	27.67	-3.42	-24.58	6.42	-24.92	9.42
0.599	1.1360	808	-3.38	4.50	-2.80	3.01	-6.84	-4.42	6.53	-5.45	2.19
0.999	1.8950	1348	4.83	0.45	-1.49	-0.31	-5.84	-1.82	6.88	-3.30	0.22
1.498	2.8430	2023	4.77	0.15	-1.73	-0.17	-5.63	-1.65	6.55	-2.63	0.85
1.998	3.7920	2698	4.54	0.11	-2.16	-0.25	-5.33	-1.68	6.39	-3.15	0.11

Table 5. Boundary-layer profile at $x/L = 0.400$, $\phi = 120^\circ$.

$x/L = 0.400$ $\alpha = 10 \text{ deg.}$
 $Re = 4.2E+06$ $\phi = 130 \text{ deg.}$

Local-Freestream Coordinates

r		y+	(deg.)	(/ Ue)			(/ Ue ² x1000)					
(cm)	(/ δ)		Beta bs	U	V	W	uu	vv	ww	-uv	-uw	-vw
0.005	0.0090	7	-9.18	0.289	0.001	0.017	12.030	0.172	1.738	0.564	-0.521	0.033
0.009	0.0158	12	-9.38	0.381	0.000	0.021	14.670	0.438	2.311	1.292	-0.459	0.062
0.013	0.0226	18	-9.31	0.435	-0.001	0.024	14.370	0.650	2.743	1.491	-0.327	0.045
0.019	0.0328	25	-9.82	0.497	0.000	0.023	12.200	1.035	3.158	1.647	-0.209	0.049
0.025	0.0431	33	-9.93	0.534	0.000	0.024	10.710	1.386	3.502	1.791	-0.196	0.098
0.032	0.0550	43	-9.97	0.568	0.003	0.025	8.777	1.651	3.539	1.671	-0.199	0.084
0.042	0.0720	56	-10.25	0.593	0.004	0.023	7.203	1.840	3.519	1.548	-0.001	0.050
0.057	0.0975	76	-10.32	0.623	0.005	0.024	6.504	2.067	3.507	1.599	-0.052	0.034
0.077	0.1315	102	-10.64	0.652	0.002	0.021	5.637	2.088	3.249	1.513	-0.038	0.056
0.122	0.2081	161	-10.91	0.708	0.008	0.020	5.059	2.226	3.166	1.477	-0.034	0.020
0.197	0.3358	260	-11.59	0.770	0.010	0.012	4.571	2.081	2.966	1.295	0.067	0.018
0.297	0.5059	392	-12.04	0.842	0.013	0.007	3.770	1.811	2.496	1.083	-0.012	0.025
0.397	0.6761	524	-12.51	0.905	0.015	-0.000	2.856	1.339	1.879	0.818	0.024	0.037
0.597	1.0160	788	-12.49	0.993	0.016	-0.000	0.718	0.466	0.453	0.171	-0.043	0.024
0.997	1.6970	1316	-12.15	1.008	0.020	0.006	0.075	0.091	0.093	-0.026	-0.028	-0.028
1.497	2.5480	1974	-11.76	1.002	0.024	0.013	0.095	0.109	0.081	-0.045	-0.026	-0.015
1.997	3.3990	2605	-11.54	0.999	0.030	0.017	0.183	0.292	0.103	0.052	-0.044	0.004

r		y+	(/Ue ³ x10 ⁶)								
(cm)	(/δ)		U ³	V ³	W ³	U ² V	U ² W	UV ²	V ² W	UW ²	VW ²
0.005	0.0090	7	773.60	-6.82	15.25	-46.75	29.52	7.40	0.35	87.10	2.09
0.009	0.0158	12	288.90	-9.83	8.50	-32.97	-2.40	12.56	-0.17	85.80	3.81
0.013	0.0226	18	19.49	-11.24	9.04	10.73	-6.76	7.09	0.42	81.07	2.46
0.019	0.0328	25	-262.60	-10.81	9.41	68.98	-6.39	-4.77	-1.07	46.87	6.35
0.025	0.0431	33	-304.00	-9.46	-3.08	92.88	-7.62	-12.53	-3.55	27.33	7.64
0.032	0.0550	43	-230.10	-0.35	2.32	82.18	-10.50	-19.21	-4.47	7.55	12.59
0.042	0.0720	56	-99.14	4.15	-4.73	48.24	-6.29	-12.91	-2.74	5.70	12.69
0.057	0.0975	76	-50.31	11.54	-8.43	38.92	-7.61	-14.09	-1.08	3.36	11.98
0.077	0.1315	102	3.22	6.48	-6.36	11.06	-1.16	-3.94	1.37	4.41	5.84
0.122	0.2081	161	-5.92	8.62	-4.37	9.61	3.28	-1.85	1.31	3.52	4.63
0.197	0.3358	260	-26.51	7.87	-4.31	7.80	-2.30	-6.41	0.03	-3.37	6.62
0.297	0.5059	392	-59.59	14.11	1.32	20.56	-0.30	-16.07	0.36	-10.54	7.75
0.397	0.6761	524	-70.22	21.58	1.94	24.38	4.48	-22.25	0.87	-18.61	9.63
0.597	1.0160	788	-28.28	9.12	-1.97	9.84	-1.85	-8.98	-1.09	-6.92	3.46
0.997	1.6970	1316	-0.18	-0.11	-0.04	-0.13	-0.08	-0.12	0.06	-0.05	0.11
1.497	2.5480	1974	-0.36	-0.36	-0.48	-0.27	-0.25	-0.27	-0.04	0.09	0.18
1.997	3.3990	2605	19.12	-19.59	0.47	-20.08	4.63	19.34	4.71	0.68	-1.32

Table 6. Boundary-layer profile at $x/L = 0.400$, $\phi = 130^\circ$.

$x/L = 0.400$ $\alpha = 10 \text{ deg.}$
 $Re = 4.2E+06$ $\phi = 140 \text{ deg.}$

Local-Freestream Coordinates

r		y+	(deg.)	(/ Ue)			(/ Ue ² x1000)					
(cm)	(/δ)		Beta bs	U	V	W	uu	vv	ww	-uv	-uw	-vw
0.008	0.0127	11	-6.44	0.346	0.002	0.024	13.460	0.325	2.106	0.947	-0.646	0.077
0.012	0.0188	16	-6.50	0.419	-0.001	0.028	13.990	0.613	2.588	1.452	-0.543	0.117
0.016	0.0249	21	-6.97	0.465	0.000	0.027	12.900	0.864	2.995	1.629	-0.444	0.096
0.022	0.0341	29	-6.66	0.511	0.002	0.033	11.260	1.223	3.347	1.767	-0.309	0.133
0.028	0.0432	37	-7.07	0.543	-0.001	0.031	10.060	1.535	3.559	1.834	-0.131	0.126
0.035	0.0539	46	-6.98	0.566	0.002	0.033	8.877	1.695	3.465	1.753	-0.114	0.103
0.045	0.0692	59	-7.29	0.592	0.002	0.031	7.371	1.941	3.502	1.660	-0.124	0.106
0.060	0.0921	78	-7.44	0.620	0.003	0.031	6.423	2.076	3.488	1.589	0.042	0.030
0.080	0.1226	104	-7.76	0.645	-0.001	0.029	5.573	2.074	3.327	1.469	0.041	0.044
0.125	0.1913	162	-7.93	0.697	0.004	0.029	5.056	2.165	3.134	1.375	0.047	0.016
0.200	0.3059	259	-8.72	0.757	0.007	0.021	4.524	1.967	2.995	1.199	0.073	-0.038
0.300	0.4586	389	-9.38	0.828	0.012	0.014	3.875	1.732	2.558	1.047	0.075	-0.020
0.400	0.6113	518	-10.01	0.889	0.015	0.005	2.853	1.360	2.034	0.775	0.078	-0.037
0.600	0.9167	777	-10.52	0.975	0.021	-0.003	1.112	0.618	0.702	0.324	-0.008	0.022
1.000	1.5270	1295	-10.33	1.008	0.022	-0.000	0.068	0.082	0.112	-0.004	-0.017	-0.027
1.500	2.2910	1943	-9.94	1.002	0.029	0.007	0.064	0.075	0.071	-0.019	-0.016	-0.013
2.001	3.0550	2588	-9.78	0.999	0.036	0.010	0.063	0.137	0.086	-0.011	-0.013	-0.021

r		y+	(Ue ³ x10 ⁶)								
(cm)	(/ δ)		u ³	v ³	w ³	u ² v	u ² w	uv ²	v ² w	uw ²	vw ²
0.008	0.0127	11	555.50	-12.72	13.44	-47.75	10.99	9.49	1.27	83.09	1.26
0.012	0.0188	16	74.40	-14.07	8.78	0.47	-10.04	8.69	-0.48	81.43	3.14
0.016	0.0249	21	-157.30	-11.33	15.40	40.91	-20.14	-0.85	0.11	57.35	5.35
0.022	0.0341	29	-271.00	-9.41	11.28	85.92	-22.33	-11.57	-0.37	39.34	7.18
0.028	0.0432	37	-268.10	-3.24	-0.54	85.91	-13.71	-17.44	-3.29	19.84	10.59
0.035	0.0539	46	-214.20	-1.74	-9.78	80.60	-10.08	-17.34	-1.76	15.62	5.93
0.045	0.0692	59	-143.50	9.75	-6.50	68.99	-7.02	-22.92	0.28	2.97	8.96
0.060	0.0921	78	-77.66	11.66	-0.93	41.57	-3.17	-14.86	0.59	0.67	9.08
0.080	0.1226	104	-24.77	15.84	-7.80	29.13	-7.19	-17.18	-0.27	0.86	11.22
0.125	0.1913	162	-15.78	14.00	-8.95	22.31	-1.01	-12.43	-2.03	-2.42	7.79
0.200	0.3059	259	-28.01	11.81	1.75	16.03	0.02	-8.81	2.66	-7.50	6.87
0.300	0.4586	389	-48.17	14.36	0.86	15.70	-3.76	-14.23	2.89	-15.03	8.14
0.400	0.6113	518	-54.91	14.08	4.16	17.37	-0.17	-16.03	5.19	-16.90	9.01
0.600	0.9167	777	-36.89	10.62	-0.70	13.92	-4.58	-12.25	4.08	-12.68	5.40
1.000	1.5270	1295	2.55	0.42	-0.65	-0.00	-4.89	-1.09	5.35	-1.89	0.27
1.500	2.2910	1943	2.40	0.06	-0.44	-0.05	-4.64	-0.94	5.09	-1.75	0.28
2.001	3.0550	2588	2.34	1.25	-1.04	-0.01	-4.51	-1.21	4.93	-1.81	0.01

Table 7. Boundary-layer profile at $x/L = 0.400$, $\phi = 140^\circ$.

$x/L = 0.400$ $\alpha = 10 \text{ deg.}$
 $Re = 4.2E+06$ $\phi = 150 \text{ deg.}$

Local-Freestream Coordinates

r		y+	(deg.)	(/ Ue)			(/ Ue ² x1000)					
(cm)	(/ δ)		Beta_bs	U	V	W	uu	vv	ww	-uv	-uw	-vw
0.006	0.0082	7	-3.86	0.288	0.002	0.020	12.390	0.187	1.675	0.615	-0.655	0.060
0.010	0.0138	12	-3.74	0.366	0.002	0.026	14.620	0.377	2.199	1.151	-0.692	0.115
0.014	0.0194	18	-3.91	0.426	-0.000	0.029	14.160	0.639	2.670	1.474	-0.562	0.112
0.020	0.0279	25	-4.10	0.486	0.002	0.032	12.260	0.973	3.153	1.567	-0.405	0.130
0.026	0.0363	33	-4.14	0.522	0.001	0.034	10.770	1.296	3.356	1.677	-0.180	0.089
0.033	0.0462	42	-4.26	0.553	0.002	0.035	9.003	1.549	3.513	1.632	-0.131	0.101
0.043	0.0602	54	-4.42	0.582	0.001	0.035	7.256	1.763	3.466	1.549	-0.049	0.086
0.058	0.0813	73	-4.59	0.612	0.003	0.035	6.384	1.921	3.422	1.470	-0.023	0.078
0.078	0.1095	99	-4.78	0.635	0.000	0.034	5.590	2.052	3.309	1.439	0.005	0.025
0.123	0.1728	156	-5.07	0.690	0.004	0.033	5.187	2.029	3.078	1.304	-0.008	-0.014
0.198	0.2783	251	-5.74	0.749	0.006	0.027	4.596	1.955	2.949	1.193	0.077	0.011
0.298	0.4190	378	-6.43	0.814	0.011	0.020	3.991	1.781	2.602	1.109	0.084	-0.079
0.398	0.5597	504	-7.19	0.874	0.015	0.010	3.123	1.448	2.150	0.923	0.073	0.009
0.598	0.8410	758	-7.88	0.960	0.016	-0.001	1.404	0.714	0.943	0.447	0.021	0.010
0.998	1.4040	1265	-7.83	1.007	0.020	0.000	0.065	0.071	0.081	0.010	-0.017	-0.006
1.498	2.1070	1899	-7.54	1.004	0.027	0.005	0.050	0.067	0.063	-0.003	-0.012	-0.005
1.998	2.8110	2533	-7.43	0.999	0.036	0.007	0.054	0.104	0.058	0.006	-0.011	-0.003

r		y+	(/Ue ³ x10 ⁶)								
(cm)	(/δ)		u ³	v ³	w ³	u ² v	u ² w	uv ²	v ² w	uw ²	vw ²
0.006	0.0082	7	869.70	-7.55	12.90	-56.10	50.67	9.25	0.60	84.42	1.37
0.010	0.0138	12	461.50	-11.10	13.31	-55.71	8.85	15.26	1.31	89.38	0.88
0.014	0.0194	18	-43.38	-12.28	16.89	9.74	-14.76	9.26	0.22	79.17	4.18
0.020	0.0279	25	-256.80	-13.20	6.38	64.87	-30.16	-2.85	-1.22	54.90	5.61
0.026	0.0363	33	-283.20	-7.39	-8.45	87.78	-27.50	-10.65	-1.64	22.90	8.02
0.033	0.0462	42	-225.80	0.42	-12.42	81.49	-13.17	-16.82	-1.85	9.48	12.93
0.043	0.0602	54	-139.10	7.59	-5.81	69.49	-8.52	-22.07	-1.50	5.24	11.41
0.058	0.0813	73	-57.71	10.73	-6.01	45.55	-10.58	-15.99	-0.39	0.96	10.47
0.078	0.1095	99	-29.04	14.85	-8.30	33.06	-3.10	-13.15	-0.40	-1.43	11.23
0.123	0.1728	156	-6.08	8.02	-1.61	14.92	-3.14	-4.36	2.67	1.30	5.87
0.198	0.2783	251	-18.44	8.35	1.81	9.37	-4.55	-5.57	0.20	-2.94	3.66
0.298	0.4190	378	-53.61	13.05	-0.37	12.75	-2.14	-11.40	3.59	-11.66	4.62
0.398	0.5597	504	-63.63	14.34	3.71	17.80	-0.52	-14.52	2.96	-16.46	9.12
0.598	0.8410	758	-38.20	9.81	2.41	14.12	-1.16	-11.78	4.24	-13.20	6.39
0.998	1.4040	1265	1.62	0.05	-0.29	-0.12	-3.94	-0.56	4.21	-1.16	0.10
1.498	2.1070	1899	1.48	-0.03	-0.19	-0.11	-3.80	-0.56	3.99	-1.09	0.17
1.998	2.8110	2533	1.45	0.71	-0.39	-0.01	-3.64	-0.73	3.71	-1.10	0.01

Table 8. Boundary-layer profile at $x/L = 0.400$, $\phi = 150^\circ$.

$$x/L = 0.400 \quad \alpha = 10 \text{ deg.}$$

$$Re = 4.2E+06 \quad \phi = 160 \text{ deg.}$$

Local-Freestream Coordinates

r		y+	(deg.)	(/ Ue)			(/ Ue ² x1000)					
(cm)	(/δ)		Beta bs	U	V	W	uu	vv	ww	-uv	-uw	-vw
0.008	0.0096	10	-1.43	0.346	0.001	0.023	14.240	0.314	2.069	0.944	-0.778	0.090
0.012	0.0147	15	-1.53	0.410	0.001	0.027	14.320	0.521	2.475	1.350	-0.658	0.131
0.016	0.0197	20	-1.77	0.455	-0.000	0.028	13.160	0.752	2.912	1.459	-0.520	0.124
0.022	0.0273	28	-1.83	0.508	0.002	0.031	11.200	1.111	3.171	1.605	-0.442	0.117
0.028	0.0349	36	-2.00	0.539	0.000	0.031	9.882	1.422	3.379	1.729	-0.294	0.124
0.035	0.0438	45	-1.79	0.564	0.002	0.034	8.589	1.628	3.480	1.623	-0.131	0.133
0.045	0.0564	58	-1.86	0.580	0.004	0.035	7.531	1.824	3.529	1.612	-0.077	0.122
0.060	0.0754	77	-1.97	0.609	0.006	0.035	6.302	1.925	3.456	1.404	-0.072	0.074
0.080	0.1007	103	-2.31	0.633	0.001	0.033	5.433	1.999	3.230	1.332	-0.017	0.063
0.125	0.1576	161	-2.36	0.689	0.006	0.035	4.973	2.040	2.938	1.236	-0.107	0.046
0.200	0.2524	258	-3.03	0.743	0.008	0.029	4.450	1.947	2.747	1.095	0.018	-0.004
0.300	0.3788	387	-3.54	0.805	0.013	0.024	3.860	1.676	2.572	0.946	0.046	-0.074
0.400	0.5053	516	-4.20	0.861	0.015	0.016	3.263	1.458	2.119	0.854	0.033	-0.050
0.600	0.7582	774	-5.01	0.943	0.016	0.004	1.708	0.836	1.184	0.496	0.028	-0.014
1.000	1.2640	1291	-5.28	1.006	0.019	-0.000	0.120	0.139	0.134	0.008	-0.044	-0.018
1.499	1.8960	1937	-5.02	1.003	0.027	0.004	0.080	0.101	0.104	0.003	-0.017	-0.009
1.999	2.5280	2582	-5.03	0.999	0.035	0.004	0.084	0.152	0.086	0.013	-0.027	0.002

r		y+	(/ Ue ³ x10 ⁶)								
(cm)	(/δ)		u ³	v ³	w ³	u ² v	u ² w	uv ²	v ² w	uw ²	vw ²
0.008	0.0096	10	588.70	-11.12	16.69	-57.27	17.10	11.87	0.55	86.37	1.31
0.012	0.0147	15	98.83	-14.39	9.46	-7.38	-8.73	10.43	1.45	77.45	3.20
0.016	0.0197	20	-175.20	-15.18	3.73	39.11	-18.12	3.76	0.70	69.70	3.10
0.022	0.0273	28	-324.20	-9.77	0.94	80.65	-31.64	-9.86	-2.35	32.90	6.49
0.028	0.0349	36	-257.10	-2.40	-4.61	90.50	-15.47	-19.61	-1.47	15.99	6.23
0.035	0.0438	45	-191.70	2.73	-9.55	79.55	-14.63	-20.69	-3.67	2.32	10.11
0.045	0.0564	58	-141.20	13.36	-10.54	69.25	-9.32	-24.65	-2.65	3.89	9.83
0.060	0.0754	77	-68.94	15.68	-4.88	46.35	-9.33	-21.99	-3.62	11.63	12.08
0.080	0.1007	103	-20.24	15.57	-0.17	29.41	-5.88	-13.09	-0.62	2.51	8.42
0.125	0.1576	161	-15.49	12.27	-5.32	23.90	0.42	-9.25	0.35	0.33	5.76
0.200	0.2524	258	-27.80	12.14	-4.19	18.68	0.36	-9.33	-0.79	-5.46	6.07
0.300	0.3788	387	-30.31	11.46	0.20	8.08	-0.71	-9.33	2.60	-9.62	6.30
0.400	0.5053	516	-53.85	12.76	-2.08	11.87	-0.94	-12.39	3.26	-10.27	7.00
0.600	0.7582	774	-39.34	10.39	3.44	13.36	0.61	-10.82	3.98	-13.73	6.98
1.000	1.2640	1291	0.56	0.50	-0.23	-0.01	-2.83	-0.05	3.10	-0.62	0.39
1.499	1.8960	1937	0.42	0.10	0.00	-0.01	-2.69	-0.23	2.72	-0.45	0.46
1.999	2.5280	2582	0.67	1.22	-0.53	-0.10	-2.58	-0.58	2.50	-0.57	0.01

Table 9. Boundary-layer profile at $x/L = 0.400$, $\phi = 160^\circ$.

$x/L = 0.400$ $\alpha = 10 \text{ deg.}$
 $Re = 4.2E+06$ $\phi = 170 \text{ deg.}$
Local-Freestream Coordinates

r		y+	(deg.)	(/ Ue)			(/ Ue ² x1000)					
(cm)	(/ δ)		Beta _{bs}	U	V	W	uu	vv	ww	-uv	-uw	-vw
0.006	0.0061	8	-0.09	0.308	0.001	0.012	13.359	0.226	1.765	0.820	-0.515	0.057
0.010	0.0105	13	-0.16	0.397	-0.001	0.015	14.588	0.460	2.397	1.286	-0.530	0.100
0.014	0.0148	18	-0.20	0.460	-0.000	0.017	13.918	0.740	2.901	1.593	-0.482	0.110
0.020	0.0212	26	-0.07	0.516	-0.001	0.020	12.323	1.164	3.303	1.834	-0.401	0.132
0.026	0.0277	34	-0.39	0.555	0.001	0.018	10.433	1.449	3.598	1.742	-0.226	0.130
0.033	0.0353	44	-0.39	0.584	0.000	0.019	9.226	1.751	3.698	1.787	-0.253	0.146
0.043	0.0461	57	-0.34	0.614	-0.001	0.021	7.729	1.983	3.645	1.748	-0.183	0.157
0.058	0.0622	77	-0.29	0.645	0.000	0.023	6.793	2.113	3.575	1.632	-0.134	0.090
0.078	0.0838	103	-0.45	0.678	0.002	0.022	6.311	2.228	3.522	1.635	-0.114	0.103
0.123	0.1324	163	-0.64	0.694	0.001	0.020	4.999	2.038	2.981	1.407	-0.043	0.047
0.198	0.2133	263	-0.85	0.749	0.003	0.019	4.366	1.858	2.704	1.173	-0.029	-0.008
0.298	0.3212	396	-1.42	0.804	0.003	0.012	3.687	1.643	2.414	1.031	-0.012	0.014
0.398	0.4290	529	-1.43	0.856	0.004	0.013	2.930	1.313	1.959	0.800	0.031	-0.013
0.598	0.6446	795	-2.06	0.934	0.010	0.004	1.656	0.784	1.098	0.405	-0.008	-0.016
0.998	1.0763	1331	-2.34	1.000	0.017	-0.001	0.105	0.145	0.145	-0.032	-0.021	-0.024
1.498	1.6158	1992	-2.13	0.996	0.027	0.003	0.059	0.075	0.115	-0.026	-0.011	-0.016
1.998	2.1548	2658	-2.29	0.993	0.035	0.000	0.063	0.081	0.096	-0.027	-0.016	-0.010

r		y+	(/ Ue ³ x10 ⁶)								
(cm)	(/ δ)		u ³	v ³	w ³	u ² v	u ² w	uv ²	v ² w	uw ²	vw ²
0.006	0.0061	8	724.32	-14.47	11.11	-62.25	21.16	9.69	0.04	81.77	1.55
0.010	0.0105	13	189.22	-15.14	9.69	-27.92	-9.08	12.66	0.41	94.77	2.92
0.014	0.0148	18	-170.69	-14.37	2.94	34.34	-7.73	3.66	0.27	67.75	5.26
0.020	0.0212	26	-282.40	-8.27	8.07	85.09	-6.92	-10.18	1.52	44.11	5.34
0.026	0.0277	34	-275.95	-6.28	3.90	86.98	-13.06	-14.61	-2.04	18.59	10.35
0.033	0.0353	44	-236.73	4.11	-1.42	85.77	-8.36	-24.97	-3.55	16.97	9.79
0.043	0.0461	57	-134.24	11.61	-0.72	70.26	-5.31	-26.57	-4.96	3.48	9.05
0.058	0.0622	77	-57.57	9.66	-5.41	43.75	-3.06	-17.17	0.81	1.76	11.45
0.078	0.0838	103	-45.66	17.86	-14.31	38.55	-1.75	-20.69	-2.15	-6.36	12.02
0.123	0.1324	163	-23.61	13.98	-4.04	19.77	-1.97	-10.60	-2.94	1.14	9.27
0.198	0.2133	263	-36.72	11.99	3.98	19.14	-0.46	-12.66	0.55	-2.66	5.28
0.298	0.3212	396	-54.83	13.55	1.35	20.40	-1.35	-13.24	1.28	-9.25	5.43
0.398	0.4290	529	-52.14	12.79	0.74	18.49	0.11	-13.90	1.51	-6.77	12.03
0.598	0.6446	795	-39.12	10.43	2.06	12.58	0.16	-10.40	1.05	-4.27	10.90
0.998	1.0763	1331	-0.70	0.90	-0.37	0.15	-1.36	-0.41	1.17	-0.31	0.25
1.498	1.6158	1992	-0.01	-0.07	0.56	-0.05	-1.13	-0.09	1.21	-0.05	0.24
1.998	2.1548	2658	0.03	-0.06	-0.56	-0.07	-1.22	-0.12	1.19	-0.28	-0.05

Table 10. Boundary-layer profile at $x/L = 0.400$, $\phi = 170^\circ$.

$x/L = 0.400$ $\alpha = 10 \text{ deg.}$
 $Re = 4.2E+06$ $\phi = 180 \text{ deg.}$

Local-Freestream Coordinates

r		y+	(deg.)	(/ Ue)			(/ Ue ² x1000)					
(cm)	(/ δ)		Beta bs	U	V	W	uu	vv	ww	-uv	-uw	-vw
0.008	0.0116	11	0.72	0.351	-0.002	-0.001	14.360	0.325	2.058	1.096	0.076	0.027
0.012	0.0172	16	0.73	0.419	-0.003	-0.001	13.840	0.556	2.448	1.383	-0.042	0.039
0.016	0.0229	21	0.64	0.468	-0.002	-0.002	12.880	0.818	2.851	1.553	-0.019	0.051
0.022	0.0313	29	0.65	0.514	-0.001	-0.002	11.000	1.128	3.245	1.594	-0.005	0.078
0.028	0.0398	37	0.52	0.543	-0.002	-0.003	9.714	1.407	3.424	1.661	-0.044	0.061
0.035	0.0496	46	0.67	0.569	-0.002	-0.002	8.438	1.644	3.378	1.703	-0.008	0.024
0.045	0.0637	58	0.61	0.596	-0.002	-0.003	7.209	1.814	3.439	1.633	-0.047	0.070
0.060	0.0849	78	0.74	0.627	-0.001	-0.001	6.379	2.030	3.287	1.580	-0.039	0.085
0.080	0.1131	104	0.58	0.653	-0.001	-0.003	5.626	2.056	3.250	1.499	-0.052	0.072
0.125	0.1766	162	0.60	0.703	-0.002	-0.003	5.081	2.060	2.996	1.355	-0.032	0.069
0.200	0.2823	259	0.70	0.761	-0.001	-0.002	4.581	1.950	2.703	1.278	-0.069	0.067
0.300	0.4233	389	0.66	0.824	0.001	-0.003	3.771	1.669	2.390	1.044	-0.039	0.064
0.400	0.5644	518	0.91	0.875	0.004	0.001	3.099	1.389	1.980	0.853	-0.058	0.065
0.600	0.8464	777	0.93	0.959	0.010	0.001	1.653	0.778	1.064	0.396	-0.043	0.018
1.000	1.4100	1297	0.87	1.019	0.016	0.000	0.098	0.133	0.135	-0.027	-0.016	-0.014
1.500	2.1160	1943	0.91	1.013	0.026	0.001	0.066	0.085	0.127	-0.034	-0.014	-0.013
2.000	2.8210	2590	0.64	1.012	0.036	-0.004	0.072	0.090	0.124	-0.028	-0.025	-0.007

r		y+	(/Ue ³ x10 ⁶)								
(cm)	(/δ)		u ³	v ³	w ³	u ² v	u ² w	uv ²	v ² w	uw ²	vw ²
0.008	0.0116	11	525.50	-14.68	-0.95	-48.05	2.88	9.69	-0.23	92.33	1.98
0.012	0.0172	16	-29.38	-15.55	-4.61	8.04	-8.36	7.00	-0.64	73.79	3.37
0.016	0.0229	21	-171.70	-14.33	4.42	47.94	-12.02	0.16	-0.79	61.99	3.89
0.022	0.0313	29	-270.80	-8.07	0.81	78.27	0.38	-10.05	0.11	26.54	9.23
0.028	0.0398	37	-239.30	-3.19	-5.46	81.94	3.15	-16.17	0.44	20.67	9.10
0.035	0.0496	46	-217.60	2.04	-5.71	79.06	-6.28	-19.55	0.52	10.76	9.45
0.045	0.0637	58	-119.40	9.39	3.96	57.47	-6.81	-21.86	0.31	5.60	10.46
0.060	0.0849	78	-71.57	17.70	5.13	45.31	1.03	-24.30	-0.89	3.90	8.87
0.080	0.1131	104	-35.08	13.53	0.99	31.72	-6.44	-16.16	1.16	-6.59	11.68
0.125	0.1766	162	-13.64	15.08	-3.38	18.20	-2.99	-11.65	0.94	-2.16	7.63
0.200	0.2823	259	-47.44	10.73	-5.49	21.60	-4.49	-10.79	-2.38	-4.86	2.68
0.300	0.4233	389	-49.44	13.34	-3.86	12.71	-3.82	-10.49	0.42	-11.18	5.86
0.400	0.5644	518	-60.93	16.42	-2.48	18.55	0.15	-15.68	-0.86	-13.31	8.08
0.600	0.8464	777	-47.83	10.86	0.02	14.50	-1.25	-11.83	-2.06	-12.91	6.44
1.000	1.4100	1297	-0.66	0.53	-0.22	0.19	0.42	-0.23	-0.51	-0.21	0.13
1.500	2.1160	1943	-0.07	0.01	0.04	-0.03	0.49	-0.02	-0.45	0.03	0.18
2.000	2.8210	2590	-0.14	-0.09	-0.69	-0.05	0.24	-0.11	-0.38	-0.33	-0.15

Table 11. Boundary-layer profile at $x/L = 0.400$, $\phi = 180^\circ$.

$x/L = 0.600$ $\alpha = 10 \text{ deg.}$
 $Re = 4.2E+06$ $\phi = 90 \text{ deg.}$

Local-Freestream Coordinates

r		y+	(deg.)	(/ Ue)			(/ Ue ² x1000)					
(cm)	(/ δ)		Beta bs	U	V	W	uu	vv	ww	-uv	-uw	-vw
0.006	0.0086	8	-18.60	0.297	0.001	-0.008	10.500	0.264	1.810	0.736	0.532	-0.020
0.011	0.0163	15	-18.70	0.424	-0.002	-0.012	11.800	0.581	2.720	1.280	0.538	-0.077
0.018	0.0270	25	-18.60	0.492	-0.004	-0.012	12.800	1.050	3.270	1.860	0.397	-0.094
0.026	0.0393	36	-18.50	0.549	-0.005	-0.013	10.300	1.490	3.670	1.920	0.422	-0.115
0.036	0.0546	50	-18.60	0.586	-0.005	-0.015	8.450	1.780	3.690	1.880	0.434	-0.154
0.056	0.0853	78	-18.80	0.631	-0.007	-0.018	6.600	2.050	3.510	1.770	0.369	-0.108
0.096	0.1470	133	-19.00	0.684	-0.009	-0.022	5.640	2.120	3.220	1.560	0.280	-0.090
0.145	0.2230	203	-19.00	0.735	-0.007	-0.024	5.170	2.070	3.030	1.460	0.171	-0.075
0.246	0.3770	342	-18.80	0.812	-0.008	-0.024	4.180	1.840	2.610	1.180	0.133	0.014
0.496	0.7610	691	-18.10	0.949	-0.009	-0.017	1.690	0.884	1.010	0.463	-0.071	0.124
0.743	1.1400	1040	-17.10	0.998	-0.008	0.000	0.197	0.242	0.154	-0.002	0.004	0.034
0.998	1.5300	1390	-16.70	1.000	-0.004	0.007	0.090	0.141	0.082	-0.013	0.015	0.032
1.500	2.3000	2080	-16.10	1.000	-0.002	0.019	0.080	0.134	0.071	-0.001	0.009	0.026
1.995	3.0600	2780	-15.40	0.999	0.003	0.031	0.083	0.123	0.069	0.002	0.008	0.023
2.497	3.8300	3480	-14.90	0.999	0.005	0.040	0.095	0.143	0.074	-0.007	0.009	0.020

r		y+	(/ Ue ³ x10 ⁶)								
(cm)	(/ δ)		u ³	v ³	w ³	u ² v	u ² w	uv ²	v ² w	uw ²	vw ²
0.006	0.0086	8	623.00	10.60	-11.30	-50.00	-19.10	7.48	-6.70	63.40	5.05
0.011	0.0163	15	74.40	-10.80	-4.48	-8.91	-23.00	8.55	-1.43	68.90	4.89
0.018	0.0270	25	-243.00	-16.60	-13.20	65.30	5.55	0.07	-0.49	47.90	4.35
0.026	0.0393	36	-332.00	-4.05	-2.97	97.10	1.63	-19.20	0.94	18.30	8.64
0.036	0.0546	50	-192.00	5.46	-1.08	75.70	9.30	-21.30	0.71	4.54	11.50
0.056	0.0853	78	-62.50	13.30	1.18	39.90	9.04	-18.00	4.00	0.38	12.50
0.096	0.1470	133	-25.90	12.60	0.84	20.40	8.53	-10.20	2.44	-5.45	9.09
0.145	0.2230	203	-36.10	10.60	-1.70	20.00	7.16	-10.40	1.47	-6.80	11.70
0.246	0.3770	342	-62.90	15.80	-6.14	22.50	-1.89	-14.90	0.51	-17.00	9.50
0.496	0.7610	691	-60.00	15.60	-7.83	21.20	-2.68	-17.30	-3.06	-14.50	8.10
0.743	1.1400	1040	-1.97	1.30	-0.65	0.76	-0.27	-1.56	-0.19	-0.45	0.44
0.998	1.5300	1390	-0.15	-0.16	0.11	-0.02	0.09	-0.17	0.11	-0.06	-0.09
1.500	2.3000	2080	-0.07	0.21	0.17	0.04	0.04	0.19	0.02	-0.06	-0.12
1.995	3.0600	2780	-0.03	0.28	0.24	0.09	-0.00	0.29	-0.02	-0.06	-0.15
2.497	3.8300	3480	0.02	0.62	0.17	0.19	-0.06	0.53	-0.10	0.00	-0.18

Table 12. Boundary-layer profile at $x/L = 0.600$, $\phi = 90^\circ$.

$$x/L = 0.600 \quad \alpha = 10 \text{ deg.}$$

$$Re = 4.2E+06 \quad \phi = 100 \text{ deg.}$$

Local-Freestream Coordinates

r		y+	(deg.)	(/ Ue)			(/ Ue ² x1000)					
(cm)	(/δ)		Beta bs	U	V	W	uu	vv	ww	-uv	-uw	-vw
0.008	0.0098	10	-19.70	0.326	-0.002	-0.018	10.800	0.280	3.660	0.946	-1.370	0.195
0.013	0.0164	16	-18.00	0.419	-0.005	-0.011	12.100	0.640	3.590	1.460	-0.835	0.164
0.019	0.0255	26	-17.50	0.490	-0.006	-0.008	10.300	1.060	3.940	1.670	-0.938	0.264
0.028	0.0360	36	-17.30	0.536	-0.006	-0.007	8.670	1.500	4.040	1.700	-0.641	0.260
0.038	0.0491	49	-17.20	0.567	-0.006	-0.006	7.230	1.770	3.890	1.640	-0.320	0.210
0.058	0.0753	75	-17.40	0.610	-0.009	-0.009	5.850	2.000	3.700	1.510	-0.191	0.224
0.098	0.1280	128	-17.70	0.661	-0.009	-0.013	5.100	2.110	3.430	1.440	-0.100	0.159
0.147	0.1930	193	-18.10	0.707	-0.008	-0.019	4.960	2.150	3.020	1.450	0.218	-0.107
0.248	0.3240	325	-18.40	0.782	-0.006	-0.025	4.260	1.900	2.700	1.160	0.214	-0.055
0.497	0.6510	653	-18.10	0.917	-0.004	-0.025	2.170	1.140	1.360	0.551	0.028	0.045
0.747	0.9780	981	-17.10	0.987	-0.002	-0.010	0.438	0.481	0.284	-0.014	-0.001	0.017
1.001	1.3100	1310	-16.50	0.997	0.001	-0.000	0.129	0.250	0.099	-0.084	0.028	0.010
1.497	1.9600	1970	-15.90	0.999	0.011	0.011	0.072	0.170	0.085	-0.046	0.025	0.018
1.994	2.6100	2620	-15.40	0.999	0.016	0.021	0.063	0.126	0.086	-0.043	0.026	0.034
2.498	3.2700	3290	-14.90	0.999	0.021	0.029	0.077	0.139	0.091	-0.062	0.031	0.042

r		y+	(/ Ue ³ x10 ⁶)								
(cm)	(/δ)		u ³	v ³	w ³	u ² v	u ² w	uv ²	v ² w	uw ²	vw ²
0.008	0.0098	10	392.00	-1.80	-60.40	-38.10	108.00	7.71	1.64	45.80	-0.00
0.013	0.0164	16	-40.70	-11.00	-32.30	18.90	21.50	5.39	1.85	38.20	3.09
0.019	0.0255	26	-181.00	-8.40	-5.65	60.90	-36.40	-7.69	-0.89	6.72	5.59
0.028	0.0360	36	-240.00	-4.21	-5.87	76.00	-29.30	-13.20	-2.59	0.68	11.60
0.038	0.0491	49	-124.00	4.39	3.50	52.20	-8.64	-15.00	-2.68	-0.52	6.55
0.058	0.0753	75	-53.60	9.22	-1.26	29.30	-0.24	-11.30	-3.77	0.40	5.29
0.098	0.1280	128	-18.00	11.50	-3.63	17.80	-0.02	-8.29	-2.37	-0.45	4.08
0.147	0.1930	193	-26.90	13.60	2.29	15.40	3.22	-7.93	1.83	-4.67	6.53
0.248	0.3240	325	-42.80	13.10	-0.40	15.00	7.20	-12.40	1.32	-11.10	9.12
0.497	0.6510	653	-56.30	11.30	-1.63	20.10	-0.03	-16.90	-0.77	-13.70	8.75
0.747	0.9780	981	-12.90	2.08	-2.24	2.81	-1.45	-6.66	-0.03	-2.57	2.24
1.001	1.3100	1310	-1.14	-1.20	0.28	-1.29	0.22	-2.03	0.98	-0.16	0.16
1.497	1.9600	1970	-0.33	0.57	0.30	-0.20	0.15	-0.33	0.78	-0.18	-0.01
1.994	2.6100	2620	-0.06	0.74	0.29	0.13	0.10	0.25	0.29	-0.17	-0.15
2.498	3.2700	3290	0.16	1.16	0.31	0.44	-0.02	0.69	0.08	-0.06	0.01

Table 13. Boundary-layer profile at $x/L = 0.600$, $\phi = 100^\circ$.

$$x/L = 0.600 \quad \alpha = 10 \text{ deg.}$$

$$Re = 4.2E+06 \quad \phi = 110 \text{ deg.}$$

Local-Freestream Coordinates

r		y+	(deg.)	(/ Ue)			(/ Ue ² x1000)					
(cm)	(/ δ)		Beta bs	U	V	W	uu	vv	ww	-uv	-uw	-vw
0.010	0.0110	12	-15.00	0.345	-0.007	0.004	10.300	0.357	1.950	1.050	0.059	0.027
0.015	0.0168	18	-14.70	0.415	-0.006	0.007	11.600	0.720	2.710	1.550	0.092	-0.020
0.022	0.0249	27	-14.70	0.480	-0.008	0.008	10.100	1.170	3.080	1.700	0.204	-0.022
0.029	0.0341	37	-14.80	0.517	-0.007	0.007	8.510	1.490	3.400	1.690	0.252	-0.050
0.040	0.0457	50	-14.90	0.546	-0.009	0.007	7.030	1.750	3.460	1.640	0.296	-0.078
0.060	0.0688	75	-15.20	0.582	-0.009	0.005	5.990	1.970	3.260	1.580	0.322	-0.095
0.099	0.1150	126	-15.10	0.637	-0.015	0.007	4.720	2.030	2.920	1.240	0.103	-0.047
0.150	0.1730	189	-15.30	0.702	-0.026	0.004	3.440	1.890	2.790	0.797	-0.004	0.147
0.249	0.2880	315	-16.10	0.763	-0.015	-0.006	3.220	1.460	2.540	0.739	0.217	-0.054
0.499	0.5770	631	-16.70	0.895	-0.002	-0.016	2.030	0.947	1.500	0.399	0.091	0.034
0.749	0.8660	946	-16.30	0.972	0.005	-0.011	0.749	0.475	0.495	0.157	-0.013	0.038
1.003	1.1600	1260	-15.70	0.996	0.009	-0.000	0.089	0.172	0.074	-0.004	0.001	0.015
1.496	1.7300	1890	-15.00	0.999	0.017	0.012	0.047	0.123	0.047	0.002	0.004	0.014
1.998	2.3100	2530	-14.50	1.000	0.022	0.020	0.049	0.095	0.044	0.004	0.002	0.012
2.500	2.8900	3160	-14.00	0.999	0.029	0.028	0.066	0.090	0.041	-0.009	0.001	0.008

r		y+	(/ Ue ³ x10 ⁶)								
(cm)	(/ δ)		u ³	v ³	w ³	u ² v	u ² w	uv ²	v ² w	uw ²	vw ²
0.010	0.0110	12	93.70	-3.07	-9.56	-15.60	-10.20	8.55	-2.47	58.50	2.59
0.015	0.0168	18	-64.50	-10.50	-1.54	20.30	-3.48	6.73	0.16	61.10	4.09
0.022	0.0249	27	-220.00	-7.33	-6.76	72.80	-2.22	-10.30	-0.06	37.80	5.38
0.029	0.0341	37	-196.00	-0.84	-3.97	80.80	-9.83	-19.00	1.26	16.60	8.95
0.040	0.0457	50	-97.90	3.76	-5.25	51.70	-5.22	-15.10	-2.24	12.60	9.26
0.060	0.0688	75	-43.60	6.35	-5.64	32.80	-4.43	-12.90	-1.23	1.52	13.40
0.099	0.1150	126	55.20	-33.90	-3.88	-34.10	12.50	35.90	14.60	6.69	1.10
0.150	0.1730	189	35.30	-68.40	-12.40	-32.00	11.60	45.20	42.20	20.10	-18.00
0.249	0.2880	315	10.00	-8.64	-4.26	-16.20	-2.88	5.90	4.25	-5.55	1.46
0.499	0.5770	631	-21.10	5.74	-8.78	2.86	-4.17	-6.10	5.70	-10.80	5.10
0.749	0.8660	946	-17.30	5.63	-4.26	7.43	-6.64	-8.12	6.23	-9.86	2.77
1.003	1.1600	1260	5.44	0.39	-1.68	0.46	-5.74	-2.29	7.27	-3.72	-0.14
1.496	1.7300	1890	5.59	0.11	-1.47	0.19	-5.51	-1.88	7.11	-3.55	-0.32
1.998	2.3100	2530	5.48	0.17	-1.45	0.21	-5.44	-1.78	6.94	-3.47	-0.31
2.500	2.8900	3160	5.30	0.26	-1.40	0.24	-5.24	-1.72	6.69	-3.35	-0.29

Table 14. Boundary-layer profile at $x/L = 0.600$, $\phi = 110^\circ$.

$$x/L = 0.600 \quad \alpha = 10 \text{ deg.}$$

$$Re = 4.2E+06 \quad \phi = 120 \text{ deg.}$$

Local-Freestream Coordinates

r		y+	(deg.)	(/ Ue)			(/ Ue ² x1000)					
(cm)	(/ δ)		Beta bs	U	V	W	uu	vv	ww	-uv	-uw	-vw
0.006	0.0061	8	-10.50	0.290	-0.003	0.018	10.300	0.244	1.720	0.849	-0.306	0.022
0.011	0.0109	14	-10.50	0.320	-0.005	0.020	9.160	0.337	1.790	0.888	-0.277	0.030
0.018	0.0176	22	-10.50	0.420	-0.003	0.026	9.520	0.761	2.620	1.340	-0.085	-0.008
0.026	0.0253	31	-10.70	0.470	-0.003	0.028	7.820	1.140	2.930	1.370	0.042	-0.031
0.036	0.0349	43	-11.00	0.511	-0.009	0.027	5.450	1.250	2.930	0.911	0.132	-0.030
0.056	0.0541	67	-11.30	0.543	-0.007	0.025	4.910	1.570	2.890	1.110	0.200	-0.096
0.096	0.0924	114	-11.90	0.586	-0.003	0.022	4.680	1.810	2.810	1.270	0.216	-0.144
0.146	0.1400	173	-12.40	0.630	-0.002	0.018	4.610	1.850	2.790	1.270	0.287	-0.157
0.246	0.2360	292	-13.40	0.702	-0.002	0.007	4.030	1.710	2.720	1.110	0.365	-0.194
0.496	0.4760	587	-14.90	0.837	0.009	-0.013	2.650	1.310	2.010	0.837	0.204	-0.029
0.746	0.7150	883	-15.20	0.932	0.010	-0.019	1.460	0.774	0.964	0.350	0.088	0.004
0.996	0.9550	1180	-14.70	0.984	0.016	-0.011	0.338	0.343	0.221	0.064	-0.005	0.026
1.491	1.4300	1770	-14.00	0.995	0.027	0.000	0.067	0.163	0.055	0.001	0.002	0.018
1.992	1.9100	2360	-13.60	0.997	0.035	0.008	0.059	0.134	0.046	-0.008	0.001	0.022
2.493	2.3900	2960	-13.10	0.999	0.043	0.017	0.065	0.140	0.046	-0.021	0.002	0.023

r		y+	(/ Ue ³ x10 ⁶)								
(cm)	(/ δ)		u ³	v ³	w ³	u ² v	u ² w	uv ²	v ² w	uw ²	vw ²
0.006	0.0061	8	350.00	-0.87	8.73	-41.00	1.87	10.70	-0.93	63.40	3.38
0.011	0.0109	14	225.00	-9.80	3.30	-25.70	4.67	9.66	-1.24	50.90	1.12
0.018	0.0176	22	-55.90	-5.96	3.59	29.60	-9.59	-0.45	0.42	41.10	5.48
0.026	0.0253	31	-84.20	-5.16	2.50	33.60	-13.00	-2.92	1.22	22.20	5.30
0.036	0.0349	43	50.60	-6.55	-18.20	-9.55	3.61	9.09	2.17	19.10	6.59
0.056	0.0541	67	53.30	-0.36	-12.90	-9.91	-2.03	6.66	0.26	8.13	7.01
0.096	0.0924	114	32.70	2.98	-11.30	-3.54	-0.78	3.80	-0.84	6.23	4.05
0.146	0.1400	173	20.00	8.45	-2.42	6.59	-8.59	-5.34	1.77	5.91	0.49
0.246	0.2360	292	1.75	1.12	-0.38	-1.53	5.31	0.42	4.60	-3.28	5.59
0.496	0.4760	587	-15.00	9.07	1.77	10.80	1.59	-5.26	5.58	-10.70	6.81
0.746	0.7150	883	-24.20	5.86	-1.07	7.19	-1.69	-8.43	7.04	-13.10	4.07
0.996	0.9550	1180	-3.66	2.32	-2.23	2.70	-5.82	-4.14	6.74	-5.08	0.90
1.491	1.4300	1770	4.73	-0.01	-1.08	0.10	-5.43	-1.46	7.04	-3.04	-0.23
1.992	1.9100	2360	4.65	0.06	-1.05	0.18	-5.33	-1.27	6.75	-2.99	-0.29
2.493	2.3900	2960	4.50	0.08	-1.01	0.23	-5.22	-1.12	6.51	-2.90	-0.28

Table 15. Boundary-layer profile at $x/L = 0.600$, $\phi = 120^\circ$.

$x/L = 0.600$ $\alpha = 10 \text{ deg.}$
 $Re = 4.2E+06$ $\phi = 130 \text{ deg.}$

Local-Freestream Coordinates

r		y+	(deg.)	(/ Ue)			(/ Ue ² x1000)					
(cm)	(/δ)		Beta bs	U	V	W	uu	vv	ww	-uv	-uw	-vw
0.007	0.0055	7	-5.28	0.241	-0.001	0.031	8.170	0.153	1.430	0.608	-0.752	0.054
0.012	0.0095	13	-5.51	0.319	-0.002	0.040	9.340	0.342	1.940	0.950	-0.710	0.074
0.019	0.0152	21	-5.61	0.388	-0.003	0.048	8.630	0.655	2.390	1.140	-0.452	0.079
0.027	0.0217	30	-5.76	0.432	-0.004	0.053	7.140	0.955	2.630	1.160	-0.211	0.021
0.037	0.0299	41	-5.92	0.465	-0.006	0.055	5.610	1.180	2.710	1.030	0.019	-0.003
0.057	0.0462	63	-6.19	0.499	-0.004	0.057	4.990	1.470	2.740	1.160	0.080	-0.012
0.097	0.0787	108	-6.98	0.542	-0.002	0.054	4.480	1.660	2.670	1.170	0.238	-0.085
0.146	0.1190	163	-7.67	0.582	-0.002	0.051	4.230	1.670	2.540	1.150	0.251	-0.142
0.247	0.2010	274	-9.12	0.643	0.001	0.040	4.050	1.670	2.600	1.100	0.329	-0.184
0.496	0.4040	552	-11.60	0.770	0.010	0.014	3.420	1.510	2.300	0.934	0.331	-0.147
0.747	0.6080	830	-13.00	0.872	0.019	-0.005	2.400	1.100	1.650	0.660	0.227	-0.059
0.997	0.8120	1110	-13.40	0.950	0.025	-0.012	1.150	0.606	0.718	0.264	0.058	0.040
1.498	1.2200	1660	-12.70	0.997	0.034	-0.000	0.057	0.135	0.069	-0.017	0.005	0.026
2.002	1.6300	2220	-12.20	0.998	0.042	0.008	0.044	0.097	0.057	-0.013	0.005	0.025
2.493	2.0300	2780	-11.70	0.999	0.049	0.017	0.051	0.096	0.057	-0.020	0.006	0.018

r		y+	(/Ue ³ x10 ⁶)								
(cm)	(/δ)		u ³	v ³	w ³	u ² v	u ² w	uv ²	v ² w	uw ²	vw ²
0.007	0.0055	7	420.00	-0.66	21.30	-40.60	30.10	7.44	0.55	55.70	1.06
0.012	0.0095	13	119.00	-6.83	18.00	-13.20	-12.00	6.52	0.15	52.60	2.07
0.019	0.0152	21	-60.30	-6.48	7.87	22.00	-26.20	1.05	-0.05	31.90	5.36
0.027	0.0217	30	-48.70	-6.16	1.19	24.60	-14.50	0.54	-0.59	24.60	5.42
0.037	0.0299	41	10.20	-3.22	-3.94	9.87	-9.01	1.19	-2.52	14.80	6.13
0.057	0.0462	63	4.75	3.32	-8.41	8.40	-8.70	-0.45	-3.46	9.97	6.40
0.097	0.0787	108	17.60	5.58	-5.19	9.74	-3.29	-4.74	-1.87	5.13	5.03
0.146	0.1190	163	29.40	2.13	-8.63	-1.00	-5.84	2.31	-1.25	8.24	0.87
0.247	0.2010	274	2.20	4.39	-3.06	2.13	-4.35	-1.96	-0.63	4.34	1.26
0.496	0.4040	552	-25.50	7.09	0.90	7.12	0.72	-8.39	3.74	-7.18	4.11
0.747	0.6080	830	-35.80	8.81	2.02	13.50	0.80	-10.40	5.27	-13.70	6.59
0.997	0.8120	1110	-27.70	6.39	-0.51	9.81	-2.89	-9.45	5.46	-10.70	3.26
1.498	1.2200	1660	3.98	0.18	-0.78	0.24	-5.27	-1.34	6.39	-2.62	-0.22
2.002	1.6300	2220	3.88	0.16	-0.73	0.22	-5.11	-1.15	6.06	-2.54	-0.27
2.493	2.0300	2780	3.76	0.22	-0.68	0.25	-4.96	-1.06	5.80	-2.44	-0.26

Table 16. Boundary-layer profile at $x/L = 0.600$, $\phi = 130^\circ$.

$x/L = 0.600$ $\alpha = 10 \text{ deg.}$
 $Re = 4.2E+06$ $\phi = 140 \text{ deg.}$

Local-Freestream Coordinates

r		y+	(deg.)	(/ Ue)			(/ Ue ² x1000)					
(cm)	(/ δ)		Beta _{bs}	U	V	W	uu	vv	ww	-uv	-uw	-vw
0.008	0.0053	8	-0.98	0.234	-0.002	0.043	7.010	0.147	1.380	0.564	-0.893	0.074
0.013	0.0086	13	-1.12	0.306	-0.002	0.055	8.290	0.322	1.900	0.846	-0.982	0.099
0.020	0.0133	21	-1.32	0.366	-0.003	0.065	7.590	0.600	2.250	1.020	-0.713	0.113
0.028	0.0187	29	-1.39	0.404	-0.005	0.071	6.480	0.900	2.370	1.100	-0.489	0.109
0.038	0.0254	39	-1.59	0.432	-0.005	0.074	5.590	1.090	2.560	1.080	-0.264	0.077
0.058	0.0389	60	-1.96	0.465	-0.004	0.077	4.720	1.300	2.500	1.090	-0.047	0.038
0.098	0.0658	102	-2.44	0.506	-0.004	0.079	3.900	1.410	2.340	1.000	0.106	-0.035
0.148	0.0994	154	-3.09	0.542	-0.003	0.079	3.780	1.480	2.290	1.030	0.168	-0.092
0.248	0.1670	259	-4.41	0.598	-0.000	0.073	3.680	1.550	2.350	1.020	0.231	-0.148
0.498	0.3350	519	-7.60	0.710	0.007	0.046	3.410	1.490	2.290	0.892	0.286	-0.189
0.747	0.5030	780	-9.91	0.804	0.014	0.020	2.850	1.210	1.980	0.781	0.340	-0.135
0.997	0.6710	1040	-11.20	0.888	0.026	0.002	2.110	0.960	1.380	0.549	0.203	-0.041
1.501	1.0100	1560	-11.30	0.991	0.040	-0.000	0.208	0.231	0.164	0.031	-0.000	0.035
1.991	1.3400	2080	-10.80	0.999	0.047	0.010	0.044	0.102	0.063	-0.012	0.004	0.032
2.496	1.6800	2610	-10.20	0.998	0.055	0.020	0.050	0.105	0.059	-0.020	0.005	0.027

r		y+	(U ₀ ³ x10 ⁻⁶)								
(cm)	(/ δ)		u ³	v ³	w ³	u ² v	u ² w	uv ²	v ² w	uw ²	vw ²
0.008	0.0053	8	266.00	-1.69	26.60	-28.20	31.00	5.91	1.33	47.40	-0.51
0.013	0.0086	13	86.70	-4.47	25.80	-7.90	-12.00	4.62	0.41	42.30	2.61
0.020	0.0133	21	-47.10	-4.85	14.80	19.60	-25.20	1.53	-0.51	30.10	5.43
0.028	0.0187	29	-70.00	-3.89	4.92	31.60	-17.60	-2.79	-0.20	15.80	4.97
0.038	0.0254	39	-46.40	-3.40	4.04	25.00	-19.10	-3.22	-1.83	15.20	4.15
0.058	0.0389	60	-20.90	3.28	-12.70	22.90	-5.02	-5.79	-3.31	7.78	6.66
0.098	0.0658	102	19.30	4.90	-4.63	6.07	-7.27	-3.12	-2.89	9.11	3.22
0.148	0.0994	154	28.40	3.27	-0.90	-1.26	-6.44	0.99	-1.50	5.51	1.91
0.248	0.1670	259	10.40	2.91	-5.17	1.37	-1.39	0.63	-0.86	5.52	1.21
0.498	0.3350	519	-4.27	4.06	0.42	-0.09	-2.12	-1.95	0.01	-1.27	2.69
0.747	0.5030	780	-30.20	6.43	2.96	7.80	-0.40	-9.51	4.08	-7.61	3.72
0.997	0.6710	1040	-36.50	8.24	3.33	14.20	-0.79	-11.30	5.11	-11.00	4.66
1.501	1.0100	1560	-2.02	1.53	-1.01	1.87	-5.23	-2.58	5.61	-3.35	0.51
1.991	1.3400	2080	3.14	0.14	-0.49	0.19	-4.76	-0.89	5.44	-2.06	-0.23
2.496	1.6800	2610	3.01	0.28	-0.46	0.24	-4.56	-0.72	5.13	-1.94	-0.23

Table 17. Boundary-layer profile at $x/L = 0.600$, $\phi = 140^\circ$.

$x/L = 0.600$ $\alpha = 10 \text{ deg.}$
 $Re = 4.2E+06$ $\phi = 150 \text{ deg.}$

Local-Freestream Coordinates

r		y+	(deg.)	(/ Ue)			(/ Ue ² x1000)					
(cm)	(/ δ)		Beta bs	U	V	W	uu	vv	ww	-uv	-uw	-vw
0.008	0.0047	8	1.93	0.229	-0.002	0.045	6.780	0.149	1.450	0.567	-1.020	0.087
0.013	0.0077	13	1.85	0.304	-0.003	0.059	7.940	0.318	1.870	0.828	-1.130	0.130
0.020	0.0118	21	1.82	0.363	-0.004	0.070	7.550	0.584	2.250	1.030	-0.953	0.130
0.028	0.0166	29	1.71	0.404	-0.005	0.077	6.470	0.834	2.420	1.060	-0.618	0.123
0.038	0.0225	39	1.78	0.431	-0.004	0.083	5.520	1.030	2.440	1.040	-0.382	0.105
0.058	0.0344	60	1.52	0.466	-0.005	0.087	4.460	1.290	2.410	1.050	-0.182	0.046
0.098	0.0582	101	1.12	0.505	-0.004	0.091	3.830	1.380	2.270	1.010	-0.077	-0.004
0.148	0.0880	153	0.49	0.540	-0.003	0.091	3.570	1.390	2.100	0.954	-0.014	-0.037
0.247	0.1470	257	-0.71	0.593	-0.002	0.087	3.360	1.450	2.110	0.946	0.115	-0.148
0.498	0.2960	516	-3.64	0.692	0.004	0.066	3.030	1.370	2.080	0.822	0.217	-0.219
0.748	0.4450	775	-6.12	0.778	0.013	0.040	2.600	1.220	1.930	0.811	0.281	-0.194
0.999	0.5940	1030	-8.11	0.849	0.022	0.015	2.280	1.060	1.610	0.601	0.268	-0.122
1.498	0.8910	1550	-9.59	0.968	0.037	-0.008	0.766	0.440	0.460	0.150	0.036	0.014
2.000	1.1900	2070	-9.09	0.997	0.046	-0.000	0.055	0.113	0.084	-0.017	0.008	0.038
2.505	1.4900	2590	-8.50	0.998	0.056	0.010	0.055	0.108	0.072	-0.021	0.008	0.034

r		y+	(/ Ue ³ x10 ⁶)									
(cm)	(/ δ)		u ³	v ³	w ³	u ² v	u ² w	uv ²	v ² w	uw ²	vw ²	
0.008	0.0047	8	282.00	-1.71	28.50	-31.20	35.30	6.11	1.45	43.00	0.09	
0.013	0.0077	13	83.40	-5.09	25.90	-10.60	-1.06	5.15	0.85	37.00	2.43	
0.020	0.0118	21	-63.60	-5.22	23.10	22.90	-25.20	-0.10	0.27	22.00	3.90	
0.028	0.0166	29	-56.10	-4.38	13.70	24.70	-22.60	-2.41	-0.14	13.50	3.84	
0.038	0.0225	39	-49.80	-0.93	7.61	23.30	-9.86	-3.43	-0.89	2.85	6.35	
0.058	0.0344	60	-24.80	4.93	2.59	25.40	-8.39	-8.86	-1.33	-2.15	7.88	
0.098	0.0582	101	10.50	2.81	5.67	4.09	-2.31	-0.40	-0.17	2.12	7.93	
0.148	0.0880	153	22.10	3.18	3.61	-2.32	-1.26	1.51	-1.00	3.20	2.85	
0.247	0.1470	257	6.77	2.96	-2.58	1.49	-4.18	-0.45	-0.65	3.75	0.37	
0.498	0.2960	516	5.91	2.98	-2.77	-1.33	-0.23	0.34	0.95	0.13	1.26	
0.748	0.4450	775	-8.65	5.71	0.24	10.90	2.92	-2.92	2.57	-4.83	4.42	
0.999	0.5940	1030	-21.40	7.29	5.25	9.43	-0.12	-7.04	4.32	-7.99	4.51	
1.498	0.8910	1550	-22.20	4.16	-0.17	6.53	-3.21	-5.85	4.90	-7.23	2.11	
2.000	1.1900	2070	2.14	0.04	-0.28	0.13	-4.24	-0.51	4.75	-1.45	-0.18	
2.505	1.4900	2590	2.04	0.06	-0.24	0.15	-4.03	-0.39	4.37	-1.34	-0.14	

Table 18. Boundary-layer profile at $x/L = 0.600$, $\phi = 150^\circ$.

$x/L = 0.600$ $\alpha = 10 \text{ deg.}$
 $Re = 4.2E+06$ $\phi = 160 \text{ deg.}$
Local-Freestream Coordinates

r		y+	(deg.)	(/ Ue)			(/ Ue ² x1000)					
(cm)	(/δ)		Beta bs	U	V	W	uu	vv	ww	-uv	-uw	-vw
0.008	0.0047	9	3.01	0.226	-0.002	0.038	6.330	0.127	1.350	0.506	-0.801	0.077
0.013	0.0075	14	2.96	0.323	-0.003	0.054	8.310	0.358	2.010	0.910	-1.040	0.123
0.020	0.0114	22	2.82	0.386	-0.004	0.064	8.050	0.668	2.470	1.120	-0.798	0.152
0.028	0.0159	30	2.87	0.428	-0.006	0.071	6.970	0.931	2.660	1.140	-0.516	0.132
0.038	0.0215	41	2.75	0.455	-0.005	0.074	6.090	1.140	2.620	1.160	-0.327	0.109
0.058	0.0327	62	2.65	0.489	-0.006	0.079	4.680	1.320	2.550	1.060	-0.113	0.041
0.098	0.0551	105	2.29	0.533	-0.007	0.083	4.110	1.430	2.390	1.010	-0.057	0.018
0.148	0.0831	158	2.02	0.564	-0.005	0.085	3.980	1.540	2.280	1.040	0.017	-0.035
0.248	0.1390	265	1.18	0.622	-0.007	0.084	3.510	1.490	2.170	0.955	0.033	-0.086
0.498	0.2790	533	-0.99	0.719	-0.003	0.070	2.900	1.310	1.890	0.788	0.112	-0.193
0.748	0.4190	800	-3.15	0.797	0.004	0.047	2.340	1.110	1.670	0.664	0.156	-0.182
0.998	0.5590	1070	-4.92	0.859	0.009	0.024	1.930	0.907	1.390	0.476	0.156	-0.132
1.498	0.8390	1600	-6.79	0.960	0.023	-0.005	0.812	0.406	0.511	0.152	0.041	0.023
1.999	1.1200	2140	-6.51	0.998	0.037	0.000	0.063	0.117	0.099	-0.008	0.005	0.040
2.499	1.4000	2670	-6.03	0.999	0.049	0.008	0.063	0.093	0.075	-0.015	0.004	0.026

r		y+	(/Ue ³ x10 ⁶)								
(cm)	(/δ)		u ³	v ³	w ³	u ² v	u ² w	uv ²	v ² w	uw ²	vw ²
0.008	0.0047	9	267.00	-1.22	22.30	-25.70	32.30	3.82	1.04	38.90	0.13
0.013	0.0075	14	86.40	-5.48	24.80	-7.83	-5.32	4.68	0.68	38.40	2.32
0.020	0.0114	22	-103.00	-4.67	26.00	27.50	-19.90	-1.83	-0.21	25.60	4.96
0.028	0.0159	30	-84.50	-4.56	21.30	31.30	-15.30	-4.43	-0.70	11.50	4.47
0.038	0.0215	41	-76.00	-0.62	12.80	36.10	-15.20	-9.98	-1.82	2.21	7.20
0.058	0.0327	62	-42.50	7.16	11.80	27.30	-3.81	-11.90	-0.52	-1.73	7.40
0.098	0.0551	105	19.30	4.00	3.86	0.36	-1.54	-0.30	-1.37	-2.28	6.97
0.148	0.0831	158	-2.39	5.14	4.46	9.70	0.77	-4.30	-0.41	3.06	4.90
0.248	0.1390	265	1.11	3.15	7.06	-0.01	0.27	-1.17	-0.26	-1.26	3.02
0.498	0.2790	533	-20.20	6.72	4.33	8.75	0.28	-8.16	0.76	-8.28	4.79
0.748	0.4190	800	-15.60	4.59	-1.55	7.67	0.30	-4.60	1.12	-4.47	3.50
0.998	0.5590	1070	-23.10	5.32	0.63	7.85	-0.87	-6.69	3.14	-5.48	3.84
1.498	0.8390	1600	-19.10	3.20	-0.27	5.91	-2.31	-5.03	3.56	-6.05	1.70
1.999	1.1200	2140	0.94	0.15	-0.14	0.19	-3.31	-0.25	3.40	-0.84	-0.07
2.499	1.4000	2670	1.08	0.14	0.06	0.12	-3.06	-0.05	3.10	-0.73	-0.10

Table 19. Boundary-layer profile at $x/L = 0.600$, $\phi = 160^\circ$.

$x/L = 0.600$ $\alpha = 10 \text{ deg.}$
 $Re = 4.2E+06$ $\phi = 170 \text{ deg.}$

Local-Freestream Coordinates

r		y+	(deg.)	(/ Ue)			(/ Ue ² x1000)					
(cm)	(/ δ)		Beta bs	U	V	W	uu	vv	ww	-uv	-uw	-vw
0.007	0.0040	8	2.06	0.215	-0.033	0.022	7.310	0.218	1.430	0.824	-0.511	0.085
0.012	0.0067	14	1.97	0.340	-0.004	0.035	10.200	0.409	2.130	1.260	-0.589	0.096
0.019	0.0105	22	1.80	0.415	-0.007	0.041	9.770	0.782	2.690	1.450	-0.452	0.078
0.027	0.0148	31	1.66	0.457	-0.008	0.044	8.690	1.130	2.920	1.540	-0.400	0.087
0.037	0.0202	42	1.67	0.490	-0.008	0.047	7.220	1.360	3.050	1.410	-0.240	0.080
0.057	0.0311	65	1.61	0.528	-0.010	0.051	5.820	1.640	3.010	1.380	-0.105	0.029
0.097	0.0528	109	1.51	0.576	-0.010	0.054	4.880	1.740	2.760	1.210	0.018	-0.046
0.147	0.0799	166	1.37	0.614	-0.011	0.056	4.530	1.760	2.540	1.210	-0.003	-0.036
0.247	0.1340	278	0.98	0.669	-0.010	0.057	3.890	1.720	2.310	1.090	0.073	-0.133
0.498	0.2700	561	-0.30	0.767	-0.010	0.048	2.810	1.450	1.850	0.751	0.036	-0.169
0.746	0.4050	864	-1.57	0.846	-0.009	0.034	2.050	1.120	1.420	0.435	0.037	-0.151
0.997	0.5410	1120	-2.58	0.888	-0.003	0.020	1.410	0.844	1.040	0.280	0.076	-0.108
1.497	0.8120	1690	-3.81	0.964	0.016	0.001	0.576	0.365	0.451	0.076	0.048	-0.005
1.990	1.0800	2250	-3.85	0.994	0.031	0.000	0.083	0.130	0.142	-0.029	0.017	0.029
2.488	1.3500	2810	-3.52	0.999	0.047	0.006	0.073	0.117	0.149	-0.046	0.027	0.047

r		y+	(/ Ue ³ x10 ⁶)								
(cm)	(/ δ)		u ³	v ³	w ³	u ² v	u ² w	uv ²	v ² w	uw ²	vw ²
0.007	0.0040	8	359.00	-20.50	13.90	-29.20	20.50	10.20	2.09	41.20	-1.41
0.012	0.0067	14	109.00	-9.23	21.80	-12.90	-10.30	9.24	0.78	50.30	-0.16
0.019	0.0105	22	-154.00	-7.96	19.50	48.10	-18.00	-2.99	0.73	45.40	1.31
0.027	0.0148	31	-160.00	-4.44	9.35	57.10	-14.40	-10.90	-1.65	17.20	4.51
0.037	0.0202	42	-128.00	3.50	15.00	55.90	-13.20	-15.50	-1.99	7.57	8.38
0.057	0.0311	65	-73.30	11.80	9.37	41.50	-1.56	-18.20	-0.27	3.91	7.54
0.097	0.0528	109	-20.70	8.81	3.29	16.30	0.80	-8.71	-1.02	2.22	7.81
0.147	0.0799	166	-20.10	7.74	2.60	16.30	-1.71	-8.25	-0.26	1.72	6.25
0.247	0.1340	278	-20.00	9.95	4.03	13.60	2.73	-7.31	1.72	-7.59	4.68
0.498	0.2700	561	-31.00	9.72	0.58	12.30	0.19	-9.05	2.87	-8.82	7.11
0.746	0.4050	864	-28.00	4.58	0.23	8.09	-0.21	-9.19	2.02	-6.72	4.51
0.997	0.5410	1120	-18.40	2.78	-0.42	3.94	0.33	-6.17	1.60	-3.60	2.93
1.497	0.8120	1690	-11.20	2.26	0.61	3.11	0.33	-2.57	0.77	-3.07	0.94
1.990	1.0800	2250	-0.58	0.46	0.12	0.21	0.02	0.23	0.03	-0.22	-0.01
2.488	1.3500	2810	0.03	0.41	0.05	0.23	-0.11	0.46	-0.20	0.03	0.11

Table 20. Boundary-layer profile at $x/L = 0.600$, $\phi = 170^\circ$.

$x/L = 0.600$ $\alpha = 10 \text{ deg.}$
 $Re = 4.2E+06$ $\phi = 180 \text{ deg.}$

Local-Freestream Coordinates

r		y+	(deg.)	(/ Ue)			(/ Ue ² x1000)					
(cm)	(/δ)		Beta_bs	U	V	W	uu	vv	ww	-uv	-uw	-vw
0.011	0.0066	13	-0.75	0.339	-0.004	-0.002	11.000	0.382	2.130	1.120	0.156	-0.026
0.016	0.0095	19	-0.74	0.398	-0.004	-0.003	11.200	0.627	2.600	1.380	0.123	-0.022
0.023	0.0137	27	-0.64	0.451	-0.006	-0.002	9.990	1.000	3.060	1.510	0.196	-0.080
0.031	0.0185	36	-0.55	0.488	-0.007	-0.002	8.590	1.260	3.300	1.500	0.223	-0.095
0.041	0.0245	46	-0.55	0.508	-0.007	-0.002	7.050	1.470	3.160	1.420	0.136	-0.096
0.061	0.0364	70	-0.40	0.554	-0.008	-0.001	5.940	1.770	3.130	1.400	0.193	-0.115
0.101	0.0602	117	-0.50	0.600	-0.009	-0.002	5.190	1.900	2.920	1.340	0.114	-0.096
0.151	0.0901	174	-0.46	0.635	-0.010	-0.001	4.720	1.850	2.700	1.210	0.138	-0.091
0.252	0.1500	290	-0.36	0.694	-0.012	-0.000	4.240	1.810	2.480	1.160	0.131	-0.121
0.501	0.2990	578	-0.41	0.796	-0.012	-0.001	2.990	1.440	1.830	0.752	0.103	-0.089
0.751	0.4480	867	-0.42	0.870	-0.011	-0.001	1.840	1.040	1.250	0.419	0.054	-0.067
1.001	0.5970	1160	-0.34	0.919	-0.005	-0.000	1.120	0.717	0.815	0.213	0.034	-0.039
1.501	0.8950	1730	-0.28	0.979	0.013	0.001	0.302	0.313	0.283	0.010	0.013	-0.007
1.996	1.1900	2310	-0.33	0.995	0.028	-0.000	0.064	0.144	0.145	-0.027	0.004	0.035
2.499	1.4900	2890	-0.13	0.999	0.044	0.004	0.059	0.120	0.131	-0.022	0.005	0.045

r		y+	(/Ue ³ x10 ⁶)								
(cm)	(/δ)		u ³	v ³	w ³	u ² v	u ² w	uv ²	v ² w	uw ²	vw ²
0.011	0.0066	13	184.00	-4.38	-0.01	-24.40	-5.91	9.78	-0.22	70.60	0.88
0.016	0.0095	19	-60.10	-8.52	-5.19	19.60	-10.50	5.03	-1.33	65.00	1.39
0.023	0.0137	27	-160.00	-6.13	6.61	53.10	3.63	-6.41	0.67	37.90	5.38
0.031	0.0185	36	-186.00	-2.75	2.02	65.40	4.12	-11.30	0.62	29.10	6.57
0.041	0.0245	46	-134.00	3.60	11.60	61.60	1.02	-17.90	-0.43	2.31	7.90
0.061	0.0364	70	-54.40	9.66	3.65	38.30	4.79	-14.10	1.56	6.91	7.83
0.101	0.0602	117	-24.50	9.04	6.65	21.70	2.64	-11.30	-0.72	-2.61	10.80
0.151	0.0901	174	-18.70	8.12	5.42	15.50	-1.10	-6.36	3.08	-2.16	4.81
0.252	0.1500	290	-33.20	9.34	3.05	17.80	-1.20	-10.10	0.92	-4.77	4.85
0.501	0.2990	578	-50.20	13.00	2.28	17.20	0.62	-13.80	1.31	-10.60	6.61
0.751	0.4480	867	-34.10	6.52	2.47	9.71	1.85	-9.93	1.88	-7.96	5.11
1.001	0.5970	1160	-19.10	3.39	1.34	4.86	-0.05	-6.46	1.47	-4.55	2.35
1.501	0.8950	1730	-5.97	1.03	0.05	1.27	0.30	-1.36	1.05	-1.47	0.61
1.996	1.1900	2310	-0.23	0.29	-0.10	0.09	-0.02	0.23	0.11	-0.14	-0.13
2.499	1.4900	2890	0.02	0.04	0.08	0.08	-0.09	0.48	-0.05	0.04	-0.08

Table 21. Boundary-layer profile at $x/L = 0.600$, $\phi = 180^\circ$.

$x/L = 0.752$ $\alpha = 10 \text{ deg.}$
 $Re = 4.2E+06$ $\phi = 120 \text{ deg.}$

Local-Freestream Coordinates

r		y+	(deg.)	(/ Ue)			(/ Ue ² x1000)					
(cm)	(/ δ)		Beta bs	U	V	W	uu	vv	ww	-uv	-uw	-vw
0.011	0.0081	12	-2.09	0.282	0.008	0.058	7.484	0.220	1.872	0.406	-1.268	0.017
0.016	0.0117	17	-2.12	0.342	0.010	0.071	7.624	0.443	2.231	0.644	-1.234	0.055
0.021	0.0153	22	-2.23	0.371	0.011	0.076	7.229	0.612	2.358	0.733	-1.014	0.047
0.031	0.0224	32	-2.36	0.412	0.013	0.083	6.230	0.957	2.538	0.874	-0.729	0.051
0.041	0.0296	42	-3.08	0.440	0.013	0.083	4.975	1.172	2.768	0.856	-0.338	0.051
0.076	0.0547	78	-3.61	0.485	0.015	0.087	4.211	1.484	2.807	0.898	-0.116	-0.019
0.151	0.1084	154	-5.24	0.545	0.019	0.082	3.922	1.602	2.787	0.943	0.090	-0.133
0.251	0.1800	256	-7.21	0.603	0.024	0.069	4.043	1.681	2.903	0.988	0.159	-0.166
0.501	0.3591	511	-11.18	0.728	0.038	0.033	3.458	1.497	2.764	0.787	0.279	-0.151
0.751	0.5381	766	-13.23	0.832	0.048	0.008	2.792	1.261	2.226	0.655	0.177	0.005
1.001	0.7172	1020	-14.27	0.913	0.064	-0.008	1.778	0.836	1.405	0.473	0.018	0.091
1.501	1.0750	1531	-15.77	0.996	0.071	0.000	0.210	0.247	0.295	0.113	-0.061	0.137
2.001	1.4330	2041	-13.14	0.997	0.075	0.011	0.140	0.183	0.235	0.104	-0.059	0.133
2.502	1.7920	2551	-12.96	0.997	0.072	0.014	0.158	0.165	0.197	0.097	-0.060	0.115

r		y+	(/ Ue ³ x10 ⁶)								
(cm)	(/ δ)		u ³	v ³	w ³	u ² v	u ² w	uv ²	v ² w	uw ²	vw ²
0.011	0.0081	12	165.10	-2.91	30.90	-6.39	19.36	3.49	1.41	42.14	4.26
0.016	0.0117	17	21.15	-4.76	28.23	12.36	-3.88	3.37	1.60	35.02	5.30
0.021	0.0153	22	-24.01	-4.11	30.98	16.43	-10.98	1.22	2.00	23.03	7.03
0.031	0.0224	32	-66.45	-3.36	24.25	30.48	-17.52	-1.29	-0.05	7.96	9.44
0.041	0.0296	42	3.36	-2.33	-10.43	16.86	-11.76	-0.18	-2.05	13.19	7.08
0.076	0.0547	78	42.27	-1.53	-10.71	0.20	-7.16	4.46	-1.53	8.77	5.87
0.151	0.1084	154	39.58	-0.33	-8.99	-9.65	-3.85	8.37	-2.21	11.12	-0.14
0.251	0.1800	256	21.81	4.73	-9.33	-1.77	-6.10	1.32	-0.13	4.71	1.38
0.501	0.3591	511	0.84	2.91	-3.05	-1.22	1.65	0.05	2.85	-4.85	4.53
0.751	0.5381	766	-25.46	7.65	0.23	5.08	2.47	-6.43	5.22	-11.17	4.38
1.001	0.7172	1020	-23.94	8.14	-1.47	9.22	-1.95	-8.21	6.00	-9.98	4.75
1.501	1.0750	1531	2.71	1.05	-1.90	1.80	-5.92	-2.64	6.24	-3.14	-0.26
2.001	1.4330	2041	3.43	0.76	-0.99	1.58	-5.74	-2.50	6.01	-2.86	-0.68
2.502	1.7920	2551	2.71	0.85	-1.57	1.96	-6.15	-2.68	5.75	-3.33	-0.29

Table 22. Boundary-layer profile at $x/L = 0.752$, $\phi = 120^\circ$.

$x/L = 0.752$ $\alpha = 10 \text{ deg.}$
 $Re = 4.2E+06$ $\phi = 123 \text{ deg.}$

Local-Freestream Coordinates

r		y+	(deg.)	(/ Ue)			(/ Ue ² x1000)					
(cm)	(/ δ)		Beta bs	U	V	W	uu	vv	ww	-uv	-uw	-vw
0.008	0.0054	8	-0.25	0.240	0.007	0.058	6.288	0.148	1.589	0.263	-1.231	0.018
0.013	0.0088	13	-0.16	0.288	0.009	0.070	6.590	0.274	1.900	0.425	-1.163	0.052
0.018	0.0122	18	-0.22	0.324	0.011	0.078	7.086	0.417	2.257	0.594	-1.197	0.079
0.028	0.0189	28	-0.46	0.382	0.010	0.091	5.580	0.724	2.430	0.653	-0.736	0.074
0.038	0.0256	37	-0.52	0.409	0.011	0.097	5.026	0.978	2.542	0.756	-0.517	0.054
0.073	0.0491	72	-1.19	0.456	0.015	0.102	4.288	1.396	2.544	0.931	-0.229	0.012
0.148	0.0995	145	-2.81	0.515	0.018	0.100	4.165	1.591	2.738	0.971	0.028	-0.059
0.248	0.1667	244	-4.72	0.574	0.022	0.092	4.063	1.697	2.874	0.975	0.173	-0.123
0.498	0.3346	489	-9.16	0.693	0.036	0.056	3.781	1.619	2.941	0.845	0.318	-0.167
0.748	0.5025	734	-12.10	0.795	0.048	0.024	3.134	1.433	2.459	0.748	0.202	-0.050
0.998	0.6704	982	-13.66	0.881	0.064	0.002	2.161	1.044	1.825	0.501	0.138	0.062
1.498	1.0060	1467	-13.82	0.988	0.078	-0.000	0.418	0.402	0.439	0.093	-0.010	0.181
1.998	1.3420	1961	-13.10	0.998	0.082	0.013	0.139	0.299	0.241	0.059	-0.004	0.183
2.498	1.6780	2451	-12.92	0.997	0.081	0.016	0.145	0.268	0.229	0.054	-0.013	0.161

r		y+	(/ Ue ³ x10 ⁶)								
(cm)	(/ δ)		u ³	v ³	w ³	u ² v	u ² w	uv ²	v ² w	uw ²	vw ²
0.008	0.0054	8	190.20	-2.38	25.80	-10.96	32.02	3.73	0.85	38.31	2.22
0.013	0.0088	13	99.09	-3.03	16.73	-3.59	-1.08	3.63	1.43	29.37	3.74
0.018	0.0122	18	36.08	-3.50	21.43	6.87	-11.90	3.87	1.33	36.98	5.78
0.028	0.0189	28	7.36	-4.61	16.62	8.09	-9.43	4.00	2.03	16.77	7.60
0.038	0.0256	37	5.84	-1.88	11.43	10.18	-10.07	1.15	0.36	7.37	7.92
0.073	0.0491	72	19.77	3.55	13.46	7.79	-8.46	0.24	-0.37	1.11	7.64
0.148	0.0995	145	29.20	3.66	-10.12	1.51	-8.07	1.50	-2.57	10.08	2.55
0.248	0.1667	244	26.07	-2.64	-4.35	-5.11	-1.74	5.56	-1.79	5.11	1.99
0.498	0.3346	489	-16.55	6.42	1.79	10.37	-0.07	-5.95	2.31	-1.72	4.25
0.748	0.5025	734	-20.52	8.46	0.01	8.72	-1.03	-9.17	5.90	-7.52	4.80
0.998	0.6704	982	-27.63	7.06	4.76	8.35	-2.19	-10.39	6.18	-10.75	4.15
1.498	1.0060	1467	-3.32	0.47	-1.35	2.78	-5.79	-3.60	7.35	-4.05	-0.77
1.998	1.3420	1961	4.11	-0.33	-0.50	1.24	-5.68	-2.54	7.03	-2.72	-1.44
2.498	1.6780	2451	3.80	-0.21	-1.60	1.45	-5.68	-2.63	6.70	-2.94	-0.96

Table 23. Boundary-layer profile at $x/L = 0.752$, $\phi = 123^\circ$.

$$x/L = 0.752 \quad \alpha = 10 \text{ deg.}$$

$$Re = 4.2E+06 \quad \phi = 125 \text{ deg.}$$

Local-Freestream Coordinates

r		y+	(deg.)	(/ Ue)			(/ Ue ² x1000)					
(cm)	(/ δ)		Beta bs	U	V	W	uu	vv	ww	-uv	-uw	-vw
0.017	0.0108	17	0.57	0.316	0.007	0.074	6.668	0.391	2.095	0.626	-1.098	0.096
0.022	0.0139	21	0.69	0.338	0.008	0.080	6.531	0.516	2.255	0.703	-1.008	0.113
0.027	0.0171	26	0.46	0.368	0.008	0.086	5.706	0.723	2.335	0.759	-0.731	0.112
0.037	0.0233	36	0.52	0.392	0.010	0.092	5.125	0.927	2.439	0.826	-0.535	0.070
0.047	0.0296	45	0.46	0.412	0.010	0.096	4.454	1.093	2.441	0.844	-0.303	0.080
0.082	0.0515	79	-0.18	0.451	0.011	0.100	3.916	1.349	2.307	0.894	-0.196	0.072
0.157	0.0986	151	-1.64	0.502	0.015	0.098	3.729	1.508	2.460	0.897	0.001	-0.050
0.257	0.1613	247	-3.54	0.555	0.019	0.089	3.822	1.569	2.635	0.950	0.152	-0.143
0.507	0.3180	486	-7.81	0.669	0.033	0.057	3.615	1.537	2.756	0.814	0.309	-0.202
0.757	0.4748	728	-11.10	0.772	0.046	0.021	3.136	1.321	2.425	0.650	0.311	-0.085
1.007	0.6315	966	-12.78	0.861	0.063	-0.002	2.415	0.997	1.894	0.514	0.267	-0.035
1.507	0.9450	1445	-13.35	0.976	0.080	-0.012	0.500	0.354	0.459	0.087	0.016	0.101
2.008	1.2590	1929	-12.66	0.997	0.085	-0.000	0.080	0.184	0.169	0.028	0.010	0.100
2.507	1.5720	2409	-12.41	0.996	0.088	0.004	0.079	0.185	0.143	0.040	0.004	0.086

r		y+	(/ Ue ³ x10 ⁶)								
(cm)	(/ δ)		u ³	v ³	w ³	u ² v	u ² w	uv ²	v ² w	uw ²	vw ²
0.017	0.0108	17	11.28	-1.74	21.45	6.82	-17.57	2.63	0.92	29.33	5.24
0.022	0.0139	21	-26.68	-2.08	20.14	15.99	-21.84	1.41	0.43	22.06	6.87
0.027	0.0171	26	-15.52	-3.41	8.68	16.62	-24.72	1.05	-1.16	14.72	7.75
0.037	0.0233	36	-27.62	-1.92	8.05	19.29	-20.03	0.24	-0.73	10.38	5.61
0.047	0.0296	45	1.56	0.11	1.07	9.98	-12.64	0.43	-1.42	5.30	6.66
0.082	0.0515	79	28.29	2.63	5.87	5.19	-6.86	-0.23	-1.34	7.80	4.20
0.157	0.0986	151	18.83	3.39	-6.06	1.02	-7.05	1.80	-2.96	7.79	0.13
0.257	0.1613	247	33.36	-0.24	-9.43	-5.62	-9.76	6.26	-1.87	8.14	-1.80
0.507	0.3180	486	17.66	2.15	-2.66	-3.16	-0.83	1.07	1.92	1.25	2.77
0.757	0.4748	728	-9.26	3.93	-0.41	-2.87	-4.38	-3.38	4.32	-3.98	4.13
1.007	0.6315	966	-25.38	5.84	5.00	8.29	-1.51	-5.67	5.32	-7.67	5.04
1.507	0.9450	1445	-7.39	1.43	-2.06	3.45	-6.06	-3.91	6.13	-5.31	0.81
2.008	1.2590	1929	3.69	-1.17	-0.90	0.63	-5.21	-1.32	6.95	-2.33	-1.08
2.507	1.5720	2409	3.62	-1.03	-0.95	0.65	-5.13	-1.38	6.70	-2.30	-0.95

Table 24. Boundary-layer profile at $x/L = 0.752$, $\phi = 125^\circ$.

$x/L = 0.762$ $\alpha = 10 \text{ deg.}$
 $Re = 4.2E+06$ $\phi = 120 \text{ deg.}$

Local-Freestream Coordinates

r		y+	(deg.)	(/ Ue)			(/ Ue ² x1000)					
(cm)	(/δ)		Beta bs	U	V	W	uu	vv	ww	-uv	-uw	-vw
0.008	0.0057	8	-0.63	0.227	0.004	0.052	6.463	0.136	1.510	0.252	-1.216	-0.011
0.013	0.0092	13	-0.89	0.303	0.005	0.067	7.741	0.322	1.956	0.587	-1.297	0.045
0.018	0.0127	18	-1.29	0.344	0.005	0.074	7.391	0.504	2.135	0.757	-1.092	0.075
0.028	0.0197	28	-1.51	0.395	0.007	0.083	6.271	0.868	2.318	0.921	-0.824	0.101
0.038	0.0267	39	-2.37	0.442	0.005	0.086	4.714	1.162	2.540	0.842	-0.289	0.060
0.073	0.0513	74	-2.98	0.480	0.011	0.089	4.178	1.409	2.605	0.923	-0.044	-0.044
0.148	0.1039	150	-4.60	0.541	0.015	0.084	3.859	1.567	2.634	0.864	0.124	-0.160
0.248	0.1740	251	-6.50	0.593	0.018	0.072	3.806	1.599	2.692	0.835	0.253	-0.149
0.498	0.3493	503	-10.31	0.714	0.034	0.039	3.750	1.555	2.655	0.843	0.256	-0.155
0.748	0.5246	756	-12.63	0.815	0.048	0.011	2.746	1.173	2.165	0.569	0.261	-0.048
0.998	0.6999	1009	-13.91	0.894	0.062	-0.008	1.914	1.045	1.565	0.436	0.142	0.139
1.499	1.0510	1511	-13.43	0.997	0.086	0.000	0.332	0.471	0.414	-0.032	0.086	0.162
1.998	1.4010	2020	-13.16	1.003	0.091	0.005	0.143	0.284	0.335	-0.019	0.050	0.147
2.498	1.7520	2527	-13.02	0.996	0.085	0.007	0.139	0.512	0.228	-0.076	0.050	0.241

r		y+	(/ Ue ³ x10 ⁶)								
(cm)	(/δ)		u ³	v ³	w ³	u ² v	u ² w	uv ²	v ² w	uw ²	vw ²
0.008	0.0057	8	293.50	-2.84	29.39	-15.18	48.59	3.43	1.45	45.35	2.72
0.013	0.0092	13	80.00	-3.20	26.58	-0.70	-4.44	4.02	1.90	32.67	5.41
0.018	0.0127	18	14.52	-4.43	23.32	7.37	-17.35	3.83	1.26	23.69	6.09
0.028	0.0197	28	-56.14	-2.64	17.56	25.18	-27.46	-0.57	-0.72	4.66	7.95
0.038	0.0267	39	45.07	-3.76	-15.22	0.76	-8.58	4.08	-1.67	10.85	5.66
0.073	0.0513	74	33.37	3.12	-13.74	0.61	-5.12	2.62	-1.88	12.28	5.94
0.148	0.1039	150	44.23	-1.06	-11.79	-7.94	-7.21	6.58	-2.37	10.97	-1.08
0.248	0.1740	251	38.53	-1.17	-8.33	-8.04	-3.14	7.26	-0.08	8.83	1.24
0.498	0.3493	503	-10.26	7.55	-12.44	3.13	-2.25	-5.17	4.47	0.08	1.31
0.748	0.5246	756	-17.03	2.02	5.37	-0.86	0.75	-5.18	4.36	-11.35	4.15
0.998	0.6999	1009	-22.72	5.29	-0.91	12.51	-2.76	-8.83	7.51	-10.72	4.10
1.499	1.0510	1511	3.05	-5.75	0.69	-0.13	-5.75	-5.91	7.47	-4.81	-3.01
1.998	1.4010	2020	4.61	-2.85	1.31	0.45	-4.89	-2.51	7.52	-3.94	-4.10
2.498	1.7520	2527	3.75	-4.67	-0.81	-0.22	-5.24	-3.78	8.00	-3.07	-1.70

Table 25. Boundary-layer profile at $x/L = 0.762$, $\phi = 120^\circ$.

$$x/L = 0.762 \quad \alpha = 10 \text{ deg.}$$

$$Re = 4.2E+06 \quad \phi = 123 \text{ deg.}$$

Local-Freestream Coordinates

r		y+	(deg.)	(/ Ue)			(/ Ue ² x1000)					
(cm)	(/ δ)		Beta bs	U	V	W	uu	vv	ww	-uv	-uw	-vw
0.007	0.0047	7	0.82	0.199	0.004	0.050	5.708	0.092	1.303	0.211	-1.173	0.015
0.012	0.0078	12	1.25	0.275	0.005	0.071	7.492	0.258	1.923	0.477	-1.485	0.053
0.017	0.0110	17	0.85	0.322	0.005	0.080	7.289	0.418	2.121	0.632	-1.293	0.081
0.027	0.0173	27	0.55	0.370	0.007	0.090	6.266	0.739	2.291	0.820	-0.973	0.111
0.037	0.0235	36	0.54	0.402	0.008	0.098	5.407	0.946	2.357	0.825	-0.657	0.058
0.072	0.0456	70	-0.24	0.455	0.010	0.104	4.068	1.339	2.336	0.886	-0.267	0.025
0.147	0.0928	143	-2.08	0.514	0.015	0.101	3.751	1.455	2.526	0.857	0.023	-0.067
0.247	0.1557	240	-4.20	0.568	0.020	0.090	3.926	1.575	2.646	0.956	0.158	-0.174
0.497	0.3131	483	-8.35	0.687	0.035	0.058	3.787	1.621	2.782	0.816	0.287	-0.170
0.747	0.4704	726	-11.61	0.785	0.050	0.021	3.164	1.346	2.485	0.710	0.223	-0.065
0.997	0.6278	968	-13.22	0.867	0.061	-0.001	2.136	0.955	1.807	0.493	0.125	0.027
1.497	0.9425	1453	-13.56	0.976	0.082	-0.007	0.413	0.293	0.475	0.111	-0.015	0.097
1.997	1.2570	1940	-13.15	0.995	0.082	0.000	0.086	0.123	0.265	0.036	-0.009	0.092
2.497	1.5720	2424	-13.06	0.996	0.087	0.002	0.111	0.144	0.225	0.051	-0.048	0.103

r		y+	(/ Ue ³ x10 ⁶)								
(cm)	(/ δ)		u ³	v ³	w ³	u ² v	u ² w	uv ²	v ² w	uw ²	vw ²
0.007	0.0047	7	233.80	-0.59	23.93	-13.38	38.29	2.31	0.49	38.46	1.51
0.012	0.0078	12	125.00	-1.95	29.07	-12.48	1.70	5.67	1.77	37.63	4.35
0.017	0.0110	17	50.71	-3.64	25.50	0.94	-12.77	4.48	1.32	29.51	4.93
0.027	0.0173	27	-49.64	-2.55	14.10	19.69	-28.50	0.73	-0.94	12.13	6.56
0.037	0.0235	36	-16.78	-1.81	8.57	15.48	-19.55	-0.57	-0.23	7.12	8.00
0.072	0.0456	70	22.04	1.33	7.98	3.48	-5.68	1.81	-1.72	0.66	8.16
0.147	0.0928	143	44.96	-0.50	-12.53	-8.52	-4.10	6.24	-2.02	9.81	2.45
0.247	0.1557	240	31.45	-0.10	-4.69	-3.56	-4.58	1.73	-0.03	7.44	0.62
0.497	0.3131	483	11.77	0.59	-1.57	-7.00	-3.29	1.60	2.12	0.41	1.52
0.747	0.4704	726	-29.63	7.30	-0.89	10.17	0.37	-8.60	5.00	-5.88	4.16
0.997	0.6278	968	-17.35	4.66	3.04	2.22	-0.53	-7.30	5.81	-10.68	4.76
1.497	0.9425	1453	-4.56	1.21	-0.45	3.03	-5.91	-3.79	6.19	-4.94	-0.05
1.997	1.2570	1940	4.15	-0.32	1.60	0.60	-5.12	-1.42	6.75	-2.60	-1.62
2.497	1.5720	2424	4.16	-0.23	-0.75	0.52	-5.29	-1.36	6.63	-2.45	-1.15

Table 26. Boundary-layer profile at $x/L = 0.762$, $\phi = 123^\circ$.

$x/L = 0.762$ $\alpha = 10 \text{ deg.}$
 $Re = 4.2E+06$ $\phi = 125 \text{ deg.}$
Local-Freestream Coordinates

r		y+	(deg.)	(/ Ue)			(/ Ue ² x1000)					
(cm)	(/ δ)		Beta bs	U	V	W	uu	vv	ww	-uv	-uw	-vw
0.007	0.0045	7	2.55	0.214	0.003	0.058	5.802	0.126	1.492	0.356	-1.295	0.043
0.012	0.0075	12	2.68	0.259	0.004	0.071	6.751	0.240	1.801	0.561	-1.346	0.080
0.017	0.0106	17	2.45	0.309	0.005	0.084	6.660	0.402	2.068	0.659	-1.171	0.080
0.027	0.0167	26	2.20	0.361	0.007	0.096	6.255	0.706	2.377	0.822	-0.969	0.135
0.037	0.0228	36	1.87	0.386	0.006	0.101	4.980	0.873	2.309	0.797	-0.575	0.086
0.072	0.0440	69	1.20	0.434	0.009	0.108	3.992	1.282	2.338	0.896	-0.245	0.087
0.147	0.0896	142	-0.59	0.491	0.011	0.106	3.636	1.404	2.359	0.816	0.056	-0.038
0.247	0.1505	238	-2.63	0.544	0.017	0.097	3.816	1.547	2.554	0.902	0.116	-0.127
0.497	0.3025	478	-7.15	0.652	0.033	0.064	3.765	1.527	2.781	0.801	0.320	-0.200
0.747	0.4545	718	-10.55	0.752	0.048	0.029	3.299	1.344	2.461	0.702	0.293	-0.134
0.997	0.6066	957	-12.34	0.847	0.067	0.006	2.435	1.036	1.883	0.532	0.208	-0.000
1.497	0.9107	1441	-13.18	0.968	0.079	-0.007	0.674	0.313	0.518	0.128	0.041	0.042
1.998	1.2150	1917	-12.74	1.000	0.085	0.000	0.168	0.066	0.139	0.009	0.050	0.013
2.498	1.5190	2397	-12.53	0.996	0.094	0.004	0.099	0.107	0.083	0.007	0.015	0.035

r		y+	(/ Ue ³ x10 ⁶)								
(cm)	(/ δ)		u ³	v ³	w ³	u ² v	u ² w	uv ²	v ² w	uw ²	vw ²
0.007	0.0045	7	204.70	-1.27	31.63	-18.83	38.75	4.21	1.31	42.87	1.46
0.012	0.0075	12	137.00	-2.74	29.64	-14.25	10.16	5.77	1.92	37.14	2.71
0.017	0.0106	17	39.93	-4.03	26.08	-2.29	-12.10	5.33	2.16	27.61	5.41
0.027	0.0167	26	-23.49	-3.20	15.08	16.50	-30.86	0.96	-0.06	12.56	7.61
0.037	0.0228	36	-4.61	-3.21	5.87	9.32	-15.36	1.72	-0.86	10.09	5.74
0.072	0.0440	69	14.84	3.43	-2.13	9.57	-5.86	-1.20	-1.81	1.65	6.72
0.147	0.0896	142	46.99	-1.65	-12.25	-9.84	-5.03	8.96	-2.62	11.16	2.25
0.247	0.1505	238	34.88	0.97	-4.30	-7.83	-9.46	5.23	-1.29	7.91	-0.99
0.497	0.3025	478	18.05	0.25	-7.97	-5.89	-6.24	3.65	1.06	0.82	0.92
0.747	0.4545	718	-16.47	3.90	0.59	1.69	-0.83	-5.28	4.60	-5.74	2.54
0.997	0.6066	957	-18.95	6.25	8.99	6.39	0.97	-5.56	4.91	-9.36	4.42
1.497	0.9107	1441	-12.56	3.02	-1.74	4.99	-5.28	-5.12	5.16	-6.31	1.46
1.998	1.2150	1917	3.35	-0.09	-1.42	0.66	-5.37	-1.36	6.22	-2.23	-0.47
2.498	1.5190	2397	4.01	-0.67	-0.87	0.58	-5.18	-1.26	6.26	-2.41	-0.67

Table 27. Boundary-layer profile at $x/L = 0.762$, $\phi = 125^\circ$.

$$x/L = 0.772 \quad \alpha = 10 \text{ deg.}$$

$$Re = 4.2E+06 \quad \phi = 105 \text{ deg.}$$

Local-Freestream Coordinates

r		y+	(deg.)	(/ Ue)			(/ Ue ² x1000)					
(cm)	(/ δ)		Beta bs	U	V	W	uu	vv	ww	-uv	-uw	-vw
0.007	0.0073	8	-11.10	0.285	-0.001	0.028	8.097	0.206	1.715	0.593	-0.538	-0.025
0.012	0.0126	14	-11.01	0.360	-0.004	0.036	9.542	0.417	2.376	0.865	-0.529	-0.038
0.017	0.0180	20	-11.40	0.432	-0.001	0.040	9.946	0.853	2.918	1.241	-0.389	-0.057
0.027	0.0287	32	-11.82	0.488	-0.004	0.041	7.823	1.295	3.297	1.338	-0.203	-0.067
0.037	0.0394	44	-12.46	0.513	-0.004	0.038	6.594	1.492	3.278	1.238	-0.110	-0.037
0.072	0.0769	85	-12.92	0.569	-0.001	0.037	5.457	1.823	3.271	1.273	-0.001	-0.060
0.147	0.1573	175	-14.11	0.651	0.002	0.029	4.821	2.047	3.421	1.285	0.121	-0.108
0.247	0.2644	294	-15.26	0.717	0.003	0.018	4.390	1.943	3.272	1.129	0.129	-0.061
0.497	0.5322	591	-16.91	0.849	0.013	-0.004	3.016	1.512	2.438	0.805	0.084	0.097
0.747	0.8001	890	-17.21	0.954	0.033	-0.009	1.324	0.720	1.103	0.511	0.024	0.100
0.997	1.0680	1185	-16.67	0.993	0.032	-0.000	0.413	0.284	0.315	0.087	-0.024	0.066
1.497	1.6040	1780	-15.88	1.002	0.041	0.014	0.062	0.115	0.095	0.013	0.005	0.057
1.997	2.1390	2378	-15.49	1.000	0.047	0.021	0.098	0.107	0.081	0.028	0.003	0.047
2.497	2.6750	2973	-15.28	0.998	0.053	0.024	0.081	0.069	0.061	0.010	0.010	0.023

r		y+	(Ue ³ x10 ⁶)								
(cm)	(/ δ)		u ³	v ³	w ³	u ² v	u ² w	uv ²	v ² w	uw ²	vw ²
0.007	0.0073	8	403.00	-4.54	7.02	-37.71	25.39	7.57	1.06	53.65	2.23
0.012	0.0126	14	302.70	-8.30	12.46	-39.58	21.14	14.54	2.24	64.57	4.81
0.017	0.0180	20	-16.80	-7.80	-1.83	17.32	-5.62	3.87	0.31	48.05	5.11
0.027	0.0287	32	-38.89	-5.07	10.11	29.47	-3.98	-0.29	1.05	27.67	4.58
0.037	0.0394	44	-64.82	0.11	-30.58	35.47	-7.59	-6.80	-2.25	24.72	3.62
0.072	0.0769	85	3.86	9.31	-14.76	16.84	-4.99	-7.25	-1.67	10.01	7.12
0.147	0.1573	175	4.73	8.33	-7.50	12.22	-10.95	-5.49	-1.21	3.49	4.07
0.247	0.2644	294	-5.50	3.94	-6.61	4.62	1.48	-2.99	6.14	-5.38	2.90
0.497	0.5322	591	-22.67	9.48	-7.24	6.23	-2.23	-8.56	4.73	-12.27	6.05
0.747	0.8001	890	-23.27	12.24	-3.05	18.36	-2.91	-13.20	5.96	-15.81	7.18
0.997	1.0680	1185	-4.25	2.98	-4.18	4.53	-7.11	-5.02	6.71	-6.84	0.53
1.497	1.6040	1780	6.00	-0.60	-1.55	0.92	-5.46	-2.08	7.66	-3.68	-1.22
1.997	2.1390	2378	6.12	-0.44	-1.48	0.84	-5.40	-2.08	7.43	-3.60	-1.18
2.497	2.6750	2973	5.99	-0.16	-1.63	0.78	-5.25	-2.05	7.12	-3.59	-0.97

Table 28. Boundary-layer profile at $x/L = 0.772$, $\phi = 105^\circ$.

$x/L = 0.772$ $\alpha = 10 \text{ deg.}$
 $Re = 4.2E+06$ $\phi = 110 \text{ deg.}$

Local-Freestream Coordinates

r		y+	(deg.)	(/ Ue)			(/ Ue ² x1000)					
(cm)	(/ δ)		Beta bs	U	V	W	uu	vv	ww	-uv	-uw	-vw
0.009	0.0081	10	-7.57	0.292	0.000	0.041	9.916	0.289	1.953	0.622	-1.080	-0.015
0.019	0.0173	21	-8.13	0.414	0.001	0.054	8.752	0.853	2.783	1.088	-0.606	-0.012
0.029	0.0264	33	-8.56	0.461	0.001	0.056	6.991	1.235	3.037	1.180	-0.250	-0.057
0.039	0.0356	44	-8.94	0.489	0.000	0.056	6.154	1.455	3.015	1.165	-0.058	-0.055
0.074	0.0676	83	-10.04	0.542	0.003	0.052	4.993	1.764	2.992	1.195	0.020	-0.104
0.149	0.1362	168	-11.61	0.627	-0.002	0.043	3.950	1.731	2.997	0.805	0.252	-0.217
0.249	0.2277	281	-12.85	0.681	0.007	0.031	4.327	1.876	3.108	1.067	0.243	-0.184
0.499	0.4564	564	-15.32	0.808	0.015	0.002	3.140	1.434	2.486	0.725	0.123	-0.046
0.749	0.6851	846	-16.41	0.902	0.027	-0.014	2.169	0.978	1.706	0.516	0.062	0.007
0.999	0.9138	1128	-16.22	0.972	0.037	-0.012	0.859	0.538	0.769	0.144	-0.066	0.024
1.499	1.3710	1693	-15.50	1.000	0.050	0.000	0.169	0.172	0.284	-0.065	-0.069	-0.050
1.999	1.8290	2257	-15.07	0.998	0.059	0.007	0.129	0.205	0.244	-0.046	-0.025	-0.018
2.499	2.2860	2823	-14.67	0.998	0.065	0.014	0.157	0.298	0.288	-0.106	0.023	0.031

r		y+	(/ Ue ³ x10 ⁶)								
(cm)	(/ δ)		u ³	v ³	w ³	u ² v	u ² w	uv ²	v ² w	uw ²	vw ²
0.009	0.0081	10	290.00	-3.92	17.77	-27.18	13.90	8.53	2.27	55.31	3.80
0.019	0.0173	21	-22.84	-6.04	-1.33	13.50	-18.57	4.92	1.66	36.82	7.29
0.029	0.0264	33	-11.94	-4.34	-0.31	19.15	-0.99	2.12	2.19	25.89	6.46
0.039	0.0356	44	3.53	-1.06	-10.93	19.54	-10.98	-0.25	-1.70	15.37	7.40
0.074	0.0676	83	15.07	4.25	-13.99	6.29	-5.13	-1.02	-1.14	7.98	7.67
0.149	0.1362	168	55.38	-1.92	-19.21	-18.95	0.54	12.91	3.65	6.34	2.78
0.249	0.2277	281	14.05	2.18	-5.49	-2.05	-1.61	0.49	3.00	3.35	1.29
0.499	0.4564	564	-10.45	6.61	-9.52	0.73	-0.50	-5.22	4.62	-5.44	3.57
0.749	0.6851	846	-41.47	7.95	-2.03	12.13	-3.65	-13.84	5.59	-13.28	6.33
0.999	0.9138	1128	-14.67	5.71	-2.83	8.12	-6.30	-7.12	6.87	-9.56	2.43
1.499	1.3710	1693	6.54	-0.90	1.11	1.21	-4.80	-1.61	7.92	-1.73	-0.36
1.999	1.8290	2257	6.33	-1.75	-0.48	1.07	-4.79	-1.44	8.27	-2.73	-1.61
2.499	2.2860	2823	6.14	-2.69	-1.03	0.76	-4.56	-2.09	9.41	-3.49	-2.95

Table 29. Boundary-layer profile at $x/L = 0.772$, $\phi = 110^\circ$.

$x/L = 0.772$ $\alpha = 10 \text{ deg.}$
 $Re = 4.2E+06$ $\phi = 115 \text{ deg.}$
Local-Freestream Coordinates

r		y+	(deg.)	(/ Ue)			(/ Ue ² x1000)					
(cm)	(/ δ)		Beta _{bs}	U	V	W	uu	vv	ww	-uv	-uw	-vw
0.009	0.0069	9	-3.86	0.254	0.002	0.049	8.329	0.219	1.669	0.360	-1.296	-0.026
0.014	0.0109	14	-4.47	0.334	0.000	0.061	8.695	0.468	2.263	0.739	-1.086	0.020
0.019	0.0149	20	-4.56	0.371	0.002	0.067	8.275	0.699	2.582	0.930	-0.924	-0.016
0.029	0.0229	30	-5.66	0.438	0.002	0.071	6.118	1.251	2.911	1.055	-0.429	0.019
0.039	0.0309	41	-5.37	0.455	0.000	0.076	5.745	1.350	2.927	0.988	-0.358	-0.000
0.074	0.0589	78	-6.44	0.513	0.002	0.076	4.795	1.663	3.005	1.047	-0.091	-0.108
0.149	0.1189	157	-8.10	0.578	0.006	0.068	4.427	1.810	2.908	1.067	0.106	-0.202
0.249	0.1990	262	-10.28	0.639	0.012	0.051	4.319	1.870	2.816	1.051	0.156	-0.204
0.499	0.3990	525	-13.53	0.761	0.023	0.018	3.668	1.634	2.862	0.876	0.225	-0.106
0.749	0.5991	791	-15.52	0.873	0.033	-0.010	2.684	1.209	2.320	0.539	0.204	-0.029
0.999	0.7992	1053	-15.92	0.946	0.043	-0.017	1.601	0.748	1.747	0.237	0.127	0.014
1.498	1.1990	1579	-14.86	0.998	0.063	-0.000	0.246	0.186	0.283	-0.068	-0.096	-0.006
1.998	1.5990	2106	-14.69	0.996	0.069	0.003	0.150	0.150	0.172	-0.067	-0.079	-0.034
2.499	2.0000	2633	-14.42	0.997	0.077	0.008	0.140	0.196	0.146	-0.092	-0.051	-0.013

r		y+	(/ Ue ³ x10 ⁶)								
(cm)	(/ δ)		u ³	v ³	w ³	u ² v	u ² w	uv ²	v ² w	uw ²	vw ²
0.009	0.0069	9	264.00	-2.68	22.08	-20.64	30.22	6.78	2.53	45.43	3.43
0.014	0.0109	14	130.20	-4.05	12.64	-9.93	-0.24	9.25	2.68	48.16	5.26
0.019	0.0149	20	-13.98	-3.84	9.34	10.44	-24.31	5.19	2.16	38.89	7.08
0.029	0.0229	30	-33.43	-1.62	-9.56	29.83	-20.62	-2.86	-1.69	13.89	7.99
0.039	0.0309	41	24.20	-3.05	-10.64	8.14	-10.49	3.66	-0.34	15.21	6.73
0.074	0.0589	78	44.24	0.84	-17.38	-0.35	0.41	4.46	-1.06	9.06	6.91
0.149	0.1189	157	50.81	-3.10	-11.15	-8.62	-7.79	10.61	0.16	9.74	1.42
0.249	0.1990	262	16.75	3.93	-14.95	0.86	-5.85	2.32	0.36	14.15	0.89
0.499	0.3990	525	-19.43	7.22	0.42	8.90	1.42	-8.28	3.42	-8.13	3.71
0.749	0.5991	791	-26.47	7.70	-7.52	8.27	-1.68	-10.48	5.51	-7.23	4.99
0.999	0.7992	1053	-24.81	6.22	8.97	9.93	-2.88	-8.43	5.42	-12.98	5.91
1.498	1.1990	1579	5.16	-0.04	-1.38	0.89	-5.53	-1.94	6.90	-2.55	-0.90
1.998	1.5990	2106	6.95	-0.56	-0.57	2.00	-3.95	-1.10	7.60	-2.01	-0.38
2.499	2.0000	2633	6.58	-1.12	-0.87	2.04	-4.20	-0.96	8.60	-2.46	-0.58

Table 30. Boundary-layer profile at $x/L = 0.772$, $\phi = 115^\circ$.

$x/L = 0.772$ $\alpha = 10 \text{ deg.}$
 $Re = 4.2E+06$ $\phi = 120 \text{ deg.}$

Local-Freestream Coordinates

r		y+	(deg.)	(/ Ue)			(/ Ue ² x1000)					
(cm)	(/δ)		Beta bs	U	V	W	uu	vv	ww	-uv	-uw	-vw
0.007	0.0048	7	-0.48	0.233	-0.000	0.058	6.452	0.142	1.668	0.292	-1.292	-0.023
0.013	0.0090	13	0.07	0.274	-0.000	0.072	8.065	0.270	1.964	0.596	-1.361	0.037
0.017	0.0118	17	-0.72	0.336	-0.001	0.083	7.203	0.492	2.252	0.690	-1.006	0.025
0.027	0.0189	27	-1.16	0.388	0.000	0.092	6.280	0.911	2.527	0.929	-0.656	0.061
0.037	0.0259	37	-1.74	0.421	-0.000	0.096	5.265	1.102	2.500	0.826	-0.372	-0.003
0.072	0.0506	72	-2.83	0.462	0.002	0.096	4.677	1.477	2.761	1.058	-0.092	-0.019
0.147	0.1035	148	-4.65	0.529	0.004	0.092	4.033	1.551	2.717	0.880	0.160	-0.142
0.247	0.1740	249	-6.77	0.586	0.011	0.080	4.198	1.687	2.885	0.960	0.261	-0.189
0.497	0.3502	500	-10.87	0.710	0.025	0.046	3.957	1.634	2.977	0.856	0.364	-0.151
0.747	0.5264	752	-13.81	0.819	0.037	0.011	3.029	1.299	2.882	0.675	0.485	-0.060
0.997	0.7026	1003	-14.97	0.903	0.053	-0.007	2.182	0.955	1.737	0.456	0.181	0.016
1.497	1.0550	1507	-14.55	0.996	0.070	-0.000	0.301	0.234	0.328	0.013	-0.065	0.049
1.996	1.4070	2009	-14.22	0.996	0.082	0.006	0.104	0.116	0.184	-0.008	-0.027	0.029
2.497	1.7600	2513	-14.05	0.996	0.089	0.009	0.107	0.120	0.165	-0.017	-0.008	0.015

r		y+	(/Ue ³ x10 ⁶)								
(cm)	(/δ)		u ³	v ³	w ³	u ² v	u ² w	uv ²	v ² w	uw ²	vw ²
0.007	0.0048	7	271.80	0.90	41.86	-20.60	55.79	5.83	2.67	52.52	4.62
0.013	0.0090	13	234.80	-1.18	33.69	-18.61	23.10	6.69	2.86	48.52	3.35
0.017	0.0118	17	63.63	-3.58	31.41	-0.25	-11.43	6.28	2.83	28.68	6.45
0.027	0.0189	27	-24.03	-2.84	20.34	20.07	-19.60	0.99	1.09	9.68	7.75
0.037	0.0259	37	17.50	-1.45	10.88	7.94	-4.98	3.52	1.59	6.90	7.70
0.072	0.0506	72	19.34	6.37	-11.26	10.37	-8.83	-1.39	-2.40	9.54	7.29
0.147	0.1035	148	53.80	0.27	-5.16	-8.15	-7.66	8.24	-1.42	8.02	0.84
0.247	0.1740	249	30.40	-0.30	-9.49	-1.80	-8.48	5.63	-1.57	10.20	0.86
0.497	0.3502	500	-5.54	3.27	-10.70	-0.27	-0.18	0.63	2.85	0.75	1.46
0.747	0.5264	752	-7.01	5.19	27.38	-0.16	-0.20	-3.85	3.80	-7.23	5.47
0.997	0.7026	1003	-30.56	7.81	6.98	12.03	-2.54	-8.54	5.66	-12.29	5.41
1.497	1.0550	1507	-0.03	1.32	-2.68	2.47	-6.23	-3.30	6.49	-4.35	-0.03
1.996	1.4070	2009	5.30	-0.32	-1.19	0.87	-5.03	-1.65	6.76	-2.58	-0.72
2.497	1.7600	2513	5.56	-0.62	-1.54	0.98	-4.94	-1.59	6.91	-2.48	-0.62

Table 31. Boundary-layer profile at $x/L = 0.772$, $\phi = 120^\circ$.

$$x/L = 0.772 \quad \alpha = 10 \text{ deg.}$$

$$Re = 4.2E+06 \quad \phi = 123 \text{ deg.}$$

Local-Freestream Coordinates

r		y+	(deg.)	(/ Ue)			(/ Ue ² x1000)					
(cm)	(/δ)		Beta bs	U	V	W	uu	vv	ww	-uv	-uw	-vw
0.012	0.0077	11	1.23	0.252	-0.001	0.070	6.776	0.240	1.848	0.626	-1.467	0.099
0.017	0.0109	16	1.09	0.310	-0.000	0.085	6.514	0.427	2.089	0.746	-1.193	0.102
0.022	0.0142	20	1.27	0.332	-0.000	0.093	6.363	0.558	2.194	0.835	-1.093	0.119
0.032	0.0207	30	0.94	0.372	0.001	0.101	5.882	0.849	2.354	0.994	-0.868	0.137
0.042	0.0272	39	0.73	0.396	0.001	0.107	4.912	1.019	2.343	0.932	-0.470	0.084
0.077	0.0499	72	-0.30	0.451	-0.001	0.113	3.366	1.191	2.300	0.649	-0.078	0.004
0.152	0.0987	143	-2.14	0.500	0.006	0.108	3.687	1.438	2.412	0.851	0.041	-0.024
0.252	0.1637	237	-4.13	0.555	0.010	0.100	3.890	1.596	2.567	0.964	0.172	-0.133
0.502	0.3262	471	-8.96	0.676	0.026	0.063	3.774	1.615	2.797	0.794	0.299	-0.180
0.752	0.4887	709	-12.19	0.777	0.041	0.029	3.320	1.400	2.520	0.735	0.319	-0.133
1.002	0.6512	942	-14.02	0.878	0.064	0.004	2.044	0.984	1.837	0.743	0.265	0.019
1.502	0.9762	1412	-14.87	0.983	0.076	-0.010	0.578	0.317	0.391	0.118	-0.012	0.062
2.001	1.3010	1882	-14.30	0.995	0.082	-0.000	0.074	0.071	0.067	-0.011	0.014	0.028
2.501	1.6260	2353	-13.52	1.031	0.056	0.014	0.066	0.051	0.056	-0.005	0.015	0.016

r		y+	(/Ue ³ x10 ⁶)								
(cm)	(/δ)		u ³	v ³	w ³	u ² v	u ² w	uv ²	v ² w	uw ²	vw ²
0.012	0.0077	11	122.80	-2.35	35.82	-17.61	5.26	6.55	1.92	39.53	2.25
0.017	0.0109	16	44.94	-3.60	25.68	-1.09	-13.13	4.61	1.70	28.20	4.71
0.022	0.0142	20	0.68	-3.73	16.79	6.72	-24.15	3.83	0.43	19.21	4.32
0.032	0.0207	30	-28.15	-2.28	12.37	21.63	-28.62	-1.72	-1.69	8.90	8.26
0.042	0.0272	39	-13.31	-0.89	8.85	14.24	-15.17	-0.85	-0.56	10.13	5.75
0.077	0.0499	72	57.82	-2.33	0.74	-12.52	1.69	9.05	-0.85	5.74	4.43
0.152	0.0987	143	45.13	-1.82	-10.37	-8.65	-4.21	8.56	-3.91	11.09	0.06
0.252	0.1637	237	30.36	-2.07	-14.06	-3.55	-8.78	4.79	-3.23	11.34	-1.61
0.502	0.3262	471	20.44	1.96	-14.96	-10.36	-5.00	3.64	0.26	5.88	-0.29
0.752	0.4887	709	-17.18	3.60	1.74	4.32	0.52	-2.96	4.39	-5.17	4.53
1.002	0.6512	942	-13.20	10.62	2.18	13.92	1.62	-6.79	5.89	-11.11	6.37
1.502	0.9762	1412	-11.52	3.07	-2.81	5.58	-6.35	-5.82	6.39	-7.03	0.96
2.001	1.3010	1882	4.84	-0.33	-1.13	0.70	-5.46	-1.73	6.90	-3.06	-0.84
2.501	1.6260	2353	7.29	-0.07	-1.85	1.06	-8.32	-2.62	10.28	-4.69	-1.13

Table 32. Boundary-layer profile at $x/L = 0.772$, $\phi = 123^\circ$.

$x/L = 0.772$ $\alpha = 10 \text{ deg.}$
 $Re = 4.2E+06$ $\phi = 125 \text{ deg.}$
Local-Freestream Coordinates

r		y+	(deg.)	(/ Ue)			(/ Ue ² x1000)					
(cm)	(/ δ)		Beta _{bs}	U	V	W	uu	vv	ww	-uv	-uw	-vw
0.006	0.0035	5	3.35	0.169	-0.000	0.052	4.756	0.073	1.217	0.183	-1.148	0.003
0.016	0.0096	14	2.20	0.267	0.000	0.076	6.879	0.253	1.849	0.558	-1.381	0.077
0.026	0.0157	24	2.69	0.339	-0.004	0.100	4.840	0.461	2.046	0.394	-0.687	-0.012
0.036	0.0218	33	2.06	0.365	0.003	0.104	4.841	0.911	2.263	0.807	-0.564	0.080
0.071	0.0432	64	0.96	0.417	0.003	0.110	3.740	1.229	2.151	0.819	-0.167	-0.011
0.146	0.0889	133	-0.72	0.485	0.006	0.113	3.662	1.426	2.252	0.886	-0.001	-0.059
0.246	0.1499	224	-2.73	0.522	0.009	0.102	3.483	1.418	2.577	0.763	0.121	-0.110
0.496	0.3024	452	-7.65	0.639	0.024	0.069	3.890	1.536	3.200	0.804	0.474	-0.215
0.746	0.4548	681	-10.88	0.784	0.043	0.040	3.911	1.647	3.029	0.841	0.435	-0.114
0.996	0.6073	911	-13.67	0.842	0.050	0.001	2.709	1.188	2.343	0.473	0.320	-0.066
1.496	0.9123	1369	-14.77	0.970	0.073	-0.017	1.000	0.535	0.848	0.092	0.067	-0.014
1.996	1.2170	1822	-13.77	0.991	0.092	0.000	0.118	0.134	0.183	-0.022	-0.022	0.026
2.496	1.5220	2278	-13.63	0.992	0.098	0.002	0.102	0.113	0.168	-0.025	-0.004	0.010

r		y+	(/ Ue ³ x10 ⁶)								
(cm)	(/ δ)		u ³	v ³	w ³	u ² v	u ² w	uv ²	v ² w	uw ²	vw ²
0.006	0.0035	5	232.20	0.42	29.03	-14.26	58.66	2.99	1.39	40.12	0.57
0.016	0.0096	14	142.70	-1.30	37.29	-12.33	2.52	5.64	2.11	38.89	3.25
0.026	0.0157	24	75.50	-4.25	18.46	-7.14	-0.60	6.16	2.14	21.06	4.99
0.036	0.0218	33	-33.46	1.39	8.23	23.27	-20.26	-2.82	-1.12	8.10	7.91
0.071	0.0432	64	34.67	3.18	1.62	4.22	-3.79	2.03	-1.90	7.38	6.82
0.146	0.0889	133	23.92	1.93	3.25	-0.10	-5.52	5.54	-2.99	5.67	2.28
0.246	0.1499	224	37.03	-5.39	-17.84	-8.34	-3.36	8.97	-1.02	13.50	-1.75
0.496	0.3024	452	13.85	0.64	8.33	-1.93	-7.00	-0.30	-1.54	3.99	0.41
0.746	0.4548	681	-31.36	3.87	3.51	8.73	-0.49	-7.90	3.76	-5.70	3.56
0.996	0.6073	911	-20.89	5.40	9.62	4.01	0.75	-7.35	5.42	-11.99	4.63
1.496	0.9123	1369	-13.56	3.84	0.36	6.29	-5.11	-5.79	6.92	-7.12	1.28
1.996	1.2170	1822	5.02	-0.28	-1.30	0.95	-4.96	-1.44	6.62	-2.33	-0.57
2.496	1.5220	2278	5.15	-0.28	-1.59	0.98	-4.96	-1.39	6.70	-2.35	-0.59

Table 33. Boundary-layer profile at $x/L = 0.772$, $\phi = 125^\circ$.

$$x/L = 0.772 \quad \alpha = 10 \text{ deg.}$$

$$Re = 4.2E+06 \quad \phi = 130 \text{ deg.}$$

Local-Freestream Coordinates

r		y+	(deg.)	(/ Ue)			(/ Ue ² x1000)					
(cm)	(/δ)		Beta bs	U	V	W	uu	vv	ww	-uv	-uw	-vw
0.007	0.0038	6	5.64	0.162	0.001	0.057	4.104	0.071	1.237	0.166	-1.112	-0.016
0.009	0.0049	8	5.80	0.186	0.002	0.066	4.931	0.107	1.556	0.202	-1.487	-0.011
0.013	0.0070	11	5.37	0.230	0.001	0.079	5.435	0.187	1.626	0.334	-1.431	0.032
0.023	0.0124	20	5.47	0.300	0.002	0.104	5.697	0.485	2.094	0.644	-1.262	0.088
0.033	0.0177	29	5.04	0.338	0.003	0.114	5.078	0.718	2.107	0.726	-0.831	0.064
0.068	0.0364	59	4.20	0.394	0.003	0.127	3.542	1.067	2.048	0.685	-0.271	0.049
0.143	0.0764	125	2.61	0.443	0.007	0.129	3.314	1.252	2.181	0.765	-0.063	-0.026
0.243	0.1298	211	0.76	0.497	0.006	0.128	3.055	1.270	2.290	0.644	0.114	-0.106
0.493	0.2633	428	-3.55	0.587	0.021	0.105	3.724	1.522	2.873	0.805	0.264	-0.173
0.743	0.3967	647	-8.05	0.686	0.033	0.067	3.621	1.499	2.742	0.695	0.391	-0.164
0.993	0.5302	865	-11.42	0.769	0.049	0.030	3.371	1.383	2.699	0.652	0.403	-0.111
1.493	0.7971	1298	-13.91	0.923	0.082	-0.004	1.780	0.846	1.373	0.280	0.114	0.029
1.993	1.0640	1732	-13.65	0.996	0.094	-0.000	0.343	0.305	0.443	-0.065	-0.008	-0.027

r		y+	(/Ue ³ x10 ⁶)								
(cm)	(/δ)		u ³	v ³	w ³	u ² v	u ² w	uv ²	v ² w	uw ²	vw ²
0.007	0.0038	6	189.20	0.90	32.99	-10.51	46.06	2.22	1.30	37.34	2.58
0.009	0.0049	8	205.20	0.31	40.69	-9.83	60.54	2.83	1.81	49.22	3.30
0.013	0.0070	11	120.10	-0.62	30.34	-7.71	22.73	3.48	1.73	35.66	2.74
0.023	0.0124	20	-0.21	-2.76	22.00	9.06	-14.25	2.84	2.00	15.64	5.72
0.033	0.0177	29	-23.29	-0.60	12.06	15.57	-27.86	0.46	0.70	3.23	8.56
0.068	0.0364	59	22.41	0.78	0.40	1.29	-1.18	3.30	-0.50	4.18	6.24
0.143	0.0764	125	36.14	-0.70	-14.91	-4.12	-2.52	4.67	-1.15	13.05	0.38
0.243	0.1298	211	47.83	-5.08	-19.01	-14.78	-1.75	10.95	-1.26	12.32	-2.00
0.493	0.2633	428	27.87	-1.89	-17.24	-7.14	-4.65	6.56	0.35	9.07	-2.08
0.743	0.3967	647	18.67	-2.16	-21.56	-8.39	-0.84	6.21	1.02	9.32	-1.54
0.993	0.5302	865	-18.91	5.18	7.32	3.92	2.05	-3.81	4.32	-5.98	4.55
1.493	0.7971	1298	-25.52	4.57	1.92	8.43	-1.23	-7.18	5.53	-8.71	2.48
1.993	1.0640	1732	2.90	0.66	-2.28	1.34	-5.28	-1.82	6.80	-2.80	-0.18

Table 34. Boundary-layer profile at $x/L = 0.772$, $\phi = 130^\circ$.

$x/L = 0.400$ $\alpha = 10 \text{ deg.}$
 $Re = 4.2E+06$ $\phi = 90 \text{ deg.}$
Derivatives in Local-Freestream Coordinates

r		(1/cm)			(1/cm x1000)					
(cm)	(δ)	U _y	V _y	W _y	u ² _y	v ² _y	w ² _y	uv _y	uw _y	vw _y
0.005	0.0139	37.300	0.564	-1.500	625.300	84.780	255.500	184.60	92.47	-4.79
0.009	0.0243	27.090	0.279	-0.877	22.190	94.460	183.500	126.00	25.09	0.53
0.013	0.0346	18.830	0.157	-0.528	-269.500	90.850	128.300	76.09	-4.46	0.65
0.019	0.0501	9.731	0.052	-0.256	-408.300	71.600	66.340	26.45	-22.12	1.17
0.025	0.0656	5.628	-0.006	-0.184	-290.300	48.140	27.980	1.43	-15.14	0.26
0.032	0.0836	3.301	0.002	-0.246	-173.900	27.600	4.101	-4.949	-8.479	1.044
0.042	0.1094	2.698	-0.026	-0.180	-121.000	14.870	-9.612	-6.252	-8.109	2.769
0.057	0.1481	2.188	0.009	-0.087	-75.620	6.696	-11.780	-6.990	-3.066	2.516
0.077	0.1998	1.569	0.008	0.015	-35.200	-0.159	-9.811	-5.319	-1.270	1.148
0.122	0.3159	1.147	0.019	0.026	-18.620	-2.960	-8.523	-3.846	-0.482	0.205
0.197	0.5094	0.910	0.011	0.050	-15.600	-4.721	-8.744	-4.137	-0.523	-0.169
0.297	0.7675	0.646	0.004	0.064	-13.280	-5.238	-8.324	-4.055	-0.154	-0.256
0.398	1.0260	0.396	-0.003	0.066	-10.710	-4.629	-6.580	-3.330	0.153	-0.506
0.598	1.5420	0.108	-0.010	0.039	-4.088	-1.985	-2.447	-1.272	0.229	-0.273
0.997	2.5740	0.005	-0.008	0.020	-0.714	-0.427	-0.366	-0.210	0.094	-0.046
1.497	3.8640	-0.011	-0.006	0.010	0.002	0.002	-0.028	0.002	-0.007	0.019
1.998	5.1550	-0.005	-0.008	0.002	-0.034	0.019	-0.290	0.024	-0.101	0.016

r		(1/cm ²)			(1/cm ² x1000)					
(cm)	(δ)	U _{yy}	V _{yy}	W _{yy}	u ² _{yy}	v ² _{yy}	w ² _{yy}	-uv _{yy}	-uw _{yy}	-vw _{yy}
0.005	0.0139	-2800.00	-102.70	203.50	-200900	4511	-20570	-15430.0	-23410	2401
0.009	0.0243	-2299.00	-44.23	113.30	-104700	478	-15570	-13680.0	-10990	432
0.013	0.0346	-1772.00	-13.02	54.08	-32620	-2657	-11590	-10960.0	-2817	-481
0.019	0.0501	-929.60	-17.32	23.27	30190	-5677	-7541	-5062.0	1462.0	131.7
0.025	0.0656	-336.90	1.72	-16.91	15900	-2868	-4090	-764.70	810.00	84.14
0.032	0.0836	-47.13	-2.25	7.89	5025.0	-1254.0	-1242.0	-262.80	115.50	128.80
0.042	0.1094	-42.29	2.16	8.42	3788.0	-667.7	-145.0	-22.70	372.20	46.92
0.057	0.1481	-25.32	0.15	3.35	1479.0	-245.0	85.7	77.94	67.50	-78.30
0.077	0.1998	-7.99	0.16	0.20	306.3	-55.7	25.5	25.24	11.82	-14.31
0.122	0.3159	-3.15	-0.09	0.36	43.4	-24.7	-4.5	-3.56	-0.92	-2.46
0.197	0.5094	-2.53	-0.10	0.27	0.3	-15.0	-12.4	-8.48	4.11	-3.48
0.297	0.7675	-2.63	-0.07	-0.02	33.3	8.6	22.4	9.90	3.41	-1.73
0.398	1.0260	-1.15	-0.02	-0.12	28.4	11.8	17.6	8.87	-0.04	1.20
0.598	1.5420	-0.25	0.01	-0.05	8.3	3.9	5.1	2.57	-0.36	0.58
0.997	2.5740	-0.04	0.00	-0.02	1.6	1.0	0.8	0.48	-0.22	0.15
1.497	3.8640	0.01	0.00	-0.01	0.1	0.0	-0.1	0.04	-0.09	0.02
1.998	5.1550	0.01	-0.01	-0.02	-0.1	0.0	-0.6	0.04	-0.20	-0.01

Table 35. Boundary-layer y-derivatives at $x/L = 0.400$, $\phi = 90^\circ$.

$x/L = 0.400$ $\alpha = 10 \text{ deg.}$
 $Re = 4.2E+06$ $\phi = 100 \text{ deg.}$
Derivatives in Local-Freestream Coordinates

r		(1/cm)			(1/cm x1000)					
(cm)	(δ)	U _y	V _y	W _y	u ² _y	v ² _y	w ² _y	uv _y	uw _y	vw _y
0.009	0.0216	18.310	-0.568	-1.181	-505.900	100.800	161.600	162.70	29.27	-3.26
0.013	0.0311	14.030	-0.210	-0.712	-468.400	85.920	109.600	87.69	-0.30	-1.44
0.017	0.0405	10.540	0.027	-0.452	-404.700	74.060	75.960	44.42	-15.05	0.57
0.023	0.0548	6.719	0.042	-0.227	-313.700	58.740	40.070	9.70	-24.11	3.36
0.029	0.0690	4.828	0.117	-0.105	-248.800	41.770	20.450	-0.61	-12.40	1.04
0.036	0.0856	3.423	-0.004	-0.166	-176.100	29.640	5.401	-0.225	-7.304	1.469
0.046	0.1093	2.515	0.018	-0.159	-114.900	13.860	-8.427	-5.476	-3.171	0.185
0.061	0.1449	1.870	0.058	-0.137	-58.310	2.845	-11.470	-7.797	-1.573	0.260
0.081	0.1923	1.452	0.016	-0.060	-32.260	-1.849	-9.670	-7.353	-2.573	0.886
0.126	0.2990	1.121	0.049	-0.023	-18.440	-2.669	-7.260	-4.479	-2.594	1.243
0.201	0.4768	0.891	0.013	-0.000	-14.410	-4.170	-7.774	-3.527	-1.111	0.343
0.301	0.7138	0.665	-0.002	0.031	-12.180	-4.948	-7.854	-3.468	0.084	-0.300
0.401	0.9509	0.444	-0.003	0.056	-10.300	-4.616	-6.723	-3.150	0.553	-0.662
0.601	1.4250	0.145	0.003	0.045	-4.430	-2.034	-2.803	-1.420	0.197	-0.317
1.001	2.3730	0.016	-0.002	0.022	-0.982	-0.498	-0.552	-0.304	0.098	-0.074
1.501	3.5590	-0.013	-0.002	0.011	-0.023	-0.009	-0.035	0.017	0.006	0.018
2.001	4.7440	-0.009	-0.002	0.009	-0.036	0.080	-0.238	0.003	-0.148	-0.086

r		(1/cm ²)			(1/cm ² x1000)					
(cm)	(δ)	U _{yy}	V _{yy}	W _{yy}	u ² _{yy}	v ² _{yy}	w ² _{yy}	-uv _{yy}	-uw _{yy}	-vw _{yy}
0.009	0.0216	-1167.00	103.30	156.10	3407	-4333	-16200	-24080.0	-9679	326
0.013	0.0311	-970.30	74.61	83.41	14210	-3189	-10170	-13940.0	-5254	536
0.017	0.0405	-748.40	39.26	41.59	18130	-2679	-6152	-6846.0	-1696	459
0.023	0.0548	-368.60	-26.36	36.74	11090	-3099	-3912	-1899.0	2019.0	-193.4
0.029	0.0690	-215.20	-6.14	-13.87	10730	-1843	-2445	-12.76	1033.00	-75.05
0.036	0.0856	-96.12	3.36	-0.54	6850.0	-1655.0	-1404.0	-486.40	327.10	-104.00
0.046	0.1093	-43.16	0.17	3.43	3992.0	-848.2	-233.4	-246.20	138.90	10.48
0.061	0.1449	-17.54	-0.75	2.71	990.1	-147.2	108.4	57.63	-43.02	23.85
0.081	0.1923	-6.63	0.59	0.78	264.6	-16.0	41.5	59.61	0.19	6.94
0.126	0.2990	-3.06	-0.66	0.24	57.0	-24.2	-8.9	11.76	26.97	-15.61
0.201	0.4768	-2.08	-0.29	0.35	9.4	-17.9	-14.7	-5.27	15.98	-9.06
0.301	0.7138	-2.32	0.07	0.27	22.6	6.3	15.1	4.65	2.93	-2.40
0.401	0.9509	-1.24	0.01	-0.08	26.2	11.5	17.3	7.87	-1.44	1.55
0.601	1.4250	-0.32	-0.01	-0.06	8.8	3.9	5.7	2.85	-0.24	0.72
1.001	2.3730	-0.06	-0.00	-0.02	2.2	1.1	1.2	0.73	-0.20	0.22
1.501	3.5590	0.00	0.01	-0.00	0.0	0.1	-0.1	0.04	-0.07	-0.03
2.001	4.7440	0.01	0.00	-0.00	-0.0	0.2	-0.4	-0.04	-0.34	-0.23

Table 36. Boundary-layer y-derivatives at $x/L = 0.400$, $\phi = 100^\circ$.

$x/L = 0.400$ $\alpha = 10 \text{ deg.}$
 $Re = 4.2E+06$ $\phi = 110 \text{ deg.}$
Derivatives in Local-Freestream Coordinates

r		(1/cm)			(1/cm x1000)					
(cm)	(/δ)	U _y	V _y	W _y	u ² _y	v ² _y	w ² _y	uv _y	uw _y	vw _y
0.008	0.0159	18.510	-0.168	0.111	-369.500	67.560	171.600	127.60	-6.22	-10.35
0.012	0.0242	14.540	-0.082	-0.124	-392.200	67.940	117.000	83.18	-8.13	-4.60
0.016	0.0326	11.180	0.027	-0.153	-378.600	66.260	80.360	49.29	-11.58	-1.85
0.022	0.0451	7.395	0.081	-0.102	-325.100	59.590	42.420	16.40	-9.43	-1.78
0.028	0.0576	5.191	0.023	-0.072	-261.300	46.380	20.760	4.62	-7.15	-0.83
0.035	0.0723	3.684	0.034	-0.060	-183.500	31.950	6.352	-1.773	-2.939	-1.532
0.045	0.0932	2.613	0.012	-0.150	-115.700	16.110	-2.910	-4.340	-0.275	0.240
0.060	0.1245	1.923	0.030	-0.127	-63.550	7.235	-6.381	-5.488	-0.828	1.178
0.080	0.1662	1.532	-0.014	-0.106	-30.940	1.486	-5.738	-4.094	0.704	0.422
0.125	0.2602	1.156	0.022	-0.054	-16.670	-2.024	-5.712	-3.772	-0.394	0.259
0.200	0.4169	0.888	0.016	-0.036	-12.190	-3.798	-6.198	-3.487	-0.584	0.230
0.300	0.6257	0.672	0.020	-0.000	-11.050	-4.346	-7.083	-3.409	-0.410	0.014
0.400	0.8346	0.497	0.020	0.026	-10.150	-4.350	-6.889	-3.167	-0.181	-0.270
0.599	1.2520	0.190	0.009	0.033	-5.196	-2.330	-3.355	-1.663	0.022	-0.277
1.000	2.0880	0.033	0.001	0.020	-1.414	-0.685	-0.818	-0.426	0.058	-0.065
1.500	3.1320	-0.011	0.001	0.010	-0.022	-0.026	-0.005	0.007	0.006	0.027
1.999	4.1760	-0.006	-0.003	0.000	-0.007	0.058	-0.222	-0.038	-0.136	-0.020

r		(1/cm ²)			(1/cm ² x1000)					
(cm)	(/δ)	U _{yy}	V _{yy}	W _{yy}	u ² _{yy}	v ² _{yy}	w ² _{yy}	-uv _{yy}	-uw _{yy}	-vw _{yy}
0.008	0.0159	-1061.00	9.18	-97.72	-11900	304	-16570	-12460.0	151	1918
0.012	0.0242	-916.00	29.35	-25.07	-90	-144	-10950	-9742.0	-912	994
0.016	0.0326	-743.20	24.78	15.45	7827	-770	-6906	-6855.0	-798	298
0.022	0.0451	-432.70	-28.42	16.01	12410	-2045	-3792	-2203.0	1578.0	-315.5
0.028	0.0576	-228.40	6.09	-2.62	11540	-2397	-2838	-977.70	365.60	48.73
0.035	0.0723	-114.40	-0.99	-9.87	7236.0	-1676.0	-664.1	-322.80	208.60	196.00
0.045	0.0932	-46.94	-0.29	2.99	3749.0	-570.4	-291.6	-49.11	54.54	43.32
0.060	0.1245	-16.03	-1.16	0.87	1240.0	-237.0	24.5	55.66	25.48	-26.41
0.080	0.1662	-7.95	0.77	1.07	26.5	-69.2	7.9	3.80	-19.70	-3.32
0.125	0.2602	-3.65	-0.21	0.19	60.6	-21.2	-10.8	5.73	-2.71	0.96
0.200	0.4169	-2.09	0.07	0.34	6.6	-11.5	-19.7	-0.50	1.54	-1.93
0.300	0.6257	-1.81	0.03	0.32	8.8	1.0	4.4	1.85	2.54	-3.34
0.400	0.8346	-1.32	-0.06	-0.01	23.6	9.7	16.5	7.38	0.72	0.39
0.599	1.2520	-0.40	-0.02	-0.03	10.0	4.3	6.7	3.30	0.12	0.62
1.000	2.0880	-0.10	0.00	-0.02	3.1	1.5	1.9	0.99	-0.10	0.21
1.500	3.1320	0.01	0.01	-0.01	0.3	0.3	0.0	0.02	-0.12	-0.02
1.999	4.1760	0.01	-0.01	-0.02	-0.0	0.1	-0.5	-0.10	-0.31	-0.10

Table 37. Boundary-layer y-derivatives at $x/L = 0.400$, $\phi = 110^\circ$.

$x/L = 0.400$ $\alpha = 10 \text{ deg.}$
 $Re = 4.2E+06$ $\phi = 120 \text{ deg.}$
Derivatives in Local-Freestream Coordinates

r		(1/cm)			(1/cm x1000)					
(cm)	(δ)	U _y	V _y	W _y	u ² _y	v ² _y	w ² _y	uv _y	uw _y	vw _y
0.006	0.0123	25.080	-0.078	-0.061	105.500	51.030	103.900	128.90	110.30	-9.28
0.010	0.0199	18.740	0.011	0.011	-115.200	69.900	104.900	91.56	57.75	-1.32
0.014	0.0275	13.830	0.072	0.015	-242.700	71.400	89.560	58.28	31.52	0.30
0.021	0.0389	8.458	0.081	-0.006	-319.000	60.630	59.010	21.84	9.86	-0.55
0.026	0.0503	5.575	0.065	-0.026	-270.800	45.800	30.430	4.49	5.99	-1.13
0.034	0.0636	3.826	0.034	-0.045	-196.500	29.300	8.413	-4.949	2.570	-1.594
0.043	0.0825	2.647	0.009	-0.080	-119.400	18.440	-0.597	-6.704	-1.129	0.396
0.058	0.1110	1.974	0.020	-0.108	-63.740	9.349	-5.864	-4.400	0.021	0.225
0.079	0.1490	1.438	0.021	-0.100	-30.470	2.685	-5.233	-2.174	-0.321	-0.102
0.123	0.2343	1.086	0.040	-0.084	-14.660	-1.038	-4.679	-2.568	0.119	-0.291
0.198	0.3766	0.850	0.017	-0.066	-10.890	-3.076	-5.156	-3.094	0.037	-0.058
0.298	0.5664	0.685	0.012	-0.031	-9.994	-4.003	-6.477	-3.068	-0.189	-0.028
0.398	0.7561	0.547	0.017	0.003	-10.020	-4.253	-6.777	-3.026	-0.432	-0.060
0.599	1.1360	0.246	0.014	0.022	-5.831	-2.520	-3.843	-1.778	-0.099	-0.151
0.999	1.8950	0.054	0.007	0.018	-1.810	-0.827	-1.093	-0.542	0.018	-0.051
1.498	2.8430	-0.012	0.004	0.010	-0.045	-0.050	-0.026	0.000	0.001	0.008
1.998	3.7920	-0.006	0.003	0.001	0.003	0.067	-0.157	-0.023	-0.085	-0.024

r		(1/cm ²)			(1/cm ² x1000)					
(cm)	(δ)	U _{yy}	V _{yy}	W _{yy}	u ² _{yy}	v ² _{yy}	w ² _{yy}	-uv _{yy}	-uw _{yy}	-vw _{yy}
0.006	0.0123	-1799.00	24.28	30.44	-69060	7763	3233	-9582.0	-17740	3172
0.010	0.0199	-1383.00	19.29	6.89	-41970	2010	-2380	-8967.0	-9052	963
0.014	0.0275	-1027.00	9.81	-6.51	-19060	-1701	-5666	-7497.0	-3394	-304
0.021	0.0389	-605.60	-12.79	-7.60	7460	-3440	-6231	-3689.0	-580.3	-440.9
0.026	0.0503	-260.80	-0.79	2.05	12350	-2171	-3301	-1328.00	-961.00	115.60
0.034	0.0636	-119.50	-3.24	-6.14	7688.0	-1239.0	-868.8	-296.50	-162.70	170.70
0.043	0.0825	-48.72	0.26	-2.01	4075.0	-647.9	-442.1	260.10	65.83	-28.74
0.058	0.1110	-21.05	0.44	0.71	1289.0	-254.9	54.2	74.10	-21.86	-8.52
0.079	0.1490	-7.20	0.27	0.22	282.1	-76.6	8.8	-17.50	15.73	-4.47
0.123	0.2343	-3.27	-0.38	0.21	55.7	-25.4	-7.5	-4.26	-3.02	4.25
0.198	0.3766	-1.60	-0.15	0.41	10.2	-13.9	-21.1	2.30	-5.30	1.70
0.298	0.5664	-1.37	0.10	0.35	-2.8	-2.3	-2.6	-1.14	-0.98	-1.14
0.398	0.7561	-1.36	-0.03	0.06	21.3	8.8	14.8	6.48	1.36	-0.13
0.599	1.1360	-0.50	-0.02	-0.01	10.9	4.5	7.4	3.41	0.31	0.31
0.999	1.8950	-0.15	-0.01	-0.02	3.9	1.7	2.4	1.23	-0.02	0.13
1.498	2.8430	-0.01	0.01	-0.01	0.7	0.5	0.3	0.10	-0.13	0.02
1.998	3.7920	0.02	-0.00	-0.02	0.0	0.2	-0.3	-0.07	-0.18	-0.07

Table 38. Boundary-layer y-derivatives at $x/L = 0.400$, $\phi = 120^\circ$.

$x/L = 0.400$ $\alpha = 10 \text{ deg.}$
 $Re = 4.2E+06$ $\phi = 130 \text{ deg.}$
Derivatives in Local-Freestream Coordinates

r		(1/cm)			(1/cm x1000)					
(cm)	(δ)	U _y	V _y	W _y	u ² _y	v ² _y	w ² _y	uv _y	uw _y	vw _y
0.005	0.0090	24.570	-0.492	1.631	883.000	60.850	166.500	203.80	18.18	7.32
0.009	0.0158	18.630	-0.179	0.901	316.100	60.680	125.800	121.10	22.99	2.25
0.013	0.0226	13.900	-0.044	0.461	-11.690	60.700	97.560	71.14	20.61	1.72
0.019	0.0328	8.718	0.083	0.152	-263.700	56.130	61.740	22.31	13.45	1.59
0.025	0.0431	6.157	0.152	0.009	-267.600	47.170	35.210	6.58	8.74	1.48
0.032	0.0550	4.080	0.149	0.023	-206.500	33.860	14.050	-4.102	6.742	-0.080
0.042	0.0720	2.697	0.128	-0.032	-131.300	20.030	-0.833	-6.786	5.863	-1.955
0.057	0.0975	1.836	0.009	-0.073	-63.840	9.888	-5.495	-2.642	2.678	-0.706
0.077	0.1315	1.463	0.040	-0.050	-29.060	4.825	-5.183	-1.095	-0.408	-0.274
0.122	0.2081	1.077	0.049	-0.076	-13.730	0.509	-3.586	-1.993	0.772	-0.202
0.197	0.3358	0.842	0.044	-0.070	-8.363	-1.594	-3.562	-2.055	0.280	-0.112
0.297	0.5059	0.673	0.022	-0.058	-8.444	-3.353	-5.072	-2.508	0.035	0.040
0.397	0.6761	0.558	0.015	-0.033	-9.452	-4.024	-6.170	-2.753	-0.228	0.021
0.597	1.0160	0.274	0.010	-0.001	-6.187	-2.811	-4.041	-1.858	-0.059	-0.080
0.997	1.6970	0.075	0.009	0.012	-2.194	-0.978	-1.417	-0.672	-0.035	-0.050
1.497	2.5480	-0.005	0.011	0.010	0.022	0.163	-0.036	0.065	-0.016	0.024
1.997	3.3990	0.000	0.016	0.005	0.245	0.532	0.078	0.311	-0.054	0.042

r		(1/cm ²)			(1/cm ² x1000)					
(cm)	(δ)	U _{yy}	V _{yy}	W _{yy}	u ² _{yy}	v ² _{yy}	w ² _{yy}	-uv _{yy}	-uw _{yy}	-vw _{yy}
0.005	0.0090	-1643.00	112.30	-228.60	-180200	-247	-12510	-26190.0	2505	-2162
0.009	0.0158	-1326.00	48.74	-139.80	-106300	80	-8158	-15700.0	61	-507
0.013	0.0226	-998.10	14.94	-72.32	-51020	-92	-5644	-8395.0	-1433	343
0.019	0.0328	-485.40	20.09	-10.77	-2992	-1287	-5311	-3422.0	-1893.0	104.1
0.025	0.0431	-328.50	1.68	-5.31	8189	-2327	-3722	-2162.00	309.60	-404.10
0.032	0.0550	-144.00	-3.28	-4.23	8946.0	-1316.0	-1244.0	73.68	-231.70	-152.00
0.042	0.0720	-58.09	-10.34	-2.88	4635.0	-768.4	-427.8	261.90	-296.00	117.30
0.057	0.0975	-15.56	1.90	0.66	1298.0	-199.8	42.4	40.81	-80.79	8.80
0.077	0.1315	-8.01	0.10	-0.52	307.3	-84.5	36.7	-15.51	22.17	1.53
0.122	0.2081	-3.26	-0.17	0.10	66.5	-29.6	-3.5	-1.64	-9.42	2.11
0.197	0.3358	-1.73	-0.23	0.03	-0.1	-22.6	-18.3	-4.02	-3.13	2.21
0.297	0.5059	-1.15	-0.08	0.27	-11.6	-6.7	-11.4	-3.42	-1.76	-0.33
0.397	0.6761	-1.29	-0.02	0.13	17.4	6.8	11.6	4.92	0.63	-0.40
0.597	1.0160	-0.53	-0.00	0.03	11.1	5.0	7.3	3.25	0.12	0.11
0.997	1.6970	-0.18	0.00	-0.00	4.8	2.4	3.0	1.59	0.06	0.15
1.497	2.5480	-0.04	0.00	-0.01	1.7	1.3	0.9	0.70	-0.08	0.16
1.997	3.3990	0.02	0.01	-0.01	0.3	0.7	0.1	0.46	-0.08	0.02

Table 39. Boundary-layer y-derivatives at $x/L = 0.400$, $\phi = 130^\circ$.

$$x/L = 0.400 \quad \alpha = 10 \text{ deg.}$$

$$Re = 4.2E+06 \quad \phi = 140 \text{ deg.}$$

Derivatives in Local-Freestream Coordinates

r		(1/cm)			(1/cm x1000)					
(cm)	(/δ)	U _y	V _y	W _y	u ² _y	v ² _y	w ² _y	uv _y	uw _y	vw _y
0.008	0.0127	20.350	-0.845	0.303	168.500	74.150	142.600	140.70	30.30	3.31
0.012	0.0188	15.050	-0.206	0.572	-51.060	67.730	110.400	88.18	25.31	3.56
0.016	0.0249	11.120	-0.032	0.494	-164.600	62.760	83.980	53.29	24.84	2.83
0.022	0.0341	6.866	0.087	0.259	-234.000	51.810	47.140	17.40	21.63	0.40
0.028	0.0432	4.824	0.037	0.183	-200.400	40.920	21.740	4.06	14.91	0.27
0.035	0.0539	3.374	0.036	-0.027	-159.400	28.740	4.734	-4.941	8.330	-1.738
0.045	0.0692	2.380	0.082	-0.013	-114.000	16.760	-2.119	-7.774	4.308	-2.392
0.060	0.0921	1.740	-0.045	-0.077	-68.480	8.120	-2.875	-5.857	4.007	-1.649
0.080	0.1226	1.337	0.006	-0.031	-30.980	2.821	-5.032	-3.818	2.018	-0.981
0.125	0.1913	1.006	0.040	-0.062	-13.360	-0.396	-3.605	-2.710	0.209	-0.517
0.200	0.3059	0.812	0.055	-0.074	-7.906	-1.830	-3.468	-2.040	0.166	-0.335
0.300	0.4586	0.655	0.041	-0.079	-7.974	-3.001	-4.458	-2.133	0.015	-0.082
0.400	0.6113	0.544	0.035	-0.062	-8.537	-3.355	-5.611	-2.197	-0.180	0.123
0.600	0.9167	0.290	0.017	-0.024	-6.108	-2.640	-4.043	-1.668	-0.174	0.023
1.000	1.5270	0.092	0.012	0.003	-2.346	-1.086	-1.606	-0.676	-0.071	0.002
1.500	2.2910	-0.003	0.013	0.009	-0.149	-0.013	-0.099	-0.048	0.003	-0.005
2.001	3.0550	-0.004	0.013	0.001	0.002	0.190	0.083	0.040	0.007	-0.037

r		(1/cm ²)			(1/cm ² x1000)					
(cm)	(/δ)	U _{yy}	V _{yy}	W _{yy}	u ² _{yy}	v ² _{yy}	w ² _{yy}	-uv _{yy}	-uw _{yy}	-vw _{yy}
0.008	0.0127	-1529.00	249.50	138.50	-71860	-2055	-9144	-16000.0	-2311	249
0.012	0.0188	-1130.00	83.09	7.53	-39230	-1273	-7092	-10520.0	-399	-99
0.016	0.0249	-797.60	-7.09	-53.99	-14630	-1202	-5986	-6444.0	239	-288
0.022	0.0341	-421.70	0.52	-16.04	7224	-2424	3097	-2959.0	-1191.0	-272.7
0.028	0.0432	-223.00	3.27	-29.34	5112	-1822	-2665	-1562.00	-1486.00	-177.30
0.035	0.0539	-97.66	2.25	-0.38	5086.0	-1164.0	-450.1	-149.80	-145.10	-128.30
0.045	0.0692	-48.28	-10.35	-4.27	3334.0	-706.6	-154.8	114.70	-45.02	69.33
0.060	0.0921	-15.74	2.57	1.70	1447.0	-186.8	-61.4	84.98	-100.40	32.10
0.080	0.1226	-6.77	0.72	-0.74	337.3	-65.6	36.3	22.06	-27.63	5.34
0.125	0.1913	-2.74	0.13	-0.22	71.9	-20.2	0.4	10.06	-0.88	4.14
0.200	0.3059	-1.58	-0.17	-0.12	-4.9	-13.8	-11.7	-1.69	-1.18	2.77
0.300	0.4586	-1.12	-0.06	0.17	-6.3	-4.2	-11.7	-1.16	-2.09	1.82
0.400	0.6113	-1.16	-0.08	0.18	13.4	4.4	8.9	3.09	0.21	-0.48
0.600	0.9167	-0.53	-0.01	0.07	10.4	4.3	6.8	2.73	0.31	-0.07
1.000	1.5270	-0.20	0.00	0.01	4.7	2.2	3.2	1.32	0.16	-0.03
1.500	2.2910	-0.08	0.01	-0.00	2.5	1.4	1.5	0.81	0.03	0.09
2.001	3.0550	0.01	-0.00	-0.02	0.0	0.3	0.2	0.09	0.01	-0.09

Table 40. Boundary-layer y-derivatives at $x/L = 0.400$, $\phi = 140^\circ$.

$x/L = 0.400$ $\alpha = 10 \text{ deg.}$
 $Re = 4.2E+06$ $\phi = 150 \text{ deg.}$
Derivatives in Local-Freestream Coordinates

r		(1/cm)			(1/cm x1000)					
(cm)	(δ)	U _y	V _y	W _y	u ² _y	v ² _y	w ² _y	uv _y	uw _y	vw _y
0.006	0.0082	21.820	-0.485	1.789	717.800	52.590	142.600	174.60	-4.10	9.97
0.010	0.0138	17.320	-0.185	1.185	244.300	55.340	123.600	107.50	9.46	7.30
0.014	0.0194	13.360	-0.058	0.787	-34.120	56.400	98.550	64.45	20.70	3.35
0.020	0.0279	8.742	0.015	0.398	-250.700	53.540	63.450	23.98	27.40	-0.78
0.026	0.0363	5.969	0.078	0.235	-253.000	43.650	35.160	6.03	21.04	-1.12
0.033	0.0462	4.031	0.014	0.121	-205.700	32.620	13.260	-1.309	13.800	-1.534
0.043	0.0602	2.747	0.025	0.027	-136.900	19.200	1.173	-6.342	5.090	-0.582
0.058	0.0813	1.810	-0.028	-0.013	-69.880	10.370	-4.413	-4.340	2.700	-1.510
0.078	0.1095	1.361	0.017	-0.016	-27.740	3.765	-5.073	-3.021	0.549	-1.446
0.123	0.1728	1.012	0.029	-0.047	-12.340	0.163	-3.600	-2.123	0.593	-0.520
0.198	0.2783	0.795	0.046	-0.068	-7.478	-1.382	-3.178	-1.542	0.398	-0.267
0.298	0.4190	0.629	0.035	-0.079	-7.551	-2.327	-3.813	-1.499	0.188	-0.022
0.398	0.5597	0.528	0.027	-0.072	-7.937	-3.078	-4.912	-1.839	-0.134	0.051
0.598	0.8410	0.309	0.012	-0.033	-6.256	-2.717	-4.076	-1.749	-0.166	0.099
0.998	1.4040	0.109	0.011	-0.003	-2.639	-1.191	-1.780	-0.804	-0.073	-0.014
1.498	2.1070	-0.001	0.017	0.006	-0.194	-0.052	-0.140	-0.061	-0.000	0.001
1.998	2.8110	-0.009	0.022	0.001	0.028	0.114	0.003	0.040	-0.003	0.005

r		(1/cm ²)			(1/cm ² x1000)					
(cm)	(δ)	U _{yy}	V _{yy}	W _{yy}	u ² _{yy}	v ² _{yy}	w ² _{yy}	-uv _{yy}	-uw _{yy}	-vw _{yy}
0.006	0.0082	-1180.00	108.40	-183.70	-149400	804	-3396	-20720.0	3334	-290
0.010	0.0138	-1064.00	46.52	-120.70	-89710	523	-5849	-13170.0	3276	-951
0.014	0.0194	-897.30	12.99	-72.84	-44070	-67	-6789	-7718.0	2222	-1035
0.020	0.0279	-551.00	15.84	-29.51	-1942	-1528	-5362	-3465.0	-1226.0	-80.2
0.026	0.0363	-297.30	-10.86	-19.98	5979	-1818	-3568	-1406.00	-1298.00	1.16
0.033	0.0462	-130.70	1.79	-8.86	8012.0	-1395.0	-1229.0	-422.70	-813.50	76.14
0.043	0.0602	-69.07	-4.83	-2.93	4785.0	-604.3	-350.5	178.30	-179.20	-76.69
0.058	0.0813	-17.22	2.00	-0.18	1572.0	-267.2	-21.3	46.16	-76.74	8.84
0.078	0.1095	-7.07	0.27	-0.70	289.6	-68.4	36.4	18.12	3.53	21.30
0.123	0.1728	-3.20	0.18	-0.28	62.4	-18.0	6.6	10.79	-2.34	0.09
0.198	0.2783	-1.76	-0.04	-0.23	-0.4	-11.8	-6.7	1.65	-3.31	4.09
0.298	0.4190	-0.98	-0.12	0.08	-5.9	-7.7	-11.5	-4.35	-2.74	1.09
0.398	0.5597	-1.01	-0.06	0.18	10.1	2.9	5.6	1.33	0.00	-0.13
0.598	0.8410	-0.54	0.00	0.08	10.1	4.3	6.6	2.70	0.28	-0.24
0.998	1.4040	-0.23	0.01	0.02	5.1	2.4	3.5	1.55	0.15	0.03
1.498	2.1070	-0.12	0.01	0.00	3.2	1.6	2.1	1.07	0.09	0.04
1.998	2.8110	-0.00	0.01	-0.01	0.1	0.2	0.1	0.09	-0.02	0.00

Table 41. Boundary-layer y-derivatives at $x/L = 0.400$, $\phi = 150^\circ$.

$x/L = 0.400$ $\alpha = 10 \text{ deg.}$
 $Re = 4.2E-06$ $\phi = 160 \text{ deg.}$

Derivatives in Local-Freestream Coordinates

r		(1/cm)			(1/cm x1000)					
(cm)	(δ)	U _y	V _y	W _y	u ² _y	v ² _y	w ² _y	uv _y	uw _y	vw _y
0.008	0.0096	16.880	-0.553	0.712	76.520	49.670	136.200	108.10	44.15	11.09
0.012	0.0147	13.770	-0.141	0.613	-122.700	54.490	102.500	67.65	31.29	4.82
0.016	0.0197	10.900	-0.009	0.455	-218.300	56.270	76.260	43.73	24.98	1.73
0.022	0.0273	7.307	0.050	0.307	-264.700	52.010	47.370	17.16	21.89	-0.18
0.028	0.0349	5.010	0.105	0.271	-215.700	41.860	25.850	7.70	18.08	0.23
0.035	0.0438	3.121	0.102	0.191	-155.500	28.930	13.860	-2.102	15.230	0.003
0.045	0.0564	2.085	0.147	0.113	-108.100	15.610	2.016	-8.829	6.804	-1.398
0.060	0.0754	1.551	0.007	-0.022	-67.420	7.640	-5.483	-6.910	1.998	-1.643
0.080	0.1007	1.379	0.002	-0.000	-33.940	2.957	-7.959	-4.722	-0.240	-0.927
0.125	0.1576	0.997	0.025	-0.031	-12.910	0.287	-5.286	-2.213	0.309	-0.533
0.200	0.2524	0.757	0.048	-0.046	-7.060	-1.481	-3.111	-1.700	0.384	-0.550
0.300	0.3788	0.589	0.031	-0.065	-6.455	-2.331	-3.140	-1.468	0.408	-0.296
0.400	0.5053	0.501	0.021	-0.063	-6.732	-2.717	-3.904	-1.450	0.013	-0.015
0.600	0.7582	0.318	0.008	-0.040	-5.911	-2.418	-3.807	-1.466	-0.126	0.094
1.000	1.2640	0.122	0.011	-0.010	-2.791	-1.187	-1.784	-0.764	-0.060	0.031
1.499	1.8960	0.002	0.016	0.003	-0.249	-0.070	-0.189	-0.061	-0.000	0.019
1.999	2.5280	-0.010	0.019	-0.005	0.053	0.193	-0.021	0.037	-0.057	0.024

r		(1/cm ²)			(1/cm ² x1000)					
(cm)	(δ)	U _{yy}	V _{yy}	W _{yy}	u ² _{yy}	v ² _{yy}	w ² _{yy}	-uv _{yy}	-uw _{yy}	-vw _{yy}
0.008	0.0096	-793.60	156.70	-6.80	-66760	1526	-9608	-13020.0	-4333	-2088
0.012	0.0147	-756.00	56.99	-37.95	-34350	847	-7323	-7523.0	-2208	-1093
0.016	0.0197	-668.20	2.18	-41.56	-10610	-65	-5601	-4024.0	-780	-371
0.022	0.0273	-442.70	4.16	4.70	8719	-1869	-4070	-2534.0	56.8	197.2
0.028	0.0349	-312.80	6.87	-11.80	9518	-2039	-1919	-1445.00	-605.00	-34.85
0.035	0.0438	-98.26	4.17	-10.07	4846.0	-1377.0	-1187.0	-671.30	-956.70	-184.20
0.045	0.0564	-36.41	-13.40	-10.12	2800.0	-573.8	-589.6	122.40	-278.30	-4.02
0.060	0.0754	-8.45	0.80	1.13	1405.0	-177.0	-58.6	115.70	-87.45	32.39
0.080	0.1007	-8.01	0.54	-0.74	390.2	-54.4	63.8	42.76	15.85	5.39
0.125	0.1576	-3.51	0.25	-0.24	72.2	-26.2	33.9	6.37	3.10	-1.53
0.200	0.2524	-1.78	-0.14	-0.25	11.4	-9.2	-0.6	5.02	-1.59	3.44
0.300	0.3788	-0.87	-0.13	0.01	-5.0	-3.7	-8.7	-0.60	-3.08	2.90
0.400	0.5053	-0.86	-0.04	0.12	5.8	2.1	2.3	0.36	-0.50	0.19
0.600	0.7582	-0.53	0.01	0.08	9.0	3.5	5.8	2.09	0.21	-0.17
1.000	1.2640	-0.25	0.01	0.03	5.3	2.3	3.3	1.44	0.12	-0.03
1.499	1.8960	-0.16	0.01	0.01	3.8	1.8	2.5	1.19	0.14	0.03
1.999	2.5280	-0.01	0.01	-0.02	0.2	0.4	0.1	0.06	-0.15	0.01

Table 42. Boundary-layer y-derivatives at $x/L = 0.400$, $\phi = 160^\circ$.

$x/L = 0.400$ $\alpha = 10 \text{ deg.}$
 $Re = 4.2E+06$ $\phi = 170 \text{ deg.}$
Derivatives in Local-Freestream Coordinates

r		(1/cm)			(1/cm x1000)					
(cm)	(δ)	U _y	V _y	W _y	u ² _y	v ² _y	w ² _y	uv _y	uw _y	vw _y
0.006	0.0061	25.379	-0.252	0.531	366.126	52.664	190.479	125.26	-0.29	9.56
0.010	0.0105	18.949	-0.252	0.633	87.407	63.737	141.411	97.01	3.47	7.07
0.014	0.0148	14.060	-0.113	0.484	-101.690	64.773	104.941	63.31	10.67	4.60
0.020	0.0212	8.763	0.044	0.228	-247.470	59.094	63.137	24.48	14.95	2.04
0.026	0.0277	5.936	0.030	0.116	-234.264	47.615	34.164	6.20	12.24	1.60
0.033	0.0353	4.090	0.030	0.049	-186.314	33.900	13.694	-3.443	8.072	0.588
0.043	0.0461	2.788	-0.016	0.122	-112.967	20.450	-1.107	-3.077	3.108	-0.820
0.058	0.0622	1.983	0.049	0.053	-62.548	9.439	-4.570	-3.966	3.021	-1.348
0.078	0.0838	1.057	0.021	-0.014	-34.530	1.210	-8.119	-3.974	1.759	-1.229
0.123	0.1324	0.688	0.008	-0.028	-18.967	-2.130	-7.008	-3.530	0.864	-0.777
0.198	0.2133	0.582	0.007	-0.036	-11.317	-2.702	-4.912	-2.771	0.443	-0.439
0.298	0.3212	0.554	0.016	-0.033	-7.273	-2.589	-3.735	-2.102	0.182	-0.148
0.398	0.4290	0.465	0.018	-0.034	-6.794	-2.707	-4.015	-1.931	0.080	-0.035
0.598	0.6446	0.308	0.021	-0.023	-5.536	-2.306	-3.536	-1.655	-0.035	-0.053
0.998	1.0763	0.121	0.020	-0.009	-2.552	-1.089	-1.630	-0.732	-0.036	-0.004
1.498	1.6158	0.003	0.018	-0.001	-0.248	-0.139	-0.178	-0.057	0.001	0.012
1.998	2.1548	-0.004	0.016	-0.012	0.058	0.085	-0.025	-0.010	-0.023	0.011

r		(1/cm ²)			(1/cm ² x1000)					
(cm)	(δ)	U _{yy}	V _{yy}	W _{yy}	u ² _{yy}	v ² _{yy}	w ² _{yy}	-uv _{yy}	-uw _{yy}	-vw _{yy}
0.006	0.0061	-1842.46	-32.20	77.50	-81596	4529	-14314	-5358.8	-94	-554
0.010	0.0105	-1389.91	26.12	-17.80	-57763	1204	-10382	-8300.8	1709	-656
0.014	0.0148	-1007.91	45.45	-62.26	-33971	-940	-7550	-8579.2	1911	-572
0.020	0.0212	-568.87	1.35	-33.61	1642	-1944	-5383	-4000.6	-786.9	-95.3
0.026	0.0277	-288.36	-7.92	-2.61	7653	-2028	-3569	-1110.36	-808.44	-45.51
0.033	0.0353	-130.12	-1.54	6.47	7401.8	-1502.5	-1432.4	-158.38	-361.35	-233.76
0.043	0.0461	-52.74	5.54	-5.72	3934.5	-734.9	-146.0	15.27	-51.73	-11.62
0.058	0.0622	-38.51	-1.66	-2.58	990.7	-330.1	-154.8	-4.93	-44.80	9.97
0.078	0.0838	-6.20	-0.13	-0.13	317.9	-59.4	36.5	7.70	-18.56	6.71
0.123	0.1324	-1.04	0.03	-0.23	116.6	-2.4	37.5	15.36	-6.83	6.84
0.198	0.2133	-0.26	0.04	0.12	45.4	-0.3	13.0	8.34	-1.69	3.60
0.298	0.3212	-0.84	0.05	-0.02	4.1	-1.2	-3.5	0.71	-1.37	0.68
0.398	0.4290	-0.75	0.00	0.05	7.0	2.6	3.5	1.87	-0.41	0.02
0.598	0.6446	-0.51	-0.00	0.05	8.4	3.4	5.4	2.59	0.06	0.12
0.998	1.0763	-0.25	-0.00	0.02	4.7	1.9	3.0	1.39	0.08	0.03
1.498	1.6158	-0.16	-0.00	0.00	3.7	1.6	2.3	1.04	0.02	0.03
1.998	2.1548	0.00	-0.00	-0.03	0.2	0.3	0.0	-0.03	-0.05	-0.01

Table 43. Boundary-layer y-derivatives at $x/L = 0.400$, $\phi = 170^\circ$.

$x/L = 0.400$ $\alpha = 10 \text{ deg.}$
 $Re = 4.2E+06$ $\phi = 180 \text{ deg.}$
Derivatives in Local-Freestream Coordinates

r		(1/cm)			(1/cm x1000)					
(cm)	(δ)	U _y	V _y	W _y	u ² _y	v ² _y	w ² _y	uv _y	uw _y	vw _y
0.006	0.0116	19.110	-0.315	-0.202	-65.950	64.350	110.900	94.30	-32.10	0.80
0.012	0.0172	14.660	-0.005	-0.108	-182.900	60.740	97.770	57.28	-13.68	3.05
0.016	0.0229	11.010	0.066	-0.102	-234.700	56.680	79.790	33.97	-5.53	2.81
0.022	0.0313	6.988	0.034	-0.075	-249.200	49.570	49.040	14.15	0.78	0.42
0.028	0.0398	4.846	-0.007	-0.029	-213.100	39.040	24.120	5.47	-0.64	-0.44
0.035	0.0496	3.446	-0.052	-0.002	-156.900	29.070	5.674	1.802	-1.029	-0.722
0.045	0.0637	2.549	0.027	0.037	-103.400	18.290	-3.021	-2.963	-0.237	0.975
0.060	0.0849	1.830	0.029	-0.016	-58.590	9.114	-3.764	-4.336	-0.719	0.997
0.080	0.1131	1.368	-0.003	-0.016	-28.380	3.119	-5.302	-3.641	0.158	-0.078
0.125	0.1766	0.986	-0.001	-0.005	-12.780	-0.460	-4.375	-2.284	-0.142	-0.120
0.200	0.2823	0.758	0.013	0.006	-8.115	-1.796	-3.943	-1.949	-0.024	-0.030
0.300	0.4233	0.594	0.024	0.010	-7.290	-2.568	-3.791	-1.946	-0.032	-0.052
0.400	0.5644	0.494	0.027	0.010	-7.234	-2.899	-4.057	-2.169	0.051	-0.111
0.600	0.8464	0.311	0.023	0.004	-5.758	-2.408	-3.553	-1.700	0.040	-0.131
1.000	1.4100	0.118	0.019	-0.001	-2.672	-1.141	-1.628	-0.772	0.038	-0.065
1.500	2.1160	0.002	0.019	-0.005	-0.236	-0.123	-0.139	-0.057	-0.006	0.003
2.000	2.8210	0.003	0.019	-0.015	0.051	0.065	-0.001	0.027	-0.033	0.018

r		(1/cm ²)			(1/cm ² x1000)					
(cm)	(δ)	U _{yy}	V _{yy}	W _{yy}	u ² _{yy}	v ² _{yy}	w ² _{yy}	-uv _{yy}	-uw _{yy}	-vw _{yy}
0.008	0.0116	-1214.00	121.80	43.23	-39970	-890	-2490	-11450.0	6430	998
0.012	0.0172	-1010.00	38.97	7.48	-19450	-938	-4009	-7231.0	2994	177
0.016	0.0229	-789.70	-9.35	-5.90	-4681	-1110	-5114	-4042.0	823	-361
0.022	0.0313	-426.90	-17.19	15.99	6714	-1602	-5996	-1189.0	-59.9	-635.4
0.028	0.0398	-214.80	-3.57	3.36	8077	-1747	-2604	-809.50	-87.22	125.20
0.035	0.0496	-90.00	8.40	4.09	5897.0	-1031.0	-887.9	-470.60	53.01	192.30
0.045	0.0637	-52.37	-0.10	-4.28	3160.0	-680.1	-54.6	-69.10	-16.90	-38.73
0.060	0.0849	-18.86	-1.38	0.04	1176.0	-242.2	-40.4	28.64	28.50	-34.48
0.080	0.1131	-7.62	0.18	0.34	301.5	-64.4	16.2	30.51	-6.66	0.33
0.125	0.1766	-3.20	0.20	0.05	55.2	-19.8	9.6	3.43	2.27	1.00
0.200	0.2823	-1.91	0.12	0.12	9.6	-9.7	3.0	-0.41	-0.01	0.21
0.300	0.4233	-0.94	0.04	-0.00	0.7	-2.9	-3.8	-1.82	0.47	-0.73
0.400	0.5644	-0.86	-0.02	-0.03	7.9	2.9	3.6	2.54	0.02	0.00
0.600	0.8464	-0.53	-0.01	-0.01	8.8	3.6	5.5	2.65	-0.03	0.20
1.000	1.4100	-0.24	-0.00	-0.01	5.0	2.1	3.1	1.49	-0.09	0.14
1.500	2.1160	-0.14	0.00	-0.01	3.8	1.6	2.2	1.03	-0.09	0.09
2.000	2.8210	0.02	-0.00	-0.02	0.2	0.2	0.0	0.05	-0.05	0.02

Table 44. Boundary-layer y-derivatives at $x/L = 0.400$, $\phi = 180^\circ$.

$$x/L = 0.600 \quad \alpha = 10 \text{ deg.}$$

$$Re = 4.2E+06 \quad \phi = 90 \text{ deg.}$$

Derivatives in Local-Freestream Coordinates

r		(1/cm)			(1/cm x1000)					
(cm)	(/δ)	U _y	V _y	W _y	u ² _y	v ² _y	w ² _y	uv _y	uw _y	vw _y
0.006	0.0086	24.800	-0.616	-0.735	509.000	68.700	183.000	148.00	-14.00	-11.10
0.011	0.0163	17.900	-0.452	-0.461	226.000	65.700	133.000	101.00	-10.60	-7.02
0.018	0.0270	11.100	-0.261	-0.251	-21.700	57.100	78.800	52.40	-5.82	-4.44
0.026	0.0393	6.060	-0.131	-0.131	-139.000	44.700	34.500	20.10	-3.71	-2.35
0.036	0.0546	3.670	-0.055	-0.153	-167.000	26.900	5.970	-2.62	-0.57	-0.65
0.056	0.0853	2.010	-0.061	-0.132	-73.100	10.200	-6.950	-5.430	-2.150	0.594
0.096	0.1470	1.320	-0.020	-0.080	-27.700	2.200	-6.020	-3.890	-2.250	0.699
0.145	0.2230	0.960	-0.002	-0.033	-12.500	-1.080	-4.620	-2.970	-1.310	0.623
0.246	0.3770	0.730	0.000	0.005	-10.300	-3.070	-5.630	-2.850	-0.964	0.680
0.496	0.7610	0.390	0.000	0.038	-7.430	-2.800	-4.400	-2.180	-0.293	0.174
0.743	1.1400	0.199	0.004	0.040	-4.420	-1.840	-2.720	-1.300	-0.101	-0.006
0.998	1.5300	0.052	0.008	0.036	-1.640	-0.775	-0.956	-0.473	0.085	-0.098
1.500	2.3000	0.001	0.008	0.023	-0.062	-0.063	-0.049	0.003	0.001	-0.008
1.995	3.0600	-0.001	0.006	0.021	0.015	0.012	0.003	-0.005	-0.001	-0.007
2.497	3.8300	0.000	0.002	0.015	0.034	0.069	0.019	-0.028	0.003	-0.008

r		(1/cm ²)			(1/cm ² x1000)					
(cm)	(/δ)	U _{yy}	V _{yy}	W _{yy}	u ² _{yy}	v ² _{yy}	w ² _{yy}	-uv _{yy}	-uw _{yy}	-vw _{yy}
0.006	0.0086	-1470.00	30.30	65.40	-62800.0	791.0	-8640.0	-9050.0	423	1030
0.011	0.0163	-1160.00	30.50	40.70	-45100.0	-820.0	-8650.0	-8010.0	700	520
0.018	0.0270	-703.00	22.80	14.90	-21600.0	-1810.0	-6520.0	-5340.0	645	154
0.026	0.0393	-214.00	5.17	-1.85	414.0	-1670.0	-2510.0	-1680.0	141.0	191.0
0.036	0.0546	-64.80	-0.14	1.30	3850.0	-676.0	-422.0	-84.10	-55.30	42.80
0.056	0.0853	-17.70	1.37	1.42	1180.0	-206.0	38.4	48.70	-2.23	-2.92
0.096	0.1470	-6.07	0.28	0.83	225.0	-52.4	22.6	15.20	17.70	0.34
0.145	0.2230	-1.92	-0.01	0.30	13.6	-12.8	-7.1	0.70	2.83	-0.57
0.246	0.3770	-1.44	-0.00	0.17	10.3	0.1	4.0	2.13	3.10	-2.60
0.496	0.7610	-1.13	0.04	0.03	16.9	5.1	9.8	4.94	1.55	-1.27
0.743	1.1400	-0.52	0.01	-0.03	10.8	4.3	6.7	3.24	0.41	-0.13
0.998	1.5300	-0.11	0.00	-0.03	3.4	1.6	2.0	1.03	-0.19	0.19
1.500	2.3000	-0.00	-0.00	-0.01	0.2	0.2	0.1	-0.01	-0.01	0.00
1.995	3.0600	-0.00	-0.00	-0.00	0.0	0.1	0.0	-0.04	0.01	0.00
2.497	3.8300	0.00	-0.01	-0.01	0.0	0.1	0.0	-0.05	0.01	-0.00

Table 45. Boundary-layer y-derivatives at $x/L = 0.600$, $\phi = 90^\circ$.

$$x/L = 0.600 \quad \alpha = 10 \text{ deg.}$$

$$Re = 4.2E+06 \quad \phi = 100 \text{ deg.}$$

Derivatives in Local-Freestream Coordinates

r		(1/cm)			(1/cm x1000)					
(cm)	(δ)	U _y	V _y	W _y	u ² _y	v ² _y	w ² _y	uv _y	uw _y	vw _y
0.008	0.0098	19.700	-0.507	1.450	188.000	69.700	8.810	108.00	67.00	3.14
0.013	0.0164	14.700	-0.341	0.936	7.890	66.200	19.400	68.80	44.80	4.70
0.019	0.0255	9.410	-0.170	0.461	-123.000	56.000	16.700	30.90	31.50	3.04
0.028	0.0360	5.520	-0.073	0.132	-181.000	42.300	9.950	5.65	19.60	1.75
0.038	0.0491	3.180	-0.092	-0.017	-121.000	25.400	-7.130	-4.45	20.90	-1.33
0.058	0.0753	1.880	-0.062	-0.094	-55.700	9.450	-8.780	-4.310	7.640	-0.978
0.098	0.1280	1.240	-0.013	-0.113	-19.400	2.920	-7.400	-1.830	4.250	-2.520
0.147	0.1930	0.910	0.019	-0.091	-7.820	-0.439	-5.440	-1.670	2.480	-1.770
0.248	0.3240	0.695	0.015	-0.043	-7.330	-2.390	-5.070	-2.280	0.340	-0.220
0.497	0.6510	0.416	0.010	0.019	-6.830	-2.570	-4.180	-2.150	-0.349	0.193
0.747	0.9780	0.231	0.011	0.033	-4.530	-1.820	-2.840	-1.360	-0.194	0.061
1.001	1.3100	0.084	0.014	0.036	-2.160	-1.010	-1.320	-0.621	0.003	-0.029
1.497	1.9600	0.007	0.014	0.023	-0.218	-0.216	-0.111	-0.011	0.016	0.015
1.994	2.6100	0.001	0.010	0.018	0.003	-0.029	0.006	-0.015	0.006	0.022
2.498	3.2700	0.001	0.007	0.015	0.049	0.084	0.015	-0.059	0.012	0.008

r		(1/cm ²)			(1/cm ² x1000)					
(cm)	(δ)	U _{yy}	V _{yy}	W _{yy}	u ² _{yy}	v ² _{yy}	w ² _{yy}	-uv _{yy}	-uw _{yy}	-vw _{yy}
0.008	0.0098	-1080.00	35.90	-122.00	-45800.0	4.2	3940.0	-8840.0	-6000	742
0.013	0.0164	-882.00	29.60	-84.80	-26800.0	-1130.0	593.0	-6600.0	-2910	-42
0.019	0.0255	-579.00	17.10	-44.00	-7250.0	-1910.0	-1800.0	-3740.0	-471	-515
0.028	0.0360	-197.00	-2.93	-13.30	5720.0	-1620.0	-1320.0	-778.0	-308.0	-174.0
0.038	0.0491	-51.90	1.81	-2.87	2720.0	-628.0	-15.3	44.70	-523.00	2.86
0.058	0.0753	-16.70	1.48	-0.52	957.0	-162.0	22.6	75.10	-56.60	-60.80
0.098	0.1280	-5.57	0.45	0.46	168.0	-57.4	37.3	-3.25	-35.50	20.80
0.147	0.1930	-1.73	-0.04	0.43	-0.7	-12.8	2.1	-4.11	-15.40	10.80
0.248	0.3240	-1.13	-0.03	0.29	-0.6	-1.5	1.6	-0.33	-2.68	1.29
0.497	0.6510	-1.02	0.00	0.11	11.3	3.3	6.7	0.0	1.23	-0.95
0.747	0.9780	-0.56	0.01	-0.01	10.0	3.6	6.4	3.22	0.61	-0.21
1.001	1.3100	-0.17	0.00	-0.03	4.3	1.8	2.7	1.36	0.01	0.11
1.497	1.9600	-0.02	-0.01	-0.01	0.5	0.4	0.3	0.02	-0.03	0.02
1.994	2.6100	-0.00	-0.01	-0.00	0.1	0.2	0.0	-0.12	0.02	-0.00
2.498	3.2700	0.00	-0.01	-0.01	0.1	0.2	0.0	-0.09	0.01	-0.03

Table 46. Boundary-layer y-derivatives at $x/L = 0.600$, $\phi = 100^\circ$.

$x/L = 0.600$ $\alpha = 10 \text{ deg.}$
 $Re = 4.2E+06$ $\phi = 110 \text{ deg.}$
Derivatives in Local-Freestream Coordinates

r		(1/cm)			(1/cm x 1000)					
(cm)	(δ)	U _y	V _y	W _y	u ² _y	v ² _y	w ² _y	uv _y	uw _y	vw _y
0.010	0.0110	15.300	-0.160	0.702	195.000	78.500	135.000	96.60	12.20	-6.29
0.015	0.0168	12.000	-0.081	0.411	29.900	70.000	104.000	62.80	11.80	-4.78
0.022	0.0249	7.840	-0.071	0.140	-108.000	52.900	61.300	25.90	9.44	-3.38
0.029	0.0341	4.830	-0.097	-0.022	-168.000	37.700	26.400	2.87	7.26	-2.18
0.040	0.0457	2.720	-0.038	-0.082	-113.000	21.700	4.870	-3.10	3.32	-2.01
0.060	0.0688	1.740	-0.091	-0.022	-55.500	8.620	-7.500	-5.860	-1.740	-0.270
0.099	0.1150	1.360	-0.133	-0.026	-30.500	0.932	-6.160	-7.350	-2.750	1.680
0.150	0.1730	0.977	-0.044	-0.060	-15.300	-2.740	-3.640	-4.740	-0.608	0.459
0.249	0.2880	0.682	0.040	-0.072	-6.410	-2.980	-3.380	-2.080	0.266	-0.020
0.499	0.5770	0.411	0.046	-0.016	-4.310	-2.150	-3.610	-1.050	-0.091	-0.087
0.749	0.8660	0.251	0.029	0.012	-3.410	-1.400	-2.680	-0.788	-0.239	0.069
1.003	1.1600	0.109	0.019	0.029	-2.120	-0.881	-1.540	-0.431	-0.086	-0.025
1.496	1.7300	0.017	0.014	0.023	-0.392	-0.226	-0.256	-0.086	0.008	-0.016
1.998	2.3100	-0.001	0.012	0.017	0.016	-0.033	-0.008	-0.012	-0.003	-0.006
2.500	2.8900	-0.011	0.013	0.017	0.048	0.014	-0.004	-0.041	-0.002	-0.010

r		(1/cm ²)			(1/cm ² x 1000)					
(cm)	(δ)	U _{yy}	V _{yy}	W _{yy}	u ² _{yy}	v ² _{yy}	w ² _{yy}	-uv _{yy}	-uw _{yy}	-vw _{yy}
0.010	0.0110	-804.00	27.70	-74.10	-41600.0	-2650.0	-8090.0	-8900.0	-151	473
0.015	0.0168	-682.00	6.70	-50.10	-27400.0	-2630.0	-7100.0	-6660.0	-299	279
0.022	0.0249	-457.00	-6.12	-22.50	-8660.0	-2190.0	-4820.0	-3330.0	-387	87
0.029	0.0341	-175.00	4.72	-4.50	5600.0	-1440.0	-1980.0	-429.0	-335.0	45.7
0.040	0.0457	-38.10	-2.49	2.70	2290.0	-543.0	-418.0	-127.00	-219.00	82.30
0.060	0.0688	-8.45	-1.98	-0.11	573.0	-199.0	56.8	-56.10	-28.60	65.30
0.099	0.1150	-7.26	2.02	-0.73	281.0	-60.2	43.0	58.10	46.40	-28.50
0.150	0.1730	-2.21	0.52	0.05	55.8	1.4	-0.9	17.70	2.91	-2.26
0.249	0.2880	-1.06	0.01	0.25	6.0	3.5	-2.4	3.77	-2.29	0.27
0.499	0.5770	-0.83	-0.09	0.19	1.9	2.7	3.2	0.87	-0.59	0.48
0.749	0.8660	-0.56	-0.03	0.05	6.3	2.5	5.3	1.57	0.62	-0.27
1.003	1.1600	-0.21	-0.01	-0.02	4.0	1.5	2.9	0.82	0.20	0.03
1.496	1.7300	-0.04	-0.00	-0.01	1.0	0.5	0.6	0.20	-0.03	0.03
1.998	2.3100	-0.01	-0.00	-0.01	0.1	0.1	0.0	-0.04	-0.01	-0.01
2.500	2.8900	-0.02	0.00	0.00	0.1	0.1	0.0	-0.06	0.00	-0.01

Table 47. Boundary-layer y-derivatives at $x/L = 0.600$, $\phi = 110^\circ$.

$x/L = 0.600$ $\alpha = 10 \text{ deg.}$
 $Re = 4.2E+06$ $\phi = 120 \text{ deg.}$
Derivatives in Local-Freestream Coordinates

r		(1/cm)			(1/cm x1000)					
(cm)	(/δ)	U _y	V _y	W _y	u ² _y	v ² _y	w ² _y	uv _y	uw _y	vw _y
0.006	0.0061	12.900	-0.400	0.845	-83.100	34.700	88.000	52.80	18.90	0.18
0.011	0.0109	10.500	-0.098	0.633	-76.500	40.000	69.600	38.80	17.10	-1.93
0.018	0.0176	8.740	-0.086	0.434	-125.000	41.300	56.800	19.30	17.10	-2.51
0.026	0.0253	6.890	-0.098	0.250	-135.000	35.300	40.500	3.81	14.90	-2.65
0.036	0.0349	3.340	-0.153	-0.006	-132.000	20.600	6.580	-9.39	7.69	-2.16
0.056	0.0541	1.690	0.018	-0.077	-45.100	10.900	-1.830	-0.296	2.650	-1.880
0.096	0.0924	1.060	0.067	-0.086	-7.290	5.110	-1.310	3.040	1.240	-1.100
0.146	0.1400	0.842	0.027	-0.095	-4.370	0.728	-0.771	-0.014	0.941	-0.507
0.246	0.2360	0.667	0.028	-0.097	-5.180	-1.150	-1.590	-1.030	0.115	0.232
0.496	0.4760	0.466	0.023	-0.051	-5.170	-1.770	-3.050	-1.440	-0.387	0.297
0.746	0.7150	0.305	0.022	-0.016	-4.030	-1.550	-2.780	-1.170	-0.390	0.222
0.996	0.9550	0.167	0.018	0.013	-2.770	-1.210	-2.080	-0.886	-0.223	0.053
1.491	1.4300	0.039	0.020	0.021	-0.843	-0.399	-0.549	-0.218	-0.046	0.008
1.992	1.9100	0.005	0.017	0.017	-0.028	-0.035	-0.024	-0.028	0.001	0.004
2.493	2.3900	0.005	0.017	0.019	0.023	0.045	0.010	-0.031	0.004	0.000

r		(1/cm ²)			(1/cm ² x1000)					
(cm)	(/δ)	U _{yy}	V _{yy}	W _{yy}	u ² _{yy}	v ² _{yy}	w ² _{yy}	-uv _{yy}	-uw _{yy}	-vw _{yy}
0.006	0.0061	-21.10	97.00	-12.20	268.0	6400.0	3840.0	2800.0	1430	-871
0.011	0.0109	-184.00	19.60	-24.40	-5730.0	1350.0	-551.0	-1690.0	299	-215
0.018	0.0176	-336.00	-23.80	-34.20	-8610.0	-1470.0	-3620.0	-4340.0	-433	107
0.026	0.0253	-298.00	1.19	-20.50	2890.0	-1240.0	-2690.0	-557.0	-634.0	14.0
0.036	0.0349	-64.30	7.39	-2.39	3570.0	-385.0	-270.0	403.00	-199.00	17.30
0.056	0.0541	-15.30	0.79	-0.16	881.0	-163.0	18.3	46.70	-31.50	24.90
0.096	0.0924	-3.72	-0.74	-0.18	33.3	-73.5	8.5	-52.10	-4.44	9.42
0.146	0.1400	-1.40	0.04	0.05	-5.7	-11.9	-8.7	-6.09	-6.81	5.13
0.246	0.2360	-0.81	-0.04	0.18	0.3	-2.9	-7.4	-2.19	-2.28	0.31
0.496	0.4760	-0.70	-0.02	0.22	2.0	-0.5	-1.9	-0.11	-0.29	-0.54
0.746	0.7150	-0.59	-0.00	0.10	6.0	1.9	4.1	1.74	0.76	-0.58
0.996	0.9550	-0.30	0.00	0.02	4.6	1.9	3.6	1.56	0.42	-0.10
1.491	1.4300	-0.08	-0.01	-0.01	1.9	0.8	1.2	0.45	0.12	-0.02
1.992	1.9100	-0.02	-0.01	-0.00	0.6	0.4	0.3	0.10	-0.01	0.02
2.493	2.3900	0.00	0.00	0.00	0.1	0.1	0.0	-0.02	0.01	-0.01

Table 48. Boundary-layer y-derivatives at $x/L = 0.600$, $\phi = 120^\circ$.

$$x/L = 0.600 \quad \alpha = 10 \text{ deg.}$$

$$Re = 4.2E+06 \quad \phi = 130 \text{ deg.}$$

Derivatives in Local-Freestream Coordinates

r		(1/cm)			(1/cm x1000)					
(cm)	(δ)	U _y	V _y	W _y	u ² _y	v ² _y	w ² _y	uv _y	uw _y	vw _y
0.007	0.0055	17.200	-0.101	2.010	249.000	41.400	116.000	76.20	15.50	8.77
0.012	0.0095	13.000	-0.104	1.500	74.700	41.600	85.700	50.00	22.80	2.81
0.019	0.0152	8.690	-0.131	0.954	-70.100	38.000	53.200	21.80	27.30	-1.56
0.027	0.0217	5.370	-0.118	0.540	-137.000	31.600	27.900	3.99	26.10	-3.05
0.037	0.0299	2.970	-0.057	0.235	-101.000	21.600	9.420	-0.66	14.80	-2.39
0.057	0.0462	1.610	0.029	0.035	-39.000	11.100	0.793	0.879	6.350	-1.410
0.097	0.0787	1.040	0.034	-0.045	-11.900	4.220	-1.460	0.907	2.240	-1.280
0.146	0.1190	0.764	0.026	-0.086	-4.890	0.989	-0.869	-0.332	1.230	-0.928
0.247	0.2010	0.594	0.030	-0.104	-2.400	-0.177	-0.547	-0.517	0.373	-0.246
0.496	0.4040	0.462	0.034	-0.087	-3.260	-1.060	-1.770	-0.904	-0.128	0.180
0.747	0.6080	0.346	0.030	-0.052	-3.530	-1.330	-2.260	-0.996	-0.311	0.235
0.997	0.8120	0.235	0.025	-0.017	-3.420	-1.390	-2.310	-0.980	-0.350	0.195
1.498	1.2200	0.082	0.018	0.014	-1.570	-0.674	-1.050	-0.444	-0.136	0.041
2.002	1.6300	0.006	0.015	0.018	-0.113	-0.079	-0.075	-0.032	-0.004	-0.010
2.493	2.0300	0.001	0.016	0.020	0.032	0.033	0.012	-0.024	0.005	-0.020

r		(1/cm ²)			(1/cm ² x1000)					
(cm)	(δ)	U _{yy}	V _{yy}	W _{yy}	u ² _{yy}	v ² _{yy}	w ² _{yy}	-uv _{yy}	-uw _{yy}	-vw _{yy}
0.007	0.0055	-868.00	3.06	-107.00	-40900.0	862.0	-5810.0	-5050.0	2050	-1480
0.012	0.0095	-712.00	-3.69	-88.90	-27300.0	-197.0	-5180.0	-4610.0	1110	-870
0.019	0.0152	-489.00	-4.24	-61.80	-11300.0	-980.0	-3880.0	-3180.0	-8	-277
0.027	0.0217	-207.00	7.65	-26.10	4400.0	-931.0	-1550.0	-174.0	-1110.0	110.0
0.037	0.0299	-53.10	3.21	-8.09	2510.0	-441.0	-323.0	55.40	-328.00	27.20
0.057	0.0462	-14.50	-0.14	-1.93	648.0	-187.0	-62.3	-14.60	-102.00	1.82
0.097	0.0787	-4.67	-0.10	-0.68	115.0	-51.4	15.4	-17.90	-18.30	8.02
0.146	0.1190	-1.23	0.04	-0.10	13.0	-8.0	-0.2	-1.57	-5.79	5.03
0.247	0.2010	-0.53	0.02	0.06	-3.8	-3.9	-5.3	-1.48	-2.20	1.86
0.496	0.4040	-0.41	-0.02	0.14	-5.0	-2.9	-5.6	-1.73	-1.70	0.80
0.747	0.6080	-0.48	-0.02	0.15	1.3	0.2	0.6	0.36	0.08	-0.34
0.997	0.8120	-0.36	-0.02	0.07	4.4	1.7	3.1	1.31	0.53	-0.37
1.498	1.2200	-0.17	-0.01	0.01	3.1	1.3	2.1	0.90	0.30	-0.13
2.002	1.6300	-0.09	-0.00	-0.01	2.2	0.9	1.3	0.55	0.11	0.01
2.493	2.0300	-0.00	0.00	0.00	0.1	0.1	0.0	-0.04	0.01	-0.02

Table 49. Boundary-layer y-derivatives at $x/L = 0.600$, $\phi = 130^\circ$.

$x/L = 0.600$ $\alpha = 10 \text{ deg.}$
 $Re = 4.2E+06$ $\phi = 140 \text{ deg.}$

Derivatives in Local-Freestream Coordinates

r		(1/cm)			(1/cm x1000)					
(cm)	(δ)	U _y	V _y	W _y	u ² _y	v ² _y	w ² _y	uv _y	uw _y	vw _y
0.008	0.0053	15.500	0.056	2.600	243.000	33.800	119.000	58.50	-6.30	5.41
0.013	0.0086	11.700	-0.082	1.950	84.000	37.400	79.600	41.90	10.30	3.67
0.020	0.0133	7.670	-0.132	1.240	-41.700	35.200	45.000	22.60	22.10	1.08
0.028	0.0187	4.650	-0.109	0.694	-103.000	29.000	21.900	8.63	26.60	-0.91
0.038	0.0254	2.650	-0.038	0.326	-77.300	18.700	7.610	1.47	18.10	-2.08
0.058	0.0389	1.530	0.014	0.129	-39.500	8.030	-0.666	-1.320	9.150	-2.100
0.098	0.0658	0.976	0.017	0.035	-15.900	3.270	-2.440	-0.619	3.690	-1.510
0.148	0.0994	0.702	-0.022	-0.021	-5.150	1.310	-0.781	-0.253	1.440	-0.998
0.248	0.1670	0.532	0.028	-0.077	-1.080	0.401	0.105	-0.235	0.499	-0.476
0.498	0.3350	0.423	0.031	-0.096	-1.690	-0.519	-0.740	-0.499	0.169	-0.017
0.747	0.5030	0.349	0.033	-0.077	-2.440	-0.941	-1.510	-0.701	-0.092	0.147
0.997	0.6710	0.280	0.033	-0.049	-3.020	-1.190	-2.040	-0.817	-0.275	0.228
1.501	1.0100	0.134	0.025	-0.002	-2.040	-0.803	-1.370	-0.574	-0.236	0.109
1.991	1.3400	0.016	0.016	0.018	-0.315	-0.173	-0.206	-0.096	-0.016	0.000
2.496	1.6800	-0.012	0.016	0.019	0.184	0.137	0.089	0.017	0.000	-0.011

r		(1/cm ²)			(1/cm ² x1000)					
(cm)	(δ)	U _{yy}	V _{yy}	W _{yy}	u ² _{yy}	v ² _{yy}	w ² _{yy}	-uv _{yy}	-uw _{yy}	-vw _{yy}
0.008	0.0053	-831.00	-41.10	-139.00	-39600.0	1380.0	-9410.0	-3480.0	4240	-295
0.013	0.0086	-677.00	-15.60	-117.00	-24600.0	104.0	-6270.0	-3140.0	2470	-385
0.020	0.0133	-446.00	4.91	-80.30	-8530.0	-905.0	-3080.0	-2210.0	563	-348
0.028	0.0187	-170.00	6.94	-31.90	2790.0	-986.0	-1250.0	-559.0	-801.0	-84.6
0.038	0.0254	-44.90	1.67	-7.62	1560.0	-430.0	-332.0	-96.30	-380.00	5.34
0.058	0.0389	-14.10	0.09	-2.39	625.0	-123.0	-31.6	21.40	-142.00	14.80
0.098	0.0658	-4.65	0.09	-1.01	177.0	-30.7	31.9	7.52	-36.00	9.73
0.148	0.0994	-1.21	0.03	-0.40	21.9	-7.2	3.7	-0.86	-6.00	3.95
0.248	0.1670	-0.46	0.00	-0.10	-2.6	-4.3	-3.4	-0.86	-1.01	1.97
0.498	0.3350	-0.27	0.03	0.03	-3.5	-2.1	-4.4	-0.87	-1.47	1.23
0.747	0.5030	-0.28	-0.00	0.13	-2.9	-1.1	-2.3	-0.72	-0.83	0.20
0.997	0.6710	-0.34	-0.02	0.11	2.2	0.8	1.5	0.56	0.13	-0.29
1.501	1.0100	-0.24	-0.02	0.05	3.4	1.2	2.3	0.94	0.45	-0.23
1.991	1.3400	-0.21	-0.01	0.02	3.8	1.5	2.4	1.02	0.41	-0.16
2.496	1.6800	-0.04	0.00	-0.00	0.7	0.5	0.4	0.14	-0.01	-0.01

Table 50. Boundary-layer y-derivatives at $x/L = 0.600$, $\phi = 140^\circ$.

$x/L = 0.600$ $\alpha = 10 \text{ deg.}$
 $Re = 4.2E+06$ $\phi = 150 \text{ deg.}$
Derivatives in Local-Freestream Coordinates

r		(1/cm)			(1/cm x1000)					
(cm)	(δ)	U _y	V _y	W _y	u ² _y	v ² _y	w ² _y	uv _y	uw _y	vw _y
0.008	0.0047	15.800	-0.135	3.060	250.000	36.800	96.000	62.60	-27.60	8.19
0.013	0.0077	12.000	-0.166	2.270	95.900	36.300	71.300	42.00	0.60	4.48
0.020	0.0118	7.860	-0.110	1.470	-30.200	32.600	42.500	21.10	21.20	1.15
0.028	0.0166	4.740	-0.051	0.875	-94.000	27.100	20.200	7.44	28.50	-1.20
0.038	0.0225	2.710	-0.018	0.467	-83.200	18.900	4.070	0.32	20.80	-2.18
0.058	0.0344	1.520	0.006	0.213	-41.300	8.760	-2.030	-0.555	8.340	-2.010
0.098	0.0582	0.964	0.007	0.071	-16.400	2.910	-2.900	-0.755	3.110	-1.280
0.148	0.0880	0.675	0.015	0.002	-5.720	0.788	-1.720	-0.559	1.550	-1.000
0.247	0.1470	0.488	0.016	-0.055	-2.040	0.107	-0.422	-0.473	0.853	-0.678
0.498	0.2960	0.380	0.028	-0.088	-1.530	-0.345	-0.393	-0.345	0.401	-0.181
0.748	0.4450	0.321	0.032	-0.087	-1.780	-0.669	-0.982	-0.521	0.074	0.084
0.999	0.5940	0.272	0.033	-0.075	-2.110	-0.874	-1.500	-0.644	-0.143	0.225
1.498	0.8910	0.153	0.026	-0.024	-1.850	-0.796	-1.350	-0.585	-0.211	0.163
2.000	1.1900	0.037	0.020	0.016	-0.720	-0.329	-0.429	-0.184	-0.046	0.028
2.505	1.4900	-0.024	0.019	0.023	0.710	0.314	0.338	0.155	0.027	-0.038

r		(1/cm ²)			(1/cm ² x1000)					
(cm)	(δ)	U _{yy}	V _{yy}	W _{yy}	u ² _{yy}	v ² _{yy}	w ² _{yy}	-uv _{yy}	-uw _{yy}	-vw _{yy}
0.008	0.0047	-809.00	-17.90	-175.00	-37300.0	338.0	-4830.0	-4430.0	7150	-866
0.013	0.0077	-678.00	3.28	-135.00	-24000.0	-325.0	-4550.0	-3540.0	4200	-596
0.020	0.0118	-465.00	14.60	-85.30	-9550.0	-815.0	-3510.0	-2210.0	1170	-306
0.028	0.0166	-172.00	1.63	-35.50	1690.0	-767.0	-1330.0	-510.0	-874.0	-90.0
0.038	0.0225	-47.30	0.97	-10.30	1770.0	-433.0	-217.0	-31.70	-498.00	16.70
0.058	0.0344	-14.50	0.14	-3.65	650.0	-157.0	-27.8	-8.90	-133.00	22.20
0.098	0.0582	-4.86	0.07	-1.21	170.0	-30.5	25.8	5.20	-23.20	3.53
0.148	0.0880	-1.33	0.03	-0.41	22.3	-5.0	8.2	0.65	-5.14	3.01
0.247	0.1470	-0.44	0.06	-0.15	1.8	-2.1	0.2	0.98	-1.89	2.21
0.498	0.2960	-0.27	0.03	-0.06	0.4	-1.1	-2.2	-0.63	-1.29	1.53
0.748	0.4450	-0.18	0.00	0.06	-2.0	-1.0	-2.6	-0.80	-1.05	0.51
0.999	0.5940	-0.26	-0.02	0.12	0.1	-0.1	0.1	0.06	-0.18	-0.13
1.498	0.8910	-0.23	-0.01	0.08	2.0	0.9	1.7	0.78	0.30	-0.27
2.000	1.1900	-0.24	-0.01	0.07	3.0	1.2	2.3	0.89	0.46	-0.28
2.505	1.4900	-0.11	-0.00	0.01	2.8	1.3	1.5	0.65	0.11	-0.12

Table 51. Boundary-layer y-derivatives at $x/L = 0.600$, $\phi = 150^\circ$.

$x/L = 0.600$ $\alpha = 10 \text{ deg.}$
 $Re = 4.2E+06$ $\phi = 160 \text{ deg.}$
Derivatives in Local-Freestream Coordinates

r		(1/cm)			(1/cm x1000)					
(cm)	(δ)	U _y	V _y	W _y	u ² _y	v ² _y	w ² _y	uv _y	uw _y	vw _y
0.008	0.0047	19.800	-0.100	3.140	406.000	50.200	141.000	88.70	-40.90	12.20
0.013	0.0075	14.500	-0.152	2.330	190.000	45.900	102.000	57.10	-7.47	7.10
0.020	0.0114	8.960	-0.144	1.430	9.120	37.800	55.700	27.20	16.70	2.15
0.028	0.0159	4.910	-0.093	0.762	-89.700	28.900	21.800	7.79	27.00	-0.97
0.038	0.0215	2.720	-0.048	0.406	-89.500	17.700	1.770	-1.26	18.30	-2.89
0.058	0.0327	1.570	-0.018	0.182	-46.400	7.530	-3.990	-2.380	7.300	-1.860
0.098	0.0551	0.975	-0.002	0.087	-17.600	3.270	-3.100	-1.100	2.710	-1.170
0.148	0.0831	0.694	-0.003	0.028	-5.890	1.030	-2.030	-0.457	0.819	-0.701
0.248	0.1390	0.498	0.004	-0.023	-3.280	-0.258	-1.290	-0.579	0.426	-0.595
0.498	0.2790	0.368	0.016	-0.067	-2.530	-0.742	-1.040	-0.638	0.212	-0.204
0.748	0.4190	0.293	0.023	-0.076	-2.150	-0.828	-1.170	-0.631	0.085	0.019
0.998	0.5590	0.238	0.026	-0.073	-2.030	-0.874	-1.300	-0.628	-0.054	0.199
1.498	0.8390	0.140	0.026	-0.030	-1.600	-0.705	-1.130	-0.467	-0.116	0.159
1.999	1.1200	0.041	0.026	0.010	-0.711	-0.308	-0.444	-0.168	-0.041	0.015
2.499	1.4000	-0.037	0.023	0.021	0.748	0.216	0.340	0.138	0.034	-0.057

r		(1/cm ²)			(1/cm ² x1000)					
(cm)	(δ)	U _{yy}	V _{yy}	W _{yy}	u ² _{yy}	v ² _{yy}	w ² _{yy}	-uv _{yy}	-uw _{yy}	-vw _{yy}
0.008	0.0047	-1200.00	-18.30	-179.00	-53400.0	-741.0	-8470.0	-7560.0	8610	-1210
0.013	0.0075	-944.00	-3.31	-148.00	-34400.0	-1080.0	-7500.0	-5330.0	4980	-871
0.020	0.0114	-590.00	7.43	-98.00	-13800.0	-1260.0	-5300.0	-2780.0	1290	-474
0.028	0.0159	-186.00	4.84	-30.90	685.0	-1040.0	-1600.0	-723.0	-855.0	-144.0
0.038	0.0215	-45.50	0.87	-8.71	1890.0	-409.0	-183.0	-23.20	-449.00	50.90
0.058	0.0327	-15.80	0.61	-2.48	785.0	-102.0	24.6	44.50	-116.00	18.30
0.098	0.0551	-4.70	-0.04	-1.01	170.0	-38.6	20.4	7.69	-28.70	6.95
0.148	0.0831	-1.41	0.06	-0.40	16.4	-8.8	4.7	-1.05	-2.66	1.28
0.248	0.1390	-0.56	0.07	-0.20	3.2	-1.9	1.2	0.01	-0.76	1.67
0.498	0.2790	-0.36	0.03	-0.10	2.6	-0.2	0.2	0.00	-0.48	1.25
0.748	0.4190	-0.20	0.01	0.02	0.2	-0.3	-1.0	-0.08	-0.63	0.69
0.998	0.5590	-0.20	0.00	0.10	0.5	0.2	0.1	0.29	-0.17	-0.08
1.498	0.8390	-0.20	0.00	0.08	1.7	0.8	1.3	0.59	0.13	-0.28
1.999	1.1200	-0.20	-0.00	0.07	2.2	1.0	1.7	0.63	0.23	-0.34
2.499	1.4000	-0.15	-0.01	0.02	3.0	1.1	1.6	0.61	0.14	-0.12

Table 52. Boundary-layer y-derivatives at $x/L = 0.600$, $\phi = 160^\circ$.

$x/L = 0.600$ $\alpha = 10 \text{ deg.}$
 $Re = 4.2E+06$ $\phi = 170 \text{ deg.}$
Derivatives in Local-Freestream Coordinates

r		(1/cm)			(1/cm x1000)					
(cm)	(δ)	U _y	V _y	W _y	u ² _y	v ² _y	w ² _y	uv _y	uw _y	vw _y
0.007	0.0040	26.500	4.880	2.630	547.000	43.500	163.000	86.50	-2.70	-0.52
0.012	0.0067	18.400	2.690	1.750	268.000	46.200	114.000	58.70	2.38	-0.34
0.019	0.0105	10.700	0.921	0.968	27.100	43.000	66.600	28.10	8.23	-0.26
0.027	0.0148	5.510	-0.159	0.461	-112.000	35.800	32.300	6.17	12.50	-0.77
0.037	0.0202	3.010	-0.082	0.255	-108.000	22.800	8.790	-2.52	9.76	-1.24
0.057	0.0311	1.770	-0.049	0.150	-58.800	9.810	-2.240	-4.470	6.410	-2.090
0.097	0.0528	1.100	-0.018	0.076	-23.100	3.260	-4.680	-2.110	2.170	-1.150
0.147	0.0799	0.746	-0.001	0.033	-9.860	0.455	-3.720	-1.410	0.836	-0.778
0.247	0.1340	0.505	0.001	-0.009	-5.550	-0.800	-2.340	-1.150	0.131	-0.426
0.498	0.2700	0.357	0.005	-0.040	-3.920	-1.090	-1.810	-1.220	0.046	-0.129
0.746	0.4050	0.266	0.015	-0.047	-2.970	-1.140	-1.590	-0.960	-0.010	0.069
0.997	0.5410	0.195	0.025	-0.046	-2.260	-1.080	-1.400	-0.679	0.022	0.157
1.497	0.8120	0.105	0.033	-0.022	-1.340	-0.690	-0.880	-0.321	-0.018	0.133
1.990	1.0800	0.037	0.031	0.004	-0.488	-0.251	-0.299	-0.123	-0.017	0.057
2.488	1.3500	-0.017	0.032	0.018	0.463	0.195	0.331	0.054	0.060	0.019

r		(1/cm ²)			(1/cm ² x1000)					
(cm)	(δ)	U _{yy}	V _{yy}	W _{yy}	u ² _{yy}	v ² _{yy}	w ² _{yy}	-uv _{yy}	-uw _{yy}	-vw _{yy}
0.007	0.0040	-1820.00	-533.00	-205.00	-64800.0	1560.0	-10300.0	-5510.0	1010	41
0.012	0.0067	-1330.00	-337.00	-141.00	-44200.0	19.5	-7990.0	-4980.0	983	26
0.019	0.0105	-750.00	-133.00	-70.60	-20500.0	-1160.0	-5100.0	-3500.0	629	-9
0.027	0.0148	-209.00	4.77	-17.10	1270.0	-1190.0	-1970.0	-642.0	-240.0	-70.5
0.037	0.0202	-49.90	1.74	-4.50	2210.0	-537.0	-424.0	-45.40	-170.00	-23.80
0.057	0.0311	-17.40	0.86	-1.87	932.0	-172.0	-56.1	63.40	-115.00	31.60
0.097	0.0528	-6.08	0.24	-0.76	206.0	-43.3	22.1	13.10	-20.30	5.18
0.147	0.0799	-1.70	0.01	-0.32	27.4	-7.3	9.3	0.64	-4.46	2.67
0.247	0.1340	-0.58	0.01	-0.14	7.2	-2.3	2.1	-0.58	-0.58	1.41
0.498	0.2700	-0.47	0.04	-0.06	4.4	-0.5	0.8	1.14	0.04	1.05
0.746	0.4050	-0.27	0.05	0.01	2.7	0.3	0.8	1.20	0.04	0.34
0.997	0.5410	-0.19	0.02	0.05	1.8	0.8	1.0	0.76	-0.14	-0.05
1.497	0.8120	-0.13	-0.00	0.05	1.7	0.9	1.2	0.40	-0.02	-0.15
1.990	1.0800	-0.14	-0.01	0.05	1.6	0.9	1.2	0.37	0.08	-0.17
2.488	1.3500	-0.10	0.00	0.03	1.9	0.9	1.3	0.35	0.16	-0.06

Table 53. Boundary-layer y-derivatives at $x/L = 0.600$, $\phi = 170^\circ$.

$x/L = 0.600$ $\alpha = 10 \text{ deg.}$
 $Re = 4.2E+06$ $\phi = 180 \text{ deg.}$
Derivatives in Local-Freestream Coordinates

r		(1/cm)			(1/cm x1000)					
(cm)	(/δ)	U _y	V _y	W _y	u ² _y	v ² _y	w ² _y	uv _y	uw _y	vw _y
0.011	0.0066	12.600	-0.138	-0.080	14.600	60.300	103.000	58.80	-3.36	-3.30
0.016	0.0095	9.880	-0.166	-0.007	-66.000	52.400	81.600	36.80	2.20	-3.97
0.023	0.0137	6.670	-0.152	0.028	-131.000	41.600	48.700	15.10	2.27	-3.39
0.031	0.0185	4.230	-0.116	0.042	-154.000	31.700	21.200	1.51	1.30	-2.73
0.041	0.0245	2.690	-0.052	0.043	-111.000	20.400	0.824	-3.31	-0.76	-0.88
0.061	0.0364	1.740	-0.028	0.008	-51.400	10.300	-4.950	-2.100	-1.160	-0.119
0.101	0.0602	1.110	-0.023	0.002	-19.700	3.170	-4.180	-1.760	-0.232	0.083
0.151	0.0901	0.733	-0.022	0.002	-8.940	0.141	-3.510	-1.380	-0.253	-0.030
0.252	0.1500	0.526	-0.011	0.003	-5.550	-1.020	-2.720	-1.380	-0.011	-0.027
0.501	0.2990	0.366	0.002	0.000	-4.580	-1.370	-2.350	-1.300	-0.131	0.064
0.751	0.4480	0.264	0.014	0.000	-3.680	-1.340	-1.990	-1.090	-0.116	0.099
1.001	0.5970	0.183	0.024	0.002	-2.710	-1.130	-1.560	-0.752	-0.091	0.085
1.501	0.8950	0.087	0.032	0.002	-1.210	-0.615	-0.759	-0.298	-0.033	0.070
1.996	1.1900	0.023	0.031	0.003	-0.277	-0.202	-0.179	-0.044	-0.008	0.047
2.499	1.4900	-0.004	0.032	0.011	0.226	0.100	0.096	0.053	0.013	-0.013

r		(1/cm ²)			(1/cm ² x1000)					
(cm)	(/δ)	U _{yy}	V _{yy}	W _{yy}	u ² _{yy}	v ² _{yy}	w ² _{yy}	-uv _{yy}	-uw _{yy}	-vw _{yy}
0.011	0.0066	-518.00	-11.60	21.00	-19800.0	-1050.0	-3010.0	-4660.0	1940	-322
0.016	0.0095	-504.00	-1.20	8.80	-12800.0	-1500.0	-4660.0	-3690.0	411	-5
0.023	0.0137	-393.00	6.45	-0.29	-4310.0	-1620.0	-4760.0	-2250.0	-558	207
0.031	0.0185	-124.00	5.67	0.36	4520.0	-969.0	-1600.0	-284.0	-84.3	133.0
0.041	0.0245	-39.70	0.72	-1.57	2510.0	-436.0	-176.0	51.40	-12.60	32.40
0.061	0.0364	-17.60	0.19	-0.20	790.0	-197.0	9.1	-0.65	20.50	6.31
0.101	0.0602	-6.15	0.02	0.08	172.0	-45.9	16.5	9.00	2.31	-3.24
0.151	0.0901	-1.52	0.09	-0.01	20.6	-7.6	5.0	-0.42	0.90	0.43
0.252	0.1500	-0.67	0.05	-0.02	3.1	-1.9	1.1	-0.10	-0.57	0.44
0.501	0.2990	-0.49	0.05	0.01	3.5	-0.3	1.3	0.80	-0.00	0.20
0.751	0.4480	-0.31	0.04	0.01	4.2	1.0	1.8	1.42	0.14	-0.06
1.001	0.5970	-0.22	0.02	-0.00	3.3	1.1	1.8	1.02	0.13	-0.02
1.501	0.8950	-0.13	-0.00	0.00	1.9	0.8	1.2	0.53	0.05	-0.05
1.996	1.1900	-0.11	-0.00	0.01	1.6	0.8	1.0	0.42	0.04	-0.04
2.499	1.4900	-0.05	0.00	0.02	0.9	0.6	0.5	0.17	0.04	-0.13

Table 54. Boundary-layer y-derivatives at $x/L = 0.600$, $\phi = 180^\circ$.

$x/L = 0.752$ $\alpha = 10 \text{ deg.}$
 $Re = 4.2E+06$ $\phi = 120 \text{ deg.}$
Derivatives in Local-Freestream Coordinates

r		(1/cm)			(1/cm x1000)					
(cm)	(δ)	U _y	V _y	W _y	u ² _y	v ² _y	w ² _y	uv _y	uw _y	vw _y
0.011	0.0081	12.720	0.394	2.453	30.090	41.550	76.750	45.84	19.00	6.37
0.016	0.0117	9.150	0.311	1.801	-21.740	39.630	50.350	33.84	23.45	3.50
0.021	0.0153	6.548	0.232	1.231	-62.440	36.300	33.990	23.01	28.08	1.64
0.031	0.0224	3.672	0.115	0.490	-97.500	27.940	19.110	8.46	32.15	-0.25
0.041	0.0296	2.176	0.081	0.211	-61.490	17.110	9.257	2.76	18.19	-1.20
0.076	0.0547	1.163	0.058	0.014	-20.260	8.032	1.771	0.691	6.991	-1.745
0.151	0.1084	0.766	0.053	-0.070	-4.115	2.153	0.493	0.571	2.304	-1.041
0.251	0.1800	0.590	0.053	-0.127	-1.443	0.216	0.176	-0.148	1.043	-0.406
0.501	0.3591	0.460	0.050	-0.118	-2.256	-0.750	-1.225	-0.560	0.073	0.235
0.751	0.5381	0.364	0.044	-0.079	-3.014	-1.121	-2.041	-0.683	-0.192	0.309
1.001	0.7172	0.269	0.035	-0.037	-3.174	-1.234	-2.438	-0.646	-0.357	0.297
1.501	1.0750	0.112	0.016	0.006	-1.859	-0.754	-1.394	-0.397	-0.150	0.077
2.001	1.4330	0.010	0.001	0.013	-0.194	-0.130	-0.201	-0.050	-0.008	-0.018
2.502	1.7920	0.001	-0.012	-0.001	0.123	0.011	-0.054	-0.009	-0.007	-0.051

r		(1/cm ²)			(1/cm ² x1000)					
(cm)	(δ)	U _{yy}	V _{yy}	W _{yy}	u ² _{yy}	v ² _{yy}	w ² _{yy}	-uv _{yy}	-uw _{yy}	-vw _{yy}
0.011	0.0081	-882.70	-16.48	-141.50	-11990.0	-107.4	-7132.0	-2534.0	752	-760
0.016	0.0117	-559.00	-16.24	-118.60	-8706.0	-621.9	-3635.0	-2240.0	960	-409
0.021	0.0153	-318.80	-13.76	-90.05	-5194.0	-892.7	-1384.0	-1772.0	756	-175
0.031	0.0224	-89.02	-2.06	-15.98	2527.0	-703.1	-620.3	-308.8	-885.5	-59.7
0.041	0.0296	-20.59	-0.42	-4.06	856.7	-227.3	-145.5	-34.60	-232.20	-6.44
0.076	0.0547	-5.20	-0.08	-1.20	202.4	-50.0	-10.7	-1.84	-57.97	10.72
0.151	0.1084	-1.30	-0.00	-0.37	12.9	-13.8	-4.0	-5.97	-9.27	5.29
0.251	0.1800	-0.53	-0.03	0.03	-3.5	-3.9	-6.0	-1.73	-4.13	2.99
0.501	0.3591	-0.36	0.01	0.14	-4.9	-2.5	-6.0	-0.48	-2.25	0.89
0.751	0.5381	-0.39	-0.04	0.18	-0.9	-0.5	-1.3	-0.05	-0.33	-0.28
1.001	0.7172	-0.37	-0.04	0.11	3.1	1.1	2.5	0.59	0.51	-0.50
1.501	1.0750	-0.22	-0.03	0.02	3.4	1.3	2.4	0.69	0.32	-0.21
2.001	1.4330	-0.16	-0.02	-0.01	3.2	1.1	2.1	0.71	0.16	-0.13
2.502	1.7920	-0.00	-0.03	-0.03	0.4	0.2	0.1	0.01	-0.02	-0.06

Table 55. Boundary-layer y-derivatives at $x/L = 0.752$, $\phi = 120^\circ$.

$$x/L = 0.752 \quad \alpha = 10 \text{ deg.}$$

$$Re = 4.2E+06 \quad \phi = 123 \text{ deg.}$$

Derivatives in Local-Freestream Coordinates

r		(1/cm)			(1/cm x1000)					
(cm)	(/δ)	U _y	V _y	W _y	u ² _y	v ² _y	w ² _y	uv _y	uw _y	vw _y
0.008	0.0054	9.806	0.596	2.544	219.300	23.060	91.520	49.07	-20.85	9.74
0.013	0.0088	8.512	0.324	2.076	71.430	26.730	65.000	32.31	5.73	5.99
0.018	0.0122	7.079	0.163	1.645	-18.940	28.460	44.590	21.11	21.15	3.02
0.028	0.0189	4.624	0.066	1.001	-70.580	26.990	22.080	11.46	26.90	-0.15
0.038	0.0256	2.479	0.089	0.463	-53.490	19.420	5.280	6.95	18.44	-1.31
0.073	0.0491	1.165	0.070	0.097	-13.340	8.155	2.315	3.083	6.888	-1.153
0.148	0.0995	0.768	0.050	-0.029	-3.964	3.115	1.667	0.889	3.160	-0.829
0.248	0.1667	0.577	0.049	-0.101	-1.087	0.719	1.223	-0.149	1.480	-0.521
0.498	0.3346	0.451	0.053	-0.124	-1.944	-0.453	-0.678	-0.473	0.234	0.059
0.748	0.5025	0.371	0.049	-0.097	-2.721	-0.941	-1.700	-0.652	-0.121	0.257
0.998	0.6704	0.295	0.043	-0.059	-3.265	-1.187	-2.395	-0.730	-0.314	0.350
1.498	1.0060	0.139	0.022	-0.005	-2.113	-0.805	-1.592	-0.487	-0.153	0.153
1.998	1.3420	0.017	0.004	-0.013	-0.392	-0.180	-0.311	-0.073	-0.020	-0.010
2.498	1.6780	-0.015	-0.007	-0.003	0.294	0.012	0.162	0.021	-0.034	-0.066

r		(1/cm ²)			(1/cm ² x1000)					
(cm)	(/δ)	U _{yy}	V _{yy}	W _{yy}	u ² _{yy}	v ² _{yy}	w ² _{yy}	-uv _{yy}	-uw _{yy}	-vw _{yy}
0.008	0.0054	-222.30	-75.03	-98.28	-39940.0	1072.0	-6342.0	-4347.0	7331	-880
0.013	0.0088	-285.60	-36.27	-88.50	-20250.0	423.4	-4336.0	-2453.0	3504	-628
0.018	0.0122	-290.80	-10.62	-74.21	-6745.0	-61.4	-2753.0	-1138.0	896	-405
0.028	0.0189	-126.20	1.36	-32.08	1706.0	-538.3	-857.1	-246.8	-659.6	-49.1
0.038	0.0256	-25.63	-0.59	-7.32	778.4	-241.2	-49.7	-88.73	-226.90	4.92
0.073	0.0491	-5.21	-0.27	-1.64	120.9	-66.3	-6.7	-28.87	-48.84	4.25
0.148	0.0995	-1.41	0.01	-0.53	15.5	-16.7	-6.1	-6.93	-12.62	2.94
0.248	0.1667	-0.52	0.01	-0.12	-3.3	-4.7	-8.3	-1.07	-5.66	2.66
0.498	0.3346	-0.30	0.02	0.06	-5.1	-2.9	-6.0	-1.02	-2.23	1.51
0.748	0.5025	-0.30	-0.03	0.17	-2.3	-1.0	-2.7	-0.47	-0.54	0.18
0.998	0.6704	-0.36	-0.05	0.13	2.6	0.9	1.8	0.58	0.38	-0.45
1.498	1.0060	-0.25	-0.04	0.04	3.4	1.3	2.5	0.83	0.26	-0.34
1.998	1.3420	-0.22	-0.03	0.01	3.5	1.2	2.7	0.81	0.28	-0.28
2.498	1.6780	-0.05	-0.02	-0.04	1.1	0.3	0.7	0.12	-0.06	-0.09

Table 56. Boundary-layer y-derivatives at $x/L = 0.752$, $\phi = 123^\circ$.

$x/L = 0.752$ $\alpha = 10 \text{ deg.}$
 $Re = 4.2E+06$ $\phi = 125 \text{ deg.}$
Derivatives in Local-Freestream Coordinates

r		(1/cm)			(1/cm x1000)					
(cm)	(δ)	U _y	V _y	W _y	u ² _y	v ² _y	w ² _y	uv _y	uw _y	vw _y
0.017	0.0108	6.454	0.154	1.460	-92.360	36.480	32.860	16.86	39.96	6.69
0.022	0.0139	5.084	0.152	1.151	-87.660	31.990	24.520	13.39	34.28	1.65
0.027	0.0171	3.986	0.132	0.902	-82.680	27.690	17.110	10.08	30.07	-0.88
0.037	0.0233	2.708	0.072	0.581	-73.300	21.200	6.725	5.37	24.64	-1.60
0.047	0.0296	1.589	0.035	0.281	-36.290	12.340	-1.178	2.58	10.61	-0.46
0.082	0.0515	0.966	0.042	0.066	-12.640	5.407	-0.413	0.661	4.379	-0.962
0.157	0.0986	0.670	0.048	-0.037	-2.748	2.118	1.088	0.407	2.159	-1.105
0.257	0.1613	0.526	0.053	-0.095	-0.490	0.592	1.323	-0.073	1.340	-0.775
0.507	0.3180	0.437	0.054	-0.124	-1.241	-0.432	-0.291	-0.456	0.426	-0.031
0.757	0.4748	0.373	0.053	-0.102	-2.268	-0.871	-1.381	-0.642	0.014	0.189
1.007	0.6315	0.307	0.048	-0.071	-2.947	-1.145	-2.167	-0.682	-0.257	0.289
1.507	0.9450	0.155	0.027	-0.012	-2.203	-0.803	-1.638	-0.453	-0.232	0.132
2.008	1.2590	0.027	0.009	0.013	-0.529	-0.200	-0.405	-0.077	-0.036	-0.003
2.507	1.5720	-0.021	0.002	0.001	0.414	0.173	0.212	0.094	-0.011	-0.042

r		(1/cm ²)			(1/cm ² x1000)					
(cm)	(δ)	U _{yy}	V _{yy}	W _{yy}	u ² _{yy}	v ² _{yy}	w ² _{yy}	-uv _{yy}	-uw _{yy}	-vw _{yy}
0.017	0.0108	-319.60	3.65	-71.77	945.8	-918.2	-1794.0	-697.3	-1427	-1476
0.022	0.0139	-231.20	-3.56	-52.39	962.8	-872.6	-1532.0	-677.2	-888	-594
0.027	0.0171	-158.80	-6.92	-36.93	1165.0	-791.5	-1213.0	-580.8	-602	-44
0.037	0.0233	-61.49	-2.07	-17.75	2128.0	-522.8	-407.1	-159.7	-787.0	58.7
0.047	0.0296	-13.21	0.27	-4.52	496.9	-148.0	34.2	-37.03	-123.90	-13.97
0.082	0.0515	-3.91	0.06	-1.35	126.7	-43.5	21.8	-2.53	-26.16	-1.51
0.157	0.0986	-1.06	0.03	-0.44	11.9	-11.1	-1.7	-4.02	-7.06	3.77
0.257	0.1613	-0.36	-0.00	-0.16	-3.3	-4.3	-7.0	-1.87	-3.98	3.52
0.507	0.3180	-0.21	0.03	0.03	-4.7	-2.6	-5.6	-0.64	-2.03	1.35
0.757	0.4748	-0.27	-0.03	0.15	-3.3	-1.1	-3.4	-0.34	-1.12	0.26
1.007	0.6315	-0.34	-0.05	0.14	1.5	0.7	1.1	0.47	0.06	-0.34
1.507	0.9450	-0.26	-0.04	0.06	3.2	1.2	2.4	0.72	0.36	-0.26
2.008	1.2590	-0.23	-0.03	0.03	3.8	1.3	2.8	0.88	0.49	-0.30
2.507	1.5720	-0.08	-0.01	-0.03	1.7	0.7	1.1	0.28	0.00	-0.05

Table 57. Boundary-layer y-derivatives at $x/L = 0.752$, $\phi = 125^\circ$.

$$x/L = 0.762 \quad \alpha = 10 \text{ deg.}$$

$$Re = 4.2E+06 \quad \phi = 120 \text{ deg.}$$

Derivatives in Local-Freestream Coordinates

r		(1/cm)			(1/cm x1000)					
(cm)	(°δ)	U _y	V _y	W _y	u ² _y	v ² _y	w ² _y	uv _y	uw _y	vw _y
0.008	0.0057	16.800	0.025	3.221	261.000	36.180	99.250	70.79	-0.64	11.57
0.013	0.0092	11.900	0.132	2.307	105.000	36.820	64.180	51.30	9.72	8.74
0.018	0.0127	8.553	0.133	1.587	-8.476	36.330	41.540	33.44	21.28	5.54
0.028	0.0197	5.080	0.039	0.717	-110.300	31.490	20.670	10.17	35.51	0.50
0.038	0.0267	2.648	0.097	0.282	-65.850	17.870	9.586	2.71	21.80	-2.46
0.073	0.0513	1.233	0.081	0.022	-19.840	6.226	2.499	-0.100	7.885	-2.488
0.148	0.1039	0.719	0.060	-0.071	-4.064	1.954	0.644	-0.140	2.407	-1.004
0.248	0.1740	0.564	0.053	-0.116	-0.813	0.515	0.322	-0.146	0.851	-0.302
0.498	0.3493	0.441	0.056	-0.117	-1.889	-0.601	-0.940	-0.443	0.100	0.237
0.748	0.5246	0.362	0.056	-0.082	-2.737	-0.871	-1.685	-0.648	-0.128	0.315
0.998	0.6999	0.281	0.051	-0.044	-3.318	-1.023	-2.160	-0.817	-0.186	0.349
1.499	1.0510	0.128	0.029	-0.001	-1.851	-0.585	-1.337	-0.458	-0.133	0.139
1.998	1.4010	0.008	-0.000	0.007	-0.314	0.044	-0.296	-0.099	-0.034	0.093
2.498	1.7520	-0.025	-0.023	0.002	0.177	0.870	-0.240	-0.185	0.036	0.297

r		(1/cm ²)			(1/cm ² x1000)					
(cm)	(°δ)	U _{yy}	V _{yy}	W _{yy}	u ² _{yy}	v ² _{yy}	w ² _{yy}	-uv _{yy}	-uw _{yy}	-vw _{yy}
0.008	0.0057	-1262.00	42.31	-214.80	-38280.0	311.4	-9274.0	-4041.0	1649	-467
0.013	0.0092	-727.70	3.44	-152.40	-24530.0	-47.1	-4989.0	-3690.0	2344	-639
0.018	0.0127	-363.10	-16.03	-100.00	-13050.0	-364.2	-2126.0	-2962.0	2147	-643
0.028	0.0197	-144.30	3.23	-25.30	3114.0	-873.8	-665.0	-374.6	-925.6	-146.6
0.038	0.0267	-28.20	-0.47	-5.15	934.0	-236.2	-140.4	-50.32	-291.70	9.68
0.073	0.0513	-6.40	-0.39	-1.25	186.4	-54.4	-20.3	-2.64	-64.42	21.24
0.148	0.1039	-1.18	-0.01	-0.31	19.8	-10.7	-3.5	0.44	-11.34	5.15
0.248	0.1740	-0.49	0.02	-0.01	-5.9	-5.6	-5.6	-1.81	-3.04	2.12
0.498	0.3493	-0.32	0.00	0.09	-6.2	-1.3	-4.7	-1.15	-1.51	1.34
0.748	0.5246	-0.32	-0.01	0.18	-1.7	-0.5	-1.8	-0.61	-0.18	-0.15
0.998	0.6999	-0.35	-0.04	0.10	3.3	0.7	2.0	0.85	0.14	-0.60
1.499	1.0510	-0.25	-0.06	0.02	3.1	1.2	2.1	0.69	0.22	-0.15
1.998	1.4010	-0.22	-0.06	-0.01	3.2	1.6	2.1	0.82	0.11	0.14
2.498	1.7520	-0.05	-0.04	-0.01	0.7	1.7	-0.1	-0.28	0.14	0.44

Table 58. Boundary-layer y-derivatives at $x/L = 0.762$, $\phi = 120^\circ$.

$x/L = 0.762$ $\alpha = 10 \text{ deg.}$
 $Re = 4.2E+06$ $\phi = 123 \text{ deg.}$

Derivatives in Local-Freestream Coordinates

r		(1/cm)			(1/cm x1000)					
(cm)	(δ)	U _y	V _y	W _y	u ² _y	v ² _y	w ² _y	uv _y	uw _y	vw _y
0.007	0.0047	17.140	0.152	4.626	386.500	30.840	133.100	55.83	-56.76	7.32
0.012	0.0078	12.320	0.150	3.127	172.700	32.620	84.620	42.71	-16.31	6.65
0.017	0.0110	8.714	0.138	2.074	32.540	31.910	50.320	30.41	10.11	4.60
0.027	0.0173	4.701	0.098	0.993	-81.810	26.610	15.550	13.32	30.92	0.41
0.037	0.0235	2.564	0.088	0.488	-64.430	18.170	3.685	4.62	20.35	-1.25
0.072	0.0456	1.283	0.067	0.110	-24.380	6.837	1.708	0.382	9.045	-1.407
0.147	0.0928	0.773	0.060	-0.046	-6.187	2.650	1.501	0.460	3.688	-1.082
0.247	0.1557	0.560	0.058	-0.106	-0.360	0.867	1.260	-0.031	1.478	-0.605
0.497	0.3131	0.437	0.057	-0.127	-1.374	-0.340	-0.360	-0.377	0.245	0.067
0.747	0.4704	0.363	0.052	-0.100	-2.594	-0.938	-1.424	-0.634	-0.101	0.251
0.997	0.6278	0.288	0.046	-0.068	-3.294	-1.300	-2.217	-0.685	-1.296	0.273
1.497	0.9425	0.145	0.024	-0.012	-2.152	-0.849	-1.589	-0.470	-0.174	0.107
1.997	1.2570	0.027	0.008	-0.007	-0.407	-0.179	-0.346	-0.082	-0.052	0.014
2.497	1.5720	-0.015	0.017	-0.002	0.399	0.232	0.087	0.117	-0.125	0.036

r		(1/cm ²)			(1/cm ² x1000)					
(cm)	(δ)	U _{yy}	V _{yy}	W _{yy}	u ² _{yy}	v ² _{yy}	w ² _{yy}	-uv _{yy}	-uw _{yy}	-vw _{yy}
0.007	0.0047	-1170.00	1.78	-379.00	-55820.0	829.5	-12160.0	-2674.0	10550	161
0.012	0.0078	-771.10	-2.08	-227.90	-30900.0	-56.6	-7424.0	-2527.0	5837	-375
0.017	0.0110	-463.70	-3.83	-119.40	-13040.0	-585.7	-3923.0	-2112.0	2389	-593
0.027	0.0173	-121.80	-1.06	-30.07	1490.0	-572.8	-625.5	-477.5	-698.9	-76.3
0.037	0.0235	-26.23	-0.38	-7.88	861.4	-238.1	-27.6	-75.73	-240.50	0.05
0.072	0.0456	-6.76	-0.11	-2.04	243.0	-54.8	-1.9	2.47	-69.97	3.06
0.147	0.0928	-1.50	-0.01	-0.41	32.3	-12.2	-4.2	-4.02	-15.78	4.66
0.247	0.1557	-0.50	0.01	-0.12	-4.4	-5.3	-6.5	-1.46	-5.32	3.11
0.497	0.3131	-0.31	-0.02	0.05	-7.8	-3.9	-6.3	-1.32	-2.22	1.33
0.747	0.4704	-0.29	-0.02	0.16	-2.7	-1.2	-3.2	-0.35	-0.61	-0.07
0.997	0.6278	-0.32	-0.05	0.13	2.5	1.0	1.4	0.47	0.33	-0.40
1.497	0.9425	-0.24	-0.03	0.04	3.5	1.3	2.5	0.77	0.25	-0.20
1.997	1.2570	-0.22	-0.03	0.02	3.5	1.4	2.6	0.79	0.20	-0.12
2.497	1.5720	-0.07	0.02	-0.02	1.4	0.8	0.7	0.36	-0.18	0.06

Table 59. Boundary-layer y-derivatives at $x/L = 0.762$, $\phi = 123^\circ$.

$x/L = 0.762$ $\alpha = 10 \text{ deg.}$
 $Re = 4.2E+06$ $\phi = 125 \text{ deg.}$
Derivatives in Local-Freestream Coordinates

r		(1/cm)			(1/cm x1000)					
(cm)	(/δ)	U _y	V _y	W _y	u ² _y	v ² _y	w ² _y	uv _y	uw _y	vw _y
0.007	0.0045	11.130	0.194	3.110	178.400	21.320	66.190	38.38	3.42	1.86
0.012	0.0075	9.320	0.201	2.507	93.720	27.150	57.340	31.07	10.11	4.12
0.017	0.0106	7.490	0.169	1.924	20.790	28.540	43.930	22.77	17.70	3.92
0.027	0.0167	4.735	0.093	1.083	-63.220	24.680	19.720	9.66	27.49	0.91
0.037	0.0228	2.359	0.061	0.461	-56.340	17.270	4.234	4.34	18.92	0.01
0.072	0.0440	1.156	0.041	0.105	-23.620	6.770	-0.183	0.186	9.077	-1.302
0.147	0.0896	0.737	0.048	-0.024	-5.037	2.831	1.061	0.268	3.222	-1.076
0.247	0.1505	0.530	0.057	-0.097	-0.291	0.783	1.289	-0.118	1.418	-0.788
0.497	0.3025	0.426	0.064	-0.125	-0.929	-0.266	-0.095	-0.292	0.344	-0.075
0.747	0.4545	0.371	0.058	-0.104	-2.171	-0.836	-1.279	-0.550	0.020	0.15
0.997	0.6066	0.316	0.048	-0.073	-2.986	-1.164	-2.162	-0.643	-0.265	0.26
1.497	0.9107	0.169	0.027	-0.018	-2.232	-0.896	-1.672	-0.494	-0.186	0.096
1.998	1.2150	0.033	0.016	0.009	-0.657	-0.225	-0.501	-0.138	-0.048	0.005
2.498	1.5190	-0.046	0.022	0.004	0.297	0.001	0.213	0.114	-0.115	0.098

r		(1/cm ²)			(1/cm ² x1000)					
(cm)	(/δ)	U _{yy}	V _{yy}	W _{yy}	u ² _{yy}	v ² _{yy}	w ² _{yy}	-uv _{yy}	-uw _{yy}	-vw _{yy}
0.007	0.0045	-343.50	9.59	-119.80	-18400.0	2006.0	-755.7	-1189.0	1039	942
0.012	0.0075	-370.20	-5.27	-119.00	-15270.0	430.0	-2583.0	-1659.0	1536	35
0.017	0.0106	-344.00	-12.06	-104.60	-11010.0	-512.7	-3200.0	-1668.0	1431	-434
0.027	0.0167	-132.50	-1.39	-34.98	910.6	-499.0	-808.2	-302.7	-586.7	-57.3
0.037	0.0228	-23.88	-0.37	-7.18	739.0	-221.9	-65.9	-77.57	-218.00	-23.44
0.072	0.0440	-5.58	0.08	-1.74	237.0	-52.1	16.9	1.84	-75.72	2.26
0.147	0.0896	-1.50	0.08	-0.52	27.4	-14.1	0.1	-2.58	-12.65	3.39
0.247	0.1505	-0.44	0.02	-0.15	-2.8	-4.5	-6.0	-0.84	-4.45	3.05
0.497	0.3025	-0.15	0.02	0.04	-7.0	-3.0	-6.6	-1.15	-2.10	1.88
0.747	0.4545	-0.23	-0.05	0.14	-3.4	-1.4	-3.5	-0.53	-0.98	0.19
0.997	0.6066	-0.32	-0.05	0.13	1.5	0.4	1.0	0.28	0.23	-0.44
1.497	0.9107	-0.28	-0.02	0.06	3.1	1.3	2.3	0.69	0.28	-0.22
1.998	1.2150	-0.25	-0.01	0.03	3.4	1.5	2.6	0.80	0.26	-0.04
2.498	1.5190	-0.15	0.01	-0.01	1.7	1.2	1.3	0.47	-0.18	0.21

Table 60. Boundary-layer y-derivatives at $x/L = 0.762$, $\phi = 125^\circ$.

$x/L = 0.772$ $\alpha = 10 \text{ deg.}$
 $Re = 4.2E+06$ $\phi = 105 \text{ deg.}$
Derivatives in Local-Freestream Coordinates

r		(1/cm)			(1/cm x1000)					
(cm)	(δ)	U _y	V _y	W _y	u ² _y	v ² _y	w ² _y	uv _y	uw _y	vw _y
0.007	0.0073	19.130	0.024	1.819	465.100	62.020	162.700	86.75	5.70	-3.35
0.012	0.0126	14.420	-0.030	1.212	185.400	61.700	119.400	62.10	13.59	-3.09
0.017	0.0180	10.460	-0.054	0.693	5.293	55.620	81.200	39.76	16.83	-2.08
0.027	0.0287	5.608	-0.007	0.079	-122.800	39.910	32.690	12.73	15.70	-0.14
0.037	0.0394	2.565	-0.001	-0.055	-87.090	18.560	5.622	0.02	7.38	0.15
0.072	0.0769	1.443	0.051	-0.089	-26.710	7.222	1.231	-0.024	2.941	-0.515
0.147	0.1573	0.964	0.032	-0.098	-9.865	2.034	0.091	-0.484	1.128	-0.142
0.247	0.2644	0.687	0.027	-0.104	-5.582	-0.503	-1.577	-1.116	0.252	0.382
0.497	0.5322	0.461	0.044	-0.052	-5.536	-2.117	-3.751	-1.338	-0.171	0.313
0.747	0.8001	0.301	0.037	-0.014	-4.470	-1.893	-3.322	-1.121	-0.153	0.124
0.997	1.0680	0.159	0.027	0.017	-3.081	-1.459	-2.470	-0.863	-0.094	-0.046
1.497	1.6040	0.027	0.013	0.021	-0.767	-0.392	-0.626	-0.289	-0.003	-0.039
1.997	2.1390	-0.003	0.013	0.011	-0.025	-0.065	-0.055	-0.015	0.009	-0.036
2.497	2.6750	-0.003	0.011	0.004	-0.087	-0.104	-0.045	-0.069	0.025	-0.063

r		(1/cm ²)			(1/cm ² x1000)					
(cm)	(δ)	U _{yy}	V _{yy}	W _{yy}	u ² _{yy}	v ² _{yy}	w ² _{yy}	-uv _{yy}	-uw _{yy}	-vw _{yy}
0.007	0.0073	-1054.00	-15.99	-133.50	-73590.0	1085.0	-9357.0	-5172.0	2442	-112
0.012	0.0126	-828.60	-5.85	-108.70	-39890.0	-1040.0	-7923.0	-4621.0	814	185
0.017	0.0180	-604.50	0.56	-79.11	-15880.0	-2129.0	-6113.0	-3669.0	-216	302
0.027	0.0287	-160.80	2.17	-5.79	3053.0	-1196.0	-1365.0	-557.1	-480.9	-1.0
0.037	0.0394	-22.33	0.75	-0.69	1186.0	-231.7	-68.1	1.77	-87.84	-11.87
0.072	0.0769	-6.58	-0.31	-0.22	213.2	-71.1	-17.6	-10.11	-24.34	6.62
0.147	0.1573	-2.12	0.01	0.04	24.4	-18.8	-15.7	-4.38	-6.50	3.79
0.247	0.2644	-0.84	0.13	0.20	-2.1	-7.8	-10.9	-0.52	-1.80	-0.38
0.497	0.5322	-0.72	-0.04	0.24	1.9	-0.9	-1.5	-0.45	-0.18	-1.38
0.747	0.8001	-0.61	-0.05	0.11	7.0	2.6	4.9	1.41	0.34	-0.50
0.997	1.0680	-0.30	-0.03	0.01	5.4	2.5	4.3	1.44	0.21	0.04
1.497	1.6040	-0.07	0.00	-0.02	1.7	0.9	1.3	0.66	0.04	0.02
1.997	2.1390	-0.02	-0.01	-0.02	0.7	0.3	0.4	0.11	-0.04	-0.03
2.497	2.6750	0.00	-0.00	-0.01	-0.2	-0.1	-0.0	-0.13	0.04	-0.06

Table 61. Boundary-layer y-derivatives at $x/L = 0.772$, $\phi = 105^\circ$.

$x/L = 0.772$ $\alpha = 10 \text{ deg.}$
 $Re = 4.2E+06$ $\phi = 110 \text{ deg.}$
Derivatives in Local-Freestream Coordinates

r		(1/cm)			(1/cm x1000)					
(cm)	(δ)	U _y	V _y	W _y	u ² _y	v ² _y	w ² _y	uv _y	uw _y	vw _y
0.009	0.0081	15.580	0.161	1.753	-134.500	68.300	119.900	67.29	55.36	-1.40
0.019	0.0173	8.746	0.033	0.813	-138.700	47.400	55.710	29.27	41.28	-1.63
0.029	0.0264	5.761	0.020	0.415	-114.700	34.480	30.220	15.44	29.43	-1.58
0.039	0.0356	2.400	0.053	-0.030	-71.610	18.030	3.340	2.44	11.74	-1.53
0.074	0.0676	1.470	-0.021	-0.116	-28.600	4.665	-0.503	-3.38	4.25	-1.54
0.149	0.1362	0.921	0.019	-0.118	-8.908	1.528	0.314	-1.046	1.553	-0.668
0.249	0.2277	0.648	0.031	-0.119	-3.764	-0.459	-0.784	-0.829	0.307	0.112
0.499	0.4564	0.441	0.044	-0.084	-3.548	-1.414	-2.440	-0.752	-0.363	0.353
0.749	0.6851	0.321	0.038	-0.043	-3.915	-1.573	-2.677	-1.040	-0.319	0.189
0.999	0.9138	0.201	0.036	-0.004	-3.114	-1.284	-2.308	-0.825	-0.213	0.016
1.499	1.3710	0.060	0.024	0.018	-1.295	-0.489	-0.920	-0.378	-0.032	-0.016
1.999	1.8290	0.001	0.015	0.015	-0.070	0.092	-0.032	-0.072	0.087	0.072
2.499	2.2860	0.000	0.009	0.013	0.124	0.247	0.173	-0.200	0.100	0.114

r		(1/cm ²)			(1/cm ² x1000)					
(cm)	(δ)	U _{yy}	V _{yy}	W _{yy}	u ² _{yy}	v ² _{yy}	w ² _{yy}	-uv _{yy}	-uw _{yy}	-vw _{yy}
0.009	0.0081	-918.20	-21.97	-127.20	-3042.0	-2463.0	-8858.0	-5394.0	-1320	-45
0.019	0.0173	-473.60	-5.31	-64.30	1639.0	-1719.0	-4263.0	-2413.0	-1414	-4
0.029	0.0264	-173.90	1.53	-22.40	2943.0	-987.7	-1329.0	-650.5	-1021	11
0.039	0.0356	-19.23	-1.45	-1.50	870.3	-268.9	-57.1	-106.0	-140.3	1.3
0.074	0.0676	-7.62	0.65	0.01	274.0	-37.1	13.2	38.69	-35.11	13.46
0.149	0.1362	-2.08	0.11	0.01	29.1	-14.6	-11.2	1.31	-9.95	5.99
0.249	0.2277	-0.84	0.05	0.12	-0.1	-4.6	-7.3	-0.09	-2.54	0.97
0.499	0.4564	-0.44	-0.01	0.22	-5.3	-1.8	-4.3	-2.23	-0.18	-0.78
0.749	0.6851	-0.51	-0.02	0.16	3.9	1.4	2.3	0.92	0.48	-0.72
0.999	0.9138	-0.33	-0.03	0.05	4.4	1.8	3.3	1.16	0.45	-0.09
1.499	1.3710	-0.13	-0.02	-0.00	2.7	1.2	2.0	0.70	0.27	0.16
1.999	1.8290	-0.06	-0.02	-0.01	1.4	0.9	1.1	0.30	0.10	0.25
2.499	2.2860	0.01	-0.01	-0.00	0.3	0.2	0.3	-0.32	0.02	0.07

Table 62. Boundary-layer y-derivatives at $x/L = 0.772$, $\phi = 110^\circ$.

$x/L = 0.772$ $\alpha = 10 \text{ deg.}$
 $Re = 4.2E+06$ $\phi = 115 \text{ deg.}$
Derivatives in Local-Freestream Coordinates

r		(1/cm)			(1/cm x1000)					
(cm)	(δ)	U _y	V _y	W _y	u ² _y	v ² _y	w ² _y	uv _y	uw _y	vw _y
0.009	0.0069	15.170	-0.232	2.891	180.600	35.240	128.400	85.34	23.32	1.81
0.014	0.0109	12.000	-0.047	1.823	-2.560	48.370	92.660	57.88	38.00	1.96
0.019	0.0149	9.037	0.019	1.127	-96.410	49.360	62.530	35.41	40.82	1.53
0.029	0.0229	4.779	0.009	0.504	-122.200	35.330	24.970	9.41	29.73	-0.44
0.039	0.0309	2.613	-0.012	0.187	-64.290	17.880	7.736	1.74	15.25	-1.92
0.074	0.0589	1.268	0.032	-0.010	-16.590	5.486	0.292	0.390	5.190	-2.175
0.149	0.1189	0.852	0.054	-0.118	-6.223	2.234	-0.619	0.249	2.339	-0.934
0.249	0.1990	0.604	0.051	-0.142	-2.447	0.166	-0.289	-0.292	0.820	-0.048
0.499	0.3990	0.465	0.044	-0.118	-3.082	-1.127	-1.024	-0.913	0.110	0.288
0.749	0.5991	0.351	0.042	-0.067	-3.451	-1.429	-1.768	-1.004	-0.122	0.225
0.999	0.7992	0.243	0.039	-0.022	-3.404	-1.443	-2.439	-0.950	-0.294	0.111
1.498	1.1990	0.081	0.027	0.013	-1.750	-0.715	-1.571	-0.418	-0.203	-0.004
1.998	1.5990	0.004	0.016	0.009	-0.224	-0.035	-0.264	-0.057	0.022	-0.001
2.499	2.0000	0.006	0.019	0.011	0.065	0.175	0.033	-0.076	0.066	0.091

r		(1/cm ²)			(1/cm ² x1000)					
(cm)	(δ)	U _{yy}	V _{yy}	W _{yy}	u ² _{yy}	v ² _{yy}	w ² _{yy}	-uv _{yy}	-uw _{yy}	-vw _{yy}
0.009	0.0069	-648.30	60.04	-281.50	-53190.0	4978.0	-7998.0	-6257.0	5221	143
0.014	0.0109	-609.00	17.03	-153.00	-21970.0	594.9	-6305.0	-4733.0	956	-67
0.019	0.0149	-508.90	-7.30	-66.29	-2079.0	-1872.0	-4563.0	-3243.0	-1483	-177
0.029	0.0229	-126.30	0.10	-18.43	3712.0	-1053.0	-932.4	-364.6	-884.3	-95.6
0.039	0.0309	-26.15	0.99	-4.23	901.0	-238.6	-137.2	-22.19	-191.60	5.01
0.074	0.0589	-5.79	0.26	-1.43	142.7	-44.5	-12.8	-3.84	-40.44	17.89
0.149	0.1189	-1.77	-0.04	-0.12	20.8	-15.2	3.0	-4.44	-10.55	6.48
0.249	0.1990	-0.52	-0.03	0.07	-3.2	-5.7	-3.5	-2.91	-2.90	1.48
0.499	0.3990	-0.40	-0.01	0.20	-4.1	-2.6	-4.2	-1.36	-1.21	-0.16
0.749	0.5991	-0.48	-0.01	0.21	0.6	0.2	-2.7	0.48	-0.74	-0.51
0.999	0.7992	-0.38	-0.03	0.08	3.9	1.7	2.0	1.27	0.21	-0.30
1.498	1.1990	-0.17	-0.02	-0.00	3.1	1.4	2.5	0.76	0.44	-0.02
1.998	1.5990	-0.10	-0.02	-0.03	2.7	1.2	2.9	0.56	0.50	0.08
2.499	2.0000	0.02	0.01	0.01	0.3	0.3	0.3	-0.10	0.04	0.20

Table 63. Boundary-layer y-derivatives at $x/L = 0.772$, $\phi = 115^\circ$.

$x/L = 0.772$ $\alpha = 10 \text{ deg.}$
 $Re = 4.2E+06$ $\phi = 120 \text{ deg.}$
Derivatives in Local-Freestream Coordinates

r		(1/cm)			(1/cm x1000)					
(cm)	(δ)	U _y	V _y	W _y	u ² _y	v ² _y	w ² _y	uv _y	uw _y	vw _y
0.007	0.0048	10.450	-0.329	2.979	316.100	12.760	60.590	45.04	-6.14	5.54
0.013	0.0090	9.187	-0.062	2.215	80.130	34.010	53.270	39.32	23.92	5.42
0.017	0.0118	8.031	0.005	1.754	-6.314	37.490	43.440	30.84	32.33	3.72
0.027	0.0189	5.519	0.032	0.905	-104.600	33.560	21.370	11.11	37.32	-0.84
0.037	0.0259	2.382	0.057	0.249	-50.390	19.160	9.484	6.72	17.93	-1.02
0.072	0.0506	1.211	0.035	0.009	-19.610	6.148	2.250	0.341	7.261	-1.636
0.147	0.1035	0.787	0.051	-0.074	-5.216	2.398	1.447	0.199	2.911	-0.942
0.247	0.1740	0.600	0.055	-0.115	-1.355	0.612	0.667	-0.367	1.159	-0.405
0.497	0.3502	0.463	0.055	-0.128	-1.866	-0.547	-0.356	-0.436	0.296	0.169
0.747	0.5264	0.375	0.051	-0.091	-2.963	-1.090	-1.697	-0.718	-0.140	0.236
0.997	0.7026	0.287	0.047	-0.050	-3.505	-1.349	-2.630	-0.809	-0.440	0.207
1.497	1.0550	0.121	0.032	0.000	-2.103	-0.843	-1.861	-0.492	-0.336	0.052
1.996	1.4070	0.010	0.018	0.009	-0.342	-0.162	-0.277	-0.071	0.026	-0.028
2.497	1.7600	-0.001	0.008	0.003	0.209	0.130	0.090	-0.005	0.017	-0.023

r		(1/cm ²)			(1/cm ² x1000)					
(cm)	(δ)	U _{yy}	V _{yy}	W _{yy}	u ² _{yy}	v ² _{yy}	w ² _{yy}	-uv _{yy}	-uw _{yy}	-vw _{yy}
0.007	0.0048	-119.90	71.99	-133.60	-55680.0	6166.0	204.9	398.8	7758	430
0.013	0.0090	-280.30	21.28	-119.10	-24860.0	1310.0	-2321.0	-1993.0	2615	-375
0.017	0.0118	-317.80	1.46	-102.20	-10590.0	-622.2	-2920.0	-2542.0	370	-592
0.027	0.0189	-168.20	0.86	-35.29	3167.0	-882.6	-621.7	-260.2	-1099.0	-11.3
0.037	0.0259	-22.88	-0.33	-4.61	635.0	-263.8	-141.9	-124.40	-218.10	-8.07
0.072	0.0506	-5.53	0.21	-1.11	186.0	-48.3	-11.1	-2.95	-56.20	8.68
0.147	0.1035	-1.44	0.03	-0.31	24.1	-12.5	-4.8	-2.60	-12.43	4.98
0.247	0.1740	-0.53	-0.02	-0.09	-3.8	-5.4	-2.5	-0.59	-2.69	2.55
0.497	0.3502	-0.32	0.01	0.10	-6.4	-3.2	-9.0	-1.54	-2.94	0.67
0.747	0.5264	-0.37	-0.02	0.20	-2.1	-1.0	-3.8	-0.44	-1.25	-0.23
0.997	0.7026	-0.39	-0.03	0.12	3.1	1.1	2.0	0.74	0.36	-0.37
1.497	1.0550	-0.23	-0.03	0.02	3.5	1.3	3.3	0.84	0.78	-0.18
1.996	1.4070	-0.19	-0.02	-0.01	3.8	1.5	2.8	0.87	0.53	-0.09
2.497	1.7600	-0.00	-0.02	-0.01	0.8	0.5	0.5	0.05	-0.08	0.02

Table 64. Boundary-layer y-derivatives at $x/L = 0.772$, $\phi = 120^\circ$.

$x/L = 0.772$ $\alpha = 10 \text{ deg.}$
 $Re = 4.2E+06$ $\phi = 123 \text{ deg.}$
Derivatives in Local-Freestream Coordinates

r		(1/cm)			(1/cm x1000)					
(cm)	(δ)	U _y	V _y	W _y	u ² _y	v ² _y	w ² _y	uv _y	uw _y	vw _y
0.012	0.0077	11.450	-0.065	3.285	-53.350	33.440	46.950	20.41	57.14	-0.04
0.017	0.0109	8.280	0.011	2.299	-42.670	32.380	35.550	21.10	38.94	1.81
0.022	0.0142	5.950	0.057	1.576	-45.750	29.860	24.910	17.63	30.59	1.67
0.032	0.0207	3.332	0.068	0.782	-60.330	22.620	9.801	7.03	26.48	-0.57
0.042	0.0272	2.293	-0.017	0.402	-63.100	12.050	1.407	-4.89	20.97	-2.53
0.077	0.0499	1.161	0.028	0.076	-22.150	5.105	0.213	-2.100	8.201	-1.413
0.152	0.0987	0.725	0.049	-0.042	-3.266	2.693	1.134	0.500	2.720	-0.914
0.252	0.1637	0.542	0.061	-0.110	1.349	1.246	1.380	0.520	1.005	-0.544
0.502	0.3262	0.455	0.063	-0.130	-1.209	-0.277	-0.134	-0.236	0.368	-0.068
0.752	0.4887	0.385	0.061	-0.108	-2.497	-0.917	-1.357	-0.488	-0.014	0.174
1.002	0.6512	0.310	0.053	-0.075	-3.224	-1.281	-2.306	-0.572	-0.269	0.261
1.502	0.9762	0.158	0.019	-0.014	-2.204	-0.927	-1.747	-0.578	-0.236	0.093
2.001	1.3010	0.059	-0.023	0.022	-0.558	-0.286	-0.416	-0.159	-0.006	-0.036
2.501	1.6260	0.094	-0.084	0.033	0.482	0.186	0.292	0.146	-0.027	-0.002

r		(1/cm ²)			(1/cm ² x1000)					
(cm)	(δ)	U _{yy}	V _{yy}	W _{yy}	u ² _{yy}	v ² _{yy}	w ² _{yy}	-uv _{yy}	-uw _{yy}	-vw _{yy}
0.012	0.0077	-777.20	20.55	-243.10	4936.0	69.5	-2335.0	973.7	-5537	762
0.017	0.0109	-500.10	10.44	-155.20	-217.1	-456.6	-2187.0	-569.6	-1996	34
0.022	0.0142	-289.30	2.88	-89.14	-2694.0	-752.3	-1822.0	-1346.0	28	-350
0.032	0.0207	-66.89	-4.54	-23.06	382.3	-652.0	-445.0	-600.1	-473.0	-84.5
0.042	0.0272	-23.65	1.21	-6.74	928.2	-135.2	-8.0	88.57	-277.60	27.92
0.077	0.0499	-5.79	0.29	-1.52	245.6	-30.7	12.9	35.66	-68.26	5.23
0.152	0.0987	-1.22	0.06	-0.48	18.8	-12.1	-0.4	-3.91	-11.08	3.05
0.252	0.1637	-0.39	-0.01	-0.11	-9.6	-6.4	-6.1	-3.42	-2.73	2.03
0.502	0.3262	-0.19	0.06	0.05	-9.4	-4.0	-7.0	0.30	-1.78	1.93
0.752	0.4887	-0.31	-0.05	0.15	-2.5	-1.3	-3.8	-0.98	-1.15	0.15
1.002	0.6512	-0.38	-0.06	0.14	2.3	0.7	1.2	-0.16	0.10	-0.44
1.502	0.9762	-0.21	-0.08	0.08	3.4	1.3	2.6	0.72	0.43	-0.30
2.001	1.3010	-0.14	-0.08	0.06	2.9	1.3	2.9	1.26	0.55	-0.11
2.501	1.6260	0.09	-0.13	0.02	2.0	0.9	1.3	0.54	-0.11	0.09

Table 65. Boundary-layer y-derivatives at $x/L = 0.772$, $\phi = 123^\circ$.

$x/L = 0.772$ $\alpha = 10 \text{ deg.}$
 $Re = 4.2E+06$ $\phi = 125 \text{ deg.}$
Derivatives in Local-Freestream Coordinates

r		(1/cm)			(1/cm x1000)					
(cm)	(/δ)	U _y	V _y	W _y	u ² _y	v ² _y	w ² _y	uv _y	uw _y	vw _y
0.006	0.0035	13.040	-0.799	3.613	221.600	-9.557	67.980	7.34	-21.17	-1.98
0.016	0.0096	8.398	-0.123	2.304	35.210	20.450	43.710	16.13	15.55	0.97
0.026	0.0157	5.884	0.039	1.549	-14.820	23.780	28.170	14.52	21.32	0.81
0.036	0.0218	2.782	0.086	0.601	-57.150	20.240	5.951	6.99	22.57	-1.15
0.071	0.0432	1.320	0.077	0.130	-13.130	8.531	0.738	3.76	6.71	-0.74
0.146	0.0889	0.749	0.028	-0.009	-5.316	2.308	1.560	-0.079	2.992	-0.839
0.246	0.1499	0.512	0.044	-0.093	0.117	0.703	2.752	-0.153	1.615	-0.550
0.496	0.3024	0.463	0.057	-0.127	-0.090	0.104	0.878	-0.211	0.642	-0.085
0.746	0.4548	0.402	0.055	-0.113	-1.418	-0.417	-0.859	-0.422	0.089	0.087
0.996	0.6073	0.322	0.048	-0.089	-2.885	-1.033	2.270	-0.724	-0.392	0.204
1.496	0.9123	0.148	0.036	-0.024	-2.601	-1.038	-2.006	-0.582	-0.318	0.089
1.996	1.2170	0.031	0.024	0.014	-0.895	-0.410	-0.698	-0.132	-0.076	0.020
2.496	1.5220	-0.018	-0.001	-0.010	0.831	0.337	0.617	0.108	0.145	-0.087

r		(1/cm ²)			(1/cm ² x1000)					
(cm)	(/δ)	U _{yy}	V _{yy}	W _{yy}	u ² _{yy}	v ² _{yy}	w ² _{yy}	-uv _{yy}	-uw _{yy}	-vw _{yy}
0.006	0.0035	-576.90	104.10	-157.90	-27960.0	4965.0	-2747.0	1721.0	5901	549
0.016	0.0096	-358.20	36.57	-104.60	-10610.0	1350.0	-2072.0	191.6	1785	89
0.026	0.0157	-175.40	1.66	-54.88	-1013.0	-391.0	-1185.0	-411.8	-284	-92
0.036	0.0218	-28.59	-0.61	-8.78	832.1	-256.8	-83.9	-89.4	-304.5	5.5
0.071	0.0432	-7.95	-0.52	-1.94	111.7	-79.1	18.6	-45.37	-51.36	1.37
0.146	0.0889	-1.54	0.14	-0.62	34.0	-10.1	5.6	0.12	-8.64	2.16
0.246	0.1499	0.04	0.09	-0.12	1.9	-1.1	-7.7	0.91	-4.24	2.28
0.496	0.3024	-0.28	-0.02	-0.04	-9.1	-3.4	-10.1	-1.88	-3.50	1.34
0.746	0.4548	-0.35	-0.03	0.11	-5.8	-2.3	-5.4	-1.23	-1.62	0.21
0.996	0.6073	-0.37	-0.02	0.16	0.4	-0.2	0.3	0.36	0.11	-0.22
1.496	0.9123	-0.23	-0.02	0.09	3.4	1.3	2.5	0.94	0.47	-0.14
1.996	1.2170	-0.25	-0.03	0.04	3.4	1.3	3.0	0.76	0.54	-0.13
2.496	1.5220	-0.08	-0.05	-0.06	3.5	1.5	2.6	0.45	0.43	-0.22

Table 66. Boundary-layer y-derivatives at $x/L = 0.772$, $\phi = 125^\circ$.

$x/L = 0.772$ $\alpha = 10 \text{ deg.}$
 $Re = 4.2E+06$ $\phi = 130 \text{ deg.}$
Derivatives in Local-Freestream Coordinates

r		(1/cm)			(1/cm x1000)					
(cm)	(δ)	U _y	V _y	W _y	U ² _y	V ² _y	W ² _y	uv _y	uw _y	vw _y
0.007	0.0038	12.960	0.096	4.215	300.900	14.410	69.920	25.58	-81.48	8.76
0.009	0.0049	11.810	0.087	3.889	243.400	17.910	65.240	27.75	-59.62	8.49
0.013	0.0070	9.430	0.069	3.219	122.100	25.510	55.810	32.75	-13.16	8.02
0.023	0.0124	5.983	0.069	1.934	3.707	24.890	24.290	21.14	25.18	3.09
0.033	0.0177	3.152	0.021	0.916	-41.160	17.380	6.828	6.21	24.08	0.21
0.068	0.0364	1.277	0.033	0.241	-23.710	7.219	0.418	0.929	11.060	-0.889
0.143	0.0764	0.724	0.017	0.052	-8.108	2.479	1.051	-0.181	4.055	-0.816
0.243	0.1298	0.472	0.037	-0.040	0.095	1.094	2.029	0.198	1.403	-0.601
0.493	0.2633	0.389	0.049	-0.109	0.595	0.368	0.941	-0.027	0.635	-0.169
0.743	0.3967	0.355	0.059	-0.119	-0.350	-0.108	-0.164	-0.169	0.199	0.052
0.993	0.5302	0.331	0.059	-0.110	-1.819	-0.645	-1.343	-0.495	-0.104	0.182
1.493	0.7971	0.220	0.043	-0.031	-2.882	-1.042	-2.071	-0.679	-0.358	0.063
1.993	1.0640	0.063	0.004	0.047	-2.718	-1.086	-1.464	-0.662	-0.076	-0.305

r		(1/cm ²)			(1/cm ² x1000)					
(cm)	(δ)	U _{yy}	V _{yy}	W _{yy}	u ² _{yy}	v ² _{yy}	w ² _{yy}	-uv _{yy}	-uw _{yy}	-vw _{yy}
0.007	0.0038	-613.00	-6.40	-163.90	-32440.0	2204.0	-1931.0	1790.0	12570	24
0.009	0.0049	-532.70	-2.43	-161.30	-25190.0	1317.0	-2708.0	428.0	9363	-282
0.013	0.0070	-393.20	2.49	-147.20	-13640.0	11.3	-3498.0	-1412.0	4324	-651
0.023	0.0124	-166.70	-2.86	-60.33	-2031.0	-532.0	-1020.0	-852.4	-239.0	-152.0
0.033	0.0177	-37.19	0.28	-13.24	482.4	-216.1	-94.6	-89.64	-297.40	-18.63
0.068	0.0364	-7.08	-0.26	-2.43	206.9	-63.7	8.3	-15.52	-89.80	0.46
0.143	0.0764	-1.74	0.17	-0.68	52.5	-8.5	5.7	2.79	-17.26	2.32
0.243	0.1298	-0.33	0.05	-0.32	2.4	-2.9	-5.3	-0.99	-3.14	1.87
0.493	0.2633	-0.13	0.04	-0.16	-4.1	-2.3	-4.4	-0.68	-1.59	1.18
0.743	0.3967	-0.09	0.01	0.06	-5.9	-2.1	-4.9	-1.19	-1.49	0.54
0.993	0.5302	-0.22	-0.03	0.16	-2.2	-0.8	-1.5	-0.37	-0.54	-0.22
1.493	0.7971	-0.25	-0.06	0.17	-1.2	-0.5	-0.8	-0.36	0.00	-0.50
1.993	1.0640	-0.33	-0.08	0.15	0.6	-0.0	1.6	0.11	0.67	-0.78

Table 67. Boundary-layer y-derivatives at $x/L = 0.772$, $\phi = 130^\circ$.

$$x/L = 0.772 \quad \alpha = 10 \text{ deg.}$$

$$Re = 4.2E+06 \quad r = 0.25 \text{ cm}$$

Body-Surface Coordinates

(deg.) ϕ	(deg.) β	(/Vinf)			(/Vinf ² x1000)					
		U	V	W	u ²	v ²	w ²	uv	uw	vw
115.0	-10.54	0.646	0.006	-0.120	4.219	1.834	3.752	-0.932	-0.645	0.452
116.0	-9.96	0.641	0.007	-0.113	4.155	1.781	3.784	-0.921	-0.620	0.403
117.0	-8.82	0.631	0.007	-0.098	4.099	1.728	4.044	-0.863	-0.597	0.416
118.0	-7.95	0.621	0.007	-0.087	3.986	1.708	3.955	-0.807	-0.568	0.412
119.0	-7.36	0.614	0.007	-0.079	3.940	1.709	3.967	-0.792	-0.592	0.414
120.0	-6.39	0.597	0.009	-0.067	4.085	1.688	3.948	-0.906	-0.589	0.385
121.0	-5.67	0.594	0.010	-0.059	4.070	1.762	3.176	-0.912	-0.519	0.448
122.0	-5.04	0.583	0.009	-0.051	3.975	1.726	3.137	-0.894	-0.517	0.423
123.0	-3.70	0.575	0.012	-0.037	3.893	1.874	2.980	-0.937	-0.472	0.339
124.0	-3.24	0.568	0.010	-0.032	3.779	1.815	2.972	-0.853	-0.414	0.363
125.0	-2.73	0.561	0.009	-0.027	3.762	1.581	2.992	-0.797	-0.353	0.321
126.0	-2.14	0.554	0.009	-0.021	3.568	1.532	2.881	-0.742	-0.432	0.393
127.0	-1.46	0.547	0.007	-0.014	3.454	1.494	2.742	-0.691	-0.419	0.380
128.0	-0.56	0.538	0.008	-0.005	3.479	1.430	2.681	-0.678	-0.343	0.286
129.0	-0.05	0.548	0.008	-0.000	3.524	1.478	2.835	-0.688	-0.354	0.357
130.0	0.76	0.521	0.006	0.007	3.060	1.313	2.465	-0.621	-0.287	0.263

(deg.) ϕ	(/Vinf ³ x10 ⁶)							
	u ³	v ³	w ³	u ² v	u ² w	uv ²	v ² w	uw ²
115.0	35.40	2.83	-53.44	-4.36	-4.47	5.37	-1.53	11.64
116.0	31.99	-1.48	-59.86	-5.42	-6.84	7.81	-0.98	14.39
117.0	44.54	-5.37	30.61	-11.26	-12.85	10.44	-2.13	14.61
118.0	41.14	-0.44	16.71	-11.15	-5.28	9.53	-0.63	11.17
119.0	45.22	-1.67	0.68	-11.20	-12.28	11.19	-3.36	21.64
120.0	38.05	0.16	5.24	-5.44	-2.47	7.21	-2.23	22.30
121.0	31.70	-1.76	-26.89	-3.81	-8.91	5.92	-3.29	14.58
122.0	29.83	-2.77	-20.55	-4.38	-10.38	6.97	-3.20	15.08
123.0	28.23	-2.65	-19.03	-3.63	-12.16	5.82	-2.58	13.26
124.0	25.23	-4.04	-27.16	-6.40	-7.23	7.51	-1.60	12.49
125.0	39.59	-6.34	-31.17	-8.24	-7.20	9.96	-3.68	12.21
126.0	40.40	-2.39	-24.64	-11.49	-14.31	12.06	-3.70	10.47
127.0	45.37	-4.81	-20.70	-8.26	-9.76	9.51	-3.84	13.33
128.0	44.49	-5.81	-22.35	-9.51	-13.22	11.14	-4.16	13.29
129.0	37.62	-3.35	-27.88	-11.91	-6.90	10.16	-3.65	12.28
130.0	46.72	-5.34	-27.94	-13.68	-8.17	10.87	-4.00	9.55

Table 68. Circumferential profile at $x/L = 0.772$, $r = 0.25$ cm, $\phi = 115 - 130^\circ$.

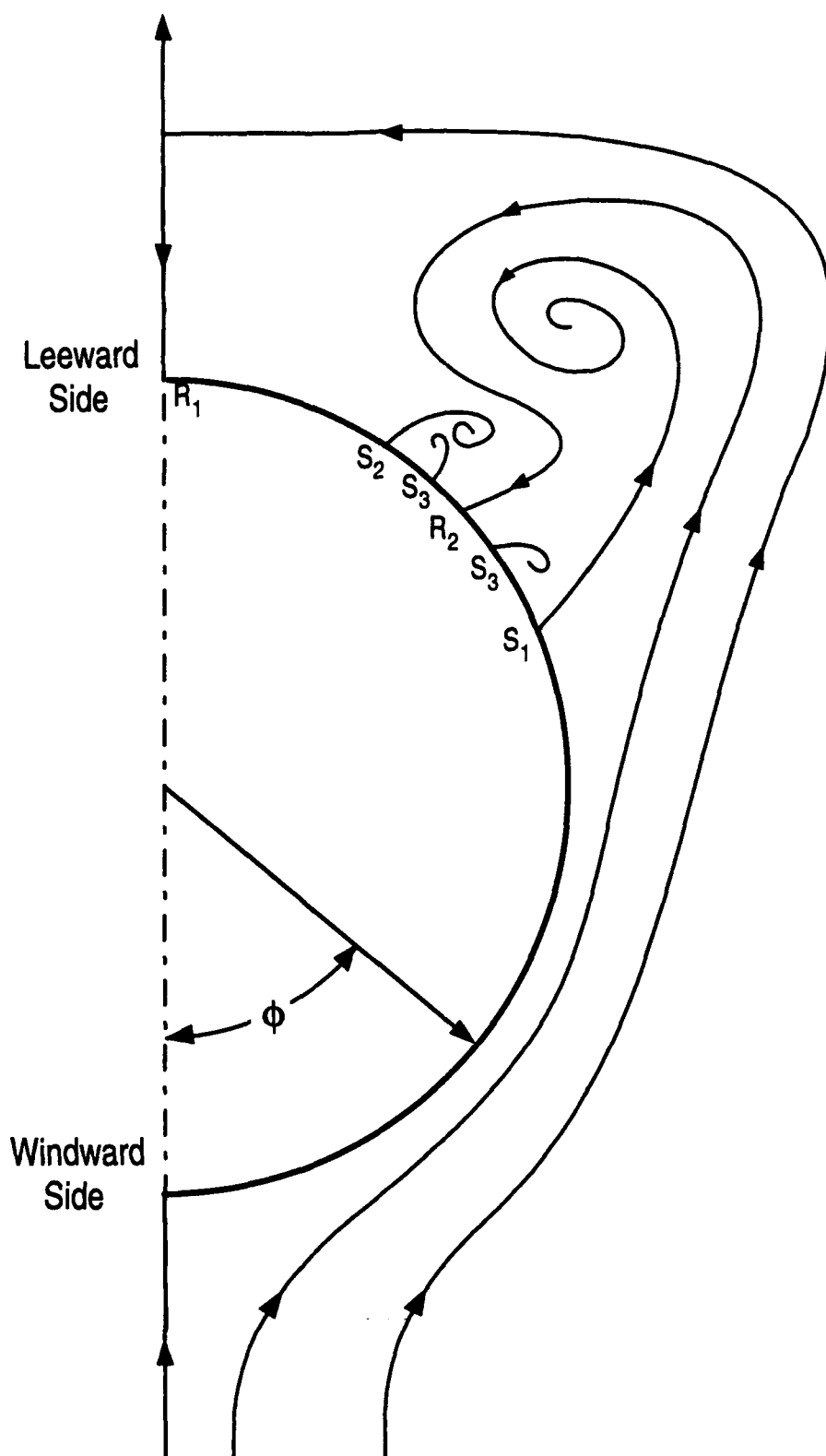


Figure 1. Flow lines in the separation region of the prolate spheroid, 2-D projection.

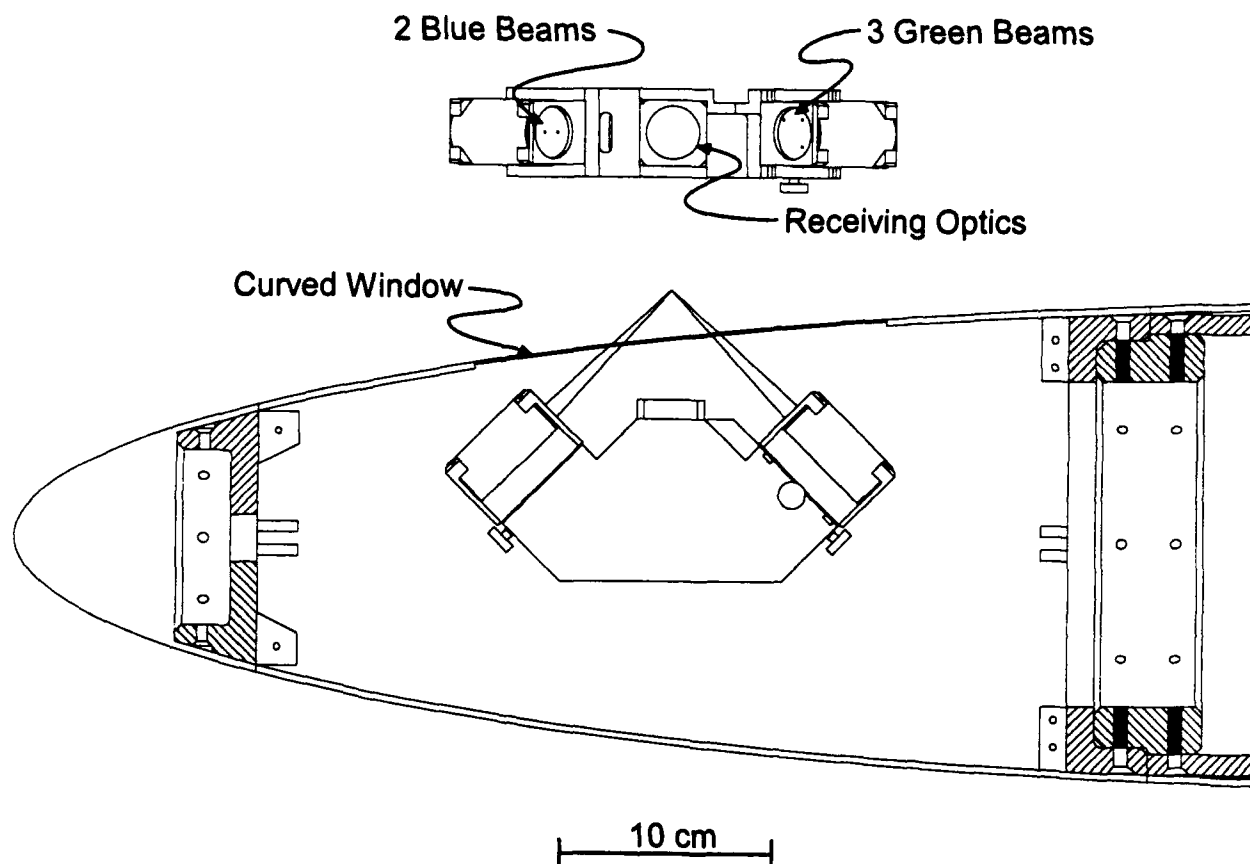


Figure 2. 3-D, fiber-optic, boundary-layer LDV probe placed inside the 6:1 prolate spheroid.

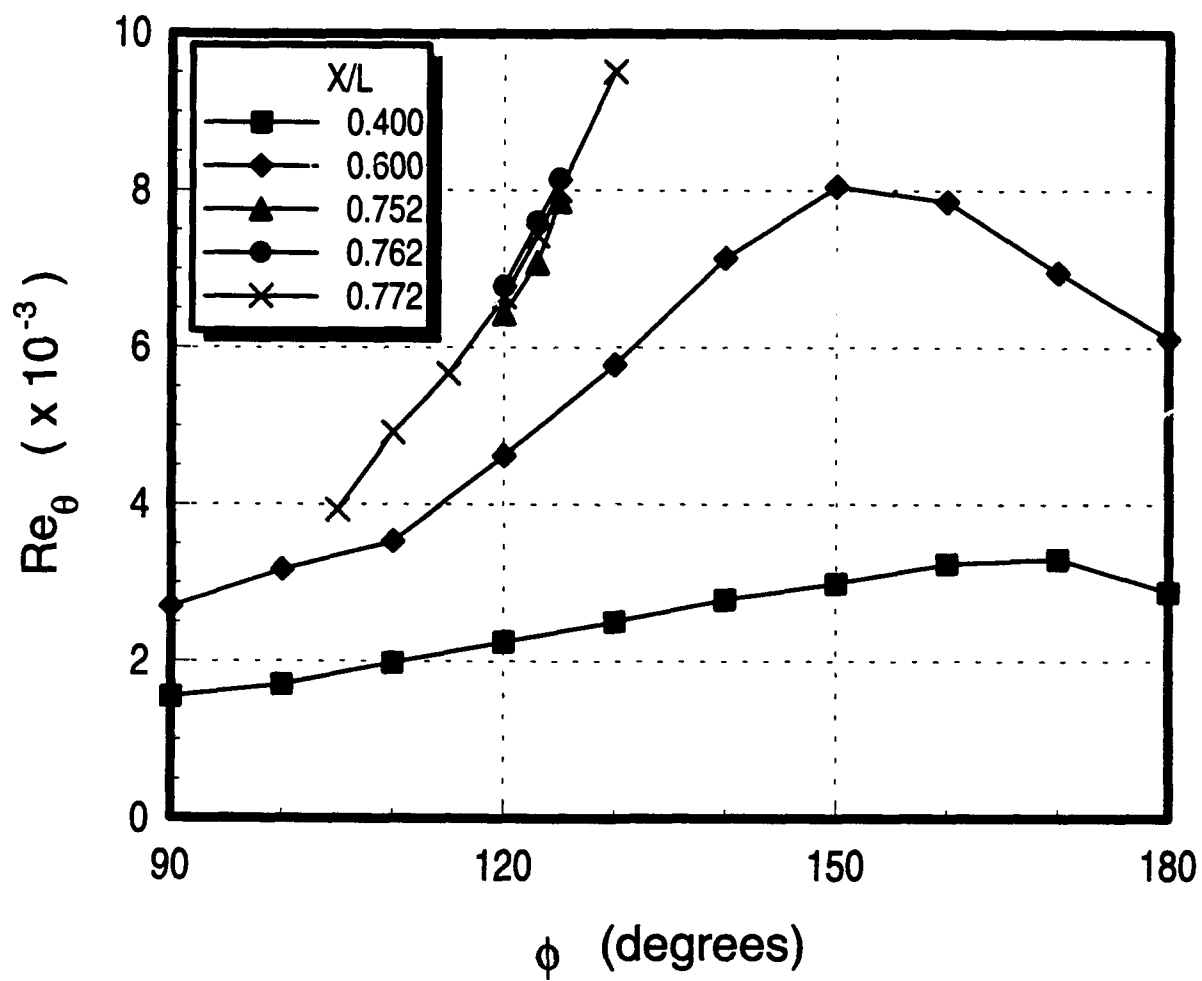


Figure 3. Prolate spheroid streamwise momentum thickness Reynolds number.

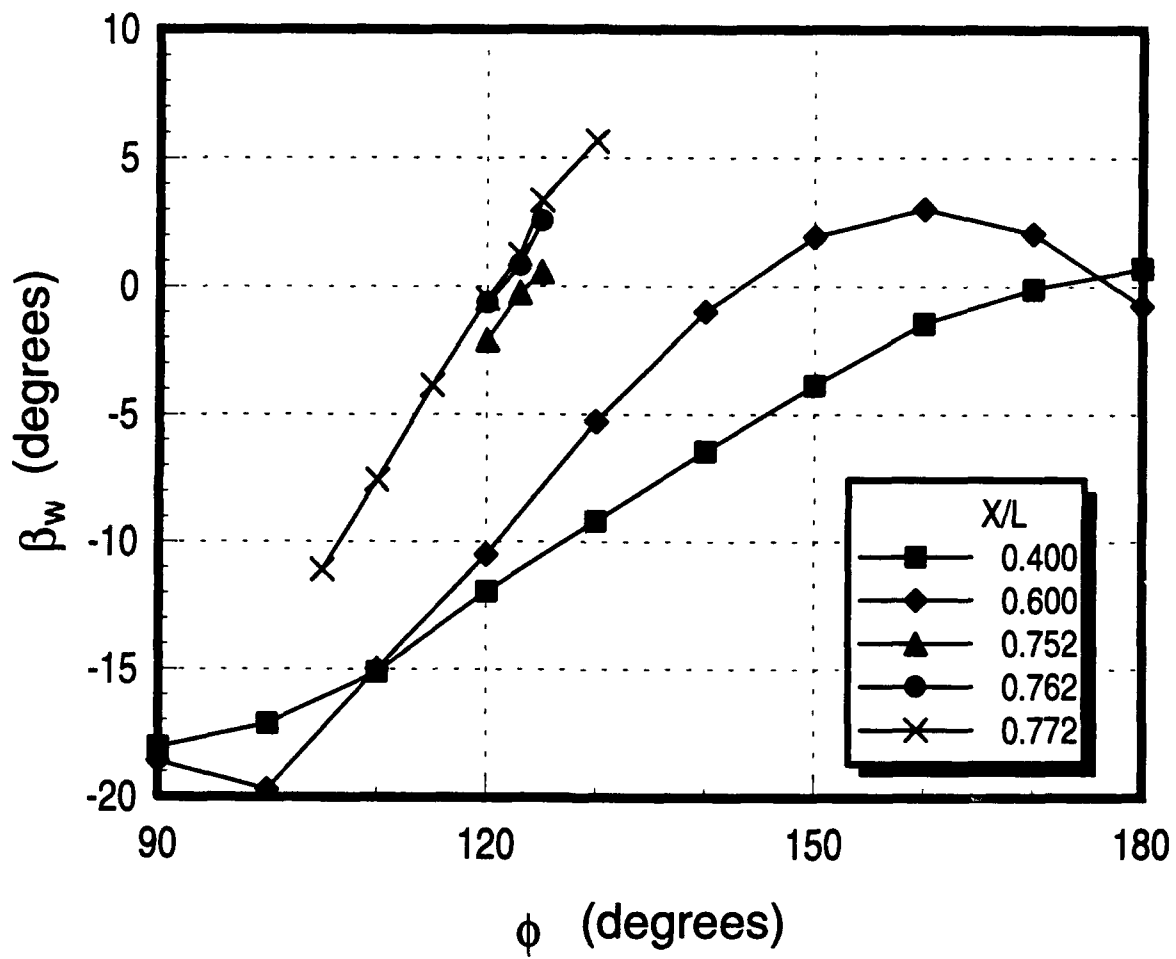


Figure 4. Prolate spheroid wall flow angle.

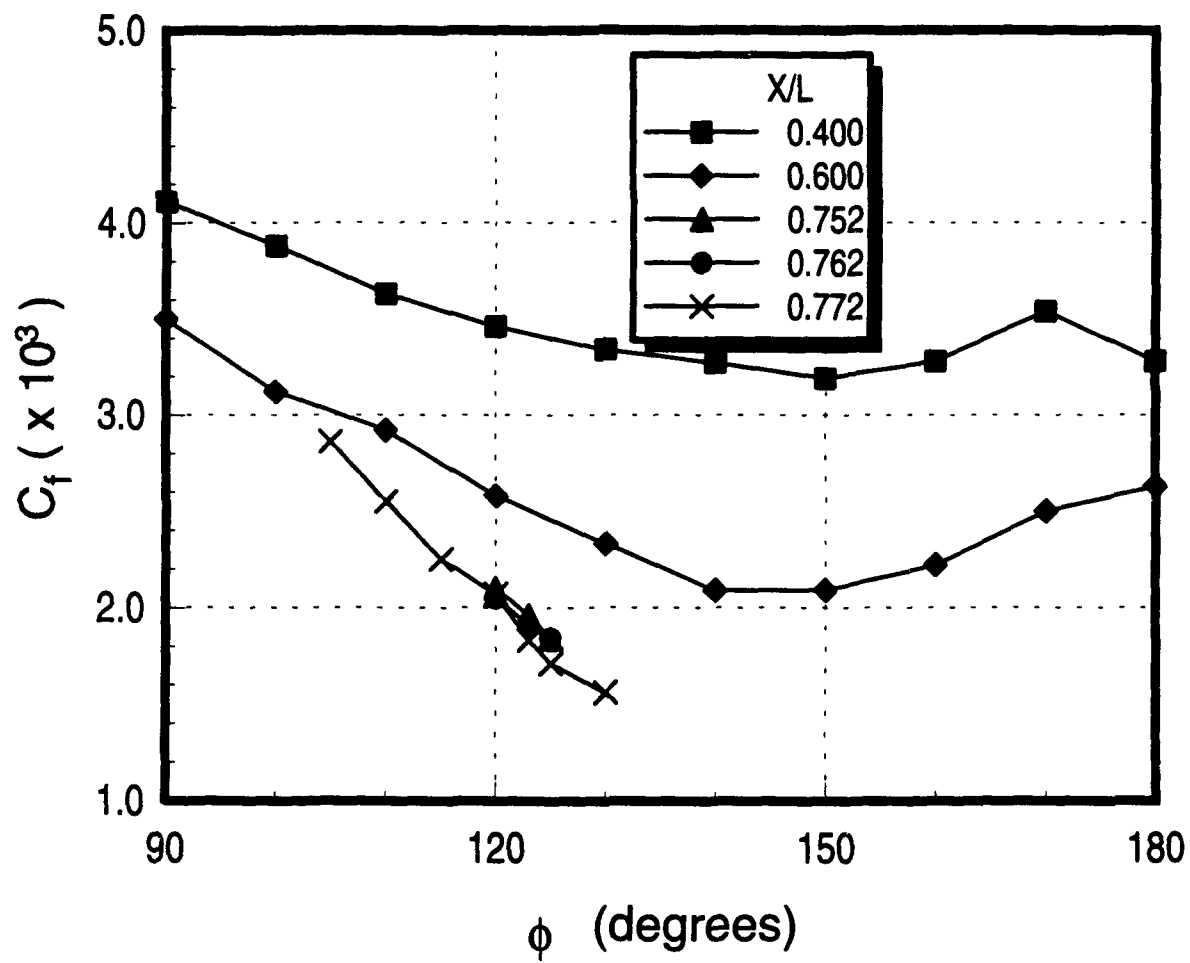


Figure 5. Prolate spheroid skin friction coefficient.

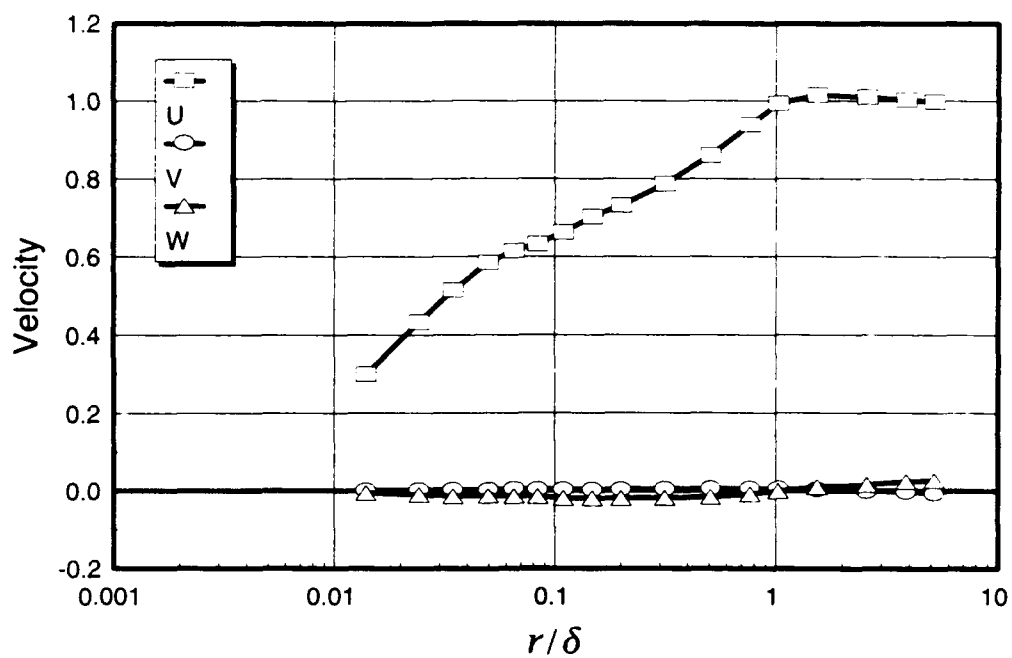


Figure 6. Boundary-layer velocity profiles, $x/L = 0.400$, $\phi = 90^\circ$.

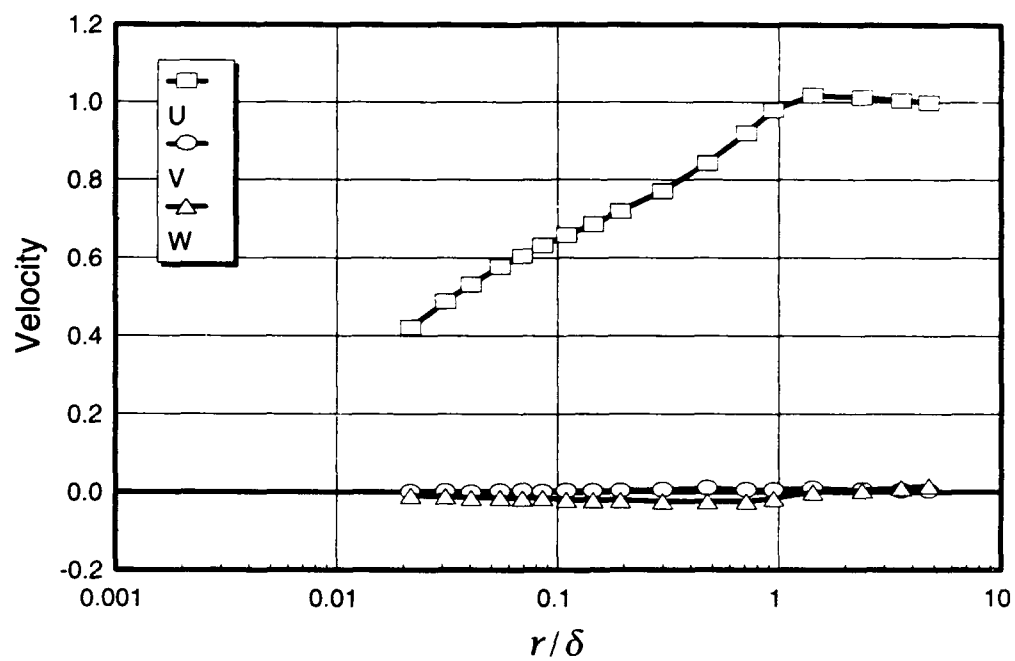


Figure 7. Boundary-layer velocity profiles, $x/L = 0.400$, $\phi = 100^\circ$.

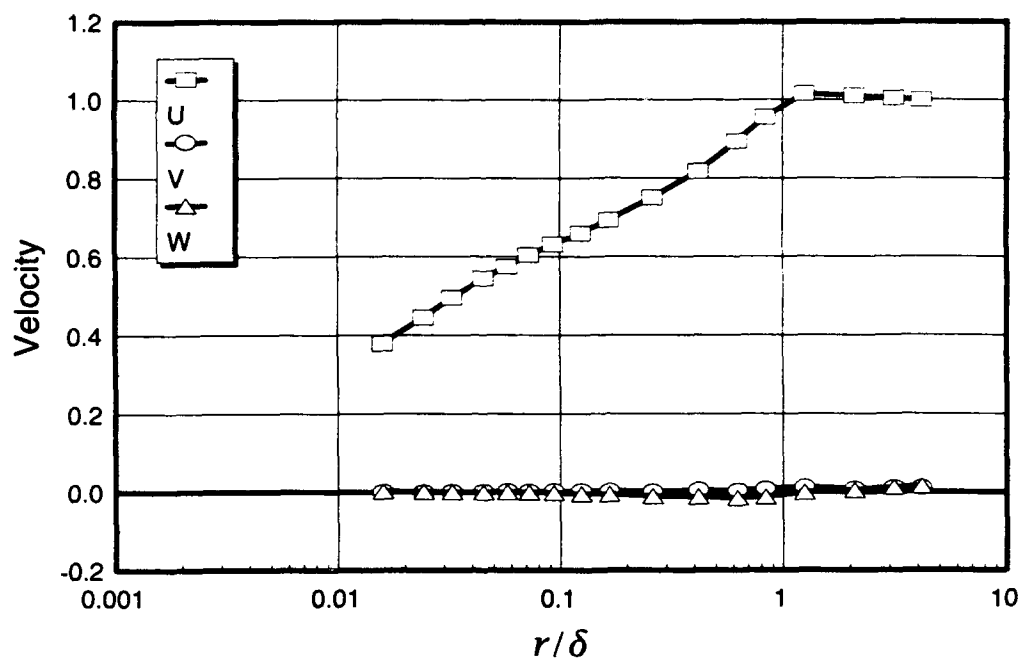


Figure 8. Boundary-layer velocity profiles, $x/L = 0.400$, $\phi = 110^\circ$.

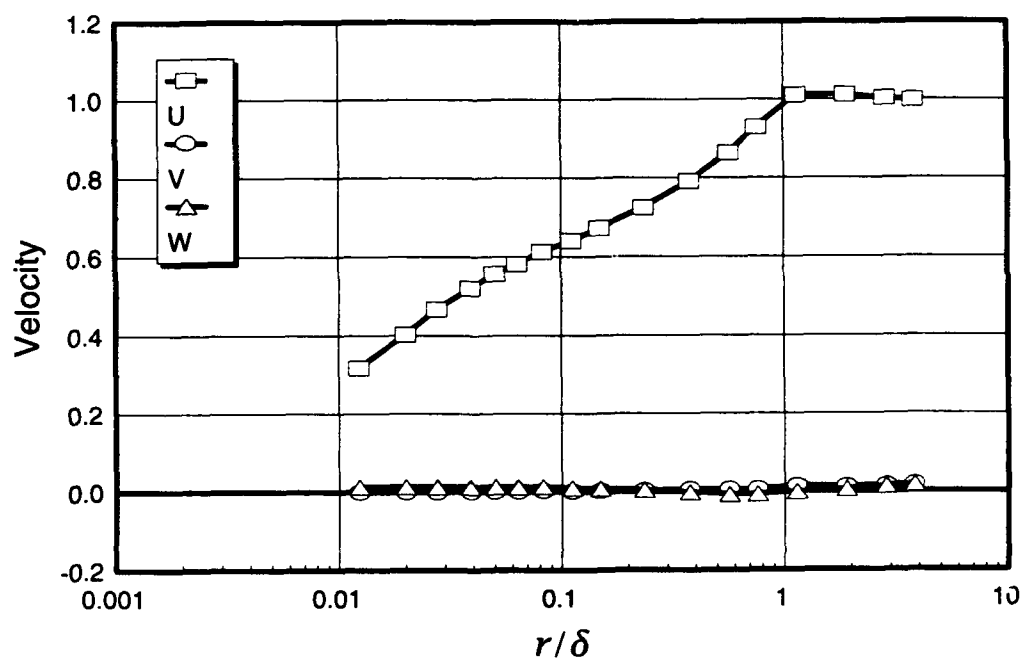


Figure 9. Boundary-layer velocity profiles, $x/L = 0.400$, $\phi = 120^\circ$.

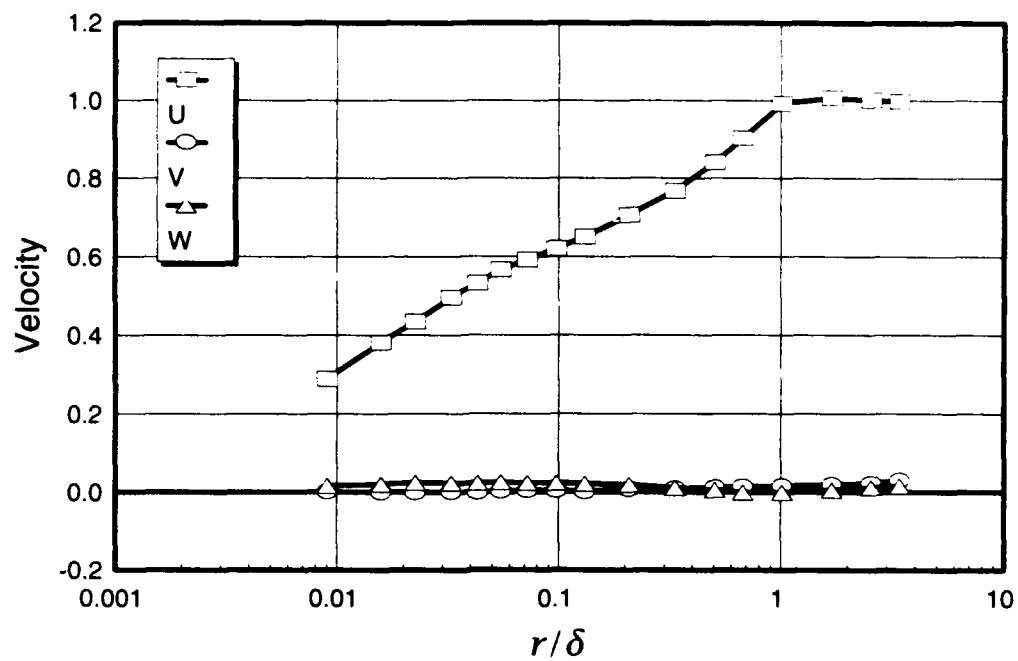


Figure 10. Boundary-layer velocity profiles, $x/L = 0.400$, $\phi = 130^\circ$.

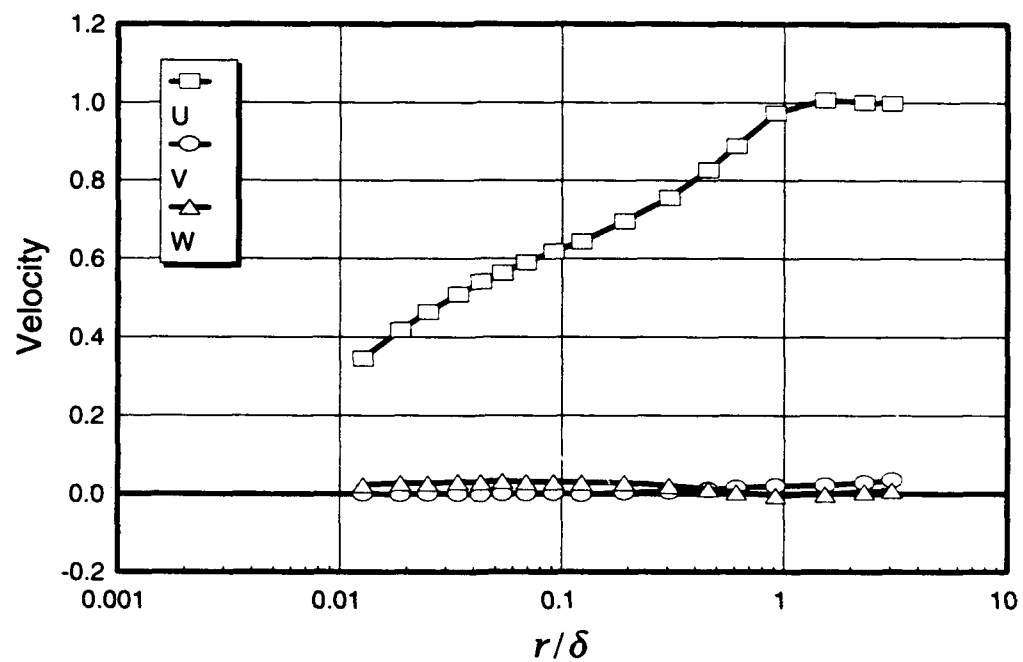


Figure 11. Boundary-layer velocity profiles, $x/L = 0.400$, $\phi = 140^\circ$.

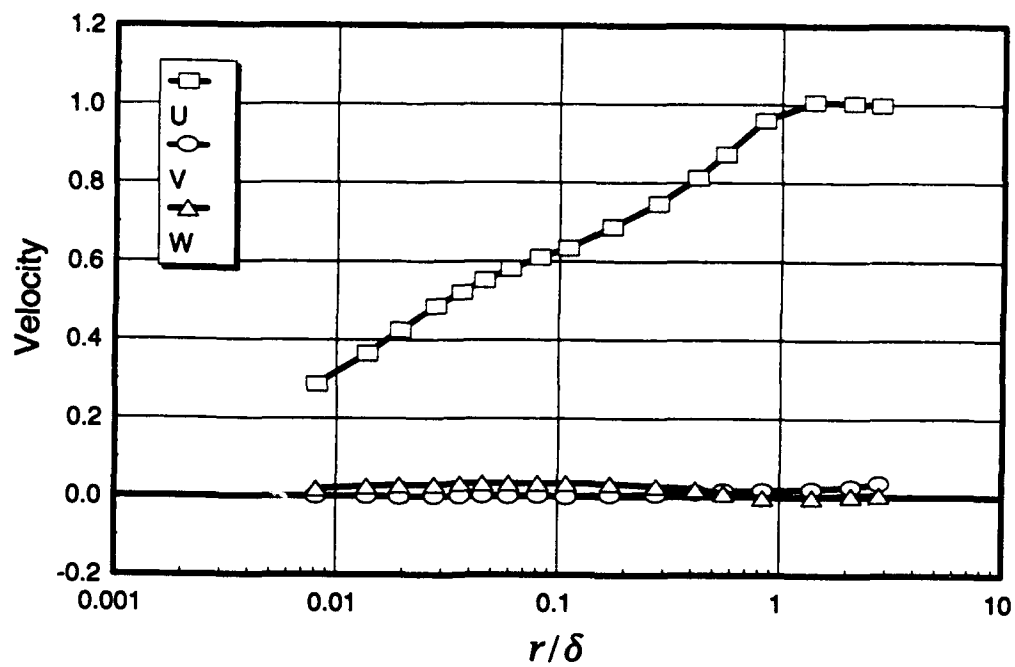


Figure 12. Boundary-layer velocity profiles, $x/L = 0.400$, $\phi = 150^\circ$.

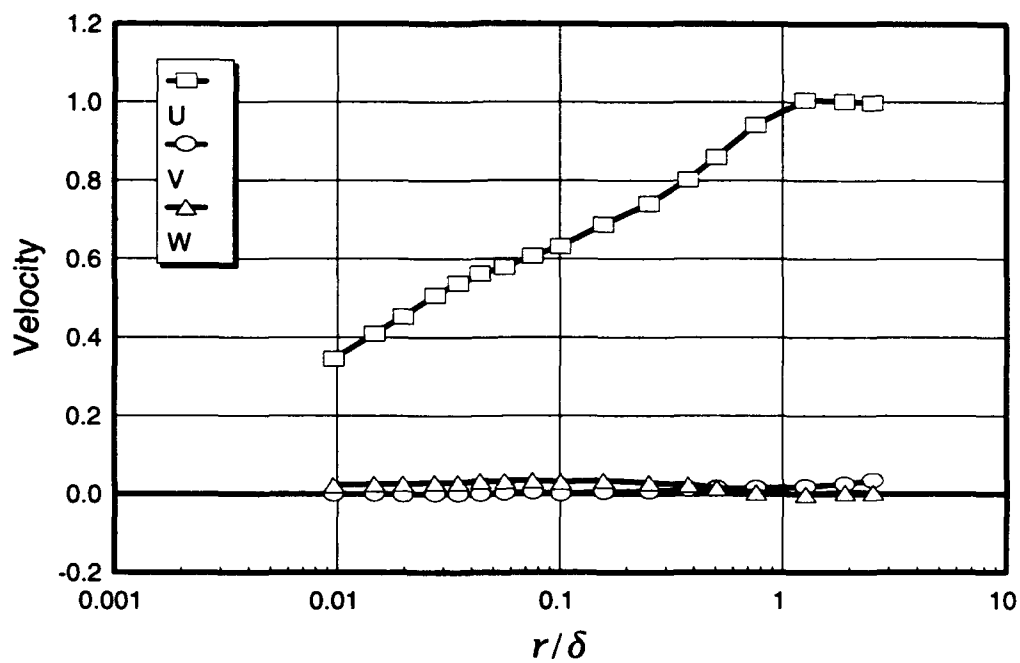


Figure 13. Boundary-layer velocity profiles, $x/L = 0.400$, $\phi = 160^\circ$.

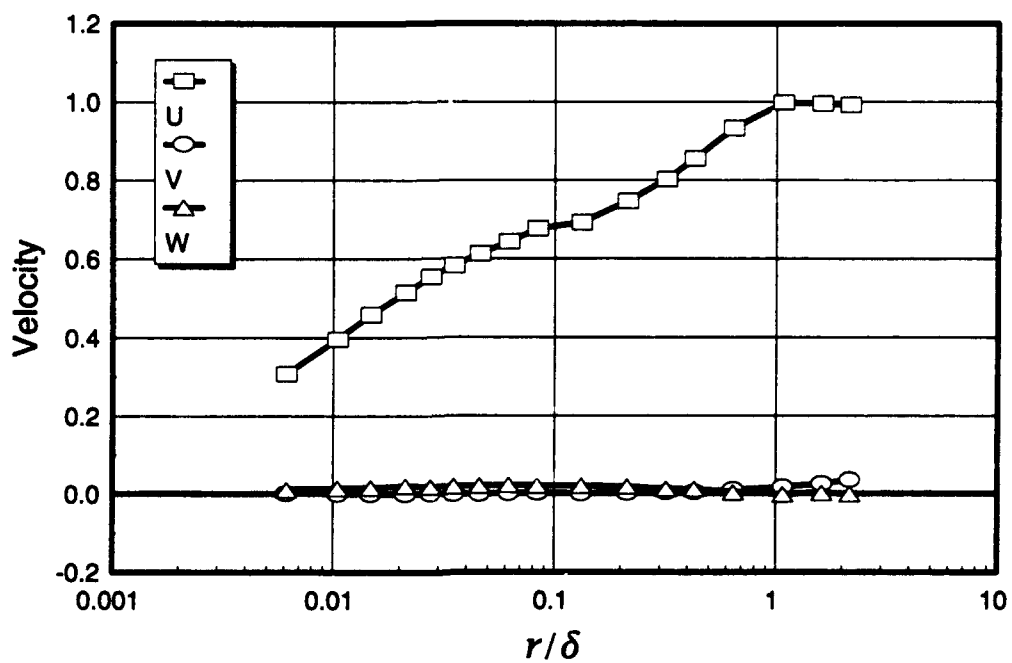


Figure 14. Boundary-layer velocity profiles, $x/L = 0.400$, $\phi = 170^\circ$.

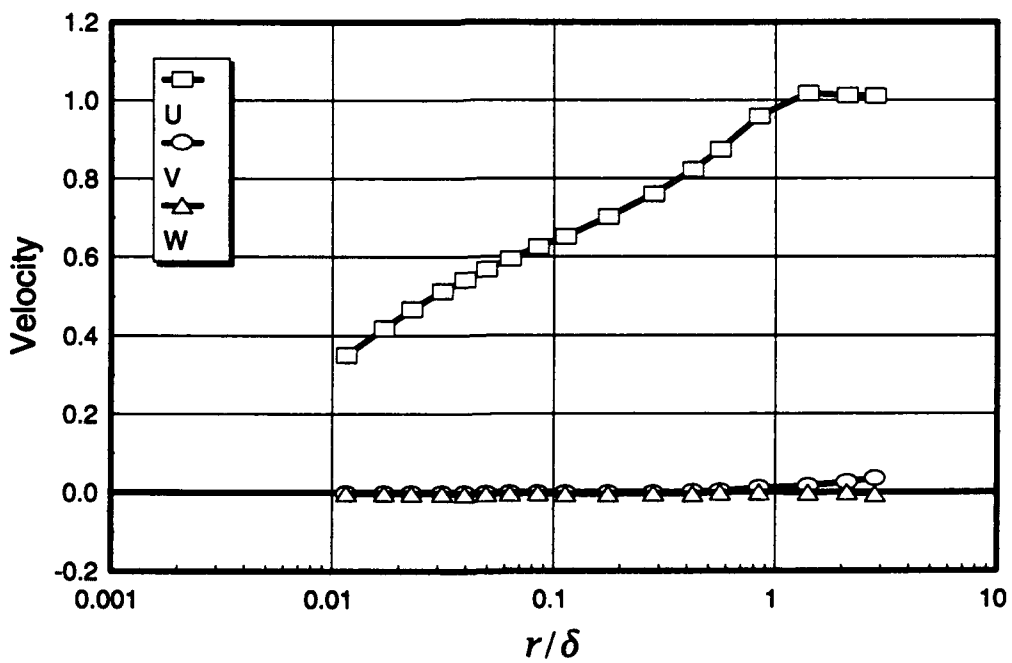


Figure 15. Boundary-layer velocity profiles, $x/L = 0.400$, $\phi = 180^\circ$.

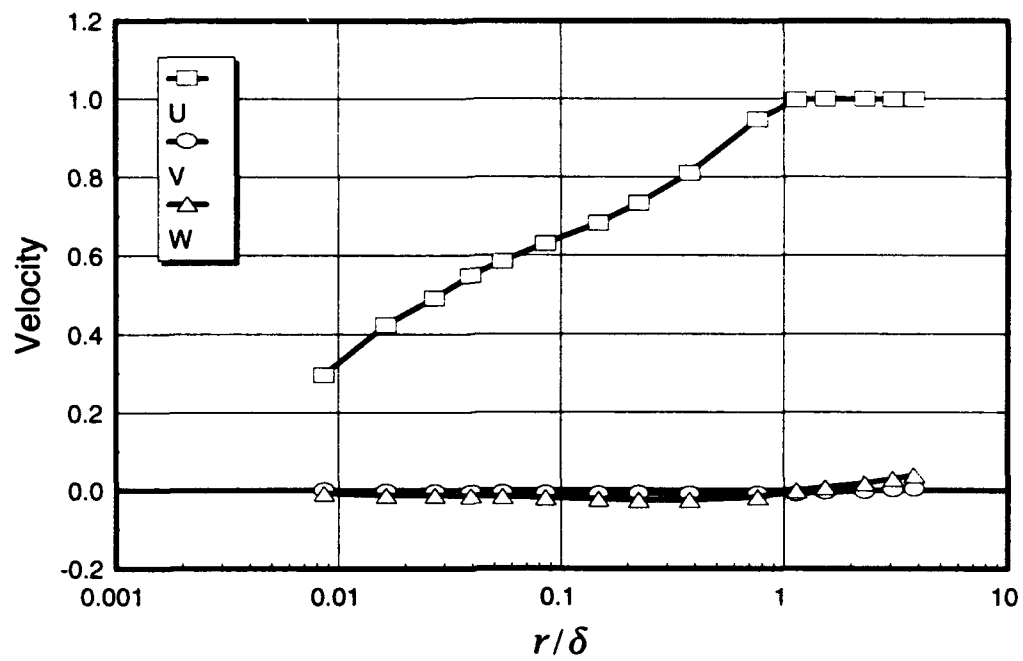


Figure 16. Boundary-layer velocity profiles, $x/L = 0.600$, $\phi = 90^\circ$.

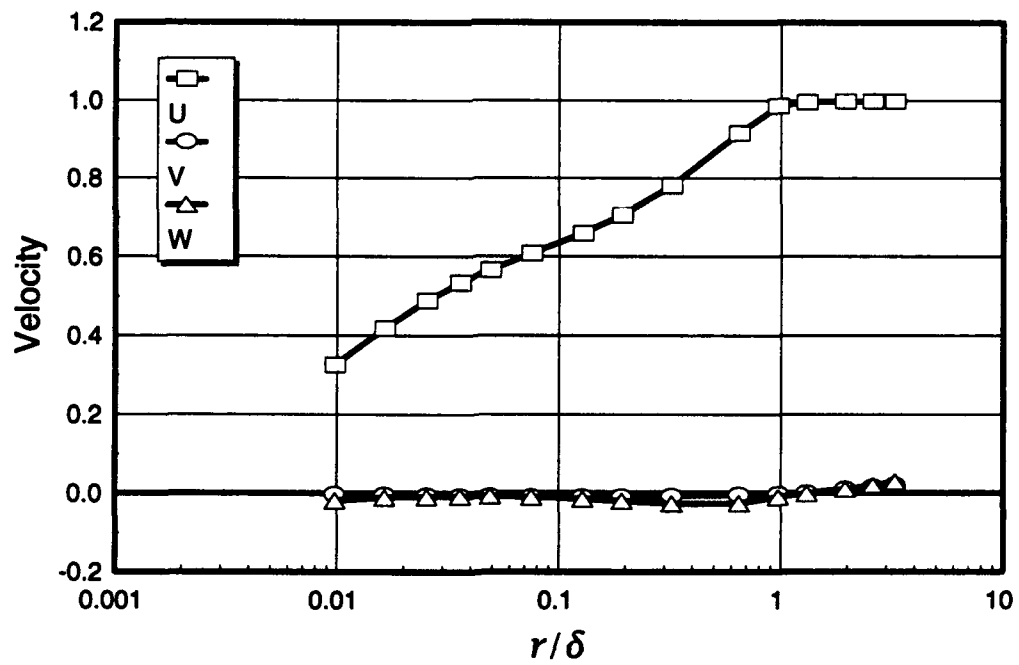


Figure 17. Boundary-layer velocity profiles, $x/L = 0.600$, $\phi = 100^\circ$.

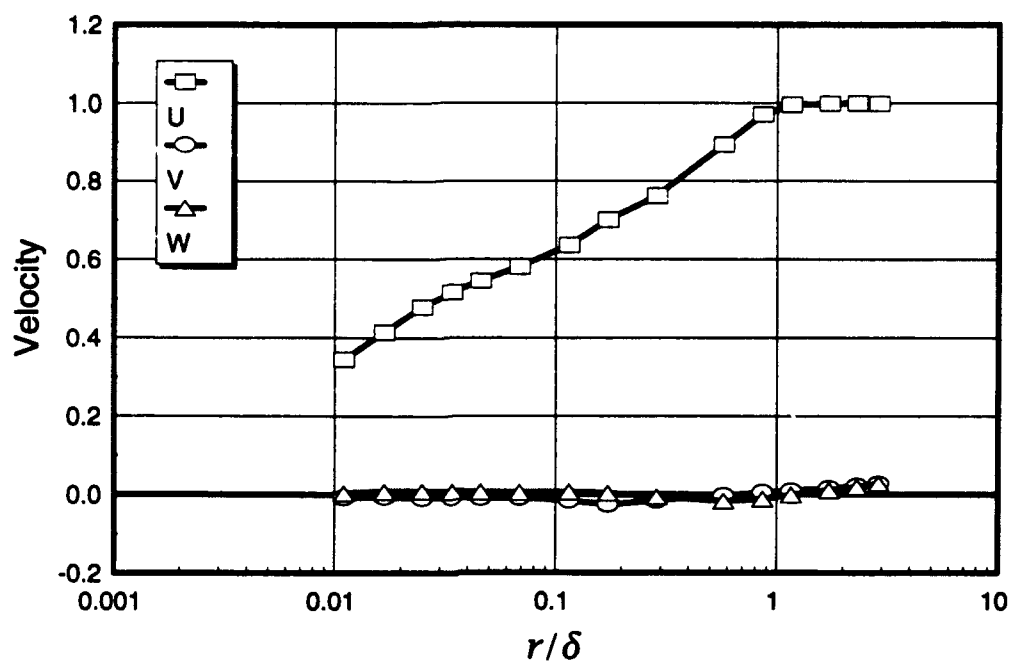


Figure 18. Boundary-layer velocity profiles, $x/L = 0.600$, $\phi = 110^\circ$.

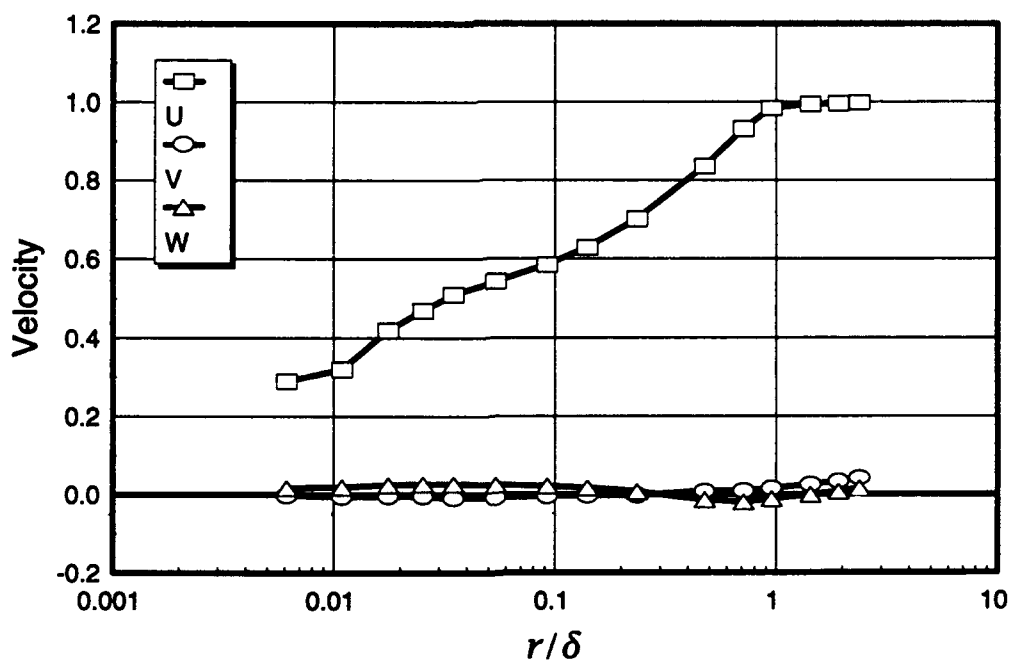


Figure 19. Boundary-layer velocity profiles, $x/L = 0.600$, $\phi = 120^\circ$.

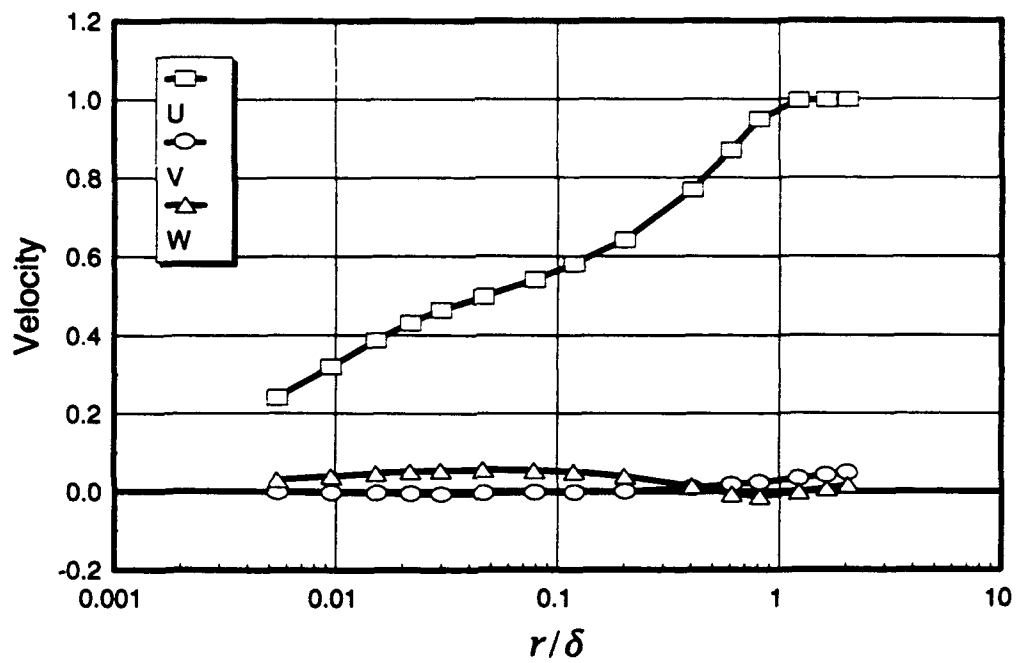


Figure 20. Boundary-layer velocity profiles, $x/L = 0.600$, $\phi = 130^\circ$.

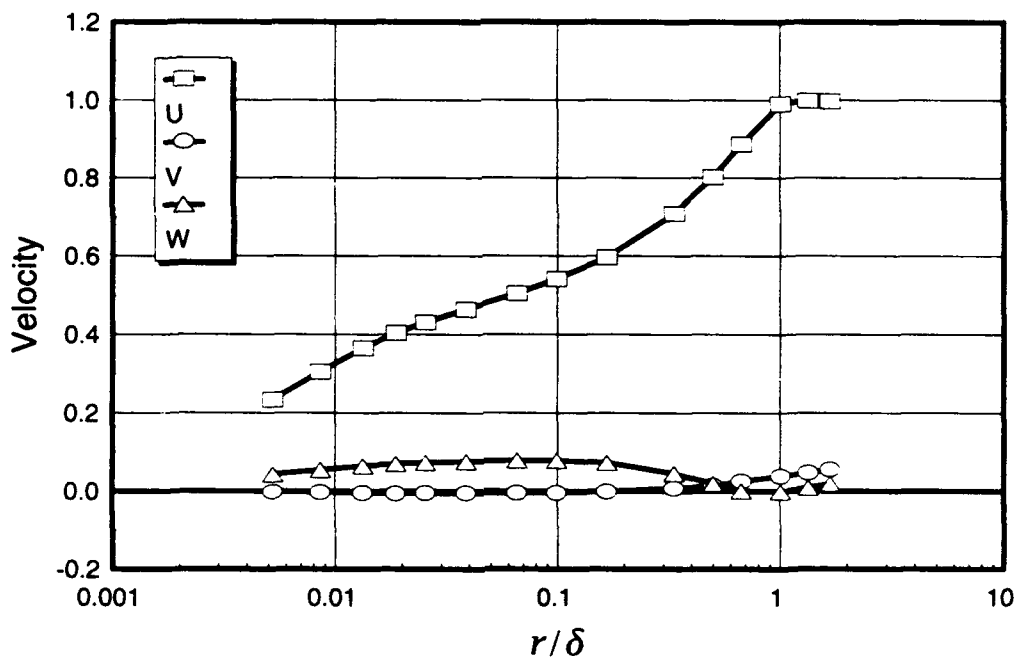


Figure 21. Boundary-layer velocity profiles, $x/L = 0.600$, $\phi = 140^\circ$.

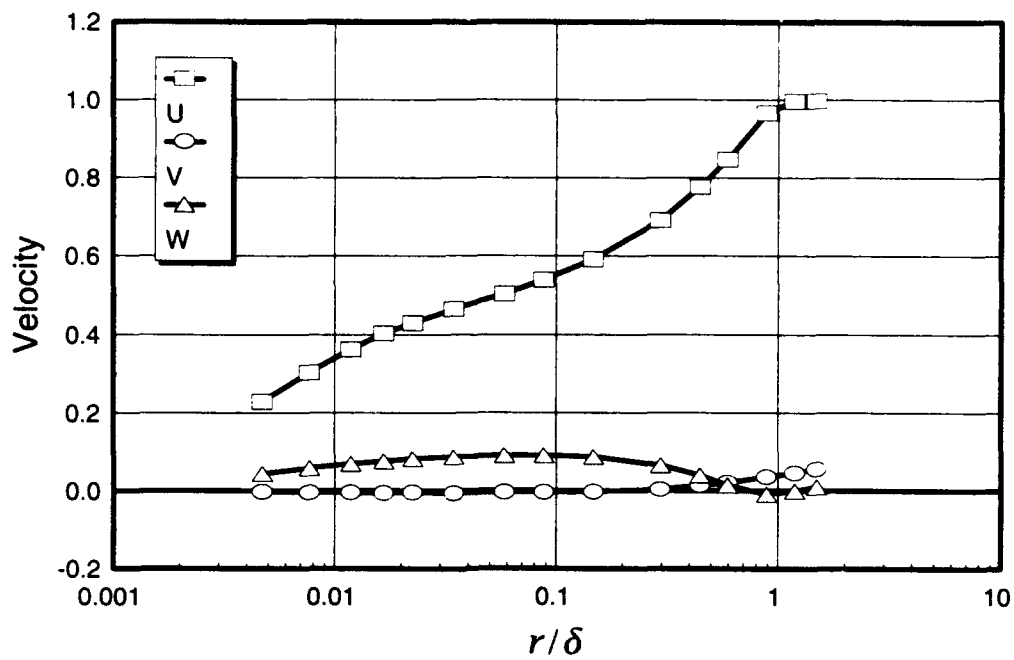


Figure 22. Boundary-layer velocity profiles, $x/L = 0.600$, $\phi = 150^\circ$.

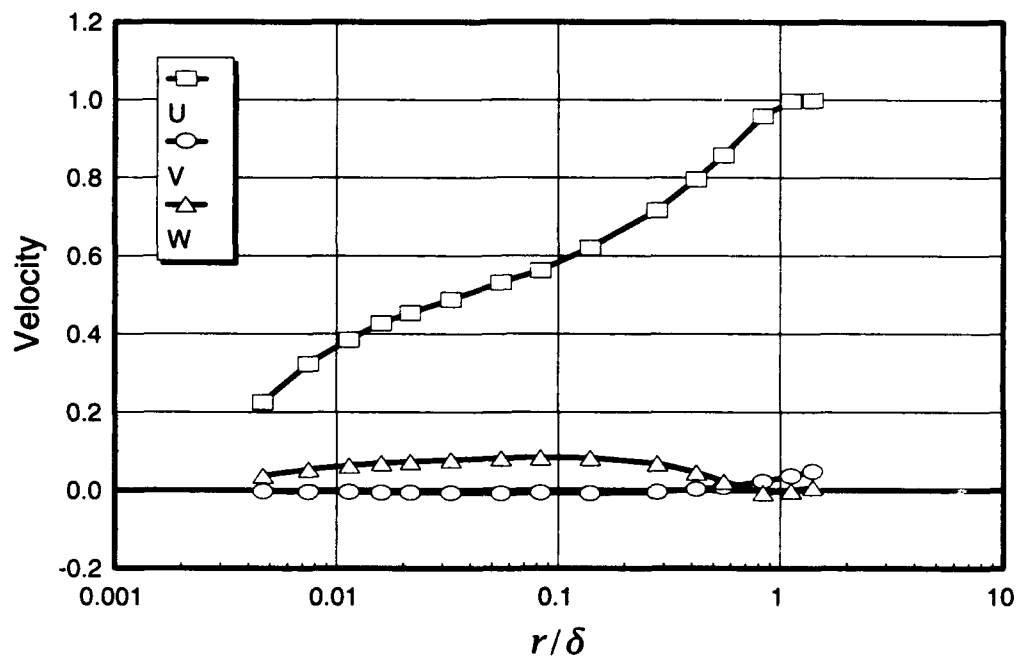


Figure 23. Boundary-layer velocity profiles, $x/L = 0.600$, $\phi = 160^\circ$.

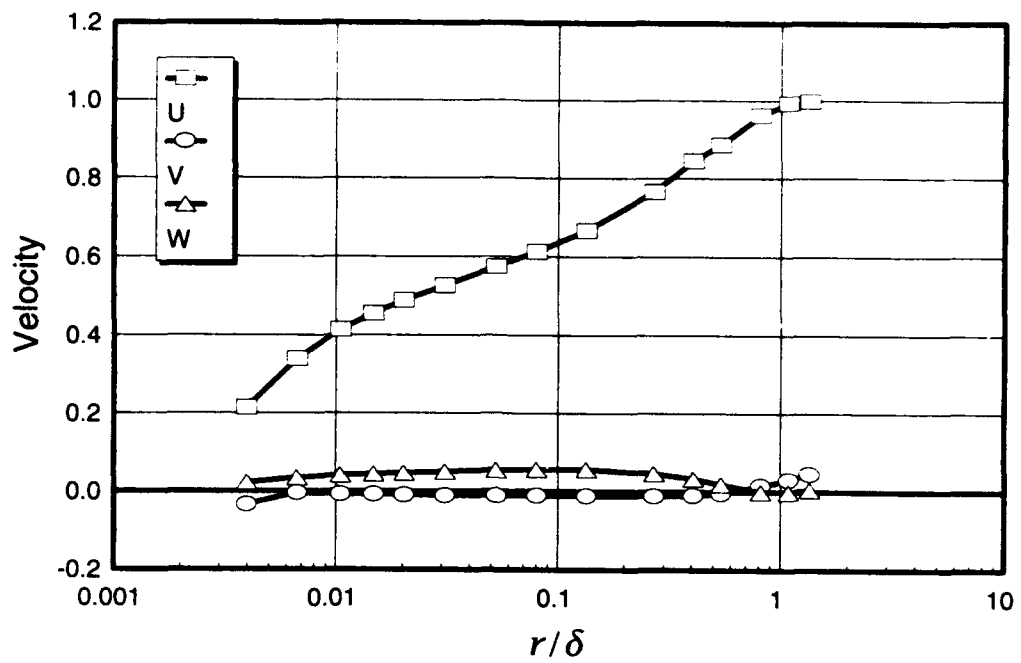


Figure 24. Boundary-layer velocity profiles, $x/L = 0.600$, $\phi = 170^\circ$.

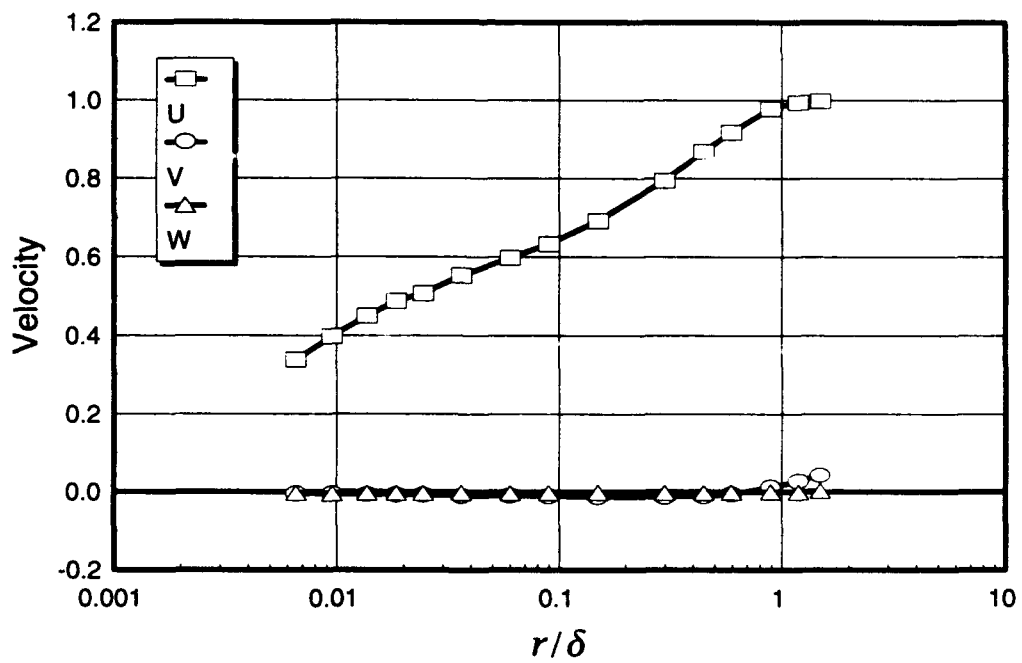


Figure 25. Boundary-layer velocity profiles, $x/L = 0.600$, $\phi = 180^\circ$.

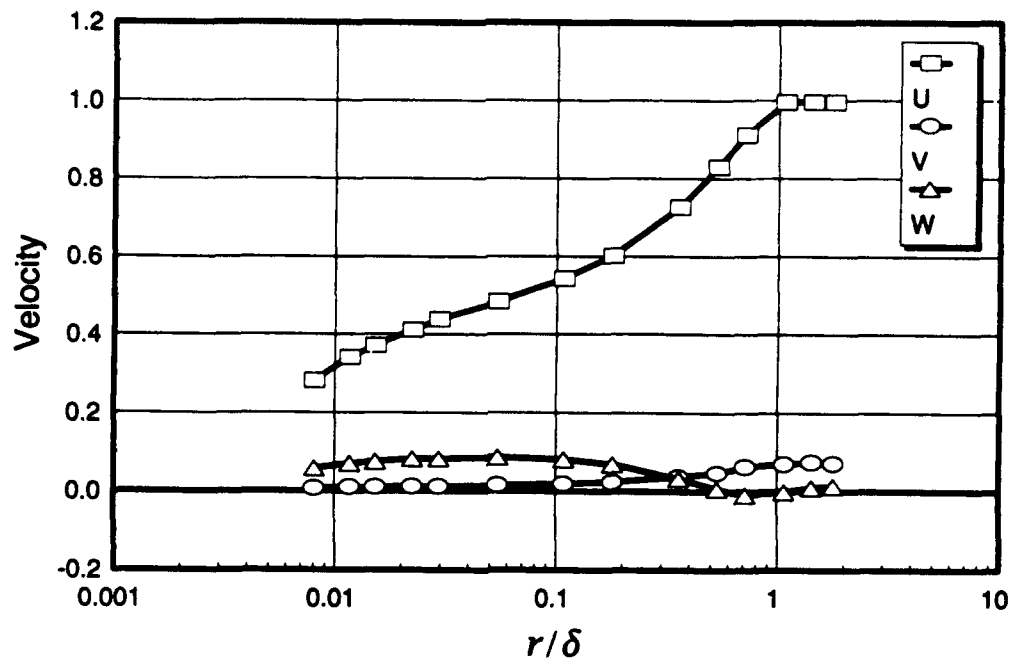


Figure 26. Boundary-layer velocity profiles, $x/L = 0.752$, $\phi = 120^\circ$.

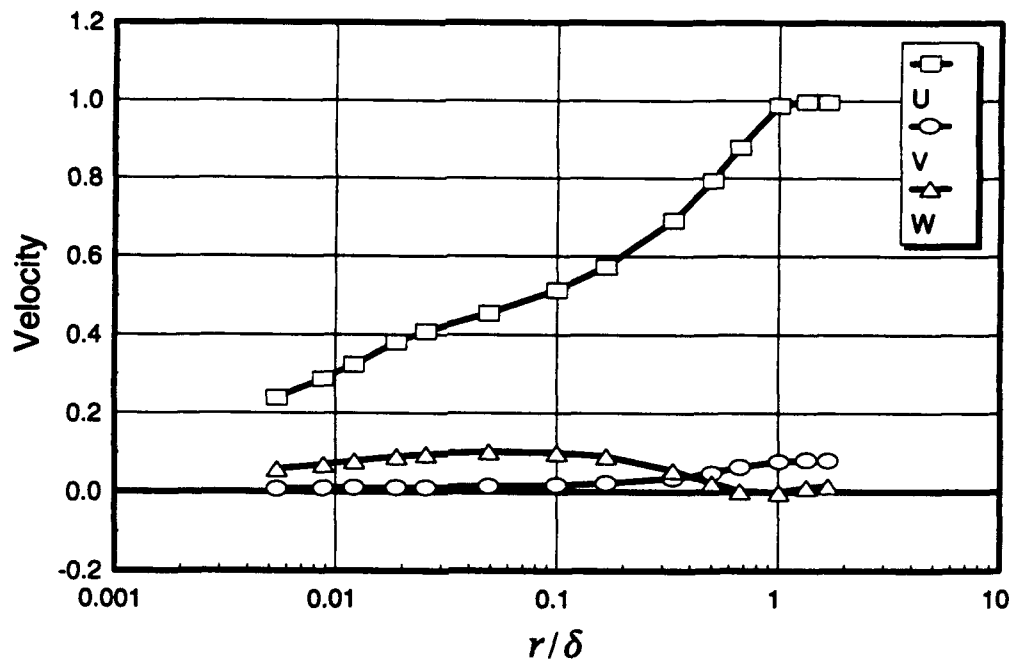


Figure 27. Boundary-layer velocity profiles, $x/L = 0.752$, $\phi = 123^\circ$.

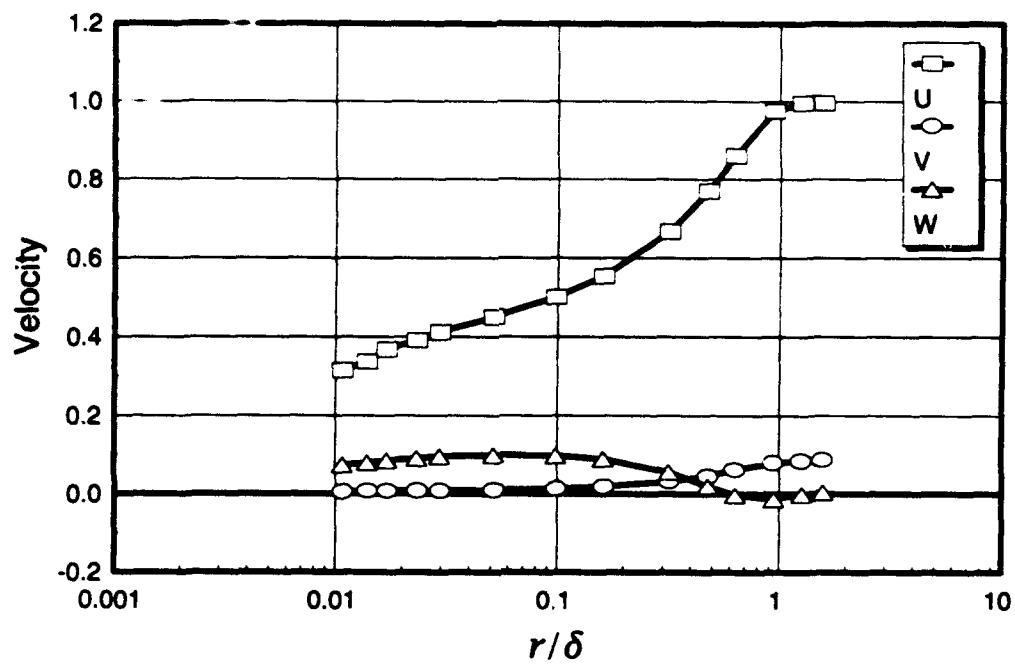


Figure 28. Boundary-layer velocity profiles, $x/L = 0.752$, $\phi = 125^\circ$.

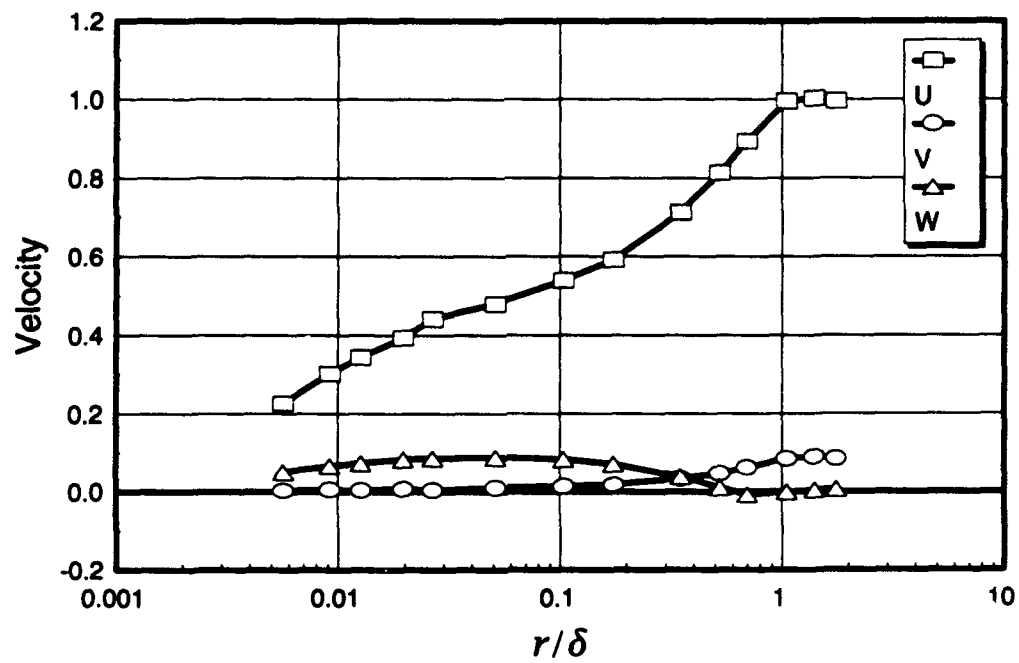


Figure 29. Boundary-layer velocity profiles, $x/L = 0.762$, $\phi = 120^\circ$.

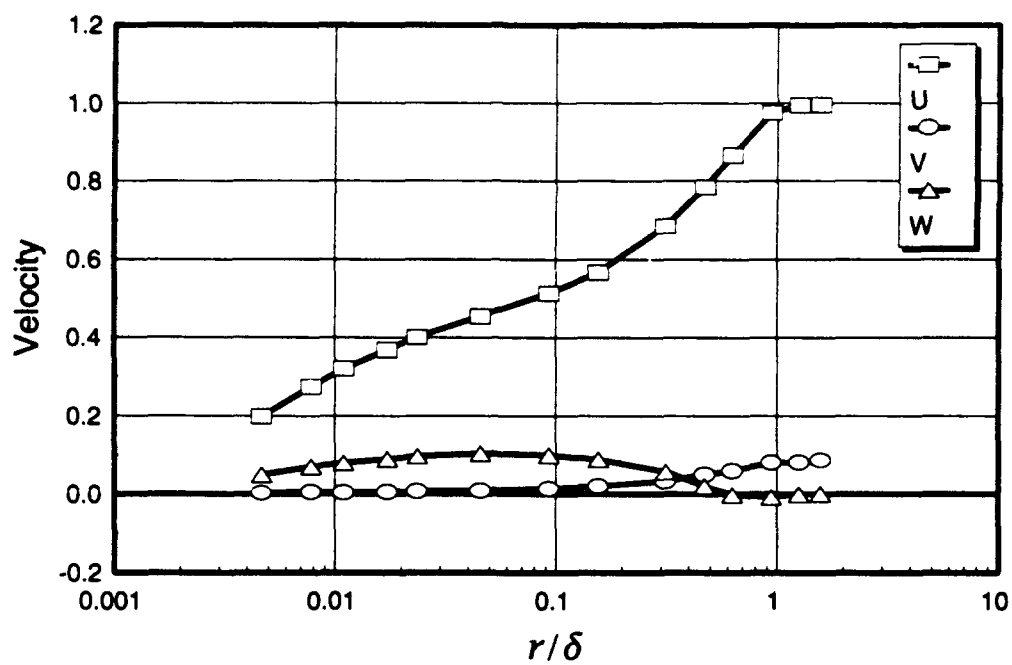


Figure 30. Boundary-layer velocity profiles, $x/L = 0.762$, $\phi = 123^\circ$.

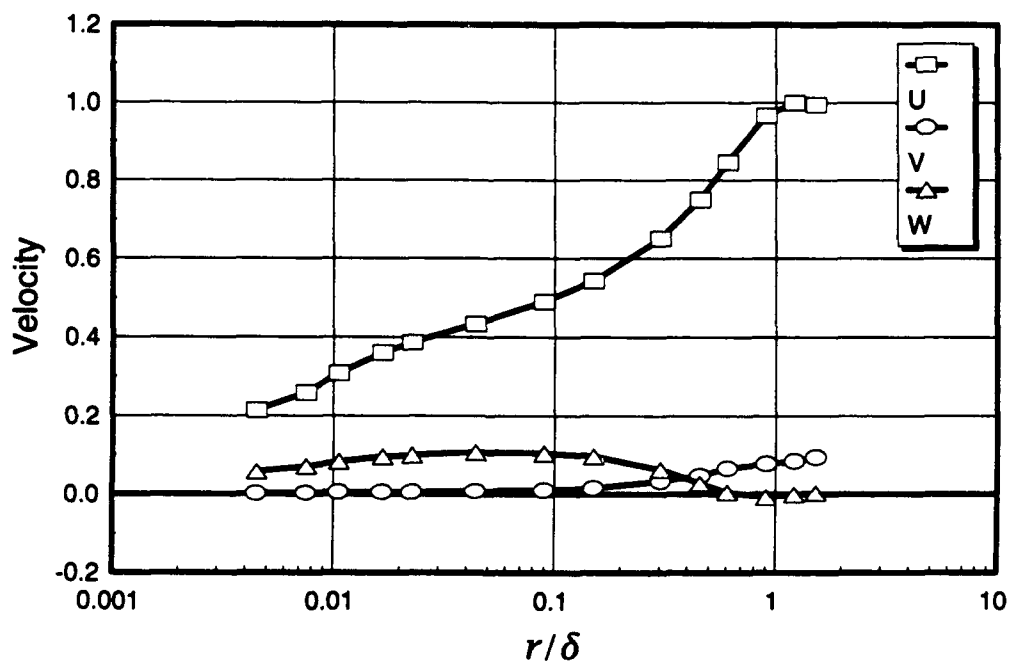


Figure 31. Boundary-layer velocity profiles, $x/L = 0.762$, $\phi = 125^\circ$.

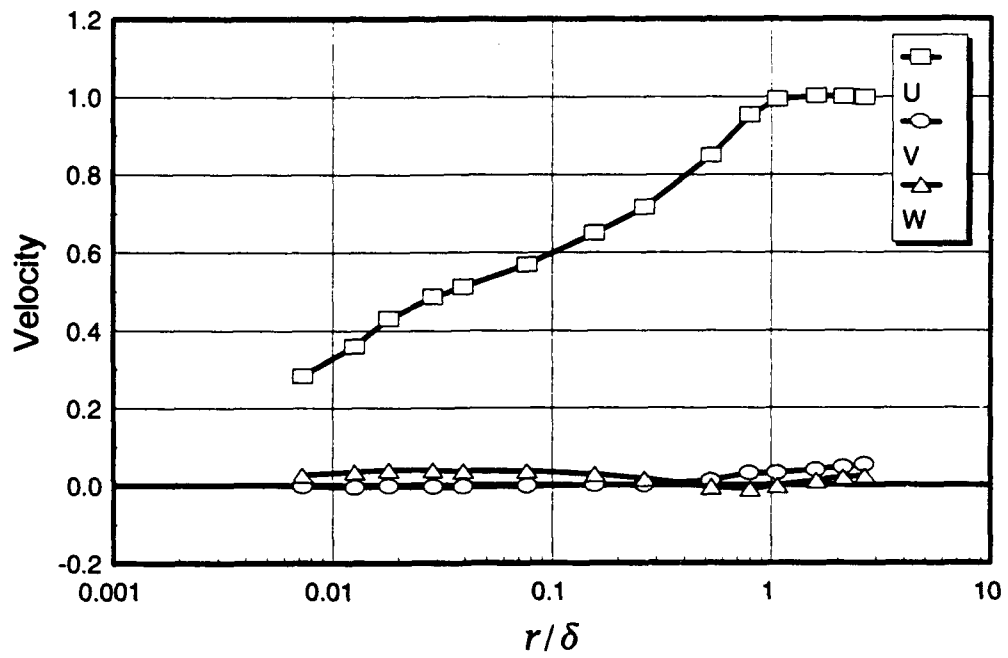


Figure 32. Boundary-layer velocity profiles, $x/L = 0.772$, $\phi = 105^\circ$.

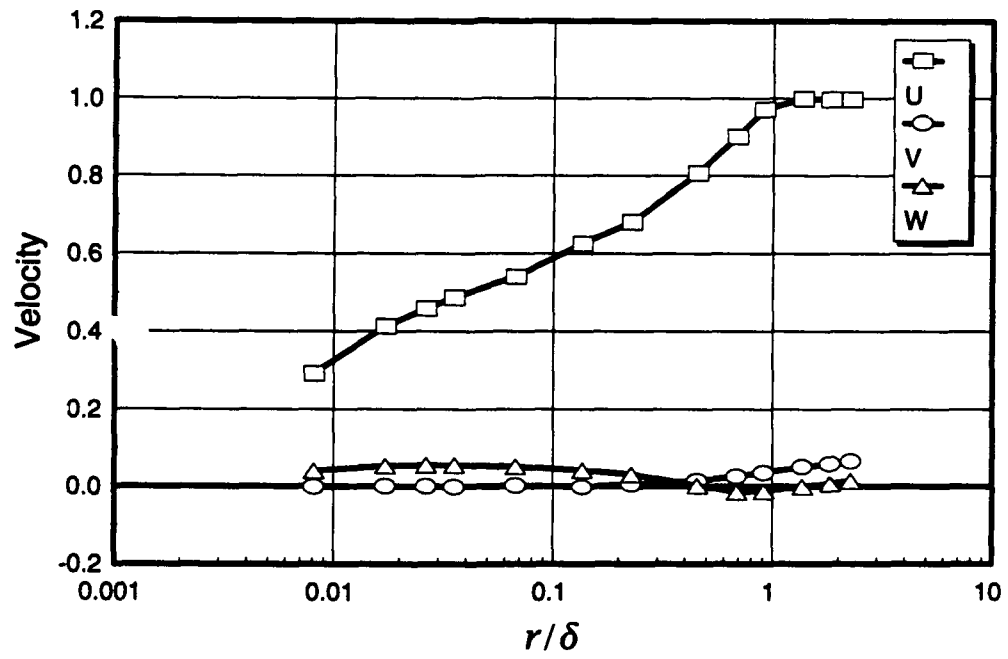


Figure 33. Boundary-layer velocity profiles, $x/L = 0.772$, $\phi = 110^\circ$.

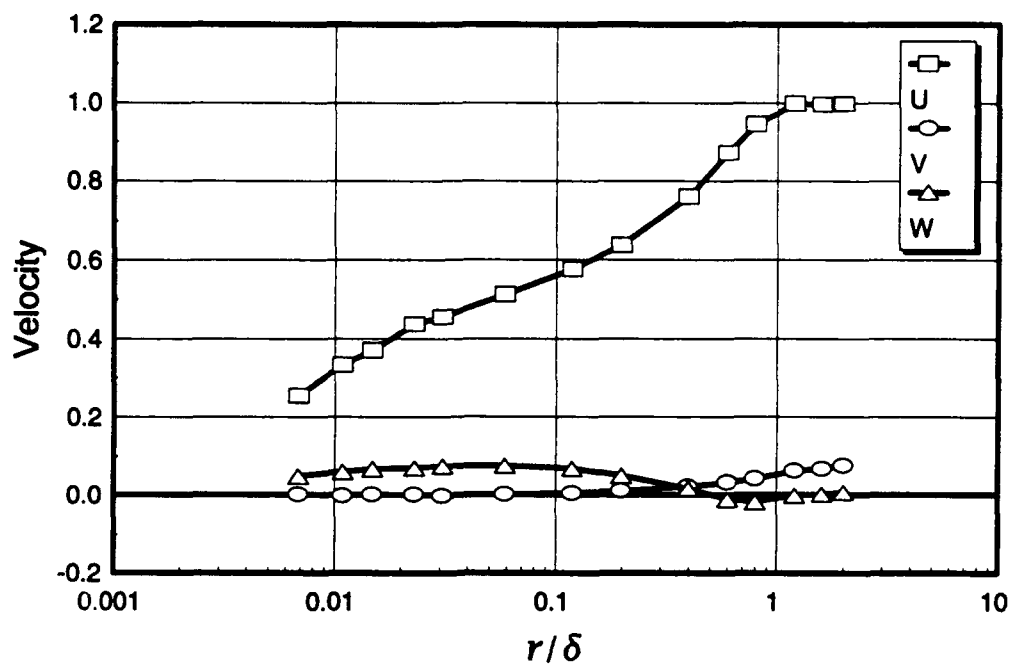


Figure 34. Boundary-layer velocity profiles, $x/L = 0.772$, $\phi = 115^\circ$.

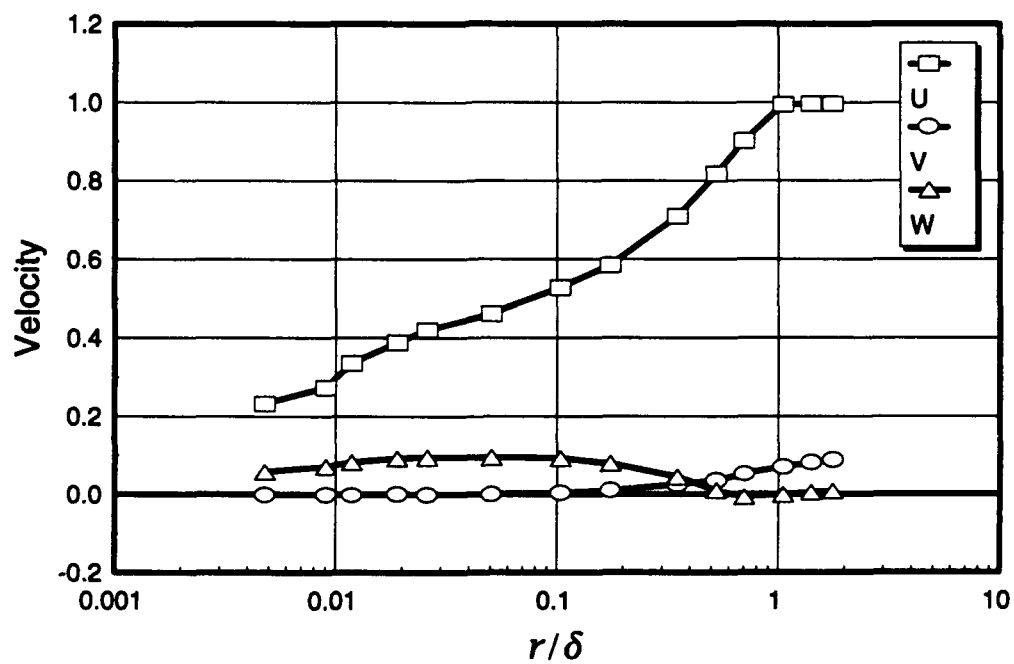


Figure 35. Boundary-layer velocity profiles, $x/L = 0.772$, $\phi = 120^\circ$.

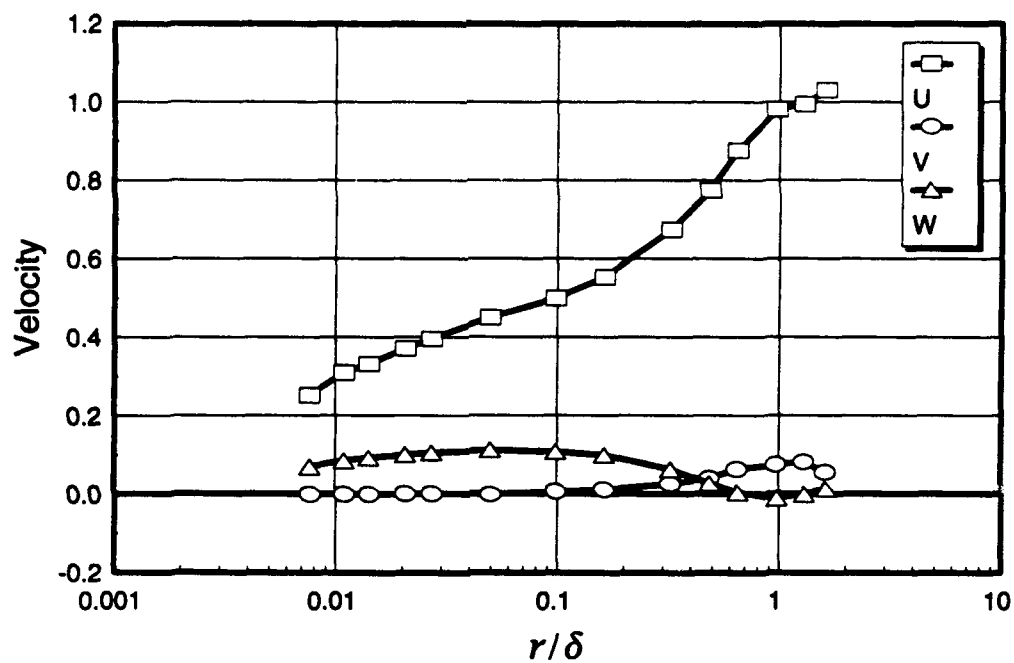


Figure 36. Boundary-layer velocity profiles, $x/L = 0.772$, $\phi = 123^\circ$.

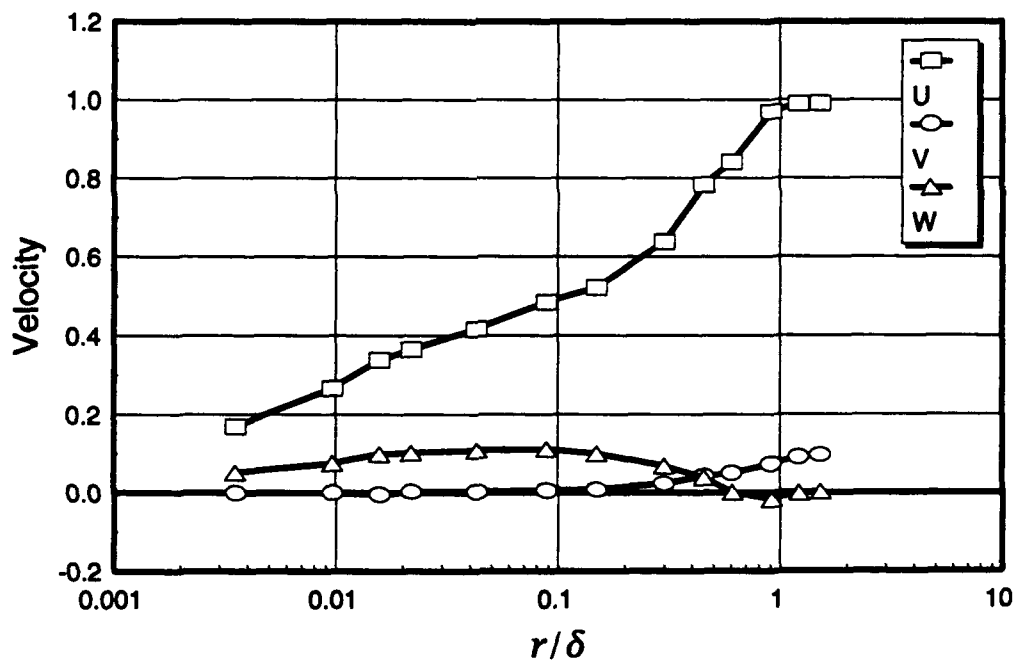


Figure 37. Boundary-layer velocity profiles, $x/L = 0.772$, $\phi = 125^\circ$.

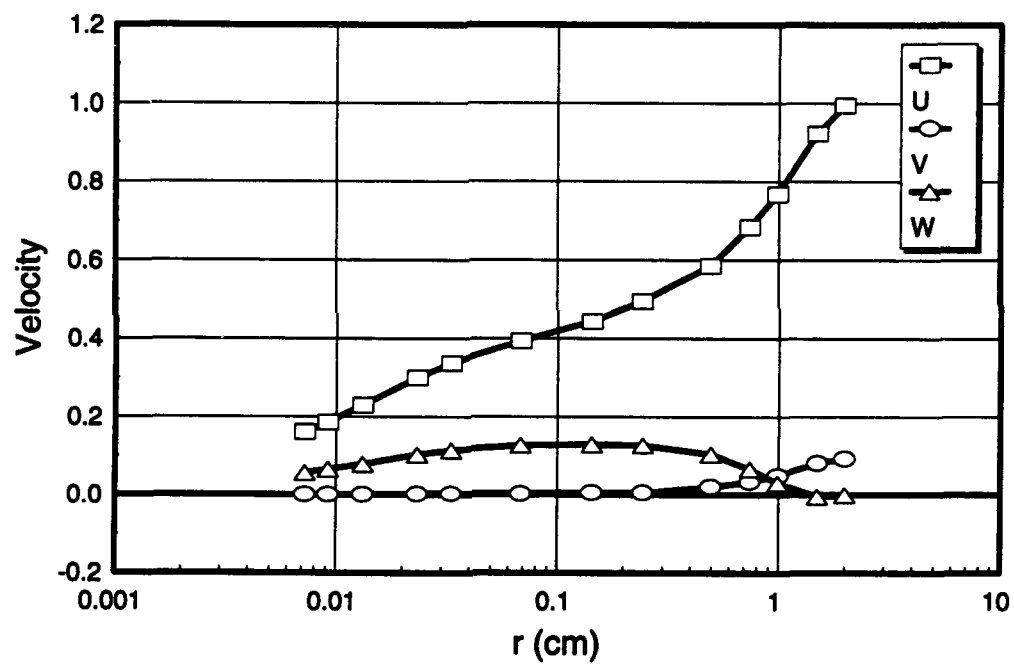


Figure 38. Boundary-layer velocity profiles, $x/L = 0.772$, $\phi = 130^\circ$.

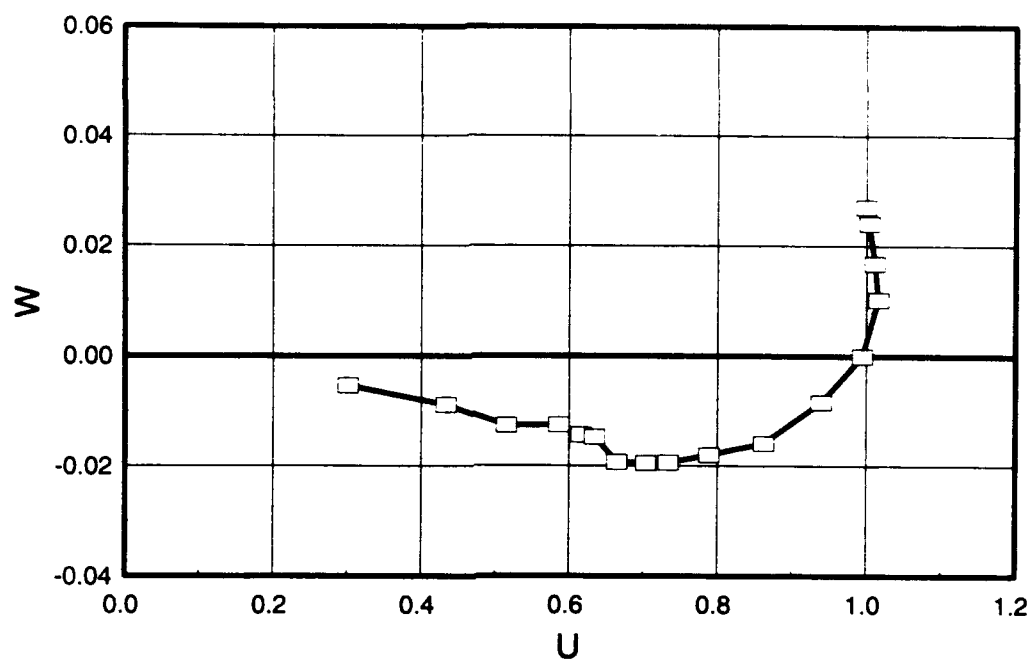


Figure 39. Johnston hodograph, $x/L = 0.400$, $\phi = 90^\circ$.

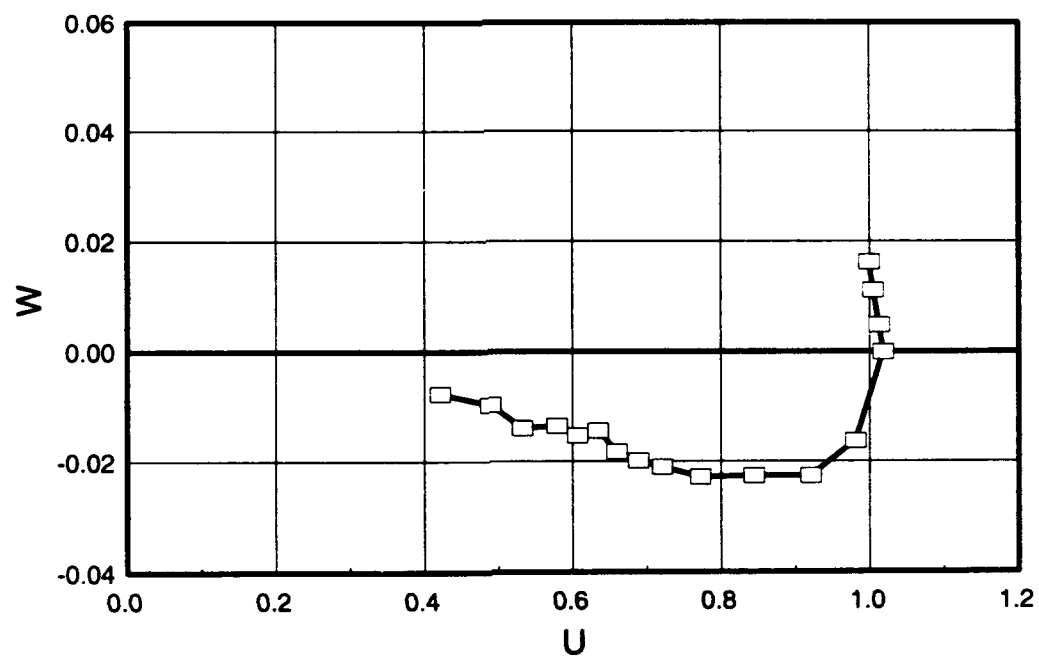


Figure 40. Johnston hodograph, $x/L = 0.400$, $\phi = 100^\circ$.

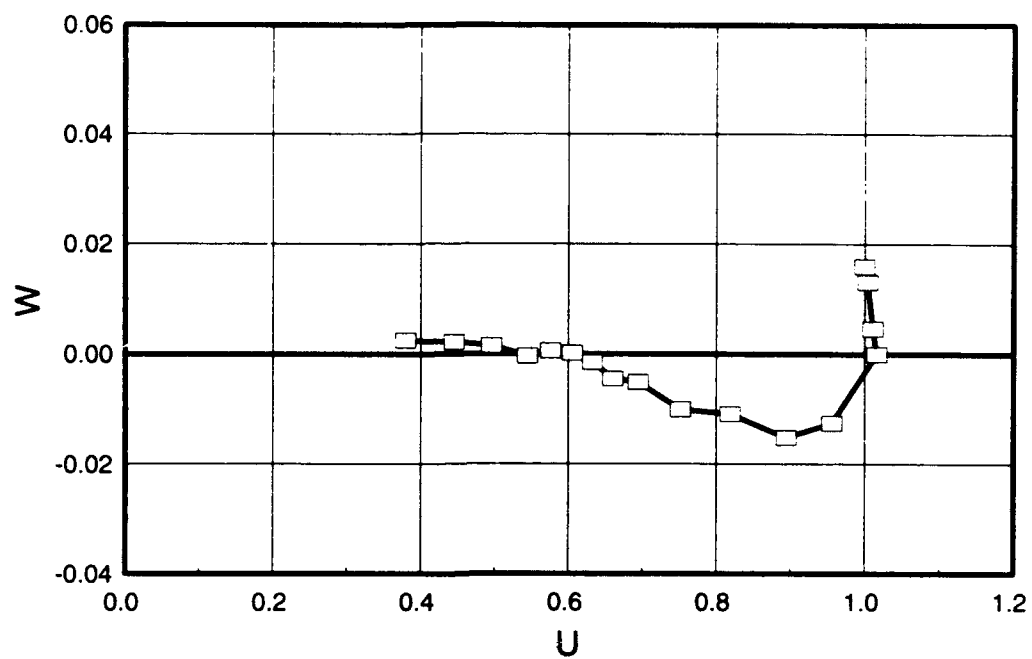


Figure 41. Johnston hodograph, $x/L = 0.400$, $\phi = 110^\circ$.

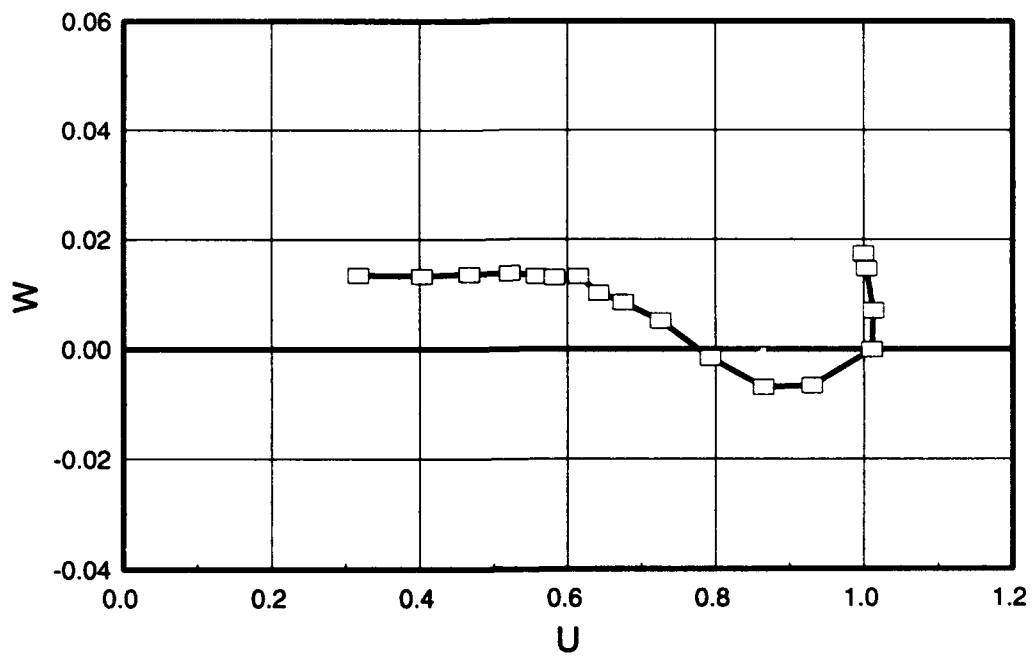


Figure 42. Johnston hodograph, $x/L = 0.400$, $\phi = 120^\circ$.

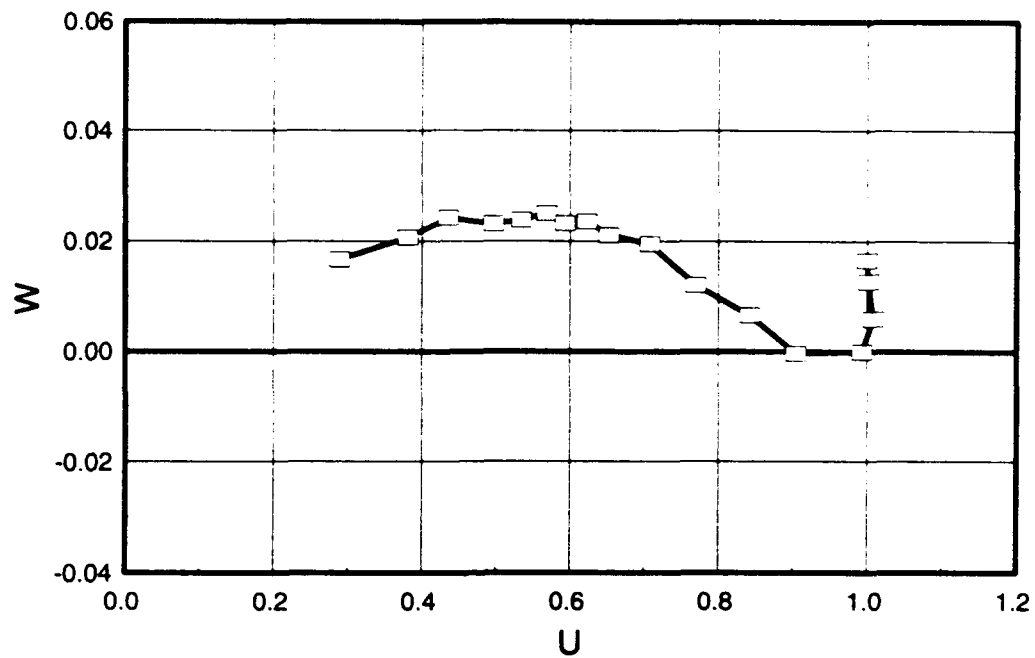


Figure 43. Johnston hodograph, $x/L = 0.400$, $\phi = 130^\circ$.

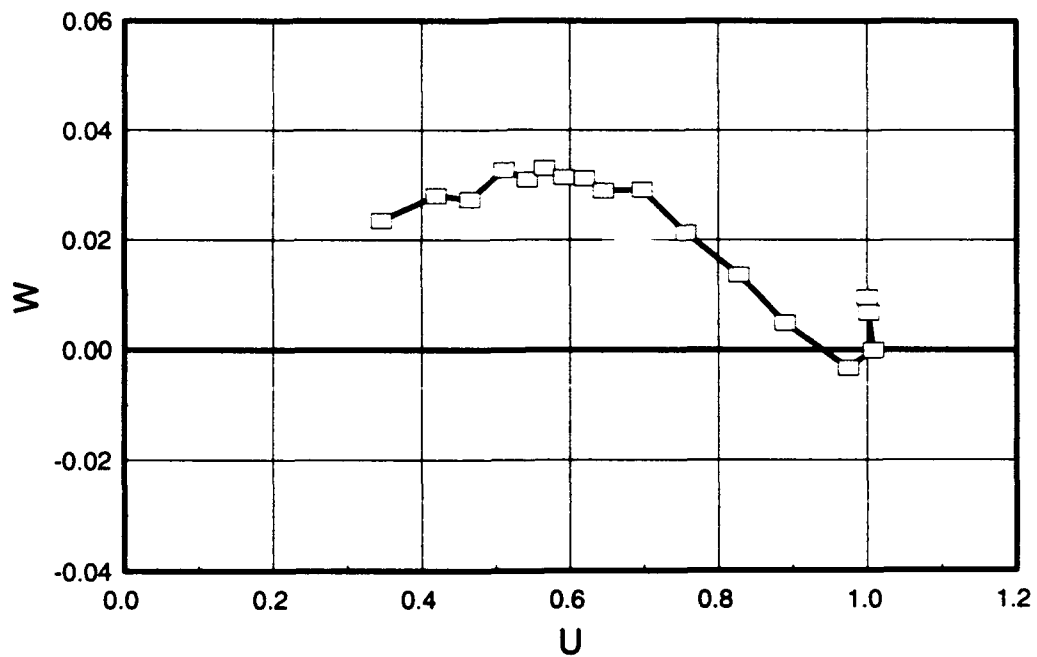


Figure 44. Johnston hodograph, $x/L = 0.400$, $\phi = 140^\circ$.

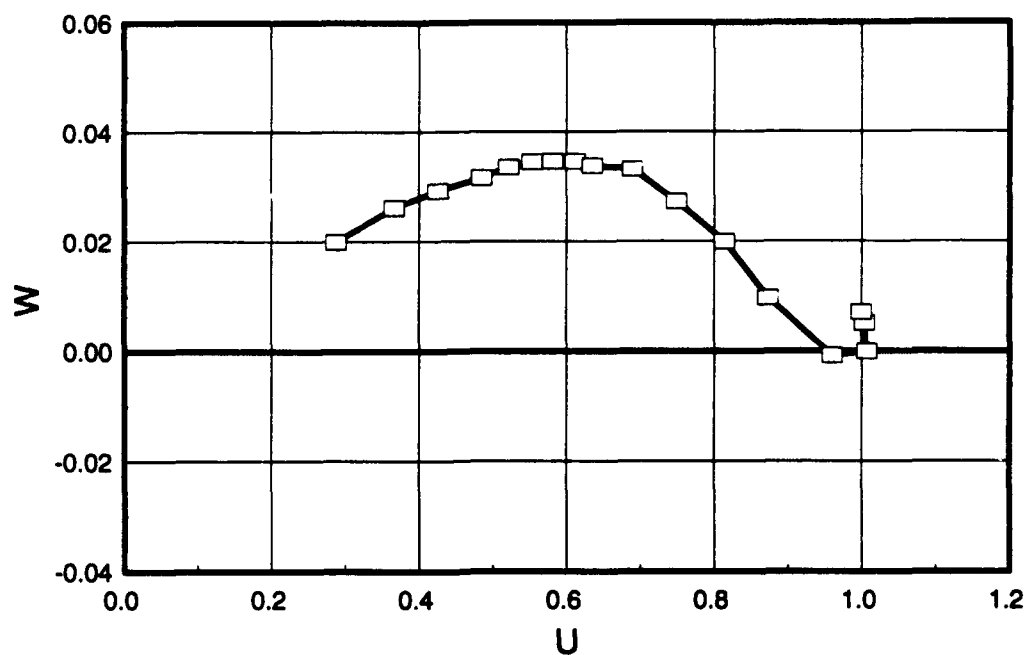


Figure 45. Johnston hodograph, $x/L = 0.400$, $\phi = 150^\circ$.

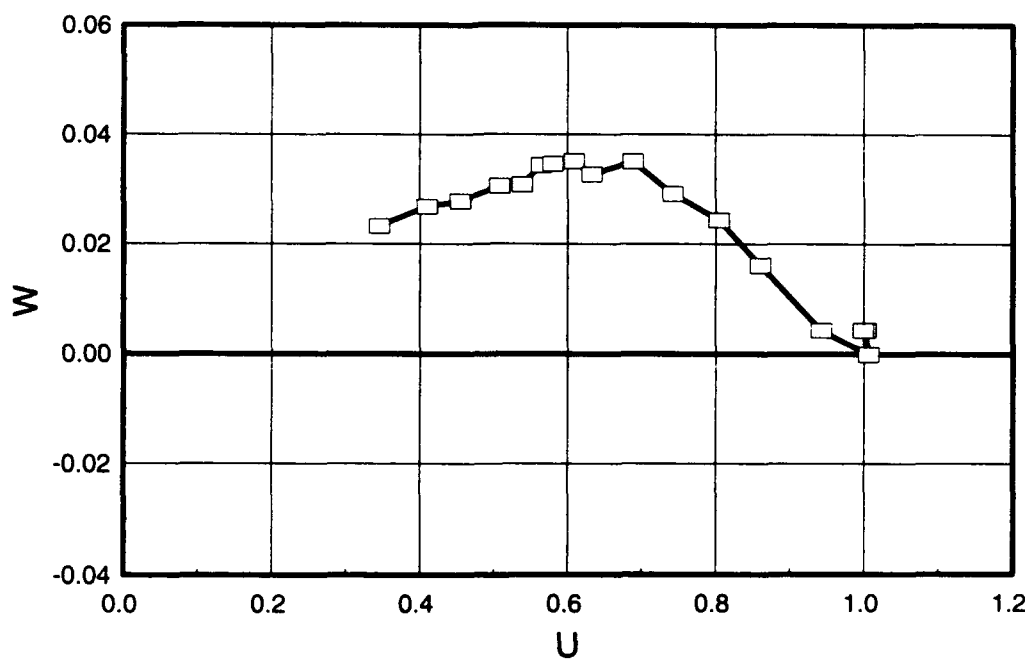


Figure 46. Johnston hodograph, $x/L = 0.400$, $\phi = 160^\circ$.

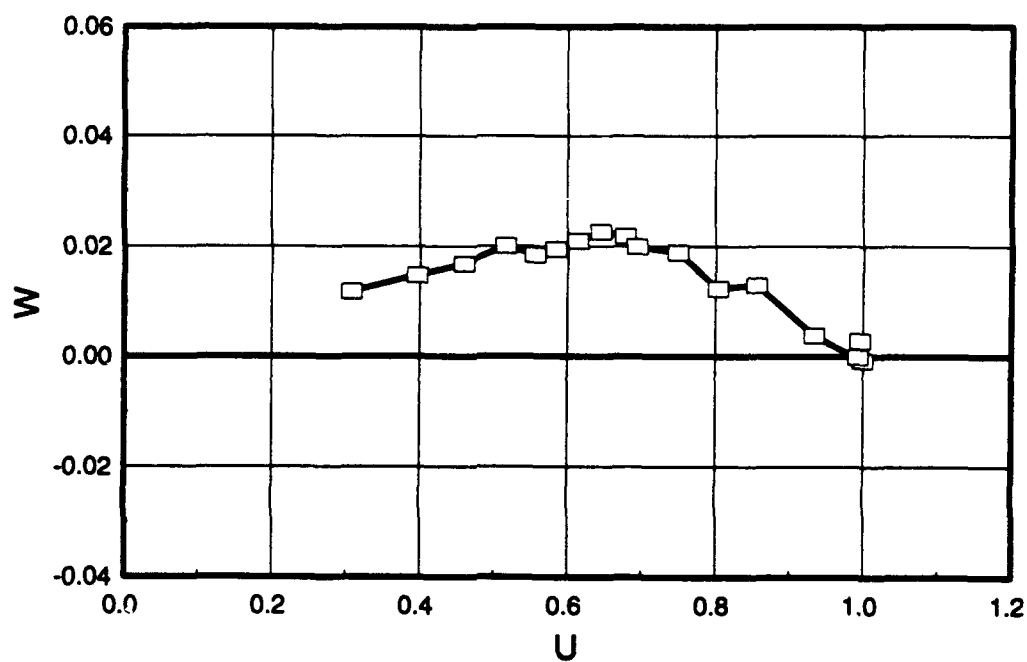


Figure 47. Johnston hodograph, $x/L = 0.400$, $\phi = 170^\circ$.

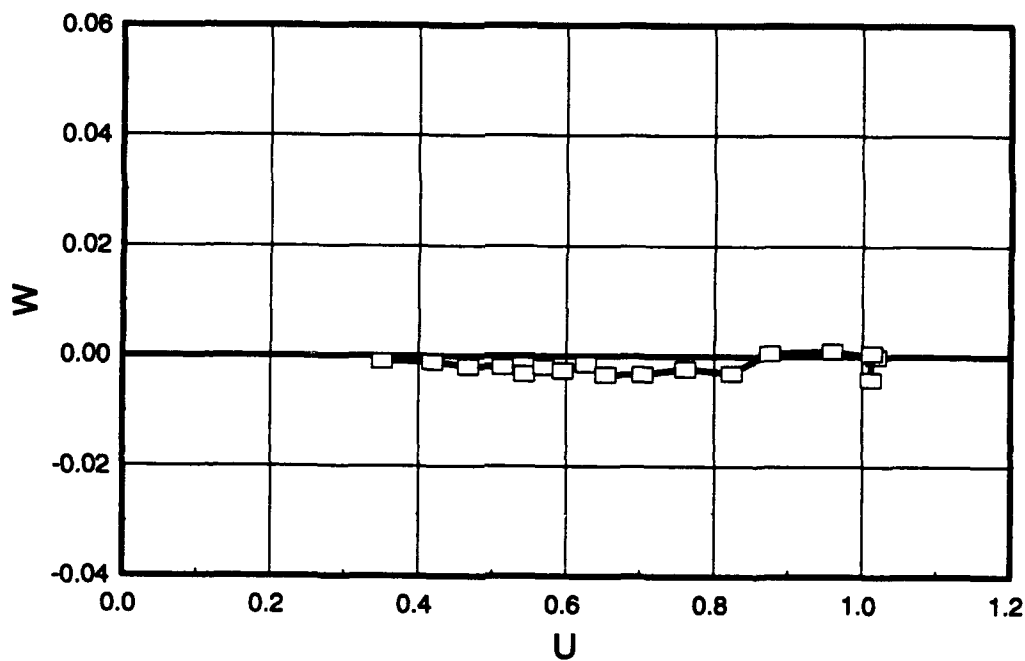


Figure 48. Johnston hodograph, $x/L = 0.400$, $\phi = 180^\circ$.

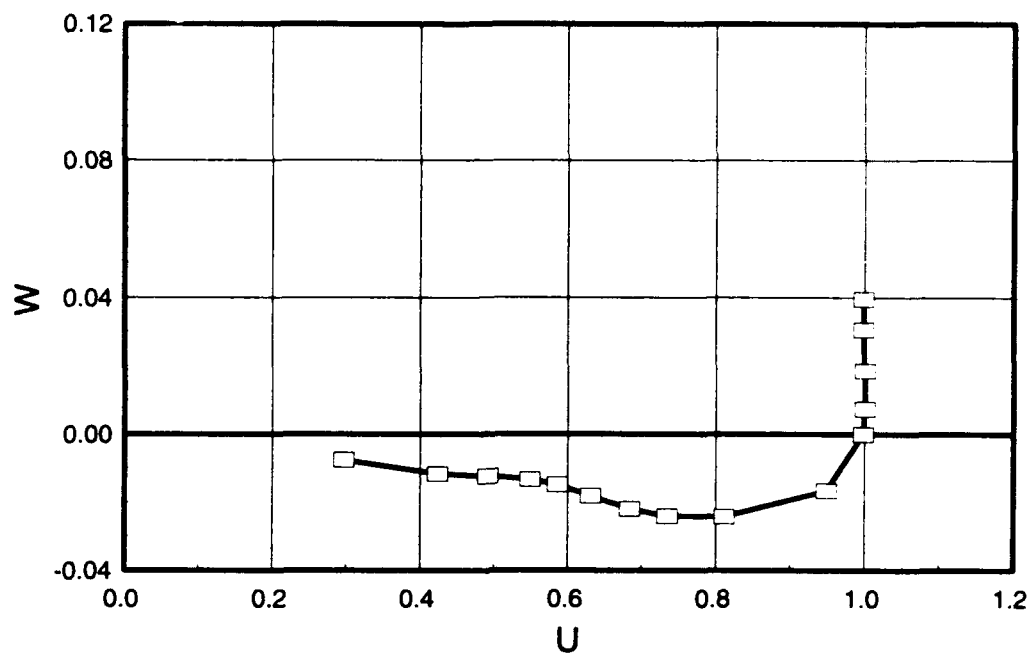


Figure 49. Johnston hodograph, $x/L = 0.600$, $\phi = 90^\circ$.

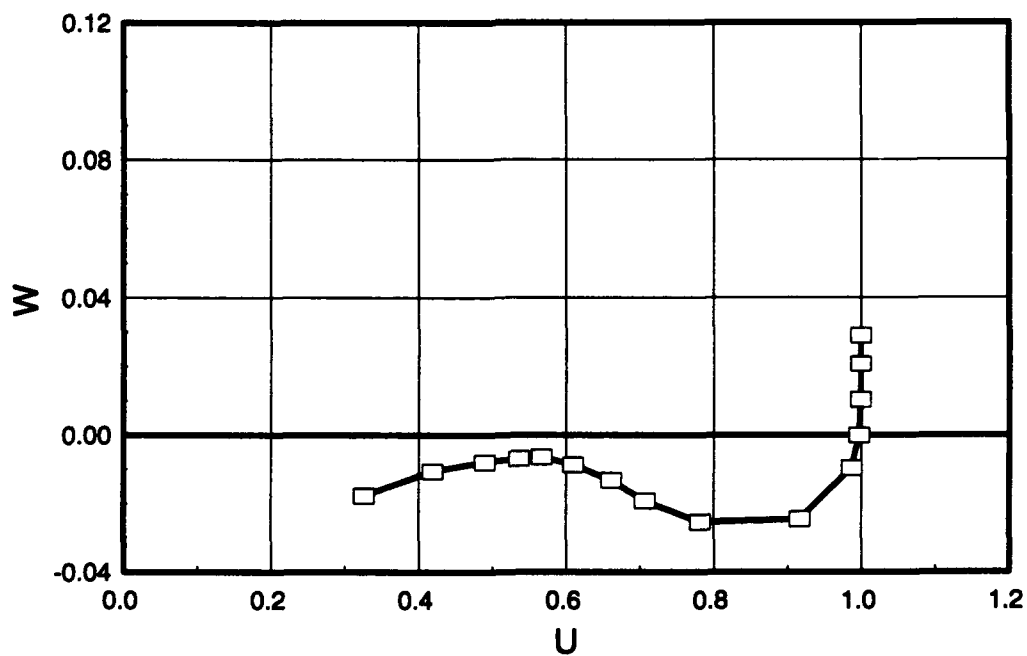


Figure 50. Johnston hodograph, $x/L = 0.600$, $\phi = 100^\circ$.

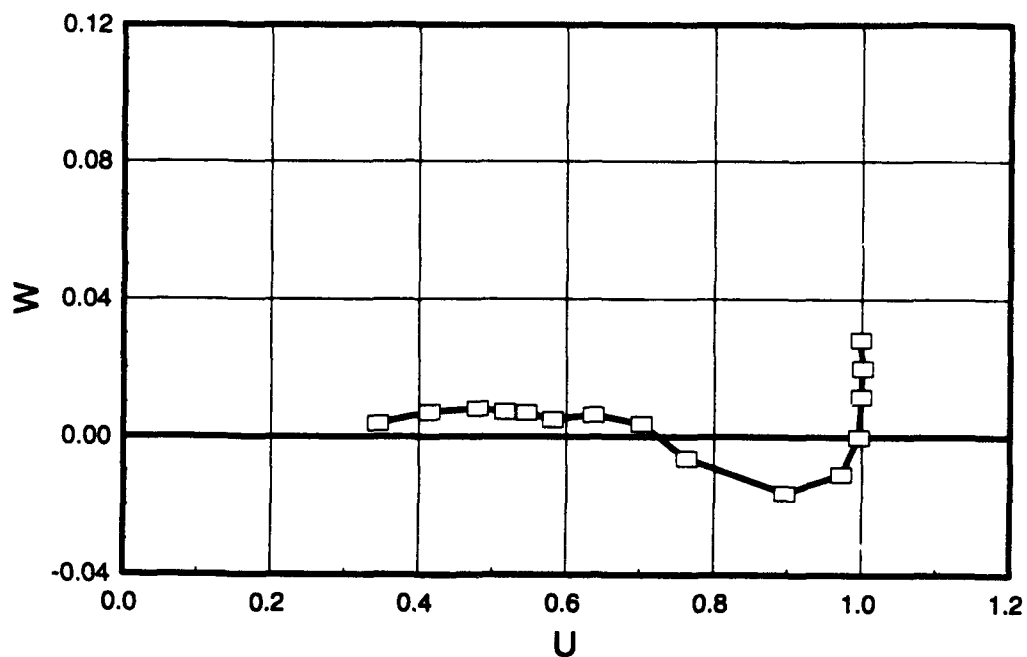


Figure 51. Johnston hodograph, $x/L = 0.600$, $\phi = 110^\circ$.

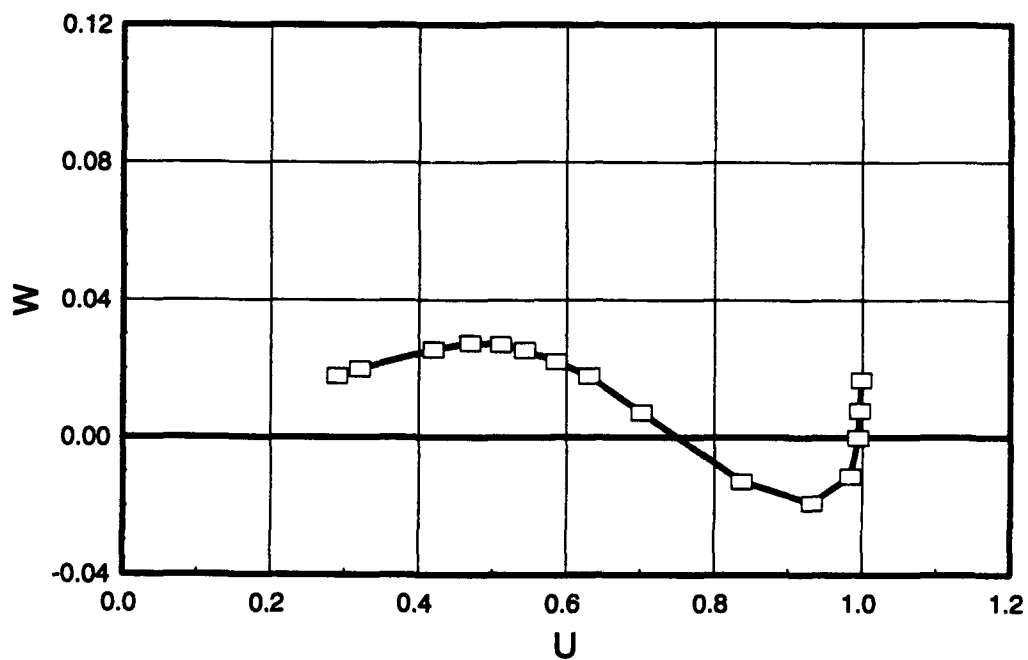


Figure 52. Johnston hodograph, $x/L = 0.600$, $\phi = 120^\circ$.

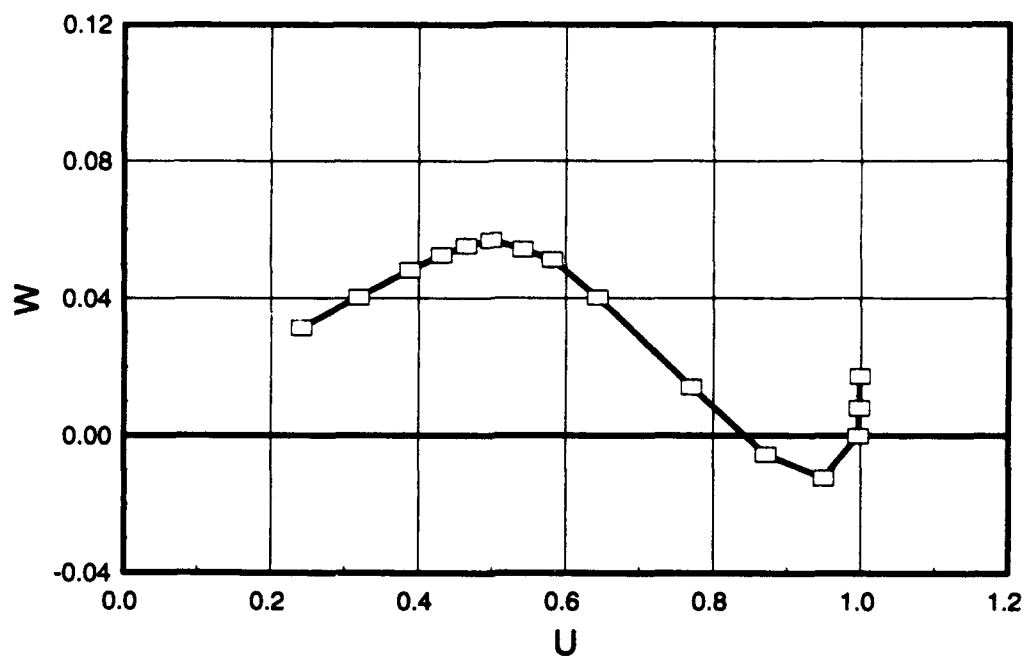


Figure 53. Johnston hodograph, $x/L = 0.600$, $\phi = 130^\circ$.

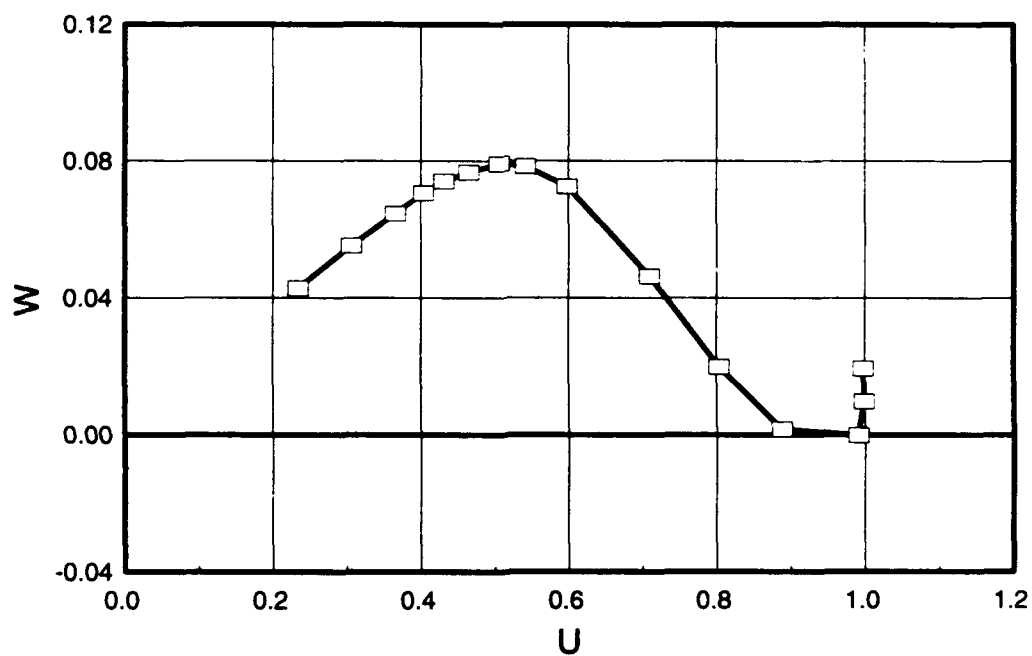


Figure 54. Johnston hodograph, $x/L = 0.600$, $\phi = 140^\circ$.

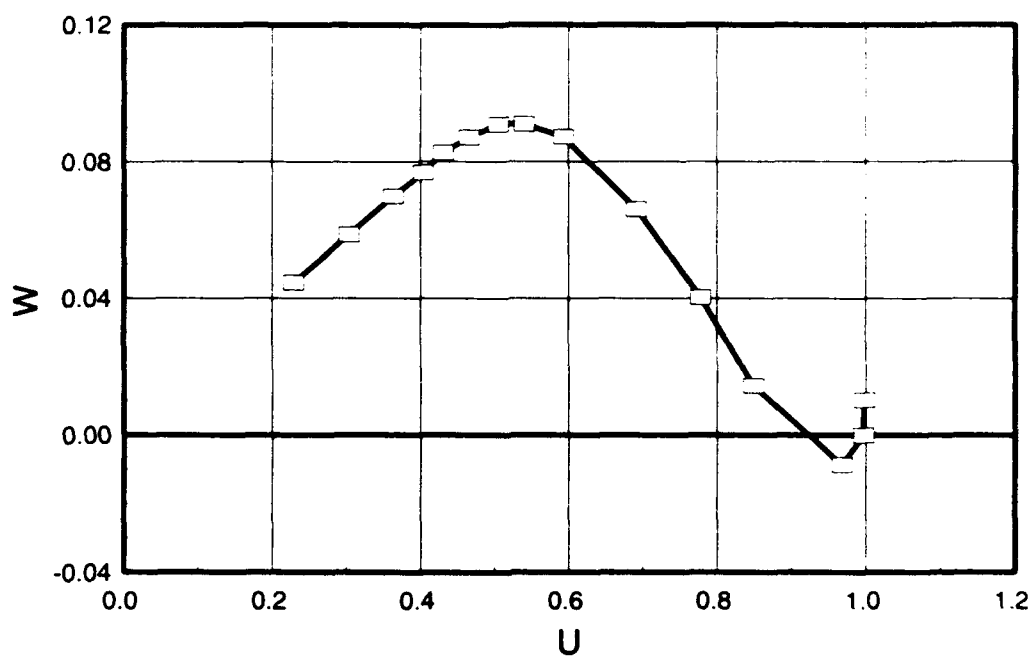


Figure 55. Johnston hodograph, $x/L = 0.600$, $\phi = 150^\circ$.

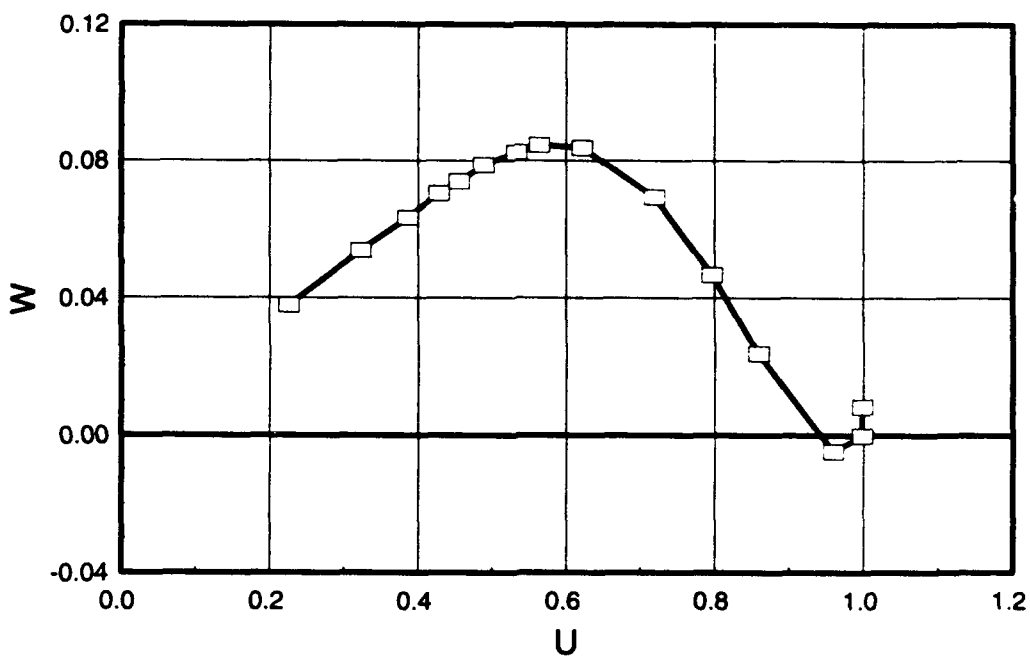


Figure 56. Johnston hodograph, $x/L = 0.600$, $\phi = 160^\circ$.

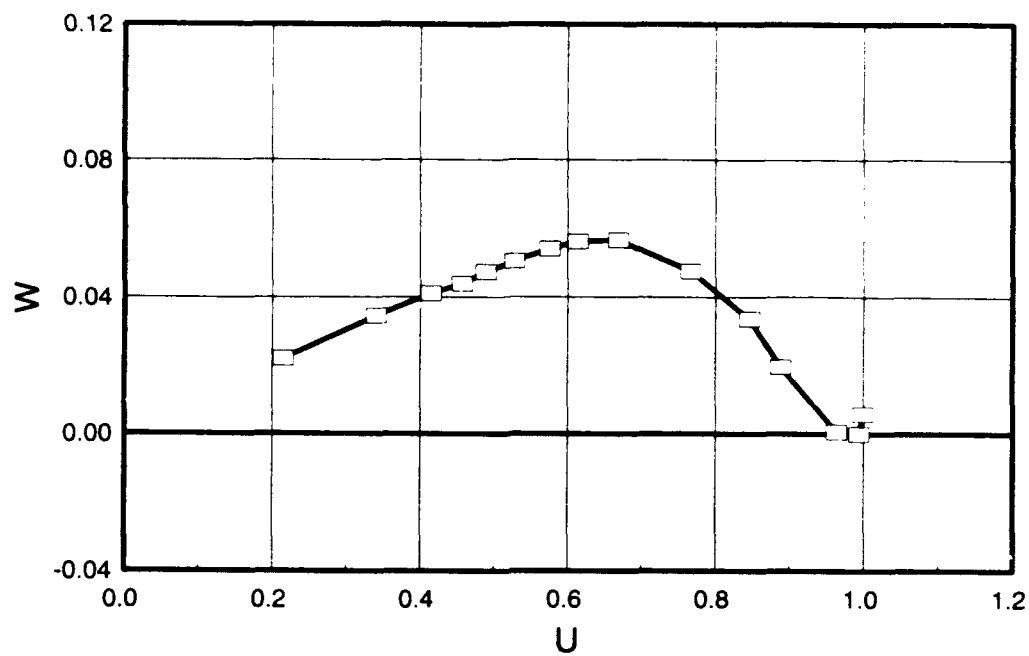


Figure 57. Johnston hodograph, $x/L = 0.600$, $\phi = 170^\circ$.

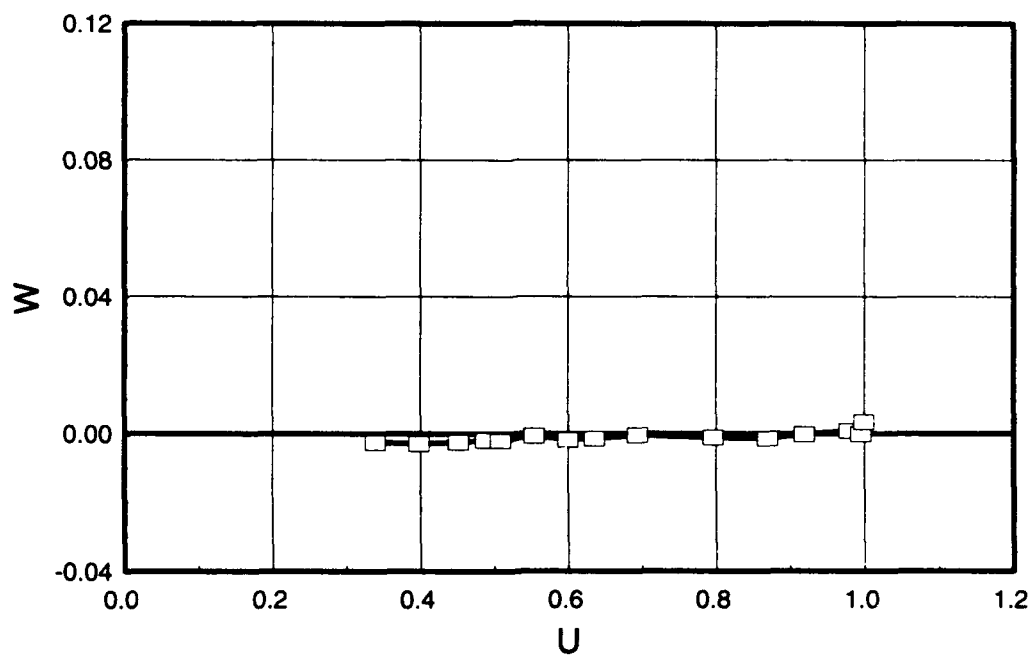


Figure 58. Johnston hodograph, $x/L = 0.600$, $\phi = 180^\circ$.

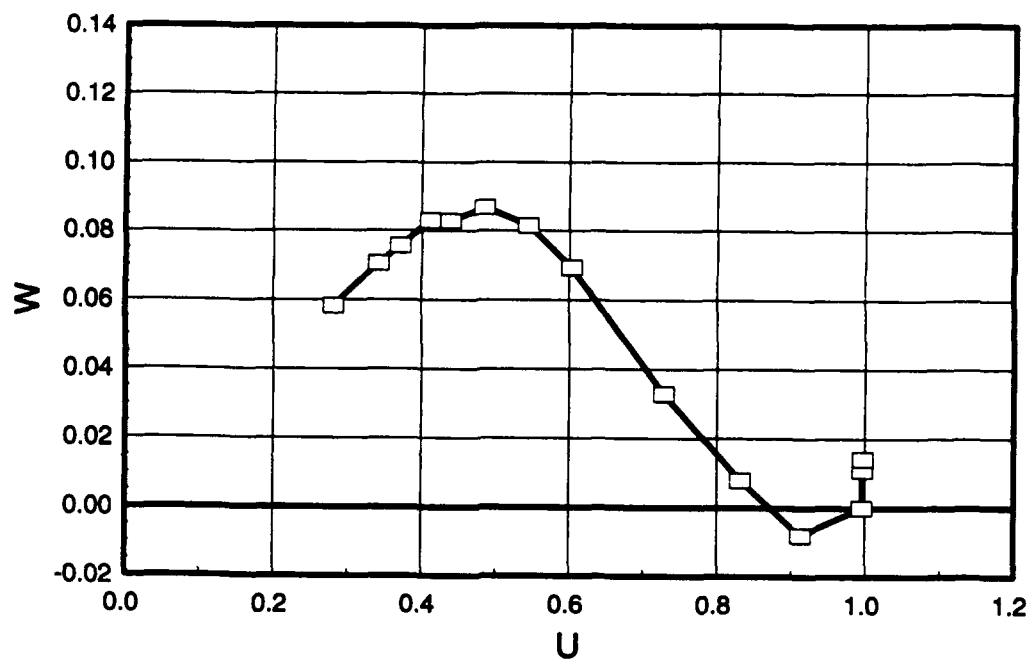


Figure 59. Johnston hodograph, $x/L = 0.752$, $\phi = 120^\circ$.

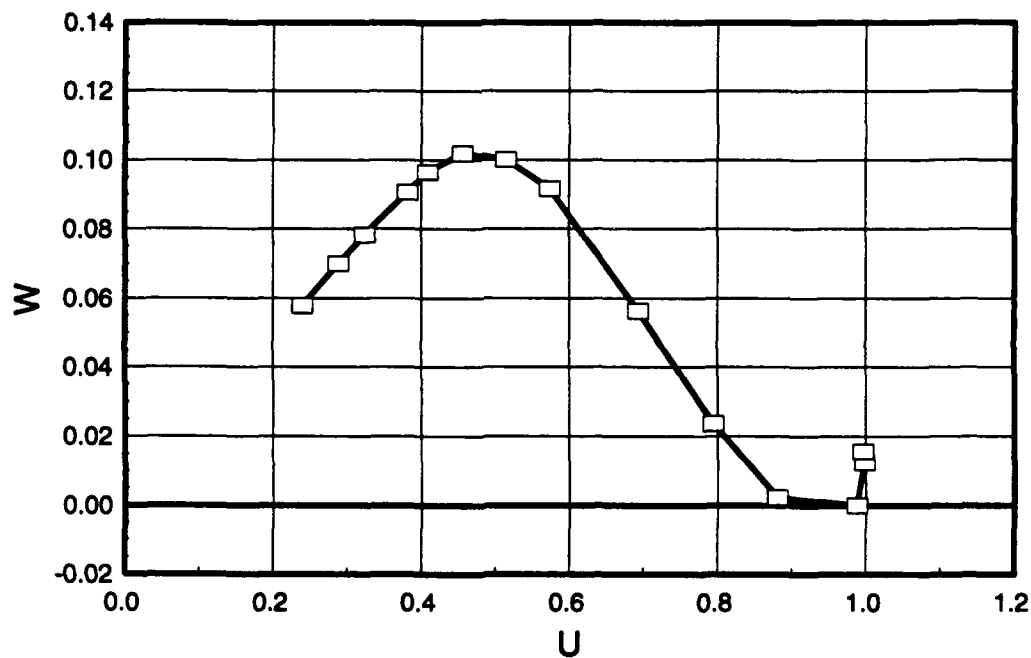


Figure 60. Johnston hodograph, $x/L = 0.752$, $\phi = 123^\circ$.

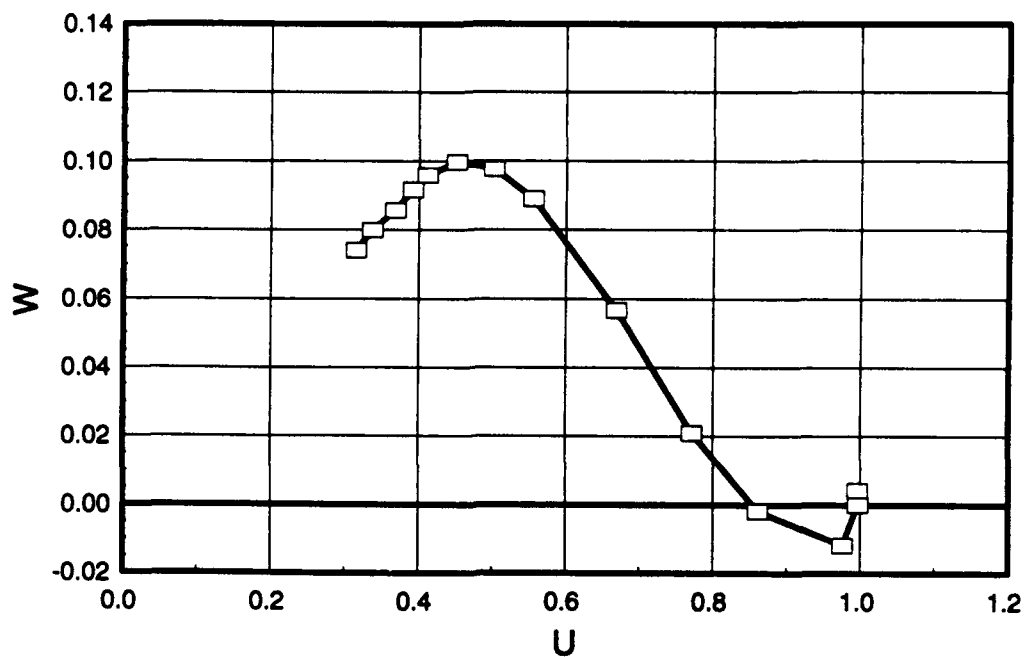


Figure 61. Johnston hodograph, $x/L = 0.752$, $\phi = 125^\circ$.

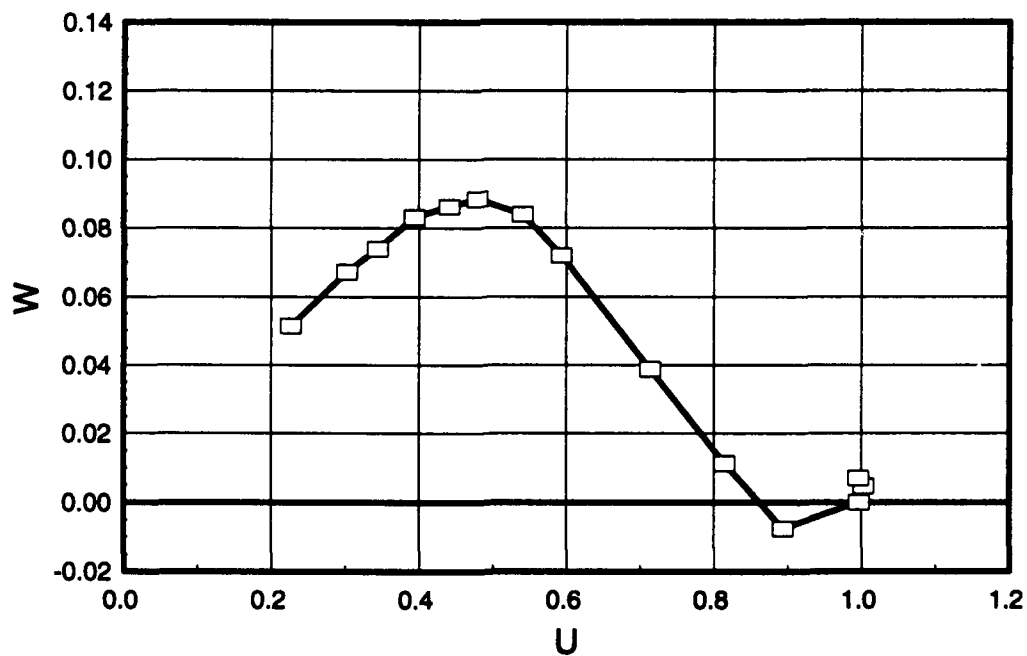


Figure 62. Johnston hodograph, $x/L = 0.762$, $\phi = 120^\circ$.



Figure 63. Johnston hodograph, $x/L = 0.762$, $\phi = 123^\circ$.

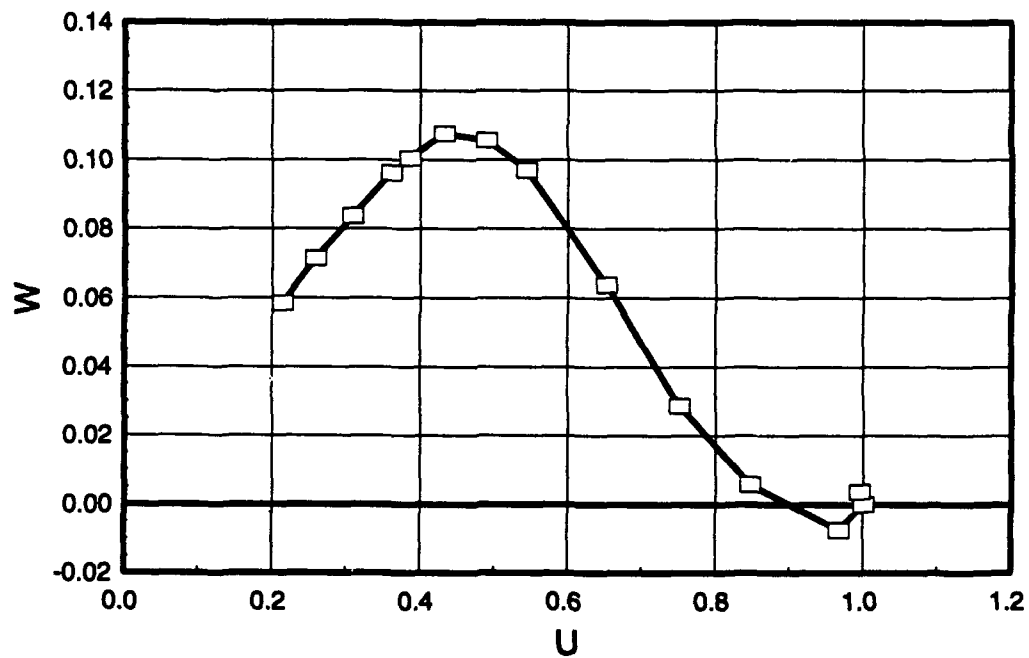


Figure 64. Johnston hodograph, $x/L = 0.762$, $\phi = 125^\circ$.

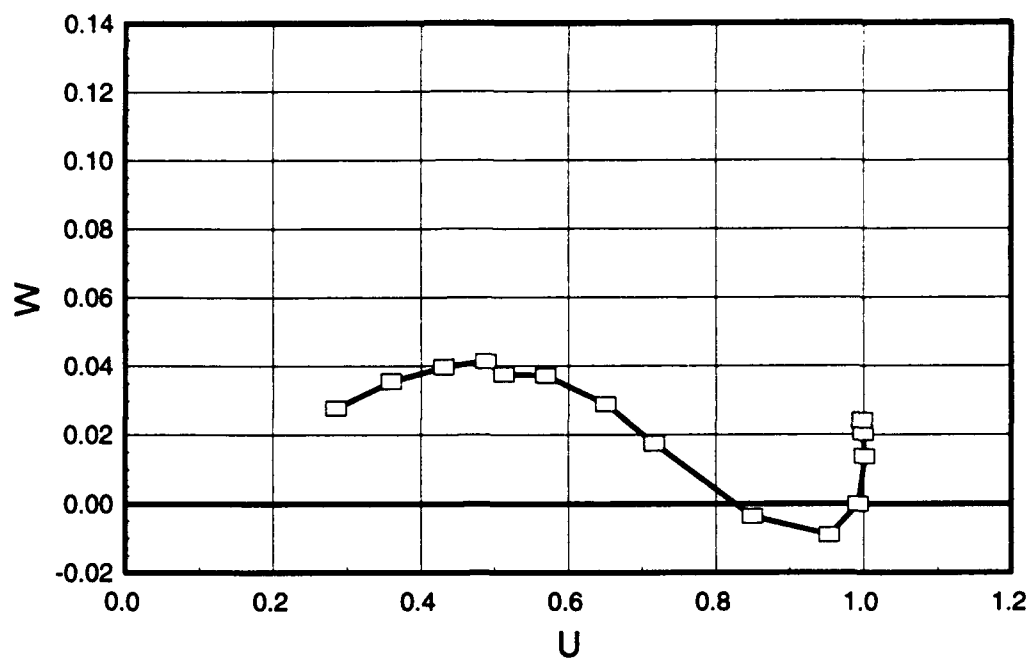


Figure 65. Johnston hodograph, $x/L = 0.772$, $\phi = 105^\circ$.

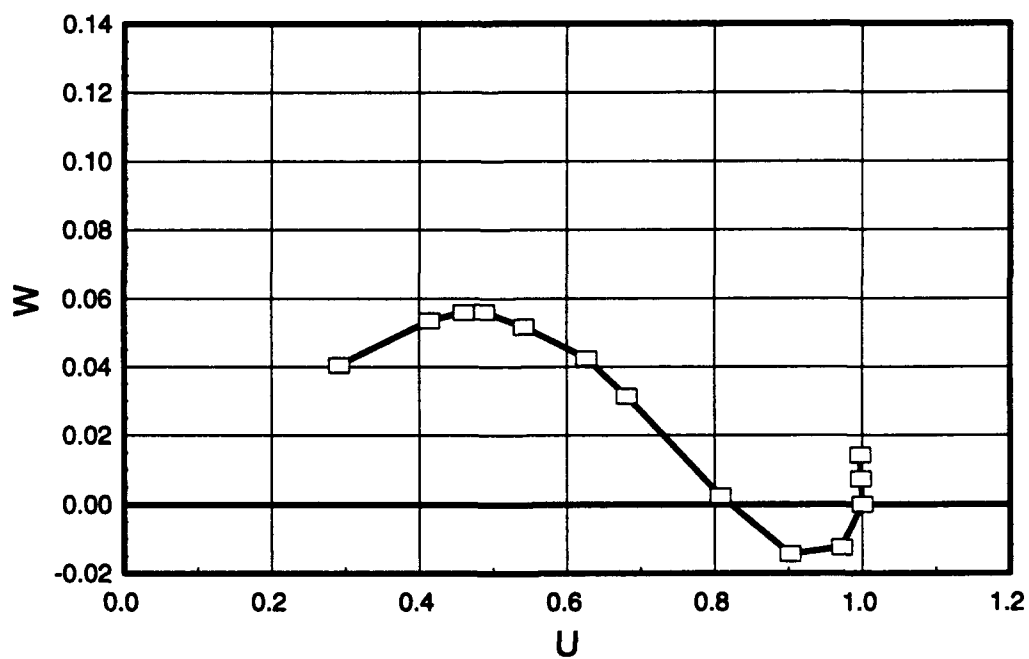


Figure 66. Johnston hodograph, $x/L = 0.772$, $\phi = 110^\circ$.

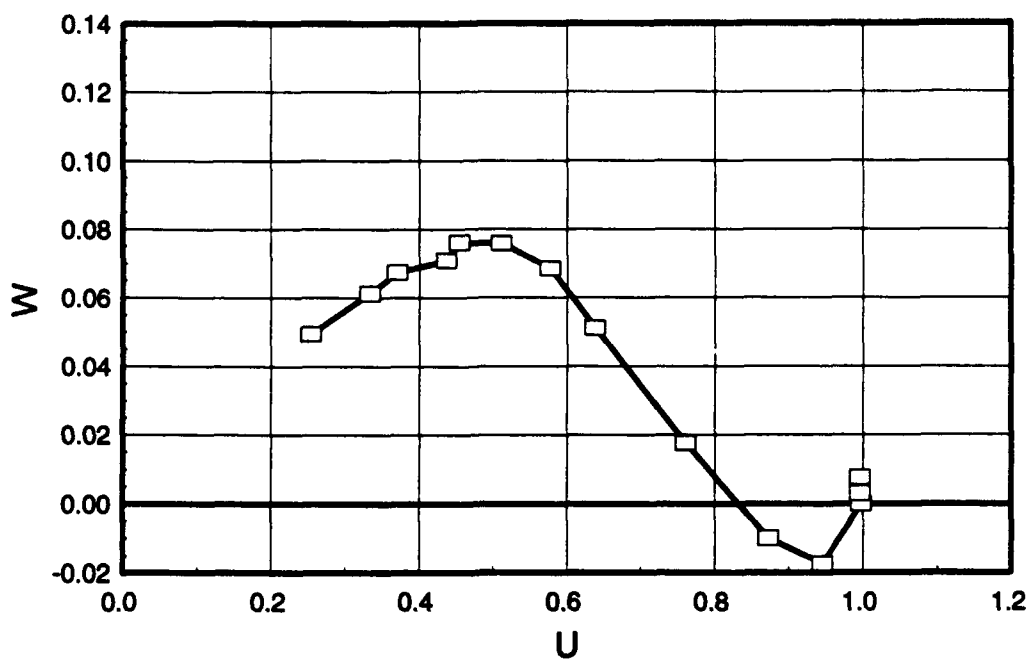


Figure 67. Johnston hodograph, $x/L = 0.772$, $\phi = 115^\circ$.

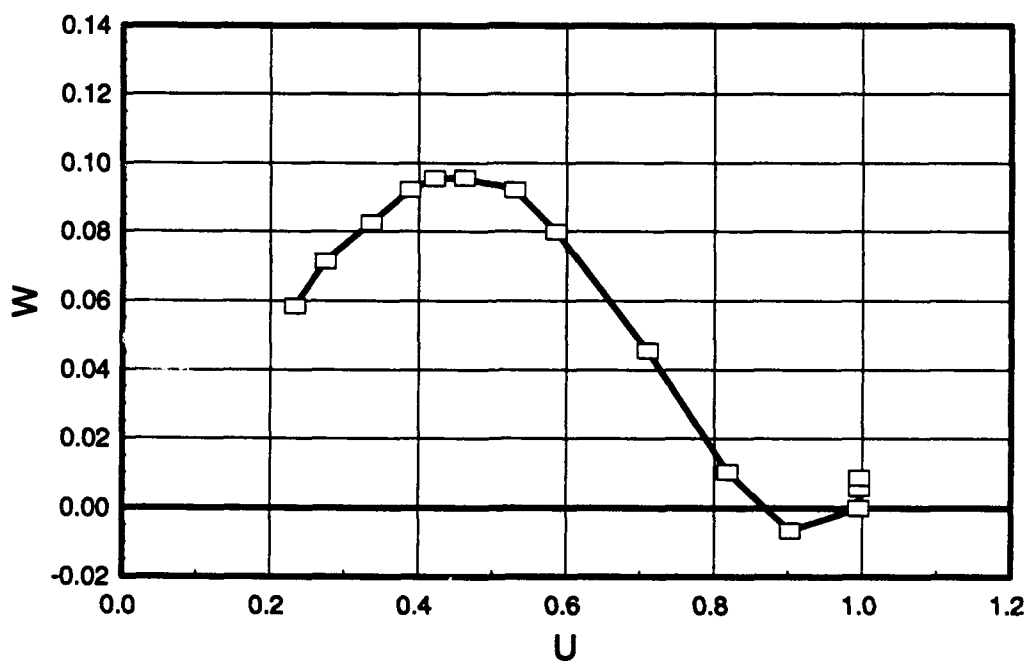


Figure 68. Johnston hodograph, $x/L = 0.772$, $\phi = 120^\circ$.

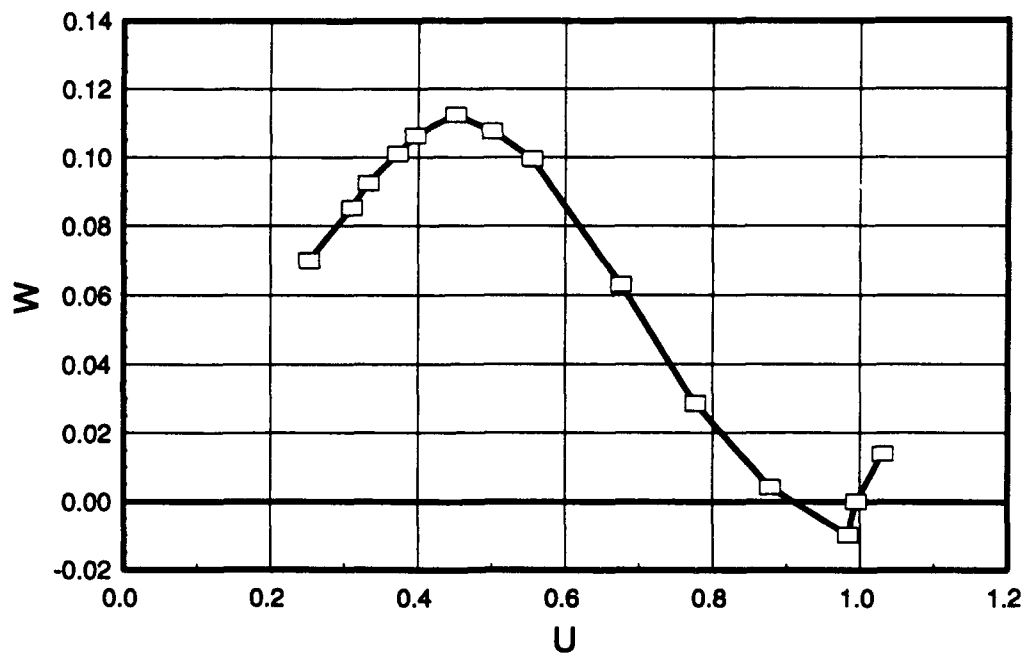


Figure 69. Johnston hodograph, $x/L = 0.772$, $\phi = 123^\circ$.

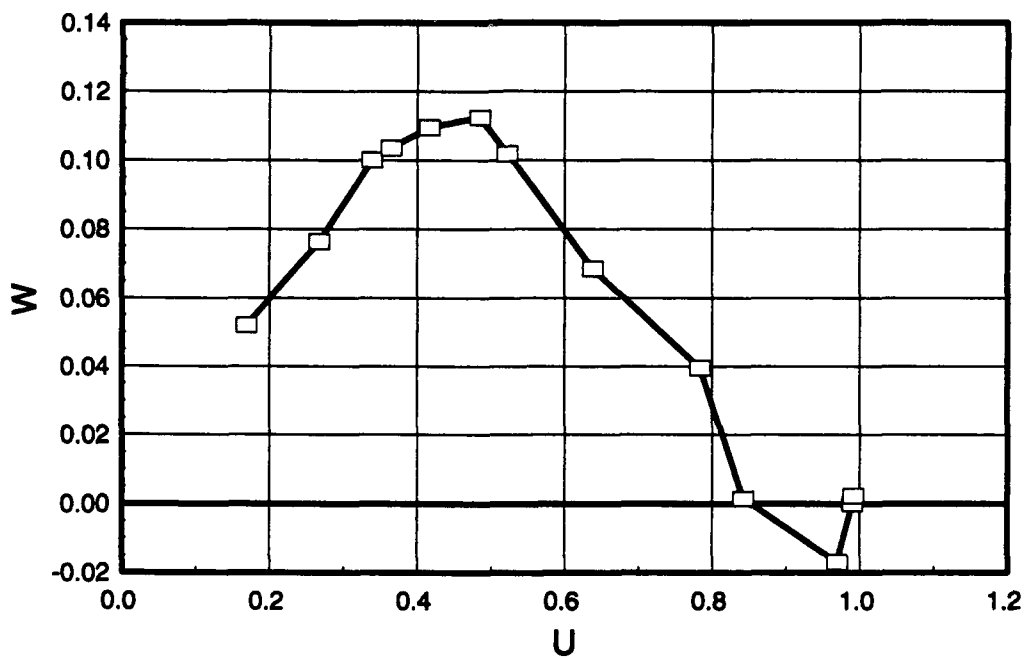


Figure 70. Johnston hodograph, $x/L = 0.772$, $\phi = 125^\circ$.



Figure 71. Johnston hodograph, $x/L = 0.772$, $\phi = 130^\circ$.

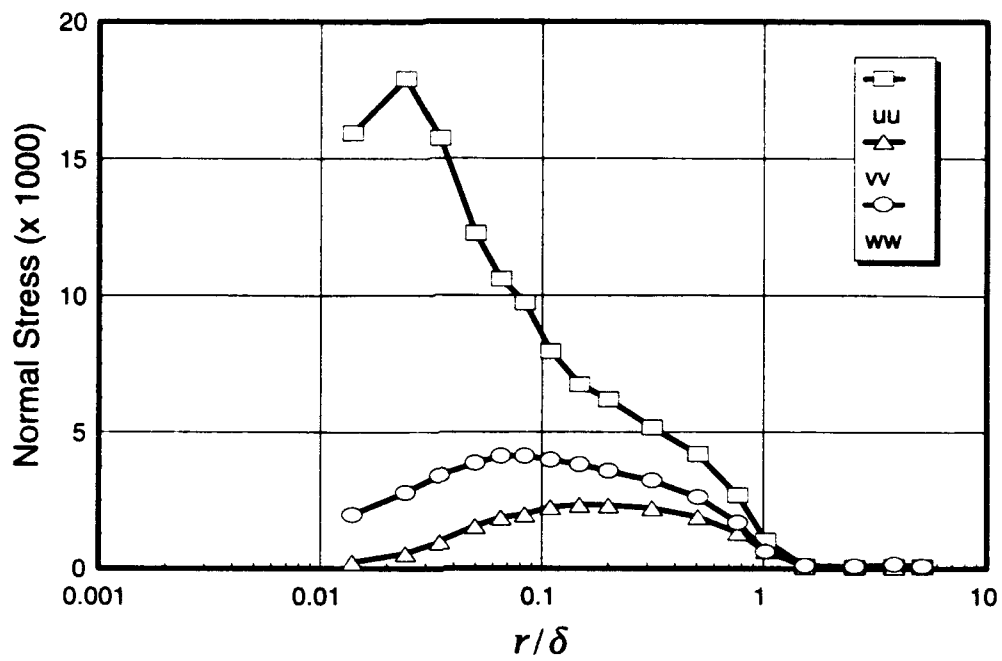


Figure 72. Boundary-layer normal-stress profiles, $x/L = 0.400$, $\phi = 90^\circ$.

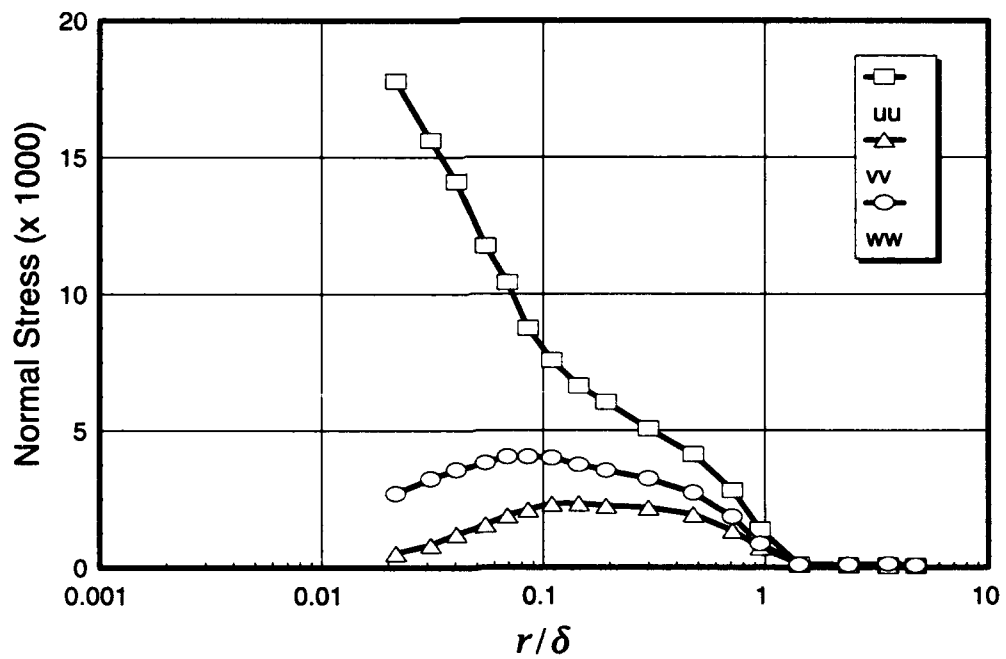


Figure 73. Boundary-layer normal-stress profiles, $x/L = 0.400$, $\phi = 100^\circ$.

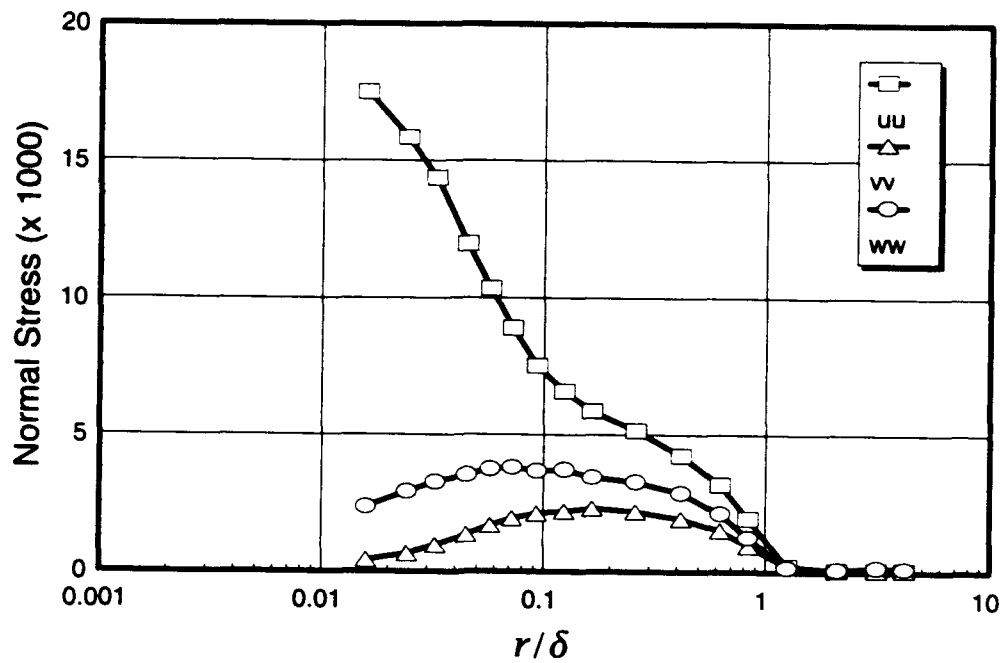


Figure 74. Boundary-layer normal-stress profiles, $x/L = 0.400$, $\phi = 110^\circ$.

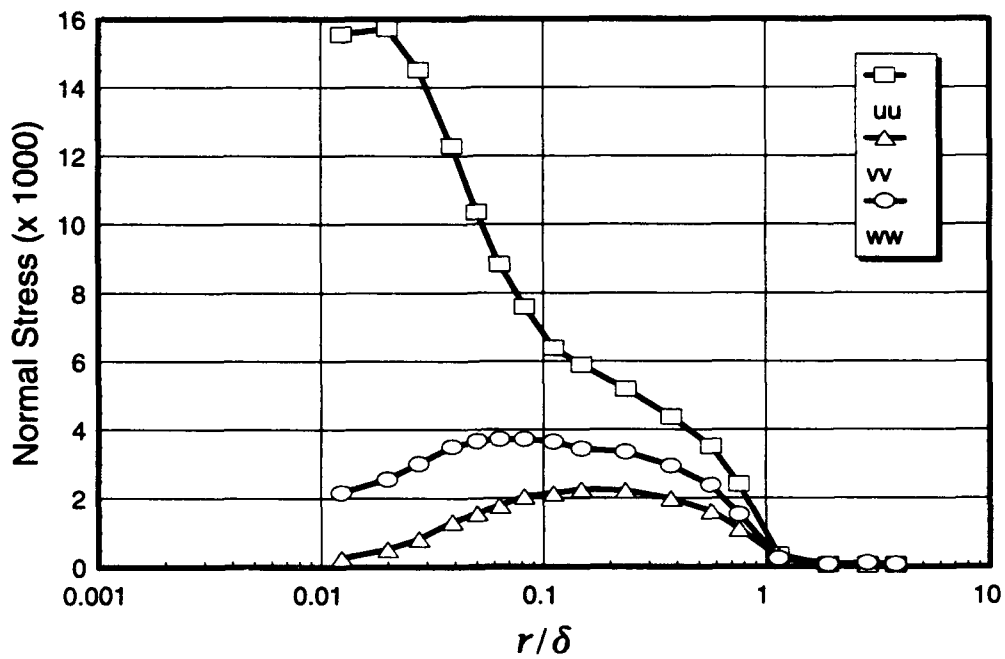


Figure 75. Boundary-layer normal-stress profiles, $x/L = 0.400$, $\phi = 120^\circ$.

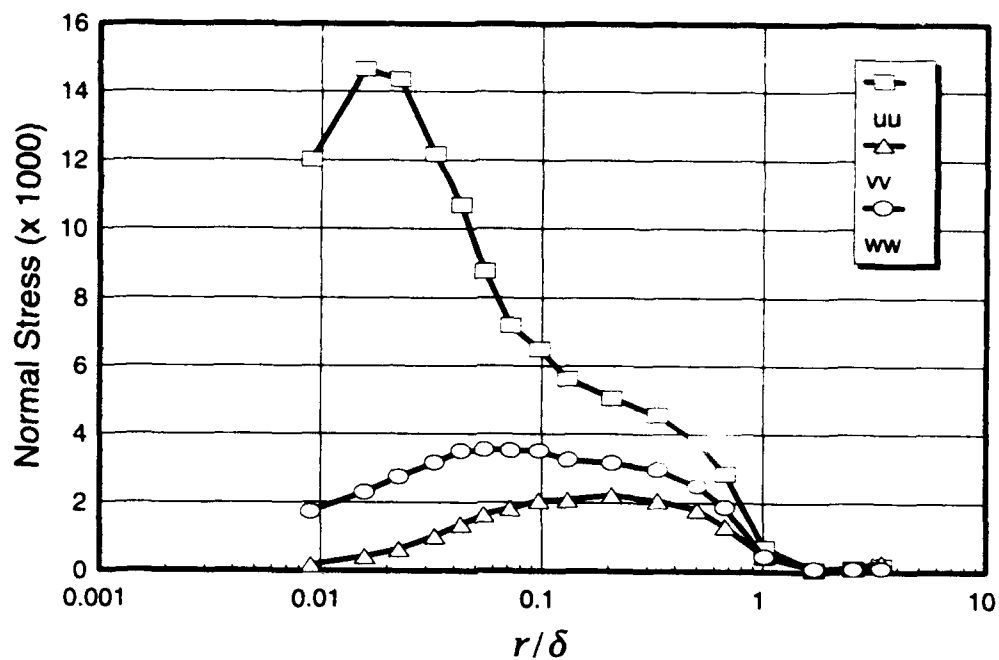


Figure 76. Boundary-layer normal-stress profiles, $x/L = 0.400$, $\phi = 130^\circ$.

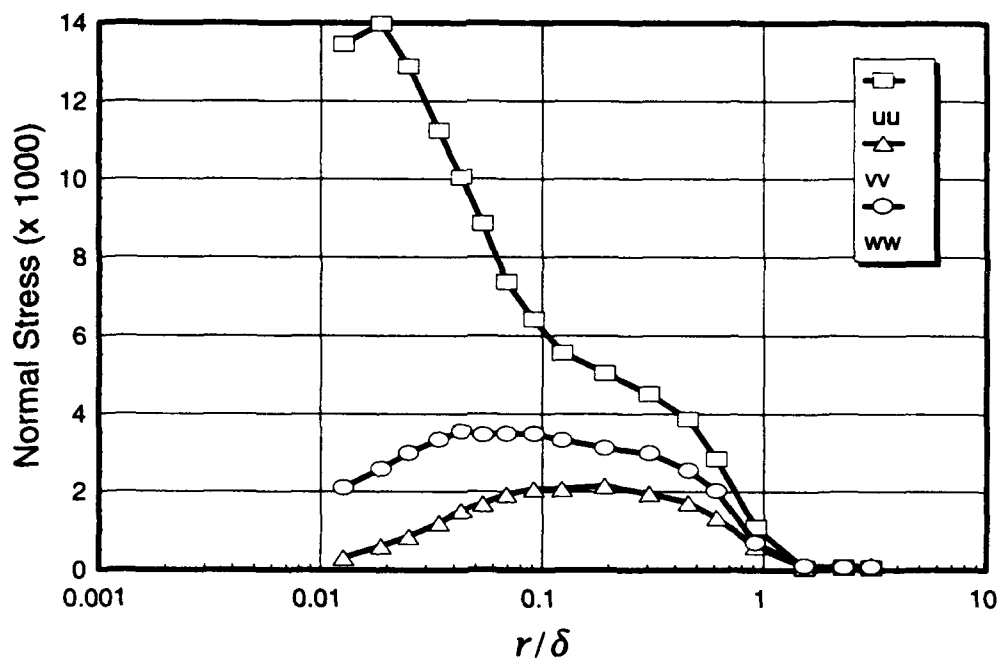


Figure 77. Boundary-layer normal-stress profiles, $x/L = 0.400$, $\phi = 140^\circ$.

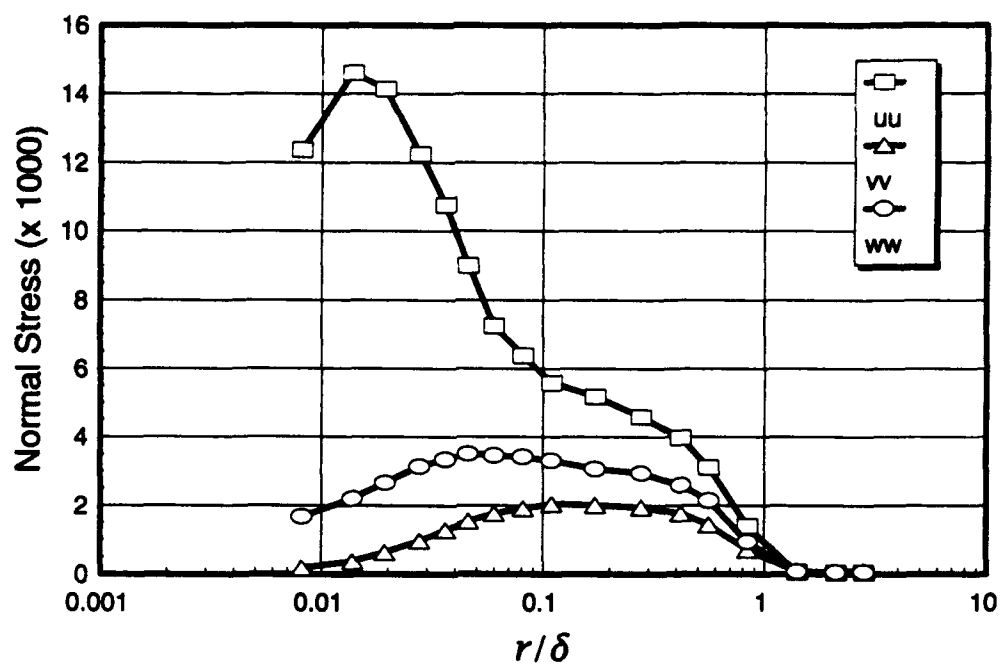


Figure 78. Boundary-layer normal-stress profiles, $x/L = 0.400$, $\phi = 150^\circ$.

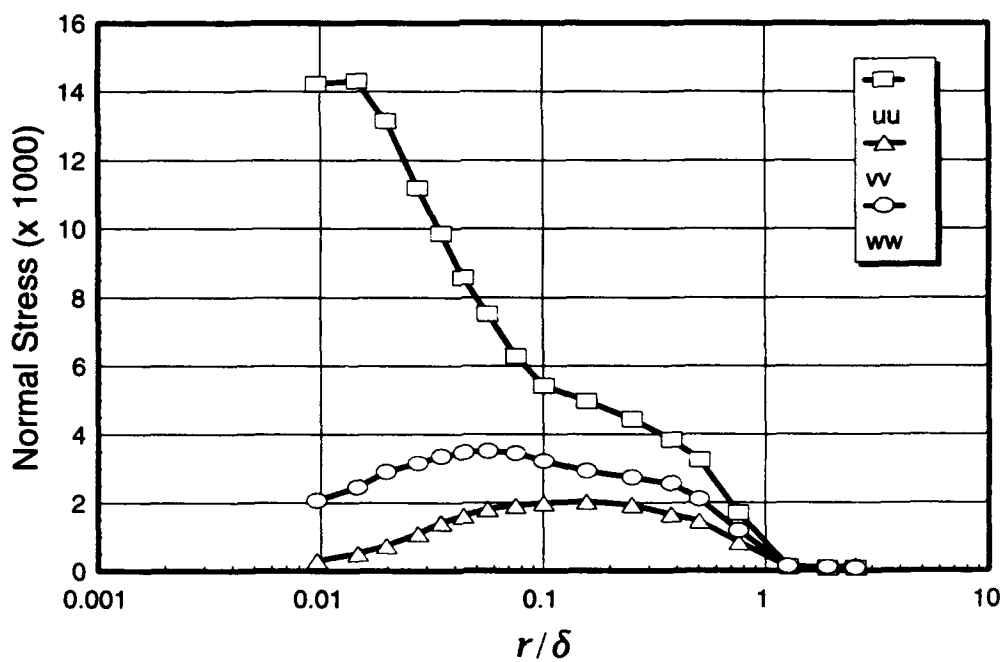


Figure 79. Boundary-layer normal-stress profiles, $x/L = 0.400$, $\phi = 160^\circ$.

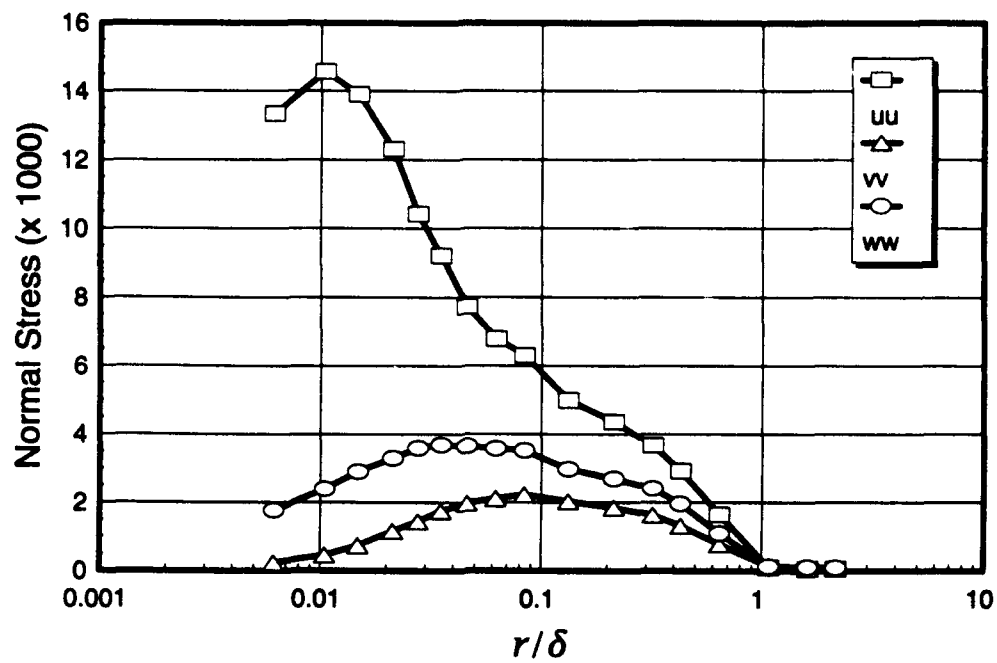


Figure 80. Boundary-layer normal-stress profiles, $x/L = 0.400$, $\phi = 170^\circ$.

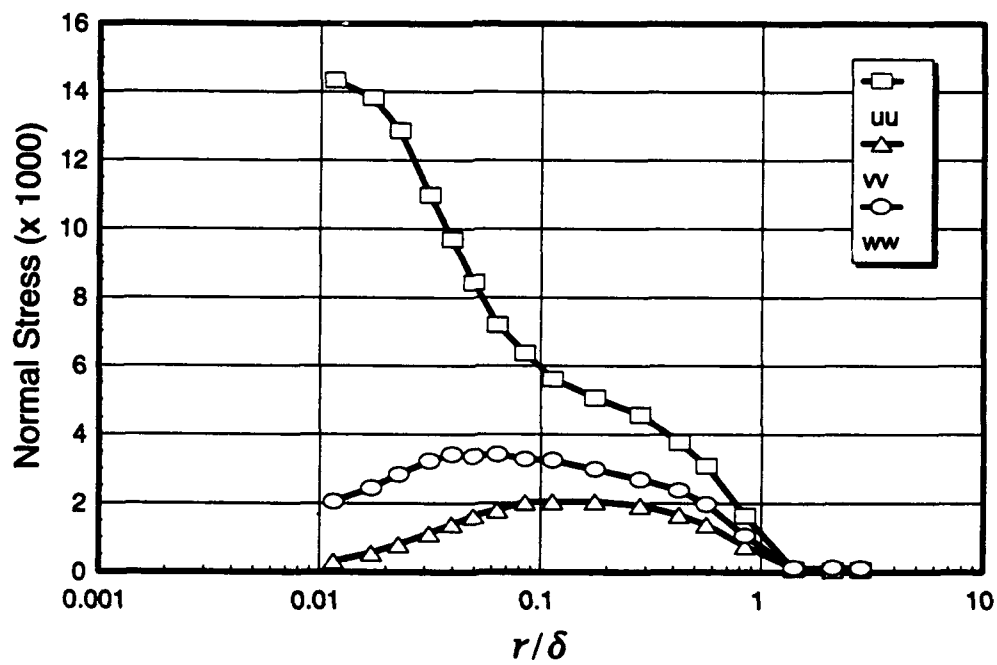


Figure 81. Boundary-layer normal-stress profiles, $x/L = 0.400$, $\phi = 180^\circ$.

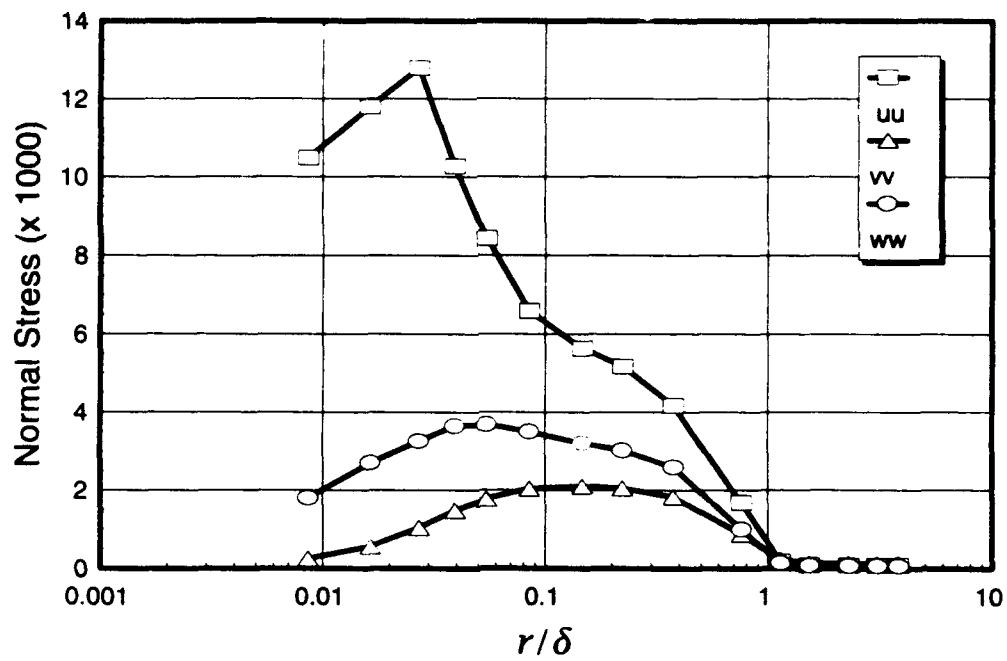


Figure 82. Boundary-layer normal-stress profiles, $x/L = 0.600$, $\phi = 90^\circ$.

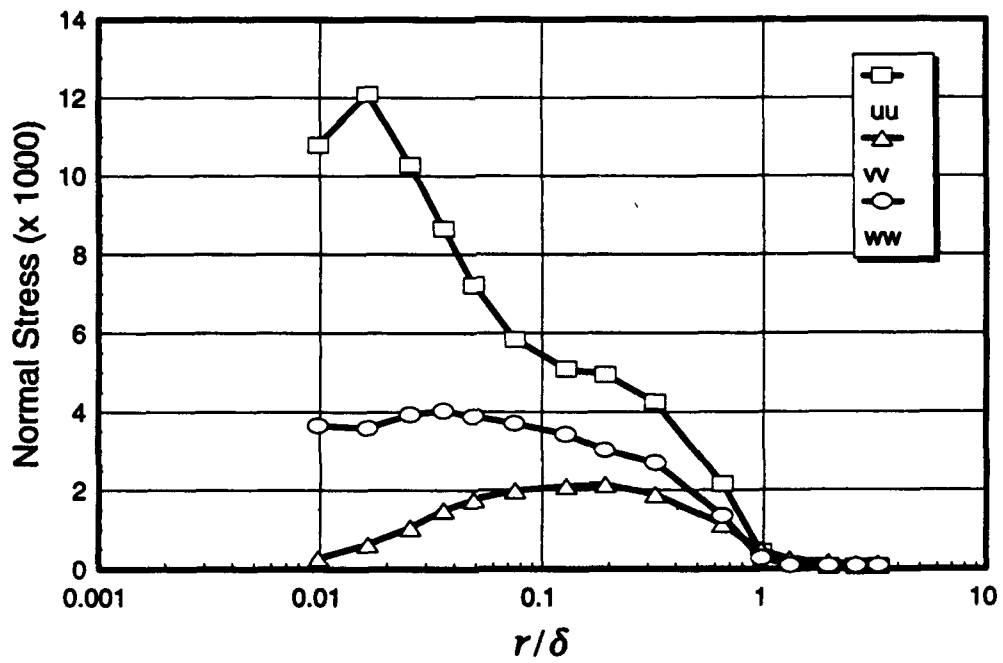


Figure 83. Boundary-layer normal-stress profiles, $x/L = 0.600$, $\phi = 100^\circ$.

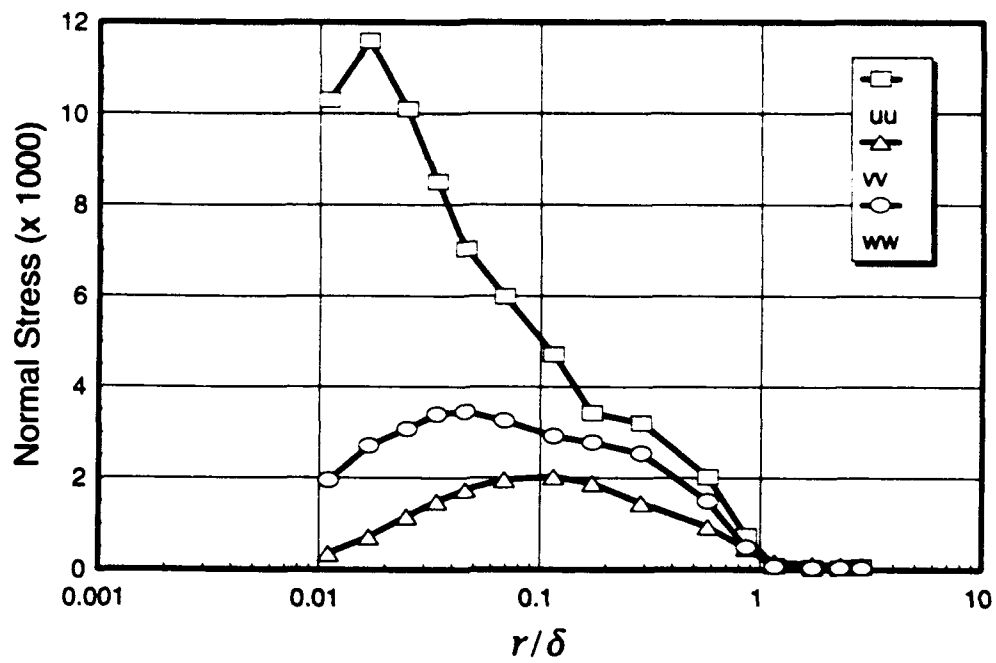


Figure 84. Boundary-layer normal-stress profiles, $x/L = 0.600$, $\phi = 110^\circ$.

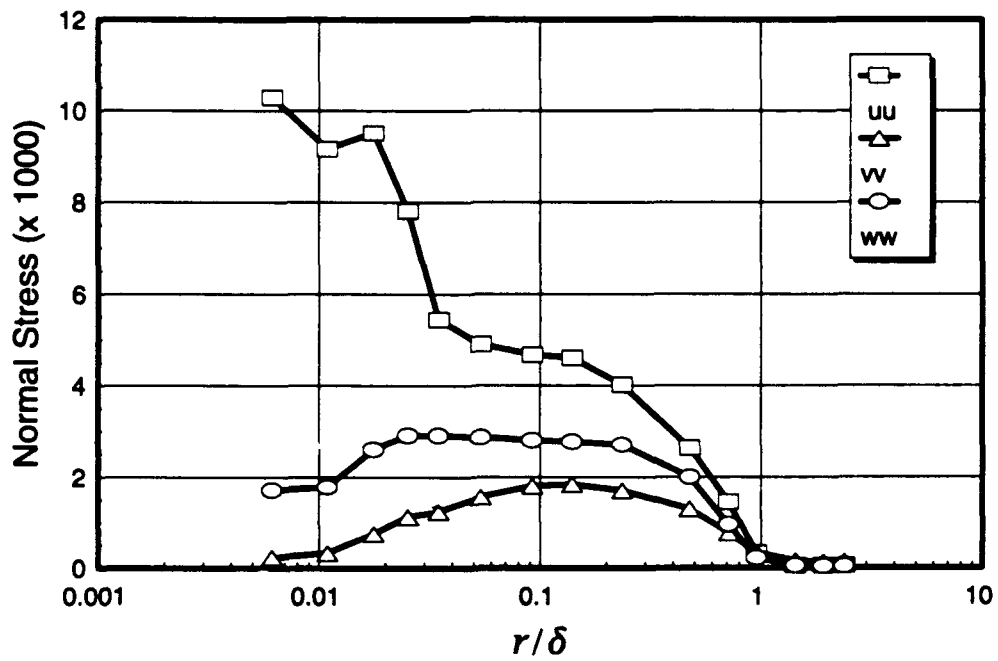


Figure 85. Boundary-layer normal-stress profiles, $x/L = 0.600$, $\phi = 120^\circ$.

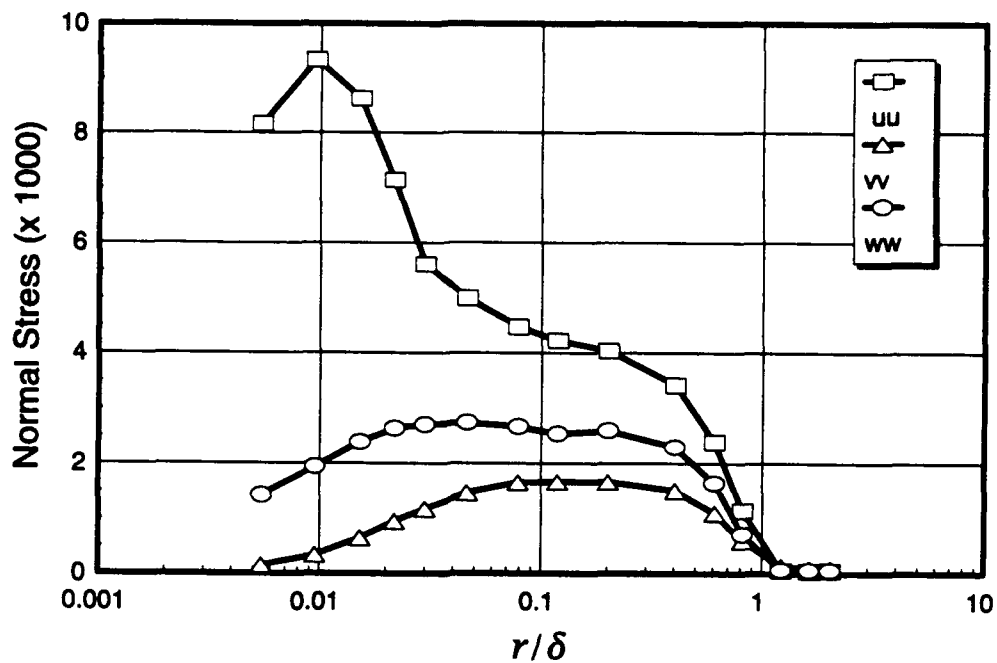


Figure 86. Boundary-layer normal-stress profiles, $x/L = 0.600$, $\phi = 130^\circ$.

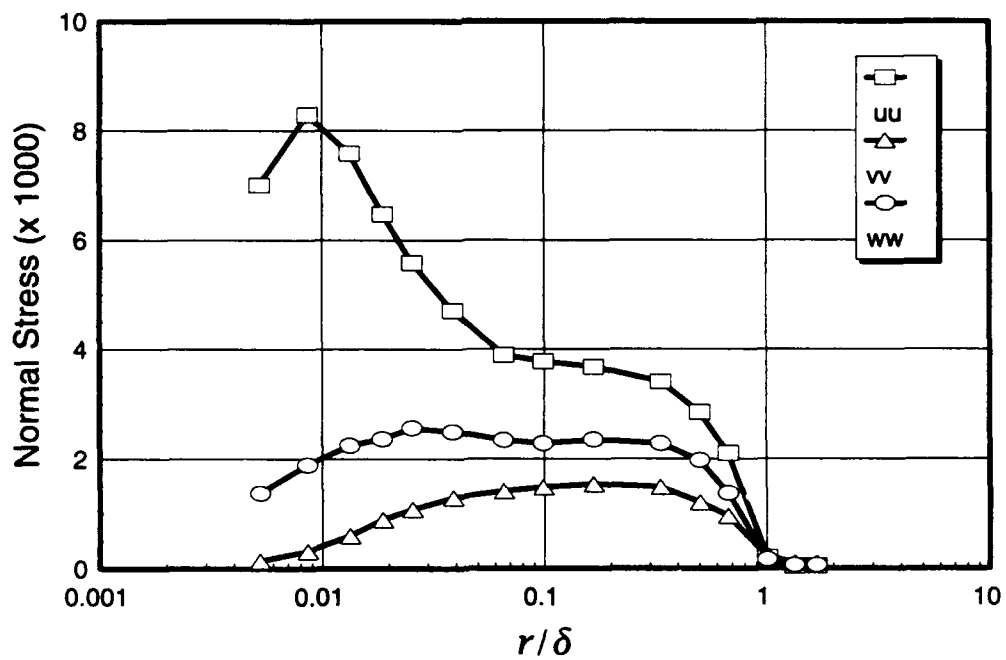


Figure 87. Boundary-layer normal-stress profiles, $x/L = 0.600$, $\phi = 140^\circ$.

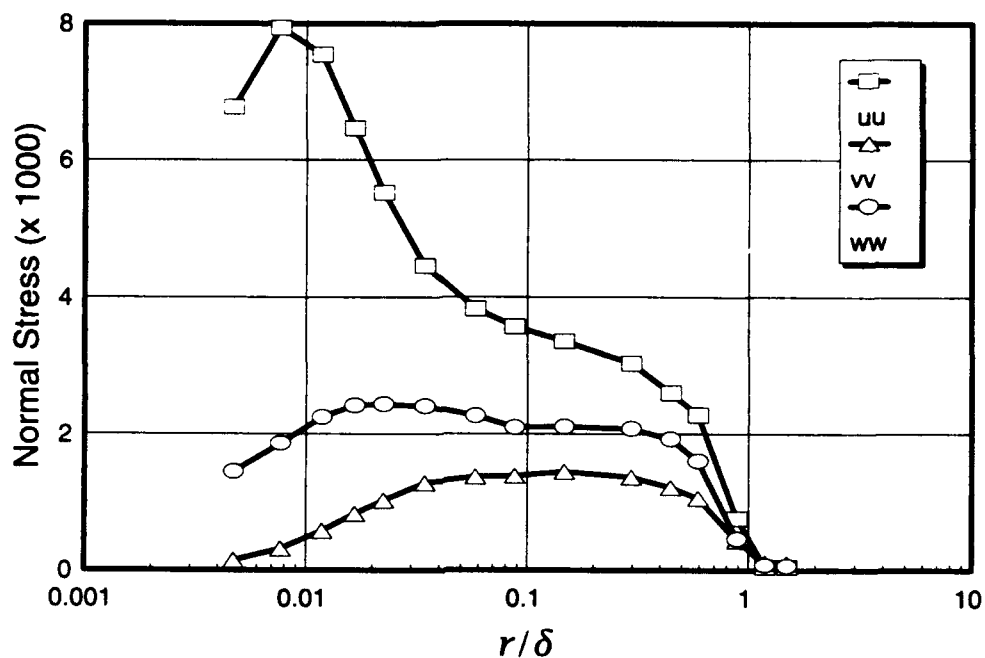


Figure 88. Boundary-layer normal-stress profiles, $x/L = 0.600$, $\phi = 150^\circ$.

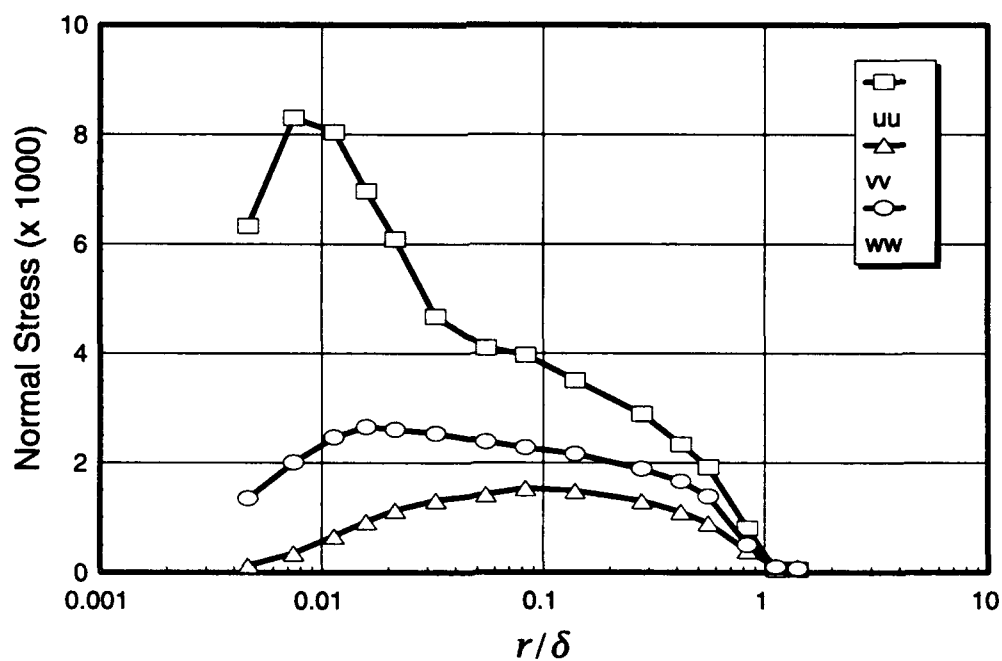


Figure 89. Boundary-layer normal-stress profiles, $x/L = 0.600$, $\phi = 160^\circ$.

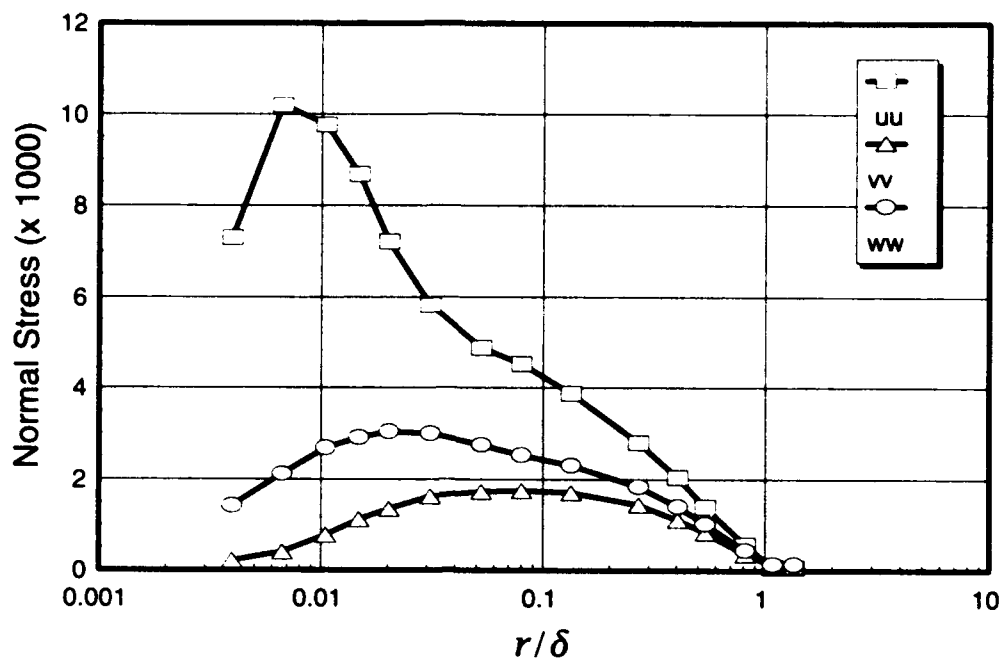


Figure 90. Boundary-layer normal-stress profiles, $x/L = 0.600$, $\phi = 170^\circ$.

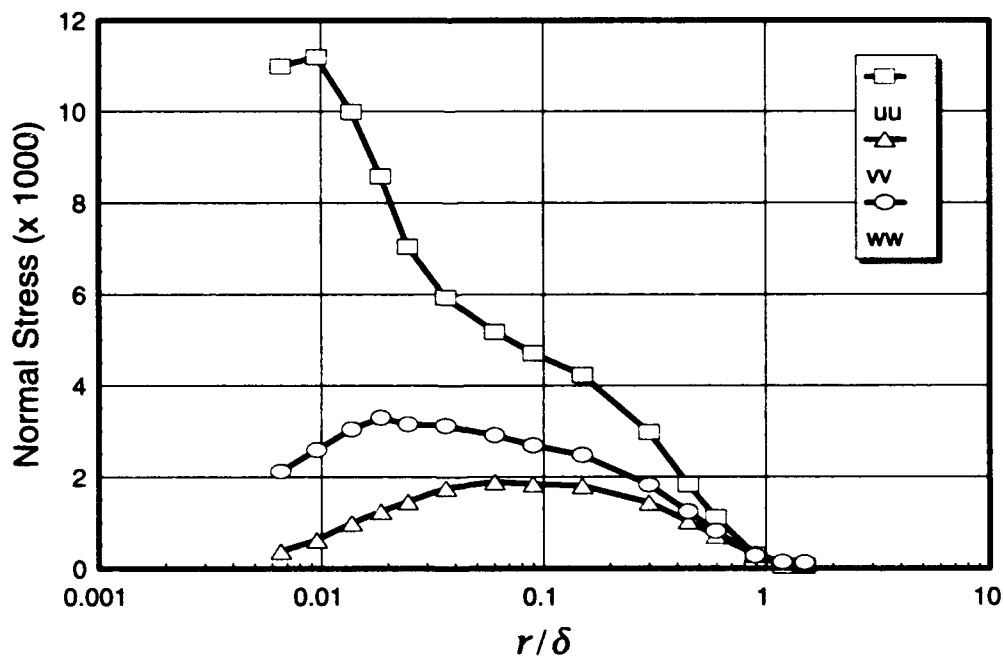


Figure 91. Boundary-layer normal-stress profiles, $x/L = 0.600$, $\phi = 180^\circ$.

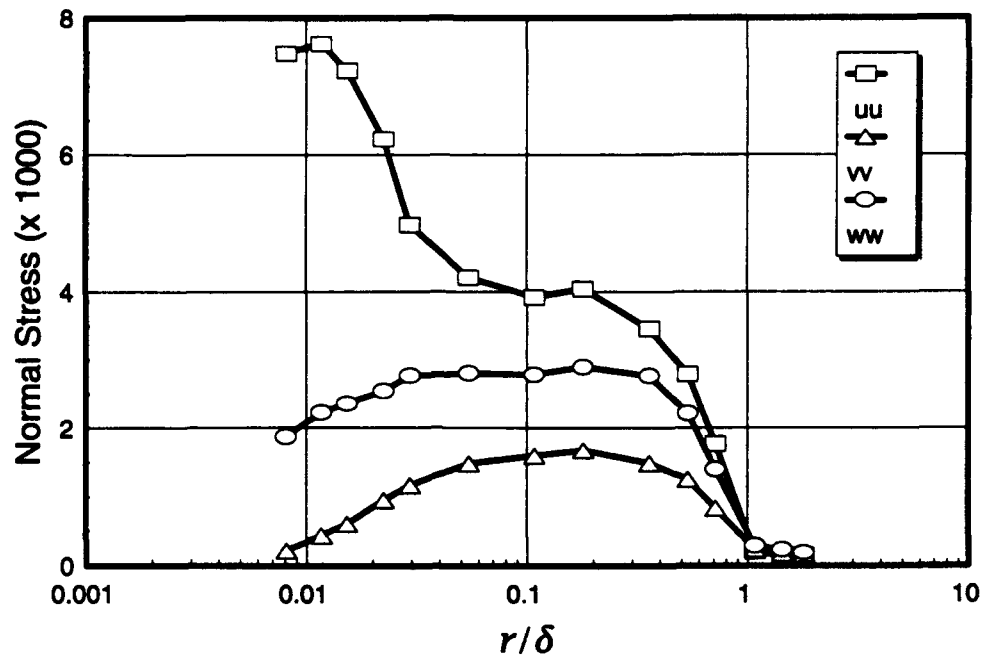


Figure 92. Boundary-layer normal-stress profiles, $x/L = 0.752$, $\phi = 120^\circ$.

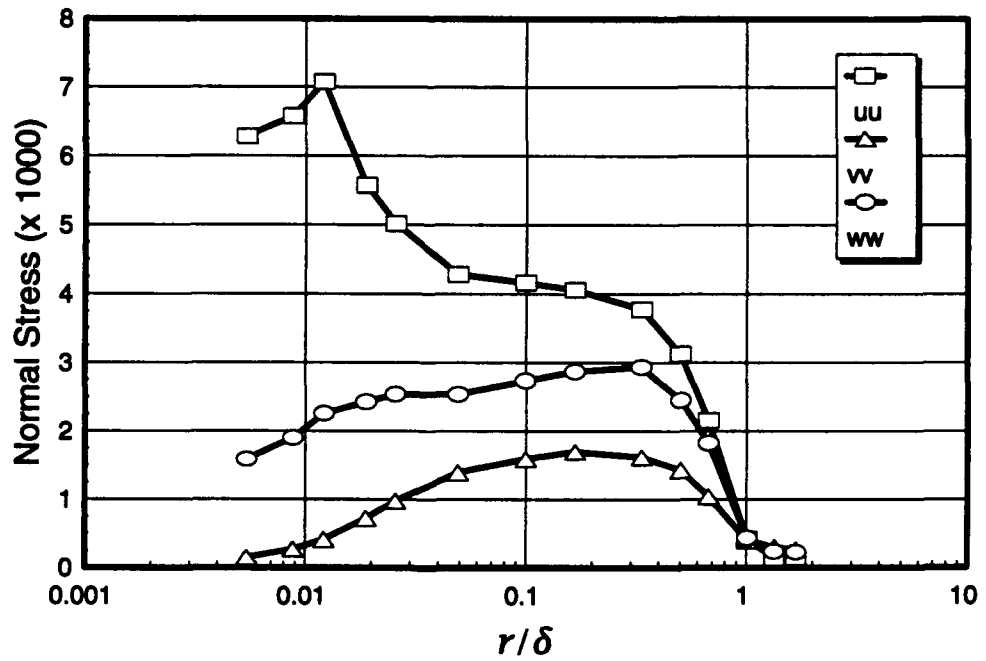


Figure 93. Boundary-layer normal-stress profiles, $x/L = 0.752$, $\phi = 123^\circ$.

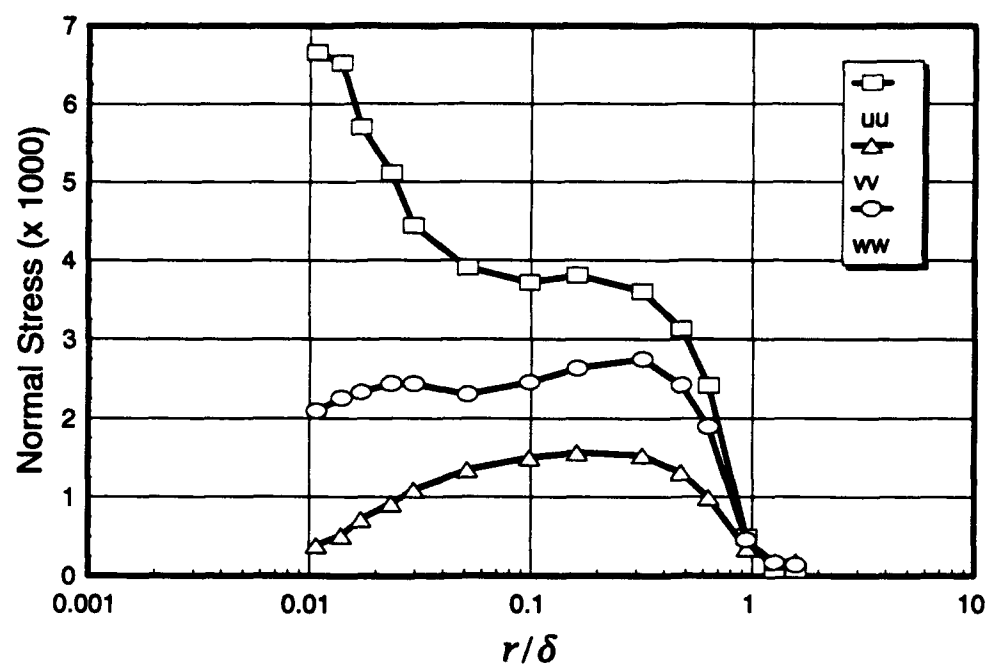


Figure 94. Boundary-layer normal-stress profiles, $x/L = 0.752$, $\phi = 125^\circ$.

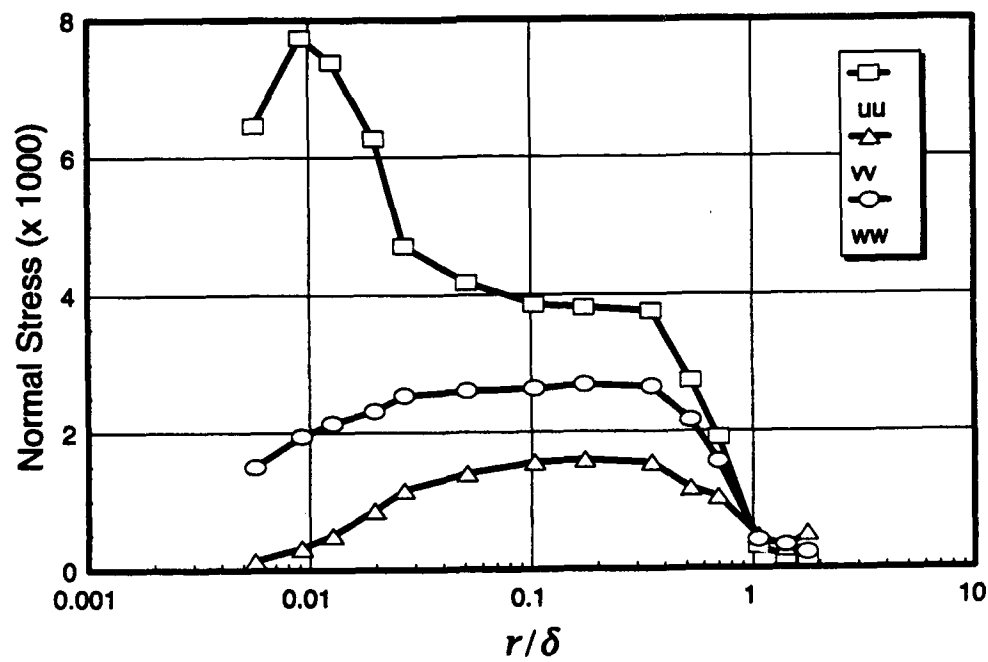


Figure 95. Boundary-layer normal-stress profiles, $x/L = 0.762$, $\phi = 120^\circ$.

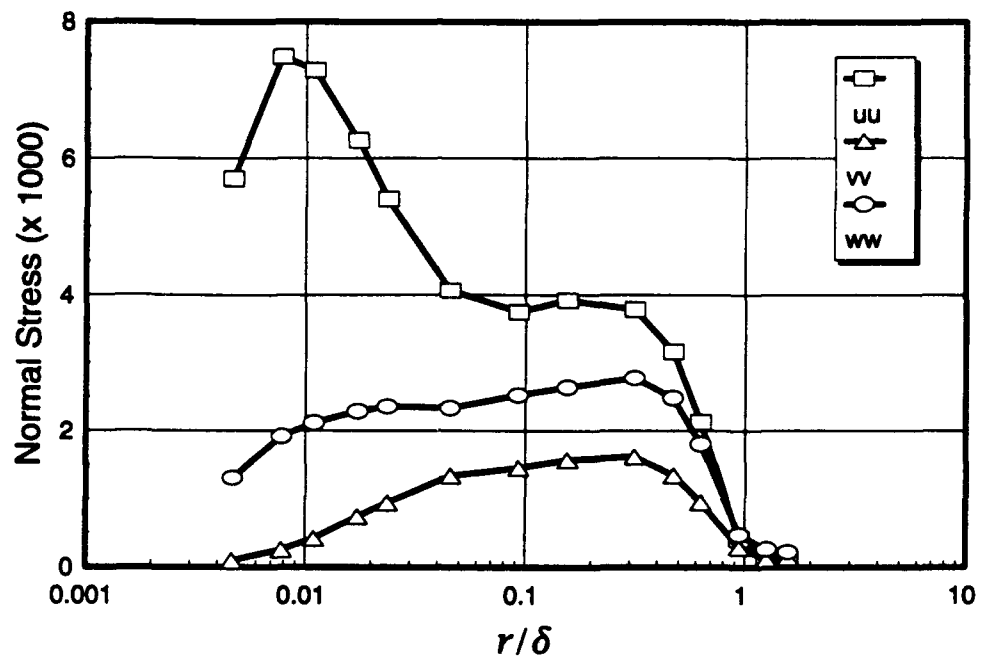


Figure 96. Boundary-layer normal-stress profiles, $x/L = 0.762$, $\phi = 123^\circ$.

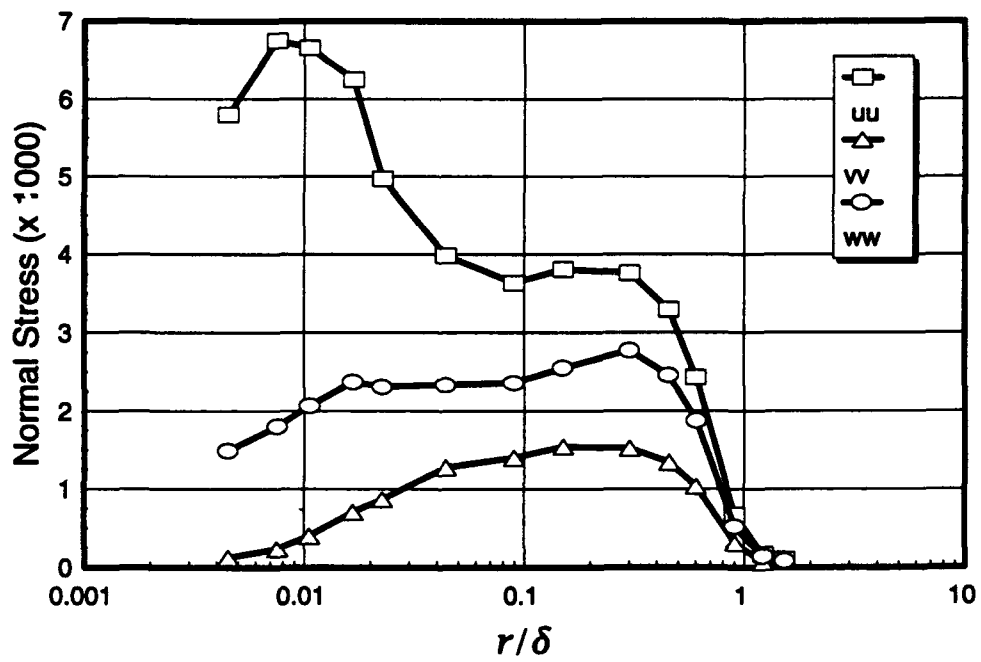


Figure 97. Boundary-layer normal-stress profiles, $x/L = 0.762$, $\phi = 125^\circ$.

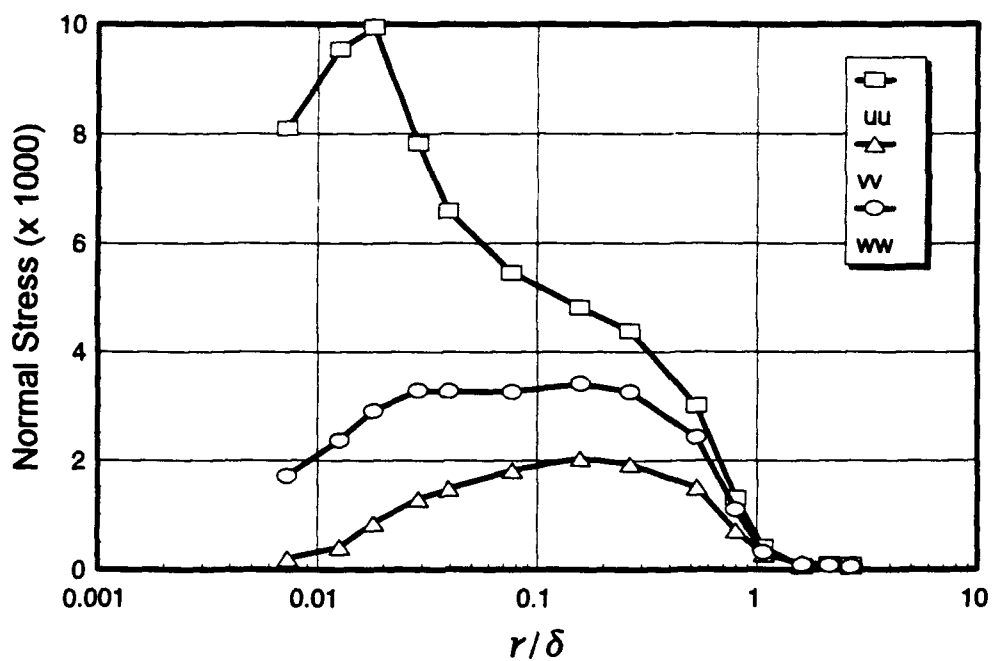


Figure 98. Boundary-layer normal-stress profiles, $x/L = 0.772$, $\phi = 105^\circ$.

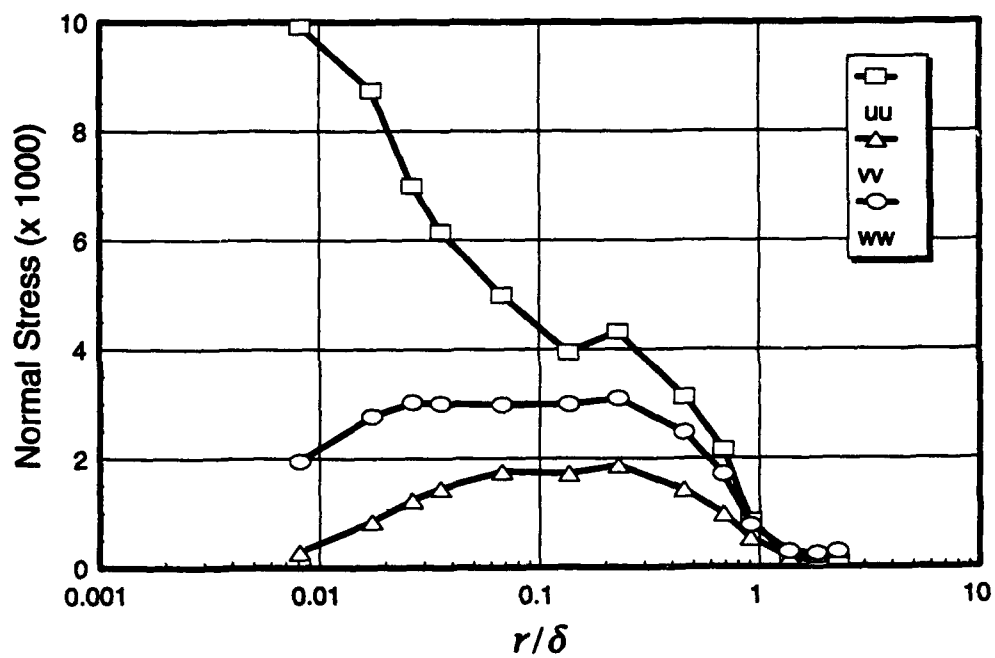


Figure 99. Boundary-layer normal-stress profiles, $x/L = 0.772$, $\phi = 110^\circ$.

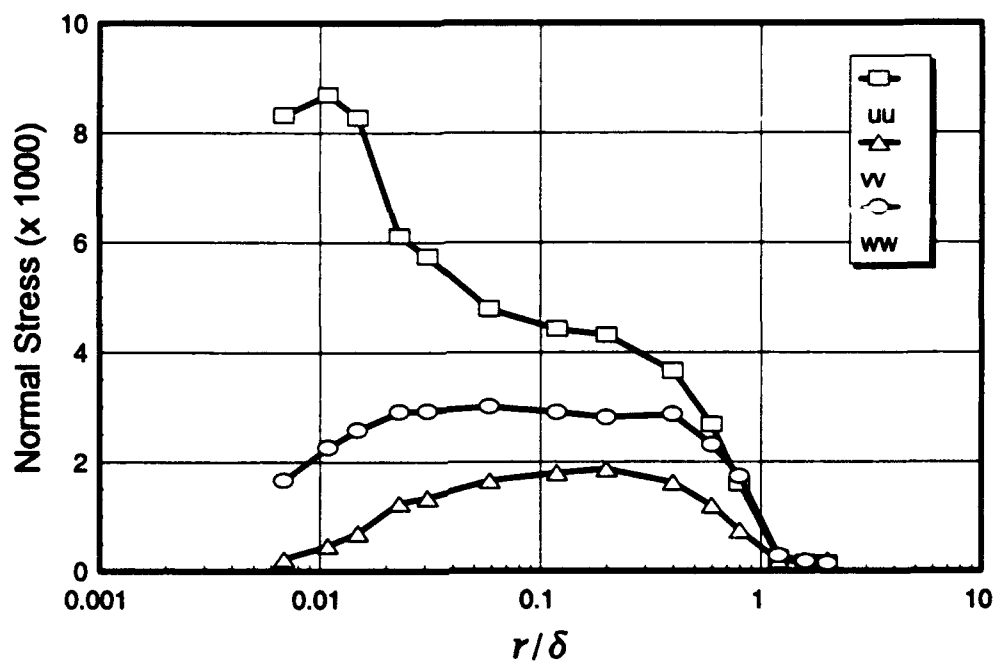


Figure 100. Boundary-layer normal-stress profiles, $x/L = 0.772$, $\phi = 115^\circ$.

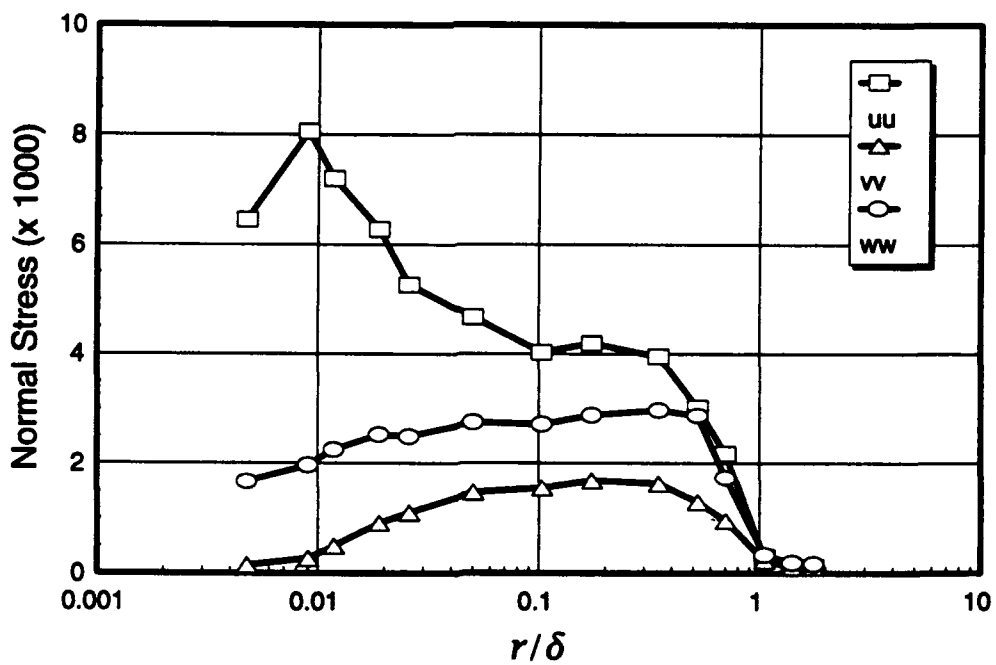


Figure 101. Boundary-layer normal-stress profiles, $x/L = 0.772$, $\phi = 120^\circ$.

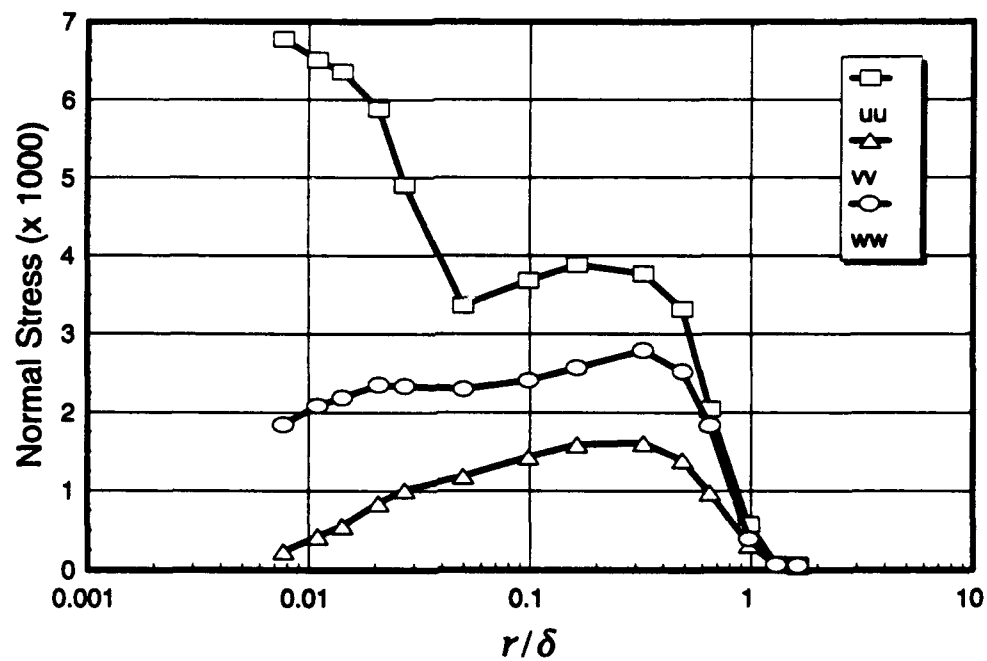


Figure 102. Boundary-layer normal-stress profiles, $x/L = 0.772$, $\phi = 123^\circ$.

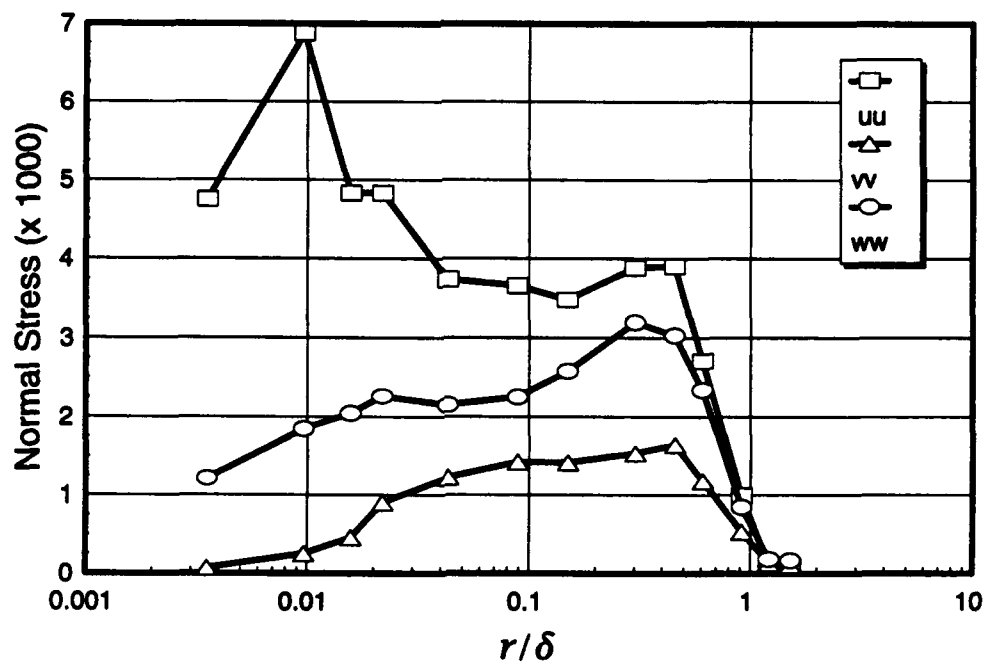


Figure 103. Boundary-layer normal-stress profiles, $x/L = 0.772$, $\phi = 125^\circ$.

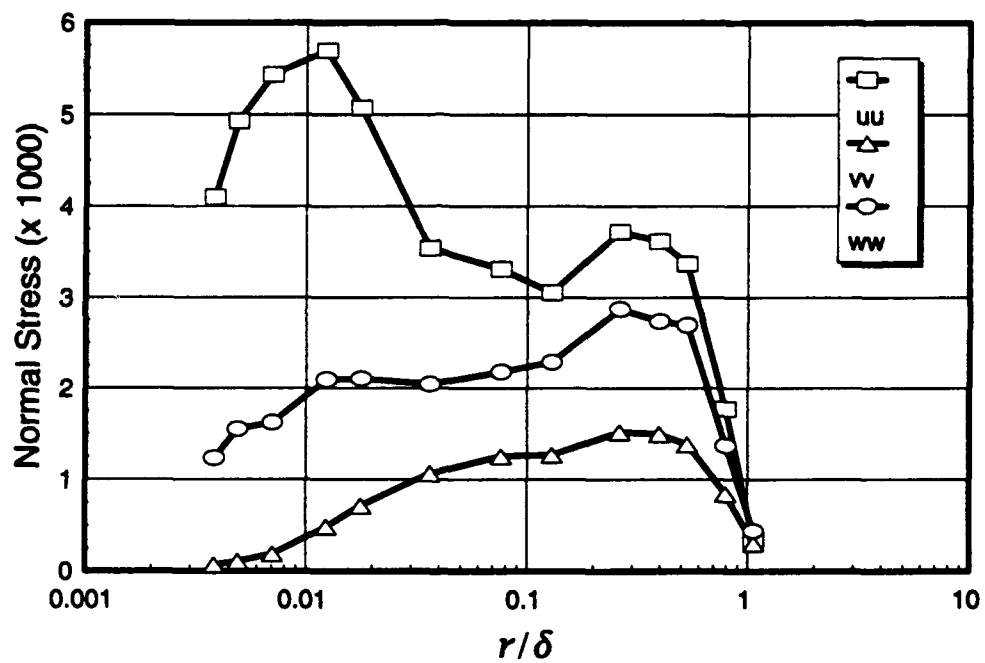


Figure 104. Boundary-layer normal-stress profiles, $x/L = 0.772$, $\phi = 130^\circ$.

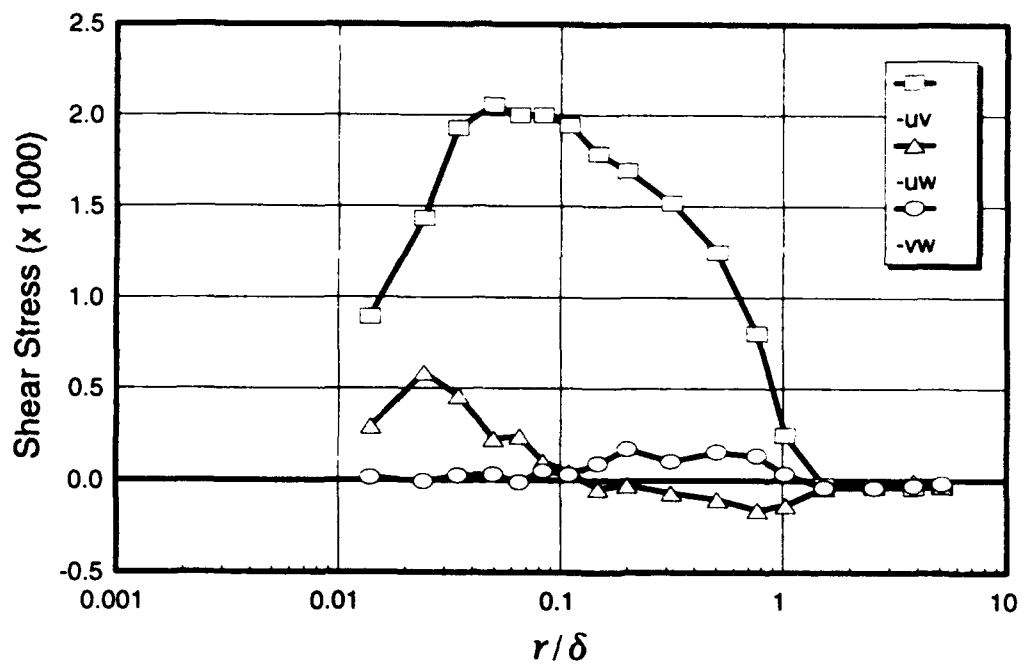


Figure 105. Boundary-layer shear-stress profiles, $x/L = 0.400$, $\phi = 90^\circ$.

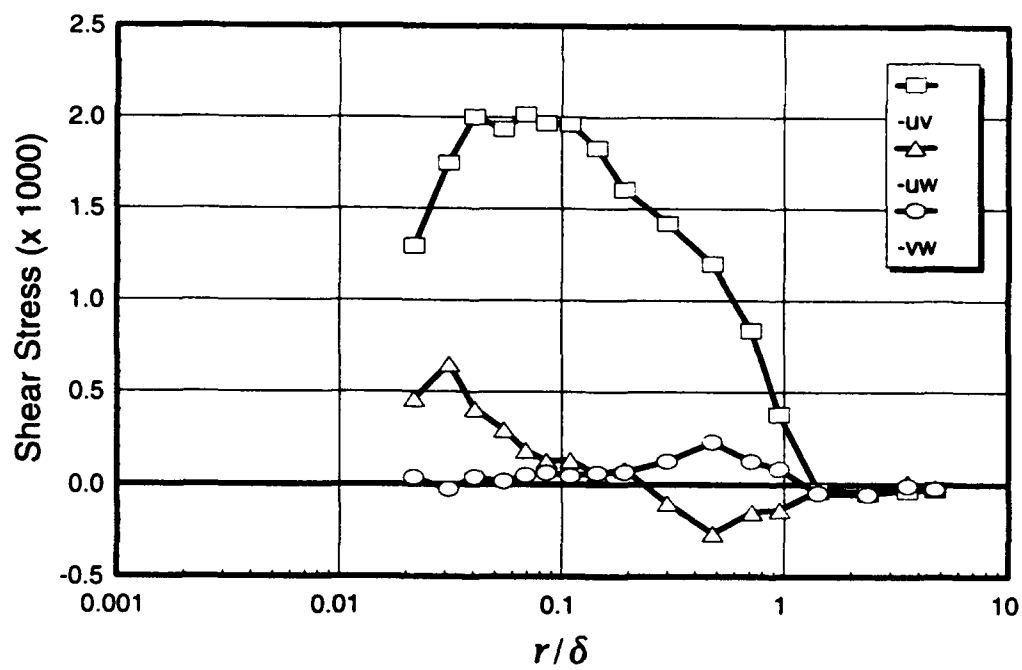


Figure 106. Boundary-layer shear-stress profiles, $x/L = 0.400$, $\phi = 100^\circ$.

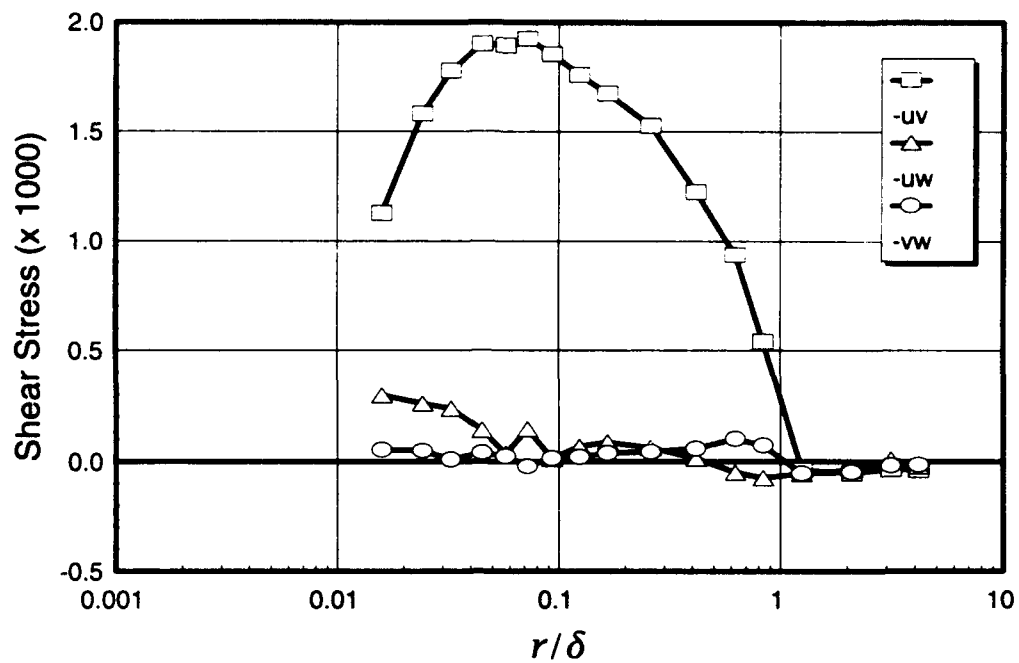


Figure 107. Boundary-layer shear-stress profiles, $x/L = 0.400$, $\phi = 110^\circ$.

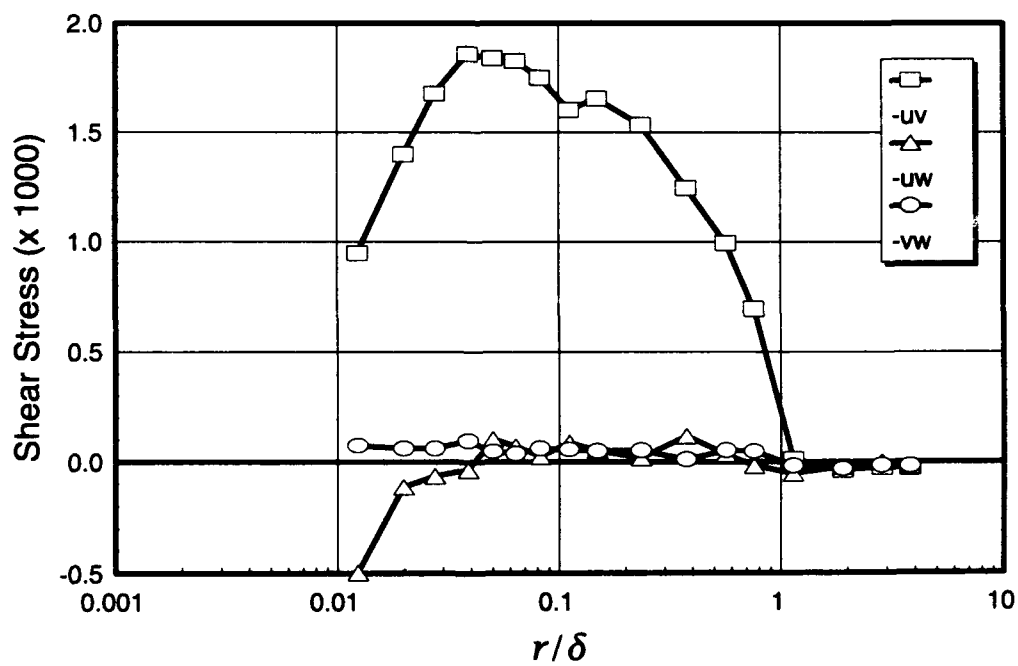


Figure 108. Boundary-layer shear-stress profiles, $x/L = 0.400$, $\phi = 120^\circ$.

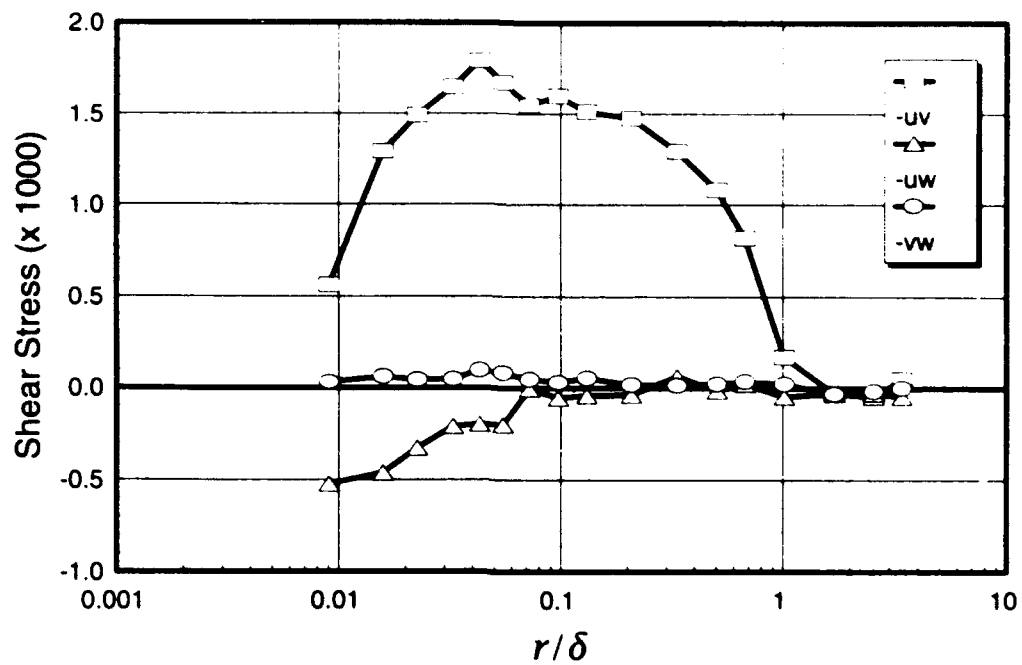


Figure 109. Boundary-layer shear-stress profiles, $x/L = 0.400$, $\phi = 130^\circ$.

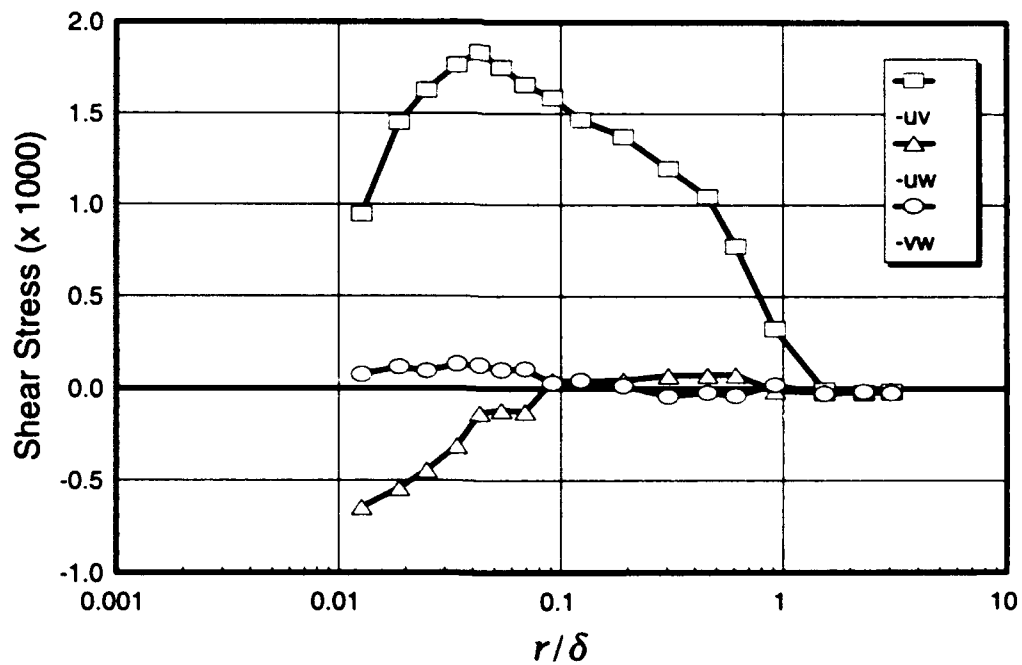


Figure 110. Boundary-layer shear-stress profiles, $x/L = 0.400$, $\phi = 140^\circ$.

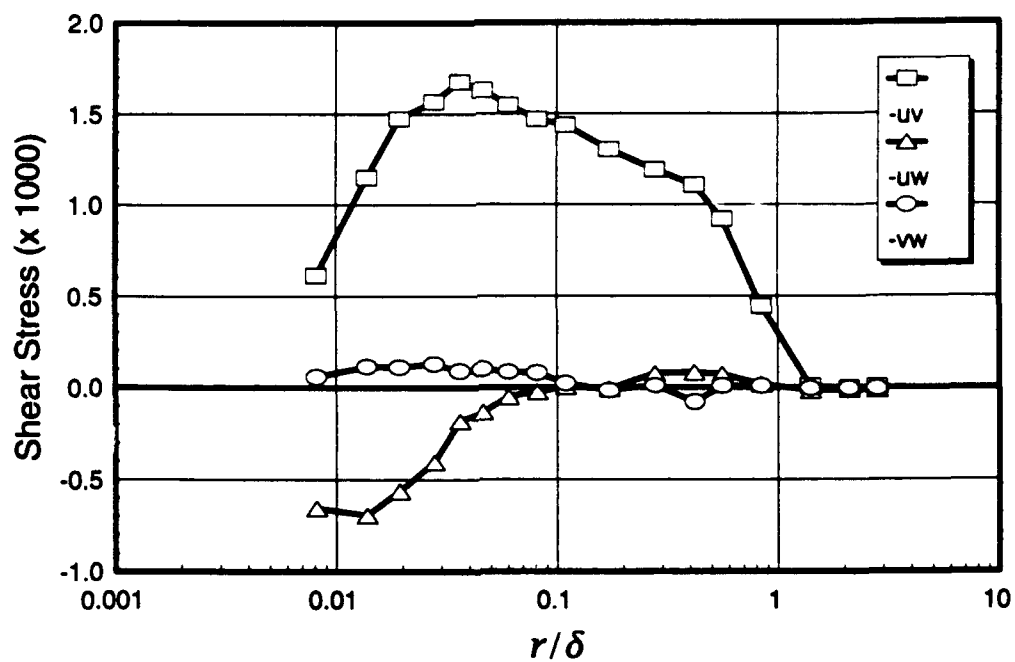


Figure 111. Boundary-layer shear-stress profiles, $x/L = 0.400$, $\phi = 150^\circ$.

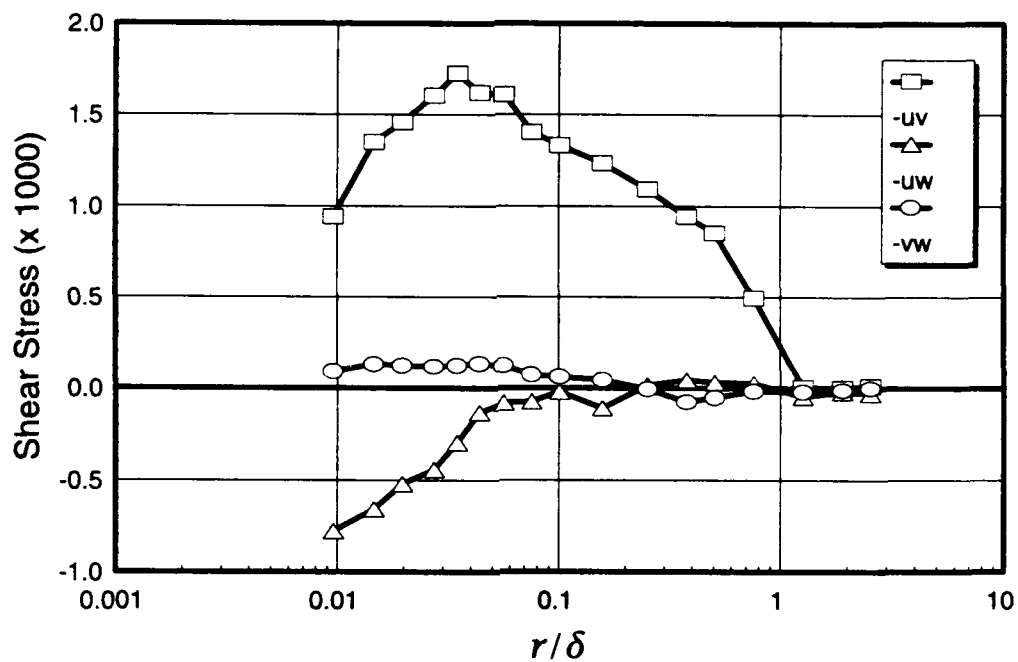


Figure 112. Boundary-layer shear-stress profiles, $x/L = 0.400$, $\phi = 160^\circ$.

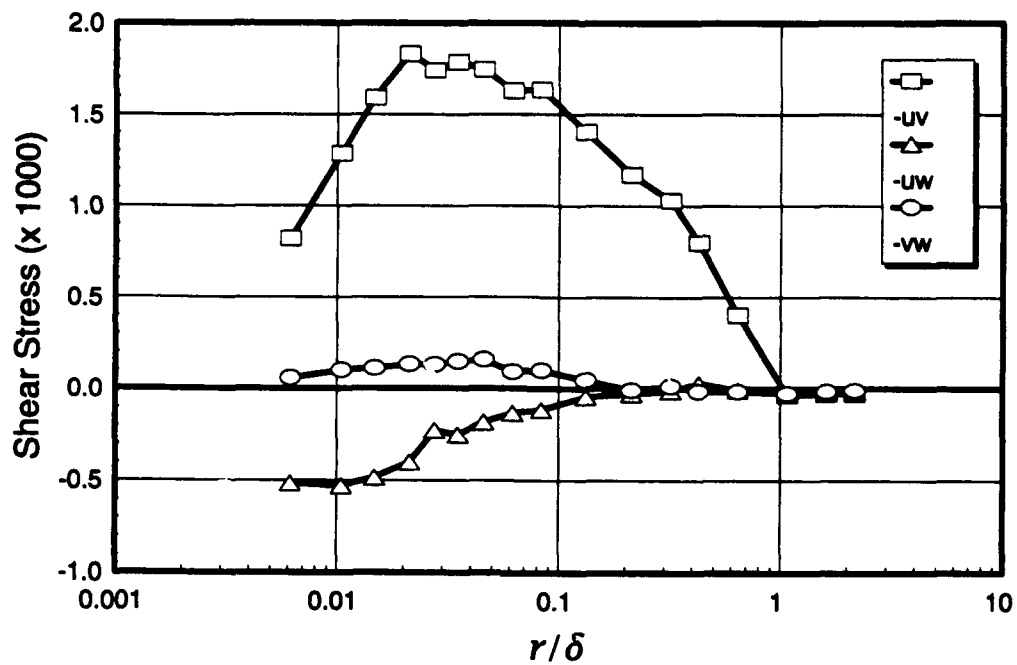


Figure 113. Boundary-layer shear-stress profiles, $x/L = 0.400$, $\phi = 170^\circ$.

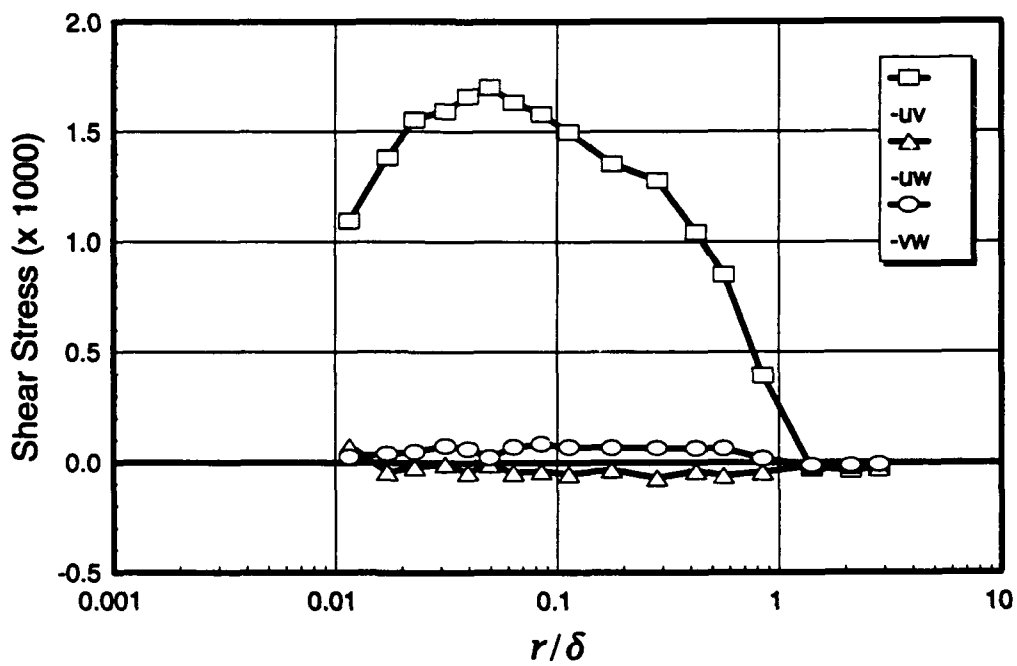


Figure 114. Boundary-layer shear-stress profiles, $x/L = 0.400$, $\phi = 180^\circ$.

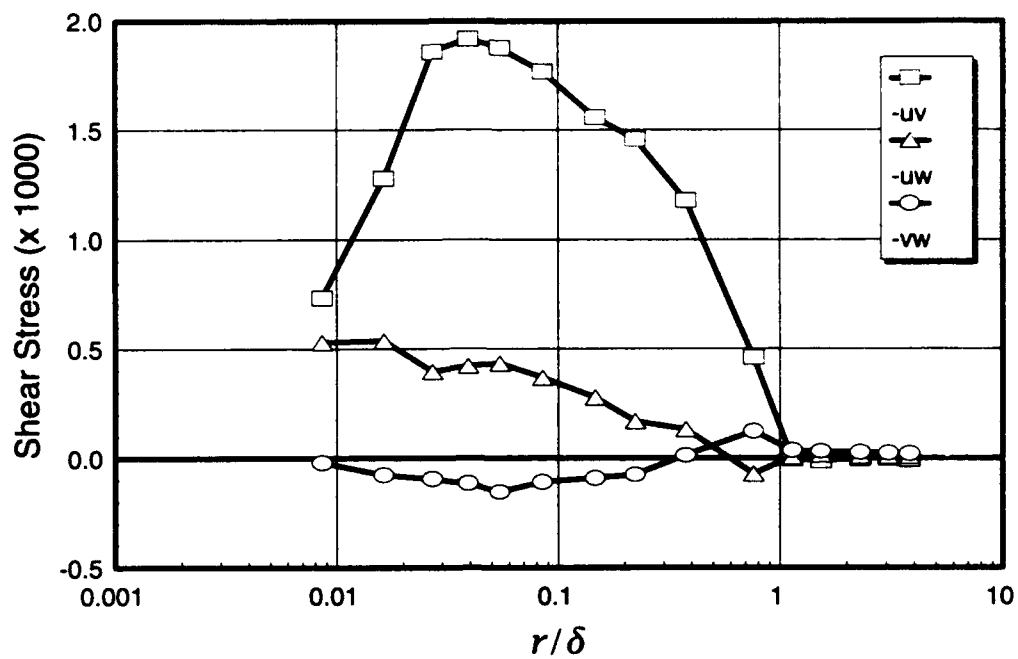


Figure 115. Boundary-layer shear-stress profiles, $x/L = 0.600$, $\phi = 90^\circ$.

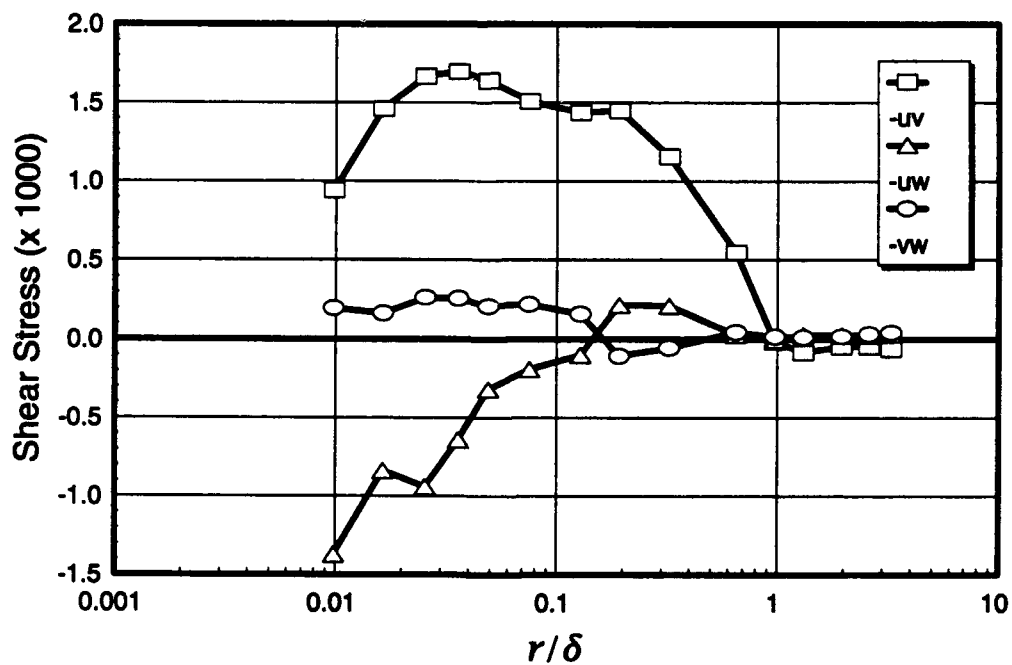


Figure 116. Boundary-layer shear-stress profiles, $x/L = 0.600$, $\phi = 100^\circ$.

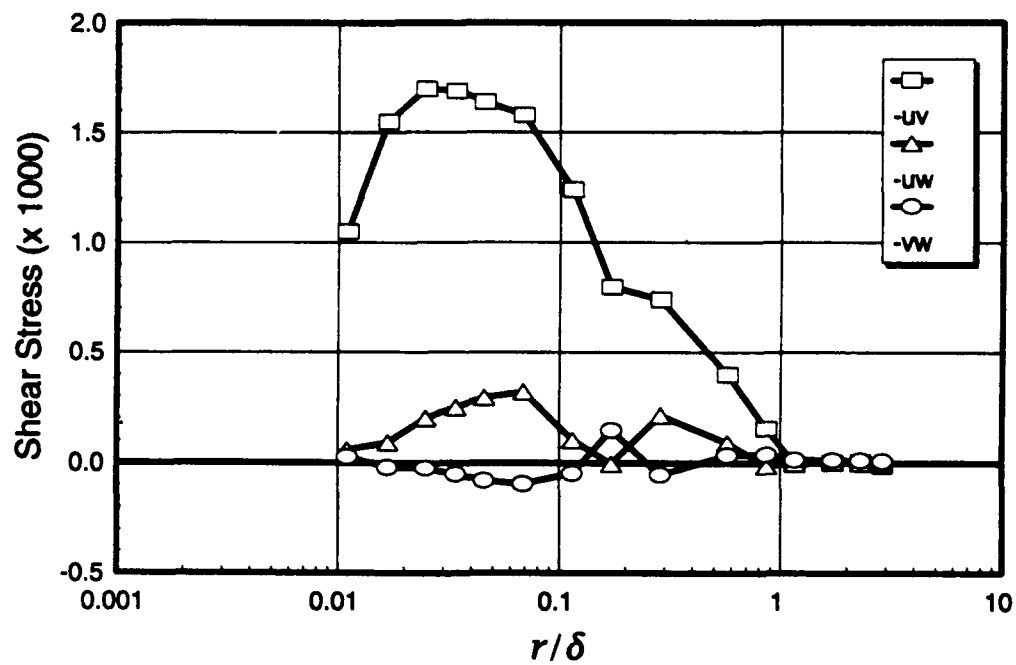


Figure 117. Boundary-layer shear-stress profiles, $x/L = 0.600$, $\phi = 110^\circ$.

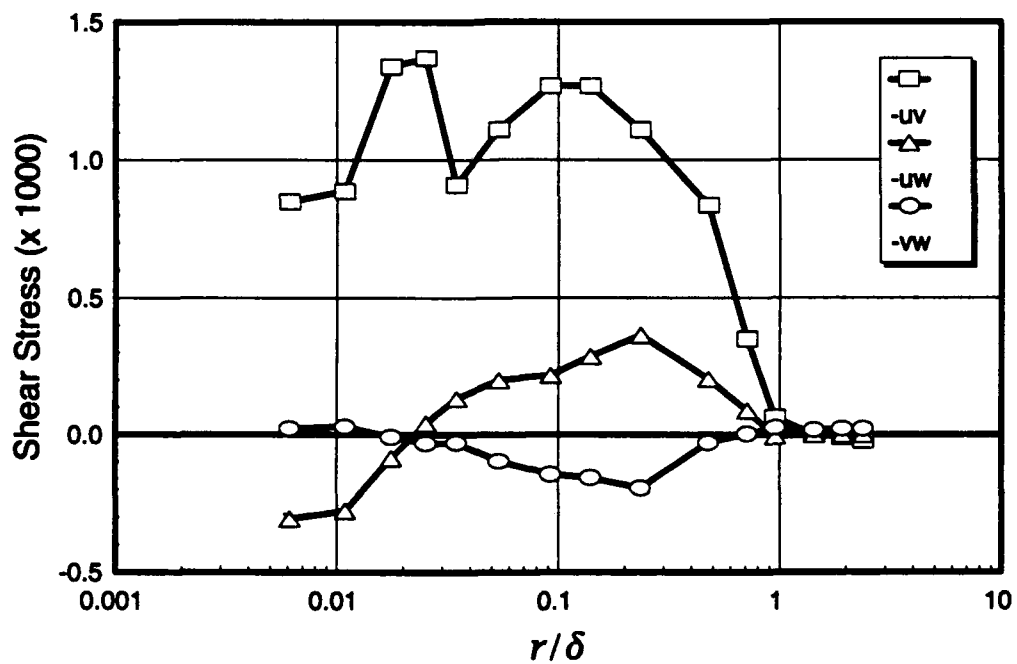


Figure 118. Boundary-layer shear-stress profiles, $x/L = 0.600$, $\phi = 120^\circ$.

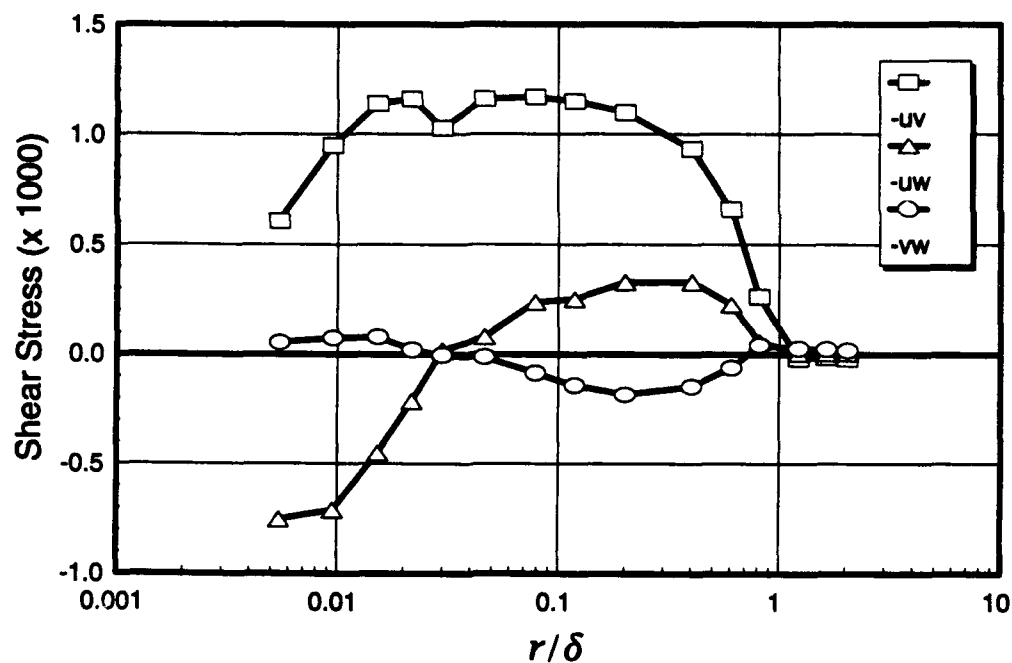


Figure 119. Boundary-layer shear-stress profiles, $x/L = 0.600$, $\phi = 130^\circ$.

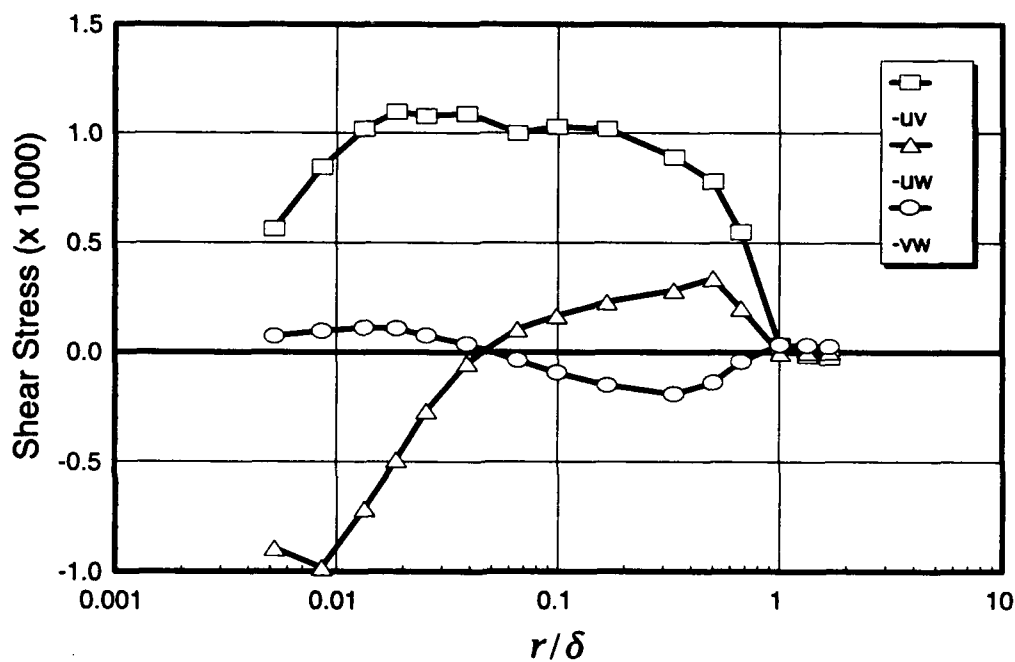


Figure 120. Boundary-layer shear-stress profiles, $x/L = 0.600$, $\phi = 140^\circ$.

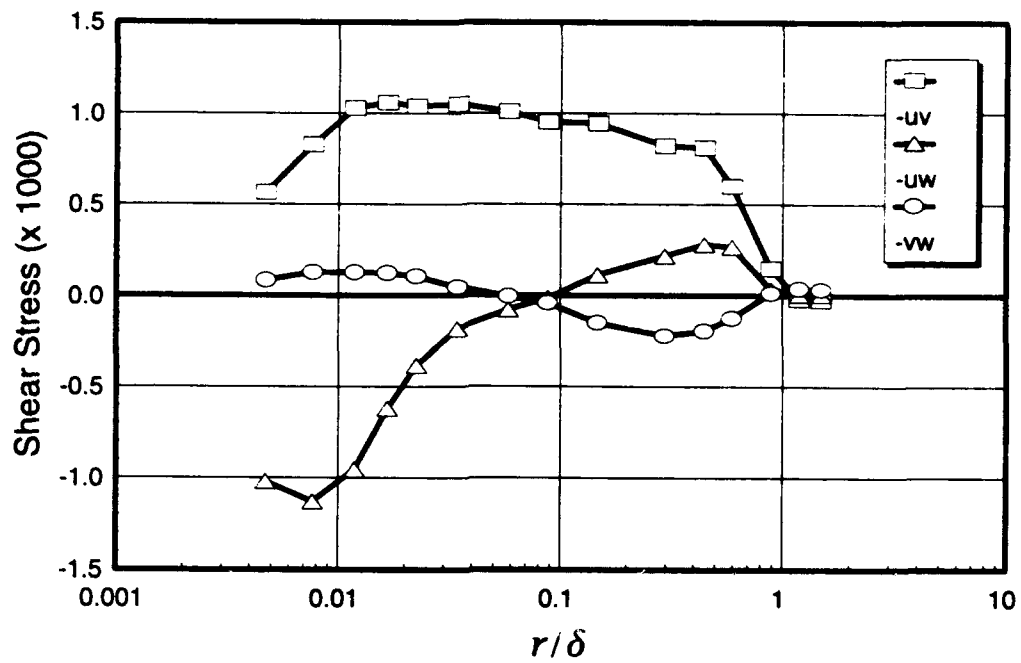


Figure 121. Boundary-layer shear-stress profiles, $x/L = 0.600$, $\phi = 150^\circ$.

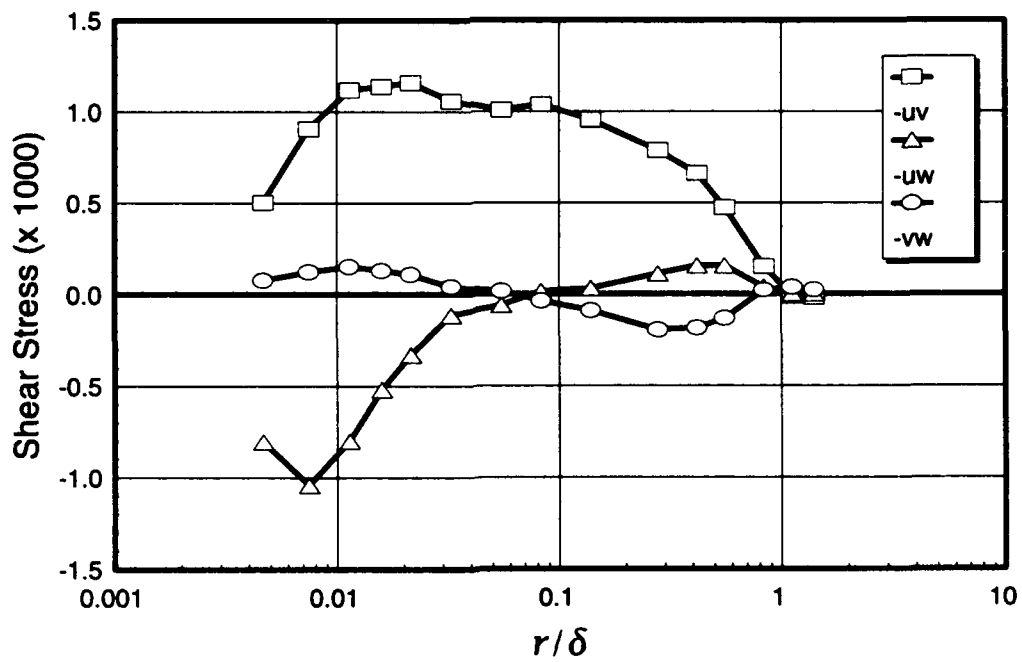


Figure 122. Boundary-layer shear-stress profiles, $x/L = 0.600$, $\phi = 160^\circ$.

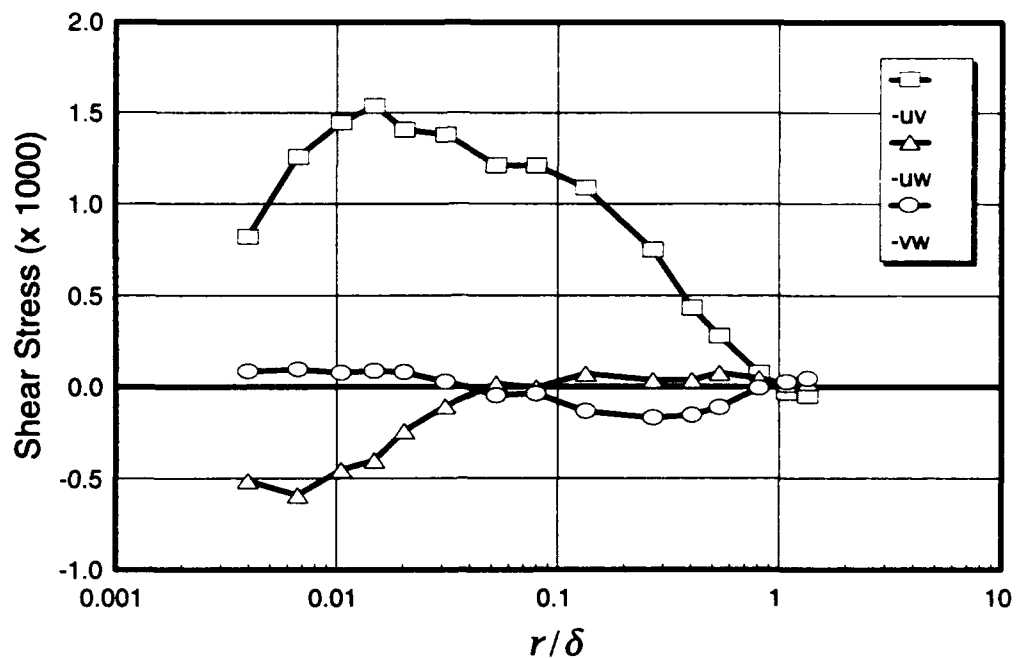


Figure 123. Boundary-layer shear-stress profiles, $x/L = 0.600$, $\phi = 170^\circ$.

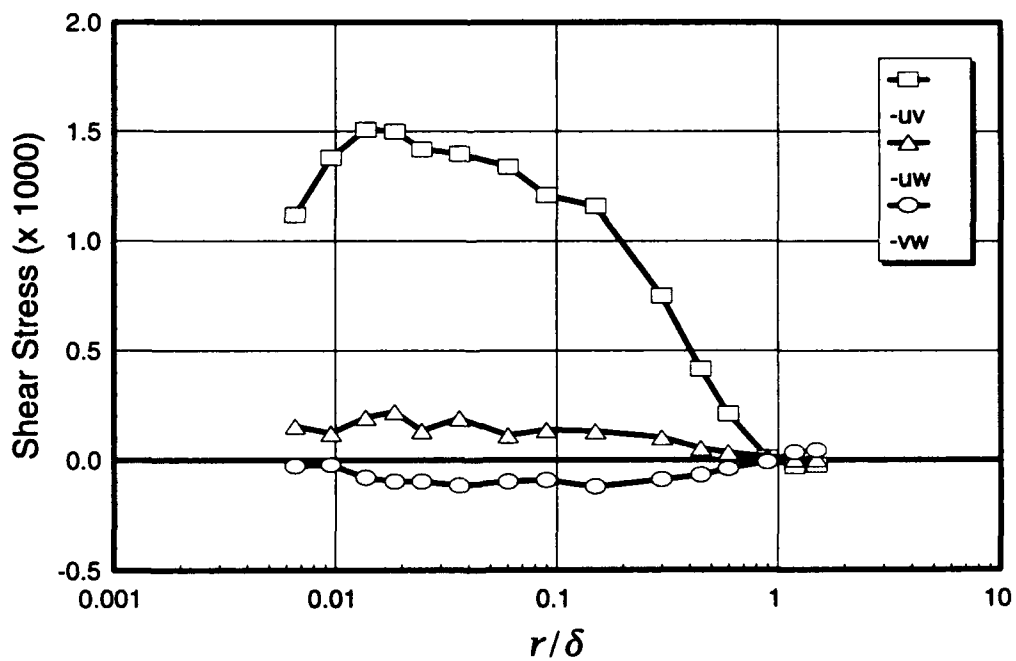


Figure 124. Boundary-layer shear-stress profiles, $x/L = 0.600$, $\phi = 180^\circ$.

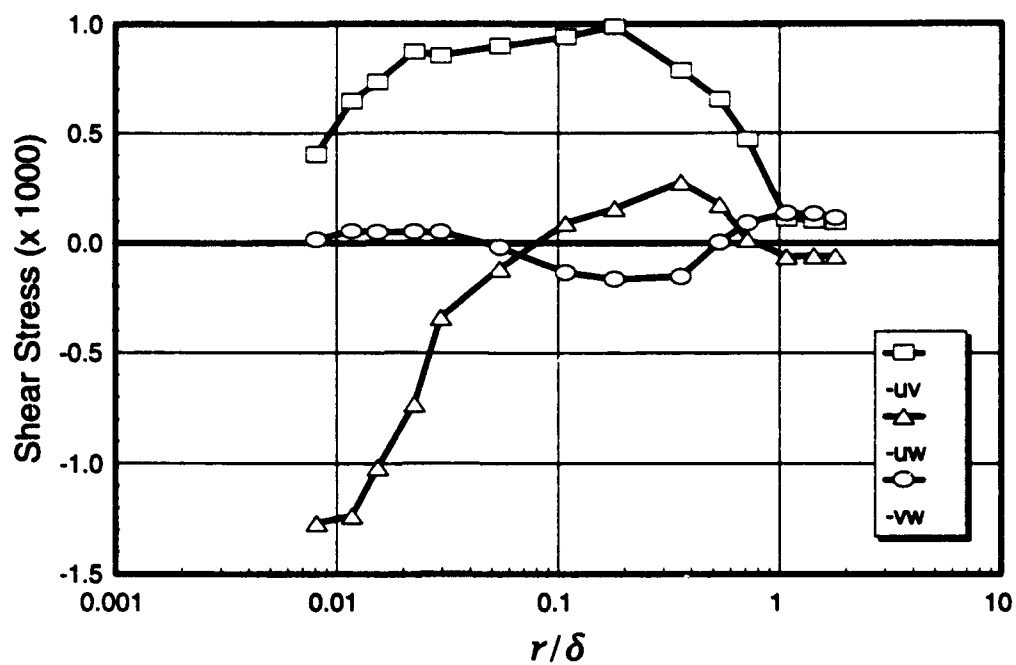


Figure 125. Boundary-layer shear-stress profiles, $x/L = 0.752$, $\phi = 120^\circ$.

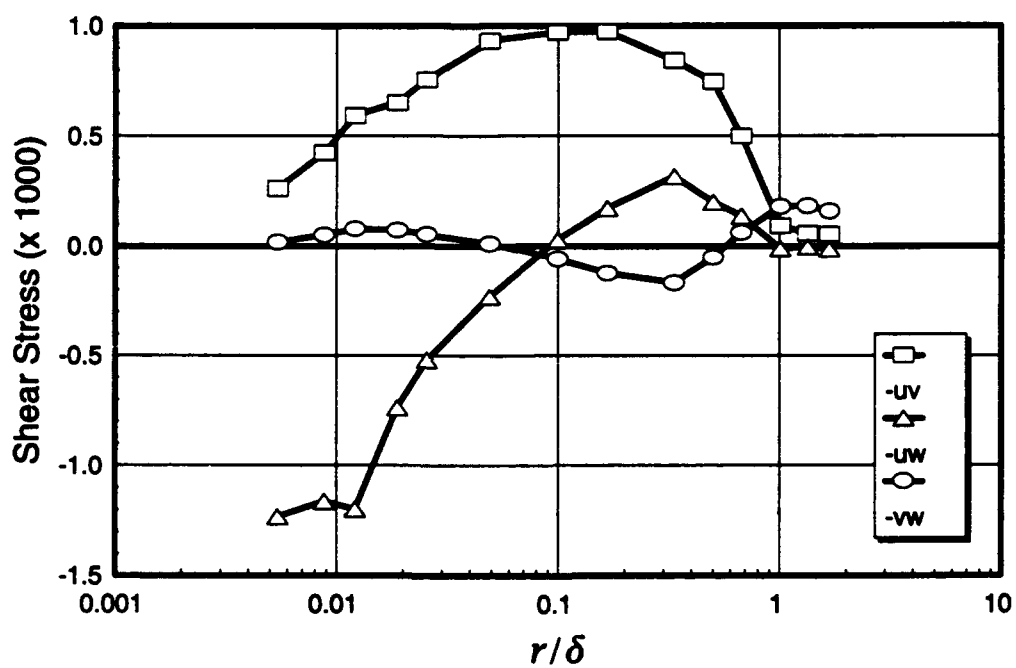


Figure 126. Boundary-layer shear-stress profiles, $x/L = 0.752$, $\phi = 123^\circ$.

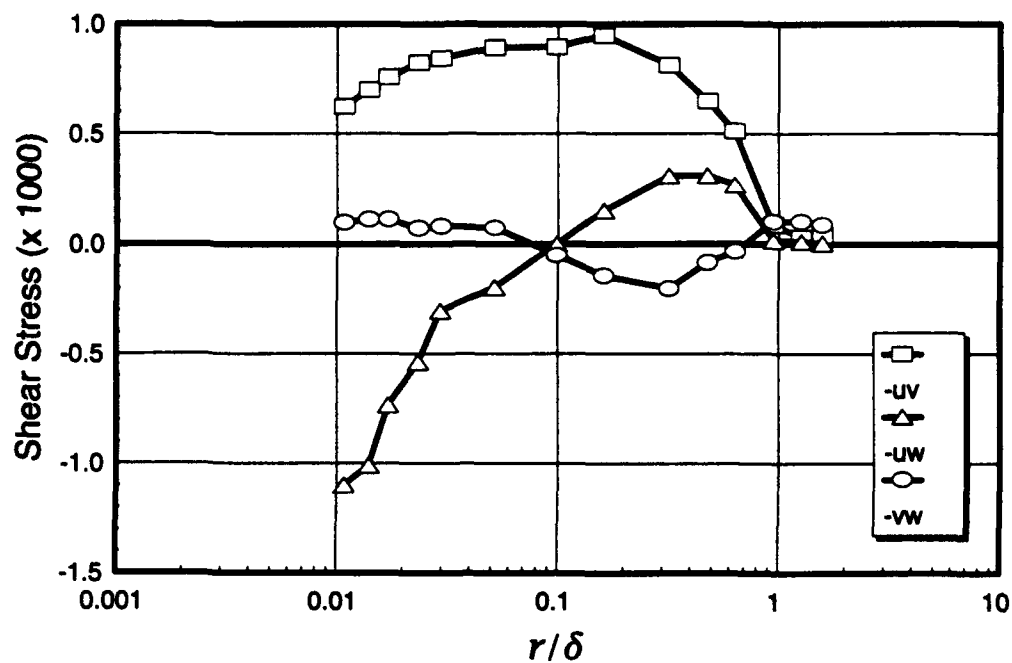


Figure 127. Boundary-layer shear-stress profiles, $x/L = 0.752$, $\phi = 125^\circ$.

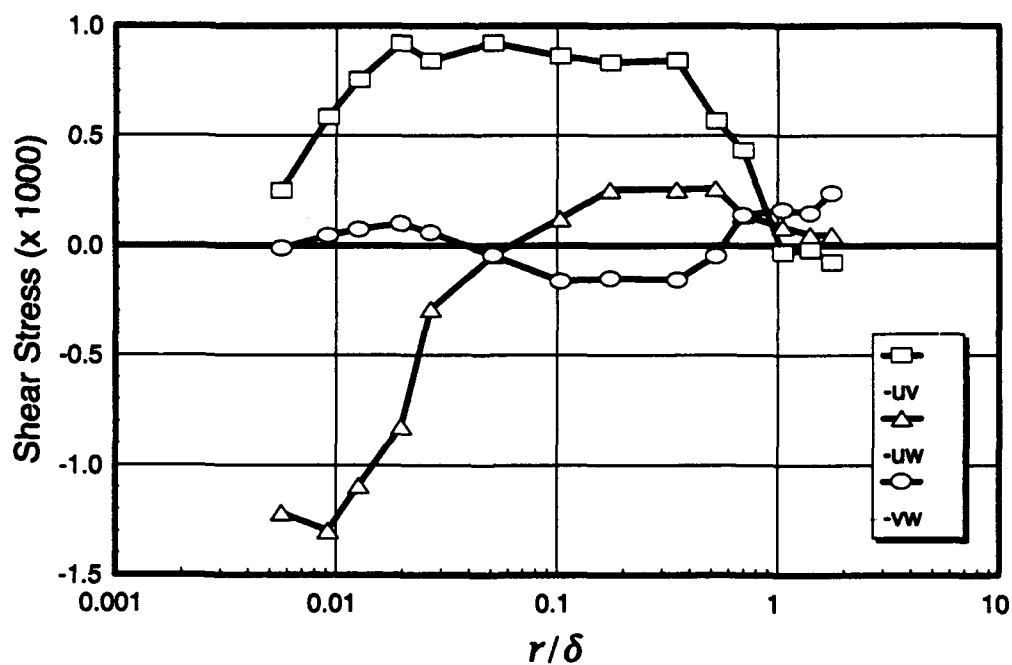


Figure 128. Boundary-layer shear-stress profiles, $x/L = 0.762$, $\phi = 120^\circ$.

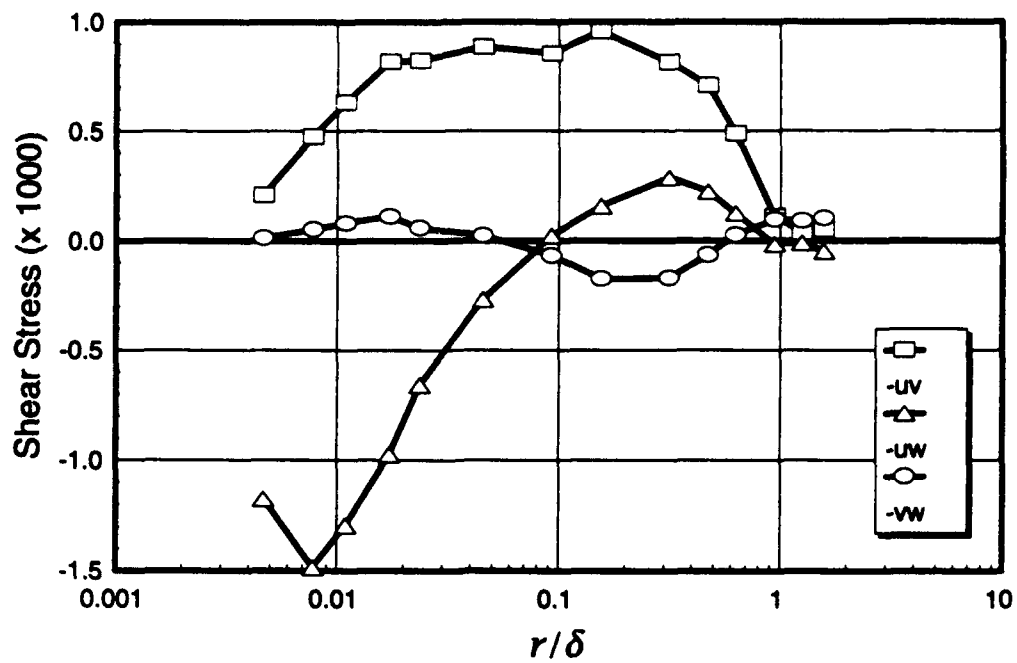


Figure 129. Boundary-layer shear-stress profiles, $x/L = 0.762$, $\phi = 123^\circ$.

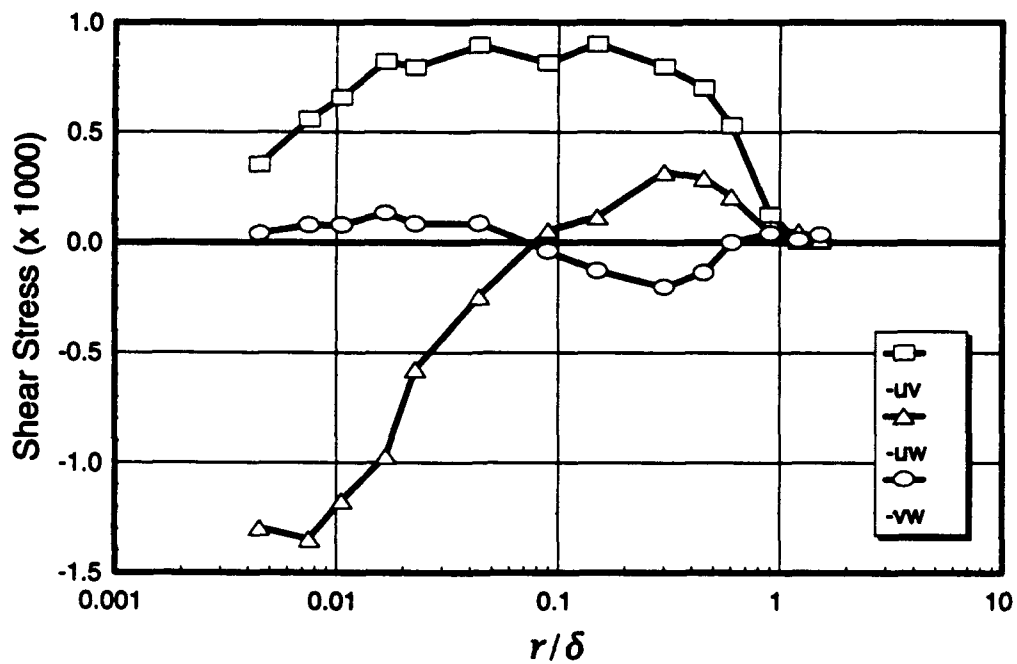


Figure 130. Boundary-layer shear-stress profiles, $x/L = 0.762$, $\phi = 125^\circ$.

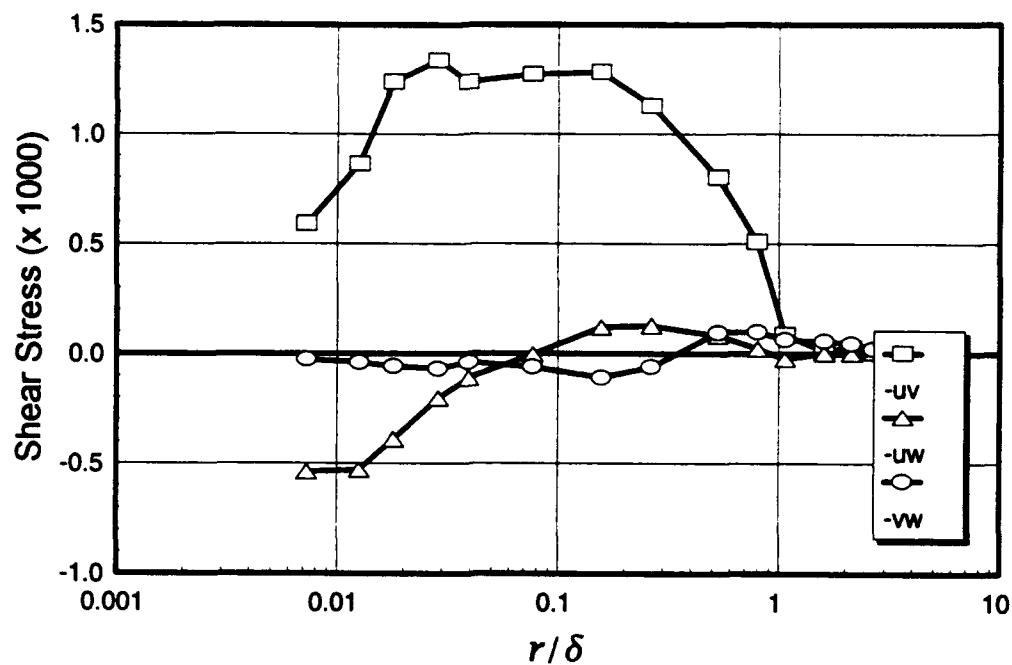


Figure 131. Boundary-layer shear-stress profiles, $x/L = 0.772$, $\phi = 105^\circ$.

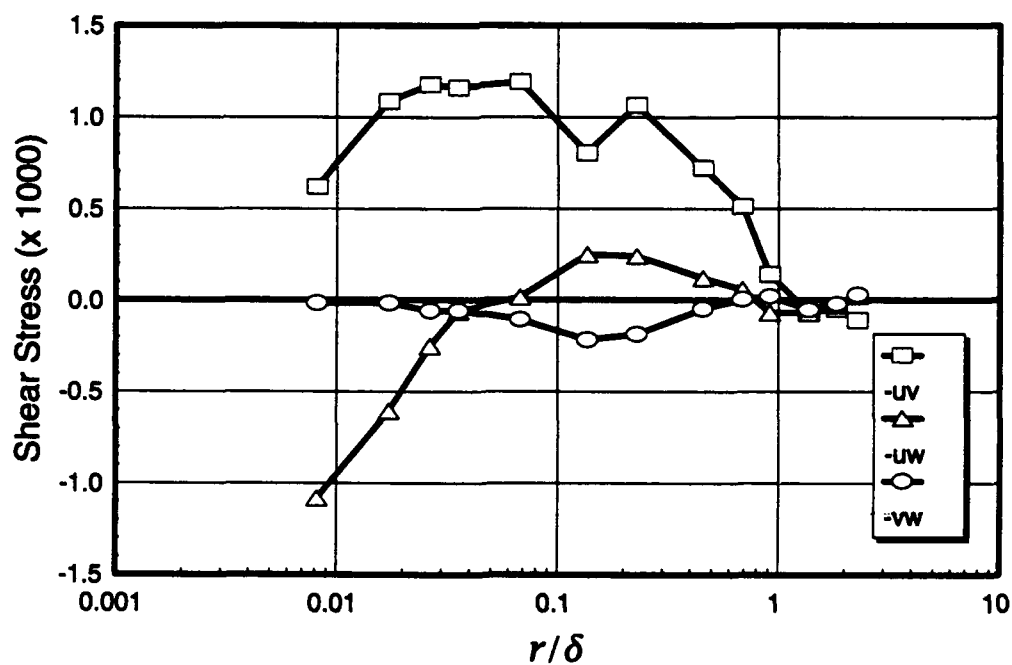


Figure 132. Boundary-layer shear-stress profiles, $x/L = 0.772$, $\phi = 110^\circ$.

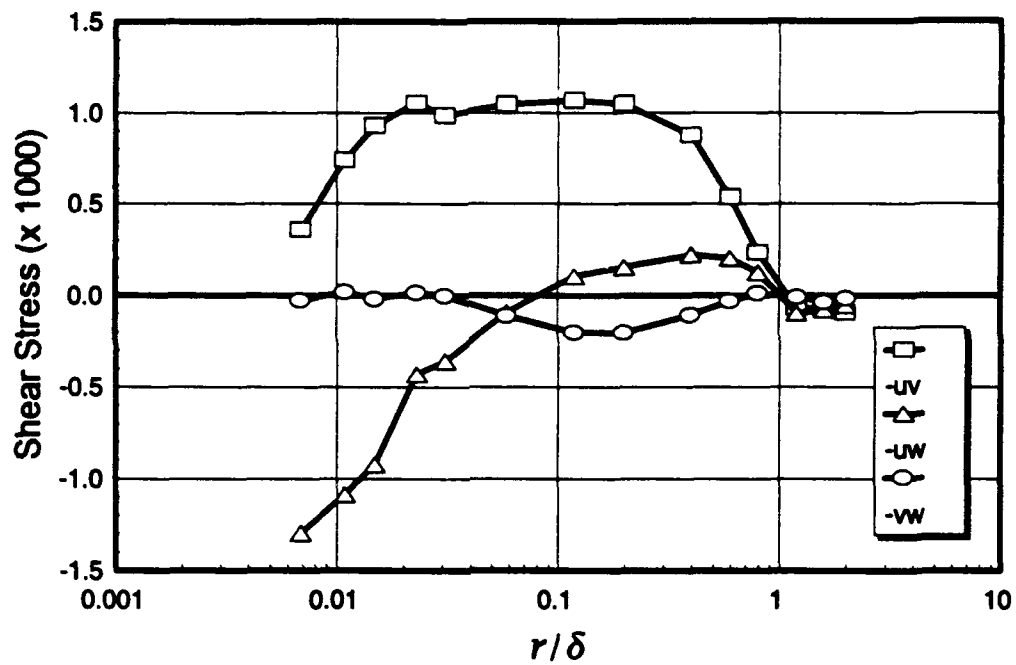


Figure 133. Boundary-layer shear-stress profiles, $x/L = 0.772$, $\phi = 115^\circ$.

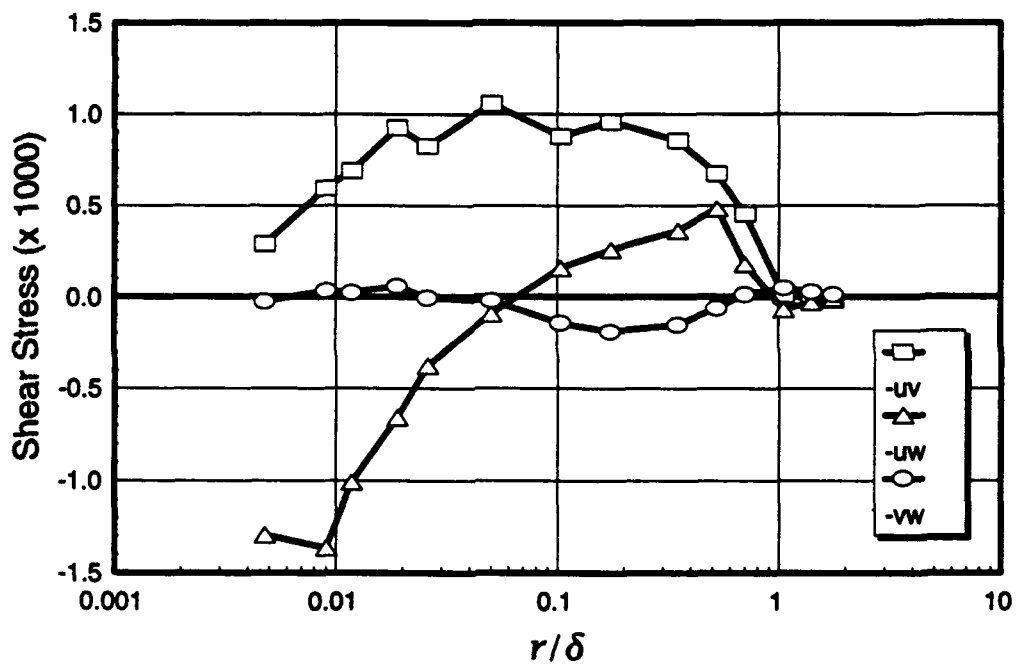


Figure 134. Boundary-layer shear-stress profiles, $x/L = 0.772$, $\phi = 120^\circ$.

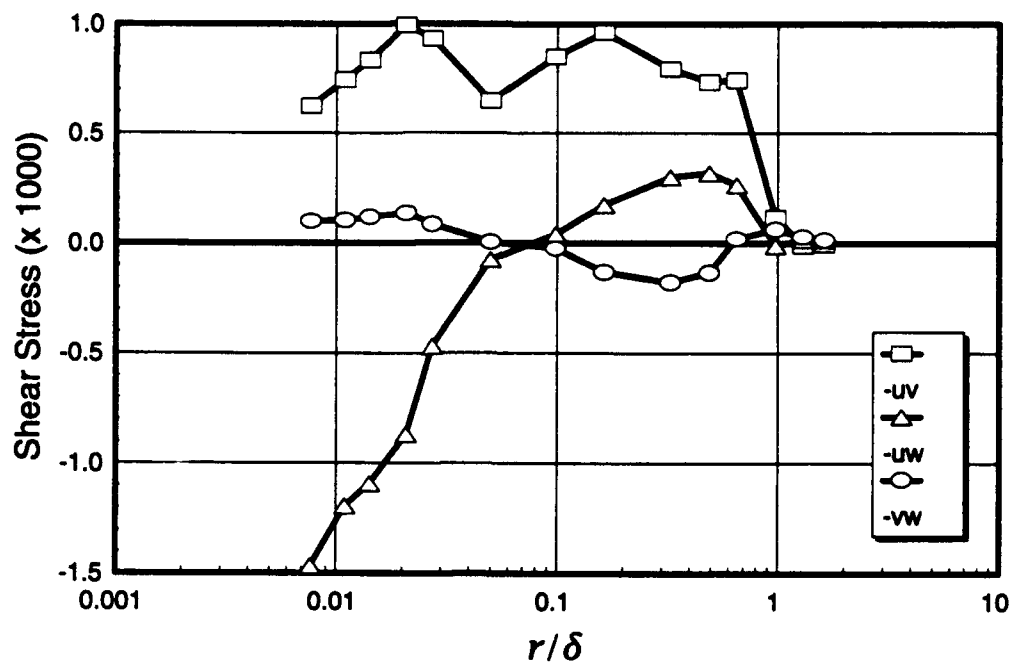


Figure 135. Boundary-layer shear-stress profiles, $x/L = 0.772$, $\phi = 123^\circ$.

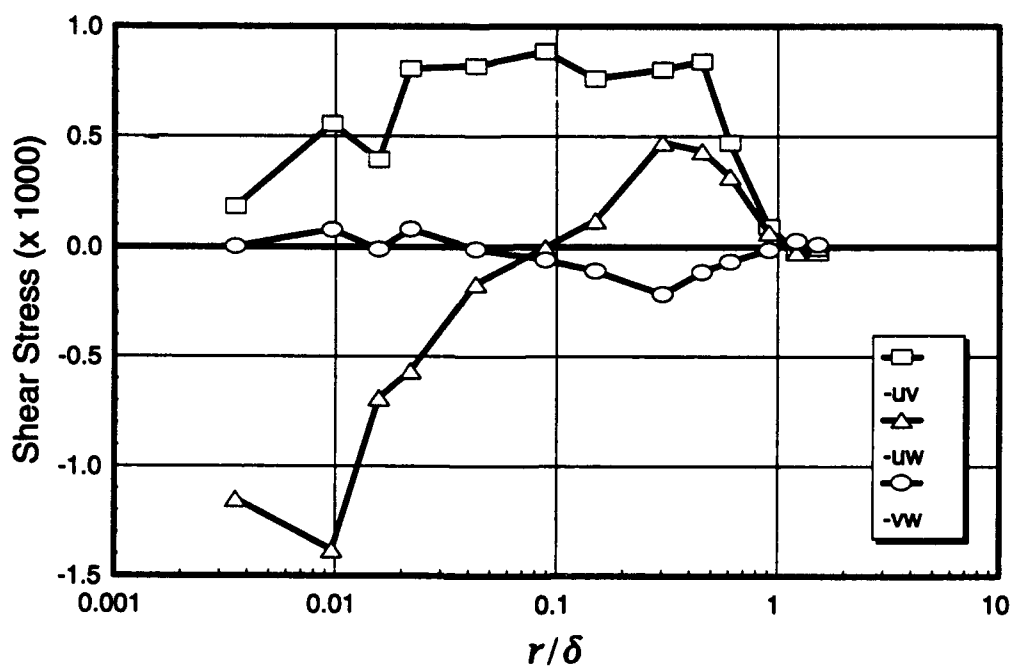


Figure 136. Boundary-layer shear-stress profiles, $x/L = 0.772$, $\phi = 125^\circ$.

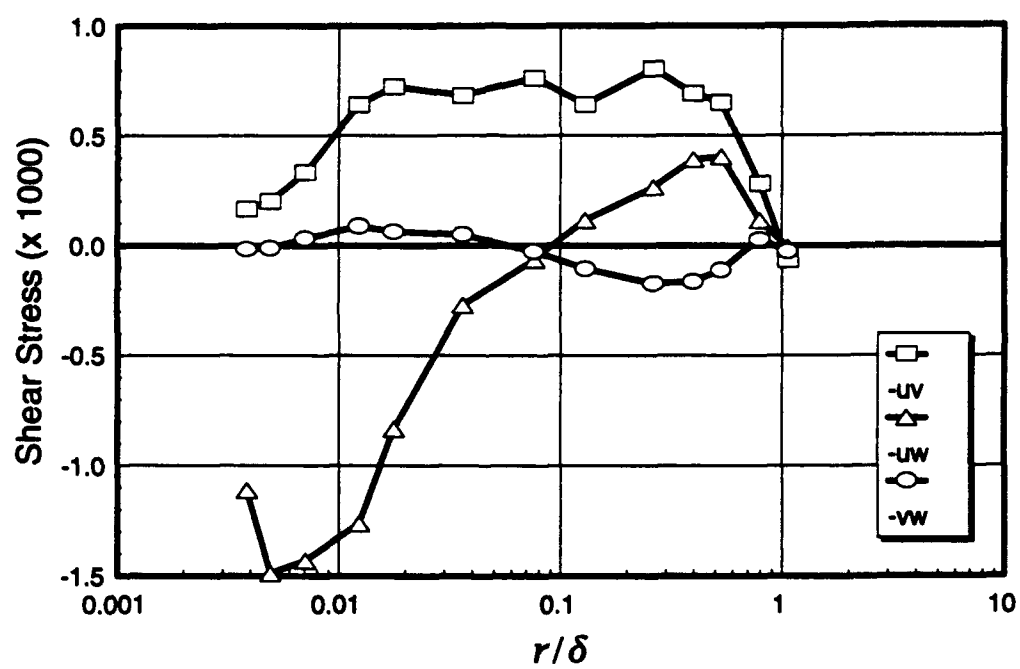


Figure 137. Boundary-layer shear-stress profiles, $x/L = 0.772$, $\phi = 130^\circ$.

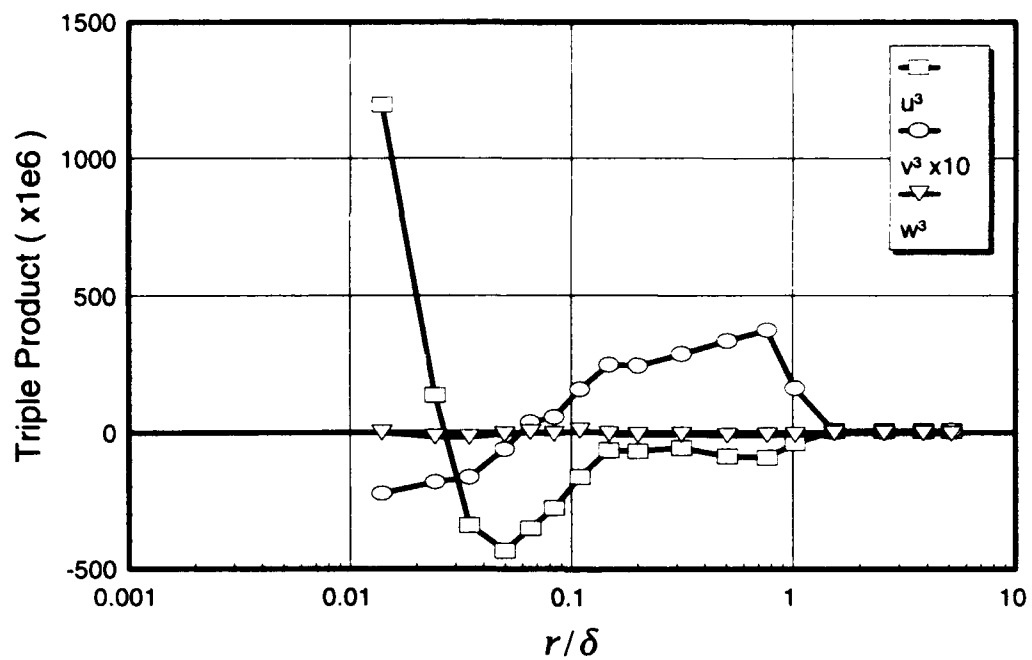


Figure 138. Boundary-layer profiles of velocity third moments, $x/L = 0.400$, $\phi = 90^\circ$.

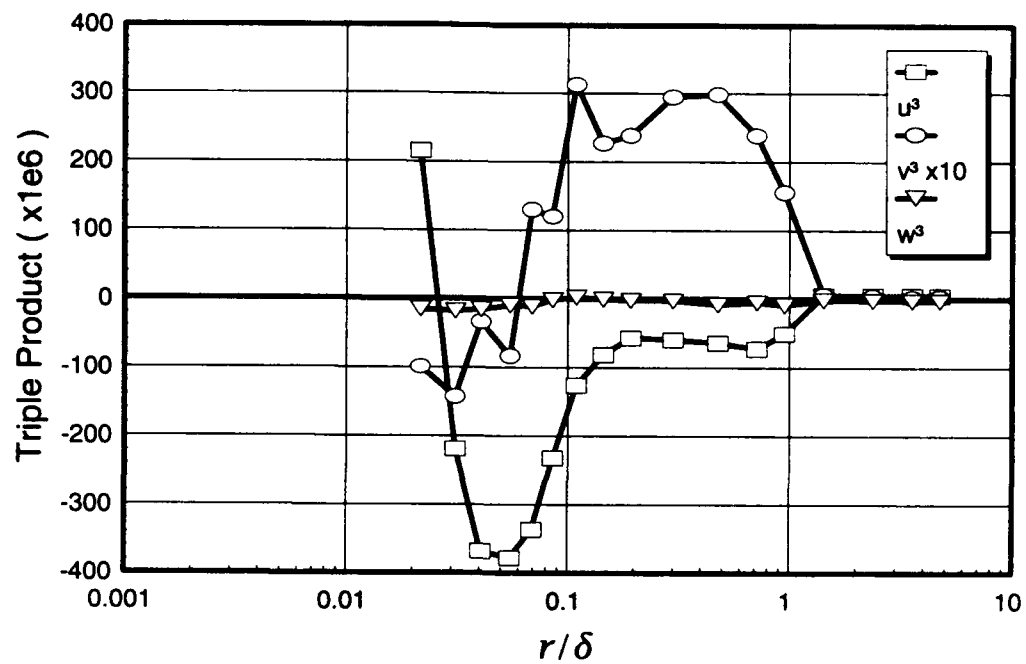


Figure 139. Boundary-layer profiles of velocity third moments, $x/L = 0.400$, $\phi = 100^\circ$.

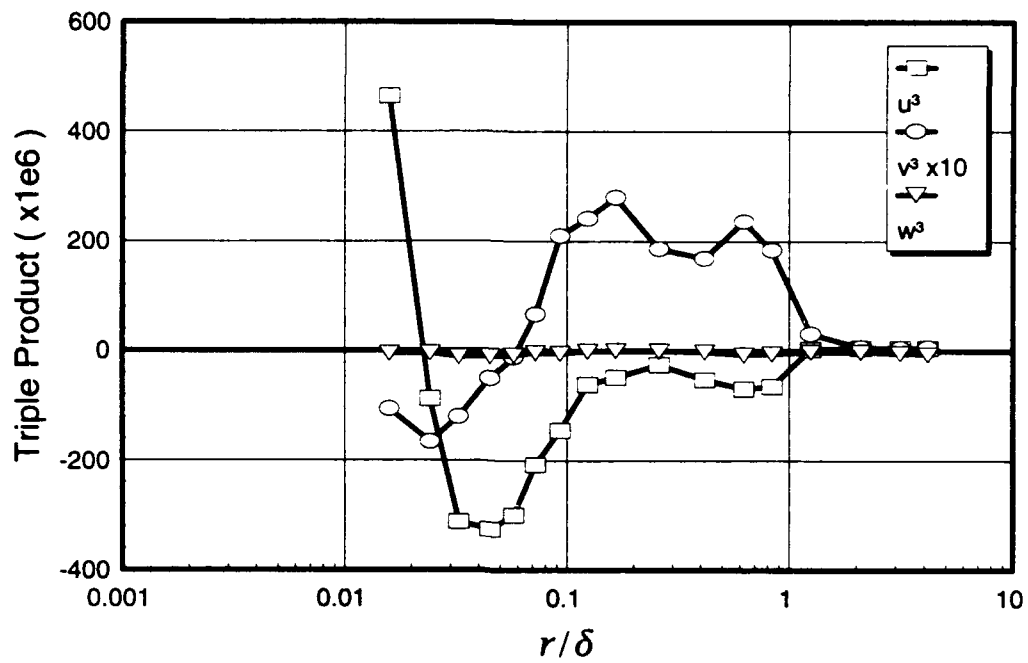


Figure 140. Boundary-layer profiles of velocity third moments, $x/L = 0.400$, $\phi = 110^\circ$.

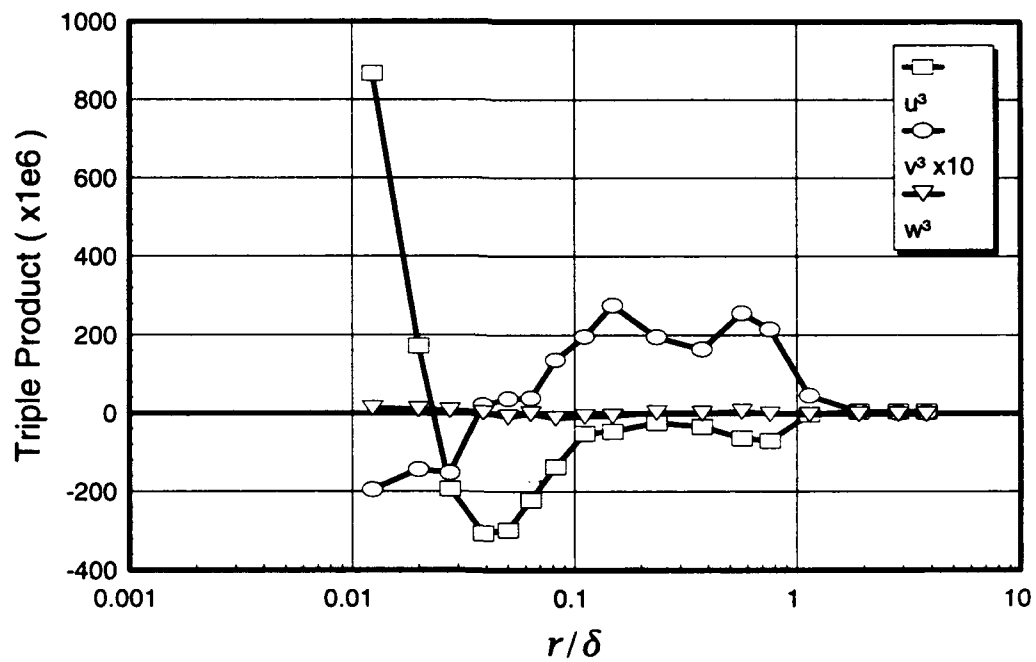


Figure 141. Boundary-layer profiles of velocity third moments, $x/L = 0.400$, $\phi = 120^\circ$.

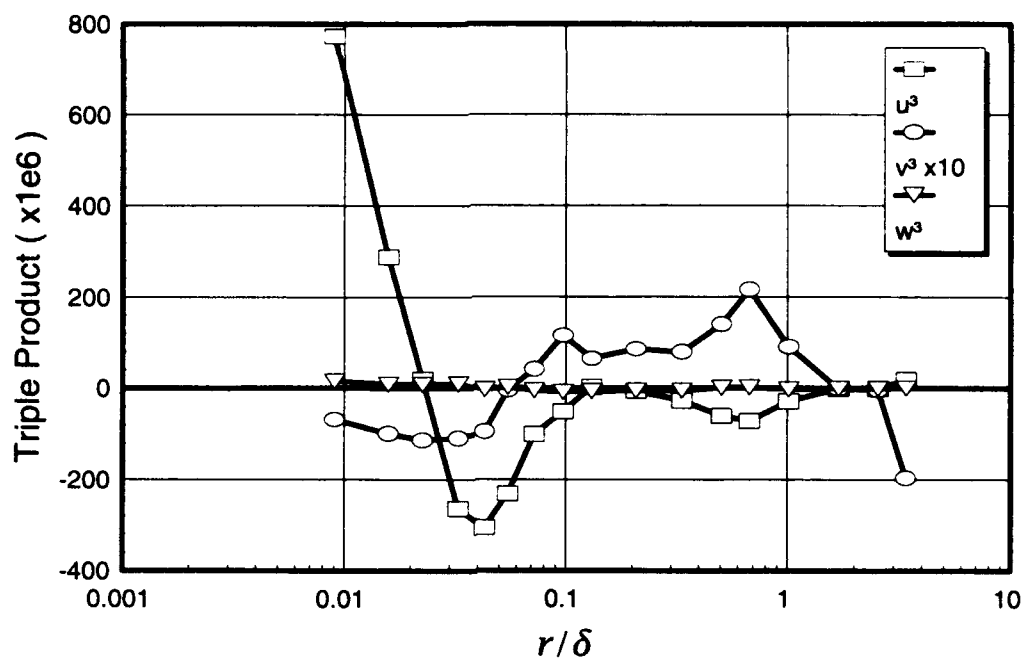


Figure 142. Boundary-layer profiles of velocity third moments, $x/L = 0.400$, $\phi = 130^\circ$.

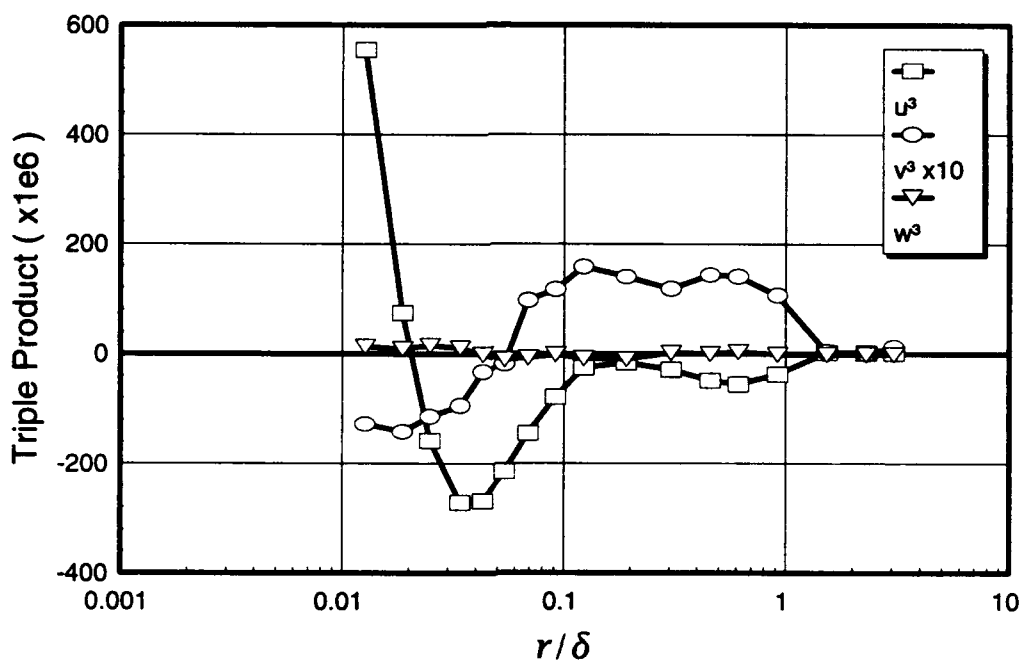


Figure 143. Boundary-layer profiles of velocity third moments, $x/L = 0.400$, $\phi = 140^\circ$.

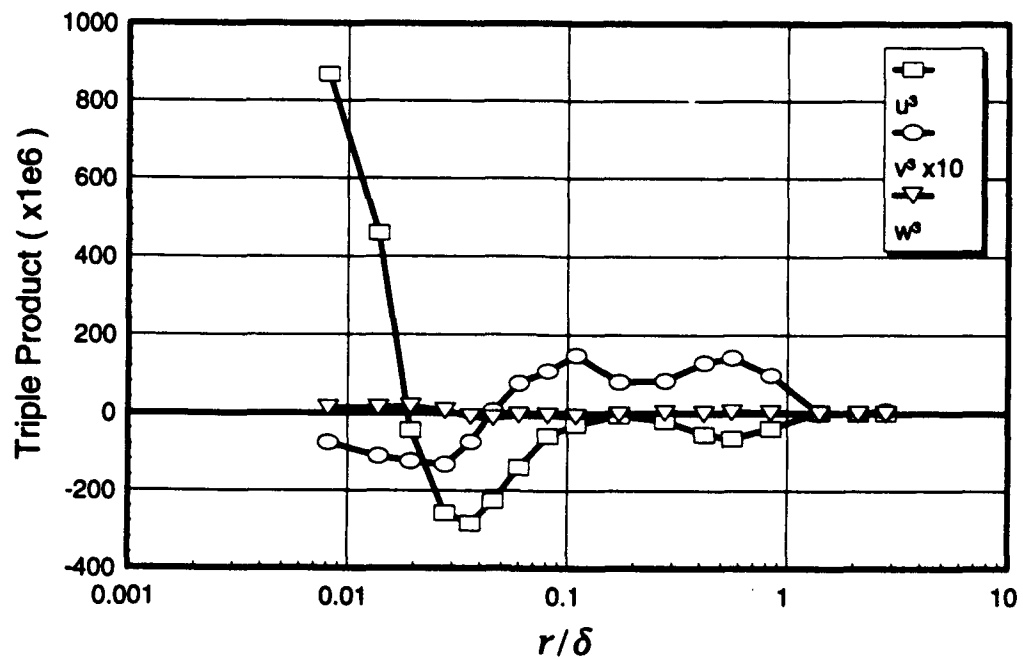


Figure 144. Boundary-layer profiles of velocity third moments, $x/L = 0.400$, $\phi = 150^\circ$.

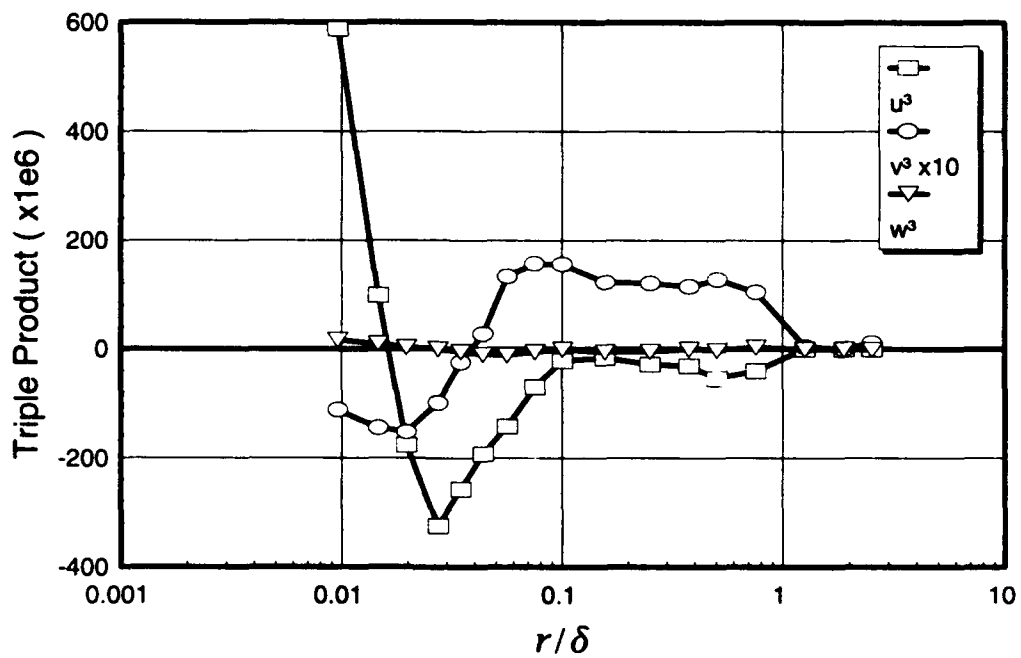


Figure 145. Boundary-layer profiles of velocity third moments, $x/L = 0.400$, $\phi = 160^\circ$.

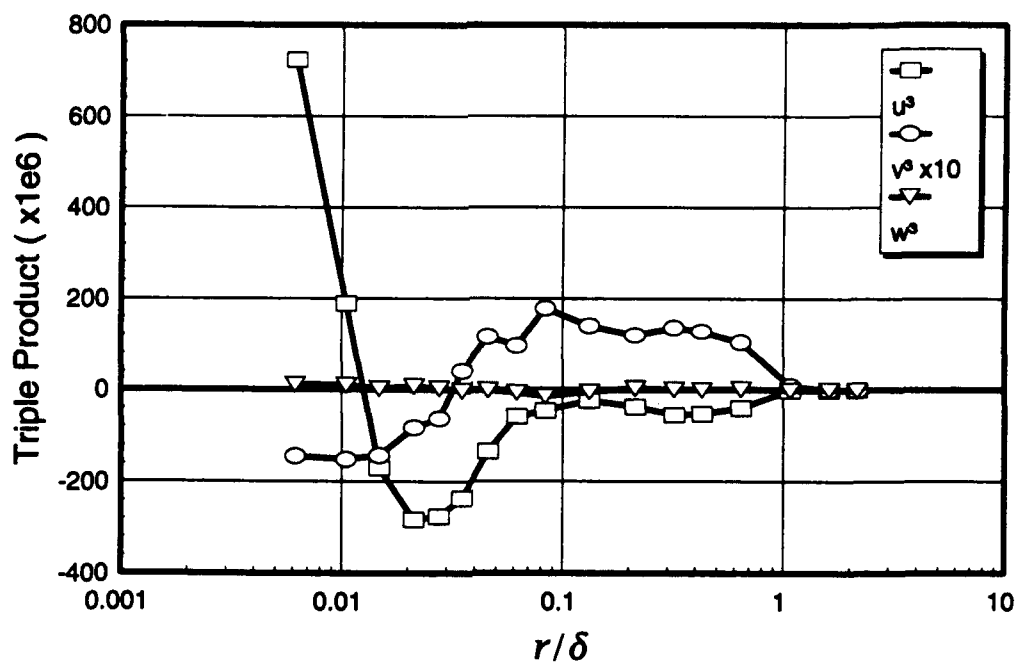


Figure 146. Boundary-layer profiles of velocity third moments, $x/L = 0.400$, $\phi = 170^\circ$.

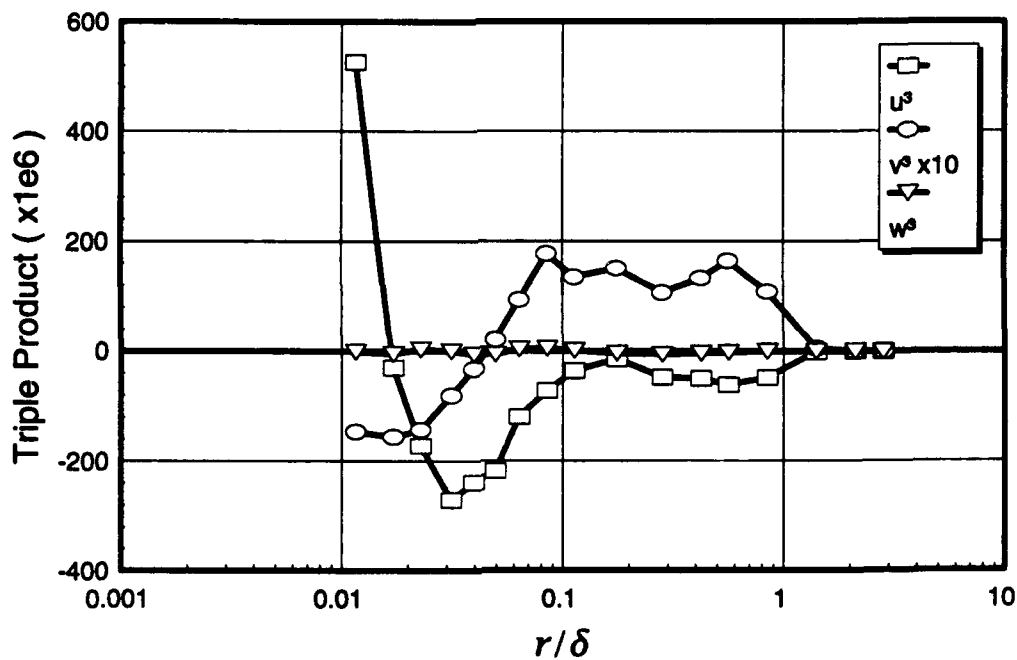


Figure 147. Boundary-layer profiles of velocity third moments, $x/L = 0.400$, $\phi = 180^\circ$.

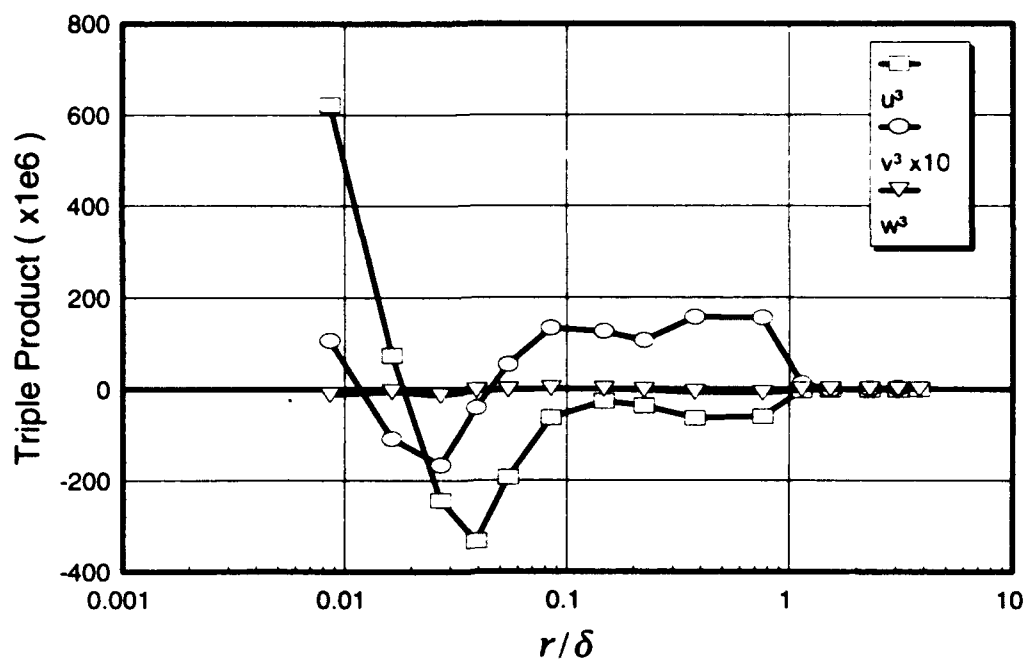


Figure 148. Boundary-layer profiles of velocity third moments, $x/L = 0.600$, $\phi = 90^\circ$.

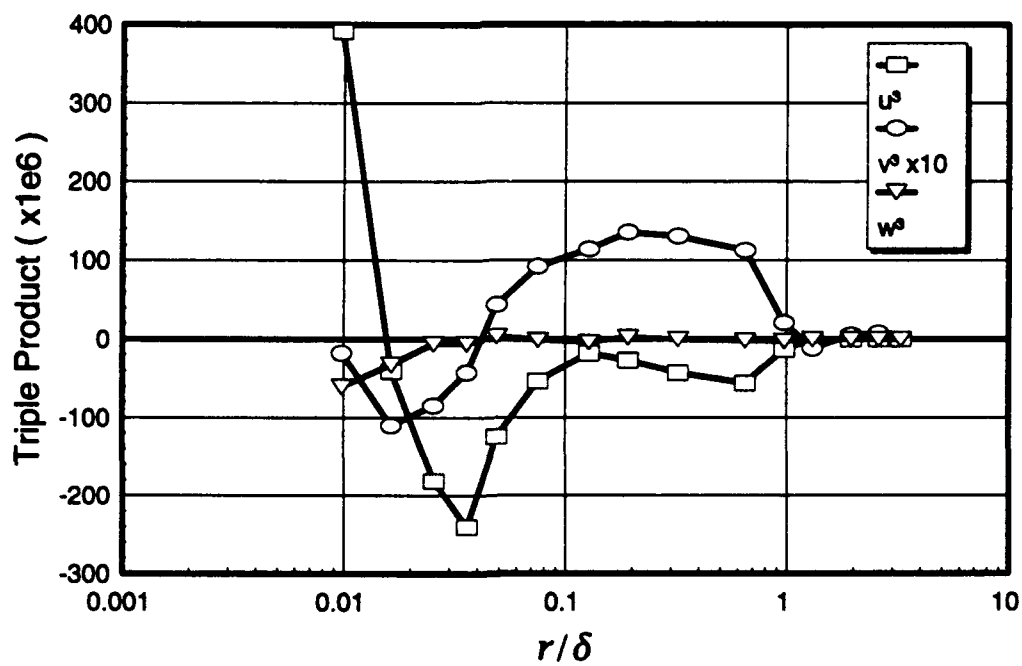


Figure 149. Boundary-layer profiles of velocity third moments, $x/L = 0.600$, $\phi = 100^\circ$.

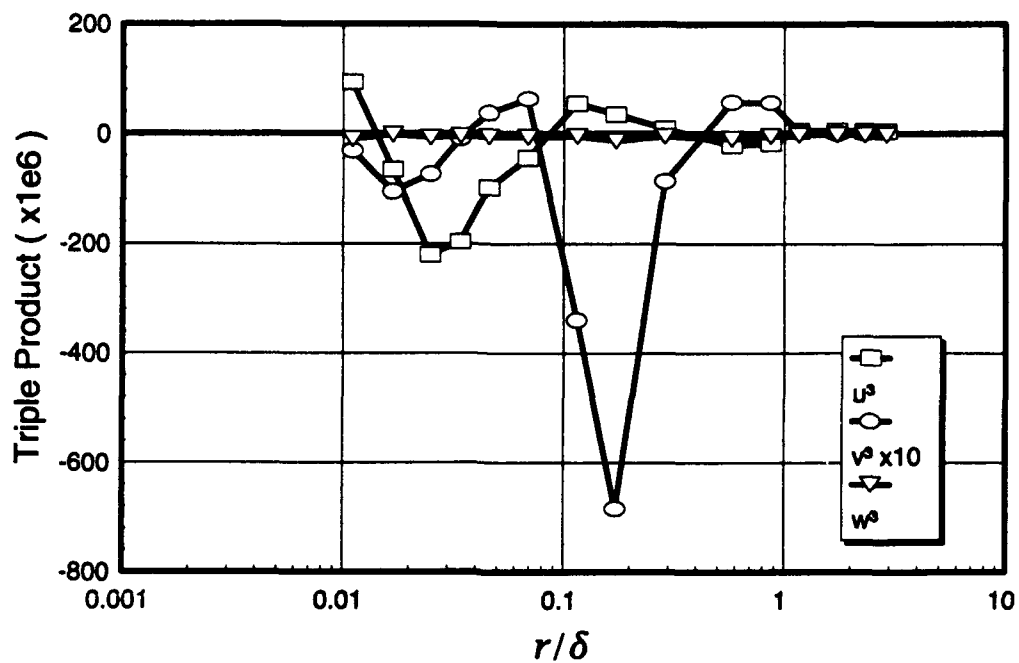


Figure 150. Boundary-layer profiles of velocity third moments, $x/L = 0.600$, $\phi = 110^\circ$.

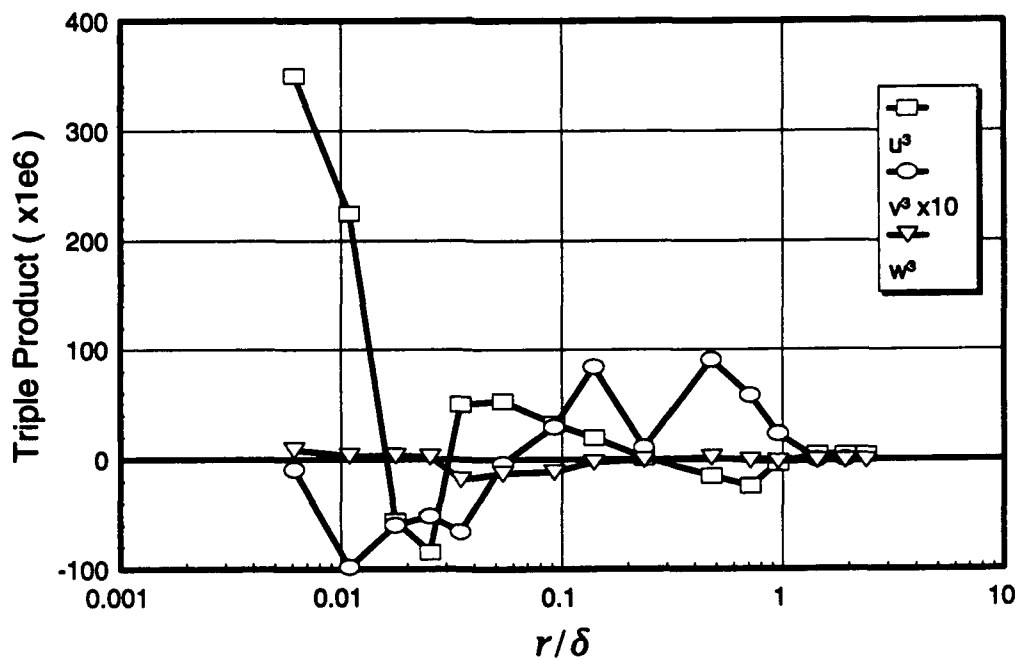


Figure 151. Boundary-layer profiles of velocity third moments, $x/L = 0.600$, $\phi = 120^\circ$.

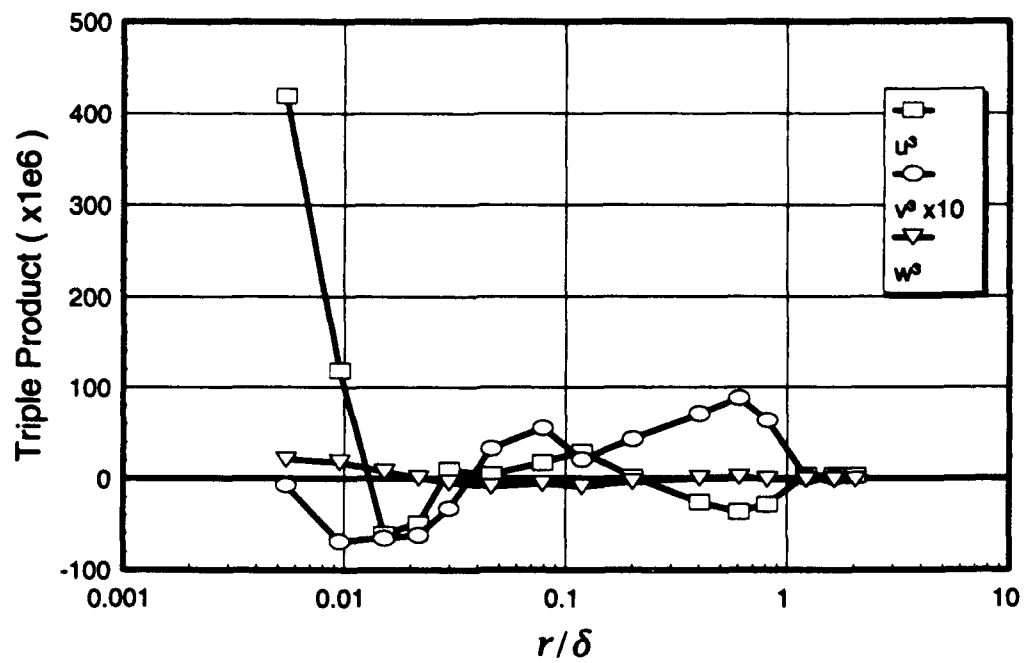


Figure 152. Boundary-layer profiles of velocity third moments, $x/L = 0.600$, $\phi = 130^\circ$.

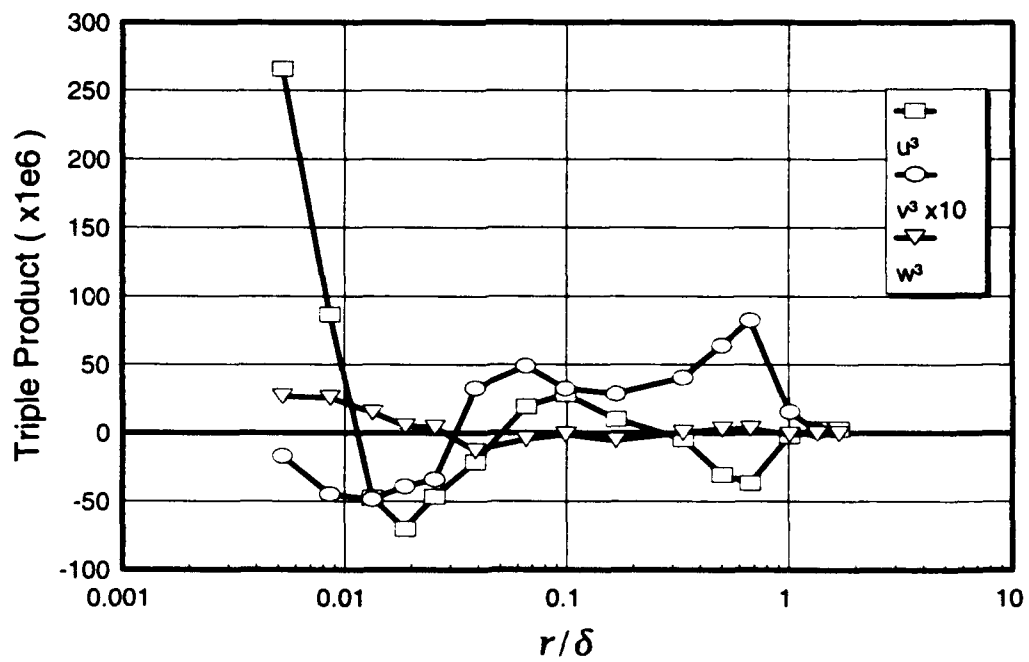


Figure 153. Boundary-layer profiles of velocity third moments, $x/L = 0.600$, $\phi = 140^\circ$.

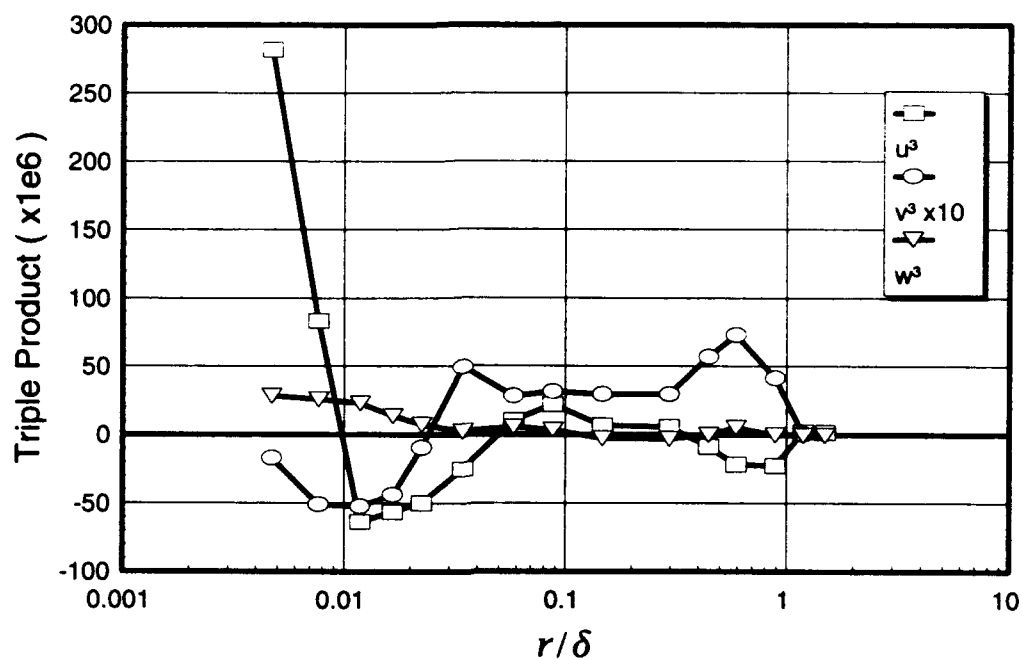


Figure 154. Boundary-layer profiles of velocity third moments, $x/L = 0.600$, $\phi = 150^\circ$.

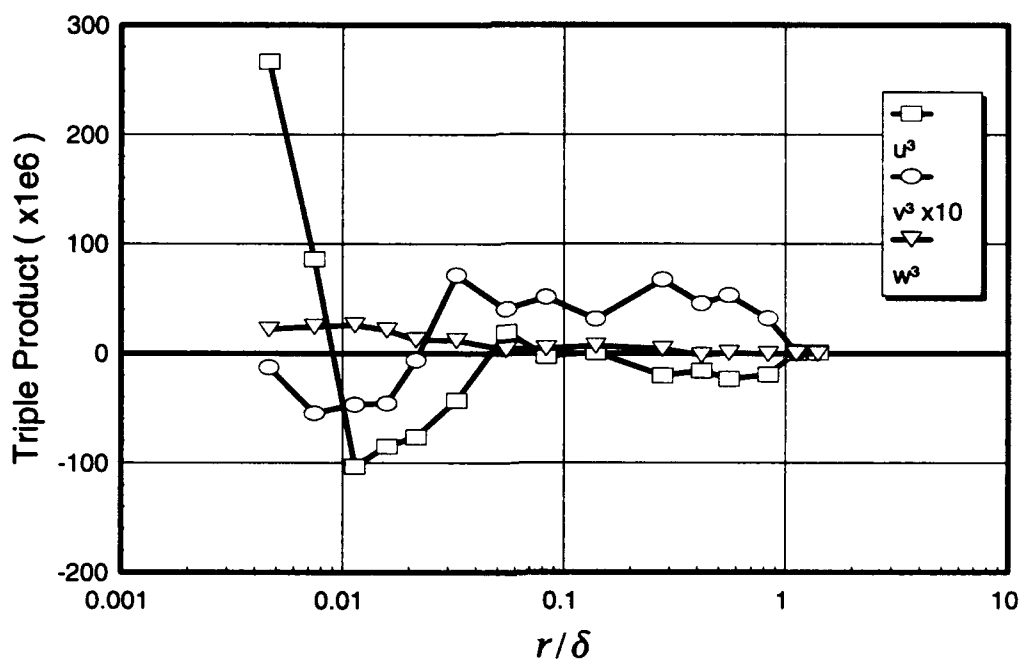


Figure 155. Boundary-layer profiles of velocity third moments, $x/L = 0.600$, $\phi = 160^\circ$.

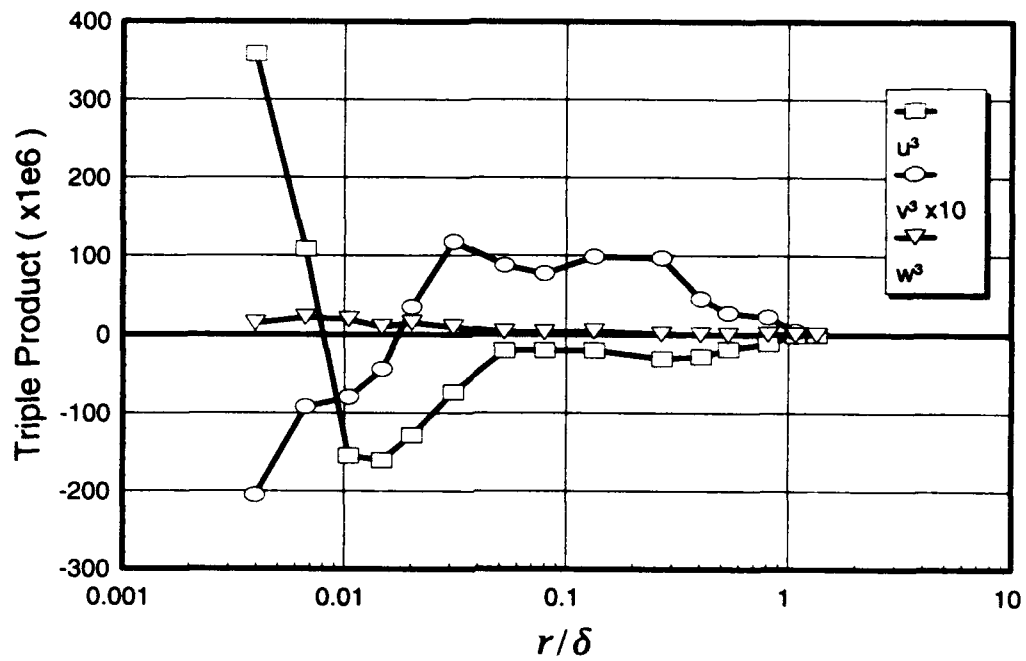


Figure 156. Boundary-layer profiles of velocity third moments, $x/L = 0.600$, $\phi = 170^\circ$.

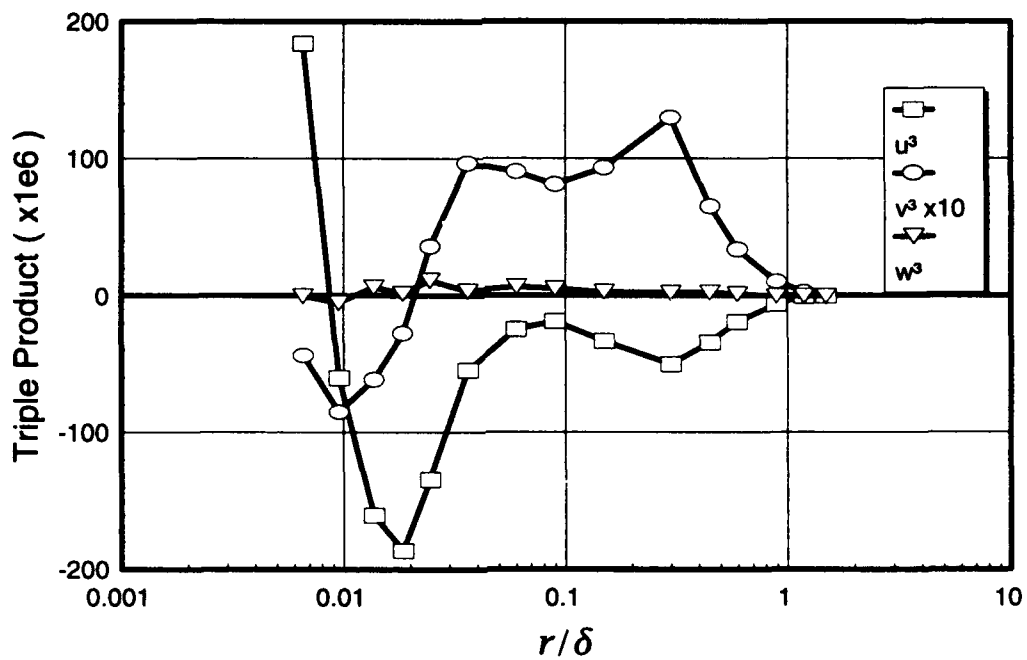


Figure 157. Boundary-layer profiles of velocity third moments, $x/L = 0.600$, $\phi = 180^\circ$.

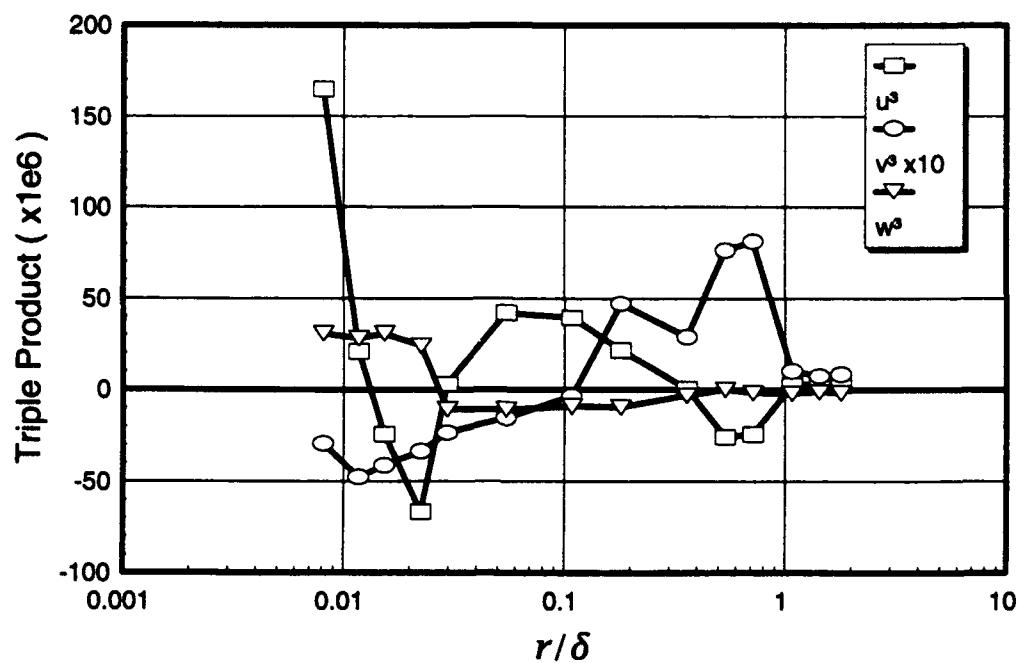


Figure 158. Boundary-layer profiles of velocity third moments, $x/L = 0.752$, $\phi = 120^\circ$.

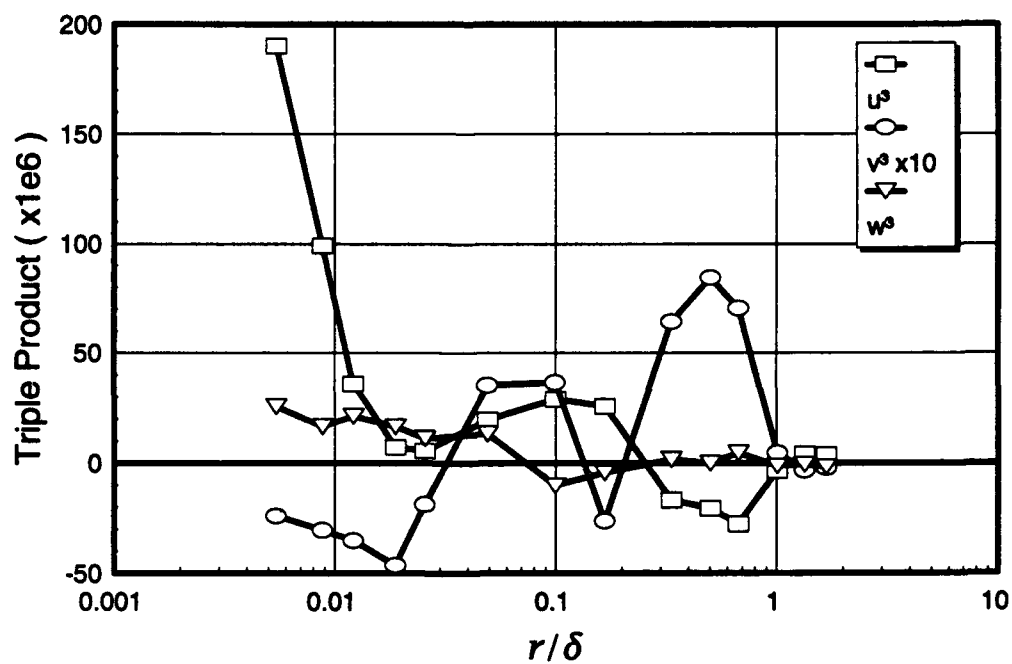


Figure 159. Boundary-layer profiles of velocity third moments, $x/L = 0.752$, $\phi = 123^\circ$.

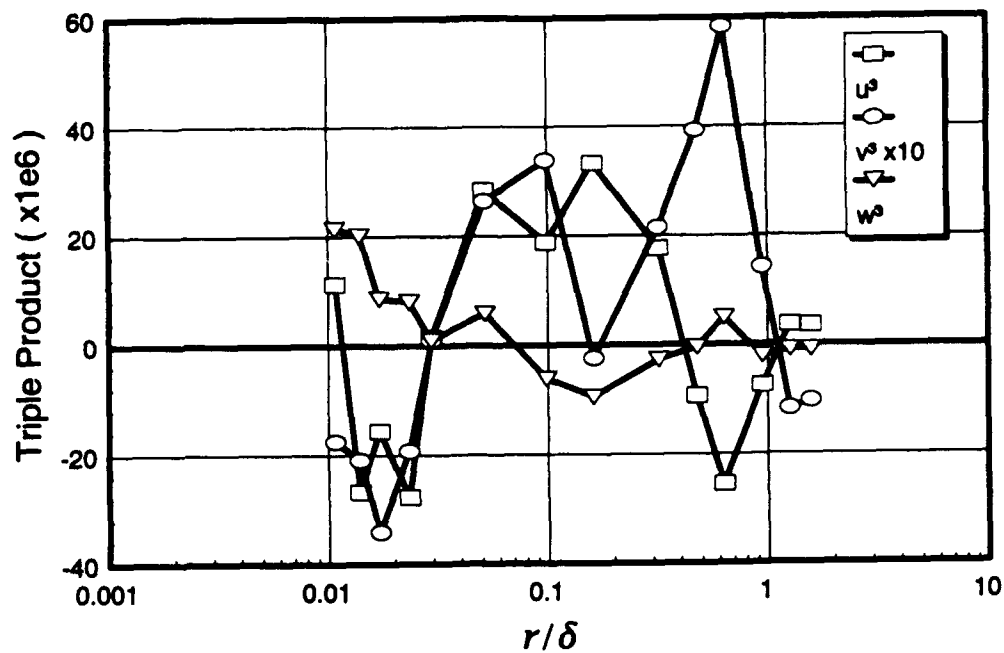


Figure 160. Boundary-layer profiles of velocity third moments, $x/L = 0.752$, $\phi = 125^\circ$.

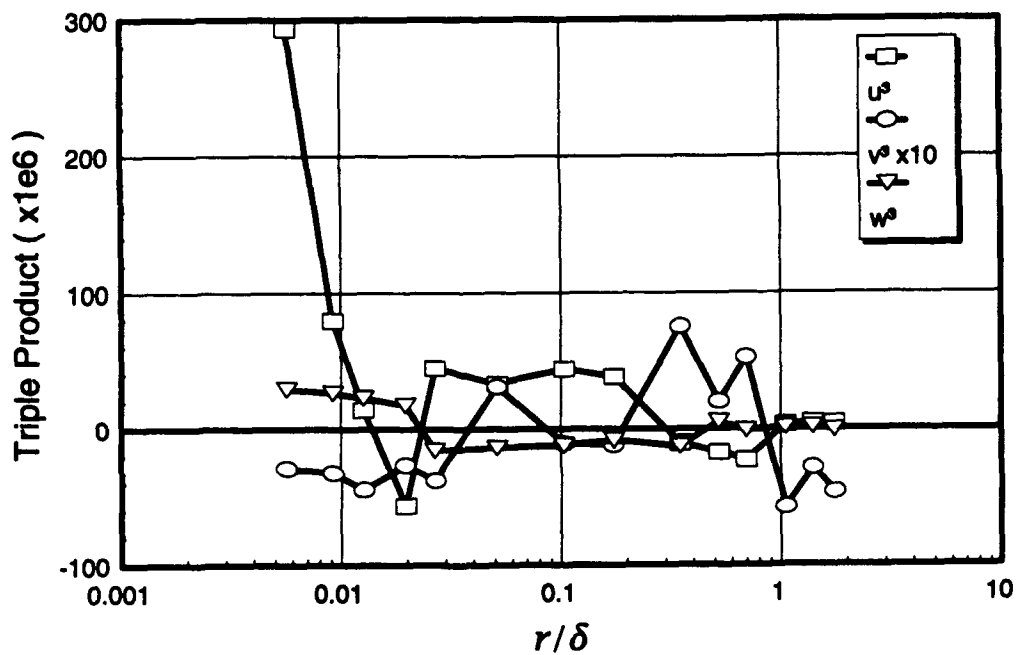


Figure 161. Boundary-layer profiles of velocity third moments, $x/L = 0.762$, $\phi = 120^\circ$.

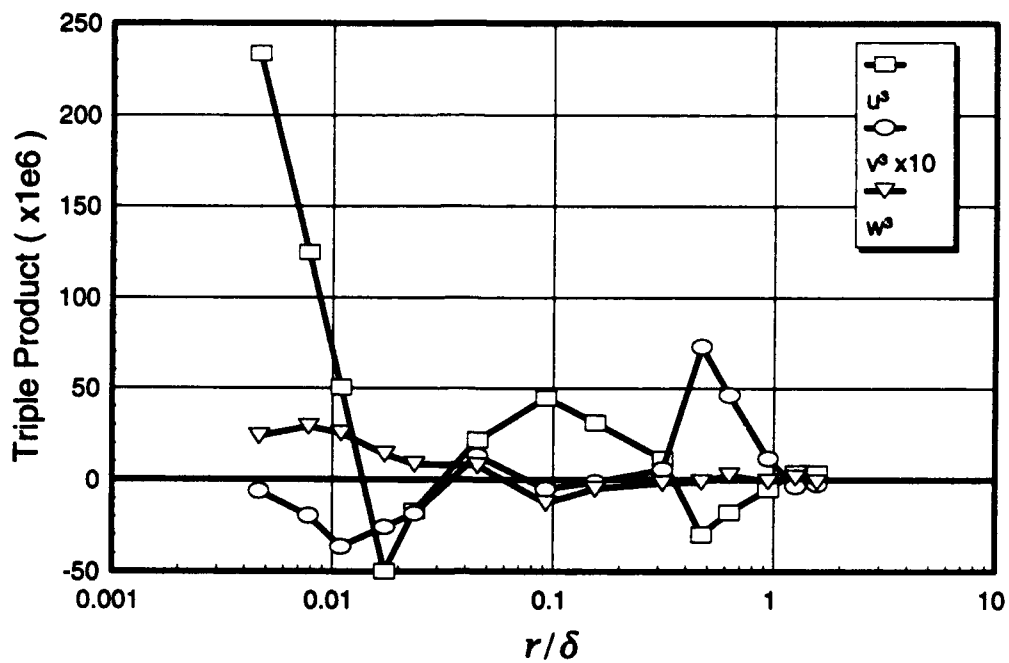


Figure 162. Boundary-layer profiles of velocity third moments, $x/L = 0.762$, $\phi = 123^\circ$.

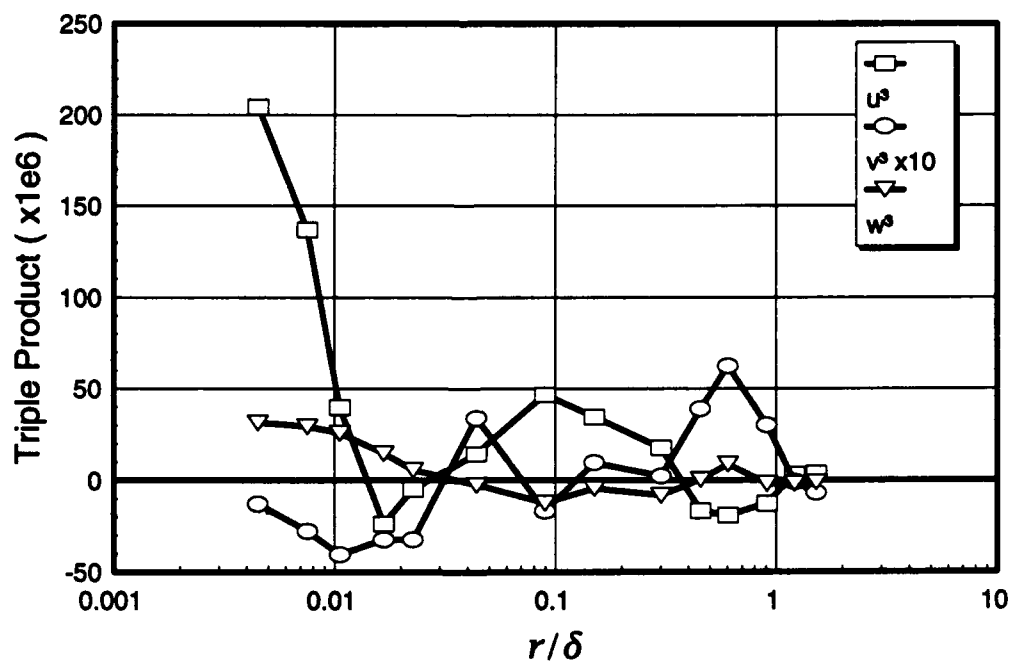


Figure 163. Boundary-layer profiles of velocity third moments, $x/L = 0.762$, $\phi = 125^\circ$.

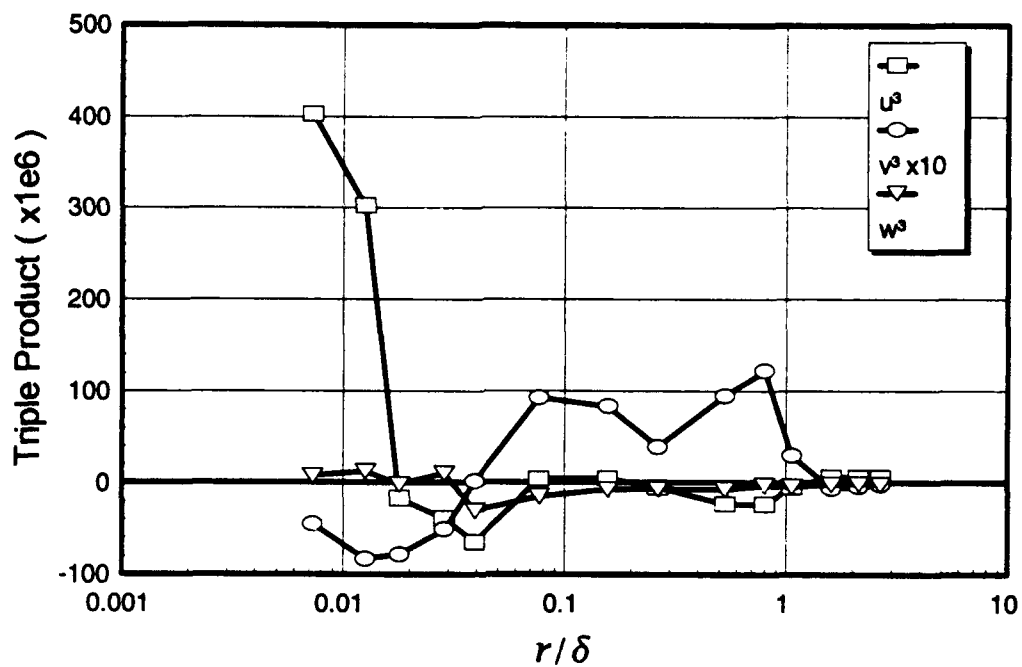


Figure 164. Boundary-layer profiles of velocity third moments, $x/L = 0.772$, $\phi = 105^\circ$.

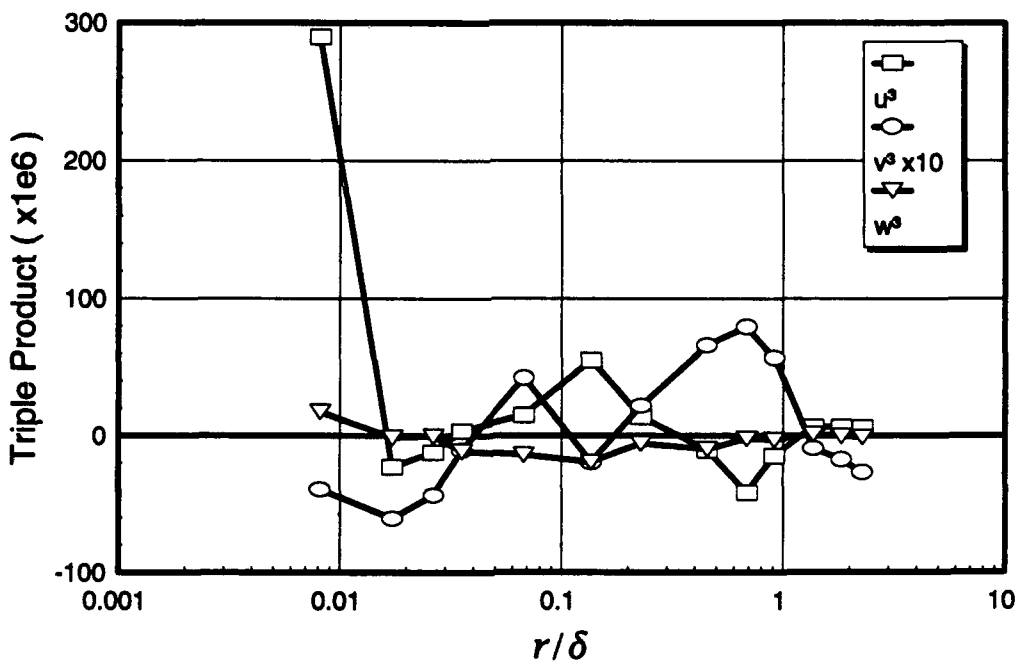


Figure 165. Boundary-layer profiles of velocity third moments, $x/L = 0.772$, $\phi = 110^\circ$.

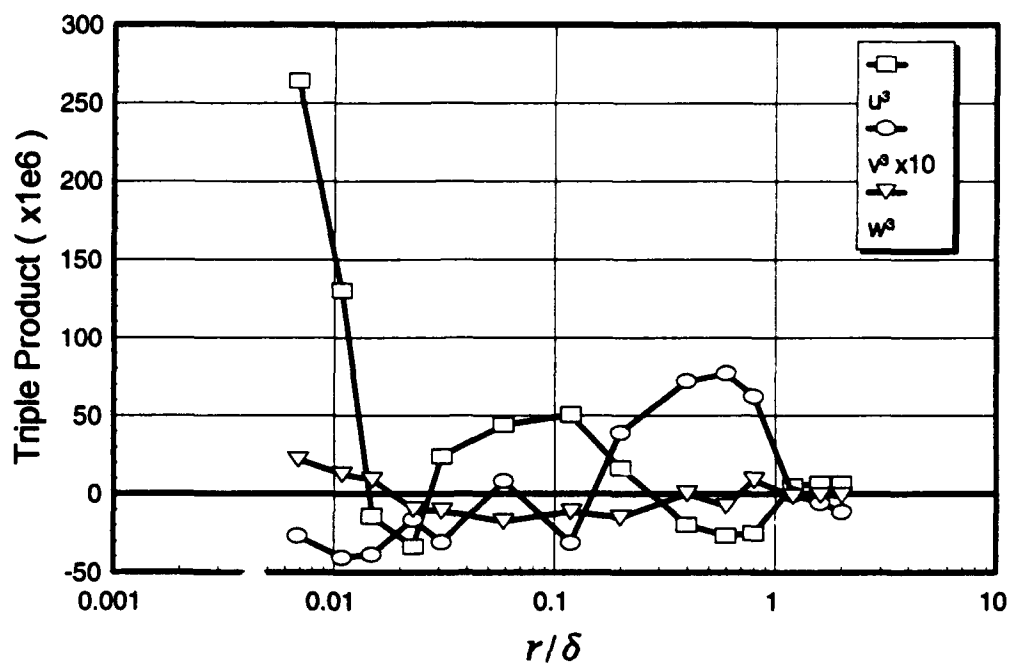


Figure 166. Boundary-layer profiles of velocity third moments, $x/L = 0.772$, $\phi = 115^\circ$.

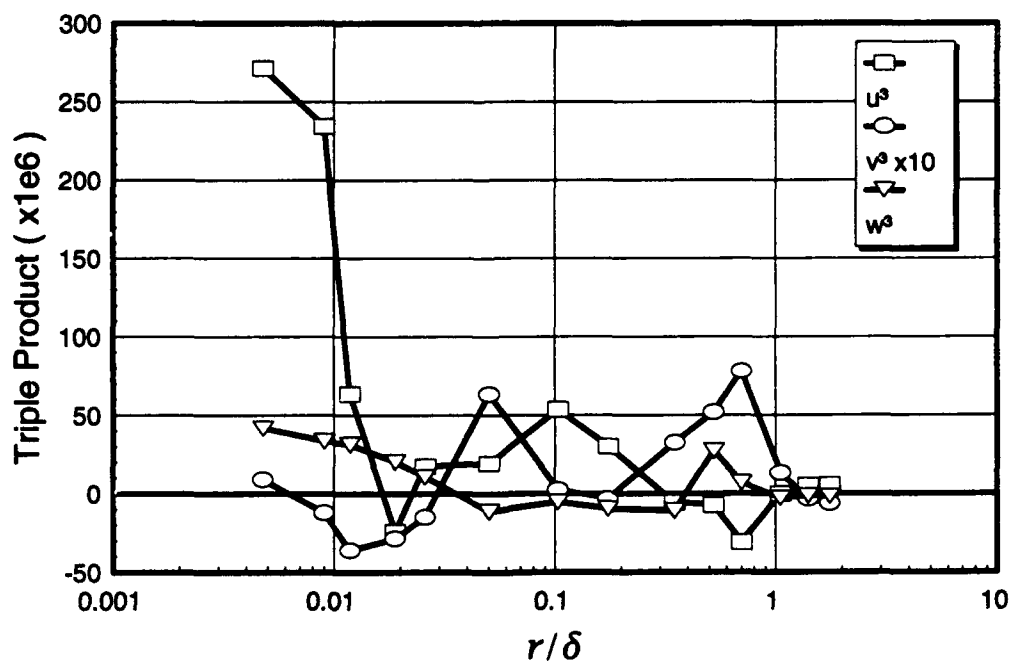


Figure 167. Boundary-layer profiles of velocity third moments, $x/L = 0.772$, $\phi = 120^\circ$.

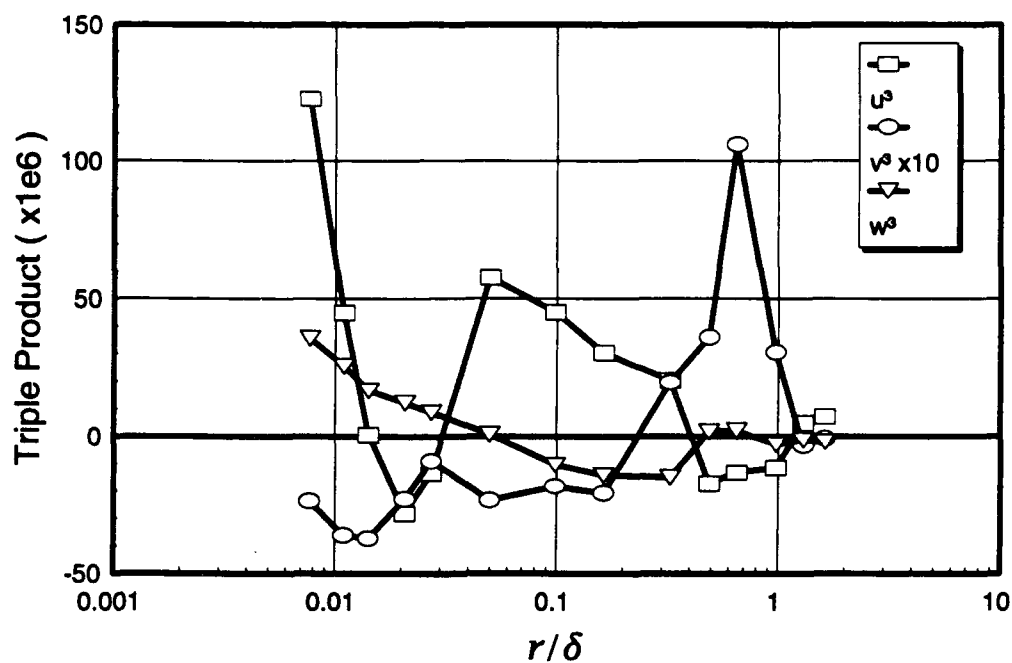


Figure 168. Boundary-layer profiles of velocity third moments, $x/L = 0.772$, $\phi = 123^\circ$.

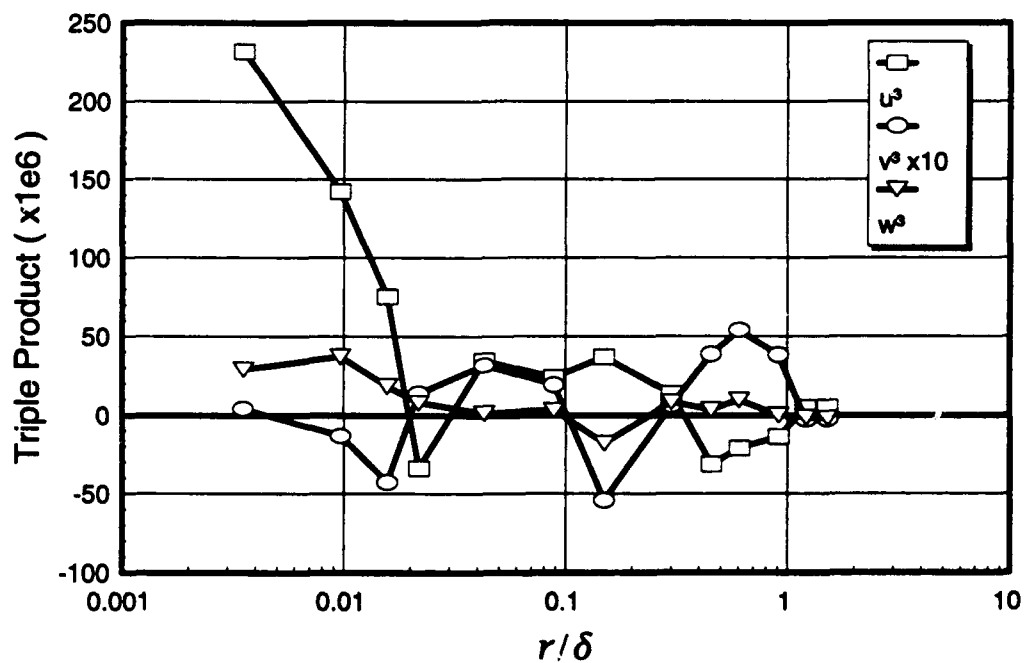


Figure 169. Boundary-layer profiles of velocity third moments, $x/L = 0.772$, $\phi = 125^\circ$.

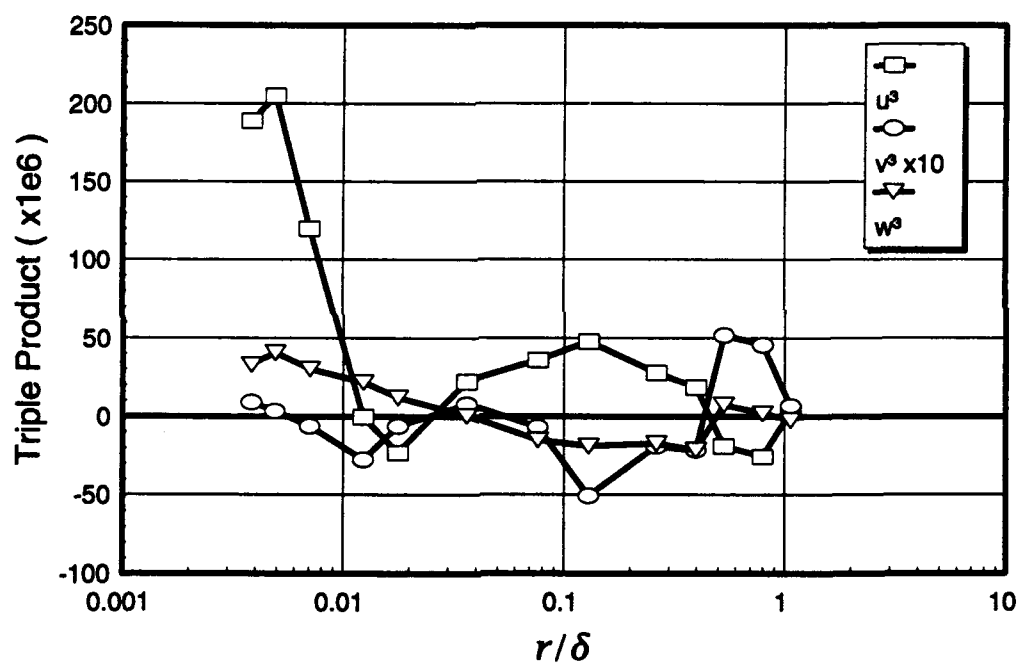


Figure 170. Boundary-layer profiles of velocity third moments, $x/L = 0.772$, $\phi = 130^\circ$.

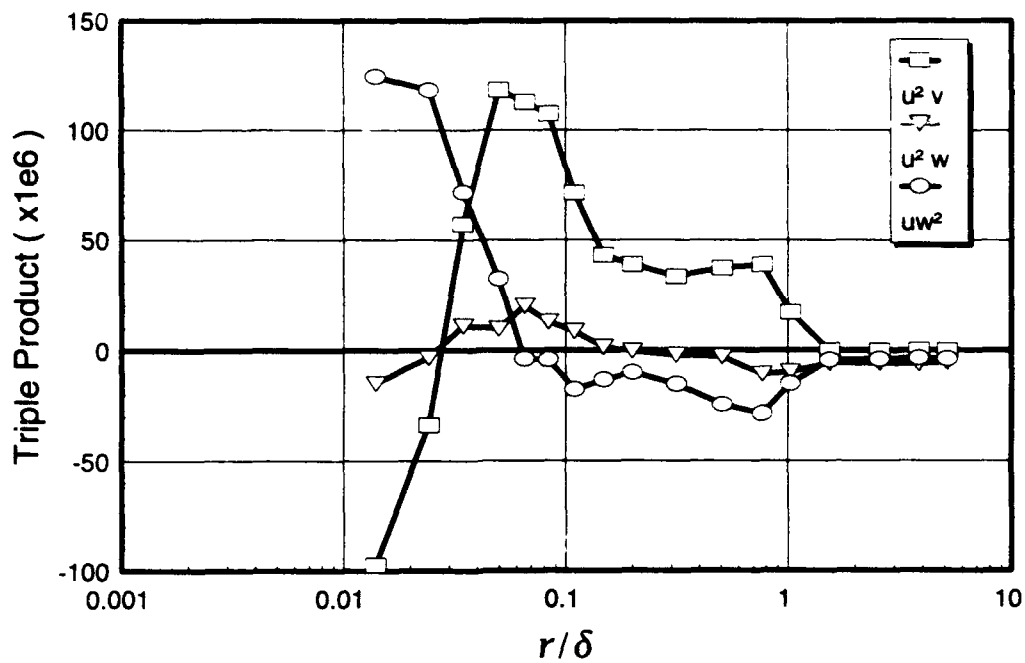


Figure 171. Boundary-layer profiles of velocity triple products (1), $x/L = 0.400$, $\phi = 90^\circ$.

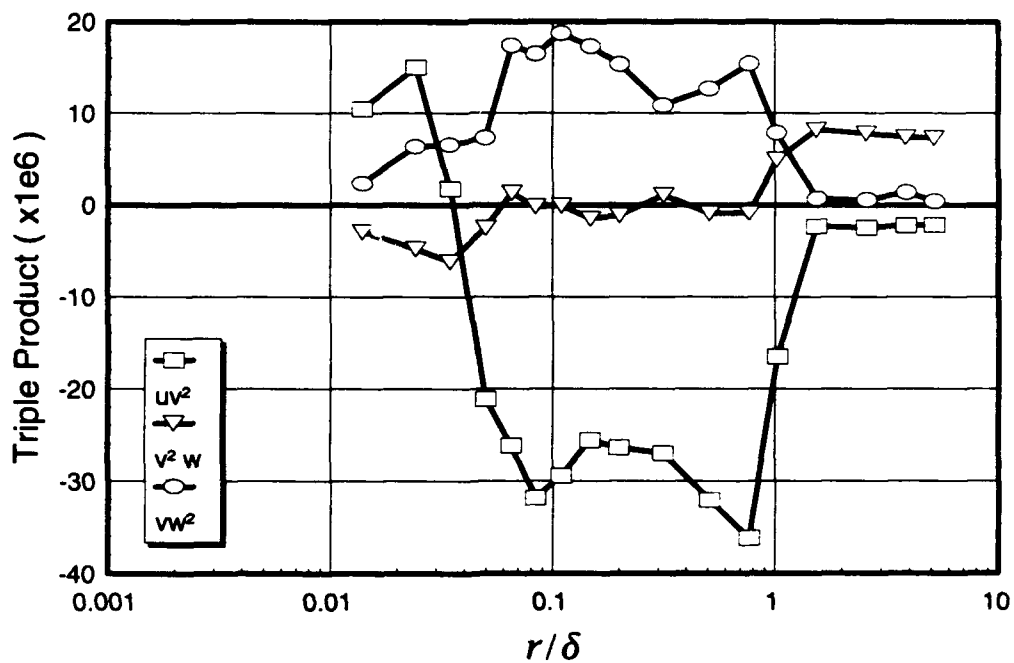


Figure 172. Boundary-layer profiles of velocity triple products (2), $x/L = 0.400$, $\phi = 90^\circ$.

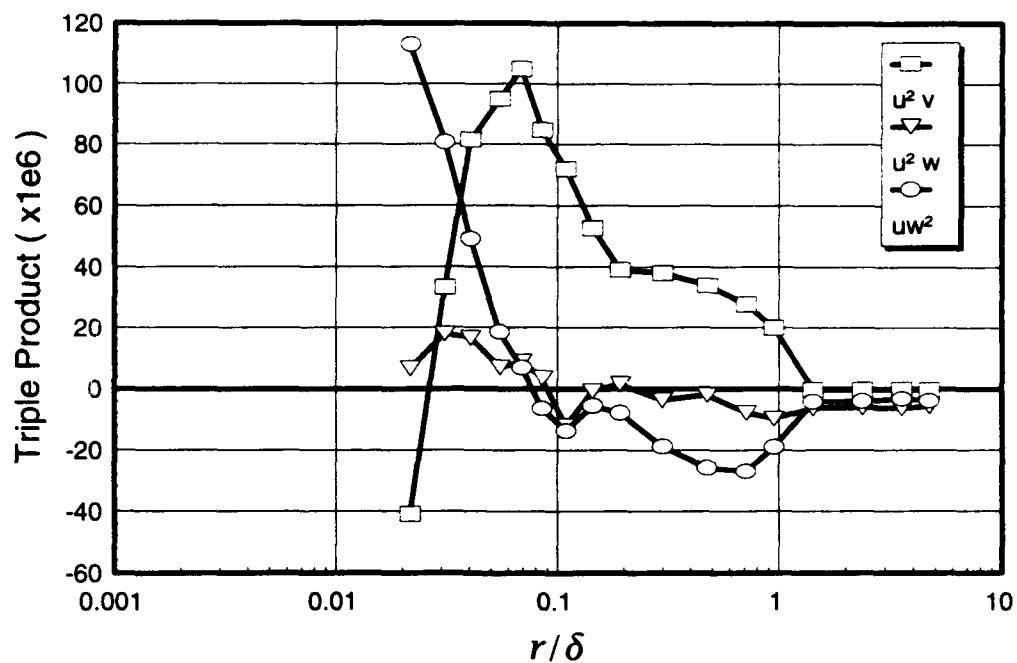


Figure 173. Boundary-layer profiles of velocity triple products (1), $x/L = 0.400$, $\phi = 100^\circ$.

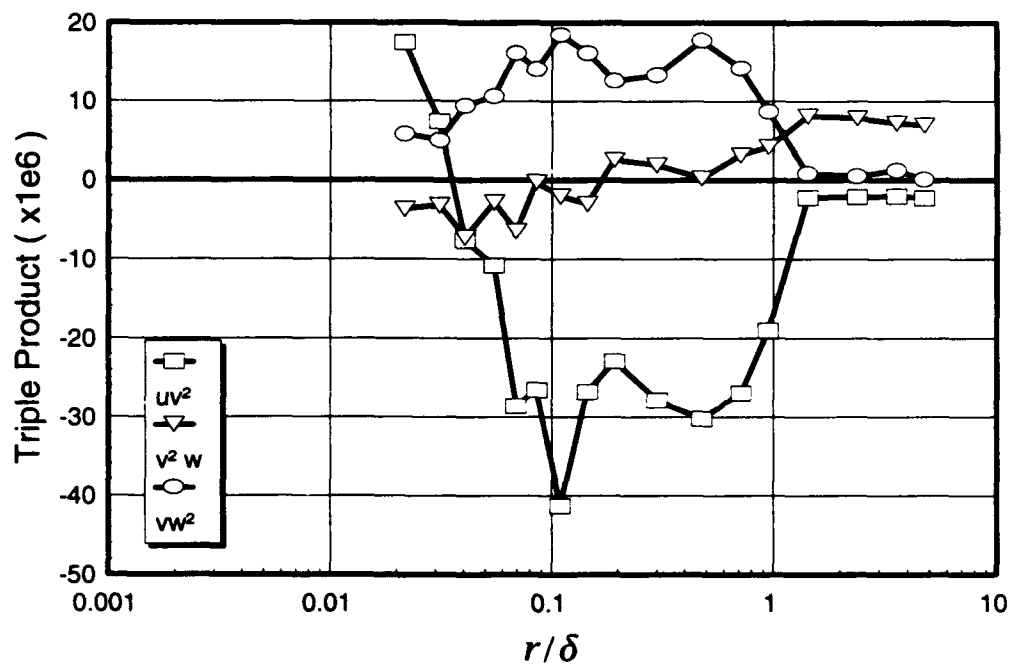


Figure 174. Boundary-layer profiles of velocity triple products (2), $x/L = 0.400$, $\phi = 100^\circ$.

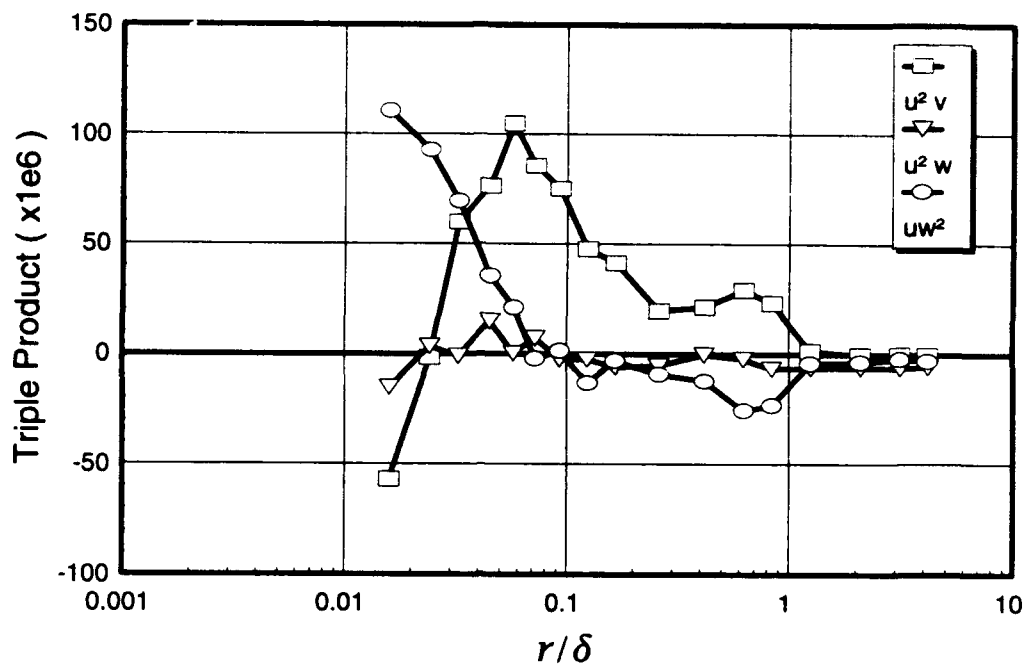


Figure 175. Boundary-layer profiles of velocity triple products (1), $x/L = 0.400$, $\phi = 110^\circ$.

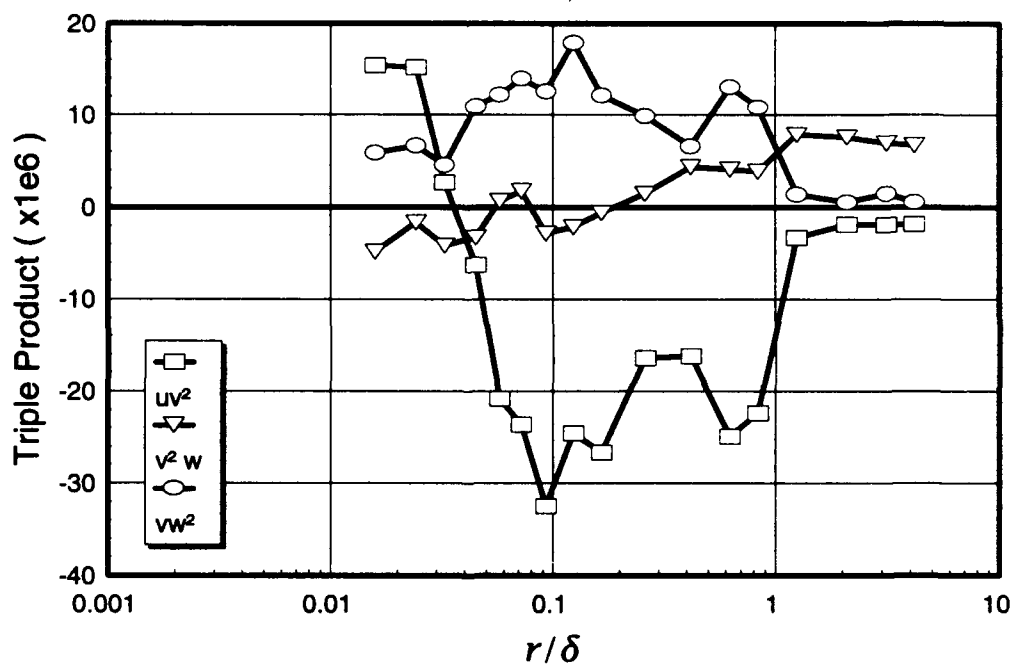


Figure 176. Boundary-layer profiles of velocity triple products (2), $x/L = 0.400$, $\phi = 110^\circ$.

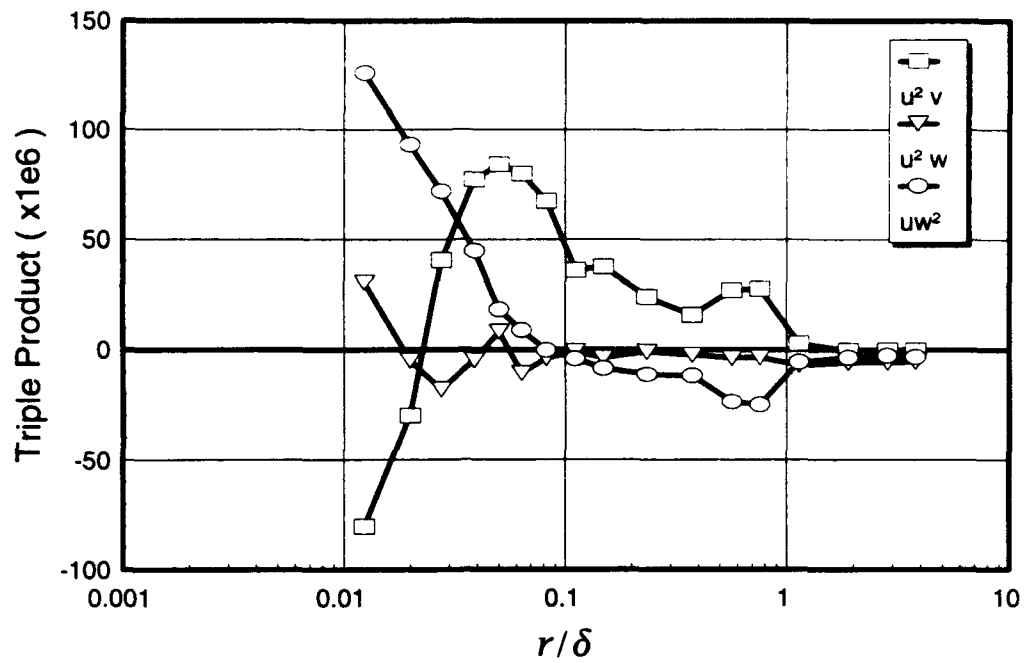


Figure 177. Boundary-layer profiles of velocity triple products (1), $x/L = 0.400$, $\phi = 120^\circ$.

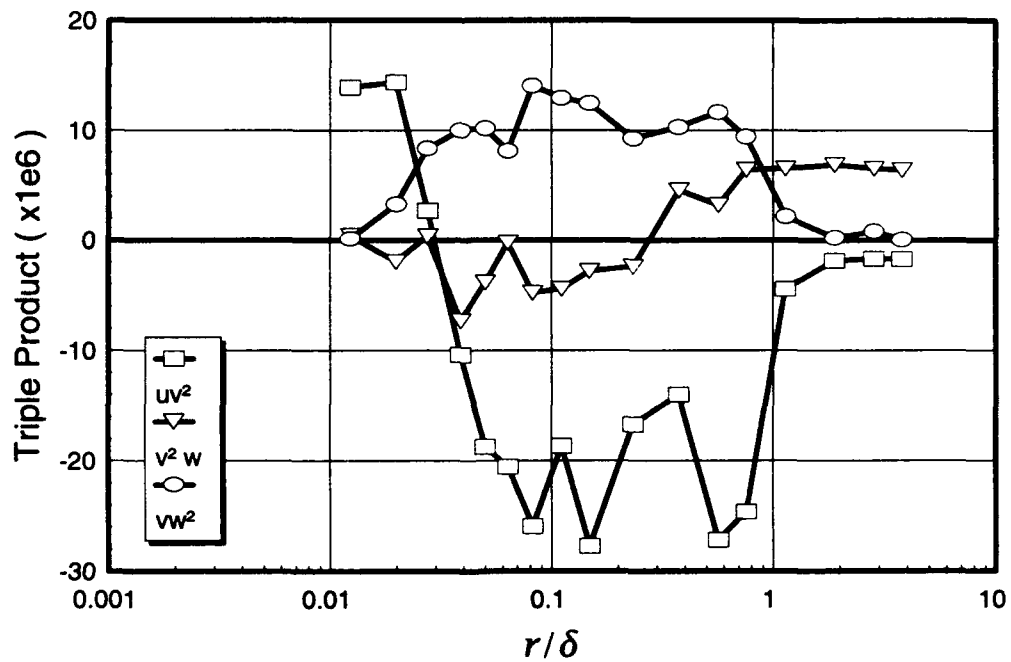


Figure 178. Boundary-layer profiles of velocity triple products (2), $x/L = 0.400$, $\phi = 120^\circ$.

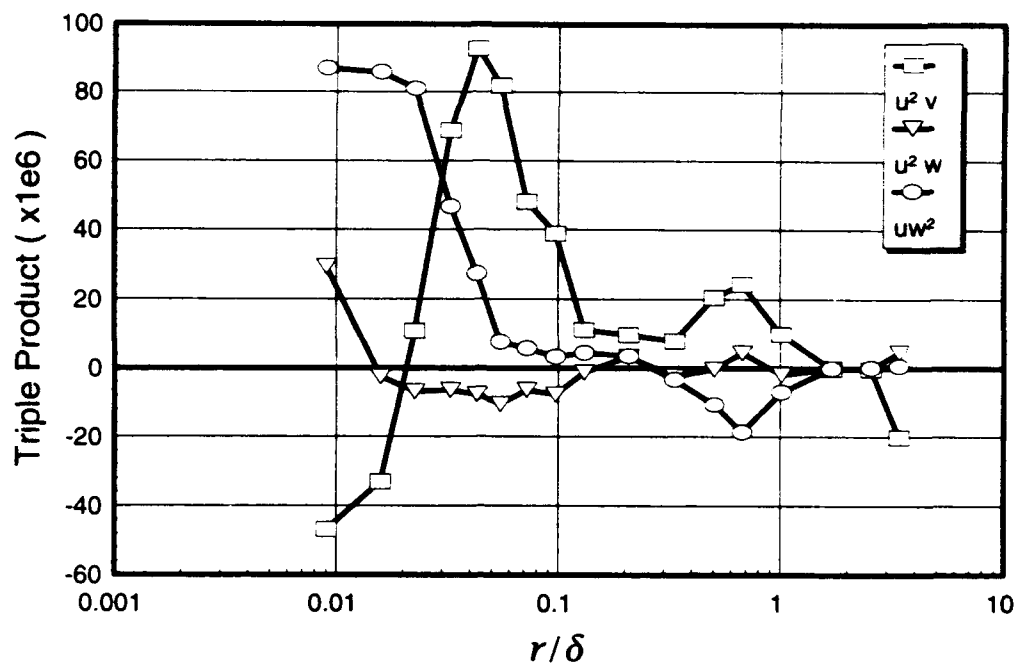


Figure 179. Boundary-layer profiles of velocity triple products (1), $x/L = 0.400$, $\phi = 130^\circ$.

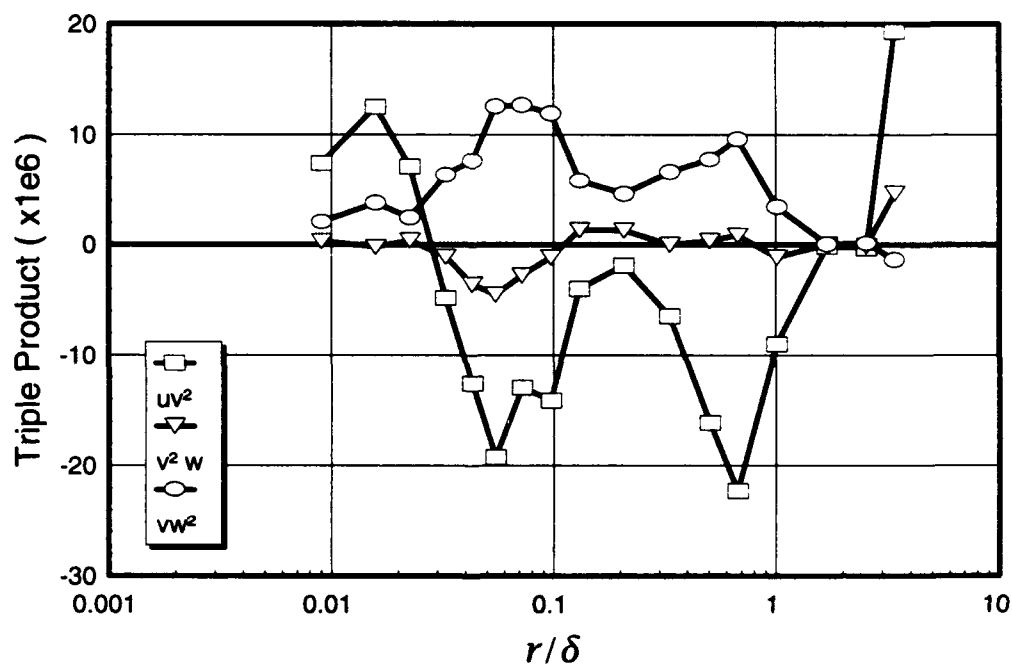


Figure 180. Boundary-layer profiles of velocity triple products (2), $x/L = 0.400$, $\phi = 130^\circ$.

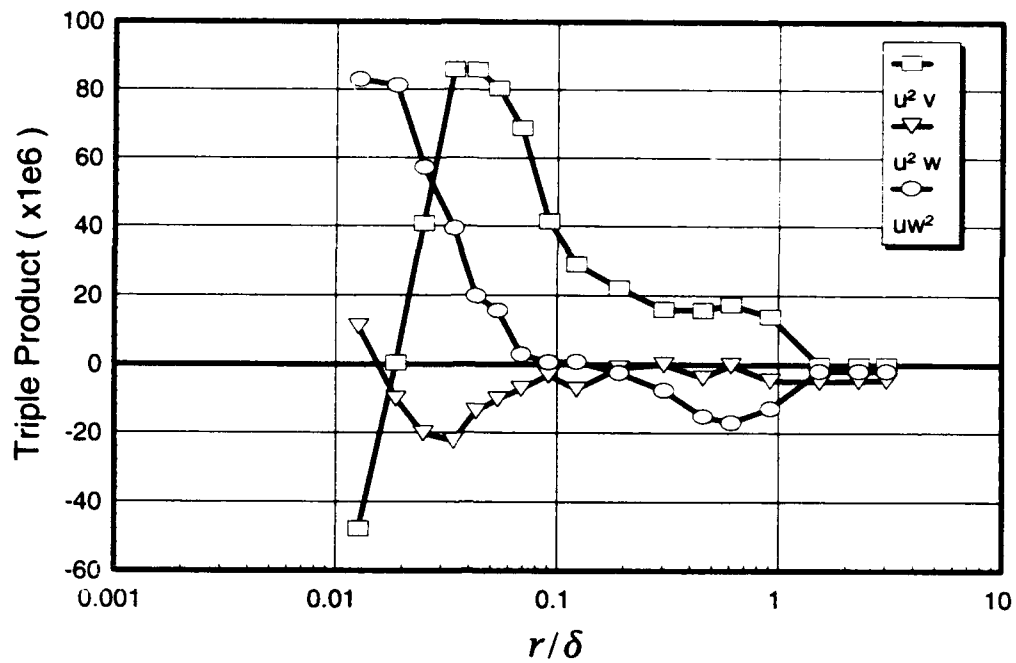


Figure 181. Boundary-layer profiles of velocity triple products (1), $x/L = 0.400$, $\phi = 140^\circ$.

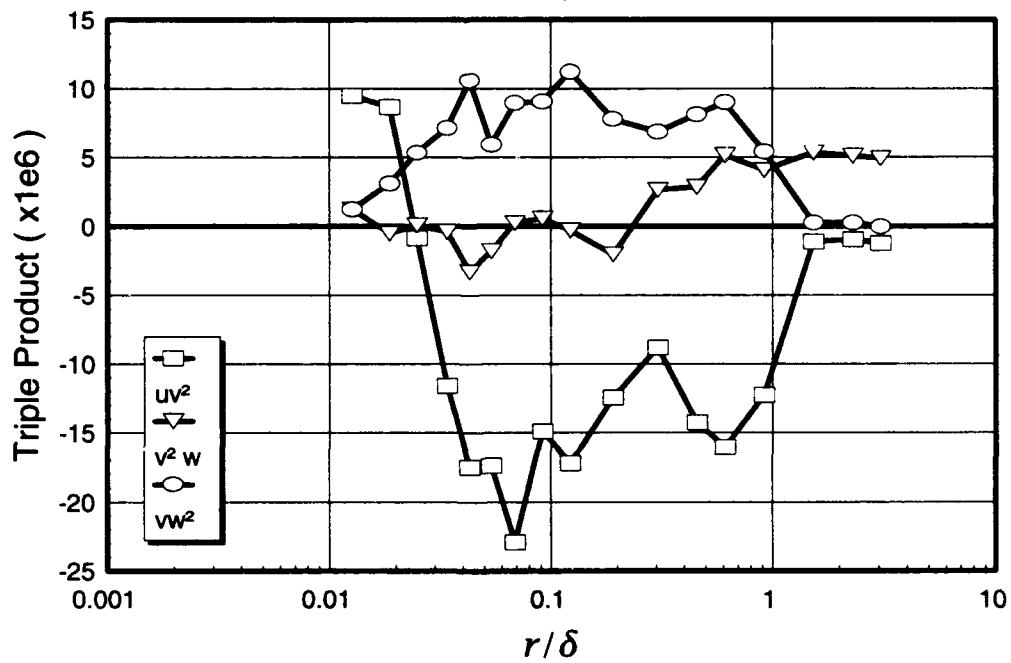


Figure 182. Boundary-layer profiles of velocity triple products (2), $x/L = 0.400$, $\phi = 140^\circ$.

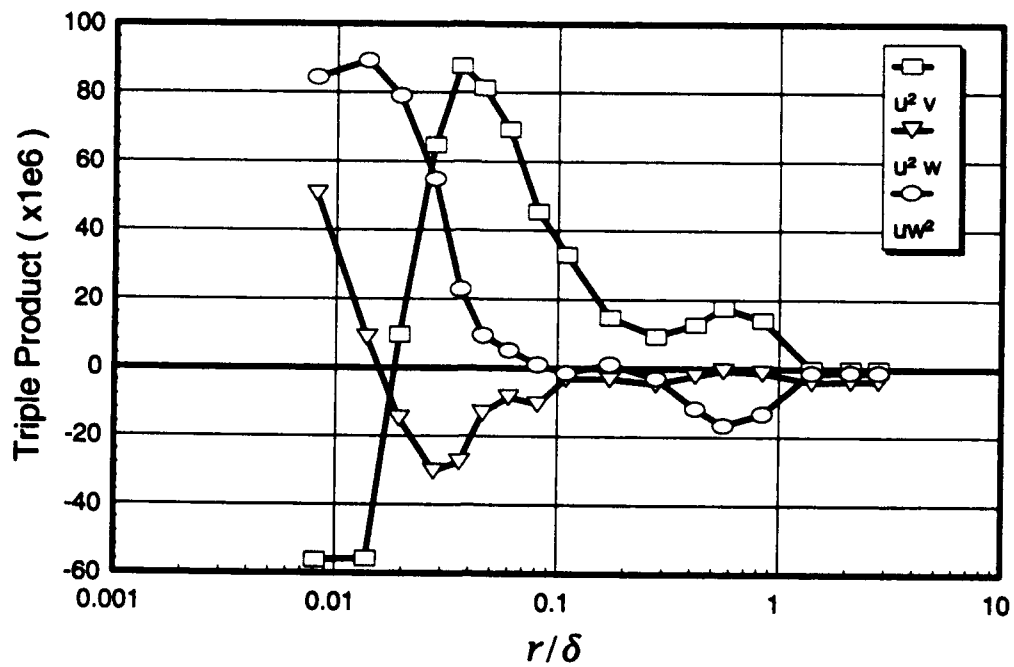


Figure 183. Boundary-layer profiles of velocity triple products (1), $x/L = 0.400$, $\phi = 150^\circ$.

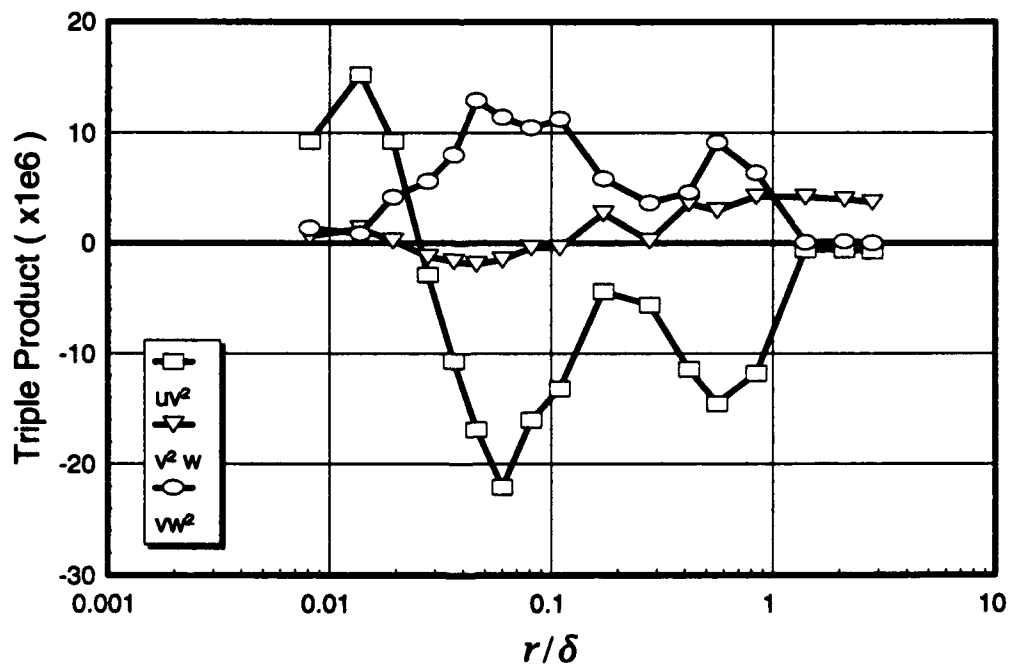


Figure 184. Boundary-layer profiles of velocity triple products (2), $x/L = 0.400$, $\phi = 150^\circ$.

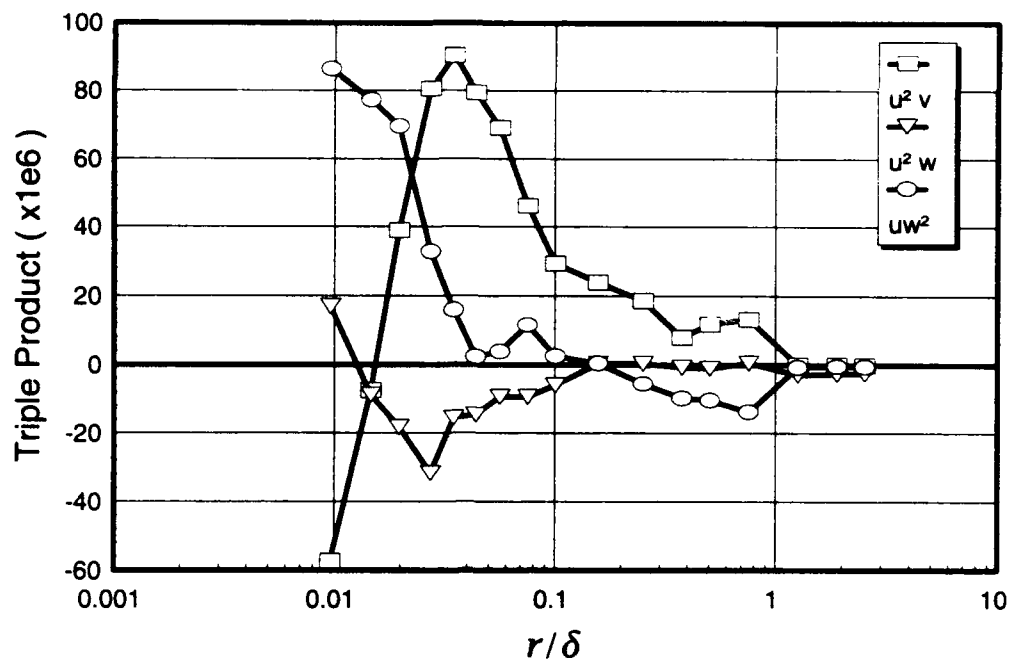


Figure 185. Boundary-layer profiles of velocity triple products (1), $x/L = 0.400$, $\phi = 160^\circ$.

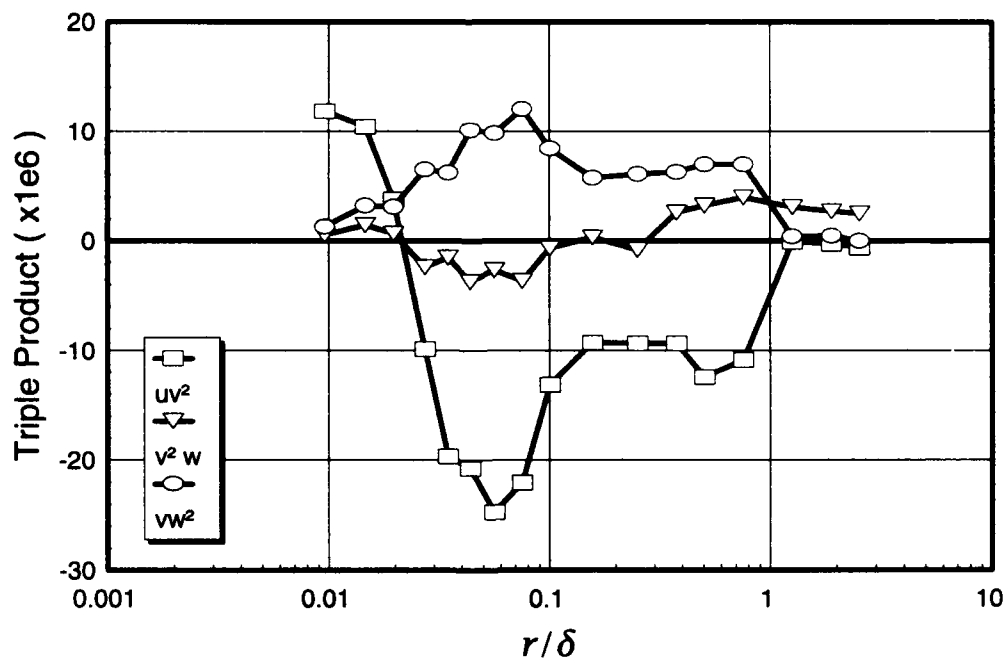


Figure 186. Boundary-layer profiles of velocity triple products (2), $x/L = 0.400$, $\phi = 160^\circ$.

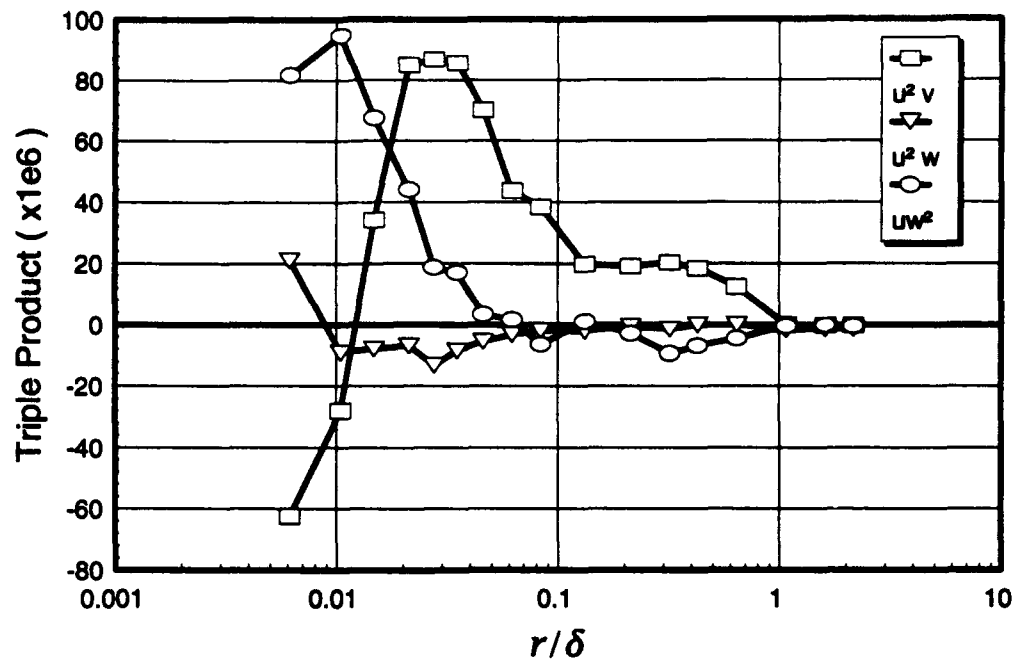


Figure 187. Boundary-layer profiles of velocity triple products (1), $x/L = 0.400$, $\phi = 170^\circ$.

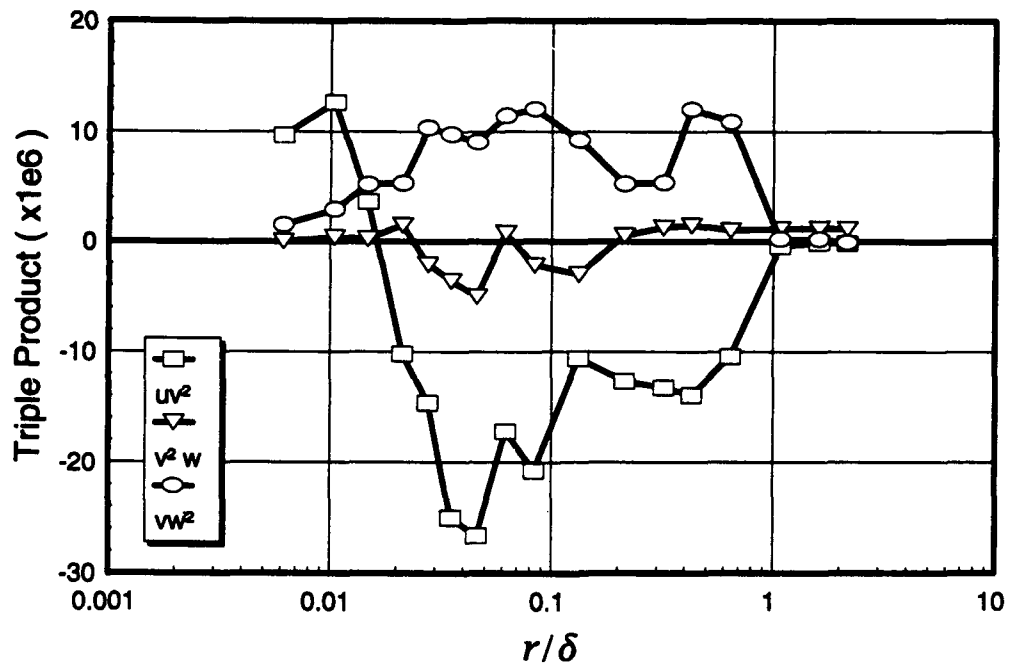


Figure 188. Boundary-layer profiles of velocity triple products (2), $x/L = 0.400$, $\phi = 170^\circ$.

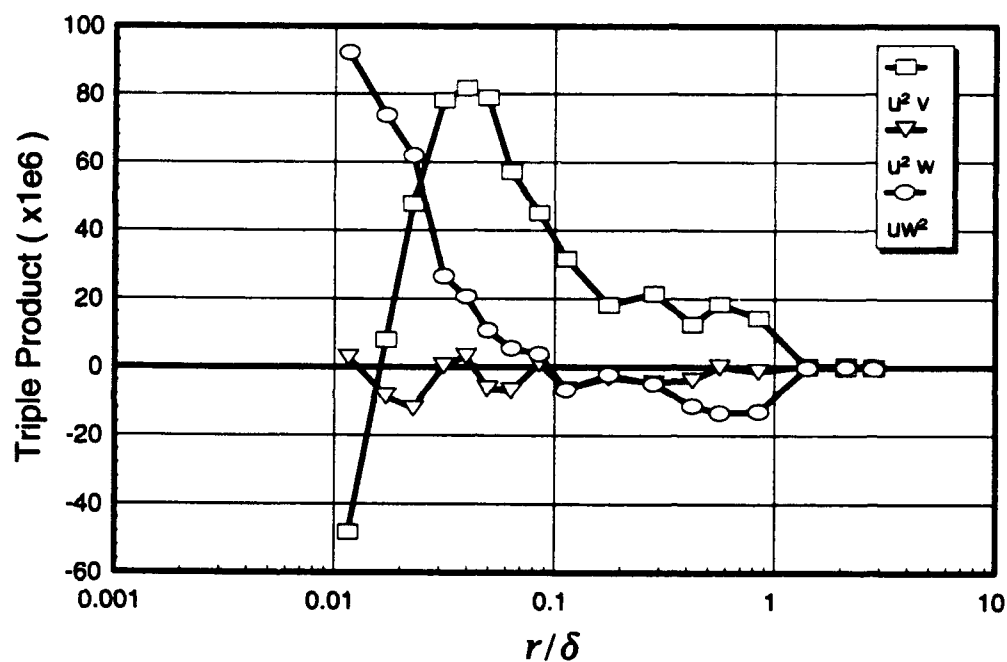


Figure 189. Boundary-layer profiles of velocity triple products (1), $x/L = 0.400$, $\phi = 180^\circ$.

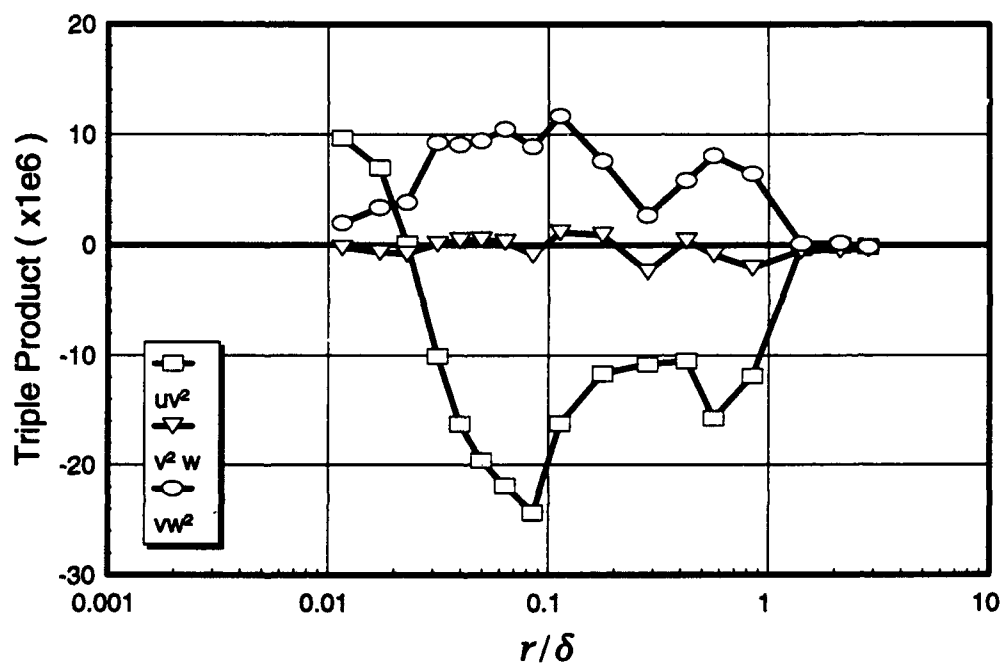


Figure 190. Boundary-layer profiles of velocity triple products (2), $x/L = 0.400$, $\phi = 180^\circ$.

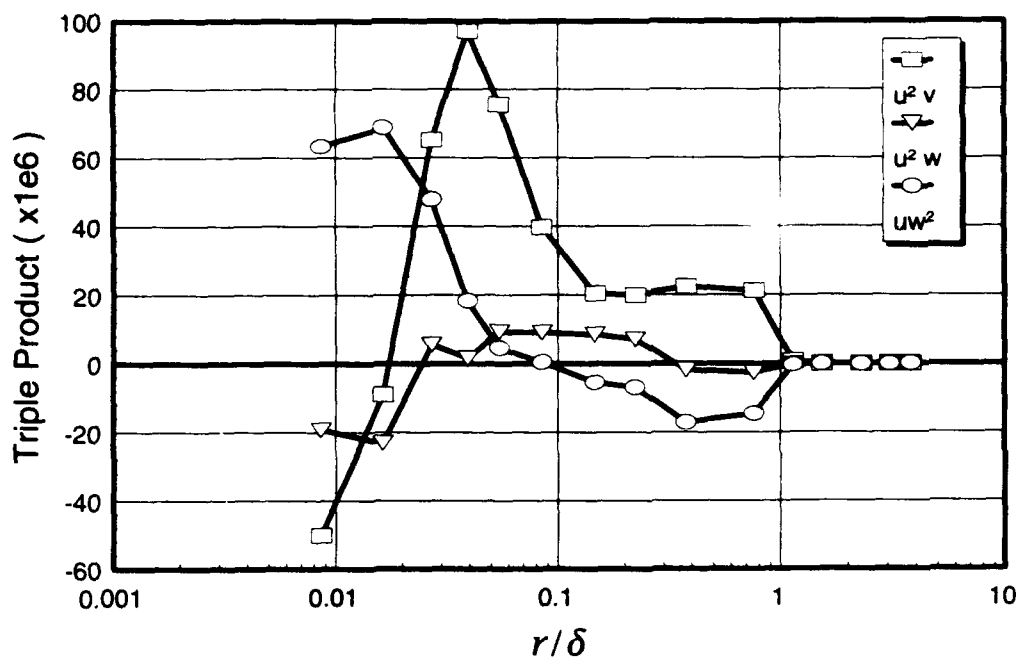


Figure 191. Boundary-layer profiles of velocity triple products (1), $x/L = 0.600$, $\phi = 90^\circ$.

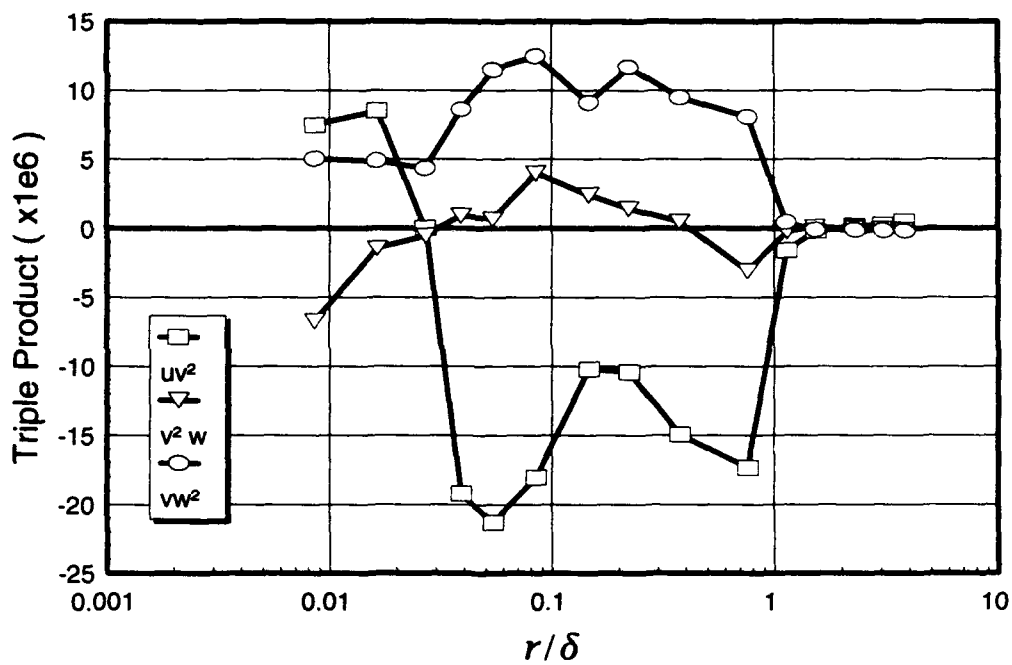


Figure 192. Boundary-layer profiles of velocity triple products (2), $x/L = 0.600$, $\phi = 90^\circ$.

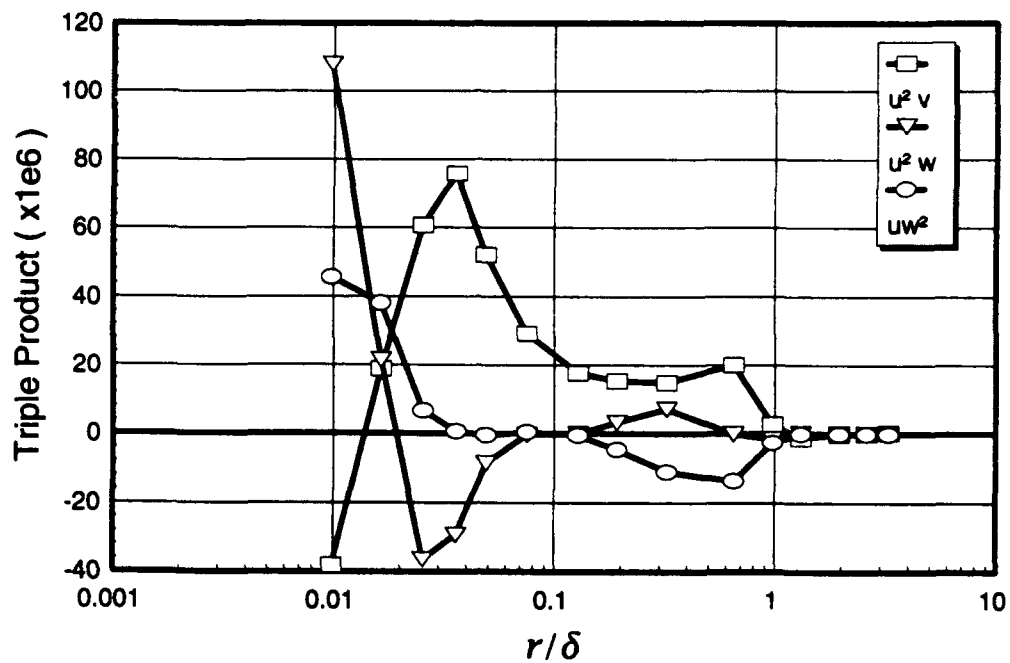


Figure 193. Boundary-layer profiles of velocity triple products (1), $x/L = 0.600$, $\phi = 100^\circ$.

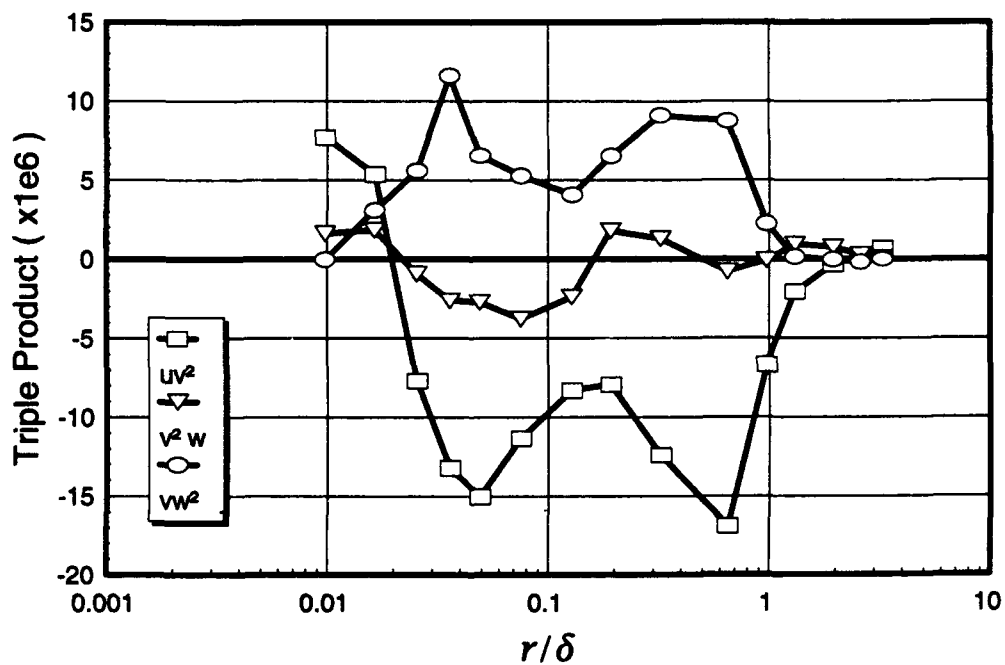


Figure 194. Boundary-layer profiles of velocity triple products (2), $x/L = 0.600$, $\phi = 100^\circ$.

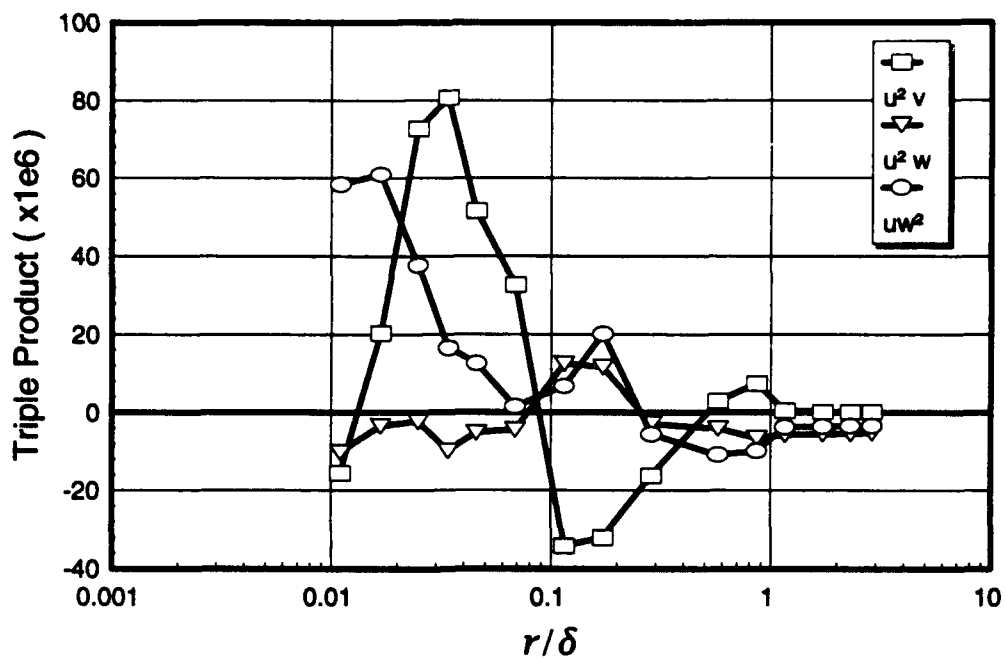


Figure 195. Boundary-layer profiles of velocity triple products (1), $x/L = 0.600$, $\phi = 110^\circ$.

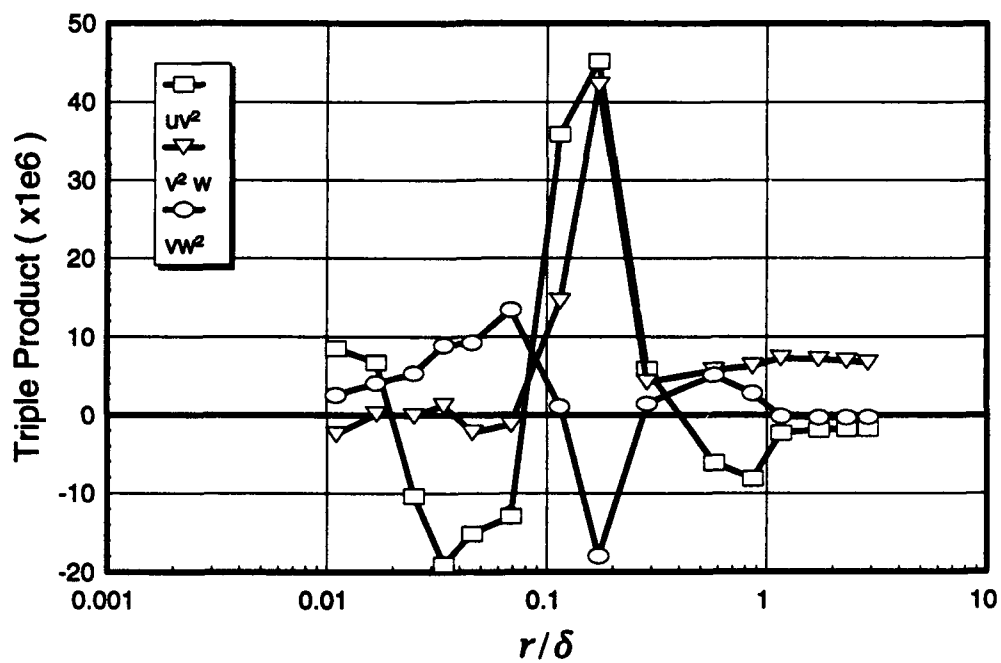


Figure 196. Boundary-layer profiles of velocity triple products (2), $x/L = 0.600$, $\phi = 110^\circ$.

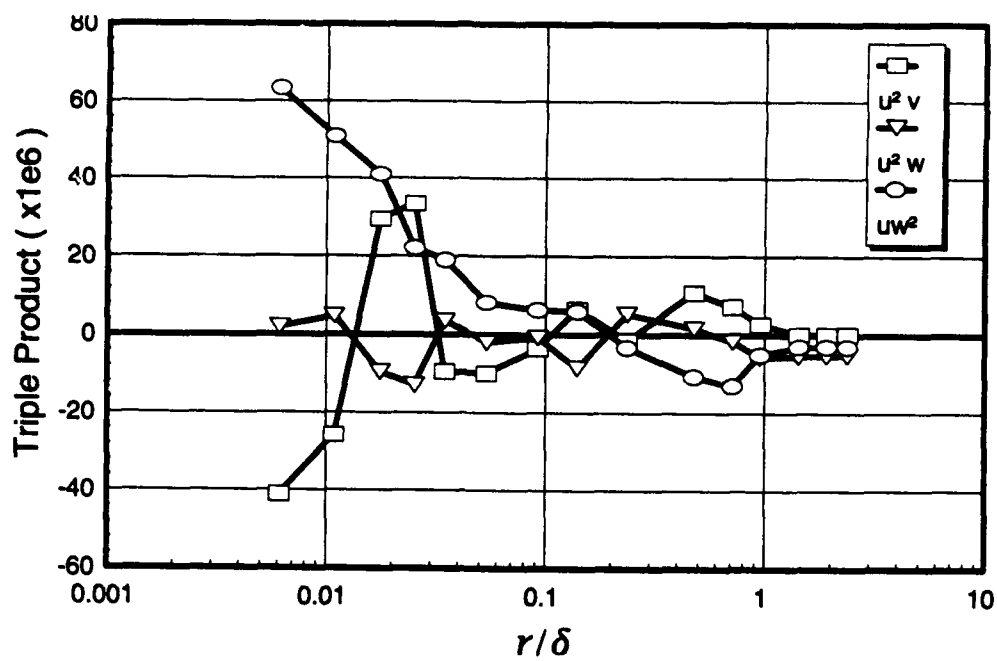


Figure 197. Boundary-layer profiles of velocity triple products (1), $x/L = 0.600$, $\phi = 120^\circ$.

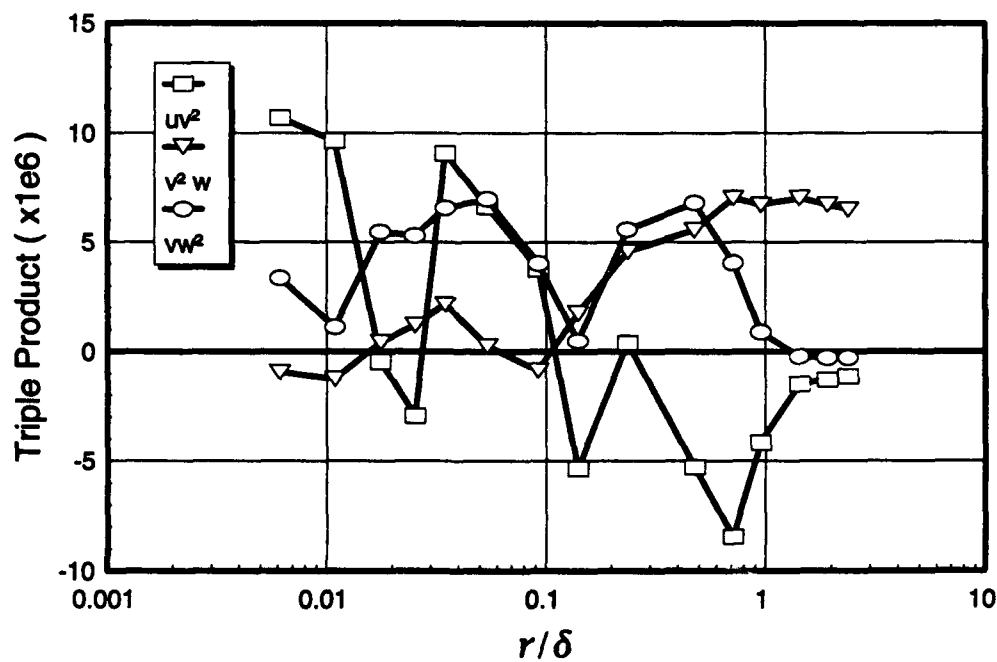


Figure 198. Boundary-layer profiles of velocity triple products (2), $x/L = 0.600$, $\phi = 120^\circ$.

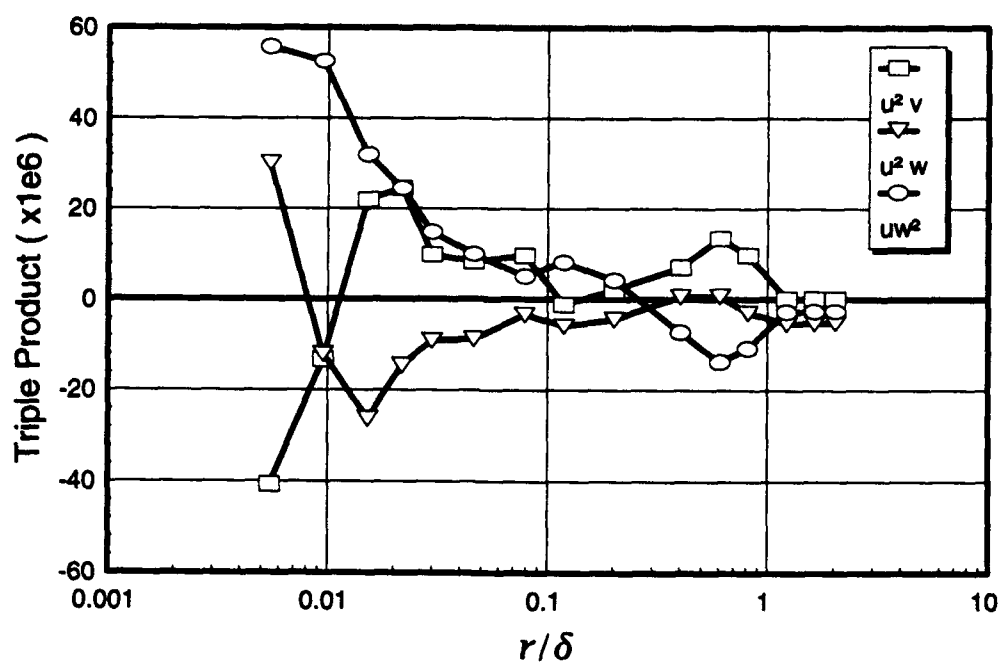


Figure 199. Boundary-layer profiles of velocity triple products (1), $x/L = 0.600$, $\phi = 130^\circ$.

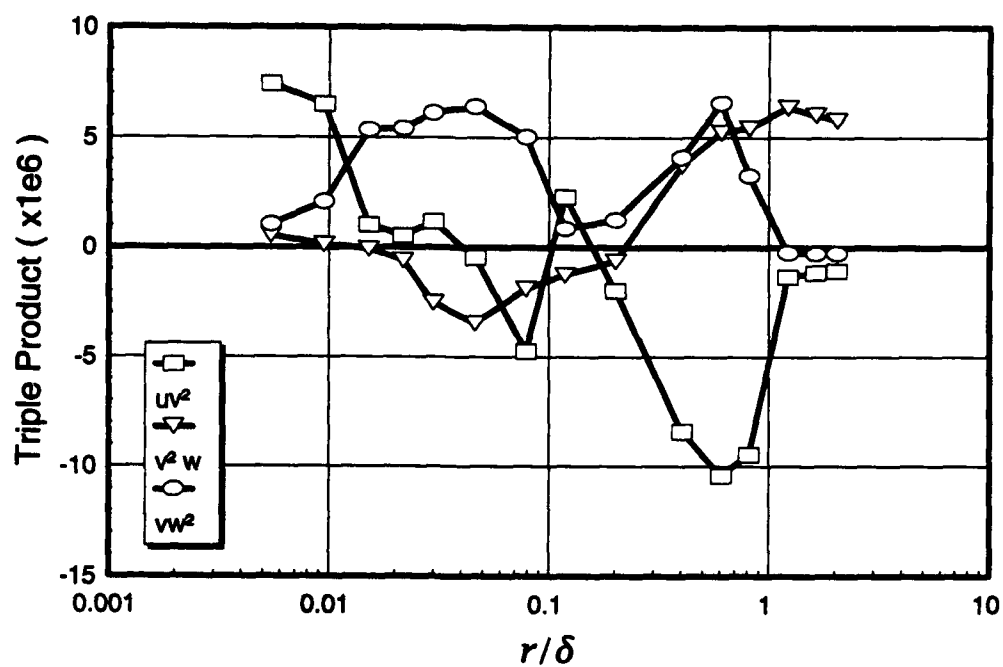


Figure 200. Boundary-layer profiles of velocity triple products (2), $x/L = 0.600$, $\phi = 130^\circ$.

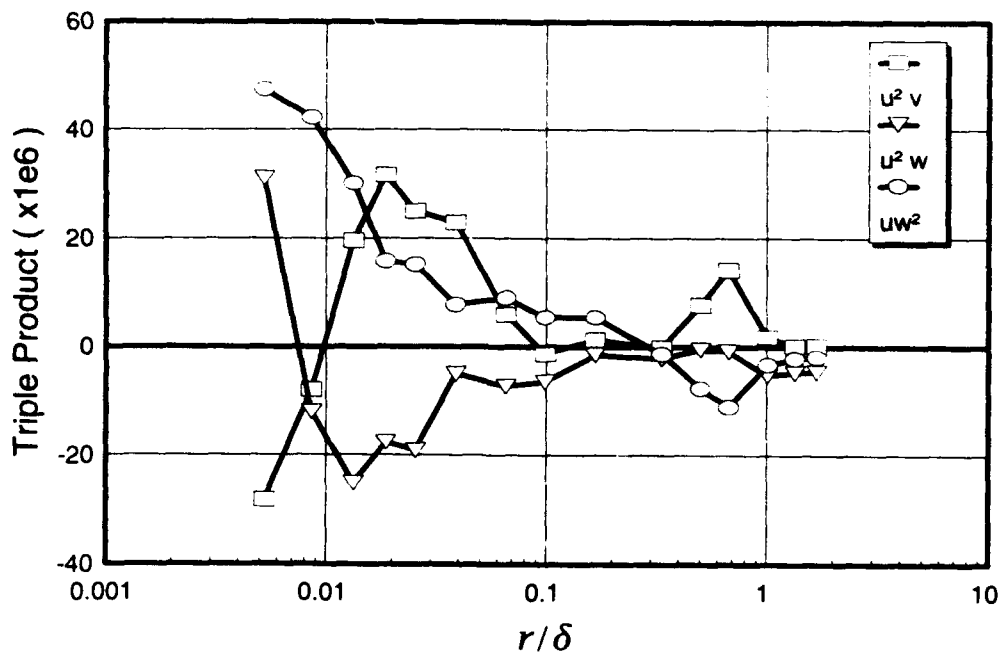


Figure 201. Boundary-layer profiles of velocity triple products (1), $x/L = 0.600$, $\phi = 140^\circ$.

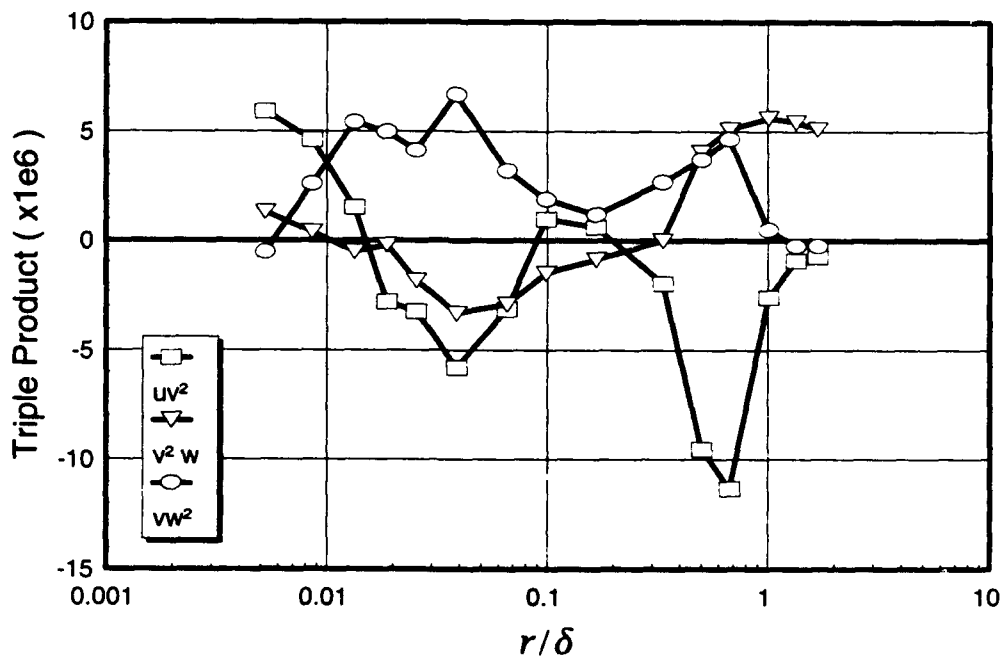


Figure 202. Boundary-layer profiles of velocity triple products (2), $x/L = 0.600$, $\phi = 140^\circ$.

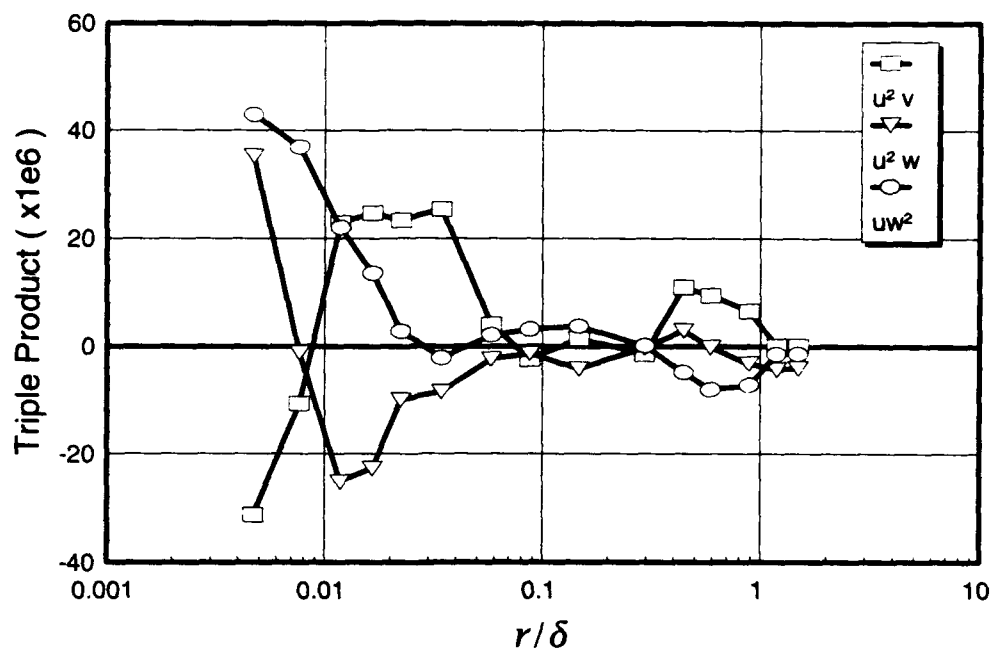


Figure 203. Boundary-layer profiles of velocity triple products (1), $x/L = 0.600$, $\phi = 150^\circ$.

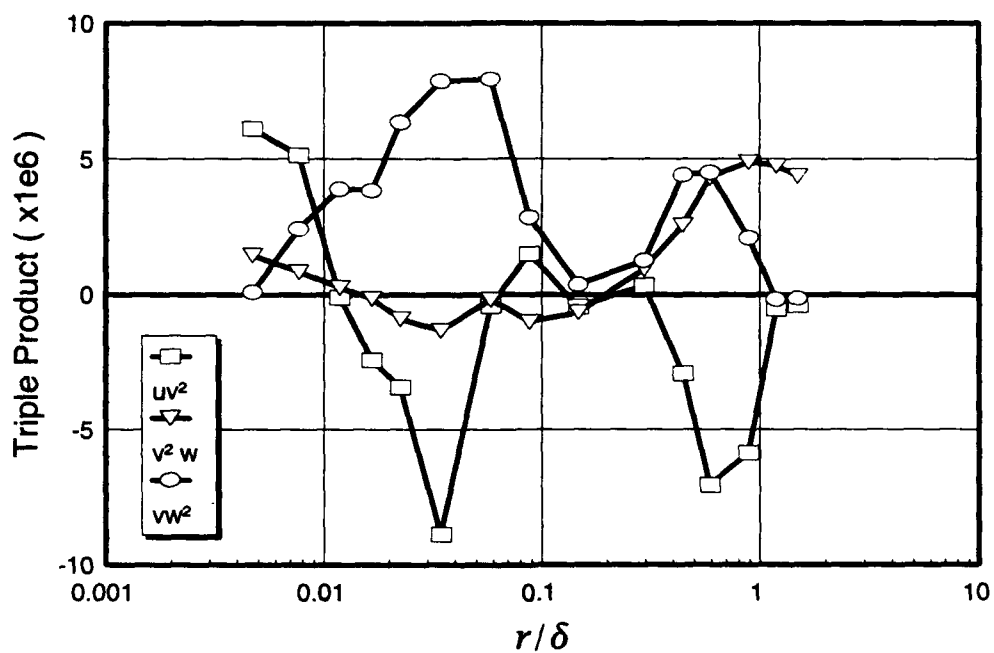


Figure 204. Boundary-layer profiles of velocity triple products (2), $x/L = 0.600$, $\phi = 150^\circ$.

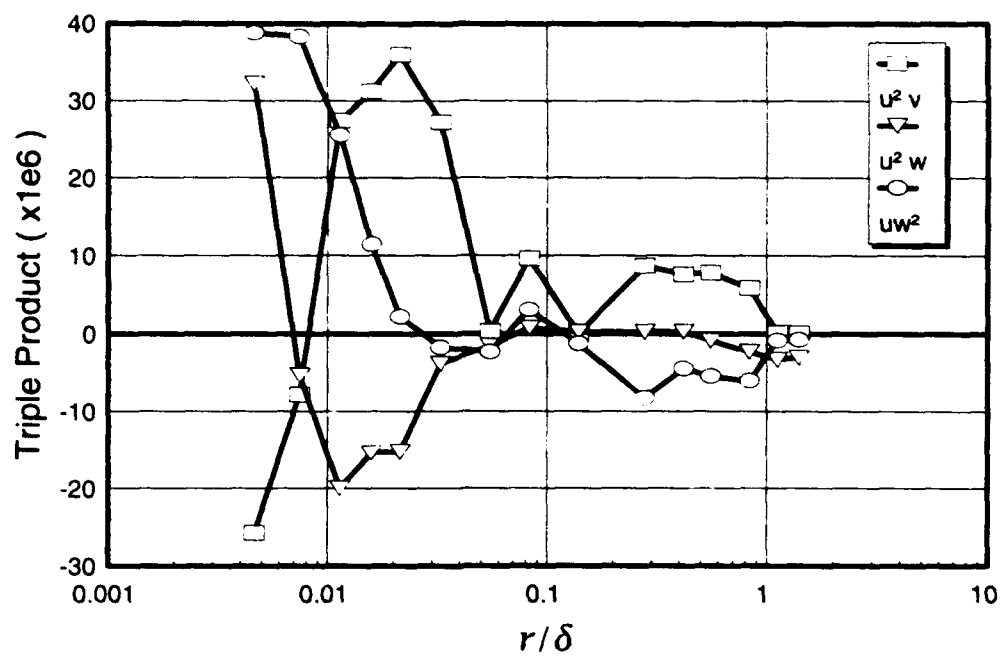


Figure 205. Boundary-layer profiles of velocity triple products (1), $x/L = 0.600$, $\phi = 160^\circ$.

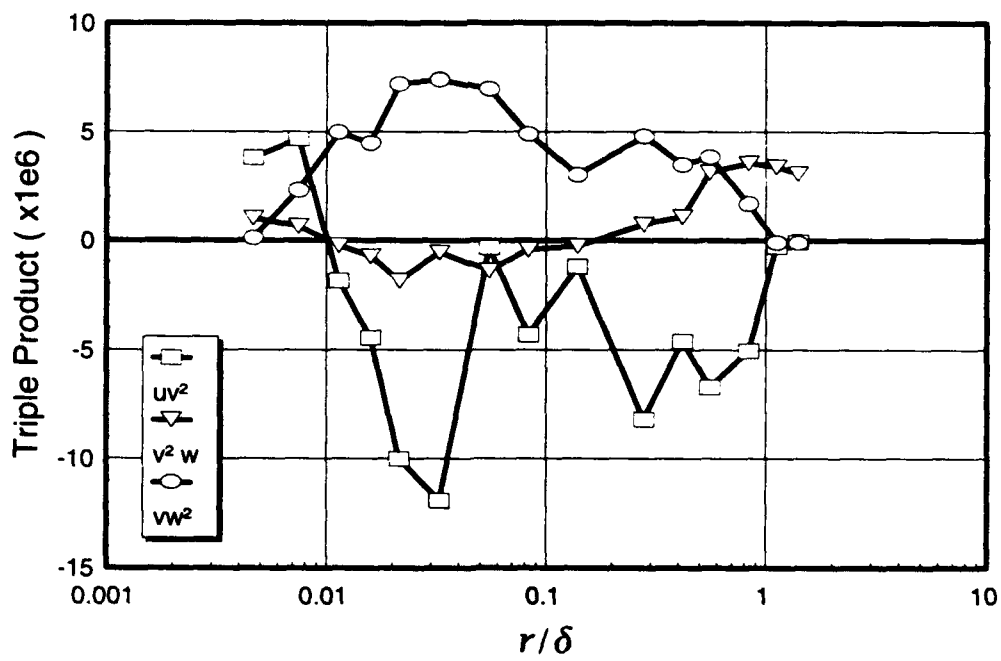


Figure 206. Boundary-layer profiles of velocity triple products (2), $x/L = 0.600$, $\phi = 160^\circ$.

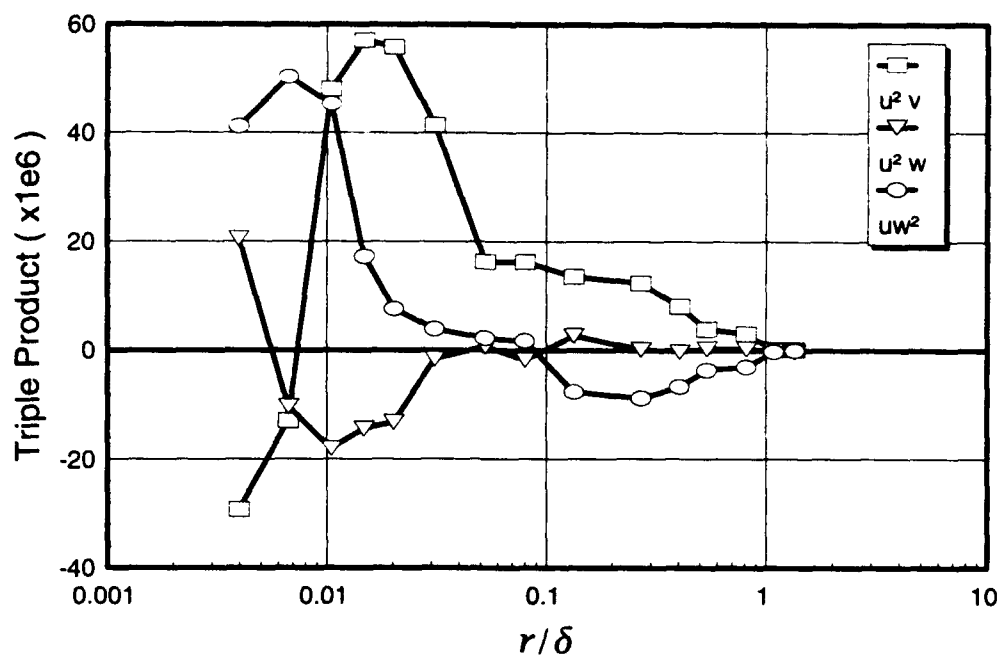


Figure 207. Boundary-layer profiles of velocity triple products (1), $x/L = 0.600$, $\phi = 170^\circ$.

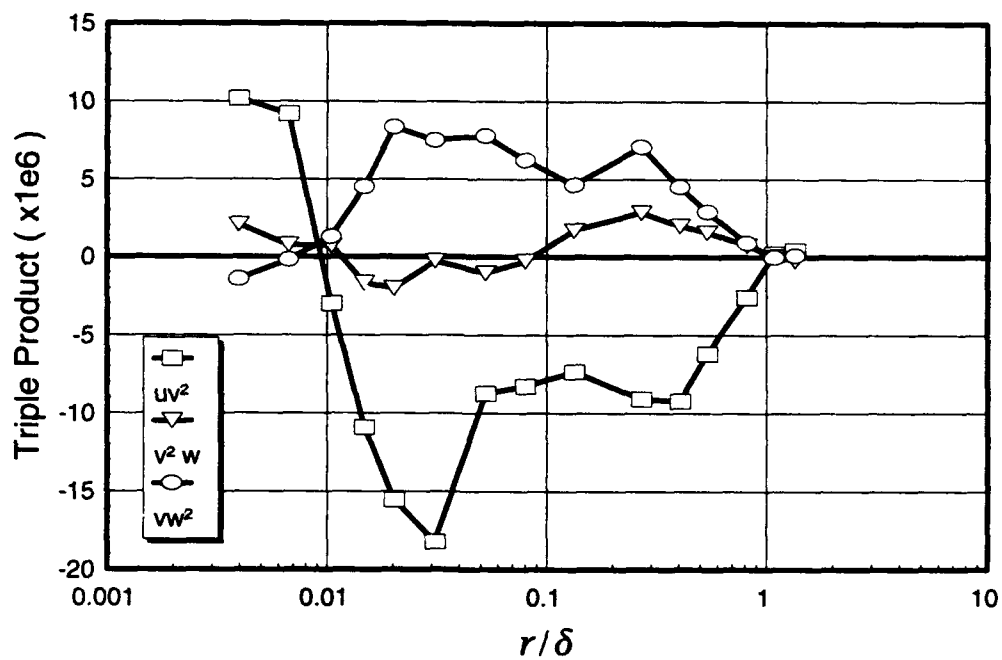


Figure 208. Boundary-layer profiles of velocity triple products (2), $x/L = 0.600$, $\phi = 170^\circ$.

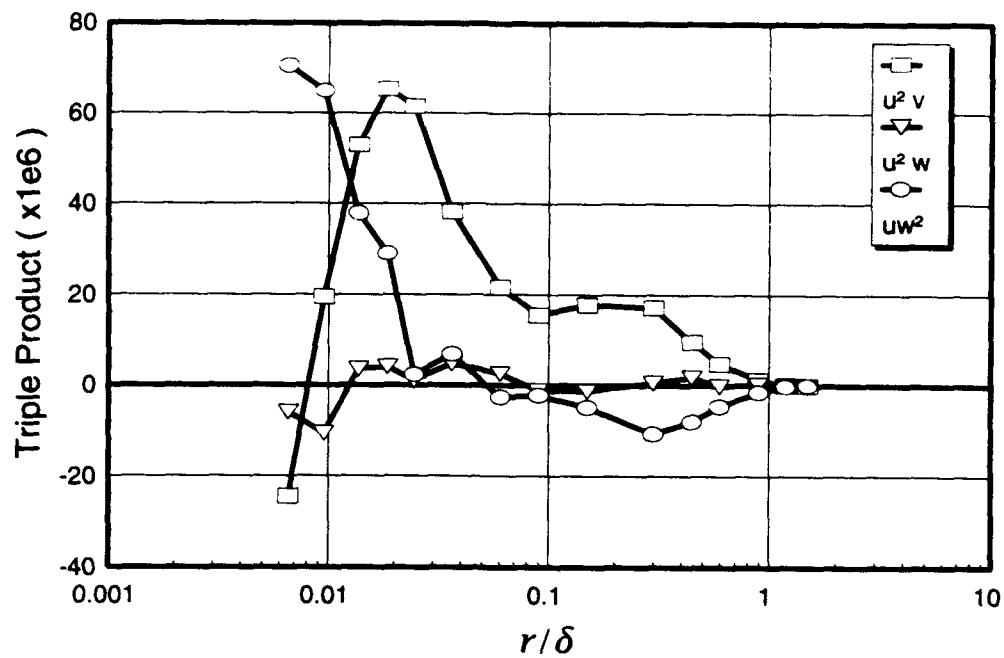


Figure 209. Boundary-layer profiles of velocity triple products (1), $x/L = 0.600$, $\phi = 180^\circ$.

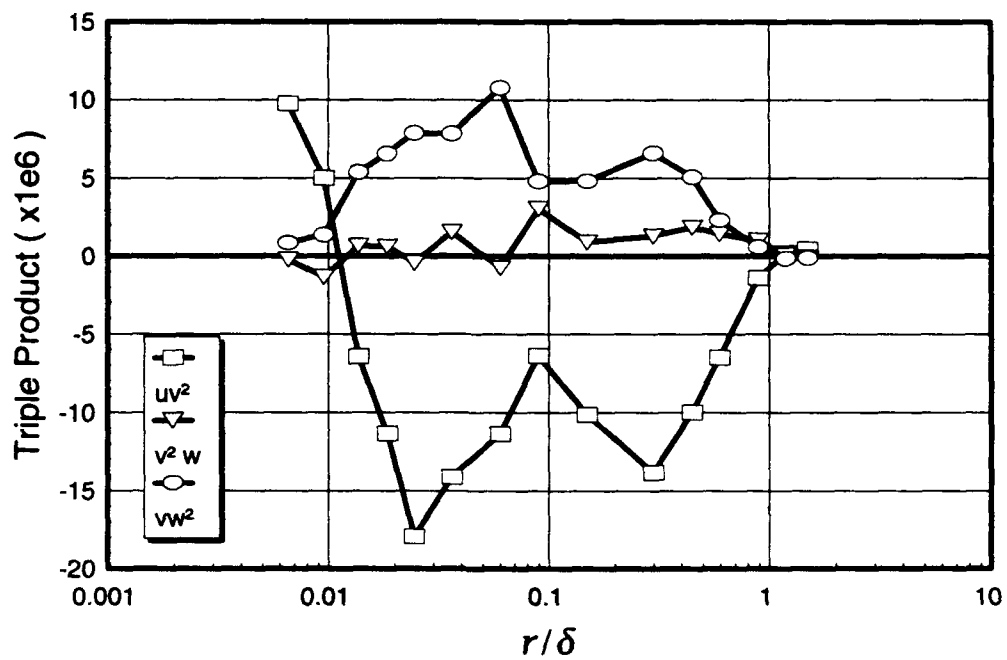


Figure 210. Boundary-layer profiles of velocity triple products (2), $x/L = 0.600$, $\phi = 180^\circ$.

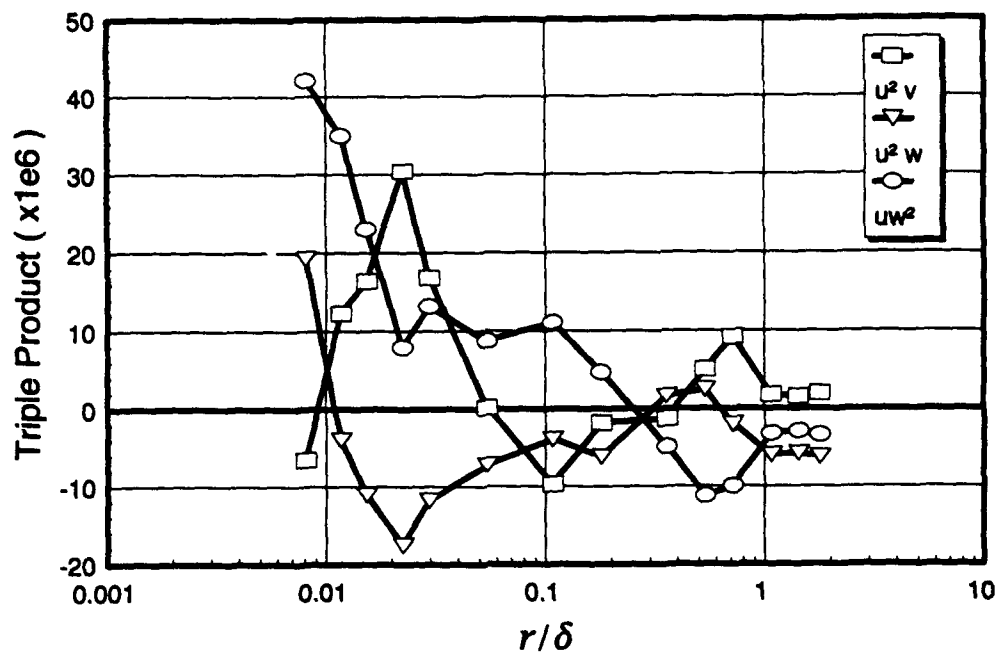


Figure 211. Boundary-layer profiles of velocity triple products (1), $x/L = 0.752$, $\phi = 120^\circ$.

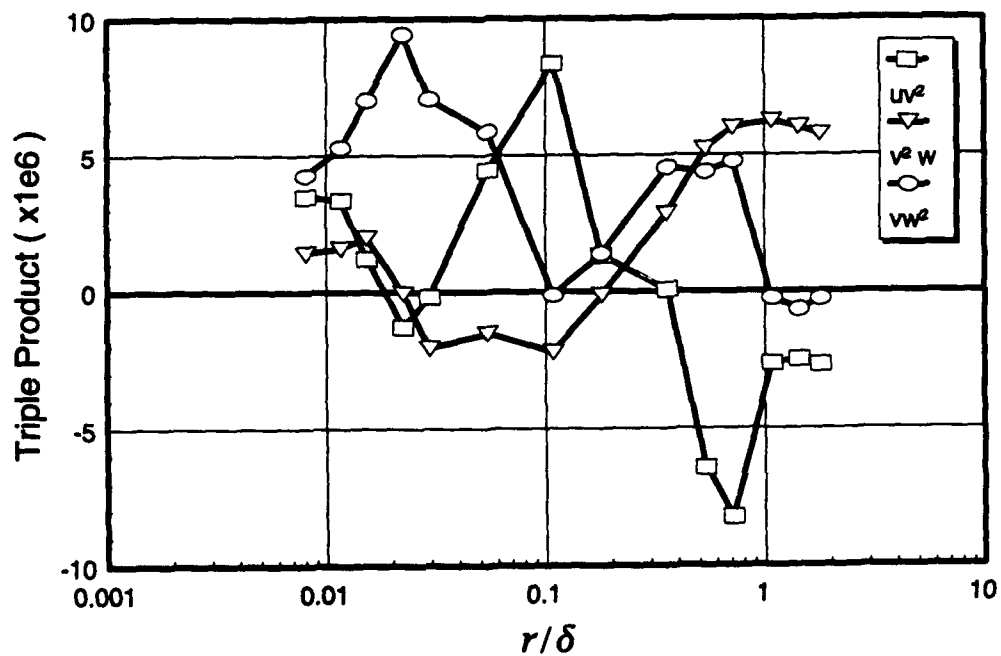


Figure 212. Boundary-layer profiles of velocity triple products (2), $x/L = 0.752$, $\phi = 120^\circ$.

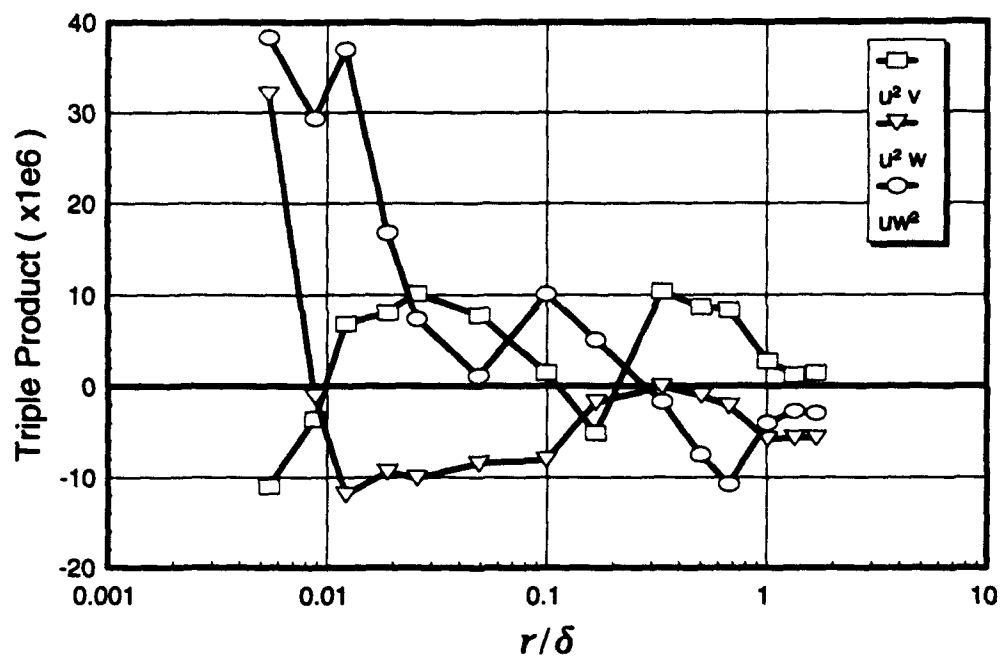


Figure 213. Boundary-layer profiles of velocity triple products (1), $x/L = 0.752$, $\phi = 123^\circ$.

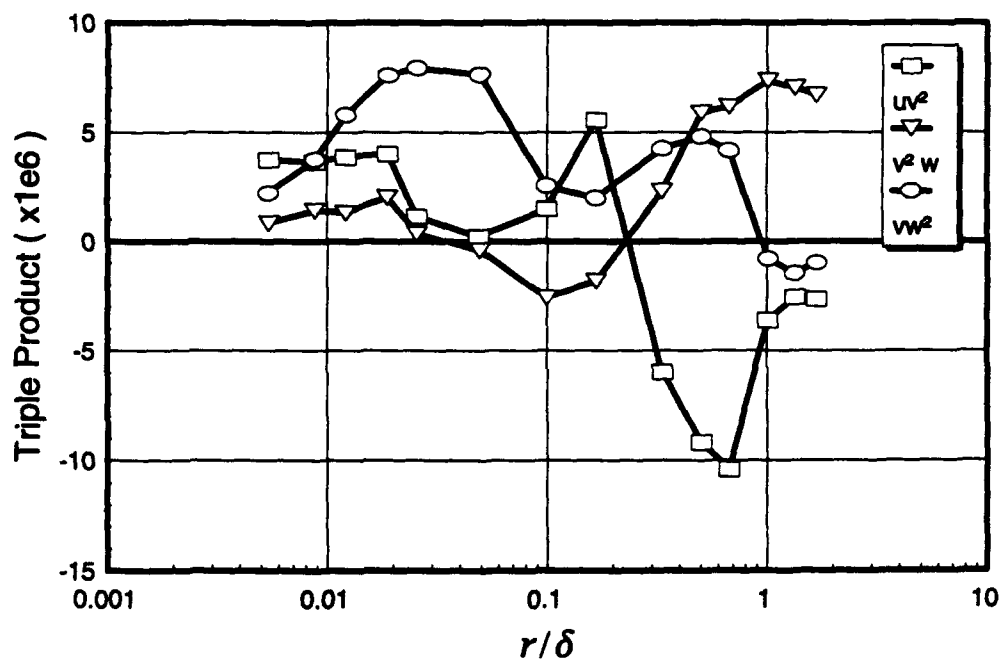


Figure 214. Boundary-layer profiles of velocity triple products (2), $x/L = 0.752$, $\phi = 123^\circ$.

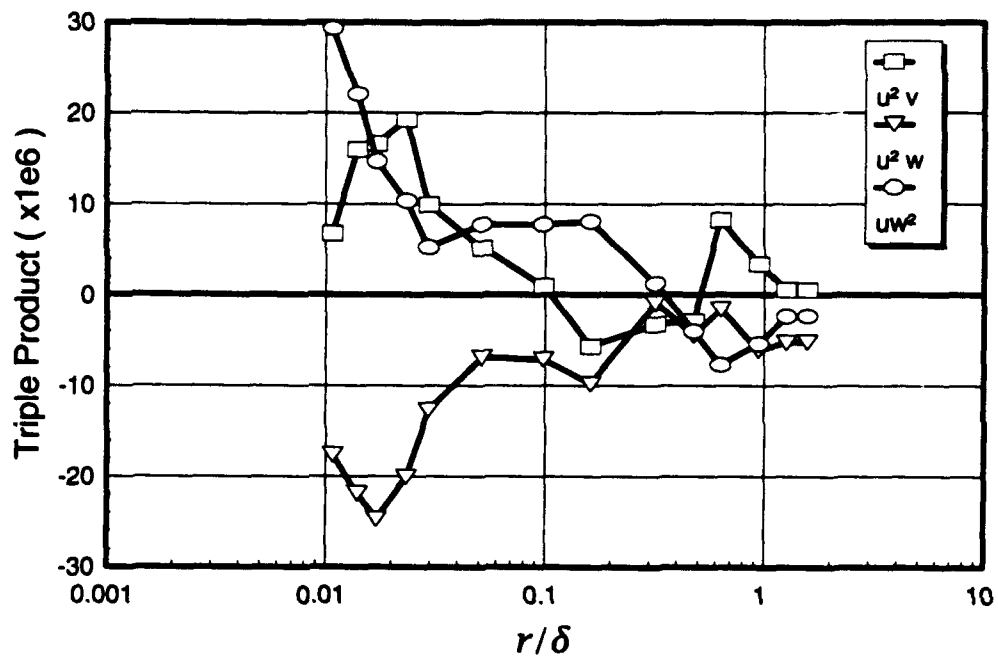


Figure 215. Boundary-layer profiles of velocity triple products (1), $x/L = 0.752$, $\phi = 125^\circ$.

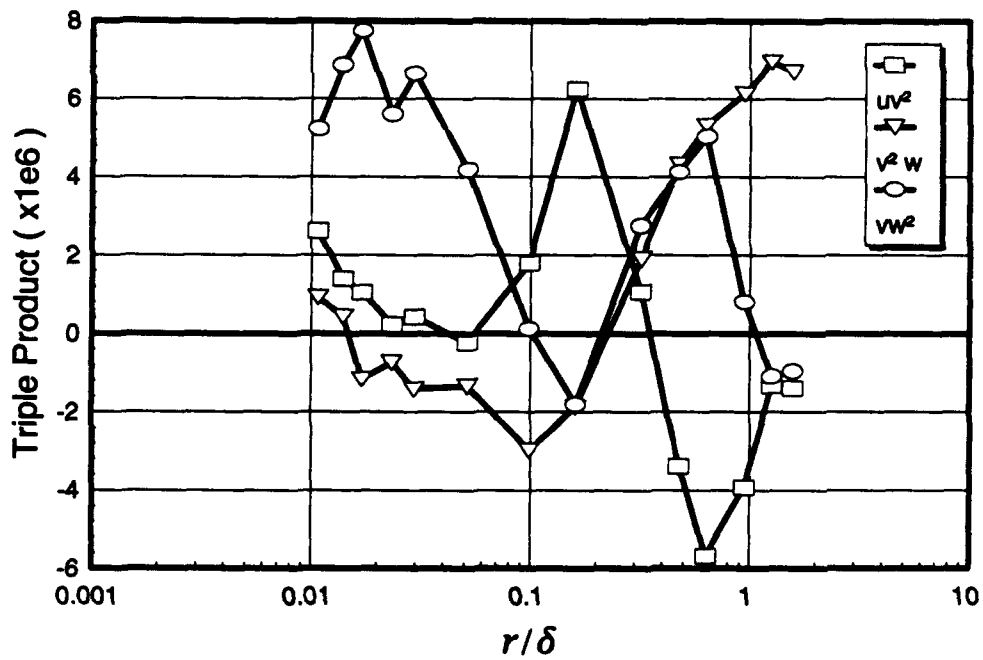


Figure 216. Boundary-layer profiles of velocity triple products (2), $x/L = 0.752$, $\phi = 125^\circ$.

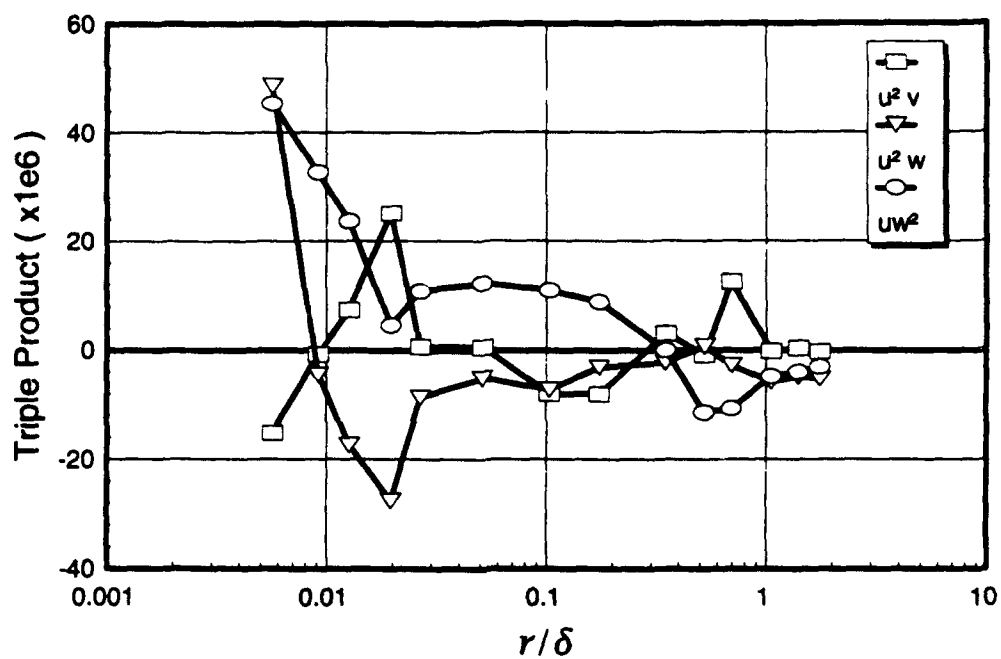


Figure 217. Boundary-layer profiles of velocity triple products (1), $x/L = 0.762$, $\phi = 120^\circ$.

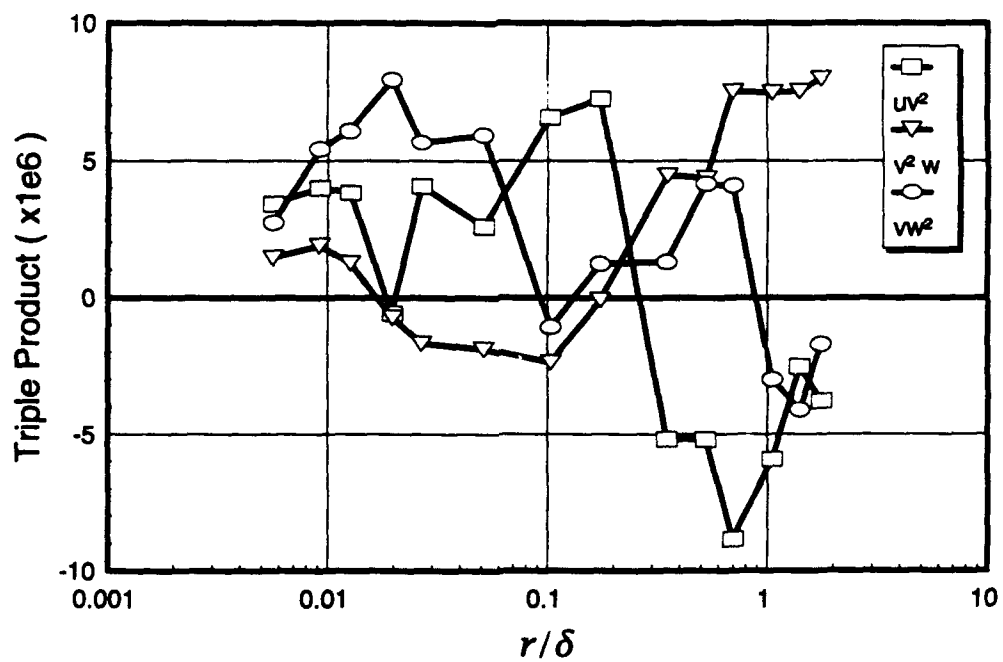


Figure 218. Boundary-layer profiles of velocity triple products (2), $x/L = 0.762$, $\phi = 120^\circ$.

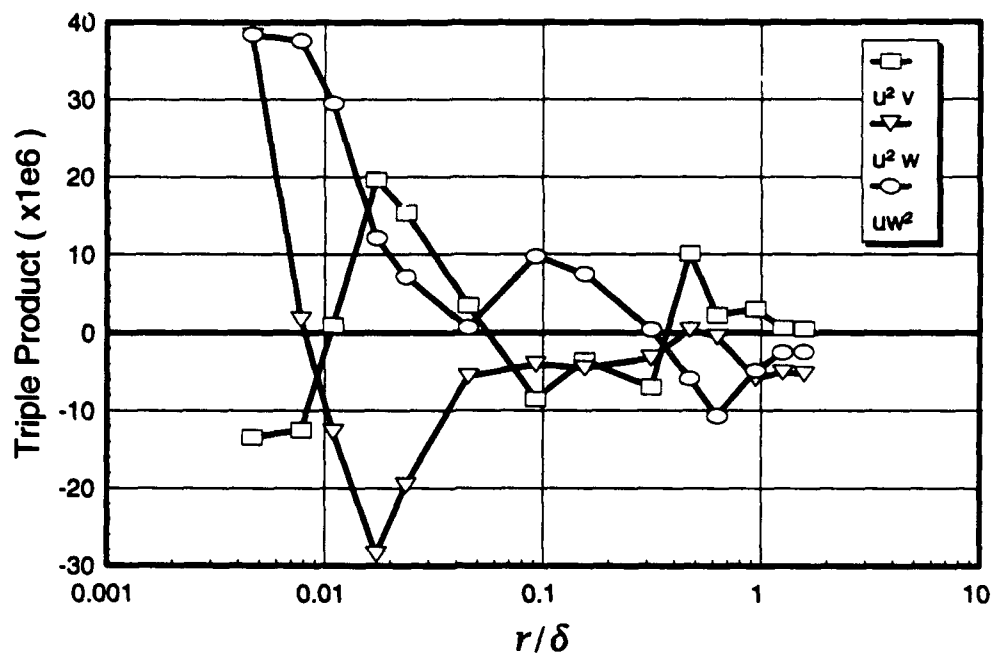


Figure 219. Boundary-layer profiles of velocity triple products (1), $x/L = 0.762$, $\phi = 123^\circ$.

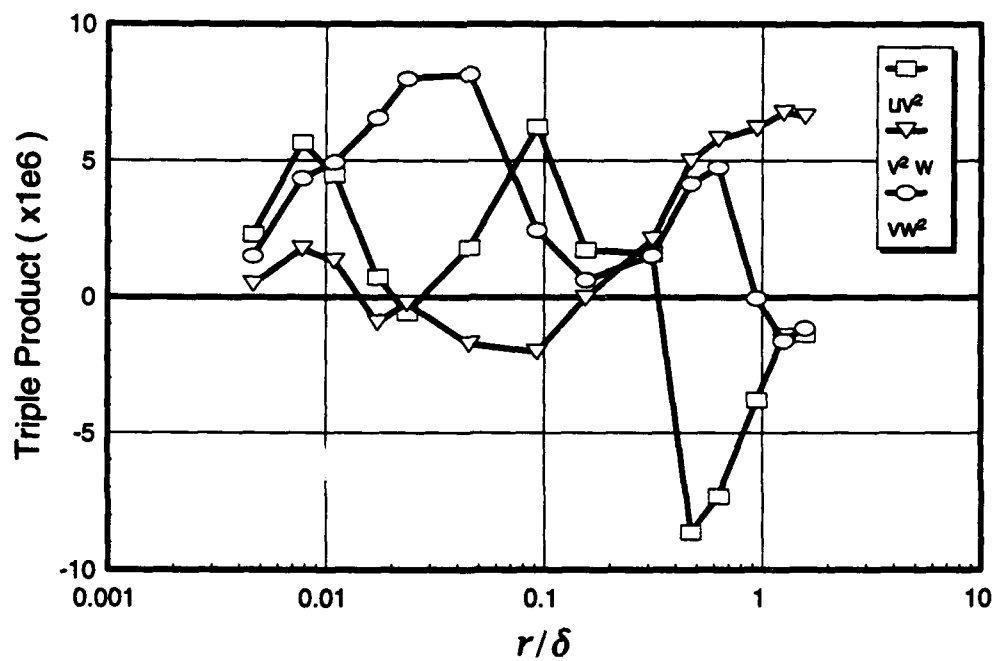


Figure 220. Boundary-layer profiles of velocity triple products (2), $x/L = 0.762$, $\phi = 123^\circ$.

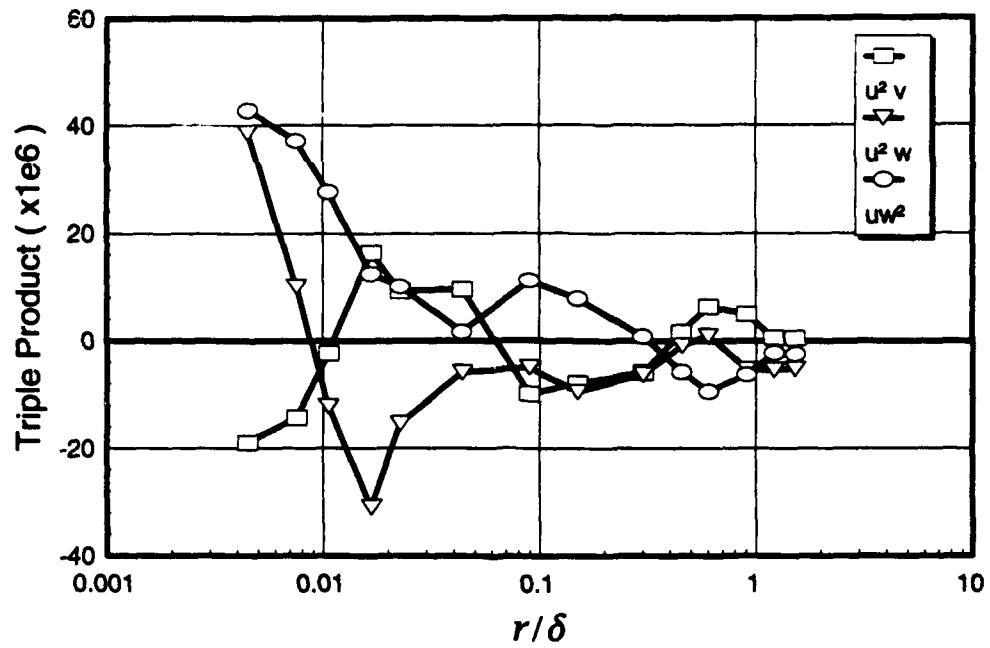


Figure 221. Boundary-layer profiles of velocity triple products (1), $x/L = 0.762$, $\phi = 125^\circ$.

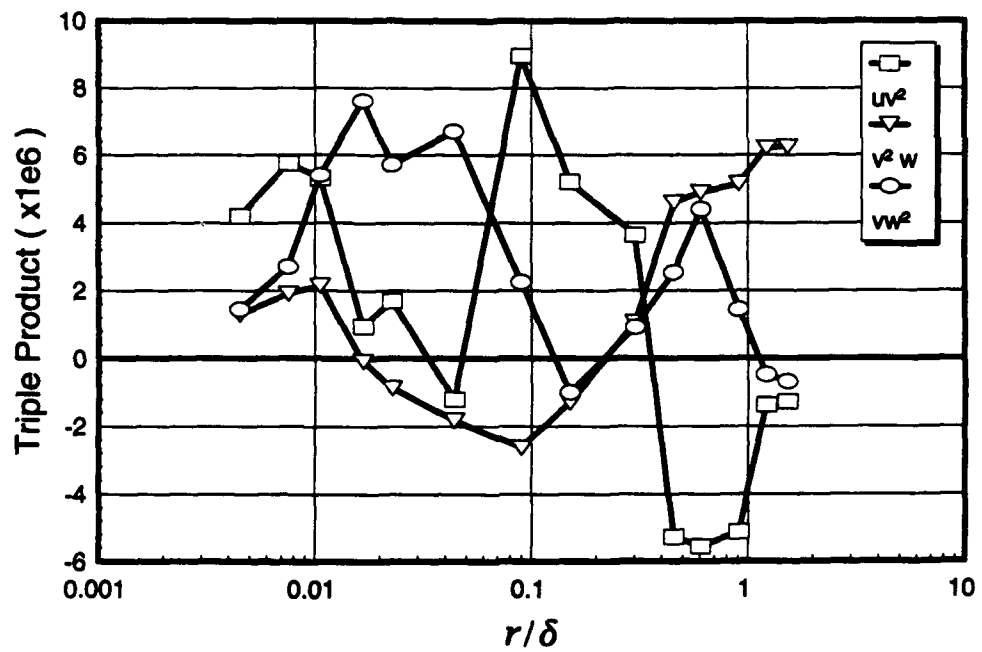


Figure 222. Boundary-layer profiles of velocity triple products (2), $x/L = 0.762$, $\phi = 125^\circ$.

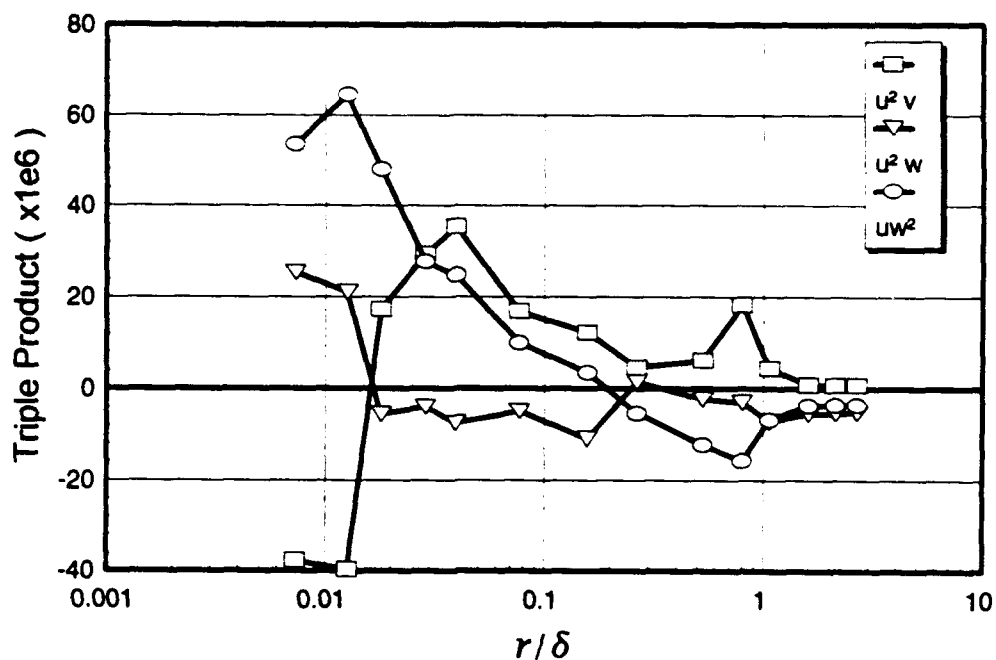


Figure 223. Boundary-layer profiles of velocity triple products (1), $x/L = 0.772$, $\phi = 105^\circ$.

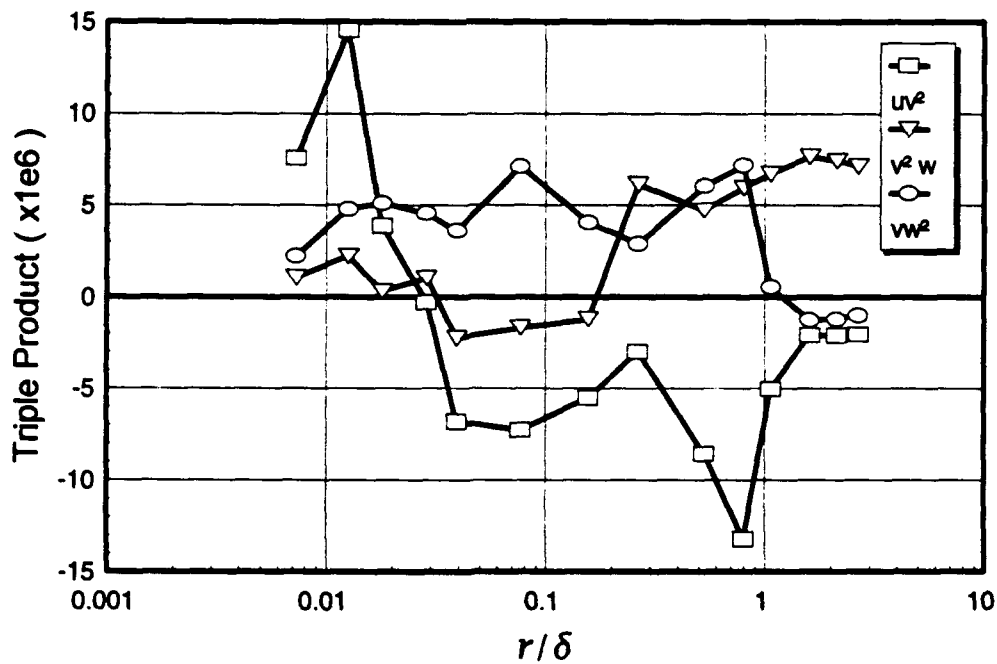


Figure 224. Boundary-layer profiles of velocity triple products (2), $x/L = 0.772$, $\phi = 105^\circ$.

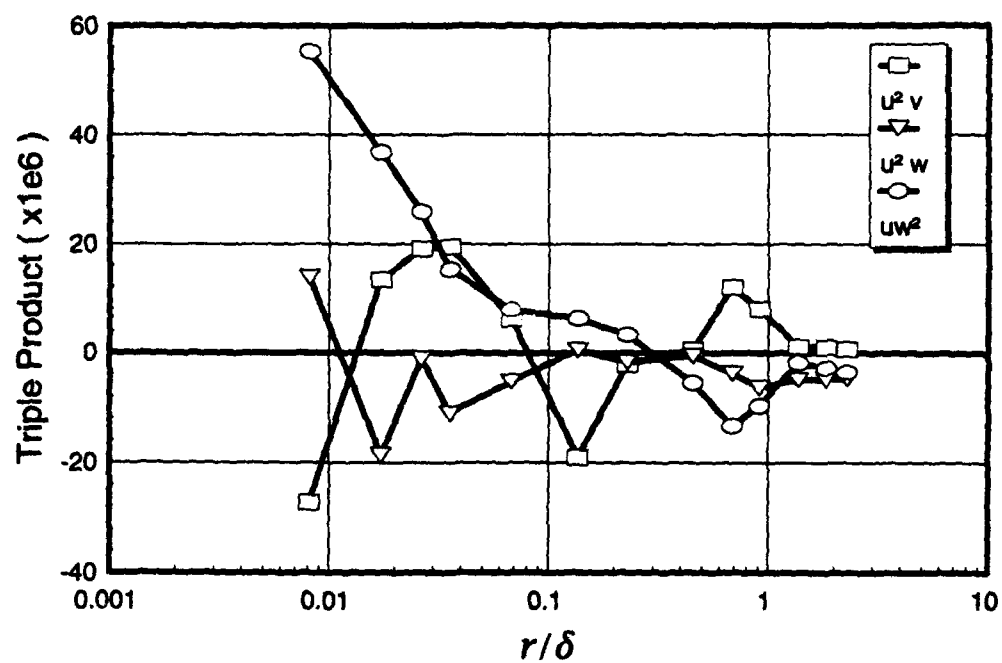


Figure 225. Boundary-layer profiles of velocity triple products (1), $x/L = 0.772$, $\phi = 110^\circ$.

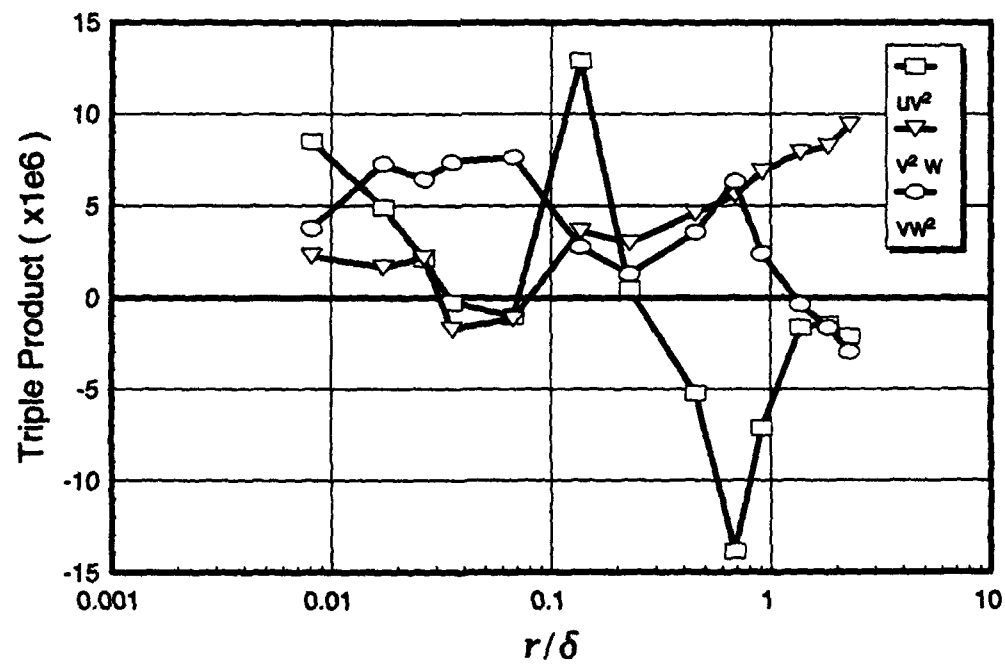


Figure 226. Boundary-layer profiles of velocity triple products (2), $x/L = 0.772$, $\phi = 110^\circ$.

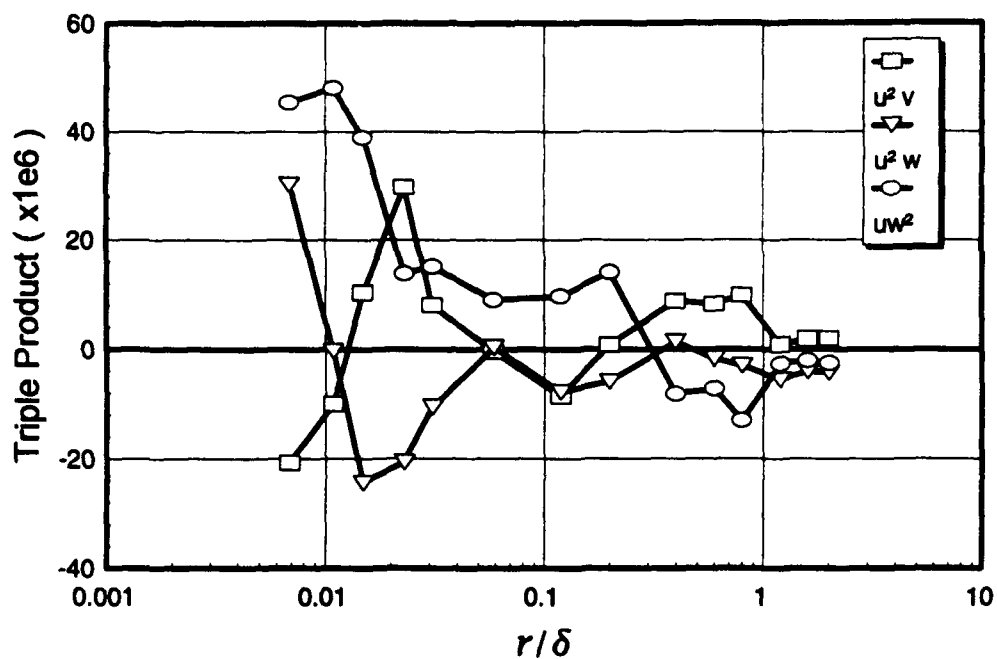


Figure 227. Boundary-layer profiles of velocity triple products (1), $x/L = 0.772$, $\phi = 115^\circ$.

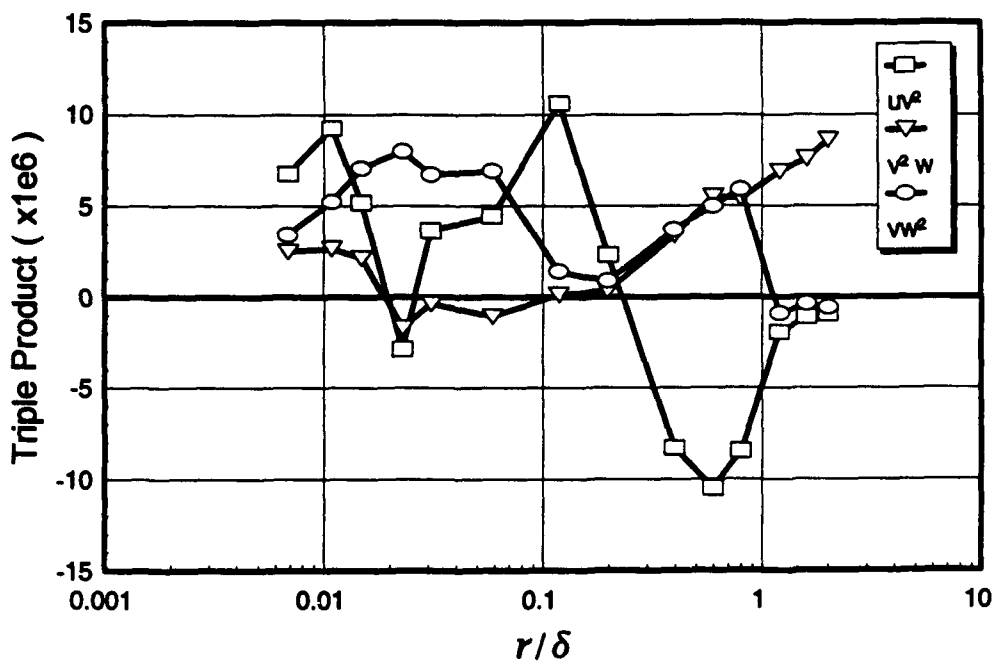


Figure 228. Boundary-layer profiles of velocity triple products (2), $x/L = 0.772$, $\phi = 115^\circ$.

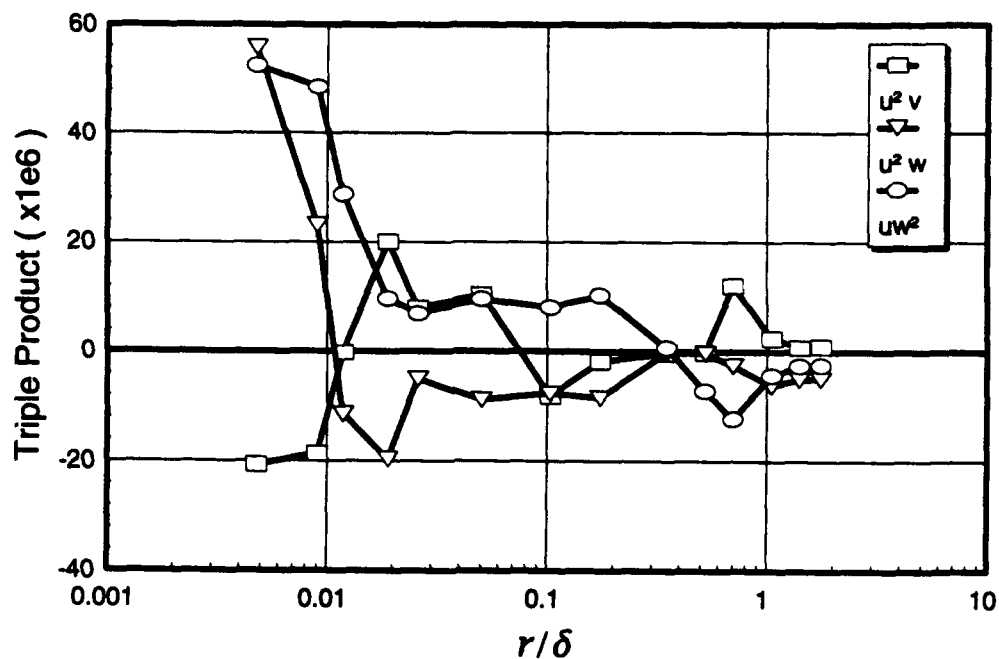


Figure 229. Boundary-layer profiles of velocity triple products (1), $x/L = 0.772$, $\phi = 120^\circ$.

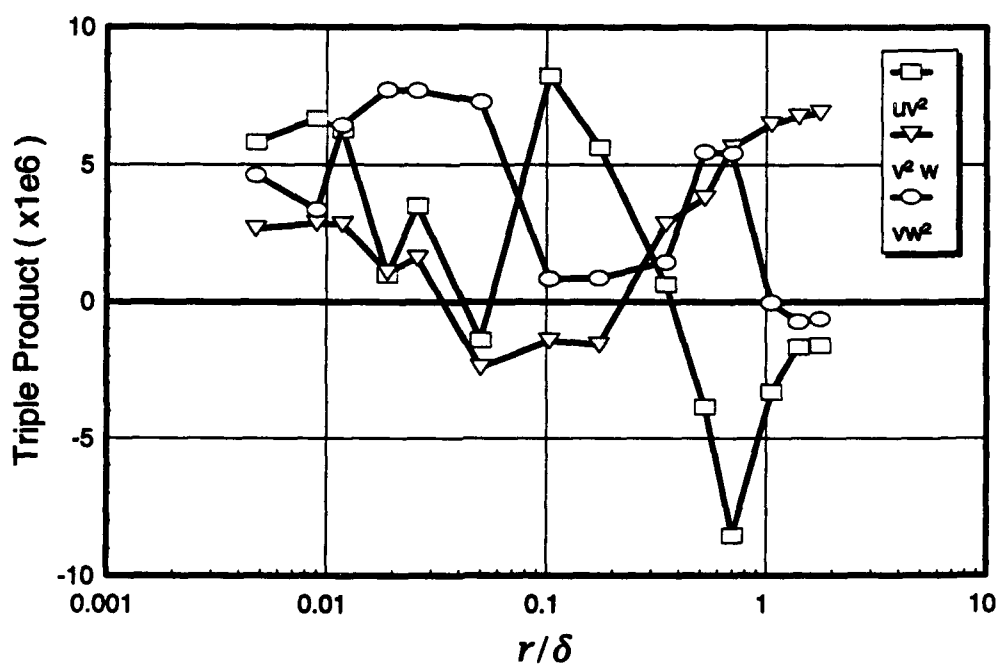


Figure 230. Boundary-layer profiles of velocity triple products (2), $x/L = 0.772$, $\phi = 120^\circ$.

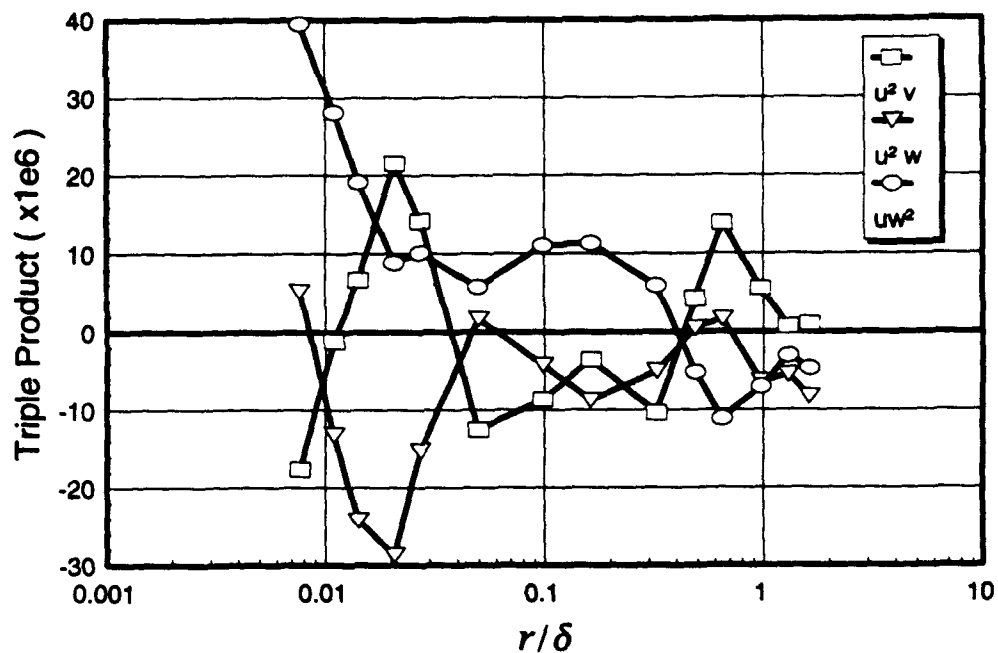


Figure 231. Boundary-layer profiles of velocity triple products (1), $x/L = 0.772$, $\phi = 123^\circ$.

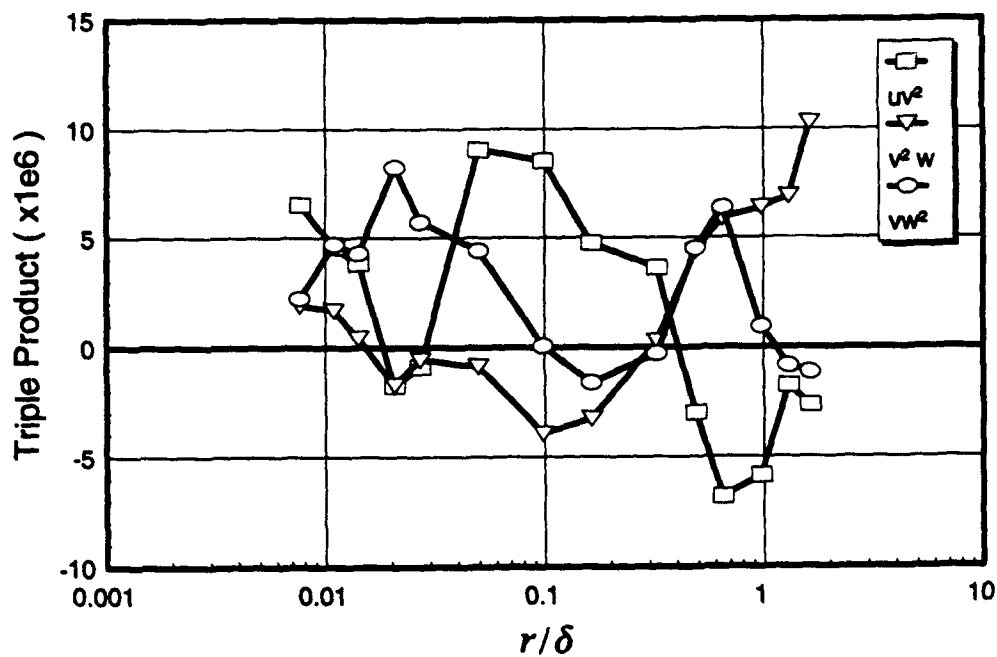


Figure 232. Boundary-layer profiles of velocity triple products (2), $x/L = 0.772$, $\phi = 123^\circ$.

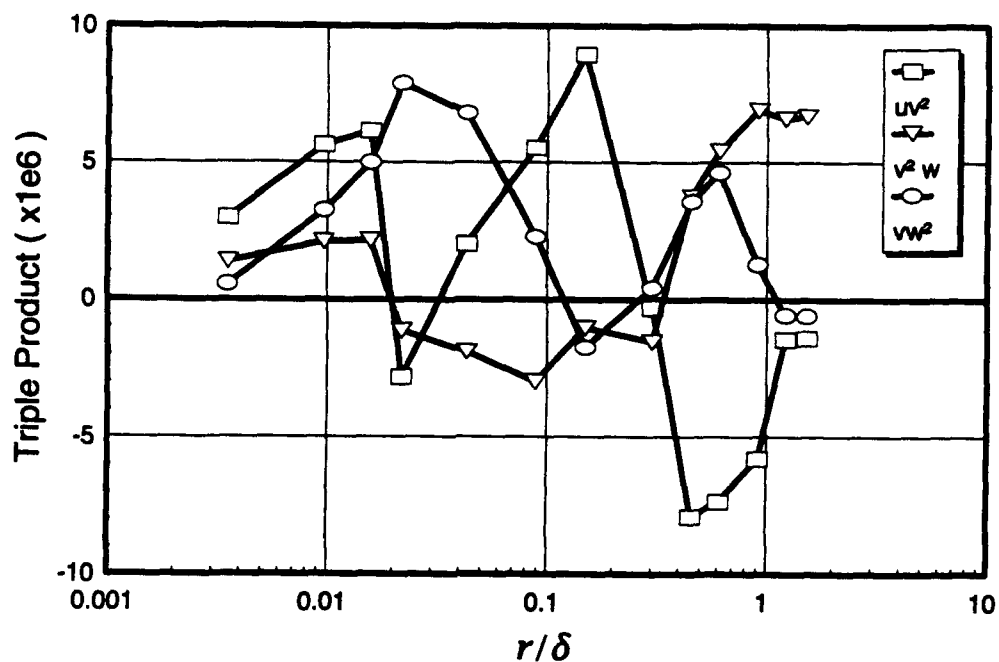


Figure 233. Boundary-layer profiles of velocity triple products (1), $x/L = 0.772$, $\phi = 125^\circ$.

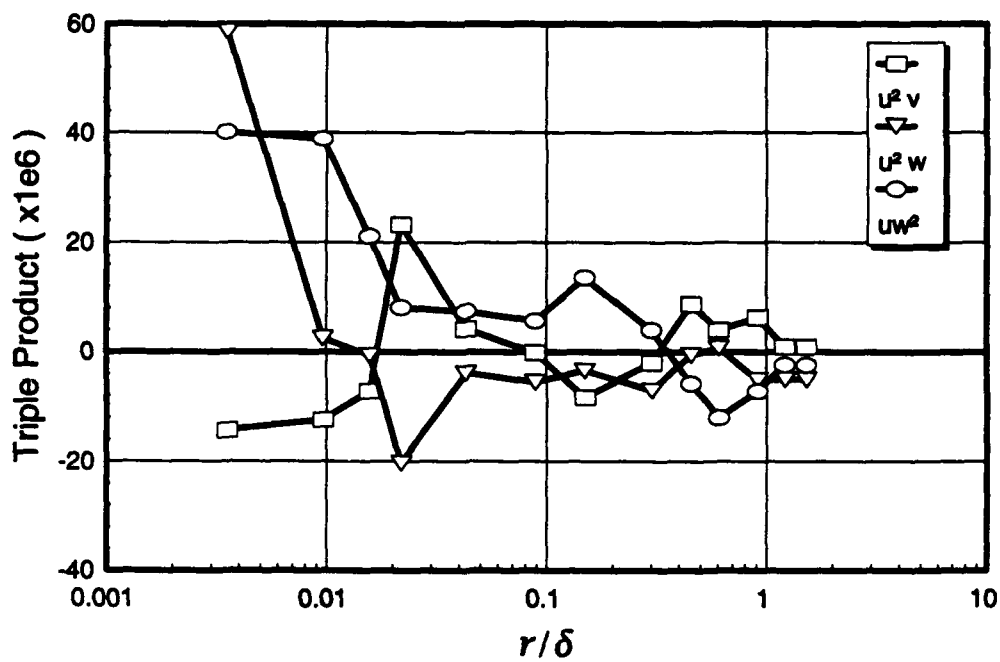


Figure 234. Boundary-layer profiles of velocity triple products (2), $x/L = 0.772$, $\phi = 125^\circ$.

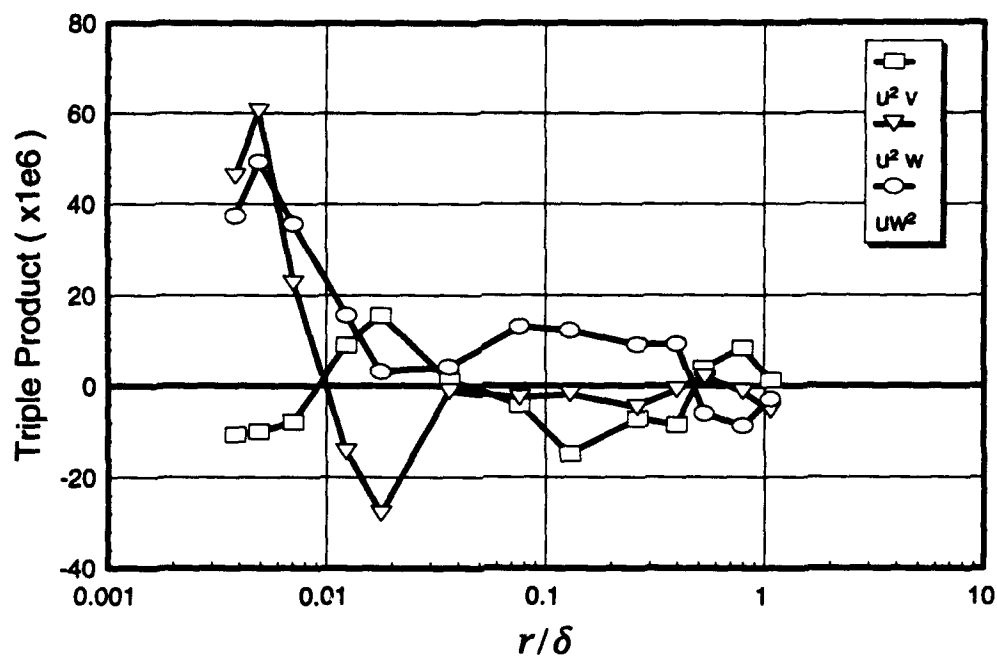


Figure 235. Boundary-layer profiles of velocity triple products (1), $x/L = 0.772$, $\phi = 130^\circ$.

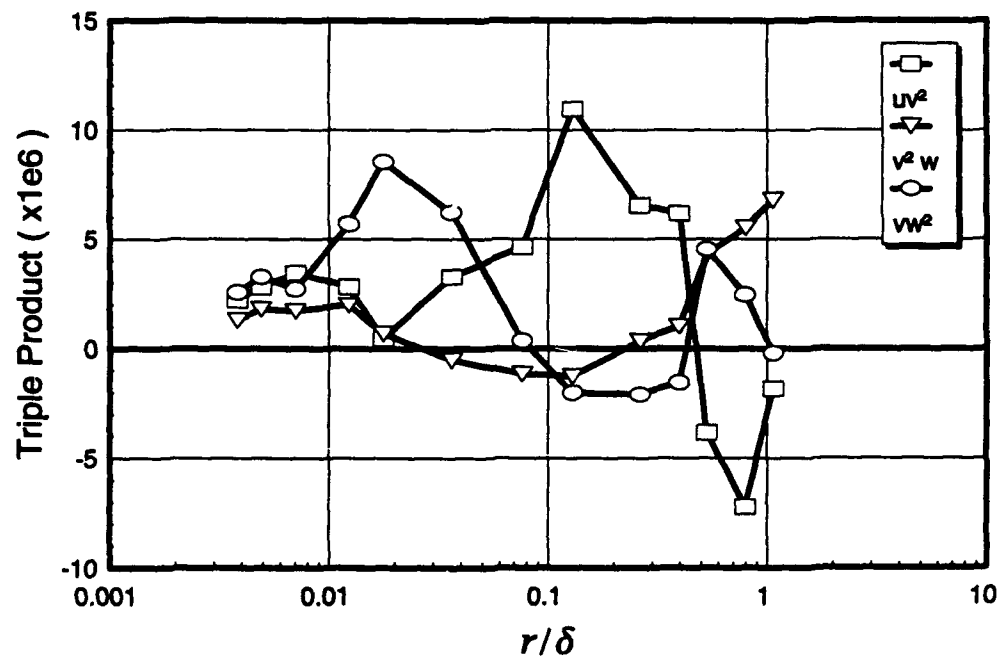


Figure 236. Boundary-layer profiles of velocity triple products (2), $x/L = 0.772$, $\phi = 130^\circ$.

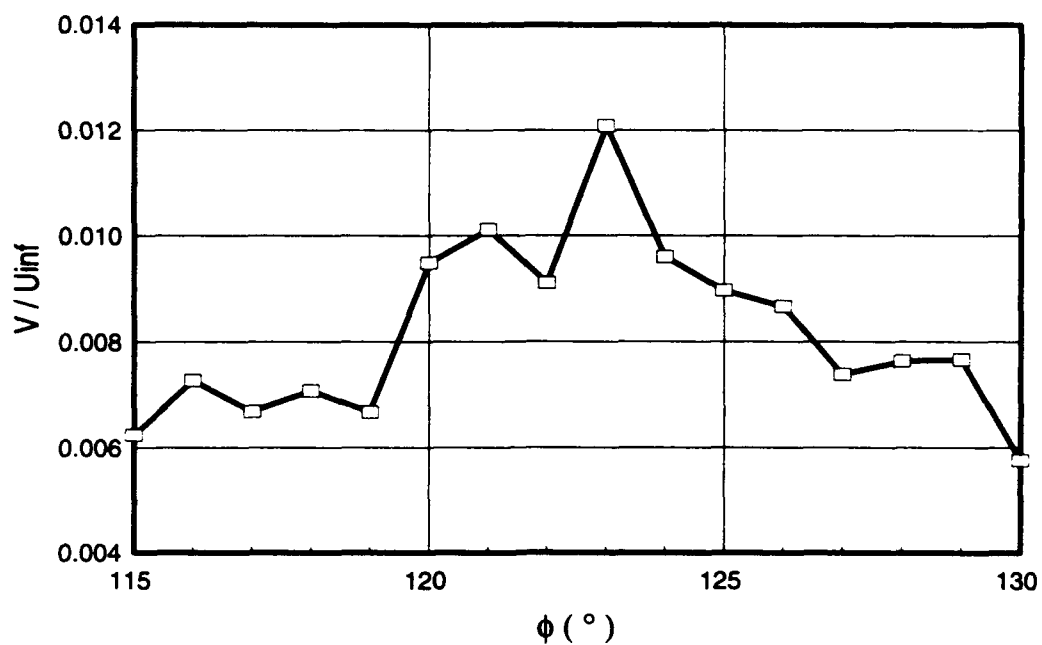


Figure 237. Circumferential profile of wall-normal velocity, $x/L = 0.772$, $r = 0.25$ cm.

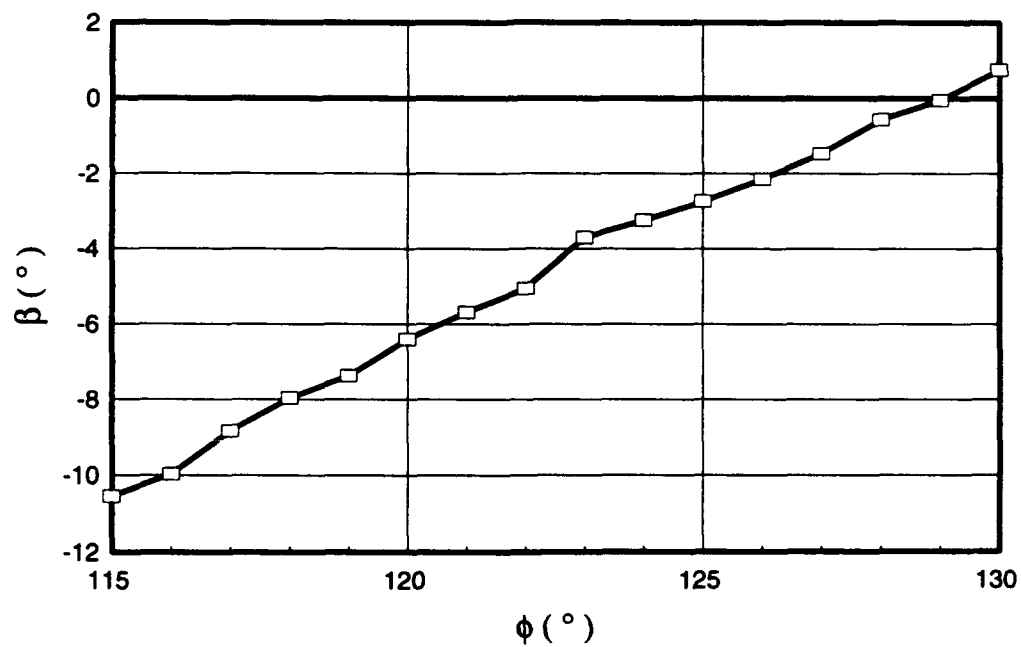


Figure 238. Circumferential profile of flow angle, $x/L = 0.772$, $r = 0.25$ cm.

APPENDIX A: OIL FLOW AND SURFACE PRESSURE MEASUREMENTS *

A.1 Surface Oil Flow Visualization

High Reynolds number simulation using a circular trip at $x/L = 0.2$ shows very close agreement [in separation line location] with the skin friction measurements of Meier and Kreplin (1980) and is shown in Figure A1. The surface oil flow results for 10 degrees angle of attack are shown in Figure A2.

A.2 Surface Pressure Measurements

The mean pressure coefficients at 10 degrees angle of attack are presented in Figures A3 to A12 along with the rms pressure fluctuations and potential flow solutions. The potential flow solution is derived in Appendix B [of Ahn (1992)]. The mean pressure coefficients are also compared to the data measured by Meier et al. (1986) at 10 degrees angle of attack.

At 10 degrees angle of attack, overall mean values are slightly higher than those of Meier et al. (1986). The difference in terms of pressure coefficient is $\Delta C_p = 0.01$. Meier et al. (1986) obtained the data in an open jet wind tunnel whereas the present data are obtained in a closed test section wind tunnel. The correction applied for an uncertain tunnel reference pressure (Meier et al., 1986) might have caused this discrepancy which is consistent throughout the measured data, even at 30 degrees angle of attack. The mean pressure distribution closely follows the potential flow solution down to $x/L = 0.565$. Starting from $x/L = 0.689$ and further downstream, the measured distribution is off from the potential flow, which indicates viscous and separating flow.

For the attached flow at 10 degrees angle of attack, the root-mean-square pressure fluctuation, p_{rms}/Q , is close to 0.01. The rms pressure fluctuation becomes higher as the separation is approached.

* The material contained within this section is reproduced from the work of Ahn (1992).

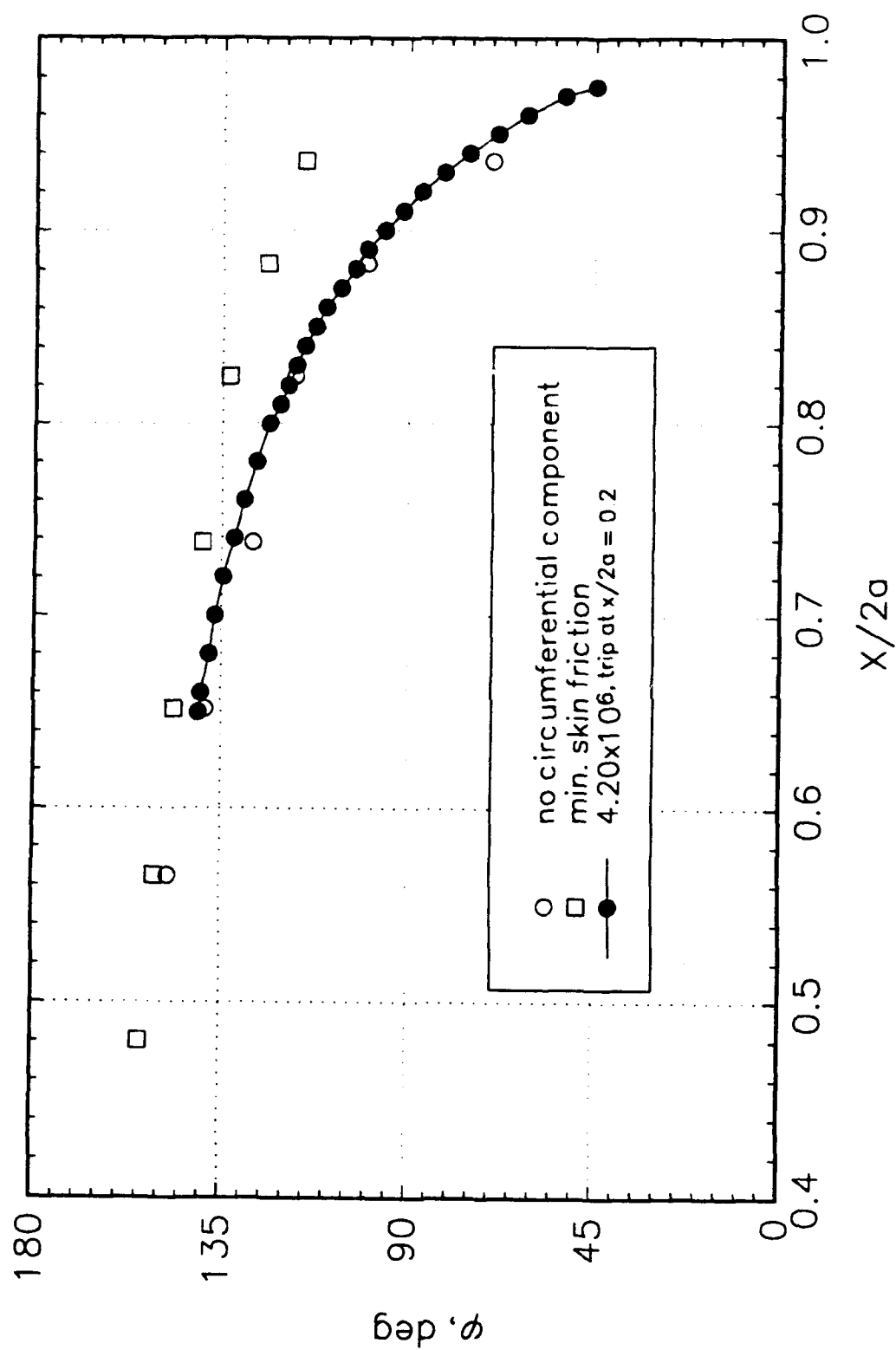


Figure A1. Primary separation location comparison, $\alpha = 10^\circ$. Open symbols are from Kreplin et al. (1985), $Re_L = 7.7 \times 10^6$.



Figure A2. Oil flow pattern at $\alpha = 10^\circ$, $Re_L = 4.20 \times 10^6$, trip at $x/L = 0.2$.

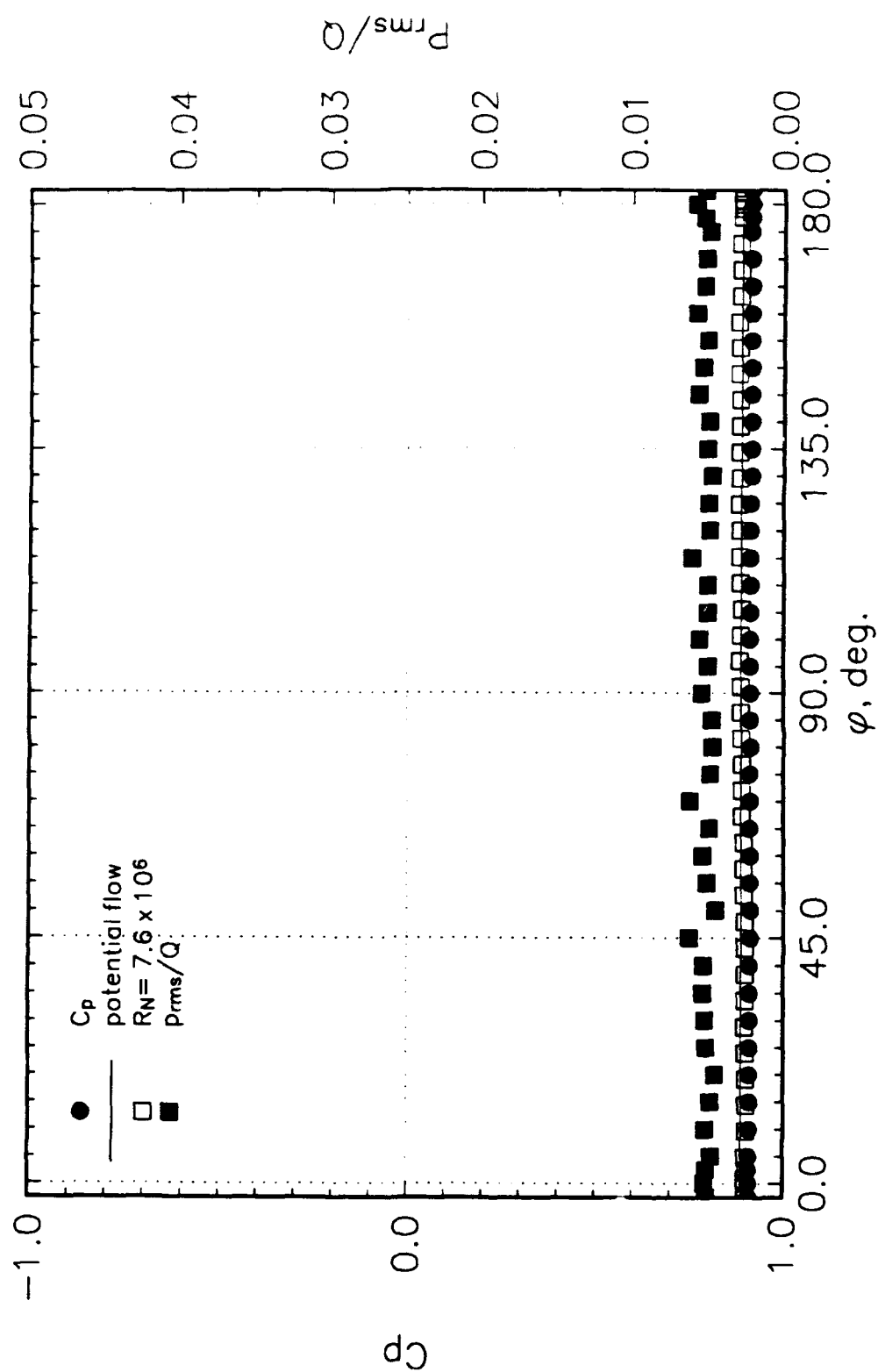


Figure A3. Mean and rms pressure distributions at $x/L = 0.0000$, $\alpha = 10^\circ$, $Re_L = 4.20 \times 10^6$. $Re_L = 7.7 \times 10^6$ data from Meier et al. (1986).

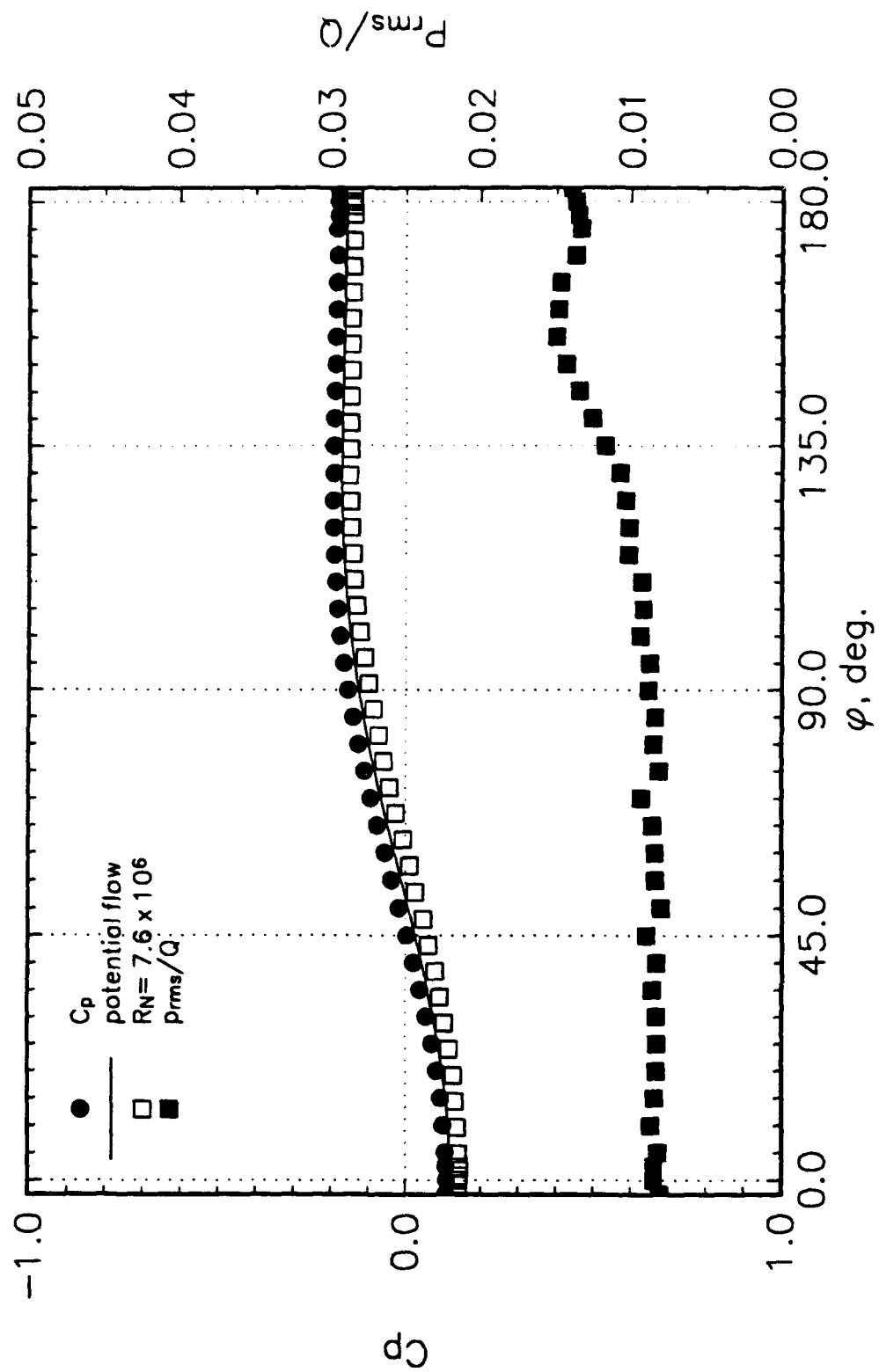


Figure A4. Mean and rms pressure distributions at $x/L = 0.1079$, $\alpha = 10^\circ$, $Re_L = 4.20 \times 10^6$.
 $Re_L = 7.7 \times 10^6$ data from Meier et al. (1986).

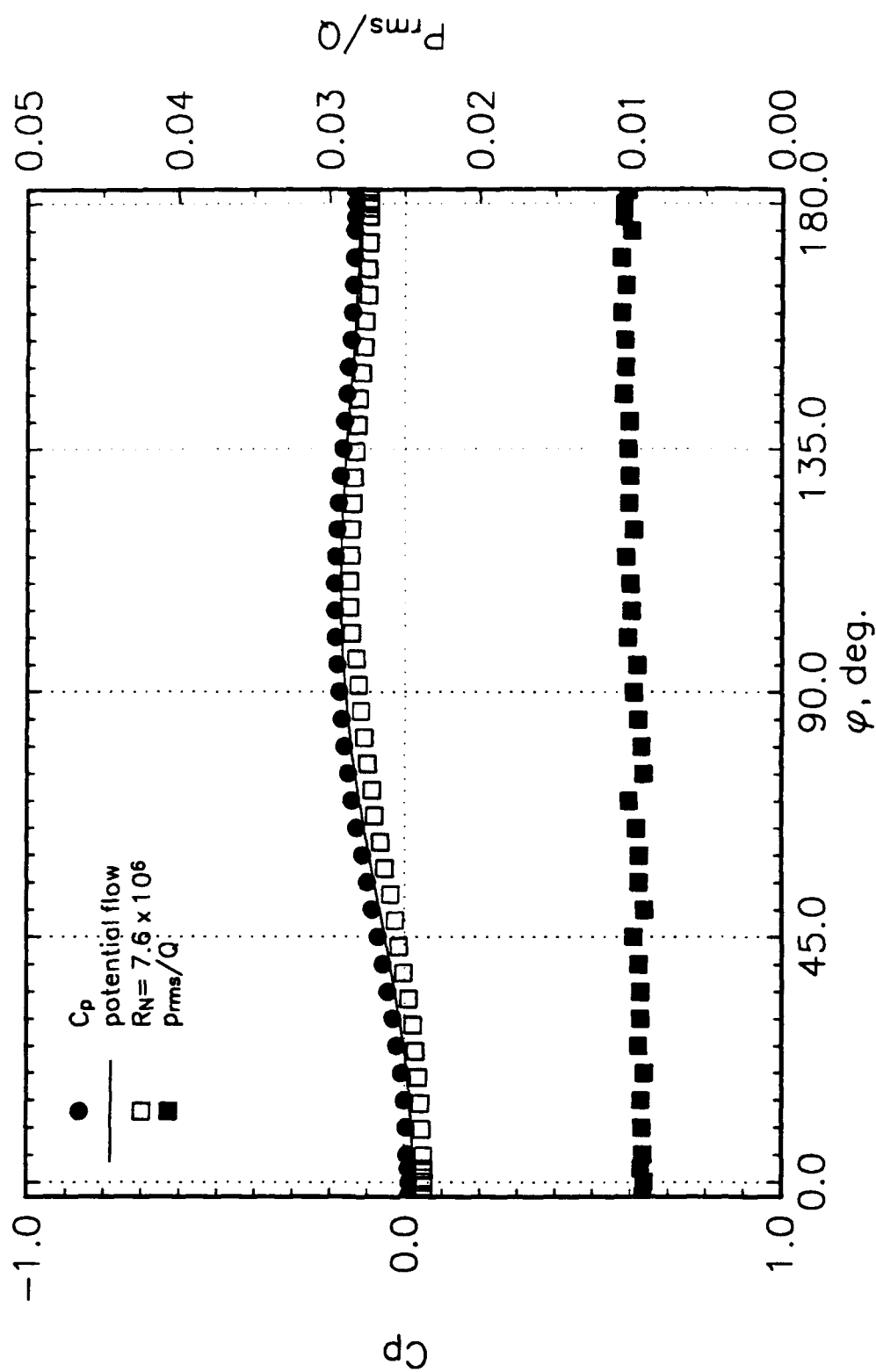


Figure A5. Mean and rms pressure distributions at $x/L = 0.2315$, $\alpha = 10^\circ$, $Re_L = 4.20 \times 10^6$.
 $Re_L = 7.7 \times 10^6$ data from Meier et al. (1986).

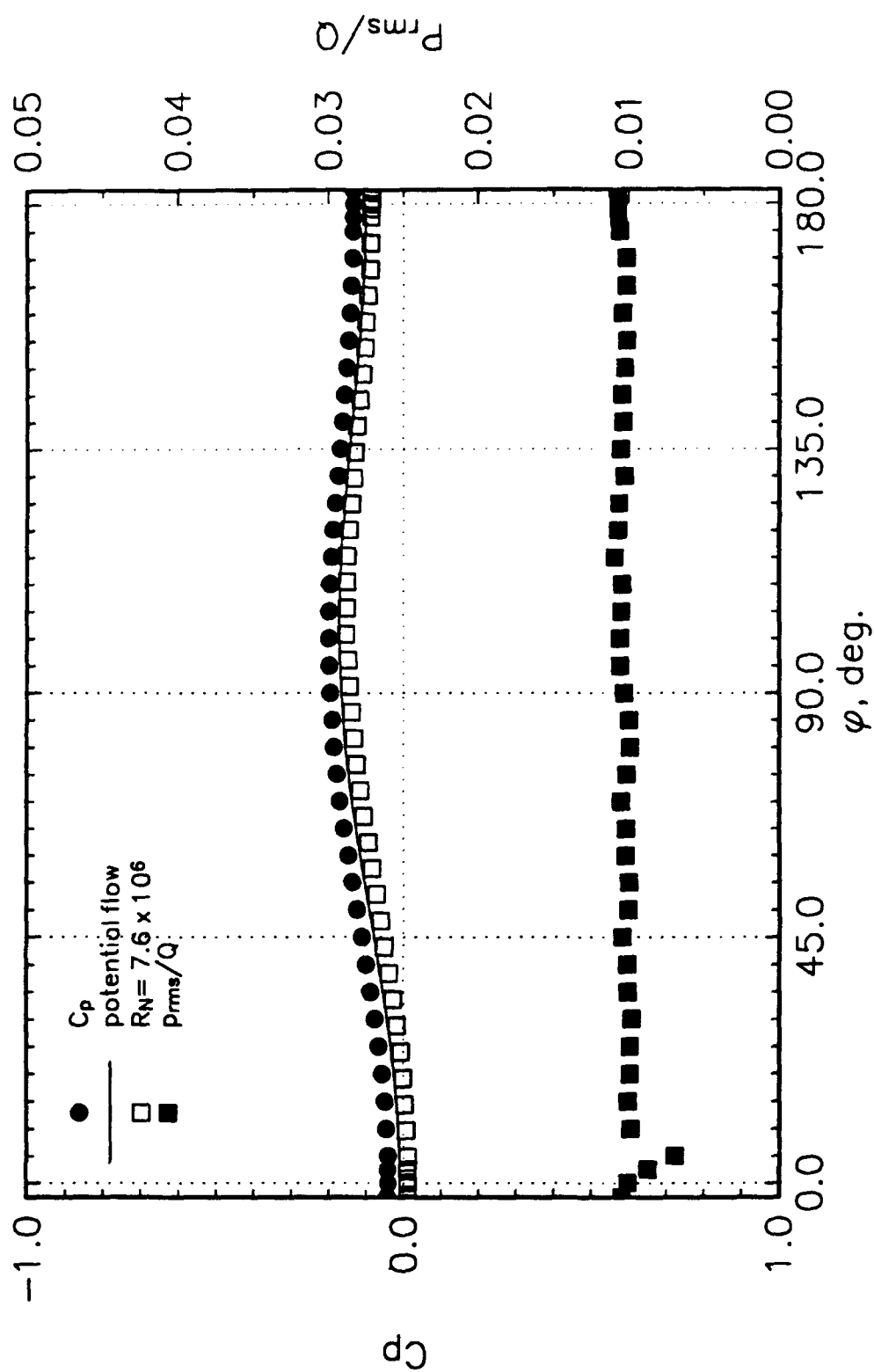


Figure A6. Mean and rms pressure distributions at $x/L = 0.3145$, $\alpha = 10^\circ$, $Re_L = 4.20 \times 10^6$. $Re_L = 7.7 \times 10^6$ data from Meier et al. (1986).

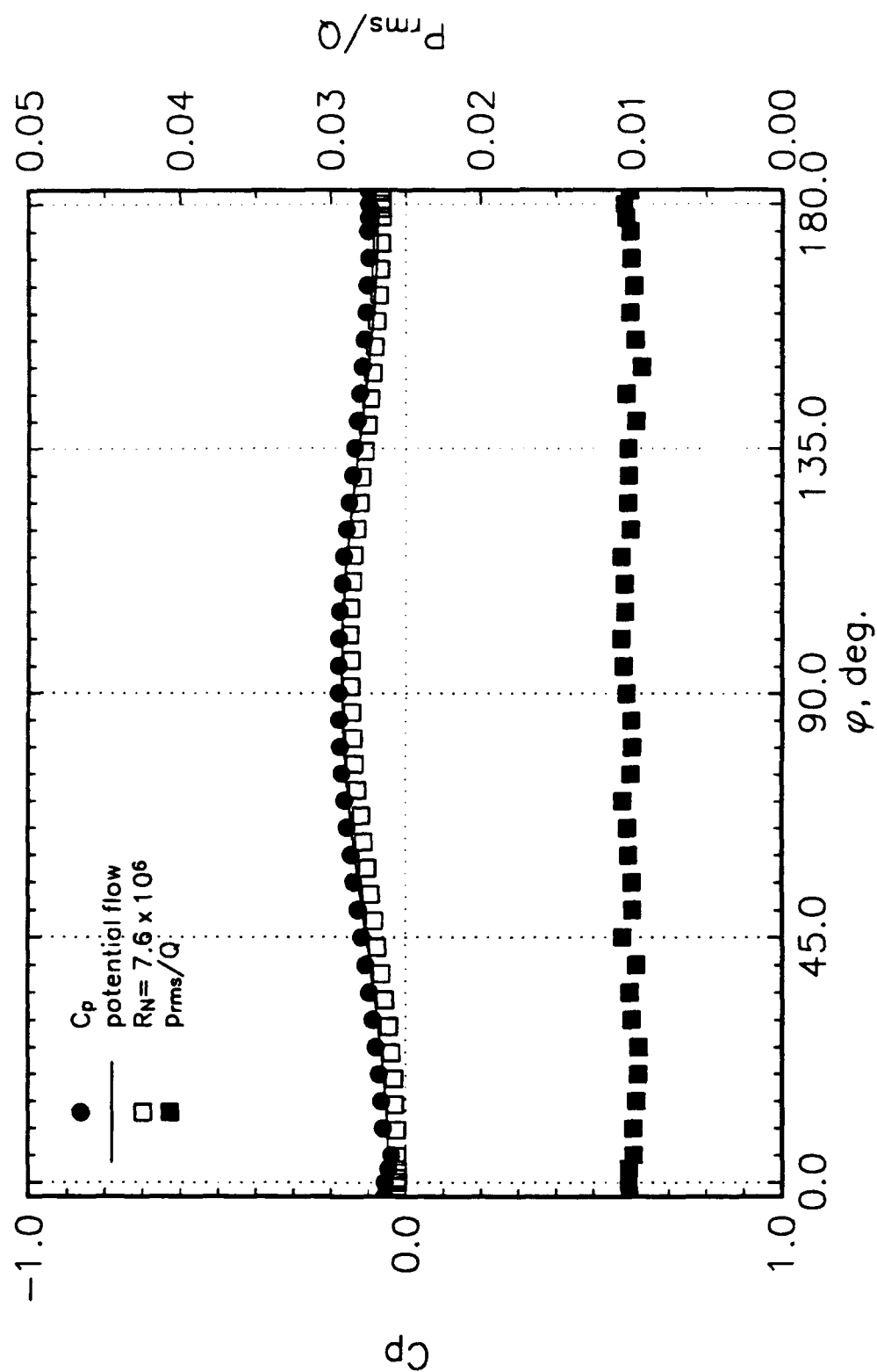


Figure A7. Mean and rms pressure distributions at $x/L = 0.4396$, $\alpha = 10^\circ$, $Re_L = 4.20 \times 10^6$.
 $Re_L = 7.7 \times 10^6$ data from Meier et al. (1986).

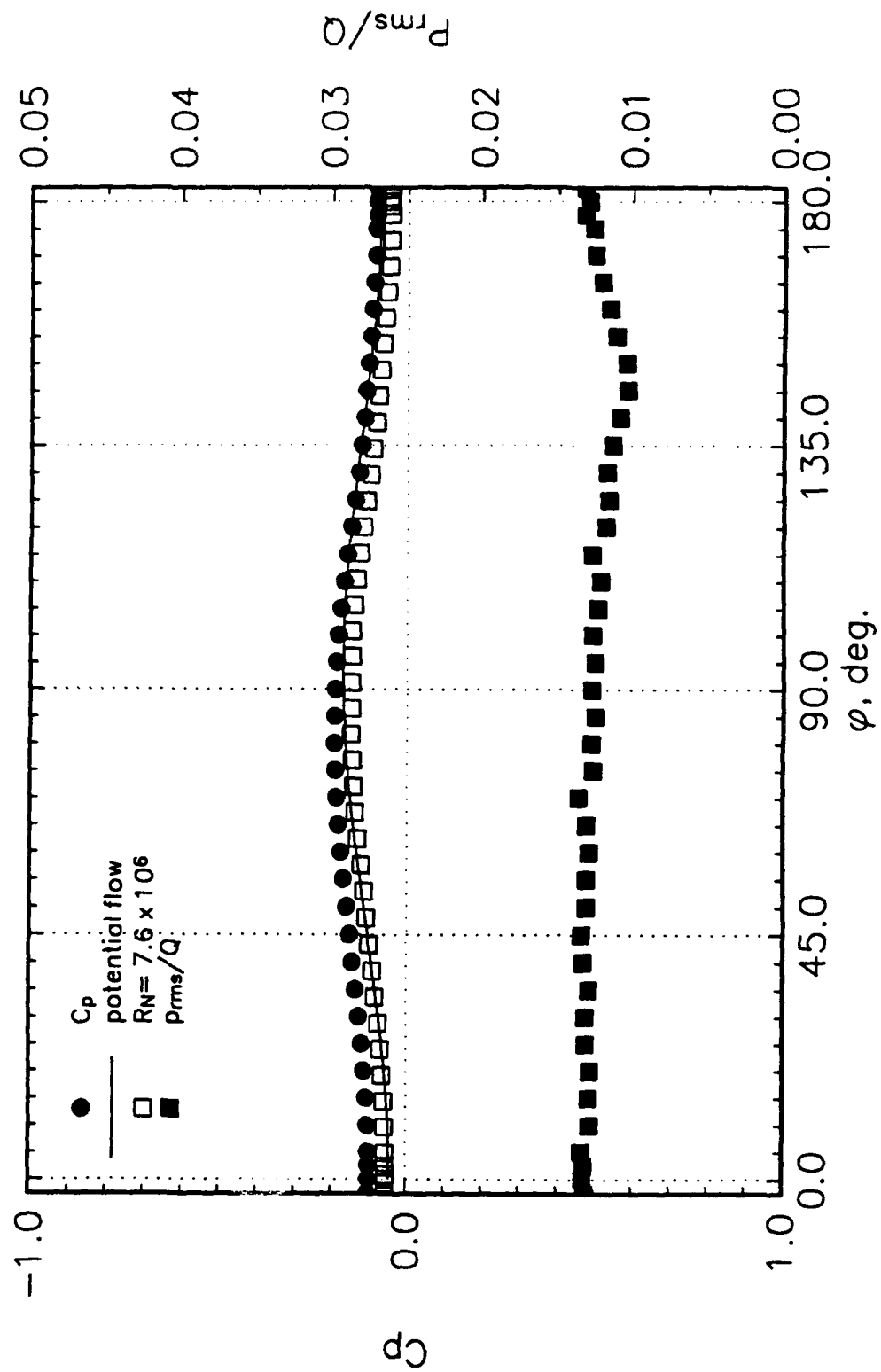


Figure A8. Mean and rms pressure distributions at $x/L = 0.5646$, $\alpha = 10^\circ$, $Re_L = 4.20 \times 10^6$.
 $Re_L = 7.7 \times 10^6$ data from Meier et al. (1986).

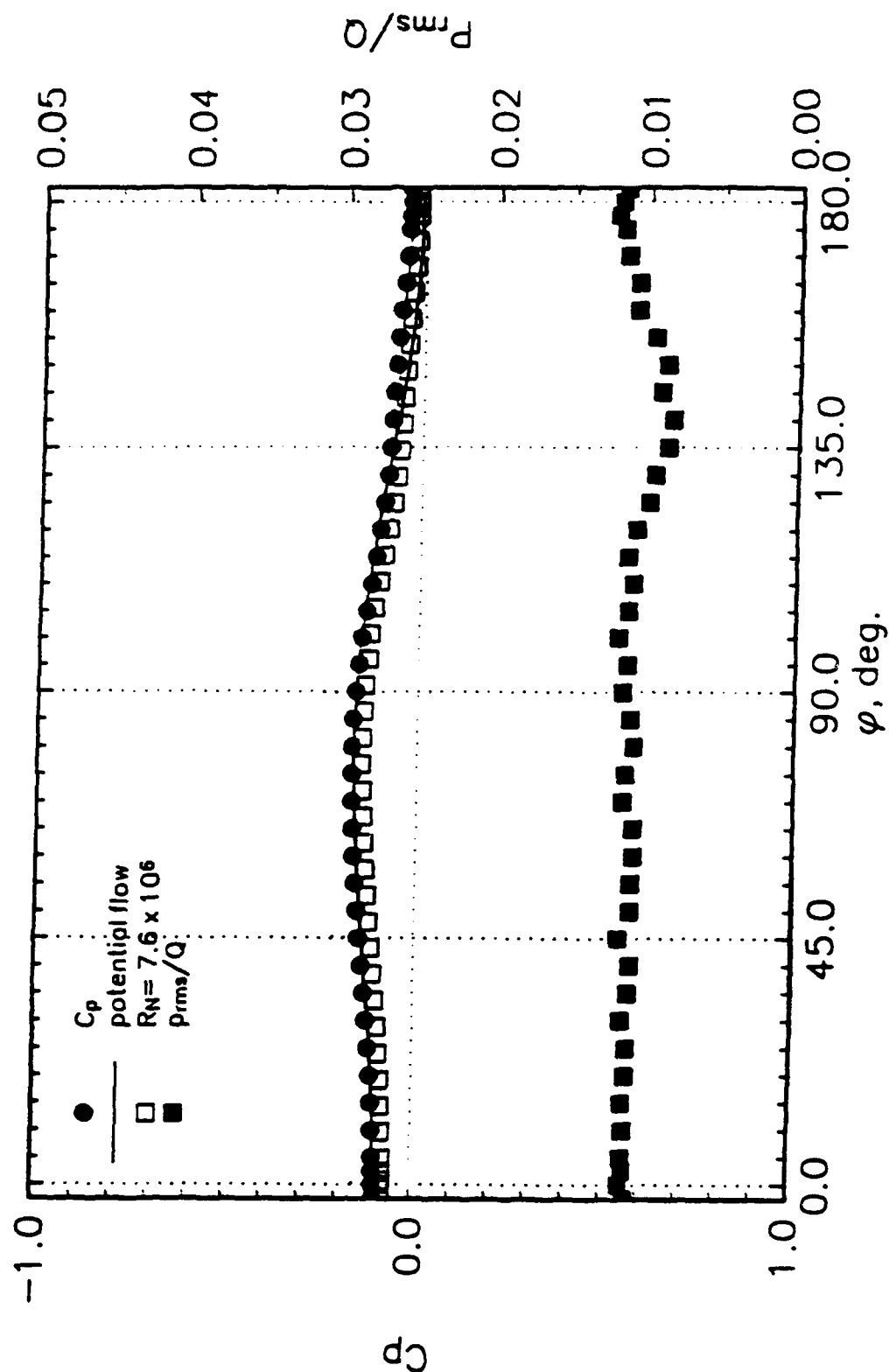


Figure A9. Mean and rms pressure distributions at $x/L = 0.6892$, $\alpha = 10^\circ$, $Re_L = 4.20 \times 10^6$.
 $Re_L = 7.7 \times 10^6$ data from Meier et al. (1986).

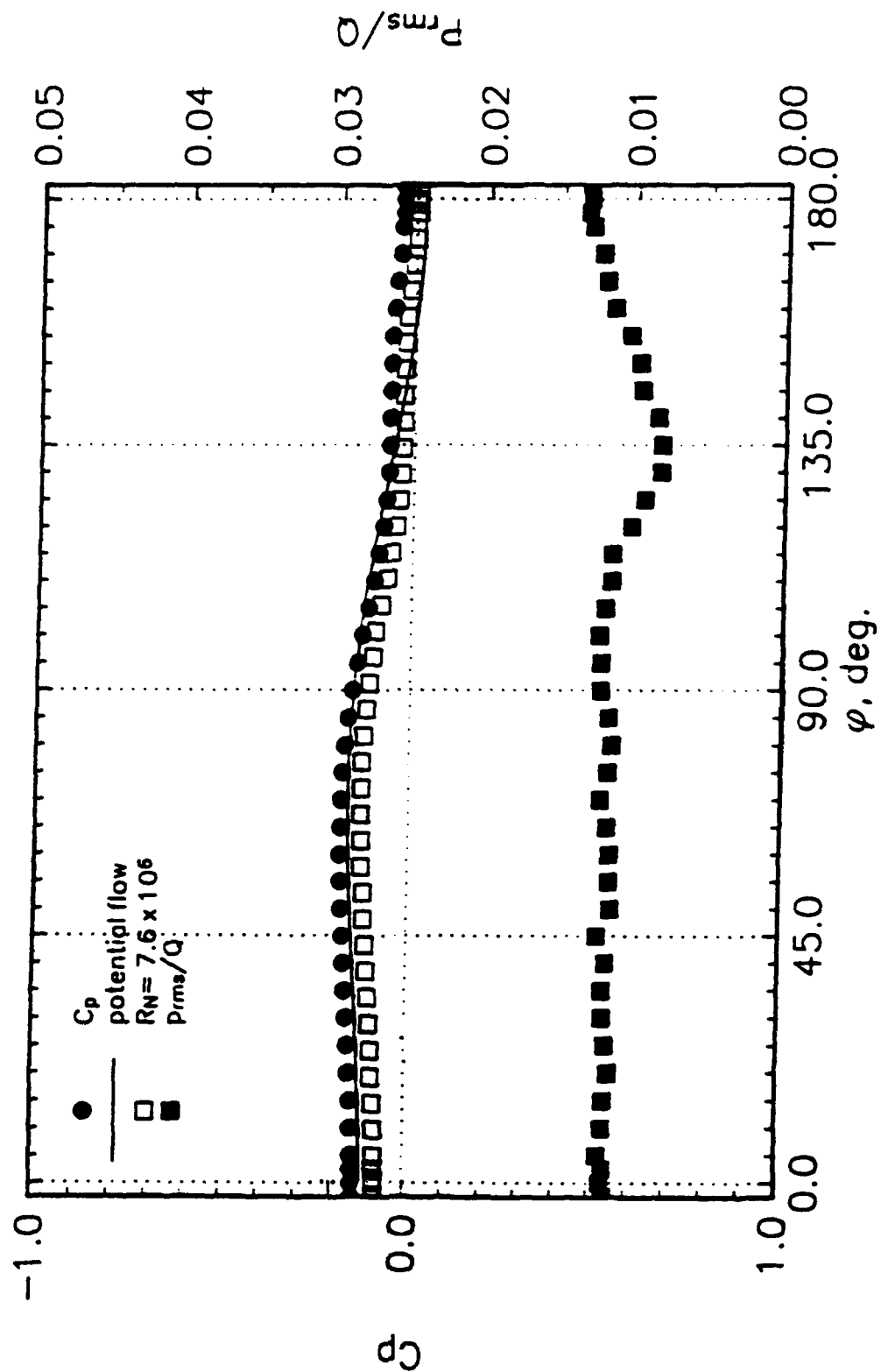


Figure A10. Mean and rms pressure distributions at $x/L = 0.7725$, $\alpha = 10^\circ$, $Re_L = 4.20 \times 10^6$.
 $Re_L = 7.7 \times 10^6$ data from Meier et al. (1986).

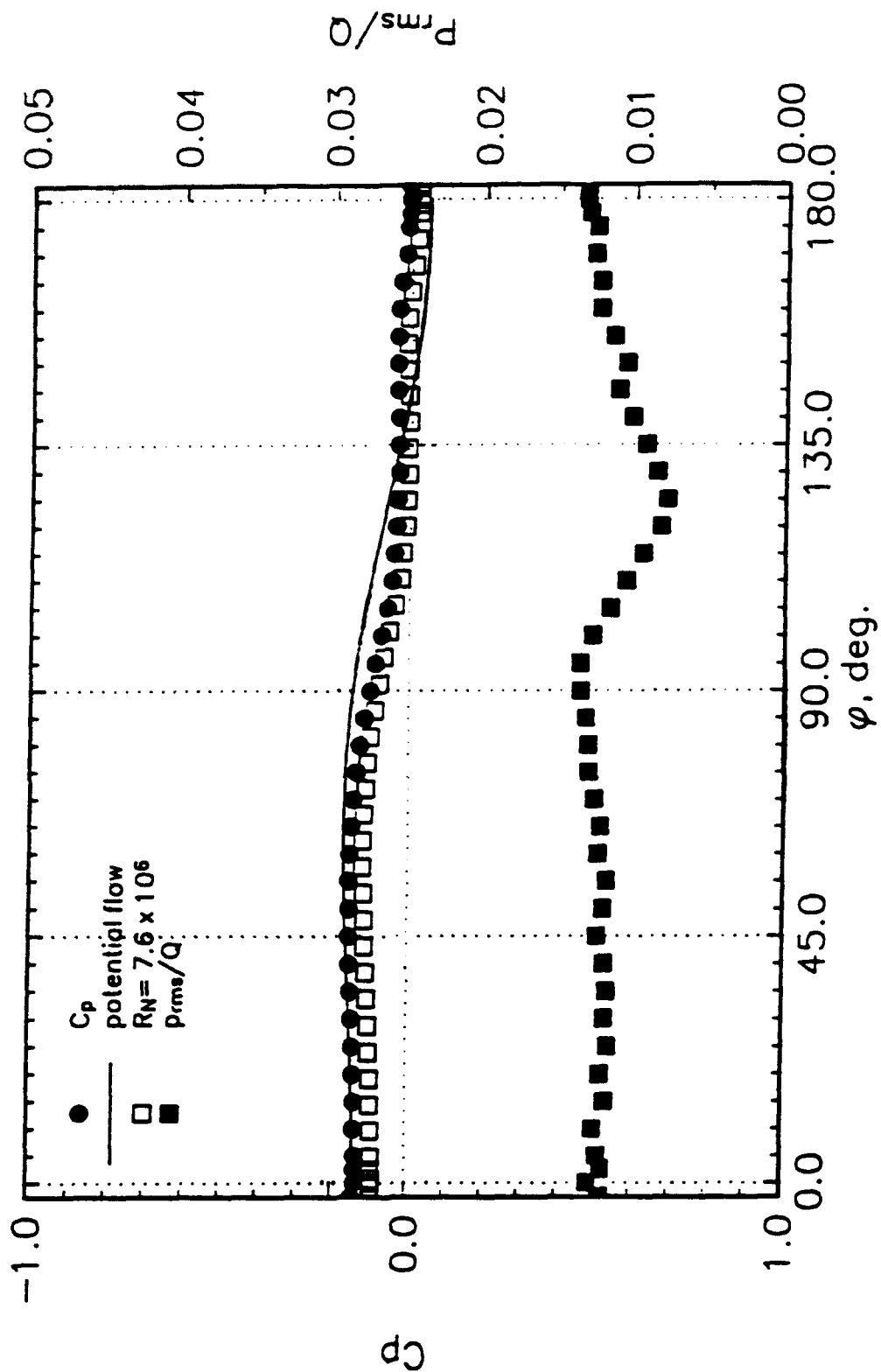


Figure A11. Mean and rms pressure distributions at $x/L = 0.8346$, $\alpha = 10^\circ$, $Re_L = 4.20 \times 10^6$.
 $Re_L = 7.7 \times 10^6$ data from Meier et al. (1986).

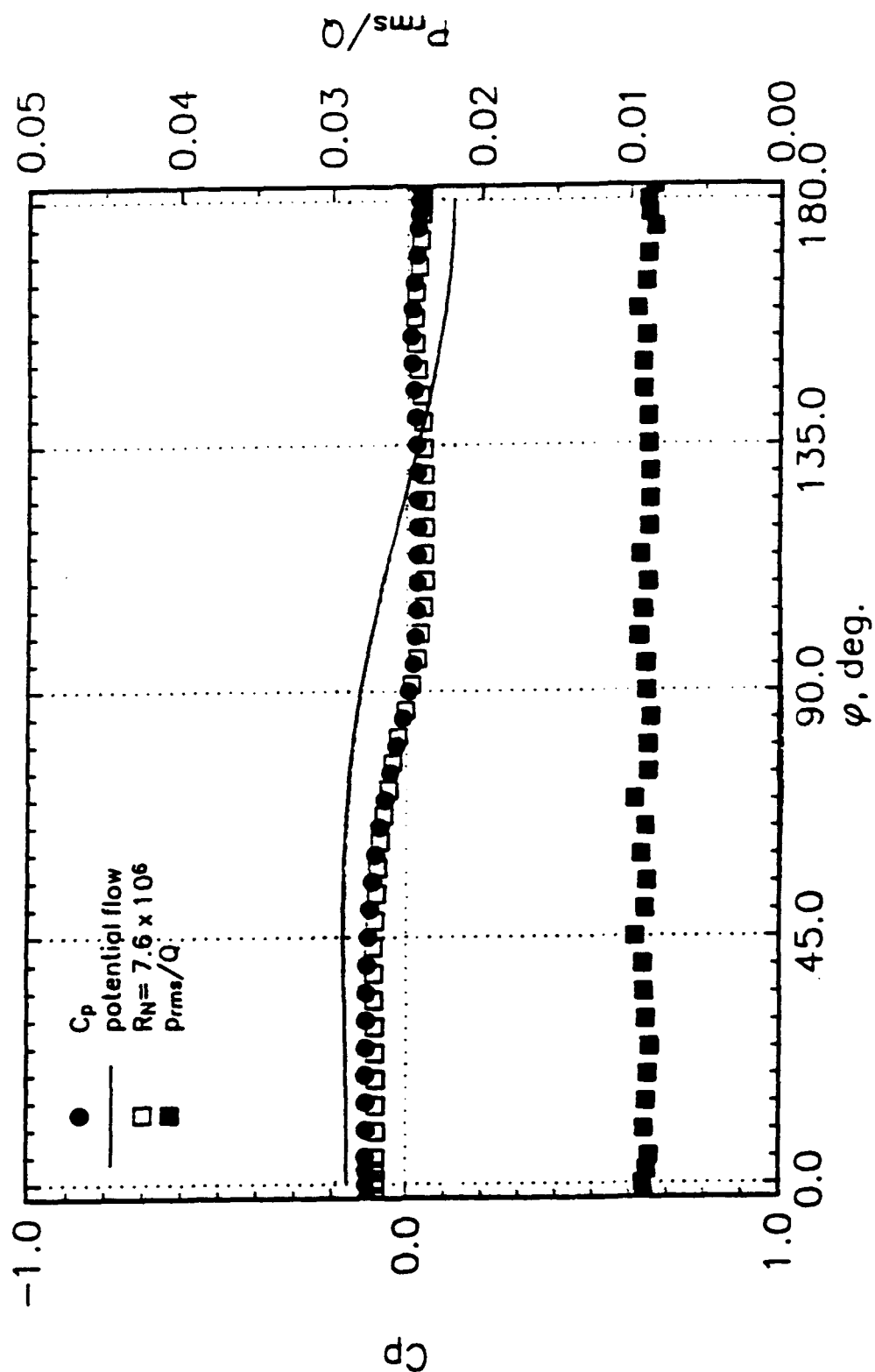


Figure A12. Mean and rms pressure distributions at $x/L = 0.8962$, $\alpha = 10^\circ$, $Re_L = 4.20 \times 10^6$.
 $Re_L = 7.7 \times 10^6$ data from Meier et al. (1986).

ACKNOWLEDGEMENTS

Development of the 6:1 prolate spheroid model was funded by the Office of Naval Research, Mr. James A. Fein, program manager. Development of the miniature, 3-D, fiber-optic, boundary-layer probe and research into the flow around this body was sponsored by the Defense Advanced Research Projects Agency, Mr. Gary W. Jones, program manager. The authors gratefully acknowledge the support of these agencies.

REFERENCES

AGARD 1990: Calculation of 3D Separate Turbulent Flows in Boundary Layer Limit. AGARD-AR-255, Neuilly sur Seine, France: AGARD

Ahn, S. 1992: An Experimental Study of Flow Over a 6 to 1 Prolate Spheroid at Incidence. PhD Dissertation, Aerospace and Ocean Engineering, Virginia Polytechnic Institute and State University, Blacksburg, Virginia

Barber, K. M.; Simpson, R. L. 1990: Mean Velocity and Turbulence Measurements of Flow Around a 6:1 Prolate Spheroid. Aerospace and Ocean Engineering Report, VPI-AOE-174. Blacksburg, Virginia: Virginia Polytechnic Institute and State University

Barber, K. M.; Simpson, R. L. 1991: Mean Velocity and Turbulence Measurements of Flow Around a 6:1 Prolate Spheroid. In: 29th Aerospace Sciences Meeting, January 7-10, Reno Nevada. AIAA Paper 91-0255

Barveris, D.; Chanetz, B. 1986: Decollement en Ecoulement Incompressible Tridimensionnel: Experiences de Validation et Modelisation. In: 23^{ème} Colloque D'Aérodynamique Appliquée, Aussois, November, 1986

Chanetz, B.; Détery, J. 1988: Experimental Analysis of Turbulent Separation on an Oblate Ellipsoid-Cylinder. *La Recherche Aéronautique* 3, 59-77

Cooke, J. C.; Hall, M. G. 1962: Boundary Layers in Three Dimensions. In: *Progress in Aeronautical Sciences*. (ed. Ferri, A.; Küchemann, D.; Sterne, L. H. G.). Vol. 2, pp. 221-282. New York: The MacMillan Company

Durst, F.; Martinuzzi, R.; Sender, J.; Thevenin, D. 1992: LDA Measurements of Mean Velocity, RMS-Values and Higher Order Moments of Turbulence Intensity Fluctuations in Flow Fields with Strong Velocity Gradients. In: *Proceedings of the Sixth International Symposium on Applications of Laser Techniques to Fluid Mechanics*, Lisbon, Portugal, 5.1.1-5.1.6

Fu, T. C.; Shekariz, A.; Katz, J.; and Huang, T. T. 1992: The Flow Structure in the Lee Side of and Inclined Prolate Spheroid. In: *Nineteenth Symposium on Naval Hydrodynamics*, Seoul, Korea, August 24-28, 1992

Gee, Ken; Cummings, Russell M.; and Schiff, Lewis B. 1992: Turbulence Model Effects on Separated Flow About a Prolate Spheroid. *AIAA Journal* 30, No.3, pp. 655-664

Kreplin, H. P.; Vollmers, H.; Meier, H. U. 1985: Wall Shear Stress Measurements on an Inclined Prolate Spheroid in the DFVLR 3m x 3m Low Speed Wind Tunnel. Data Report, DFVLR IB 222-84/A 33. Göttingen

Meier, H. U.; Kreplin, H. P. 1980: Experimental Study of Boundary Layer Transition and Separation on a Body of Revolution. *Z. Flugwiss. Weltraumforschung*, Vol. 4, No. 2, pp. 65-71

Meier, H. U.; Kreplin, H. P.; Landhauser, A.; Baumgarten, D. 1984: Mean Velocity Distributions in Three-Dimensional Boundary Layers Developing on a 1:6 Prolate Spheroid with Natural Transition. Data Report, DFVLR IB 222-4/A 10. Göttingen

Meier, H. U.; Kreplin, H. P.; and Landhauser, A. 1986: Wall Pressure Measurements on a 1:6 Prolate Spheroid in the DFVLR 3m x 3m Low Speed Wind Tunnel ($\alpha=10^\circ$, $U_\infty=55\text{m/s}$, Artificial Transition). Data Report, DFVLR IB 222-86 A 04. Göttingen

Sendstad, O.; and Moin, P. 1992: The Near Wall Mechanics of Three-Dimensional Turbulent Boundary Layers. TF-57. Stanford, California: Department of Mechanical Engineering, Stanford University

Vollmers, H.; Kreplin, H. P.; Meier, H. U.; Kühn, A. 1985: Measured Mean Velocity Field Around a 1:6 Prolate Spheroid at Various Cross Sections. Data Report, DFVLR IB 221-85 A 08. Göttingen